UC Berkeley
UC Berkeley Electronic Theses and Dissertations

Title
Development of Gold-Catalyzed Oxidative Alkene Heteroarylation and of Enantioselective Reactions Enabled by Phase Separation

Permalink
https://escholarship.org/uc/item/8w83k1js

Author
Lackner, Aaron D.

Publication Date
2013

Peer reviewed|Thesis/dissertation

eScholarship.org Powered by the California Digital Library
University of California

Development of Gold-Catalyzed Oxidative Alkene Heteroarylation and of Enantioselective Reactions Enabled by Phase Separation

by

Aaron Daniel Lackner

A dissertation submitted in partial satisfaction of the

requirements for the degree of

Doctor of Philosophy

in

Chemistry

in the

Graduate Division

of the

University of California, Berkeley

Committee in charge:

Professor F. Dean Toste
Professor Peter Vollhardt
Professor Stuart Linn

Spring 2013

Development of Gold-Catalyzed Oxidative Alkene Heteroarylation and of Enantioselective Reactions Enabled by Phase Separation

© 2013

by Aaron Daniel Lackner

Abstract

Development of Gold-Catalyzed Oxidative Alkene Heteroarylation and of Enantioselective Reactions Enabled by Phase Separation

by

Aaron Daniel Lackner

Doctor of Philosophy in Chemistry

University of California, Berkeley

Prof. F. Dean Toste, Chair

As with many bodies of research compiled through the course of a graduate career, this thesis reflects an uneven progression of aim based on the accumulation of unexpected results. Three main topics will be discussed in this thesis' chapters that may appear somewhat disparate. In particular, a significant conceptual gap exists between the first topic, oxidative gold catalysis, and the second topic, chiral anion phase-transfer catalysis. However, these fields are united by the realization that the characteristics of a reagent integral to the former might also be uniquely suitable for implementation in the latter.

Chapter 1 discusses the development of a redox-active Au(I)-Au(III) catalytic system for the functionalization of alkenes. Based on early precedent, we hoped to show that the strong dicationic oxidant Selectfluor could generate a catalytically active cationic Au(III) center that enables reactivity that cannot be achieved through Au(I) catalysis, terminating in an arylation rather than protonation to return the catalyst. Methods for the intra- and intermolecular heteroarylation of alkenes were developed and experiments were performed suggesting an unusual reaction mechanism. Attempts to expand the types of transformations that could be accomplished under this mode of reactivity unexpectedly led us to consider instead the properties of Selectfluor and how it could be effectively employed as a reagent in enantioselective transformations.

Chapter 2 addresses this very topic. The dicationic nature of the electrophilic fluorination reagent Selectfluor imparts on it many favorable qualities, but solubility in organic solvents is not one of them. Using a concept developed earlier within our laboratories, we hoped to show that this insolubility could be used to suppress racemic background reaction in enantioselective fluorination reactions, a class of transformation that remains largely underdeveloped in the literature. Lipophilic chiral phosphate anions, which can undergo anion exchange with the reagent salt, serve to solubilize the cationic fluorinating agent, rendering it both chiral and available for reaction with a suitable substrate. This mode of reactivity, chiral anion phase-transfer catalysis, was used to develop the enantioselective fluorocyclization of alkenes. Studies in the use of another type of cationic electrophile for the enantioselective oxidation of alcohols will also be discussed.

An extension of the concept of phase-separation for suppression of unwanted reactivity was applied to the deracemization of chiral amines, which is presented in Chapter 3. Single-operation deracemization, in which a racemic substrate is dynamically resolved to

its enantioenriched form, generally employs an oxidant to destroy a stereocenter and a reductant to reform it, as well as a chiral element to impart enantioselectivity on at least one of these steps. The highly reactive nature of oxidants and reductants towards one another has thus far precluded the development of such a deracemization by purely chemical means. We hypothesized that by separating the oxidant, substrate, and reductant into different phases, we could use a single catalyst to promote both the oxidation and subsequent enantioselective reduction of chiral substrates. This concept was used in the development of a deracemization protocol for 3H indolines and other chiral amine substrates.

Table of Contents

Abstract……..……1
Table of contents…….……i
Acknowledgements…….……ii

Chapter 1. Oxidative gold-catalyzed heteroarylation of alkenes
Abstract…….……...…....1
Introduction…….……...…….2
Results and discussion…….…….……...…….……5
Conclusion…….....…….....14
Experimental details…….…….…15
Notes and references……..…….…...35
NMR and HPLC spectra……..……..36

Chapter 2. Enantioselective electrophilic fluorination through chiral anion phase-transfer catalysis
Abstract……...…...83
Introduction…….....…...84
Results and discussion…….…….……87
Conclusion…….....…….....97
Experimental details……..……98
Notes and references…….…...121
NMR and HPLC spectra……..122

Chapter 3. Single-operation chemically catalyzed deracemization of racemic 3H indolines enabled by phase separation
Abstract……...….192
Introduction…….....….193
Results and discussion……..…...…195
Conclusion…….....…….....202
Experimental details…….…203
Notes and references…….…...217
NMR and HPLC spectra……..218

Acknowledgements

Five years of academic research can feel like a very long time, and at least in my case, would not have been such a positive experience, or even possible, if not for the support and opportunities afforded by a number of individuals. They have kept me sane and happy, and I am lucky to have had and continue to have such intelligent, thoughtful and caring people in my life.

First, I would like to thank my advisor, Dean Toste. Over the course of my research career here, he helped me move to more productive routes and projects when I lacked the context to see a dead end on my own. And when I had gained a little more perspective, he gave me the freedom to explore what I wanted, even when it was a long shot. I value my time working with Dean and hope

One of the greatest attributes of the Toste lab is the personnel. I have been fortunate to work alongside people who have taught me what I know about chemistry (and some other things). When I first arrived, about as green as could be, Heather Burks was kind enough to take the time (and it was a lot of time) to make sure I had proper lab technique. I had the great fortune of collaborating with two immensely talented postdocs, Skip Brenzovich and Vivek Rauniyar, from whom I learned not just chemical techniques but how to navigate through a project. I am greatly indebted to Greg Hamilton. He has acted as a mentor to me in his time in the group and thereafter, and really helped guide me towards taking on interesting projects (in some instances more directly than others), and helped me learn to write scientifically. My fellow classmates, Jeff Wu, Yiming Wang and Mika Shiramizu have shared my fear and pain at the board in group meeting and it has been, though sometimes stressful, a great experience to grow as scientists together.

I am fortunate to have had Sunghee Son in my life for the last four years. I have found in her someone who has helped me grow, someone I feel like I truly understand and who truly understands me. Even though we have spent the majority of our time together separated by thousands of miles, I feel lucky to have someone whose support I can feel so tangibly. I look forward to getting rid of those thousands of miles.

I would like lastly to thank my parents, Robin and Jim Lackner, and my brother, Josh Lackner. They have always supported me and given me every opportunity to succeed, and created a positive and supportive environment in which to live and develop. I am privileged that they have provided such an enabling and loving upbringing, and I thank them for getting me to where I am.

Chapter 1. Oxidative gold-catalyzed heteroarylation of alkenes

Gold-catalyzed activation of π-bonds toward nucleophilic attack is generally terminated in protodeauration, resulting in an overall hydrofunctionalization reaction. The diversion of this termination pathway to coincide with another bond-forming event would increase the complexity of products that can be obtained through gold catalysis in a single transformation. Here we report the development of the heteroarylation of terminal alkenes, in which both a carbon-heteroatom and a carbon-carbon bond are formed. Both intramolecular and intermolecular variants are demonstrated. Use of the electrophilic fluorine source Selectfluor as oxidant is necessary to drive a Au(I)-Au(III) catalytic cycle. Mechanistic experiments suggest a catalytic cycle in which concerted transmetallation/reductive elimination results in the carbon-carbon bond-forming event.

Portions of this chapter are based on work done in collaboration with William Brenzovich, Jr., Hunter Shunatona, and Asa Melhado.

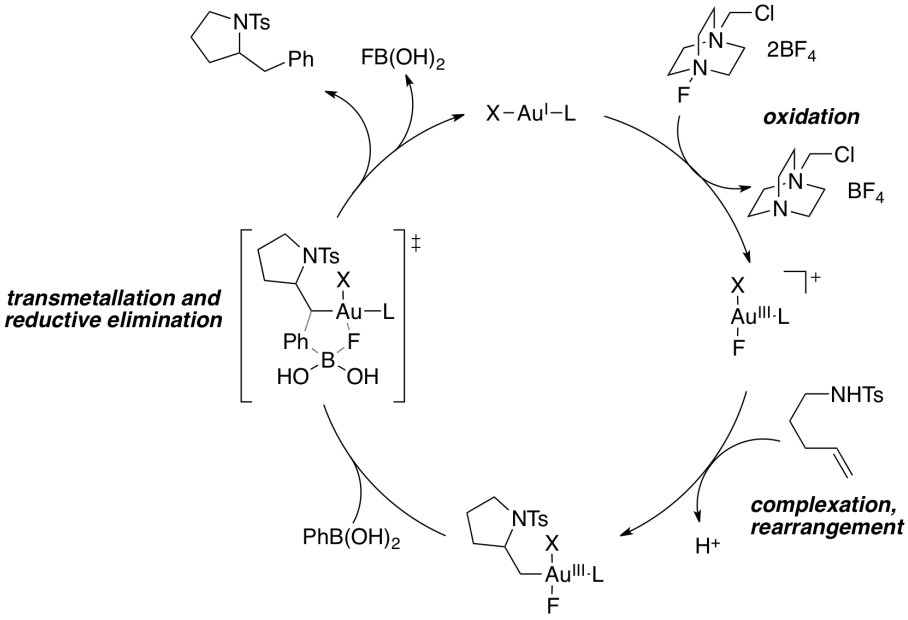

Introduction

The development of homogeneous gold-catalyzed reactions over the past 15 years has been remarkable, as indicated by the sheer rate of expansion of the field.[1a] Until the 1998 report by Teles on the addition of alcohol nucleophiles into alkyne substrates,[1b] only a handful of reports of homogeneous catalysis appeared in the literature on a yearly basis. The past several years, by comparison, have averaged greater than 200 publications on the topic. In the majority of these reported reactions, gold is thought of as a π-acid in its cationic form and +1 oxidation state. As such, it is used to activate alkynes, allenes, and, less frequently, alkenes, towards attack by a nucleophile. The resultant organogold complex generally undergoes protodeauration to regenerate the cationic Au(I) catalyst and complete an overall hydrofunctionalization such as the hydroamination shown in Scheme 1.[2]

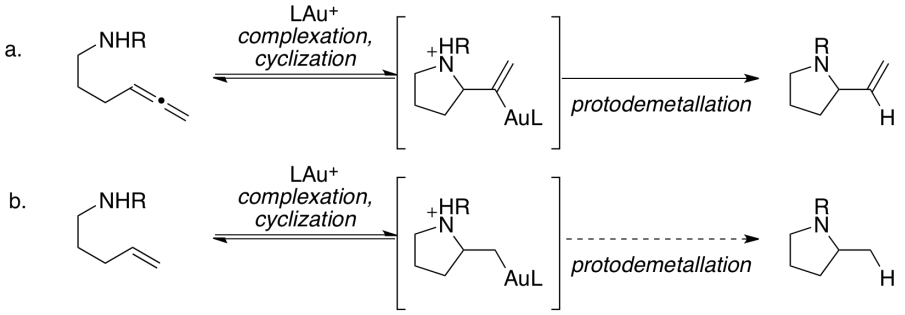

Scheme 1. Gold-catalyzed functionalization of allenes proceeds more readily than of alkenes.

Studies of the kinetic basicities of organogold complexes indicate that vinylgold complexes protdeaurate much more readily than do alkylgold complexes, suggesting one major reason that allenes and alkynes undergo gold-catalyzed addition and rearrangement reactions more facilely than do alkenes (Scheme 1, a vs b).[3] In fact, in the case of alkene functionalization protocols employing a gold catalyst, the actual role of gold has been called into question. Under the elevated reaction temperatures employed by He, Hartwig has shown that nearly identical results are achieved using the conjugate acid of the gold counterion, trifluoromethanesulfonic acid, implying that strong acid generated *in situ* may be the active catalyst, rather than the gold complex (Scheme 2).[4]

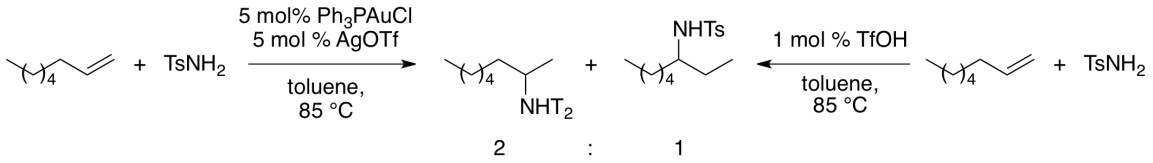

Scheme 2. The role of gold in alkene functionalization is unclear, as a potential byproduct, triflic acid, similarly catalyzes the transformation (ref. 4).

It is in the interest of the field to demonstrate as clearly as possible that gold-catalyzed transformations are indeed gold-catalyzed. And while appropriate control experiments must be undertaken to confirm the gold complex as the active catalyst in each transformation, the value of gold catalysis might also be effectively demonstrated through

the development of transformations that cannot be catalyzed by simple acid. The demonstration of unique reactivity (which is evident in many other classes of gold-catalyzed reactivity) is also a practical one, as products of increasing complexity may be accessed through operationally simple transformations.

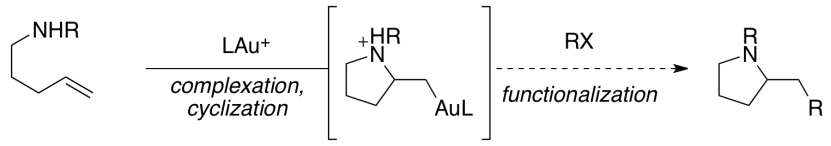

Scheme 3. Proposed gold-catalyzed heterofunctionalization of alkenes.

In this context, we were interested in exploring an oxidative cross coupling event as a final elementary step in a catalytic cycle,[5] resulting in an overall heteroarylation reaction (Scheme 3, R = Ar). Several developments in the field had paved the way for this thinking. Using $AuCl_3$ as catalyst for the 5-*endo-dig* hydroalkoxylation of allenes, Hashmi observed the formation of the diene shown in Scheme 4 as a byproduct.[6] This is suggestive of reductive elimination from a diorganogold(III) intermediate (which might be generated either through disproportionation or through a second allene activation by the monoorganogold(III) complex), and in fact the product to gold ratio indicates stoichiometric formation of dimer product, along with unactive Au(I).

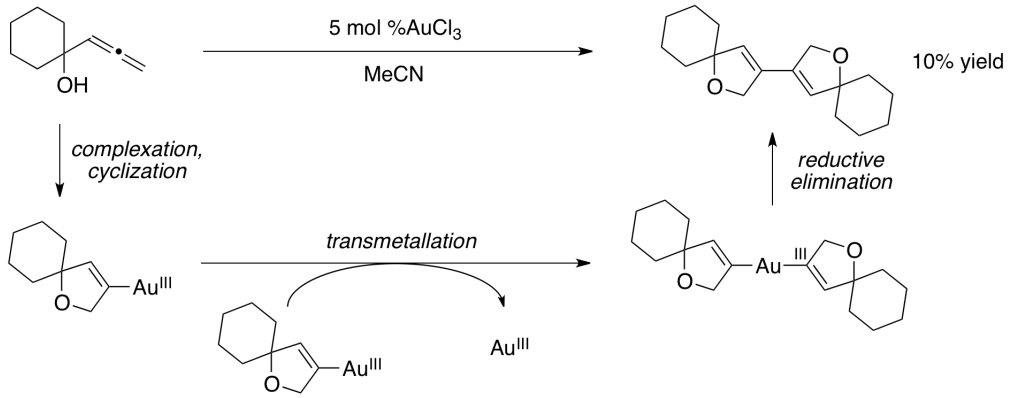

Scheme 4. Observation of Au(III) mediated cross coupling (ref. 6).

In order to render such a coupling catalytic, a suitable oxidant to regenerate Au(III) is necessary. This is not trivial, as the oxidation potential for Au(I) vs Au(III) is +1.41 V;[7] however the Zhang group demonstrated that Selectfluor, a dicationic electrophilic fluorination reagent, can be used to drive the homocoupling of rearranged propargyl esters when used in conjunction with a PPh_3AuCl catalyst (Scheme 5).[8]

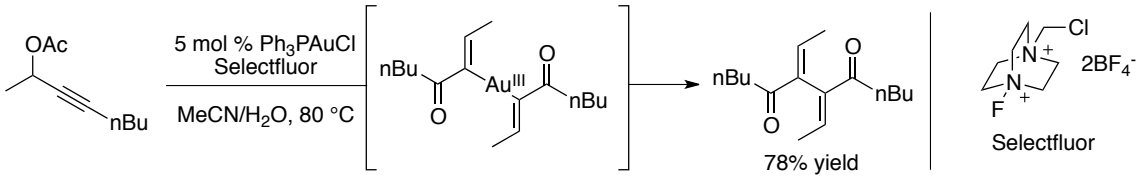

Scheme 5. Selectfluor used as stoichiometric oxidant for the gold-catalyzed homo-coupling of propargyl acetates (ref. 8).

The same authors took this concept a step further, employing a phenylboronic acid as a coupling partner, effecting a cross coupling from an analogous putative vinylgold(III) fluoride intermediate.[9] The preference for the cross-coupled product is likely driven by the formation of the very strong B-F bond that results from delivery of the arene. However, while the desired products were isolated in good overall yield, competitive homodimerization and protodemetallation products were also observed. The authors' proposed mechanism is shown in Figure 1.

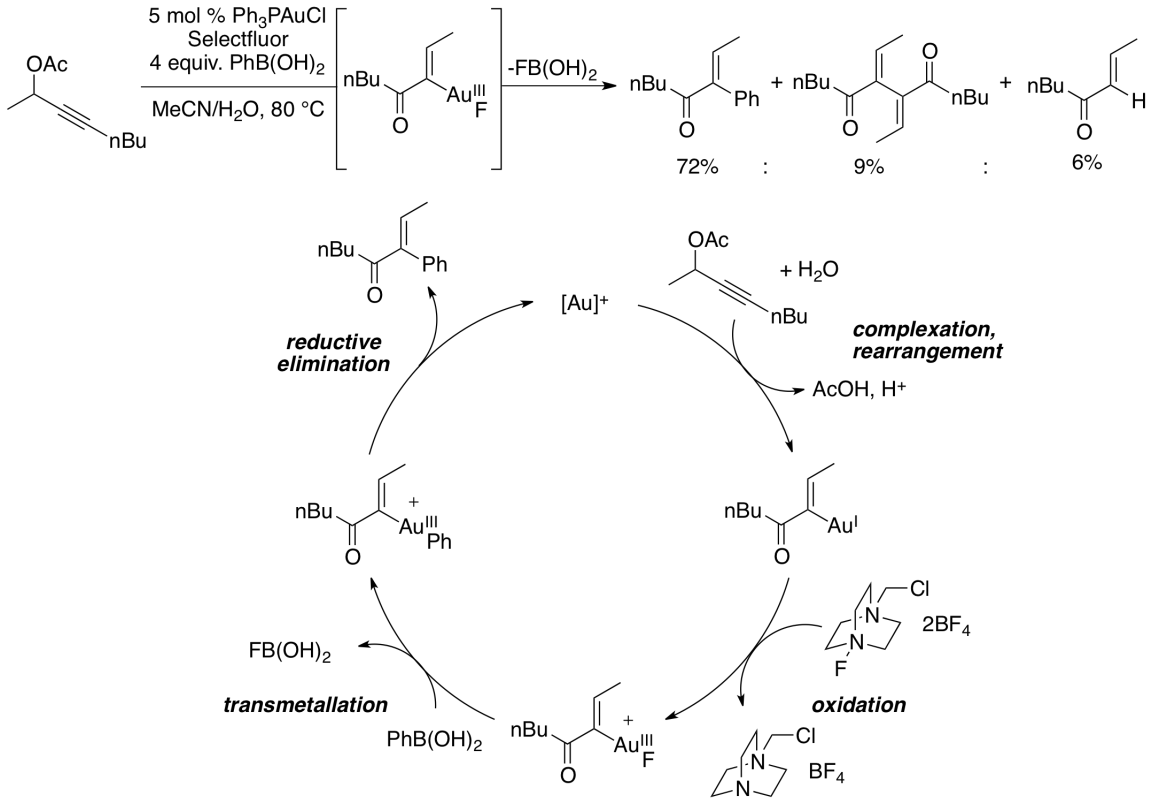

Figure 1. Gold-catalyzed oxidative cross coupling reaction and the proposed mechanism (ref. 9).

An analogous functionalization of alkenes using Selectfluor as an oxidant was particularly attractive to us. The general lack of productive reactivity of alkenes in typical cationic Au(I) chemistry seemed especially advantageous for oxidative cross coupling under the demonstrated system. Alkylgold intermediates would be much less prone to form undesired side products resulting from protodeauration and homocoupling. In fact, studies in our lab had recently led to the isolation of a stable alkylgold(I) intermediate **1.2** generated from an aminoalkene substrate, a cationic gold(I) catalyst and an organic base scavenger.[10] Notably, when this alkylgold complex was exposed to acidic conditions, reversion to starting material, rather than protodemetallation, was observed (Scheme 6).

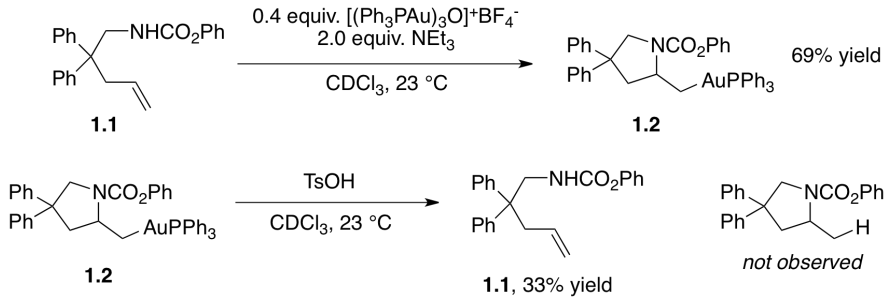

Scheme 6. Observation of aminoarylated product from alkene starting material, and the absence of protodemetallation product (ref. 10).

Thus, we hoped to show that by utilizing an oxidative mechanism to generate a reactive cationic species, transformation of alkenes by gold catalysis could be readily accomplished. Relying on a cross-coupling/deauration step to regenerate the free catalyst rather than protodeauration would lead to products of added complexity.

Results and Discussion

Substrate **1.3**, a close analog to the substrates used in the alkene aminoarylation, was chosen for initial reaction studies. We were pleased to see that using PPh_3AuCl as catalyst in the presence of Selectfluor and phenylboronic acid as a coupling partner, the aminoarylation product **1.4a** was observed in 24% yield (Table 1, entry 1). Previous research in our lab has led us to consider the importance of the counterion (in this case the X-type ligand) in gold catalysis, and by changing its nature, trends in reactivity became apparent. By employing less coordinating counterions on gold, conversion to desired product dropped (entry 2, 3). One reasonable explanation for this result is the decreasing ability to form (or stabilize) a Au(III) intermediate. If the Au(I) center already has a degree of cationic character (as would be the case for non-coordinating X-type ligands), it is unlikely to form the putative active Au(III) center as a dication. Exploring other halides as counterions, use of PPh_3AuBr led to a significant increase in desired product formation (entry 4). Using the same logic, bromide should better stabilize a developing cationic Au(III) center than should chloride.

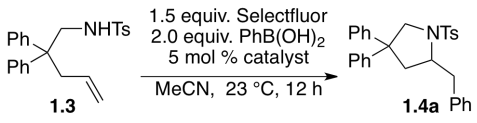

entry	catalyst	yield
1	Ph_3PAuCl	24%
2	$Ph_3PAuOBz$	18%
3	$Ph_3PAuOTf$	<5%
4	Ph_3PAuBr	47%
5	Ph_3PAuI	<5%
6	tBu_3PAuCl	<5%
7	Cy_3PAuCl	<5%
8	$[(Ph_3P)_2Au]BF_4$	22%
9	Ph_3PAuPh	31%

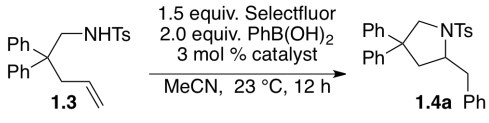

entry	catalyst	yield
1	$dppm(AuBr)_2$	72%
2	$dppm(AuCl)_2$	37%
3	$dppb(AuBr)_2$	26%
4	$XANTPHOS(AuBr)_2$	43%

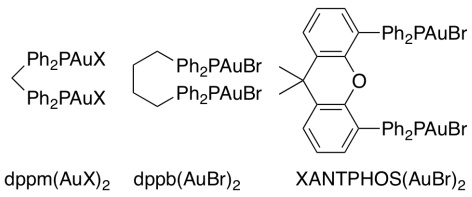

Tables 1 and 2. The exploration of counterion effect and dinuclear catalysts in aminoarylation.

Unfortunately, when gold complexes bearing more donating ligands such as the analogous iodide (entry 5) or more electron rich alkylphosphines (entry 6, 7), no desired product was observed. It is likely that this is a result of direct reaction between ligand and Selectfluor, though attempts to recover the presumed phosphine oxide byproduct were never carried out.

The presence of a catalyst byproduct, $(PPh_3)_2Au^+$, however, was observed by ^{31}P NMR as the major species during the course of the reaction with PPh_3AuBr. The cationic bisphosphinegold(I) complex, when prepared independently, however, gave the desired product in lowered yield (entry 8), indicative of a catalyst deactivation pathway. In considering further ways to avoid this nonproductive consumption of catalyst, exploitation of aurophilic interaction, in which an adjacent Au(I) center stabilizes the oxidized Au(III) center[11] offered a possible solution. The dinuclear complex $dppm(AuBr)_2$, in which the two gold centers are held together in close proximity, led to a significant improvement in isolated yield (Table 2, entry 1). The analogous chloride compound was less advantageous (entry 2), and complexes such as $dppb(AuBr)_2$, which has a longer alkyl tether that does less to reinforce geometry, and $XANTPHOS(AuBr)_2$, which is more structurally rigid but holds the two gold centers of the dinuclear complex more distally, were not significantly more effective than their mononuclear counterparts (entries 3, 4). It should be noted that through the course of optimization, no significant byproduct resulting from the substrate was observed. Having developed a catalyst that showed reasonable efficacy in the desired transformation, we set about determining the scope of the aminoarylation reaction.

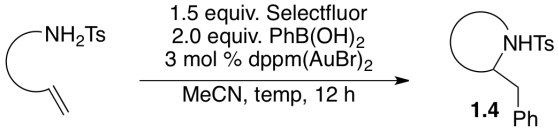

product		temp (°C)	yield	product		temp (°C)	yield
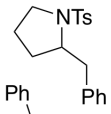	**1.4b**	23	70%	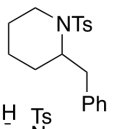	**1.4f**	40	82%
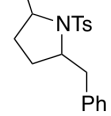	**1.4c**	23	72%[a]	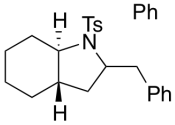	**1.4g**	23	92%[d]
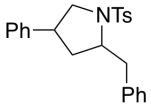	**1.4d**	23	72%[b]	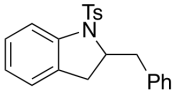	**1.4h**	23	63%
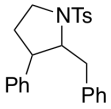	**1.4e**	23	33%[c]	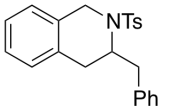	**1.4i**	40	63%

[a] diastereoselectivity: 1.1:1; [b] diastereoselectivity: 1.5:1; [c] diastereoselectivity: 1.2:1; [d] diastereoselectivity: 1.8:1

Table 3. Scope of aminoarylation reaction with regard to alkene substrate.

Terminal alkenes with amines of varying tethers proved viable substrates. The Thorpe-Ingold effect is not crucial to the success of the reaction, as unsubstituted pyrrolidine **1.4b** was isolated in good yield (Table 3). Substitution at the positions α- (**1.4c)**, β- (**1.4d**), and γ- (**1.4e)** to the amine were well tolerated, though diastereoselectivity was uniformly low. Bicyclic products, such as dihydroindoles (**1.4h)** and tetrahydroisoquinolines (**1.4i**), and six-member piperidines (**1.4f**, **1.4i**) were also accessed in good yield, though in the latter case a slightly elevated reaction temperature was necessary.

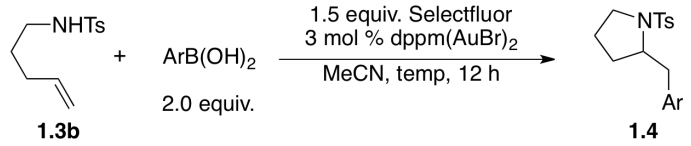

1.3b **1.4**

product		temp (°C)	yield	product		temp (°C)	yield
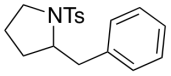	**1.4b**	23	70%	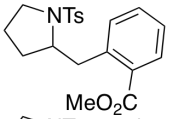	**1.4m**	40	77%
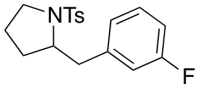	**1.4j**	40	75%	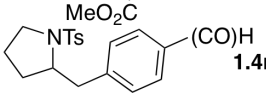	**1.4n**	23	68%
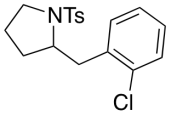	**1.4k**	40	56%	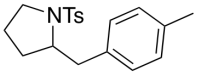	**1.4o**	23	81%
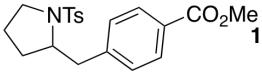	**1.4l**	40	83%	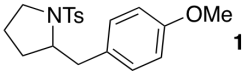	**1.4p**	23	17%

Table 4. Scope of the aminoarylation with regard to arylboronic acid coupling partner.

The nature of the arylboronic acid coupling partner was also investigated and a variety of substitutions were tolerated (Table 4). Arylboronic acids with substitution at the *ortho*-, *meta*-, and *para*- positions were effectively incorporated into aminoarylation products. Oxidation-sensitive aldehyde functionality was not compromised under reaction conditions, though in the case of highly electron rich arenes, competitive direct arene oxidation by Selectfluor limits the efficacy of the transfomation (**1.4p**).

Substrates that were not amenable to the transformation include internal alkenes and less electron-deficient amines. We believe this is a result of the decreased ability to cross-couple from a more highly substituted (secondary or tertiary) carbon center, and the propensity to react directly with Selectfluor, respectively.

During the course of optimization, assessment of different reaction solvent mixtures led to an unexpected result. While the dicationic nature of Selectfluor imparts on it a general insolubility that requires the use of acetonitrile as the main solvent, other additives were explored in order to improve the solubility of the boronic acid coupling partner. In an attempt to further optimize the reaction of substrate **1.5**, the addition of isopropyl alcohol cosolvent led not to the expected cylclized product, but instead to **1.6a**, resulting from the

incorporation of the alcohol cosolvent (Scheme 7). Thus, surreptitiously, an intermolecular three-component alkoxyarylation of alkenes had been achieved.

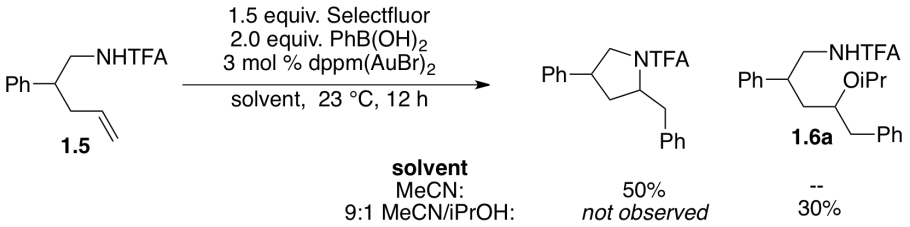

Scheme 7. Incoroporation of nucleophilic solvent constitutes an intermolecular three-component coupling.

After minor optimization of reaction conditions (increased stoichiometry of catalyst, arylboronic acid and oxidant, increased reaction temperature, as well as addition of catalyst and boronic acid in two portions over two hours) the yield of alkoxyarylation product could be improved to 72% (Table 5, entry 1).

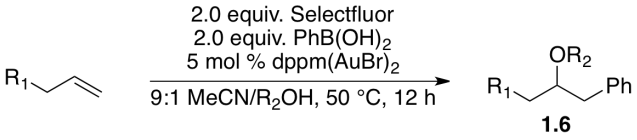

product		yield	product		yield
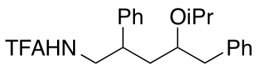	**1.6a**	72%[a]	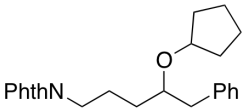	**1.6g**	85%
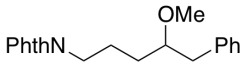	**1.6b**	79%	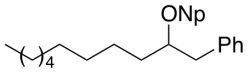	**1.6h**	66%
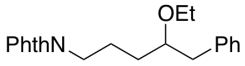	**1.6c**	85%	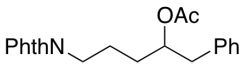	**1.6i**	62%
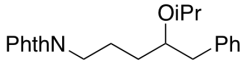	**1.6d**	90%	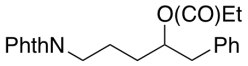	**1.6j**	69%
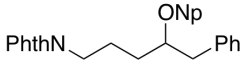	**1.6e**	91%	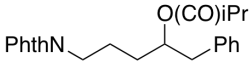	**1.6k**	50%
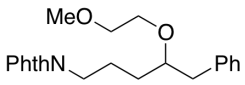	**1.6f**	85%	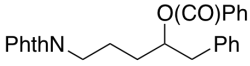	**1.6l**	48%

[a] diastereoselectivity: 1.4:1

Table 5. Scope of alcohol and carboxylic acid addition in the alkoxyarylation reaction.

We were pleased that a number of simple alkenes and alcohols could be effectively coupled with phenylboronic acid under the same protocol, including the hindered neopentyl alcohol (**1.6e**, **1.6h**). Carboxylic acids were also suitable nucleophiles (**1.6i-l**), though yields of the ester products were more modest. Similarly to the intramolecular mode, a variety of arylboronic acids were effectively coupled in high yields (Table 6).

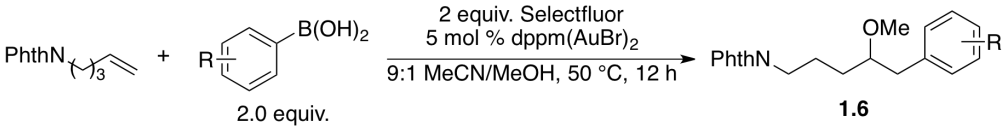

R	yield	R	yield
4-Me, **1.6m**	88%	4-CO_2Me, **1.6p**	88%
4-Br, **1.6n**	90%	4-(CO)H, **1.6q**	90%
4-F, **1.6o**	79%	3,5-bis-CF_3, **1.6r**	79%

Table 6. Scope of boronic acid coupling partner in alkoxyarylation reaction.

Employing water as a cosolvent offers the possibility of arriving directly at potentially useful alcohol (rather than ether or ester) products under mild conditions. In fact simple replacement of the alcohol cosolvent with water yielded the desired free alcohols in generally high yields, the result of alkene hydroxyarylation (Table 7).

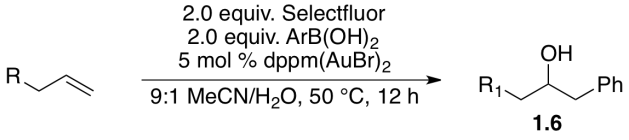

product		yield	product		yield
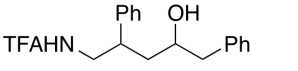	**1.6s**	88%[a]	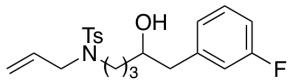	**1.6v**	85%
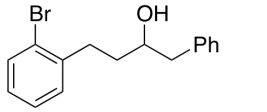	**1.6t**	79%	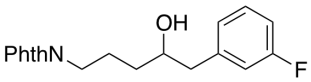	**1.6w**	62%
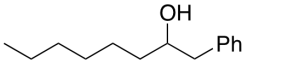	**1.6u**	85%	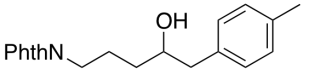	**1.6x**	62%

[a] diastereoselectivity: 1.2:1

Table 7. Alcohol products resulting from hydroxyarylation reaction.

Having demonstrated a reasonably wide scope of alkene heteroarylation, we hoped to determine a reasonable reaction mechanism, as several observations through the course of our work were inconsistent with earlier proposals. For example, when considering the initial Zhang proposal (Figure 1), prior to oxidation to Au(III), a cationic Au(I) center is believed to promote cyclization of the substrate resulting in an alkylgold(I) intermediate, in analogy to conventional Au(I) catalysis. However, our initial results in varying the counterion on gold (Table 1, entries 1-3) indicated that less coordinating counterions, that impart a greater degree of positive charge on Au(I) in fact led to diminished yields.

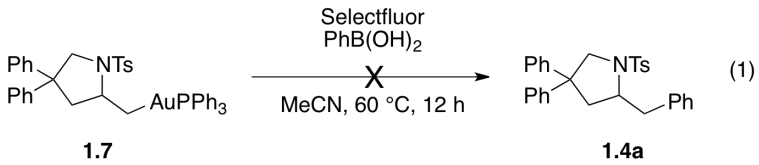

Furthermore, the putative intermediate alkylgold(I) delivered no desired product when exposed to typical reaction conditions (eq 1). As a result, we believe the data indicate that complexation and cyclization are not the first elementary steps in the heterofunctionalization reaction, preceding oxidation. It seems unlikely, too, that transmetallation of the arylboronic acid onto Au(I) is operative, as exposure of Au(I) catalyst to stoichiometric phenylboronic acid, even at elevated temperature, yielded no phenylgold(I) complex (eq 2). As discussed below, complexes of this type are shown to be catalytically active.

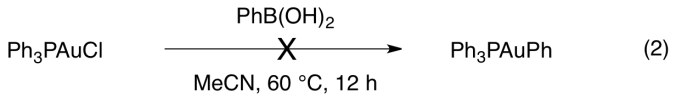

(2)

We are therefore left with oxidation of Au(I) to Au(III) by Selectfluor as the first step, prior to heteroauration. This makes sense intuitively, as electrophilic fluorination of the catalyst also renders it cationic, a general requisite for π-activation in gold catalysis. And as outlined above in the catalyst optimization, ligands that improve the stability of an electron-poor cationic Au(III) center promote conversion to desired product.

Discrete transmetallation of the arene coupling partner from boron onto gold and subsequent reductive elimination (in analogy to a palladium-catalyzed Suzuki cross-coupling) is also called into question on the basis of a set of control experiments. The complex Ph_3PAuPh, which would result from arene transmetallation, was shown to be a competent catalyst for aminoarylation (Table 1, entry 9). However, when Ph_3PAuPh was employed stoichiometrically in the absence of added phenylboronic acid, no significant product formation was observed (Table 8, entry 1). When stoichiometric phenylboronic acid was introduced, the desired reactivity was regained (entry 2). Furthermore, when the added arylboronic acid was different from the phenyl ligand on the catalyst, incorporation of the substituted arene was observed almost exclusively, regardless of their electronic properties (entry 3, 4). Taken together, these results suggest that any arene ligand on gold resulting from transmetallation would act mainly as a spectator, and not be incorporated into product as a result of reductive elimination to any significant degree.

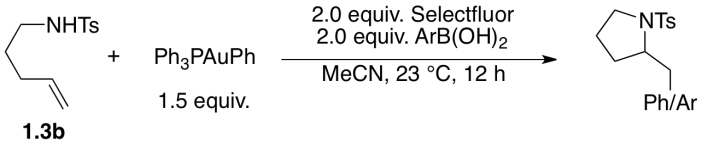

1.3b

entry	$ArB(OH)_2$	yield	Ar:Ph
1	--	<5%	--
2	$PhB(OH)_2$	52%	--
3	4-$MeC_6H_4B(OH)_2$	58%	94:6
4	4-$MeO_2CC_6H_4B(OH)_2$	37%	93:7

Table 8. Incorporation of external arylboronic acid rather than gold-bound arene.

Instead, on the basis of computations performed by the Goddard group, a concerted delivery of the arene and reductive elimination is proposed, again driven by the concomitant formation of a B-F bond. An approximately 5 kcal/mol preference for this

five-center bimolecular reductive elimination as compared to reductive elimination of an aryl ligand on the gold center was calculated. The overall proposed mechanism is presented in Figure 2.

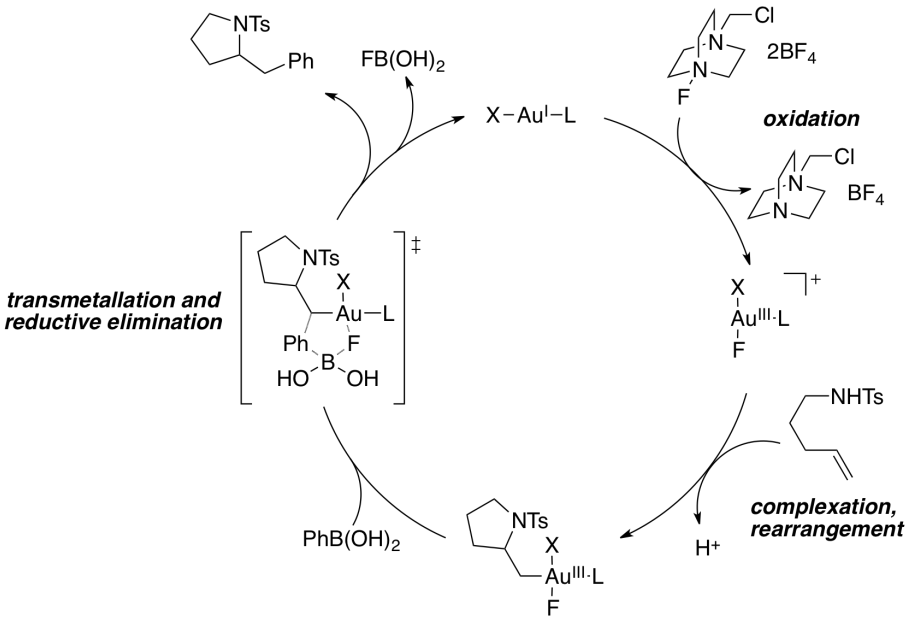

Figure 2. Proposed mechanism for the gold-catalyzed heteroarylation reaction.

Substrates of different types were also briefly explored for the development of tandem reactivity of different types. Generally speaking, we hoped to show that alkylgold(III) intermediates generated from different substrate classes could also undergo cross-coupling, or perhaps other modes of functionalization. Previous unpublished work in the Toste lab had indicated that when exposed to cationic Au(I), the silyl cyclopropyl ether substrate shown in Scheme 8 did not form any expected ketone product, which would result from ring expansion onto the activated alkene. Instead, epimerization of the starting material was observed, which suggests that the silyl cyclopropyl ether moiety itself is activated, opening to an alkylgold intermediate, which, unable to undergo protodemetallation, returns starting material.

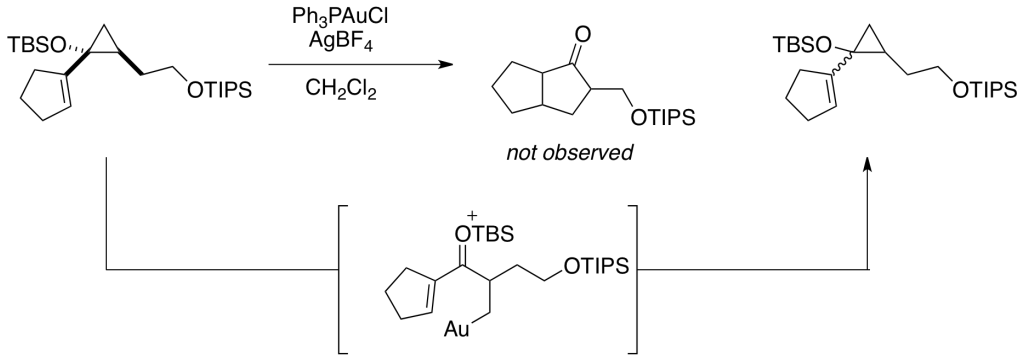

Scheme 8. Observation of epimerization of silyl cyclopropyl ether substrates in Au(I) catalysis.

We hypothesized that simple (and commercially available) cyclopropyl mixed acetals might similarly generate alkylgold intermediates, and that by employing the same oxidative conditions, cross coupling onto arylboronic acids could be accomplished (eq 3). This would represent an overall functionalized 3-carbon alkylation of arylboronic acids.

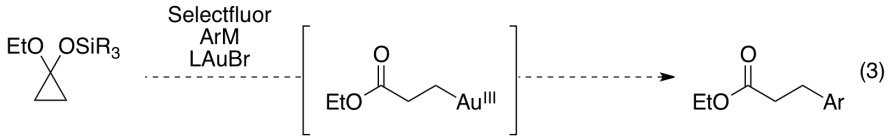

In initial attempts at the ring opening-cross coupling of substrate **1.11a**, an electron poor mononuclear gold complex that had been effective in intermolecular oxyarylation was employed and different coupling partners were examined (Table 9). Arylboronic acids gave the desired product **1.12**, though in low yield (entry 1), as did arylsilanes, which had recently been shown to be effective coupling partners (entry 2).[12] Aryl trifluoroborates, which had been ineffective in our previous studies as a result of significant arene homocoupling, proved more suitable in this context (entry 3). A brief catalyst screen showed similar trends to those observed with the alkenyl substrates, and again dppm$(AuBr)_2$ was the most effective catalyst (Table 10, entry 7), resulting in 44% yield of the desired product, though it should be noted that **1.11a** was employed as the limiting reagent in these cases, which is not ideal for an arene functionalization methodology.

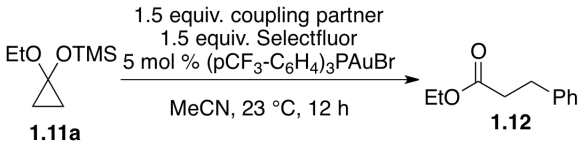

entry	coupling partner	yield
1	$PhB(OH)_2$	11%
2	PhTMS	9%
3	$PhBF_3K$	30%

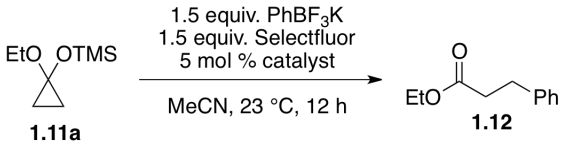

entry	catalyst	yield
1	$AuBr_3$	14%
2	Ph_3PAuCl	<5%
3	IPrAuCl	<5%
4	$(4\text{-}CF_3\text{-}C_6H_4)_3PAuBr$	30%
5	$(4\text{-}F\text{-}C_6H_4)_3PAuBr$	41%
6	$dppm(AuCl)_2$	38%
7	$dppm(AuBr)_2$	44%

Tables 9 and 10. Effect of coupling partner and catalyst on ring opening-coupling reaction.

Further increasing the stoichiometry of the aryl trifluoroborate led to slightly improved yield; conversely, using potassium phenyl trifluoroborate as the limiting reagent significantly diminished yield (Table 11, entries 1-4). Results were somewhat improved, however, by modifying the sacrificial protecting group on the acetal. When the slightly more robust triethylsilyl mixed acetal **1.11b** was employed, **1.12** was observed in 30% yield (entry 5), and using the free hemiacetal **1.11c**, a yield of 40% was achieved (entry 6).

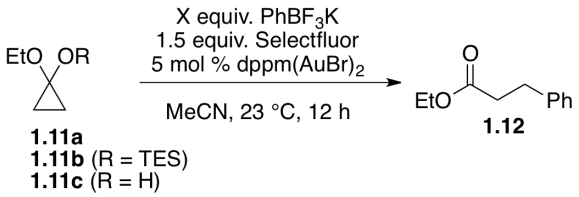

1.11a
1.11b (R = TES)
1.11c (R = H)

1.12

entry	equiv. 1.11	equiv. $PhBF_3K$	yield
1	1.0, **1.11a**	2.0	42%
2	1.0, **1.11a**	2.5	43%
3	1.0, **1.11a**	3.0	53%
4	1.5, **1.11a**	1.0	24%
5	1.5, **1.11b**	1.0	30%
6	1.5, **1.11c**	1.0	40%

Table 11. Effect of stoichiometry and acetal protecting group on ring opening-coupling reaction.

In examining the crude reaction mixtures by NMR and by GCMS, two major side products were consistently observed: 3-fluoroethyl propionate, **1.13**, and ethyl acrylate, **1.14**. These side products may result from fluorination and elimination respectively (rather than the desired cross coupling) from the presumed alkylgold(III) intermediate, though the acrylate could also result from elimination of HF from **1.13** (Scheme 9).

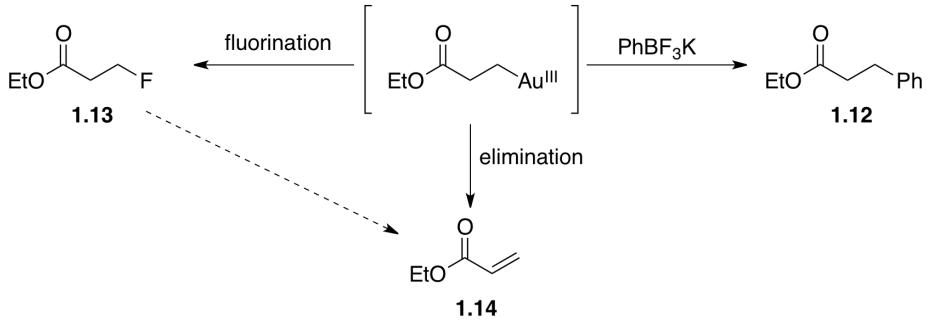

1.13 **1.12** **1.14**

Scheme 9. Products observed from the putative alkylgold(III) intermediate.

We inferred that increasing the relative concentration of the coupling partner could lessen the formation of these side products. In fact, the slow addition of Selectfluor and **1.11c** did result in an improved yield of desired product (Scheme 10). However, no further experiments were undertaken to improve the methodology.

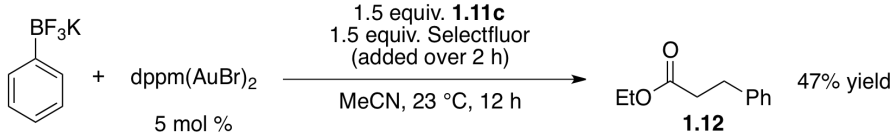

1.12

Scheme 10. Slow addition of hemiacetal and Selectfluor resulted in an increased yield.

Instead, a substrate class that we believed would not suffer from significant side product formation was explored. We hypothesized that vinylcyclopropanol substrate **1.15** could undergo activation by cationic Au(III), leading to a ring-expanded alkylgold(III) intermediate that would not undergo elimination. And in contrast to the aminoarylation reaction, the carbon-carbon bond formation onto the alkene to generate the alkylgold

intermediate is likely to be irreversible, which could allow for greater scope of dearylative functionalization. Along with cross-coupling, we were interested in exploring the possibility of nucleophilic displacement by alcohols or other heteroatom nucleophiles, as well as reductive elimination of the C-F bond for an overall carbofluorination of alkenes (Scheme 11).

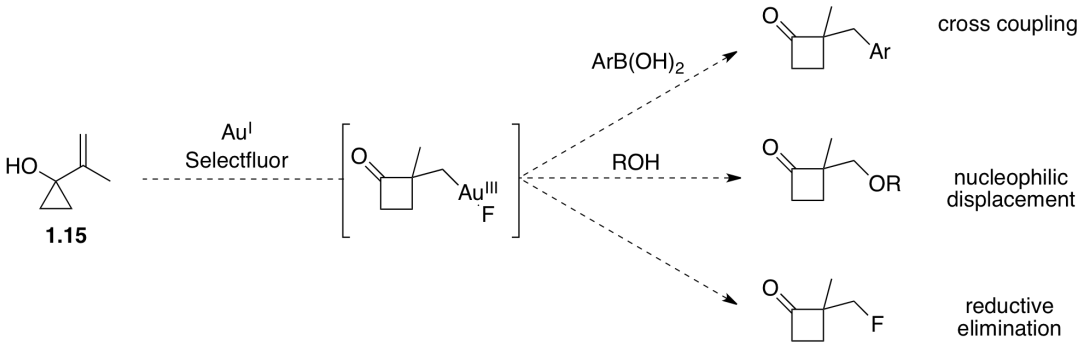

Scheme 11. Proposed use of vinyl cyclopropanol substrates to achieve different modes of reactivity from irreversible formation of an alkylgold(III) intermediate.

We were initially very pleased that under the established cross coupling reaction conditions, employing either Ph_3PAuCl or $dppm(AuBr)_2$ as catalyst, though the cross coupling product was not observed as the major product, the fluorinated product **1.16** was observed in very high yield. However, we quickly realized that this was the result of the direct reaction of the substrate with Selectfluor, as the reaction proceeded readily in the absence of gold (Scheme 12). Though the mass balance of the reaction in the presence of $dppm(AuBr)_2$ did appear to be the cross-coupled product, the reactivity of Selectfluor toward this type of substrate precluded any gold-catalyzed reaction development.

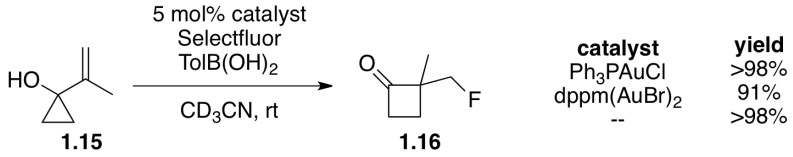

Scheme 12. Fluorination of substrate observed in the presence and absence of catalyst.

Given the potential value of fluorinated organic compounds,[13] however, this led us to consider ways to selectively form C-F bonds using Selectlfuor as an electrophilic fluorination reagent, and this will be discussed in Chapter 2.

Conclusions

The heteroarylation of alkenes, demonstrated in both intra- and intermolecular fashions, were developed using the oxidant Selectfluor to drive a Au(I)/Au(III) catalytic cycle. Employment of a catalyst with greater stability at the higher oxidation state led to improved yields of the desired bifunctionalized product under mild conditions. Furthermore, mechanistic studies indicate that the cross-coupling event may take place through a non-traditional 5-center bimolecular transition state.

Experimental details

General. Unless otherwise noted commercial materials were used without further purification. Acetonitrile (MeCN) for the gold-catalyzed reactions was distilled from CaH_2 under a nitrogen atmosphere prior to use. Gold(I)-catalyzed reactions were conducted in dram vials equipped with a magnetic stir bar and fitted with a threaded cap. All other reactions were conducted in flame-dried glassware under an inert (N_2) atmosphere with magnetic stirring and dried solvent, unless otherwise noted. Solvents were dried by passage through an activated alumina column under nitrogen. Gold chloride complexes were synthesized utilizing the procedures previously reported,[24,25] and gold(I)-bromides and iodides were synthesized according to the procedure of Schmidbaur.[26] Thin-layer chromatography (TLC) analysis was performed using Merck silica gel 60 F254 TLC plates, and visualized under UV or by staining with I_2, cerium sulfate, and/or permanganate. Flash column chromatography was carried out on Merck 60 silica
gel (32–63 μm). ^1H, ^{13}C and ^{31}P NMR spectra were recorded with Bruker AVB-400, AVQ-400, DRX-500, and AV-600 spectrometers and chemical shifts are reported in ppm, relative to $CHCl_3$ (7.26 ppm for ^1H, and 77.23 ppm for ^{13}C) unless otherwise noted. Mass spectral and analytical data were obtained *via* the Micro-Mass/Analytical Facility operated by the College of Chemistry, University of California, Berkeley.

Substrate synthesis

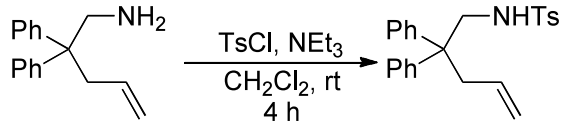

1.3. The amine substrate[14] (0.32 g, 1.3 mmol) was dissolved in DCM (5 mL) with NEt3 (0.21 mL, 1.5 mmol), then TsCl (0.29 g, 1.5 mmol) was added in one portion. After stirring for 6 hours, the reaction was quenched by the addition of sat. aq. NH_4Cl (10 mL), then extracted with Et2O (3 × 10 mL). The combined organic layers were washed with brine (10 mL), dried over $MgSO_4$, filtered, and concentrated *in vacuo*. The residue was purified by flash column chromatography on silica gel (7% EtOAc in hexanes) to give **1.3** (0.457 g, 1.17 mmol) as a colorless solid: ^1H NMR (500 MHz, $CDCl_3$) δ 7.59 (d, J = 7.6, 2H), 7.28–7.24 (m, 6H), 7.22– 7.19 (m, 2H), 7.05 (d, J = 7.8, 4H), 5.30–5.22 (m, 1H), 4.95 (d, J = 6.0, 1H), 4.92 (s, 1H), 3.82– 3.80 (m, 1H), 3.52 (d, J = 6.5, 2H), 2.90 (d, J = 7.0, 2H), 2.43 (s, 3H) ppm; ^{13}C NMR (125 MHz, $CDCl_3$) δ 144.6, 143.5, 136.2, 133.1, 129.7, 128.4, 127.8, 127.2, 126.8, 119.1, 49.4, 49.3, 41.3, 21.6 ppm; HRMS (ESI) calc for $[C_{24}H_{26}NO_2S]^+$: *m/z* 392.1684, found 392.1684.

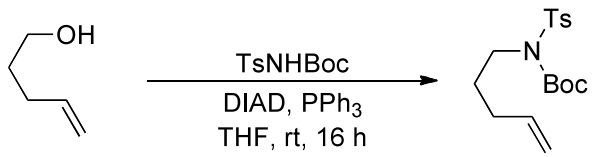

S1.1. In a flame dried flask, 4-penten-1-ol (0.77 mL, 7.5 mmol), TsNHBoc (2.03 g, 7.5 mmol), and triphenylphoshine (1.97 g, 7.5 mmol) were combined in THF (25 mL) and cooled to 0 °C. Then diisopropyldiazodicarboxylate (1.49 mL, 77.5 mL) was added dropwise over 20 minutes, and upon completion the reaction was allowed to warm to room temperature overnight before concentration *in vacuo*. The oily residue was triturated with 4:1 hexanes/Et_2O (50 mL), filtered, and the filtrate was concentrated. The residue was purified by flash chromatography on silica gel (5% Et_2O in hexanes) to provide **S1.1** (2.19 g, 86% yield) as a viscous colorless oil: ^{1}H NMR (500 MHz, $CDCl_3$) δ 7.78 (d, *J* = 8.2 Hz, 2H), 7.29 (d, *J* = 8.2 Hz, 2H), 5.83 (ddt, *J* = 16.9, 10.3, 6.8 Hz, 1H), 5.06 (dd, *J* = 15.5, 1.7 Hz, 1H), 5.00 (d, *J* = 10.2 Hz, 1H), 3.84–3.81 (m, 2H), 2.44 (s, 3H), 2.12 (q, *J* = 7.2 Hz, 2H), 1.86 (p, *J* = 7.6 Hz, 2H), 1.33 (s, 9H) ppm. ^{13}C NMR (150 MHz, $CDCl_3$) δ 151.0, 144.0, 137.6, 137.5, 129.2, 127.8, 115.2, 84.1, 46.8, 30.9, 29.2, 27.9, 21.6 ppm; HRMS (ESI) calc for $[C_{17}H2_5O_4NNaS]^+$: *m/z* 362.1397, found 362.1399.

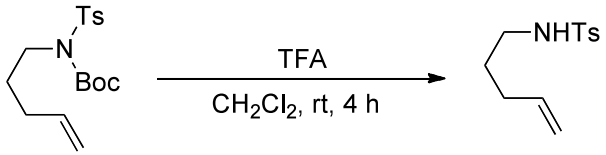

1.3b. **S1.1** (1.70 g, 5.0 mmol) was dissolved in DCM (20 mL), then trifluoroacetic acid (1.50 mL, 20.0 mmol) was added. After stirring for 4 hours, the solution was concentrated *in vacuo*. The residue was purified by flash chromatography on silica gel (10% EtOAc in hexanes) to give **1.3b** (1.13 g, 94%) as a viscous oil: ^{1}H NMR (500 MHz, $CDCl_3$) δ 7.76 (d, *J* = 8.1 Hz, 2H), 7.30 (d, *J* = 8.1 Hz, 2H), 5.70 (ddt, *J* = 17.0, 10.3, 6.8Hz, 1H), 4.99–4.94 (m, 2H), 4.49 (brs, 1H), 2.95 (q, *J* = 6.7 Hz, 2H), 2.43 (s, 3H), 2.04 (q, *J* = 7.1 Hz, 2H), 1.56 (p, *J* = 7.2 Hz, 2H) ppm. ^{13}C NMR (150 MHz, $CDCl_3$) δ 143.4, 137.2, 129.7, 127.1, 115.6, 42.7, 30.7, 28.7, 21.5 ppm; HRMS (ESI) calc for $[C_{12}H_{18}O_2NS]^+$: *m/z* 240.1053, found 240.1056.

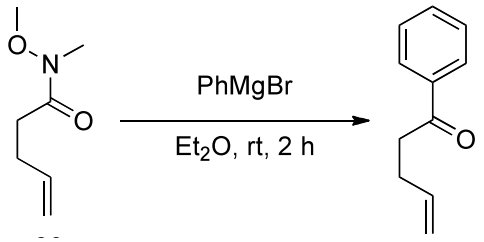

S1.2. To the Weinreb amide[15] (300 mg, 2.10 mmol) in Et_2O (20 mL) under N_2 was added slowly PhMgBr (750 mL, 2.10 mmol). After the reaction mixture became clear, it was stirred for 2 h. The reaction was quenched with sat. aq. NH_4Cl. The organic phase was dried with $MgSO_4$, filtered and concentrated. The crude product was purified by flash

column chromatography on silica gel (4% EtOAc in hexanes) to give **S1.2** (205 mg, 61%) as a clear, colorless oil: ^{1}H NMR (300 MHz, $CDCl_3$) δ 7.97–7.95 (m, 2H), 7.53–7.58 (m, 1H), 7.48–7.43 (m, 2H) 5.90 (ddt, *J* = 16.8, 10.2 and 6.6 Hz, 1H), 5.08 (dd, *J* = 17.1, 1.8 Hz, 1H), 5.01 (dd, *J* = 9.9, 1.2 Hz, 1H), 3.08 (t, *J* = 7.5 Hz, 2H), 2.53–2.46 (m, 2H) ppm; ^{13}C NMR (75 MHz, $CDCl_3$) δ 199.6, 137.6, 137.2, 133.3, 128.9, 115.6, 28.0, 28.4 ppm; HRMS (ESI) calc for $[C_{11}H_{13}O]^+$: *m/z* 161.0966, found 161.0966.

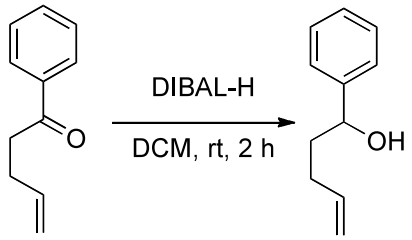

S1.3. In a flame-dried flask under N_2 at 0 °C, **S1.2** (205 mg, 1.28 mmol) was dissolved in DCM (10 mL). A 1.0 M solution of DIBAL-H in hexanes (1.41 mL, 1.41 mmol) was added and the reaction mixture was warmed to room temperature and stirred for 2 h. The reaction was quenched by stirring with solid $Na_2SO_4 \cdot 10H_2O$ for 1 h. The reaction mixture was filtered through a cotton plug, concentrated and purified by flash column chromatography on silica gel (7% EtOAc in hexanes) to give **S1.3** (199 mg, 96%) as a clear, colorless oil: ^{1}H NMR (500 MHz, CDCl) δ 7.49–7.26 (m, 5H), 5.87 (ddt, *J* = 17.0, 10.0 and 6.5 Hz), 5.09–4.99 (m, 2H), 4.75–4.71 (m, 1H), 2.20–2.12 (m, 2H), 1.97–1.90 (m, 1H), 186–1.79 (m, 2H); ^{13}C NMR (125 MHz, CDCl) δ 145.1, 138.6, 128.9, 128.0, 126.4, 115.4, 74.4, 38.5, 30.5; HRMS (ESI) calc for $[C_{11}H_{15}O]^+$: *m/z* 163.1123, found 163.1123.

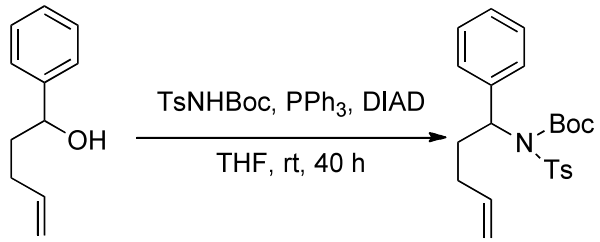

S1.4. **S1.3** (199 mg, 1.23 mmol) was dissolved in THF (15 mL), then TsNHBoc (33 mg, 1.23 mmol) and PPh_3 (322 mg, 1.2 mmol) were added. Diisopropyldicarboxylate (241 μL, 1.2 mmol) was added dropwise over 10 min. The reaction mixture was stirred at room temperature for 40 h. The reaction mixture was concentrated and triturated in 9:1 hexanes/Et_2O, then filtered. The filtrate was concentrated and purified by flash column chromatography on silica gel (10% EtOAc in hexanes) to give **S1.4** (419 mg, 82%) as a colorless solid: ^{1}H NMR (500 MHz, $CDCl_3$) δ 7.62 (d, *J* = 8.0 Hz, 2H), 7.44 (d, *J* = 7.5 Hz, 2H), 7.35 (t, *J* = 7.5 Hz, 2H), 7.30 (d, *J* = 7.0 Hz, 1H), 7.24 (d, *J* = 8.0 Hz, 2H), 5.93 (ddt, *J* = 17.0, 10.5 and 6.5 Hz, 1H), 5.68 (t, *J* = 8.0 Hz, 1H), 5.10 (dd, *J* = 17.0, 2.0 Hz, 1H), 5.06 (d, *J* = 10.0 Hz, 1H), 2.55–2.39 (m, 5H), 2.32–2.21 (m, 2H), 1.25 (s, 9H); ^{13}C NMR (125 MHz, $CDCl_3$) δ 151.0, 144.0, 139.8, 137.6, 137.3, 129.0, 128.4, 128.2, 128.1, 127.5, 115.4, 60.4, 31.7, 31.2, 27.8, 21.6; HRMS (ESI) calc for $[C_{23}H_{29}NO_4NaS]^+$: *m/z* 438.1710, found 438.1726.

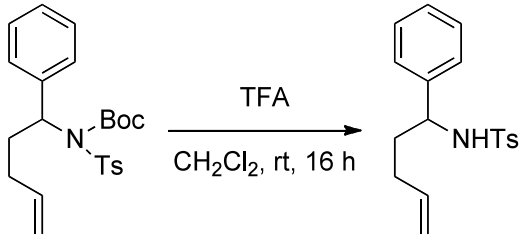

1.3c. N-Boc-tosylsulfonamide **S1.4** was dissolved in DCM, and trifluoroacetic acid (370 μL, 5.0 mmol) was added. The reaction mixture was stirred at room temperature for 5 h, then concentrated. Crude product was purified by flash column chromatography on silica gel (12% EtOAc in hexanes) to give **1.3c** (290 mg, 92%) as a colorless, crystalline solid: ^{1}H NMR (500 MHz, CDCl3) δ 7.54 (d, *J* = 8.5 Hz, 2H), 7.18–7.17 (m, 3H), 7.13 (d, *J* = 8.5 Hz, 2H), 7.01–7.00 (m, 2H), 5.73 (ddt, *J* = 16.5, 10.5 and 6.5 Hz, 1H), 4.98–4.93 (m, 2H), 4.71 (d, *J* = 7.5 Hz, 1H), 4.31 (q, *J* = 7.0 Hz, 1H), 2.37 (s, 3H), 2.02–1.78 (m, 4H); ^{13}C NMR (125 MHz, $CDCl_3$) δ 142.9, 140.7, 137.7, 137.2, 129.3, 128.4, 127.3, 126.6, 115.5, 57.8, 36.7, 30.0, 21.5 ppm; HRMS (ESI) calc for $[C_{18}H_{21}NO_2NaS]^+$: *m/z* 338.1185, found 338.1196.

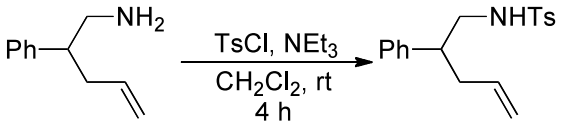

1.3d. To the amine substrate[16] (0.806 g, 5.0 mmol) was dissolved in DCM (20 mL) with NEt_3 (1.05 mL, 7.5 mmol). Then TsCl (1.05 g, 5.5 mmol) was added in one portion and the solution was allowed to stir overnight at room temperature. The reaction was quenched by the addition of sat. aq. NH_4Cl (50 mL) and then extracted with EtOAc (3 × 20 mL). The combined organic layers were washed with sat. aq. $NaHCO_3$ (20 mL) and brine (20 mL), dried over $MgSO_4$, filtered, and concentrated *in vacuo*. The residue was purified by flash column chromatography on silica gel (10 % EtOAc in hexanes) to give **1.3d** (1.149 g, 72%) as a pale orange solid: ^{1}H NMR (500 MHz, $CDCl_3$) δ 7.64 (d, *J* = 8.2 Hz, 2H), 7.27 (t, *J* = 7.4 Hz, 4H), 7.24–7.21 (m, 1H), 7.04– 7.02 (m, 2H), 5.59 (ddt, *J* = 17.1, 10.1, 7.0 Hz, 1H), 4.98–4.94 (m, 2H), 4.26–4.23 (m, 1H), 3.33–3.28 (m, 1H), 3.03–2.97 (m, 1H), 2.76 (dt, *J* = 14.5, 7.3 Hz, 1H), 2.43 (s, 3H), 2.38–2.28 (m, 2H). ppm; ^{13}C NMR (150 MHz, $CDCl_3$) δ 143.4, 141.0, 136.9, 135.4, 129.7, 128.9, 127.7, 127.22, 127.11, 117.1, 47.8, 45.3, 38.1, 21.6 ppm; HRMS (ESI) calc for $[C_{18}H_{22}NO_2S]^+$: *m/z* 316.1366, found 316.1367.

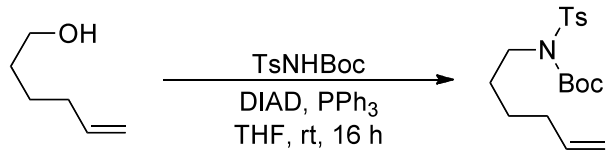

S1.5. In a flame dried flask, 5-hexen-1-ol (0.60 mL, 5.0 mmol), TsNHBoc (1.36 g, 5.0 mmol), and triphenylphoshine (1.31 g, 5.0 mmol) were combined in THF (30 mL) and

cooled to 0 °C. Then diisopropyldiazodicarboxylate (0.98 mL, 5.0 mL) was added dropwise over 20 minutes, and upon completion the reaction was allowed to warm to room temperature overnight before concentration *in vacuo*. The oily residue was triturated with 4:1 hexanes/Et_2O (50 mL), filtered, and the filtrate was concentrated. The residue was purified by flash chromatography on silica gel (5% Et_2O in hexanes) to provide **S1.5** (1.633 g, 92% yield) as a viscous colorless oil: ^{1}H NMR (500 MHz, $CDCl_3$) δ 7.76 (d, *J* = 8.3 Hz, 2H), 7.29 (d, *J* = 8.3 Hz, 1H), 5.77 (ddt, *J* = 17.1, 10.2 and 6.7 Hz, 1H), 5.02 (d, *J* = 17.1 Hz, 1H), 4.96 (d, *J* = 10.2 Hz, 1H), 3.82 (t, *J* = 7.6 Hz, 2H), 2.43 (s, 3H), 2.12–2.08 (m, 2H), 1.80–1.73 (m, 2H), 1.48–1.42 (m, 2H), 1.32 (s, 9H) ppm; ^{13}C NMR (150 MHz, $CDCl_3$) δ 151.0, 141.0, 138.4, 137.6, 129.2, 127.8, 114.8, 84.1, 47.1, 33.3, 29.7, 27.9, 26.0, 21.6 ppm; HRMS (ESI) calc for $[C_{18}H_{27}NO_4NaS]^+$: *m/z* 376.1553, found 376.1555.

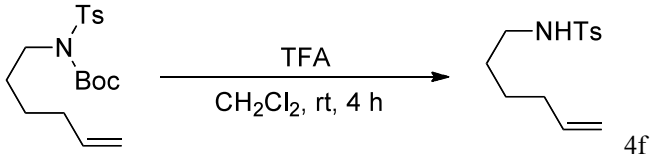

4f

1.3f. **S1.5** (1.60 g, 4.5 mmol) was dissolved in DCM (40 mL), then trifluoroacetic acid (1.70 mL, 22.5 mmol) was added. After stirring for 4 hours, the solution was concentrated *in vacuo*. The residue was purified by flash chromatography on silica gel (10% EtOAc in hexanes) to give **1.3f** (1.076 g, 95%) as a viscous oil: ^{1}H NMR (500 MHz, $CDCl_3$) δ 7.75 (d, *J* = 8.2 Hz, 2H), 7.30 (d, *J* = 8.0 Hz, 2H), 5.70 (ddt, *J* = 16.9, 10.2, 6.8Hz, 1H), 4.96–4.90 (m, 2H), 4.64 (brs, 1H), 2.93–2.92 (m, 2H), 2.42 (s, 3H), 1.97 (q, *J* = 7.0 Hz, 2H), 1.46 (p, *J* = 7.2 Hz, 2H), 1.35 (p, *J* = 7.4 Hz, 2H) ppm; ^{13}C NMR (150 MHz, $CDCl_3$) δ 143.4, 138.1, 136.9, 129.7, 127.1, 114.9, 43.1, 33.1, 29.0, 25.7, 21.5 ppm; HRMS (ESI) calc for $[C_{13}H_{20}NO_2S]^+$: *m/z* 254.1209, found 254.1209.

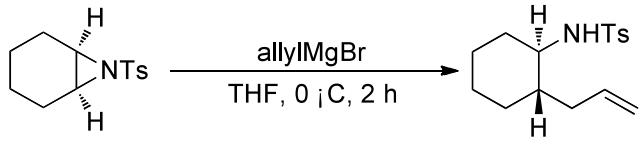

1.3g. A 50 mL two-necked flask fitted with a reflux condenser and addition funnel was charged with magnesium turnings (0.073 g, 3.0 mmol) and a single crystal of iodine. Allylbromide (0.26 mL, 3.0 mmol) in Et_2O (4.0 mL) was then added slowly over 15 minutes by addition funnel, then let stir for an additional two hours. The brown solution was then cooled to 0 °C and aziridine substrate[17] (0.587 g, 2.0 mmol) in Et_2O (10.0 mL) was added, then the solution was allowed to warm to room temperature. After 3 hours, the reaction was quenched by the careful addition of 0.5 N HCl (15 mL) at 0 °C. The layers were separated, and the aqueous layer was extracted with Et_2O (3 × 10 mL). The combined organic layers were washed with sat. aq. $NaHCO_3$ (10 mL), brine (10 mL), dried over $MgSO_4$, filtered and concentrated. The residue was purified by flash column chromatography on silica gel (gradient: 20% → 30% Et_2O in hexanes) to give **1.3g** (0.563 g, 96%) as an off-white amorphous solid: ^{1}H NMR (500 MHz, $CDCl_3$) δ 7.76 (d, *J* = 8.3 Hz, 2H), 7.29 (d, *J* = 8.1 Hz, 2H), 5.63 (ddt, *J* = 17.0, 10.1, 7.5 Hz, 1H), 4.96–4.91 (m, 2H), 4.44 (d, *J* = 8.9 Hz 1H), 2.87 (qd, *J* = 10.1, 3.9 Hz, 2H), 2.42 (s, 3H), 2.41–2.39

(m, 1H), 1.87–1.70 (m, 3H), 1.60–157 (m, 2H), 1.22–1.10 (m, 4H), 0.96–0.90 (m, 1H) ppm; ^{13}C NMR (150 MHz, $CDCl_3$) δ 143.2, 138.6, 136.6, 129.7, 127.0, 116.3, 57.1, 42.9, 36.9, 34.4, 30.8, 25.2, 25.0, 21.6 ppm; HRMS (ESI) calc for $[C_{16}H_{24}NO_2S]^+$: *m/z* 294.1522, found 294.1523.

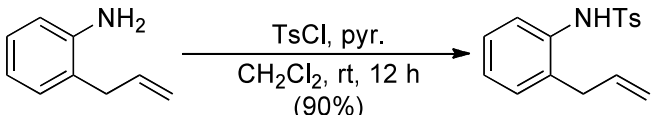

1.3h: Aniline substrate[18] (0.266 g, 2.0 mmol) and pyridine (0.32 mL, 4.0 mmol) were dissolved in DCM (10 mL) at room temperature, then TsCl (0.419 g, 2.2 mmol) was added in one portion. After stirring overnight, the reaction was quenched by the addition of sat. aq. NH_4Cl (30 mL), and the mixture was extracted with Et_2O (3 × 15 mL). The combined organic layers were washed with sat. aq. $NaHCO_3$ (20 mL) and brine (20 mL), dried over $MgSO_4$, filtered, and concentrated *in vacuo*. The residue was purified by flash column chromatography on silica gel (10% Et_2O in hexanes) to give **1.3h** (0.518 g, 90%) as a waxy colorless solid: ^{1}H NMR (500 MHz, $CDCl_3$) δ 7.60 (d, *J* = 8.3 Hz, 2H), 7.40 (d, *J* = 8.0 Hz, 1H), 7.23–7.17 (m, 3H), 7.11 (td, *J* = 7.4, 1.0 Hz, 1H), 7.06 (d, *J* = 6.4 Hz, 1H), 6.57 (brs, 1H), 5.77 (ddt, *J* = 17.3, 10.2 and 6.0 Hz, 1H), 5.11 (dd, *J* = 10.2, 1.4 Hz, 1H), 4.94 (dd, *J* = 17.3, 1.4 Hz, 1H), 3.02 (d, *J* = 6.0 Hz, 2H), 2.37 (s, 3H) ppm; ^{13}C NMR (150 MHz, $CDCl_3$) δ 143.8, 136.8, 135.6, 135.0, 132.1, 130.5, 129.6, 127.7, 127.1, 126.3, 124.5, 117.1, 36.2, 21.6 ppm; HRMS (ESI) calc for $[C_{16}H_{18}NO_2S]^+$: *m/z* 288.1053, found 288.1052.

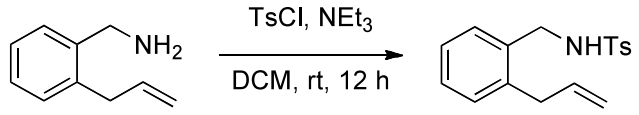

1.3i: Benzylamine **45** was prepared from 2-bromobenzyl bromide according to the literature.[19,20] Benzylamine **45** (76 mg, 0.52 mmol) and TsCl (196 mg, 1.0 mmol) were dissolved in DCM (4 mL). NEt_3 (216 µL, 1.6 mmol) was added and the reaction mixture was stirred at room temperature overnight. The reaction mixture was washed with H_2O. The organic phase was dried with $MgSO_4$, filtered and concentrated. The crude product was purified flash column chromatography on silica gel (15% EtOAc in hexanes) to give **1.3i** (88 mg, 57%) as a pale yellow solid: ^{1}H NMR (400 MHz, CDCl3) δ 7.81 (d, *J* = 8.4 Hz, 2H), 7.46 (d, *J* = 8.4 Hz, 2H), 7.28– 7.25 (m, 1H), 7.20–7.18 (m, 3H), 5.93 (ddt, *J* = 17.2, 10.4 and 5.6 Hz, 1H), 5.07 (dd, *J* = 10.0, 1.6 Hz, 1H), 4.88 (dd, *J* = 17.2, 1.6 Hz, 1H), 4.64 (t, *J* = 6.0 Hz, 1H), 4.14 (d, *J* = 5.6 Hz, 2H), 3.56 (d, *J* = 6.0 Hz, 2H), 2.49 (s, 3H) ppm; ^{13}C NMR (125 MHz, $CDCl_3$) δ 143.8, 138.4, 137.2, 136.8, 134.1, 130.4, 129.9, 129.7, 128.6, 127.4, 127.0, 116.3, 45.1, 36.9, 21.7 ppm; HRMS (ESI) calc for $[C_{17}H_{20}NO_2S]^+$: *m/z* 302.1214, found 302.1214.

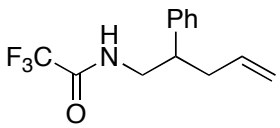

1.5. To 2-phenylpent-4-enylamine[21] (150 mg, 0.94 mmol) and trifluoroacetic anhydride (198 µl, 1.4 mmol) in dichloromethane (4.7 mL) was added triethylamine (325 µl, 2.3 mmol). The reaction mixture was stirred for 14 h at room temperature, and was then washed with sat. aq. NH_4Cl and brine. The organic phase was dried with $MgSO_4$, filtered and concentrated *in vacuo* to afford the crude product. The product was purified by flash column chromatography on silica gel (5:1 hexanes/EtOAc) to give **1.5** (140mg, 55%) as a colorless oil: ^{1}H NMR (500 MHz, $CDCl_3$) 7.39 (t, J = 7.5 Hz, 2 H), 7.33-7.29 (m, 1H), 7.21 (d, J = 7.0 Hz, 2H), 6.11 (br s, 1H), 5.72 (ddt, J = 17.0 Hz, 10.5 Hz and 6.5 Hz, 1H), 5.09 (d, J = 17.0 Hz, 1H), 5.05 (d, J = 10.0 Hz, 1H), (quintet, J = 6.5 Hz, 1H), 3.42-3.36 (m, 1H), 2.99-2.93 (m, 1H), 2.49-2.46 (m, 2H) ppm; ^{13}C NMR (126 MHz, $CDCl_3$) 157.1 (q, $J^{C\text{-}F}$ = 37 Hz), 140.9, 135.3, 129.0, 127.6, 127.4, 117.3, 115.8 (q, $J^{C\text{-}F}$ = 289 Hz), 44.8, 44.7, 38.1 ppm.

Heteroarylation procedures

Aminoarylation general procedure: Sulfonamide (100 µmol) was dissolved in anhydrous MeCN (1.0 mL) with boronic acid (200 µmol) and dppm$(AuBr)_2$ (2.8 mg, 3 µmol). Then Selectfluor® (150 µmol) was added in one portion, and the solution stirred in a sealed vial at the noted temperature for 18 hours. The reaction was quenched at room temperature by the addition of sat. aq. $Na_2S_2O_3$ (3.0 mL), then extracted with Et_2O (3 × 5 mL). The combined organic layers were washed with brine (5 mL), dried over $MgSO_4$, filtered and concentrated.

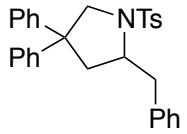

1.4a. **1.3** and phenylboronic acid were reacted at room temperature. The residue was purified by flash column chromatography on silica gel (10 % Et_2O in hexanes) to give **1.4a** (33.7 mg, 72 %) as a viscous oil that solidified upon standing: ^{1}H NMR (500 MHz, $CDCl_3$) δ 7.73 (d, J = 8.1 Hz, 2H), 7.36–7.29 (m, 7H), 7.25–7.23 (m, 3H), 7.19–7.14 (m, 3H), 7.08–7.06 (m, 4H), 4.46 (d, J = 10.2 Hz, 1H), 3.93 (ddt, J = 11.3, 7.7, 3.9 Hz, 1H), 3.69 (d, J = 10.2 Hz, 1H), 3.47–3.43 (m, 1H), 2.47–2.44 (m, 1H), 2.44 (s, 3H), 2.40–2.36 (m, 1H), 2.38 (dd, J = 12.9, 4.7 Hz, 1H); ^{13}C NMR (126 MHz; $CDCl_3$): δ 145.4, 145.0, 143.4, 138.6, 134.4, 129.7, 129.4, 128.6, 128.6, 127.5, 127.0, 126.6, 126.5, 126.4, 61.4, 58.3, 52.3, 42.0, 41.7, 21.6; HRMS (ESI) calc for $[C_{30}H_{30}O_2NS]^+$: *m/z* 468.1992, found 468.2000.

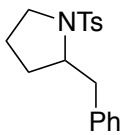

1.4b. **1.3b** and phenylboronic acid were reacted at room temperature. The residue was purified by flash column chromatography on silica gel (10% Et_2O in hexanes) to give

1.4b (22.1 mg, 70 %): ^{1}H NMR (500 MHz, $CDCl_3$) δ 7.76 (d, *J* = 8.2 Hz, 2H), 7.32–7.29 (m, 4H), 7.25–7.21 (m, 3H), 3.84–3.80 (m, 1H), 3.42–3.38 (m, 1H), 3.24 (dd, *J* = 13.3, 3.5 Hz, 1H), 3.15–3.10 (m, 1H), 2.78–2.73 (m, 1H), 2.42 (s, 3H), 1.64–1.60 (m, 2H), 1.48–1.43 (m, 2H) ppm; ^{13}C NMR (150 MHz, $CDCl_3$) δ 143.4, 138.5, 134.7, 129.7, 129.7, 128.4, 127.5, 126.4, 61.6, 49.3, 42.8, 29.9, 23.8, 21.6 ppm; HRMS (ESI) calc for $[C_{18}H_{22}NO_2S]^+$: *m/z* 316.1366, found 316.1370.

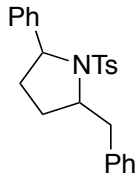

1.4c. **1.3c** and phenylboronic acid were reacted at room temperature. The crude product was purified by flash column chromatography on silica gel (15% EtOAc in hexanes) to give **1.4c** as an inseparable mixture of diastereomers (28 mg, 72%, dr 1.1:1): ^{1}H NMR (500 MHz, CDCl3) δ 7.75 (d, *J* = 8.5 H, 2H major diastereomer), 7.41–7.24 (m, 10H major + 9H minor diastereomer), 7.16–7.06 (m, 2H major + 3H minor), 6.99 (d, *J* = 8.5 Hz, 2H minor), 5.01 (d, *J* = 8.5 Hz, 1H minor), 4.73 (t, *J* = 6.5 Hz, 1H major), 4.39–4.35 (m, 1H minor), 4.03–3.98 (m, 1H major), 3.58 (dt, *J* = 13.0, 3.5 Hz, 2H minor), 2.81 (dd, *J* = 13.0, 11.0 Hz, 1H major), 2.73 (dd, *J* = 13.0, 10.5 Hz, 1H minor), 2.44 (s, 3H major), 2.37–2.29 (m, 4H minor), 2.11–2.03 (m, 1H minor), 1.90 (q, *J* = 7.0 Hz, 2H major), 1.79 (dd, *J* = 13.0, 7.0 Hz, 1H minor), 1.71–1.57 (m, 2H major), 1.51–1.45 (m, 1H major) ppm; ^{13}C NMR (125 MHz, $CDCl_3$) δ 143.5, 142.6, 142.4, 142.2, 138.9, 138.9, 138.6, 129.7, 129.6, 129.4, 129.0, 128.6, 128.4, 128.1, 127.7, 127.1, 127.0, 126.9, 126.7, 126.5, 126.5, 126.3, 65.1, 64.1, 63.8, 63.0, 43.2, 41.9, 34.3, 33.0, 29.0, 27.4, 21.5, 21.4 ppm; HRMS (ESI) calc for $[C_{24}H_{26}NO_2S]^+$: *m/z* 392.1679, found 392.1698.

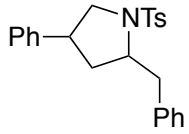

1.4d. **1.3d** and phenylboronic acid were reacted at room temperature. The residue was purified by flash column chromatography on silica gel (15% EtOAc in hexanes) to give **1.4d** as an inseparable mixture of diastereomers (28 mg, 72%, dr 1.5:1): ^{1}H NMR (500 MHz, CDCl3) δ 7.84 (d, *J* = 8.0 Hz, 1H minor diastereomer), 7.80 (d, *J* = 8.0 Hz, 1H major diastereomer), 7.39–7.19 (m, 10H major + 10H minor), 6.99 (d, *J* = 7.5 Hz, 2H major + 2H minor), 4.04 (dt, *J* = 9.0, 3.0 Hz, 1H major), 3.97–3.91 (m, 1H minor), 3.89–3.85 (m, 1H major + 1H minor), 3.49 (dd, *J* = 12.5, 3.5 Hz, 1H minor), 3.34–3.25 (m, 2H major + 1H minor), 2.99– 2.89 (m, 2H major + 1H minor), 2.59–2.50 (m, 1H minor), 2.48 (s, 3H minor), 2.56 (s, 3H major), 2.15–2.10 (m, 1H minor), 2.04 (dd, *J* = 12.5, 6.0 Hz, 1H major), 1.78 (td, *J* = 12.0, 9.5 Hz, 1H minor), 1.58 (td, *J* = 12.5, 8.5 Hz, 1H major) ppm; ^{13}C NMR (125 MHz, $CDCl_3$) δ 143..6, 143.5, 142.3, 139.7, 139.5, 138.4, 138.0, 135.2, 134.1, 129.9, 129.8, 129.7, 129.6, 128.6, 128.5, 128.4, 127.7, 127.5, 127.0,

126.9, 126.6, 126.5, 62.2, 61.6, 55.3. 55.2, 43.0, 42.8, 41.4, 39.2, 36.1, 21.6, 21.6 ppm; HRMS (ESI) calc for $[C_{24}H_{26}NO_2S]^+$: *m/z* 392.1679, found 392.1693.

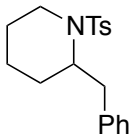

1.4f. **1.3f** and phenylboronic acid were reacted at 40°C. The residue was purified by flash column chromatography on silica gel (10 % Et_2O in hexanes) to give **1.4f** (27.0 mg, 82 %): ^{1}H NMR (500 MHz, $CDCl_3$) δ 7.61 (d, *J* = 8.1 Hz, 2H), 7.29–7.25 (m, 2H), 7.22–7.20 (m, 3H), 7.15 (d, *J* = 8.0 Hz, 2H), 4.31–4.27 (m, 1H), 3.77 (d, *J* = 13.5 Hz, 1H), 3.08 (td, *J* = 13.2, 2.5 Hz, 1H), 2.87 (dd, *J* = 13.0, 10.1 Hz, 1H), 2.78 (dd, *J* = 13.3, 5.6 Hz, 1H), 2.39 (s, 3H), 1.67–1.54 (m, 3H), 1.49–1.41 (m, 3H) ppm; ^{13}C NMR (150 MHz, $CDCl_3$) δ 142.8, 138.7, 138.4, 129.6, 129.2, 128.6, 127.0, 126.4, 54.4, 40.9, 35.7, 26.0, 24.5, 21.5, 18.3 ppm; HRMS (ESI) calc for $[C_{19}H_{24}O_2NS]^+$: *m/z* 330.1522, found 330.1527.

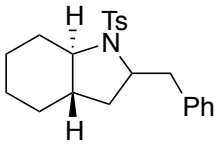

1.4g. **1.3g** and phenylboronic acid were reacted at room temperature. The residue was purified by flash column chromatography on silica gel (10 % Et_2O in hexanes) to give **1.4g** (34.0 mg, 92 %) as a viscous oil that solidified upon standing: ^{1}H NMR (500 MHz, $CDCl_3$) δ 7.73 (d, *J* = 8.0 Hz, 2H), 7.33–7.29 (m, 4H), 7.26–7.21 (m, 3H), 3.80 (td, *J* = 9.5, 2.9 Hz, 1H), 3.30 (dd, *J* = 13.2, 2.5 Hz, 1H), 2.72 (dd, *J* =13.2, 10.6 Hz, 1H), 2.53 (dd, *J* = 12.5, 2.5 Hz, 1H), 2.43 (s, 3H), 2.31 (td, *J* = 10.8 Hz, 3.1 Hz, 1H), 1.84–1.79 (m, 1H), 1.74 (d, *J* = 12.3 Hz, 1H), 1.68–1.63 (m 1H), 1.61–1.46 (m, 2H), 1.44–1.34 (m, 1H), 1.22–1.11 (m, 2H), 0.95–0.86 (m, 2H) ppm; ^{13}C NMR (150 MHz, $CDCl_3$) δ 143.3, 139.0, 133.9, 129.6, 129.6, 128.4, 127.8, 126.4, 67.0, 62.5, 43.8, 42.8, 33.2, 32.7, 29.8, 25.4, 24.7, 21.6 ppm; HRMS (ESI) calc for [C22H28NO2S]$^+$: *m/z* 370.1841, found 370.1841.

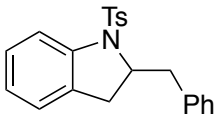

1.4h. **1.3h** and phenylboronic acid were reacted at room temperature. The residue was purified by flash column chromatography on silica gel (10 % Et_2O in hexanes) to give **1.4h** (23.3 mg, 64 %): ^{1}H NMR (500 MHz, $CDCl_3$) δ 7.71 (d, *J* = 8.0 Hz, 1H), 7.60 (d, *J* = 8.3 Hz, 2H), 7.35–7.33 (m, 2H), 7.29– 7.24 (m, 4H), 7.18 (d, *J* = 8.0 Hz, 2H), 7.05–7.04 (m, 2H), 4.51–4.46 (m, 1H), 3.39 (dd, *J* = 13.4, 4.2 Hz, 1H), 2.82 (dd, *J* = 13.4, 10.3 Hz, 1H), 2.63–2.62 (m, 2H), 2.37 (s, 3H) ppm; ^{13}C NMR (150 MHz, $CDCl_3$) δ 143.8,

141.4, 137.3, 135.4, 131.7, 129.7, 129.6, 128.5, 127.8, 127.0, 126.7, 125.3, 124.7, 117.4, 63.6, 42.6, 32.9, 21.5 ppm; HRMS (ESI) calc for $[C_{22}H_{22}O_2NS]^+$: *m/z* 364.1366, found 364.1372.

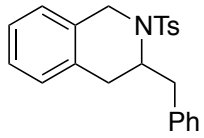

1.4i. **1.3i** and phenylboronic acid were reacted 40°C. The residue was purified by flash column chromatography on silica gel (15% EtOAc in hexanes) to give **1.4i** (21 mg, 63%) as a colorless solid: ^{1}H NMR (500 MHz, CDCl3) δ 7.69 (d, *J* = 8.5 Hz, 2H), 7.31–7.18 (m, 7H), 7.13–7.11 (m, 3H), 7.04–7.03 (m, 1H), 4.69 (d, *J* = 16.0 Hz, 1H), 4.49– 4.44 (m, 1H), 4.38 (d, *J* = 16.0 Hz, 1H), 2.81 (dd, *J* = 13.0 Hz and 5.0 Hz, 1H), 2.73 (dd, *J* = 16.0 Hz and 5.5 Hz, 1H), 2.57–2.54 (m, 2H), 2.39 (s, 3H) ppm; ^{13}C NMR (125 MHz, $CDCl_3$) δ 143.3, 138.2, 136.9, 132.3, 131.8, 129.7, 129.5, 129.3, 128.6, 127.2, 127.1, 126.6, 126.5, 126.1, 53.7, 43.8, 38.2, 21.0, 21.5 ppm; HRMS (ESI) calc for $[C_{23}H_{24}NO_2S]^+$: *m/z* 378.1522, found 378.1539.

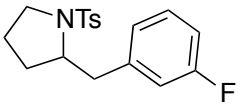

1.4j. **1.3b** and 3-fluorophenylboronic acid were reacted at 40 °C. The residue was purified by flash column chromatography on silica gel (10 % Et_2O in hexanes) to give **1.4j** (25.0 mg, 75 %) as a viscous oil that solidified upon standing: ^{1}H NMR (500 MHz, $CDCl_3$) δ 7.75 (d, *J* = 8.1 Hz, 2H), 7.32 (d, *J* = 8.0 Hz, 2H), 7.28–7.23 (m, 1H), 7.02 (d, *J* = 7.5 Hz, 1H), 6.95–6.90 (m, 2H), 3.82–3.78 (m, 1H), 3.41–3.37 (m, 1H), 3.23 (dd, *J* = 13.4, 3.5 Hz, 1H), 3.16–3.11 (m, 1H), 2.77 (dd, *J* = 13.4, 9.5 Hz, 1H), 2.43 (s, 3H), 1.65–1.57 (m, 2H), 1.49– 1.44 (m, 2H) ppm; ^{13}C NMR (150 MHz, $CDCl_3$) δ 163.8, 161.9, 143.4, 141.0 (d, $J_{19F\text{-}13C}$ = 7.2 Hz), 134.7, 129.9 (d, $J_{19F\text{-}13C}$ = 8.3 Hz), 129.7, 127.5 (d, $J_{19F\text{-}13C}$ = 5.2 Hz), 116.4 (d, $J_{19F\text{-}13C}$ = 20.8 Hz), 113.3 (d, $J_{19F\text{-}13C}$= 21.0 Hz), 61.3, 49.3, 42.4 (d, $J_{19F\text{-}13C}$ = 1.4 Hz), 30.0, 23.8, 21.6 ppm; HRMS (ESI) calc for $[C_{18}H_{21}FNO_2S]^+$: *m/z* 334.1272, found 334.1278.

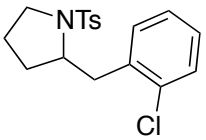

1.4k. **1.3b** and 2-chlorophenylboronic acid were reacted at 40 °C. The residue was purified by flash column chromatography on silica gel (15 % EtOAc in hexanes) to give **1.4k** (19.6 mg, 56 %): ^{1}H NMR (400 MHz, CDCl3): δ 7.77 (d, *J* = 8.2 Hz, 2H), 7.35 (dd, *J* = 7.8, 1.4 Hz, 1H), 7.33–7.30 (m, 3H), 7.23–7.14 (m, 2H), 3.96–3.90 (m, 1H), 3.49–3.44 (m, 1H), 3.41 (dd, *J* = 13.4, 4.3 Hz, 1H), 3.21– 3.16 (m, 1H), 2.92 (dd, *J* = 13.4, 9.8

Hz, 1H), 2.42 (s, 3H), 1.82–1.73 (m, 1H), 1.67–1.61 (m, 1H), 1.55–1.49 (m, 1H), 1.40–1.29 (m, 1H); ^{13}C NMR (150 MHz, $CDCl_3$) δ 143.6, 136.4, 134.7, 134.4, 132.0, 129.7, 129.6, 128.0, 127.6, 126.9, 60.3, 49.3, 39.5, 29.8, 23.9, 21.5 ppm; HRMS (ESI) calc for $[C_{18}H_{21}ClNO_2S]^+$: *m/z* 350.0982, found 350.0982.

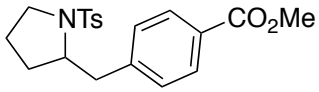

1.4l. **1.3b** and 4-(methoxycarbonyl)phenylboronic acid were reacted at 40 °C. The residue was purified by flash column chromatography on silica gel (10 % Et_2O in hexanes) to give **1.4l** (31.0 mg, 83 %): ^{1}H NMR (500 MHz, $CDCl_3$) δ 7.97 (d, *J* = 8.0 Hz, 2H), 7.75 (d, *J* = 8.1 Hz, 2H), 7.32 (d, *J* = 7.8 Hz, 4H), 3.91 (s, 3H), 3.85–3.82 (m, 1H), 3.38–3.34 (m, 1H), 3.26 (dd, *J* = 13.3, 3.4 Hz, 1H), 3.15–3.10 (m, 1H), 2.86 (dd, *J* = 13.3, 9.2 Hz, 1H), 2.42 (s, 3H), 1.60–1.56 (m, 2H), 1.47–1.45 (m, 2H) ppm; ^{13}C NMR (150 MHz, $CDCl_3$) δ 167.1, 143.9, 134.6, 129.7, 128.5, 127.5, 61.2, 52.1, 49.3, 42.7, 30.0, 23.9, 21.6 ppm; HRMS (ESI) calc for $[C_{20}H_{24}NO_4S]^+$: *m/z* 374.1421, found 374.1428.

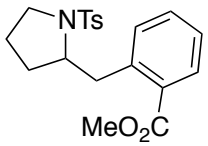

1.4m. **1.3b** and 2-(methoxycarbonyl)phenylboronic acid were reacted at 40 °C. The residue was purified by flash column chromatography on silica gel (10 % Et_2O in hexanes) to give **26** (28.8 mg, 77 %): ^{1}H NMR (500 MHz, $CDCl_3$) δ 7.84 (d, *J* = 7.9 Hz, 1H), 7.73 (d, *J* = 7.9 Hz, 2H), 7.45 (t, *J* = 7.5 Hz, 1H), 7.35 (d, *J* = 7.7 Hz, 1H), 7.28 (d, *J* = 7.6 Hz, 3H), 4.10–3.99 (m, 1H), 3.93 (s, 3H), 3.49 (dd, *J* = 13.1, 5.1 Hz, 1H), 3.44–3.40 (m, 1H), 3.23 (dd, *J* = 13.0, 8.8 Hz, 1H), 3.19–3.14 (m, 1H), 2.41 (s, 3H), 1.80–1.74 (m, 1H), 1.61–1.56 (m, 1H), 1.51–1.47 (m, 1H), 1.34–1.27 (m, 1H) ppm; ^{13}C NMR (150 MHz, $CDCl_3$) δ 168.4, 143.2, 139.7, 135.0, 132.4, 131.8, 130.7, 130.5, 129.6, 127.6, 126.5, 61.6, 52.2, 49.0, 39.5, 29.8, 23.9, 21.5 ppm; HRMS (ESI) calc for $[C_{20}H_{24}NO_4S]^+$: *m/z* 374.1430, found 374.1428.

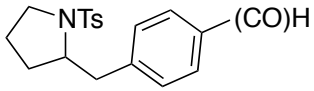

1.4n. **1.3b** and 4-formylphenylboronic acid were reacted at 40 °C. The residue was purified by flash column chromatography on silica gel (10 % Et_2O in hexanes) to give **1.4n** (23.4 mg, 68 %): ^{1}H NMR (500 MHz, $CDCl_3$) δ 9.99 (s, 1H), 7.82 (d, *J* = 7.8 Hz, 2H), 7.74 (d, *J* = 8.0 Hz, 2H), 7.42 (d, *J* = 7.8 Hz, 2H), 7.32 (d, *J* = 8.0 Hz, 2H), 3.86–3.83 (m, 1H), 3.38–3.34 (m, 1H), 3.13 (dd, *J* = 13.3, 3.4 Hz, 1H), 3.15–3.11 (m, 1H), 2.90 (dd, *J* = 13.1, 9.1 Hz, 1H), 2.42 (s, 3H), 1.59–1.56 (m, 2H), 1.50–1.44 (m, 2H) ppm; ^{13}C NMR (150 MHz, $CDCl_3$) δ 192.0, 145.8, 143.6, 135.0, 134.5, 130.4, 129.9, 129.8,

127.5, 61.1, 49.3, 42.9, 30.1, 23.9, 21.6 ppm; HRMS (ESI) calc for $[C_{19}H_{22}NO_3S]^+$: *m/z* 344.1315, found 344.1322.

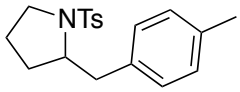

1.4o. **1.3b** and 4-tolylboronic acid were reacted at room temperature. The residue was purified by flash column chromatography on silica gel (10 % Et_2O in hexanes) to give **1.4o** (26.3 mg, 81 %) as a viscous oil that solidified upon standing: ^{1}H NMR (500 MHz, $CDCl_3$) δ 7.75 (d, *J* = 8.1 Hz, 2H), 7.30 (d, *J* = 8.1 Hz, 2H), 7.13 (d, *J* = 8.0 Hz, 2H), 7.10 (d, *J* = 8.0 Hz, 2H), 3.82–3.77 (m, 1H), 3.42–3.37 (m, 1H), 3.20 (dd, *J* = 13.3, 3.4 Hz, 1H), 3.15–3.10 (m, 1H), 2.70 (dd, *J* = 13.3, 9.7 Hz, 1H), 2.42 (s, 3H), 2.32 (s, 3H), 1.69–1.59 (m, 2H), 1.48–1.38 (m, 2H) ppm; ^{13}C NMR (150 MHz, $CDCl_3$) δ 143.3, 135.9, 135.4, 134.7, 129.7, 129.5, 129.1, 127.5, 61.8, 49.3, 42.3, 29.8, 23.8, 21.6, 21.1 ppm; HRMS (ESI) calc for $[C_{19}H_{24}NO_2S]^+$: *m/z* 330.1522, found 330.1530.

Alkoxyarylation general procedure: The alkene (100 mol), arylboronic acid (100 mol), and dppm$(AuBr)_2$ (2.5 mol) were dissolved in a mixture of 9:1 MeCN/nucleophile* (1.0 mL) at room temperature in a 1 dram vial equipped with a magnetic stir-bar. Selectfluor® (200 mol) was added in one portion and the reaction mixture was heated to 50 °C. After two hours, additional arylboronic acid (100 mol) and dppm$(AuBr)_2$ (2.5 mol) were added to the reaction mixture which then was stirred for an additional 12 hours at 50 °C. The reaction mixture was cooled to room temperature and quenched by the addition of sat. aq. $Na_2S_2O_3$ (5 mL). The materials were extracted with Et_2O (3 X 5 mL), the combined organic extracts were washed with brine, dried over $MgSO_4$ and concentrated *in vacuo*. In each case the crude product mixture was subjected to flash column chromatography to provide analytically pure product.

*N. B.: In cases where the nucleophile is a solid under ambient conditions, the first sentence of General Procedure A was subject to the following modification: The alkene (100 mol), arylboronic acid (100 mol), dppm$(AuBr)_2$ (2.5 mol), *and the nucleophile (1 mmol, 10 equiv) were dissolved MeCN (1.0 mL)* at room temperature in a 1 dram vial equipped with a magnetic stir-bar.

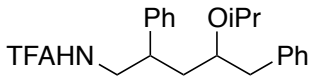

1.6a. **1.5** (25.7 mg, 0.1 mmol) was reacted with $PhB(OH)_2$ and methanol at 50 °C. The product was purified by flash column chromatography on silica gel (6:1 Hex/EtOAc) to give an inseparable mixture of diastereomers (d.r. 1.4:1) **1.6a** (30.9 mg, 72 %) as a clear oil: ^{1}H NMR (500 MHz, $CDCl_3$) 7.37-7.05 (m, 10H major + 10H minor diastereomer), 6.70 (br s, 1H major), 6.62 (br s, 1H minor), 3.62 (quintet, *J* = 6.5 Hz, 2H major), 3.47-3.40 (m, 3H minor), 3.32 (s, 3H major), 3.31 (s, 3H minor), 3.21- 3.16 (m, 1H major),

3.08-3.01 (m, 1H major + 1H minor), 2.94-2.87 (m, 1H major + 1H minor), 2.74-2.65 (m, 1H major + 1H minor), 1.92-1.82 (m, 2H major), 1.77-1.74 (m, 2H minor) ppm; ^{13}C NMR (126 MHz, $CDCl_3$) 157.3 (major), 156.9 (minor), 141.9 (major), 141.5 (minor), 138.1 (major), 137.9 (minor), 129.4 (minor), 129.4 (major), 129.1 (major), 129.0 (minor), 128.4 (major), 128.4 (minor), 127.6 (minor), 127.4 (major), 127.3, 126.4 (major), 126.3 (minor), 118.1 (q, $J^{C\text{-}F}$ = 289 Hz, minor), 115.8 (q, $J^{C\text{-}F}$ = 284 Hz, major), 57.1 (minor), 56.9 (major), 45.9 (minor), 44.9 (major), 42.1 (minor), 40.9 (major), 39.7 (minor), 39.4 (major), 38.3 (minor), 37.6 (major) ppm.

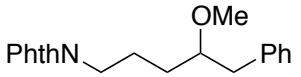

1.6b. 5-Phthalimidopentene[22] (21.5 mg, 0.10 mmol) was reacted with $PhB(OH)_2$ and MeOH at 50 °C. The product was purified by flash column chromatography on silica gel (10% EtOAc in hexanes) to give **1.6b** (25.5 mg, 79%) as a colorless viscous oil: ^{1}H NMR (500 MHz, $CDCl_3$) 7.83 (dd, *J* = 5.4, 3.1 Hz, 2H), 7.70 (dd, *J* = 5.4, 3.1 Hz, 2H), 7.25–7.22 (m, 2H), 7.17–7.14 (m, 3H), 3.70–3.64 (m, 2H), 3.42–3.37 (m, 1H), 3.31 (s, 3H), 2.85 (dd, *J* = 13.7, 6.1 Hz, 1H), 2.67 (dd, *J* = 13.7, 6.4 Hz, 1H), 1.87–1.80 (m, 1H), 1.75–1.66 (m, 1H), 1.55–1.42 (m, 2H) ppm; ^{13}C NMR (125 MHz, $CDCl)_3$ 168.4, 138.7, 133.9, 132.2, 129.4, 128.3, 126.1, 123.2, 81.7, 57.2, 40.1, 38.0, 30.7, 24.5 ppm; HRMS (ESI) calcd. for $[C_{20}H_{21}NO_3Na]$ ($[M+Na]^+$): *m/z* 346.1414, found 346.1416.

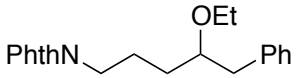

1.6c. 5-Phthalimidopentene[22] (21.5 mg, 0.10 mmol) was reacted with $PhB(OH)_2$ and ethanol at 50 °C. The product was purified by flash column chromatography on silica gel (10% EtOAc in hexanes) to give **1.6c** (28.6 mg, 85%) as a colorless viscous oil: ^{1}H NMR (500 MHz, $CDCl_3$) 7.83 (dd, *J* = 5.4, 3.0 Hz, 2H), 7.70 (dd, *J* = 5.4, 3.0 Hz, 2H), 7.25–7.21 (m, 2H), 7.18–7.13 (m, 3H), 3.71–3.62 (m, 2H), 3.49–3.44 (m, 1H), 3.42 (q, *J* = 7.0 Hz, 2H), 2.83 (dd, *J* = 13.6, 6.2 Hz, 1H), 2.67 (dd, *J* = 13.6, 6.3 Hz, 1H), 1.89–1.81 (m, 1H), 1.75–1.65 (m, 1H), 1.55–1.42 (m, 2H), 1.12 (t, *J* = 7.0 Hz, 3H) ppm; ^{13}C NMR (125 MHz, $CDCl_3$) 168.4, 138.9, 133.9, 132.2, 128.2, 126.1, 123.2, 80.1, 65.0, 40.9, 38.0, 31.3, 24.5, 15.5 ppm; HRMS (ESI) calc for $[C_{21}H_{24}O_3N]$ ($[M+H]^+$): *m/z* 338.1751, found 338.1747.

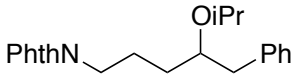

1.6d. 5-Phthalimidopentene[22] (21.5 mg, 0.10 mmol) was reacted with $PhB(OH)_2$ and isopropanol at 50 °C. The product was purified by flash column chromatography on silica gel (10% EtOAc in hexanes) to give **1.6d** (31.4 mg, 90%) as a colorless viscous oil: ^{1}H NMR (500 MHz, $CDCl_3$) 7.83 (dd, *J* = 5.4, 3.1 Hz, 2H), 7.70 (dd, *J* = 5.4, 3.1 Hz, 2H), 7.25–7.22 (m, 2H), 7.17–7.14 (m, 3H), 3.70–3.61 (m, 2H), 3.55–3.48 (m, 2H), 2.78 (dd, *J* = 13.4, 6.1 Hz, 1H), 2.67 (dd, *J* = 13.4, 6.4 Hz, 1H), 1.90–1.81 (m, 1H), 1.72–1.64 (m, 1H), 1.53–1.39 (m, 2H), 1.10 (d, *J* = 6.0 Hz, 3H), 1.00 (d, *J* = 6.1 Hz, 3H) ppm; ^{13}C NMR (125 MHz, $CDCl_3$) 168.4, 139.0, 133.9, 132.2, 129.6, 128.2, 126.0, 123.2, 77.6,

70.1, 41.8, 38.0, 31.9, 24.8, 22.9, 22.5 ppm; HRMS (ESI) calc for $[C_{22}H_{26}O_3N]$ ($[M+H]^+$): *m/z* 352.1907, found 352.1908.

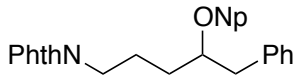

1.6e. 5-Phthalimidopentene[22] (21.5 mg, 0.10 mmol) was reacted with $PhB(OH)_2$ and neopentanol at 50 °C. The product was purified by flash column chromatography on silica gel (7% Et_2O in hexanes) to give **1.6e** (34.2 mg, 90%) as a colorless viscous oil: ^{1}H NMR (500 MHz, $CDCl_3$) 7.83 (dd, *J* = 5.4, 3.0 Hz, 2H), 7.70 (dd, *J* = 5.4, 3.0 Hz, 2H), 7.24–7.20 (m, 2H), 7.18–7.13 (m, 3H), 3.68–3.63 (m, 2H), 3.46–3.40 (m, 1H), 3.06 (d, *J* = 8.4 Hz, 1H), 3.02 (d, *J* = 8.4 Hz, 1H), 2.84 (dd, *J* = 13.6, 6.2 Hz, 1H), 2.65 (dd, *J* = 13.6, 6.3 Hz, 1H), 1.90–1.78 (m, 1H), 1.76–1.66 (m, 1H), 1.53–1.45 (m, 2H), 0.85 (s, 9H) ppm; ^{13}C NMR (125 MHz, $CDCl_3$) 168.4, 139.1, 133.9, 132.2, 129.6, 128.1, 125.9, 80.4, 80.0, 40.5, 38.1, 32.2, 31.0, 26.8, 24.5 ppm; HRMS (ESI) Calcd. for $[C_{24}H_{30}O_3N]$ ($[M+H]^+$): *m/z* 380.2220, found 380.2220.

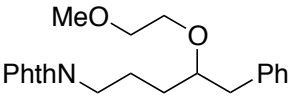

1.6f. 5-Phthalimidopentene[22] (21.5 mg, 0.10 mmol) was reacted with $PhB(OH)_2$ and 2-methoxyethanol. The product was purified by flash column chromatography on silica gel (gradient: 10% – 15% EtOAc in hexanes) to give **1.6f** (31.2 mg, 85%) as a colorless viscous oil: ^{1}H NMR (500 MHz, $CDCl_3$) 7.82 (dd, *J* = 5.4, 3.1 Hz, 2H), 7.70 (dd, *J* = 5.4, 3.1 Hz, 2H), 7.24–7.21 (m, 2H), 7.18–7.13 (m, 3H), 3.70–3.61 (m, 2H), 3.56–3.49 (m, 2H), 3.46–3.43 (m, 2H), 3.32 (s, 3H), 2.86 (dd, *J* = 13.6, 6.3, 1H), 2.68 (dd, *J* = 13.6, 6.4, 1H), 1.91–1.82 (m, 1H), 1.75–1.67 (m, 1H), 1.53–1.48 (m, 2H) ppm; ^{13}C NMR (125 MHz, $CDCl_3$) 168.4, 138.8, 133.9, 132.2, 129.5, 128.3, 126.1, 123.2, 81.1, 72.2, 68.9, 59.0, 40.8, 37.9, 31.1, 24.7 ppm; HRMS (ESI) calc for $[C_{22}H_{25}NO_4Na]$ ($[M+Na]^+$): *m/z* 390.1676, found 390.1677.

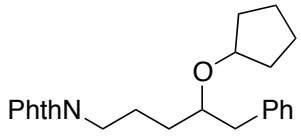

1.6g. 5-Phthalimidopentene[22] (21.5 mg, 0.10 mmol) was reacted with $PhB(OH)_3$ and cyclopentanol. The product was purified by flash column chromatography on silica gel (5% EtOAc in hexanes) to give **1.6g** (32.1, 85%) as a colorless viscous oil: ^{1}H NMR (500 MHz, $CDCl_3$) 7.83 (dd, *J* = 5.3, 3.0 Hz, 2H), 7.70 (dd, *J* = 5.3, 3.0 Hz, 2H), 7.25–7.22 (m, 2H), 7.17–7.14 (m, 3H), 3.93–3.88 (m, 1H), 3.66 (t, *J* = 7.3 Hz, 2H), 3.51–3.46 (m, 1H), 2.80 (dd, *J* = 13.5, 6.1, 1H), 2.66 (dd, *J* = 13.5, 6.4, 1H), 1.89–1.79 (m, 1H), 1.72–1.38 (m, 9H) ppm; ^{13}C NMR (125 MHz, $CDCl_3$) 168.4, 139.0, 133.9, 132.2, 129.6, 128.2, 126.0, 123.2, 79.6, 78.0, 41.2, 38.1, 32.7, 32.6, 31.6, 24.8, 23.3, 23.2 ppm; HRMS (ESI) calc for $[C_{24}H_{27}NO_3Na]$ ($[M+Na]^+$): *m/z* 400.1883, found 400.1884.

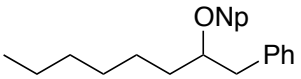

1.6h. 1-dodecene (16.8 mg, 0.1 mmol) was reacted with phenylboronic acid and neopentanol. The product was purified by flash column chromatography on silica gel (9:1 Hex/EtOAc) to give **1.6h** (22.0 mg, 66%) as a colorless oil. ^{1}H NMR (500 MHz, $CDCl_3$) 7.30-7.27 (m, 2H), 7.23-7.19 (m, 2H), 3.41-3.39 (m, 1H), 3.06 (s, 2H), 2.85 (dd, J = 13.5 Hz ad 6.5 Hz), 2.71 (dd, J = 13.5 Hz and 6.0 Hz), 1.51-1.43 (m, 3H), 1.32- 1.25 (m, 17H), 0.98-0.88 (m, 13H) ppm; ^{13}C NMR (126 MHz, $CDCl_3$) 139.7, 129.6, 128.0, 125.8, 81.2, 79.9, 40.8, 33.9, 32.3, 32.0, 29.8, 29.7, 29.7, 29.4, 26.8, 25.4, 22.7, 14.2.

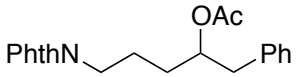

1.6i. 5-Phthalimidopentene[22] (21.5 mg, 0.10 mmol) was reacted with $PhB(OH)_2$ and acetic acid. The product was purified by flash column chromatography on silica gel (gradient: 10 – 15% EtOAc in hexanes) to give **1.6i** (21.7 mg, 62%) as a colorless viscous oil: ^{1}H NMR (500 MHz, $CDCl_3$) 7.83 (dd, J = 5.5, 3.1 Hz, 2H), 7.71 (dd, J = 5.5, 3.1 Hz, 2H), 7.26– 7.22 (m, 2H), 7.20–7.15 (m, 3H), 5.13–5.08 (m, 1H), 3.70–3.61 (m, 2H), 2.87 (dd, J = 13.7, 6.9, 1H), 2.79 (dd, J = 13.7, 6.2, 1H), 1.98 (s, 3H), 1.80–1.54 (m, 4H) ppm; ^{13}C NMR (125 MHz, $CDCl_3$) 170.6, 168.4, 137.7, 134.0, 132.1, 129.4, 128.4, 126.5, 123.2, 74.0, 40.5, 37.7, 30.7, 24.6, 21.2 ppm; HRMS (ESI) Calcd. for [$C_{21}H_{21}NO_4Na$] ([M+Na]$^+$): *m/z* 374.1363, found 374.1362.

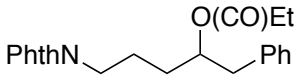

1.6j. 5-Phthalimidopentene[22] (21.5 mg, 0.10 mmol) was reacted with $PhB(OH)_2$ and propionic acid. The product was purified by flash column chromatography on silica gel (10% EtOAc in hexanes) to give **1.6j** (25.2 mg, 69%) as a colorless viscous oil: ^{1}H NMR (500 MHz, $CDCl_3$) 7.83 (dd, J = 5.4, 3.1 Hz, 2H), 7.71 (dd, J = 5.4, 3.1 Hz, 2H), 7.25–7.22 (m, 2H), 7.19–7.15 (m, 3H), 5.09–5.15 (m, 1H), 3.70–3.61 (m, 2H), 2.86 (dd, J = 13.7, 7.0, 1H), 2.79 (dd, J = 13.7, 6.2, 1H), 2.32–2.18 (m, 2H), 1.80–1.56 (m, 4H), 1.05 (t, J = 7.6 Hz, 3H) ppm; ^{13}C NMR (125 MHz, $CDCl_3$) 174.0, 168.4, 137.3, 134.0, 132.1, 129.4, 128.3, 126.5, 123.2, 73.8, 40.6, 37.7, 30.7, 27.8, 24.6, 9.2 ppm; HRMS (ESI) Calcd. for [$C_{22}H_{23}NO_4Na$] ([M+Na]$^+$): *m/z* 388.1519, found 388.1521.

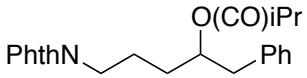

1.6k. 5-Phthalimidopentene[22] (21.5 mg, 0.10 mmol) was reacted with $PhB(OH)_2$ and isobutyric acid. The product was purified by flash column chromatography on silica gel (10% EtOAc in hexanes) to give **1.6k** (18.8 mg, 50%) as a colorless viscous oil: ^{1}H NMR (500 MHz, $CDCl_3$) 7.83 (dd, J = 5.4, 3.0 Hz, 2H), 7.71 (dd, J = 5.4, 3.0 Hz, 2H), 7.25–7.22 (m, 2H), 7.18–7.15 (m, 3H), 5.14–5.09 (m, 1H), 3.71–3.62 (m, 2H), 2.86 (dd, J = 13.7, 7.1, 1H), 2.80 (dd, J = 13.7, 6.2, 1H), 2.51–2.46 (septet, J = 7.0 Hz, 1H), 1.80–1.57 (m, 4H), 1.09 (d, J = 7.0 Hz, 3H), 1.03 (d, J = 7.0 Hz, 3H) ppm; ^{13}C NMR (125 MHz, $CDCl_3$) 176.7, 168.4, 137.3, 134.0, 132.1, 129.5, 128.3, 126.5, 123.2, 73.5, 40.6, 37.7, 34.2, 30.8, 24.5, 19.0, 18.9 ppm; HRMS (ESI) Calcd. for [$C_{23}H_{25}NO_4Na$] ([M+Na]$^+$): *m/z* 402.1676, found 402.1675.

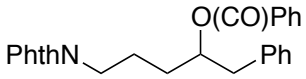

1.6l. 5-Phthalimidopentene[22] (21.5 mg, 0.10 mmol) was reacted with $PhB(OH)_2$ and benzoic acid (122.2 mg, 1.0 mmol, 10 equiv). The product was purified by flash column chromatography on silica gel (gradient: 15 – 20% EtOAc in hexanes) to give **1.6l** (19.8 mg, 48%) as a colorless viscous oil: ^{1}H NMR (500 MHz, $CDCl_3$) 7.99 (d, *J* =7.5 Hz, 2H), 7.82(dd,*J*=5.4,3.1Hz,2H),7.70(dd,*J*=5.4,3.1Hz,2H),7.54(appt,*J*=7.4 Hz, 1H), 7.42 (t, *J* = 7.6 Hz, 2H), 7.25–7.20 (m, 4H), 7.18–7.14 (m, 1H), 5.40–5.34 (m, 1H), 3.72–3.67 (m, 2H), 3.03 (dd, *J* = 13.7, 6.4, 1H), 2.93 (dd, *J* = 13.7, 6.3, 1H), 1.89– 1.70 (m, 4H) ppm; ^{13}C NMR (125 MHz, $CDCl_3$) 168.3, 166.0, 137.1, 133.9, 132.8, 132.0, 130.3, 129.5, 129.4, 128.3, 128.3, 126.5, 123.2, 74.7, 40.4, 37.6, 30.6, 24.6 ppm; HRMS (ESI) Calcd. for $[C_{26}H_{23}NNaO_4]$ ($[M+Na]^+$): *m/z* 436.1519, found 436.1531.

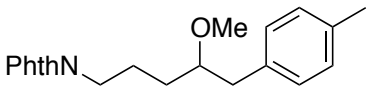

1.6m. 5-Phthalimidopentene[22] (21.5 mg, 0.10 mmol) was reacted with 4-tolylboronic acid and methanol. The product was purified by flash column chromatography on silica gel (10% EtOAc in hexanes) to give **1.6m** (29.7 mg, 88%) as a colorless viscous oil: ^{1}H NMR (500 MHz, $CDCl_3$) 7.83 (dd, *J* = 5.4, 3.1 Hz, 2H), 7.70 (dd, *J* = 5.4, 3.1 Hz, 2H), 7.06 (d, *J* = 8.7 Hz, 2H), 77.03 (d, *J* = 8.7 Hz, 2H), 3.70–3.62 (m, 2H), 3.39–3.34 (m, 2H), 3.31 (s, 3H), 2.82 (dd, *J* = 13.7, 5.9, 1H), 2.62 (dd, *J* = 13.7, 6.6, 1H), 2.78 (s, 3H), 1.89–1.79 (m, 1H), 1.74–1.65 (m, 1H), 1.55–1.40 (m, 2H) ppm; ^{13}C NMR (125 MHz, $CDCl_3$) 168.4, 135.6, 135.5, 133.9, 132.2, 129.3, 129.0, 123.2, 81.8, 57.1, 39.5, 38.0, 30.6, 24.5, 21.0 ppm; HRMS (ESI) Calcd. for $[C_{21}H_{23}NO_3Na]$ ($[M+Na]^+$): *m/z* 360.1570, found 360.1573.

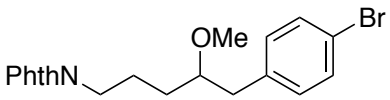

1.6n. 5-Phthalimidopentene[22] (21.5 mg, 0.10 mmol) was reacted with 4-bromophenylboronic acid and methanol. The product was purified by flash column chromatography on silica gel (gradient: 10% – 15% EtOAc in hexanes) to give **1.6n** (36.1 mg, 90%) as a colorless viscous oil: ^{1}H NMR (500 MHz, $CDCl_3$) 7.81 (dd, *J* = 5.3, 3.0 Hz, 2H), 7.70 (dd, *J* = 5.3, 3.0 Hz, 2H), 7.33 (d, *J* = 8.3 Hz, 2H), 7.03 (d, *J* = 8.3 Hz, 2H), 3.89 (s, 3H), 3.69– 3.62 (m, 2H), 3.38–3.33 (m, 1H), 3.28 (s, 3H), 2.75 (dd, *J* = 13.8, 6.3, 1H), 2.63 (dd, *J* = 13.8, 6.0, 1H), 1.87–1.77 (m, 1H), 1.74–1.66 (m, 1H), 1.51–1.39 (m, 2H) ppm; ^{13}C NMR (125 MHz, $CDCl_3$) 168.4, 137.7, 133.9, 132.1, 131.3, 131.2, 123.2, 120.0, 81.3, 57.3, 39.4, 37.9, 30.5, 24.4 ppm; HRMS (ESI) Calcd. for $[C_{20}H_{21}NO_3Br]$ ($[M+H]^+$): *m/z* 402.0699, found 402.0697.

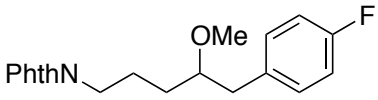

1.6o. 5-Phthalimidopentene[22] (21.5 mg, 0.10 mmol) was reacted with 3-fluorophenylboronic acid and methanol. The product was purified by flash column chromatography on silica gel (10% EtOAc in hexanes) to give **1.6o** (26.9 mg, 79%) as a

colorless viscous oil: ^{1}H NMR (500 MHz, $CDCl_3$) 7.83 (dd, J = 5.4, 3.0 Hz, 2H), 7.70 (dd, J = 5.4, 3.0 Hz, 2H), 7.21–7.16 (m, 1H), 6.94 (d, J = 7.5 Hz, 1H), 6.90–6.83 (m, 2H), 3.69–3.64 (m, 2H), 3.41–3.37 (m, 1H), 3.29 (s, 3H), 2.81 (dd, J = 13.8, 6.4, 1H), 2.68 (dd, J = 13.8, 5.9, 1H), 1.88–1.79 (m, 1H), 1.76–1.68 (m, 1H), 1.55–1.43 (m, 2H) ppm; ^{13}C NMR (125 MHz, $CDCl_3$) 168.4, 162.8 (d, $J^{C\text{-}F}$ = 245.0 Hz), 141.3 (d, $J^{C\text{-}F}$ = 7.0 Hz), 133.9, 132.1, 129.6 (d, $J^{C\text{-}F}$ = 9.3 Hz), 125.1 (d, $J^{C\text{-}F}$ = 2.8 Hz), 123.2, 116.2 (d, $J^{C\text{-}F}$ = 20.9 Hz), 113.0 (d, $J^{C\text{-}F}$ = 20.4 Hz), 81.3, 57.3, 39.8 (d, $J^{C\text{-}F}$ = 1.4 Hz), 37.9, 30.7, 24.5 ppm; HRMS (ESI) Calcd. for [$C_{20}H_{21}NO_3F$] ([M+H]$^+$): *m/z* 342.1500, found 342.1500.

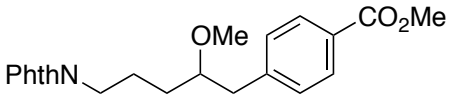

1.6p. 5-Phthalimidopentene[22] (21.5 mg, 0.10 mmol) was reacted with 4-(methoxycarbonyl)phenylboronic acid and methanol. The product was purified by flash column chromatography on silica gel (gradient: 15% – 25% EtOAc in hexanes) to give **1.6p** (30.5 mg, 80%) as a colorless viscous oil: ^{1}H NMR (500 MHz, $CDCl_3$) 7.90 (d, J = 8.1 Hz, 2H), 7.81 (dd, J = 5.3, 3.1 Hz, 2H), 7.70 (dd, J = 5.3, 3.1 Hz, 2H), 7.23 (d, J = 8.1 Hz, 1H), 3.89 (s, 3H), 3.69–3.64 (m, 2H), 3.43–3.38 (m, 1H), 3.28 (s, 3H), 2.86 (dd, J = 13.6, 6.4, 1H), 2.73 (dd, J = 13.6, 5.9, 1H), 1.87–1.78 (m, 1H), 1.75–1.66 (m, 9H), 1.53–1.41 (m, 2H) ppm; ^{13}C NMR (125 MHz, $CDCl_3$) 168.4, 167.1, 144.3, 133.9, 132.1, 129.6, 129.5, 128.1, 123.2, 81.3, 57.3, 52.0, 40.1, 37.8, 30.7, 24.4 ppm; HRMS (ESI) Calcd. for [$C_{22}H_{23}NO_5Na$] ([M+Na]$^+$): *m/z* 404.1468, found 404.1470.

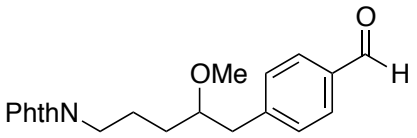

1.6q. 5-Phthalimidopentene[22] (21.5 mg, 0.10 mmol) was reacted with 4-formylphenylboronic acid and methanol. The product was purified by flash column chromatography on silica gel (20% EtOAc in hexanes) to give **1.6q** (28.9 mg, 82%) as a colorless viscous oil: ^{1}H NMR (500 MHz, $CDCl_3$) 9.96 (s, 1H), 7.85 (dd, J = 5.3, 3.0 Hz, 2H), 7.78 (d, J = 8.0 Hz, 2H), 7.70 (dd, J = 5.3, 3.0 Hz, 2H), 7.36 (d, J = 8.0 Hz, 1H), 3.749–3.66 (m, 2H), 3.49–3.44 (m, 1H), 3.32 (s, 3H), 2.91 (dd, J = 13.7, 6.5, 1H), 2.81 (dd, J = 13.7, 5.8, 1H), 1.90–1.82 (m, 1H), 1.80–1.71 (m, 1H), 1.54–1.47 (m, 2H) ppm; ^{13}C NMR (125 MHz, $CDCl_3$) 192.0, 168.4, 146.3, 134.7, 134.0, 132.1, 130.1, 129.8, 123.2, 81.2, 57.3, 40.3, 37.8, 30.7, 24.4 ppm; HRMS (ESI) Calcd. for [$C_{21}H_{20}NO_4$] ([M+H]$^+$): *m/z* 350.1387, found 350.1388.

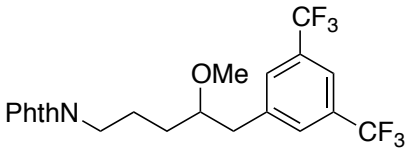

1.6r. 5-Phthalimidopentene[22] (21.5 mg, 0.10 mmol) was reacted with 3,5-bis-(trifluoromethyl)- phenylboronic acid and methanol. The product was purified by flash column chromatography on silica gel (20% EtOAc in hexanes) to give **1.6r** (35.4 mg,

77%) as a colorless viscous oil: ^{1}H NMR (500 MHz, $CDCl_3$) 7.83 (dd, J = 5.4, 3.2 Hz, 2H), 7.72– 7.70 (m, 3H), 7.64 (s, 2H), 3.72–3.67 (m, 2H), 3.44–3.39 (m, 1H), 3.27 (s, 3H), 2.88 (dd, J = 14.1, 6.9, 1H), 2.84 (dd, J = 14.1, 5.1, 1H), 1.88–1.71 (m, 2H), 1.58–1.48 (m, 2H) ppm; ^{13}C NMR (125 MHz, $CDCl_3$) 168.4, 141.3, 134.0, 132.1, 131.6 (q, $J^{C\text{-}F}$ = 33.0 Hz), 129.6 (q, $J^{C\text{-}F}$ = 2.9 Hz), 123.4 (q, $J^{C\text{-}F}$ = 272.6 Hz), 123.2, 120.3 (m), 80.8, 57.4, 39.9, 37.7, 30.8, 24.4 ppm.

Hydroxyarylation general procedure: The alkene (100 μmol), arylboronic acid (100 μmol), dppm(AuBr)$_2$ (2.5 μmol), water (1 mmol, 10 equiv) and MeCN (1.0 mL) were combined in a 1 dram vial. Selectfluor® (200 μmol) was added in one portion and the reaction mixture was heated to 50 °C. After one hour, additional arylboronic acid (100 μmol) and dppm(AuBr)$_2$ (2.5 μmol) were added and the reaction mixture was stirred for an additional 14 hours at the indicated temperature. The reaction mixture was diluted with sat. aq. $Na_2S_2O_3$ (5 mL) and water (5 mL), and then extracted with Et_2O (4 X 15 mL), the combined organic extracts were washed with water (5 mL) and brine (5 mL), dried over $MgSO_4$ and concentrated *in vacuo.* In each case the crude product mixture was subjected to flash column chromatography to provide analytically pure product.

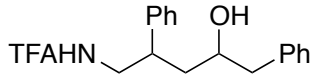

1.6s. **1.5** (25.7 mg, 0.10 mmol) was reacted with PhB(OH)$_2$ and water. The product was purified by flash column chromatography on silica gel (2:1:1 hexanes/EtOAc/PhH) to give an inseparable mixture of diastereomers (d.r. 1.2:1) **1.6s** (30.9 mg, 88%) as a clear oil: ^{1}H NMR (500 MHz, $CDCl_3$) 7.34-7.14 (m, 10H major + 10H minor diastereomer), 6.86 (br s, 1H minor), 6.65 (br s, 1H major), 3.94-3.91 (m, 1H major), 3.78-3.72 (m, 1H major), 3.72-3.66 (m, 1H major + 1H minor), 3.52-3.42 (m, 1H major + 1H minor), 3.19-3.11 (m, 1H major + 1H minor), 2.84 (dd, J = 13.5 Hz and 4.0 Hz, 1H major), 2.78 (dd, J = 13.5 Hz and 4.0 Hz, 1H minor), 2.68 (t, J = 9.0 Hz, 1H major), 2.68 (dd, J = 17.5 Hz and 8.5 Hz, 1H minor), 1.97-1.84 (m, 2H major + 2H minor), 1.78 (br s, 1H major + 1H minor) ppm;^{13}C NMR (126 MHz, $CDCl_3$) 157.2 (q, $J^{C\text{-}F}$ = 37 Hz), 157.2 (q, $J^{C\text{-}F}$ = 37 Hz), 141.7, 141.6, 137.7, 137.7, 129.4, 129.2, 129.1, 128.8, 128.7, 127.6, 127.5, 127.5, 127.4, 126.8, 115.8 (q, $J^{C\text{-}F}$ = 289 Hz), 115.8 (q, $J^{C\text{-}F}$ = 289 Hz), 70.6, 70.3, 45.8, 44.8, 44.7, 43.9, 42.5, 41.3, 40.7, 40.3 ppm.

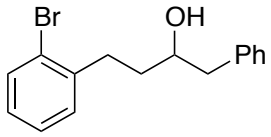

1.6t. 1-Bromo-2-(but-3-enyl)benzene[19] (24.3 μL, 31.6 mg, 0.15 mmol) was reacted with PhB(OH)$_2$ and water. The product was purified by flash column chromatography on silica gel (10 cm X 2.5 cm, gradient: pet. ether/acetone 12/1 3/1) to give alcohol **1.6t** (34.8 mg, 76%) as a clear colorless oil: ^{1}H NMR (600 MHz, $CDCl_3$) 7.54 (d, J = 8.4, 1H), 7.35 - 7.30 (m, 2H), 7.26 - 7.21 (m, 5H), 7.06 (ddd, J = 7.8, 6.6, 2.4 Hz, 1H), 3.88 (app septet, J = 4.2 Hz, 1H), 2.99 (ddd, J = 13.5, 10.8, 5.4 Hz, 1H), 2.89 (dd, J = 13.5, 4.2, 1H), 2.84

(ddd, J = 13.8, 10.2, 6.6, 1H), 2.71 (dd, J = 13.5, 8.7 Hz, 1H), 1.92 - 1.86 (m, 1H), 1.84 - 1.77 (m, 1H), 1.60 (br s, 1H) ppm; ^{13}C NMR (125 MHz, $CDCl_3$) 141.3, 138.3, 132.8, 130.4, 129.4, 128.6, 127.6, 127.5, 126.5, 124.4, 72.0, 44.1, 36.8, 23.4 ppm; HRMS (EI) Calcd. for [$C_{16}H_{15}Br$] ([M-H_2O]$^+$): *m/z* 286.0347, found 286.0345.

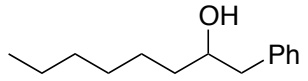

1.6u. 1-Octene (23.5 μL, 0.15 mmol) was reacted with $PhB(OH)_2$ and water. The product was purified by flash column chromatography on silica gel (10 cm X 2.5 cm, gradient: 12/1 1/1 hexanes/EtOAc) to give alcohol **1.6u** (25.6 mg, 73%) as a clear colorless oil: ^{1}H NMR (600 MHz, $CDCl_3$) 7.35 - 7.30 (m, 2H), 7.55-7.15 (m, 3H), 3.84 - 3.79 (m, 1H), 2.84 (dd, J = 13.8, 4.2 Hz, 1H), 2.65 (dd, J = 13.2, 8.4, 1H), 1.55 - 1.43 (m, 4H), 1.40 - 1.25 (m, 7H), 0.89 (t, J = 7.2 Hz, 3H) ppm; ^{13}C NMR (150 MHz, $CDCl_3$) 138.9, 129.6, 128.7, 126.6, 72.9, 44.3, 37.1, 32.0, 29.5, 25.9, 22.8, 14.3 ppm; HRMS (EI) Calcd. for [$C_{14}H_{21}O$] ([M-H]): *m/z* 205.1592, found 205.1596.

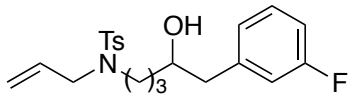

1.6v. *N*-1-Penten-4-yltoluensulfonamide[23] (37.8 μL, 41.9 mg, 0.15 mmol) was reacted with *m*-fluorophenylboronic acid and water. The product was purified by flash column chromatography on silica gel (10 cm X 2.5 cm, gradient: hexanes/EtOAc/PhH 5/1/1 1/1/1 to give alcohol **1.6v** (42.2 mg, 72%) as an off-white solid: ^{1}H NMR (600 MHz, $CDCl_3$) 7.68 (d, J = 7.8 Hz, 2H), 7.29 (d, J = 7.8 Hz, 2H), 7.29 - 7.24 (m, 2H), 6.98 (d, J = 7.2 Hz 1H), 6.96 - 6.88 (m, 2H), 5.61 (dddd, J = 16.8, 10.2, 6.6, 6.6, Hz, 1H), 5.16 (d, J = 16.8 Hz, 1H), 5.12 (d, J = 10.2 Hz, 1H), 3.82 (app septet, J = 4.2 Hz, 1H), 3.79 (d, J = 6.0 Hz, 2H), 3.14 (t, J = 7.2 Hz, 2H), 2.78 (dd, J = 13.2, 4.2 Hz, 1H), 2.64 (dd, J = 13.2, 8.4 Hz, 1H), 2.42 (s, 3H), 1.77 - 1.69 (m, 1H), 1.67 - 1.58 (m, 2H), 1.58 - 1.50 (m, 2H), 1.48 - 1.41 (m, 1H); ^{13}C ($CDCl_3$, 125 MHz): 163.1 (d, J^{C-F} = 250 Hz), 143.4, 141.2 (d, J^{C-F} = 7.5 Hz), 137.2, 133.4, 130.2 (d, J^{C-F} = 8.8 Hz), 129.9, 127.3, 125.2 (d, J^{C-F} = 2.5 Hz), 119.0, 116.4 (d, J^{C-F} = 20 Hz), 113.6 (d, J^{C-F} = 20 Hz) 72.2, 50.9, 47.3, 44.0, 33.6, 24.7, 21.7 ppm; HRMS (ESI) Calcd. for [$C_{21}H_{27}O_3NFS$] ([M+H]$^+$): *m/z* 392.1690, found 392.1677.

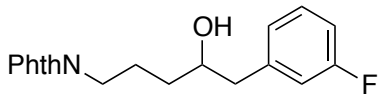

1.6w. 5-Phthalimidopentene[22] (32.2 mg, 0.15 mmol) was reacted with *m*-fluorophenylboronic acid and water in MeCN at 50°C. The product was purified by flash column chromatography on silica gel (10 cm X 2.5 cm, gradient: hexanes/EtOAc/PhH 4/1/1 1/1/1) to give alcohol **1.6w** (34.1 mg, 69%) as an off-white solid: ^{1}H NMR (600 MHz, $CDCl_3$) 7.83 (dd, J = 5.4, 4.5 Hz, 2H), 7.71 (dd, J = 6.6, 3.6 Hz, 2H), 7.24 (app q, J = 8.4 Hz, 1H), 6.97 (d, J = 4.5 Hz, 1H), 6.94 - 6.86 (m, 2H), 3.87 (app septet, J = 4.8 Hz, 1H), 3.73 (app t, J = 8.4 Hz, 1H), 2.79 (dd, J = 16.5, 4.8 Hz, 1H), 2.66 (dd, J = 16.2, 10.2 Hz, 1H), 1.96 - 1.86 (m, 1H), 1.85 - 1.71 (m, 2H), 1.63 - 1.48 (m, 2H) ppm; ^{13}C NMR (125 MHz, $CDCl_3$) 168.7, 163.1 (d, J^{C-F} = 244 Hz), 141.1 (d, J^{C-F} = 7.5 Hz), 134.1, 132.3,

130.2 (d, J = 8.8 Hz), 125.2 (d, $J^{C\text{-}F}$ = 3.8 Hz), 123.4, 116.4 (d, $J^{C\text{-}F}$ = 20 Hz), 113.6 (d, $J^{C\text{-}F}$ = 21 Hz), 72.2, 44.0, 37.9, 33.9, 25.2 ppm; HRMS (ESI) Calcd. for [$C_{19}H_{19}O_3NF$] ([M+H]$^+$): *m/z* 328.1343, found 328.1331.

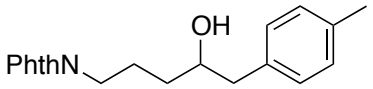

1.6x. 5-phthalimidopentene[22] (32.2 mg, 0.15 mmol) was reacted with *p*-tolylboronic acid and water. The product was purified by flash column chromatography on silica gel (15 cm X 2.5 cm, gradient: pet. ether/acetone/PhH 4/1/1 1/1/1) to give alcohol **1.6x** (37.5 mg, 83%) as an off-white solid: ^{1}H NMR (600 MHz, $CDCl_3$) 7.83 (dd, J = 6.6, 3.6 Hz, 2H), 7.70 (dd, J = 6.6, 3.6, 2H), 7.08 (dd, J = 12.0, 1.8 Hz, 4 H), 3.87 - 3.79 (br m, 1H), 3.75 (app t, J = 8.4 Hz, 2H), 2.77 (dd, J = 16.5, 5.4 Hz, 1H), 2.60 (dd, J = 16.2 Hz, 10.2 Hz, 1H), 2.31 (s, 3H), 1.95 - 1.85 (m, 1H), 1.83 - 1.70 (m, 1H), 1.71 (br s, 1H, O*H*), 1.62 - 1.47 (m, 2H) ppm; ^{13}C NMR (125 MHz, $CDCl_3$) 168.7, 136.3, 135.3, 134.1, 132.3, 129.5, 129.5 123.4, 72.4, 43.8, 38.0, 33.8, 25.2, 21.2 ppm; HRMS (ESI) Calcd. for [$C_{20}H_{21}O_3NNa$] ([M+Na]$^+$): *m/z* 346.1414, found 346.1400.

Notes and references

1. (a) Nugent, W. A. *Angew. Chem. Int. Ed.* **2012**, *51*, 8936-8949. (b) Teles, J. H.; Brode, S.; Chabanas, M. *Angew. Chem. Int. Ed.* **1998**, *37*,1415-1418.
2. (a) Gorin, D. J.; Sherry, B. D.; Toste, F. D. *Chem. Rev.* **2008**, *108*, 3351-3378. (b) Fürstner, A. *Chem. Soc. Rev.* **2009**, *38*, 3208-3221.
3. Roth, K. E.; Blum, S. A. *Organometallics* **2010**, *29*, 1712-1716.
4. Rosenfeld, D. C.; Shekhar, S.; Takemiya, A.; Utsunomiya, M.; Hartwig, J. F. *Org. Lett.* **2006**, *8*, 4179-4182.
5. Hopkinson, M. N.; Gee. A. D.; Gouverneur, V. *Chem. Eur. J.* **2011**, *17*, 8248-8262.
6. Hashmi, A. S. K.; Blanco, M. C.; Fischer, D.; Bats, J. W. *Eur. J. Org. Chem.* **2006**, *6*, 1387-1389.
7. Bratsch, S. G. *J. Phys. Chem. Ref. Data* **1989**, *18*, 1-21.
8. Cui, L.; Zhang, G.; Zhang, L. *Bioorg. Med.Chem. Let.* **2009**, *19*, 3884-3887.
9. Zhang, G.; Peng, Y.; Cui, L.; Zhang, L. *Angew. Chem. Int. Ed.* **2009**, *48*, 3112-3115.
10. LaLonde, R. L.; Brenzovich, W. E.; Benitez, D.; Tkatchouk, E.; Kelley, K.; Goddard III, W. A.; Toste, F. D. *Chem. Sci.* **2010**, *1*, 226-233.
11. (a) Schmidbaur, H.; Schier, A. *Chem. Soc. Rev.* **2008**, *37*, 1931-1951. (b) Mendizabal, F.; Pykkö, P. *Phys. Chem. Chem. Phys.* **2004,** *6*, 900-905.
12. Brenzovitch, W. E.; Brazeu, J.-F. Toste, F. D. *Org. Lett.* **2010**, *12*, 4728-4731.
13. Müller, K. Faeh, C. Diedrich, F. *Science*, **2007**, *317*, 181-1886.
14. Hong, S.; Tian, S; Metz, M. V.; Marks, T. J. *J. Am. Chem. Soc.* **2003**, *125*, 14768–14783.
15. Ng, S. M; Bader, S. J.; Snapper, M. L. *J. Am. Chem. Soc.* **2006**, *128*, 7315-7319.
16. Kim, Y. J.; Livinghouse, T. *Org. Lett.* **2005**, *7,* 4391–4393.
17. (a) Ando, T.; Kano, D.; Minakata, S.; Ryu, I.; Komatsu, M. *Tetrahedron* **1998**, *54*, 13485–13494. (b) Minakata, S.; Hotta, T.; Oderaotoshi, Y.; Komatsu, M. *J. Org. Chem.* **2006**, *71*, 7471–7472.
18. Gagne, M. R.; Marks, T. J. *J. Am. Chem. Soc.* **1989**, *111*, 4108–4109.
19. Watson, I. D. G.; Ritter, S.; Toste, F. D. *J. Am. Chem. Soc.* **2009**, *131*, 2056-2057.
20. Bennasar, M. L.; Roca, T; Monerris, M; Garcia-Diaz, D. J. *J. Org. Chem.* **2006**, *71*, 7028-7034.
21. Michael, F. E.; Cochran, B. M. *J. Am. Chem. Soc.* **2006**, *128*, 4246-4247.
22. Gagne, M. R; Stern, C. L.; Marks, T. J. *J. Am. Chem. Soc.* **1992**, *114*, 275-294.
23. Che, C.; Li, W.; Lin, S.; Chen, J.; Zheng, J.; Wu, J.-C.; Zheng, Q.; Zhang, G.; Yang, Z.; Jiang, B. *Chem. Commun.* **2009**, 5990-5992.
24. Johansson, M. J.; Gorin, D. J.; Staben, S. T.; Toste, F. D. *J. Am. Chem. Soc.* **2005**, *127*, 18002-18003.
25. Lalonde, R. L.; Sherry, B. D.; Kang, E. J.; Toste, F. D. *J. Am. Chem. Soc.* **2007**, *129*, 2452-2453.
26. Schneider, D.; Schier, A.; Schmidbaur, H. *Dalton Trans.* **2004**, *13*, 1995-2005.

NMR and HPLC spectra

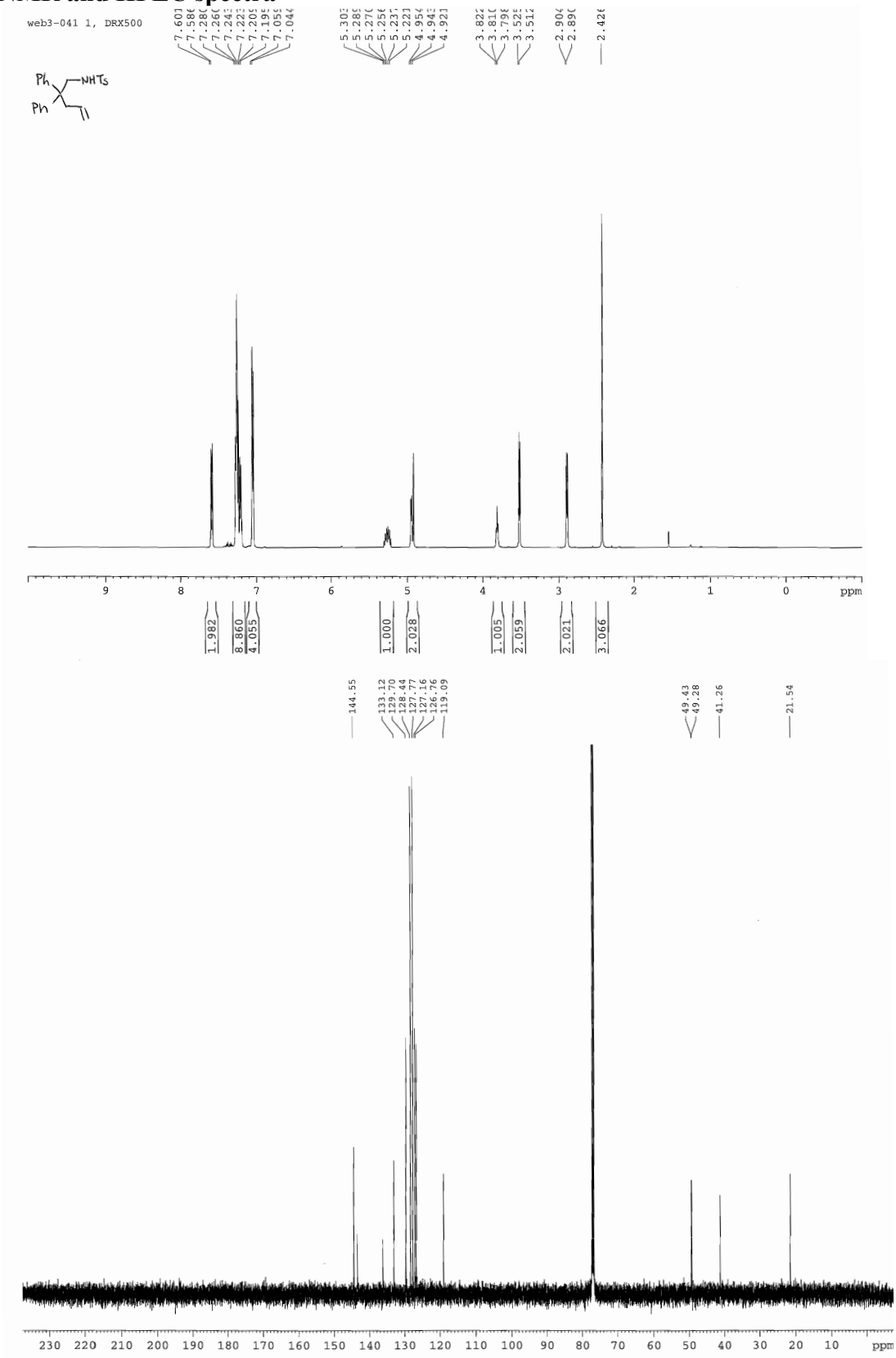

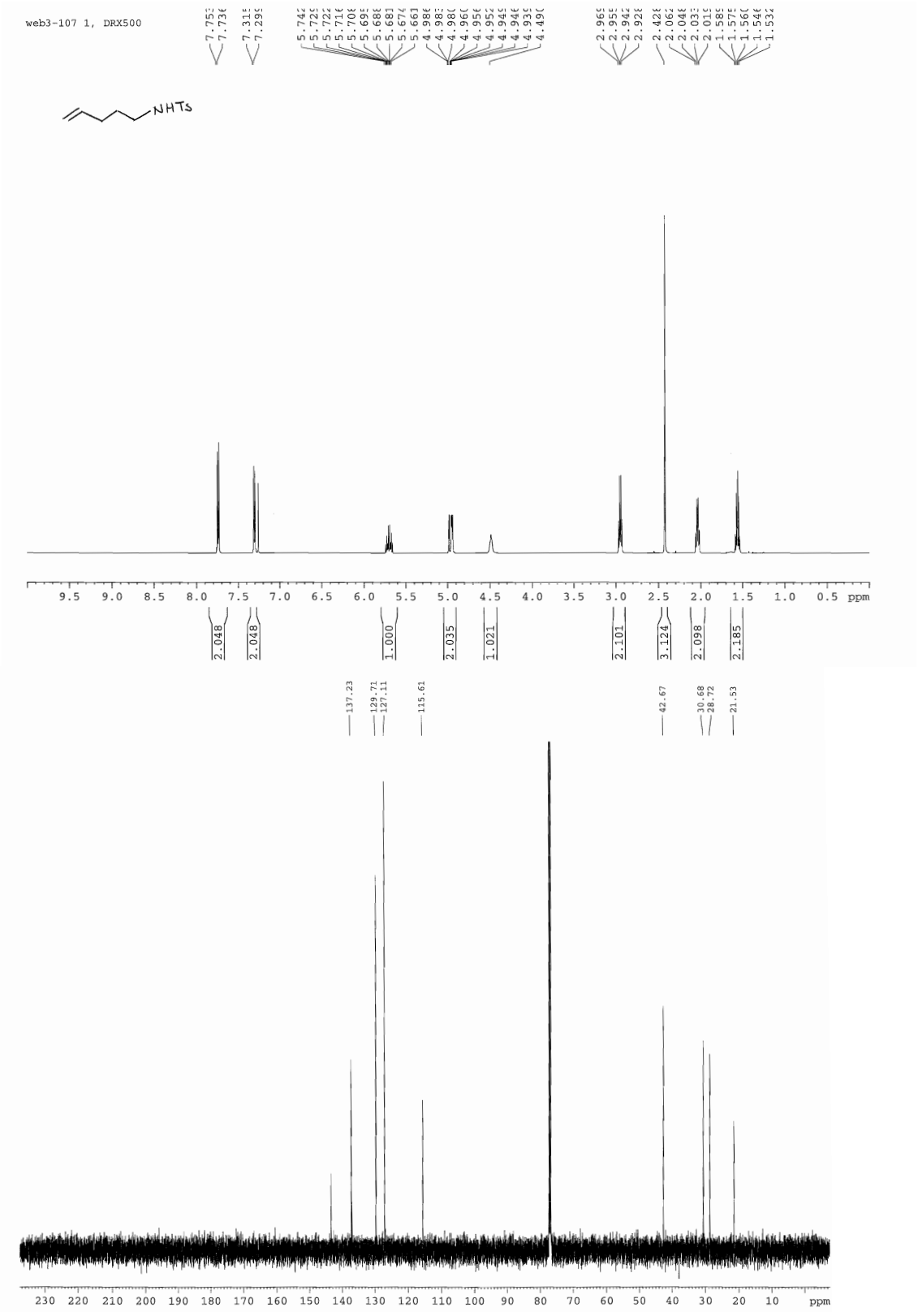
web3-107 1, DRX500
NHTs
9.5 9.0 8.5 8.0 7.5 7.0 6.5 6.0 5.5 5.0 4.5 4.0 3.5 3.0 2.5 2.0 1.5 1.0 0.5 ppm
2.048
2.048
1.000
2.035
1.021
2.101
3.124
2.098
2.185
137.23
129.71
127.11
115.61
42.67
30.68
28.72
21.53
230 220 210 200 190 180 170 160 150 140 130 120 110 100 90 80 70 60 50 40 30 20 10 ppm

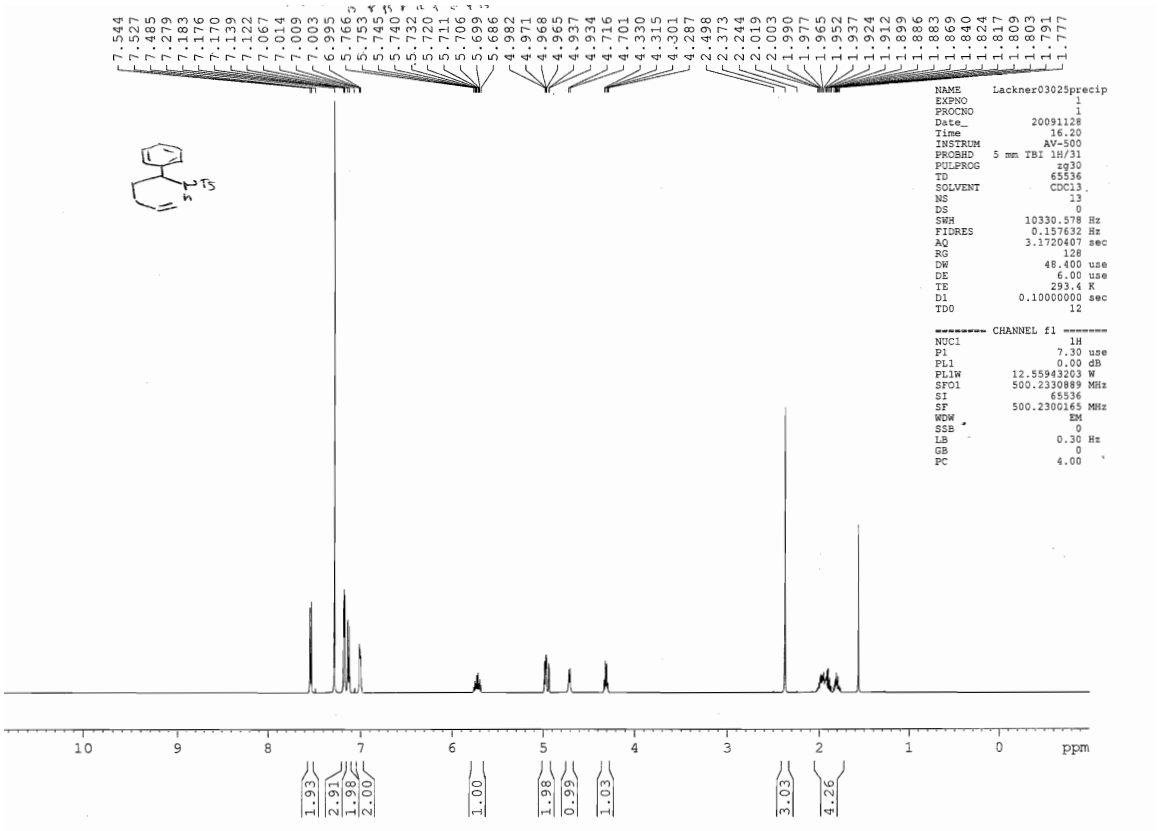
7.544
7.527
7.485
7.279
7.183
7.176
7.170
7.139
7.122
7.067
7.014
7.009
7.003
6.995
5.766
5.753
5.745
5.740
5.732
5.720
5.711
5.706
5.699
5.686
4.982
4.971
4.968
4.965
4.937
4.934
4.716
4.701
4.330
4.315
4.301
4.287
2.498
2.373
2.244
2.019
2.003
1.990
1.977
1.965
1.952
1.937
1.924
1.912
1.899
1.886
1.883
1.869
1.840
1.824
1.817
1.809
1.803
1.791
1.777
Ts
N
NAME Lackner03025precip
EXPNO 1
PROCNO 1
Date_ 20091128
Time 16.20
INSTRUM AV-500
PROBHD 5 mm TBI 1H/31
PULPROG zg30
TD 65536
SOLVENT CDCl3
NS 13
DS 0
SWH 10330.578 Hz
FIDRES 0.157632 Hz
AQ 3.1720407 sec
RG 128
DW 48.400 use
DE 6.00 use
TE 293.4 K
D1 0.10000000 sec
TD0 12
======== CHANNEL f1 ========
NUC1 1H
P1 7.30 use
PL1 0.00 dB
PL1W 12.55943203 W
SFO1 500.2330889 MHz
SI 65536
SF 500.2300165 MHz
WDW EM
SSB 0
LB 0.30 Hz
GB 0
PC 4.00
10
9
8
7
6
5
4
3
2
1
0
ppm
1.93
2.91
1.98
2.00
1.00
1.98
0.99
1.03
3.03
4.26

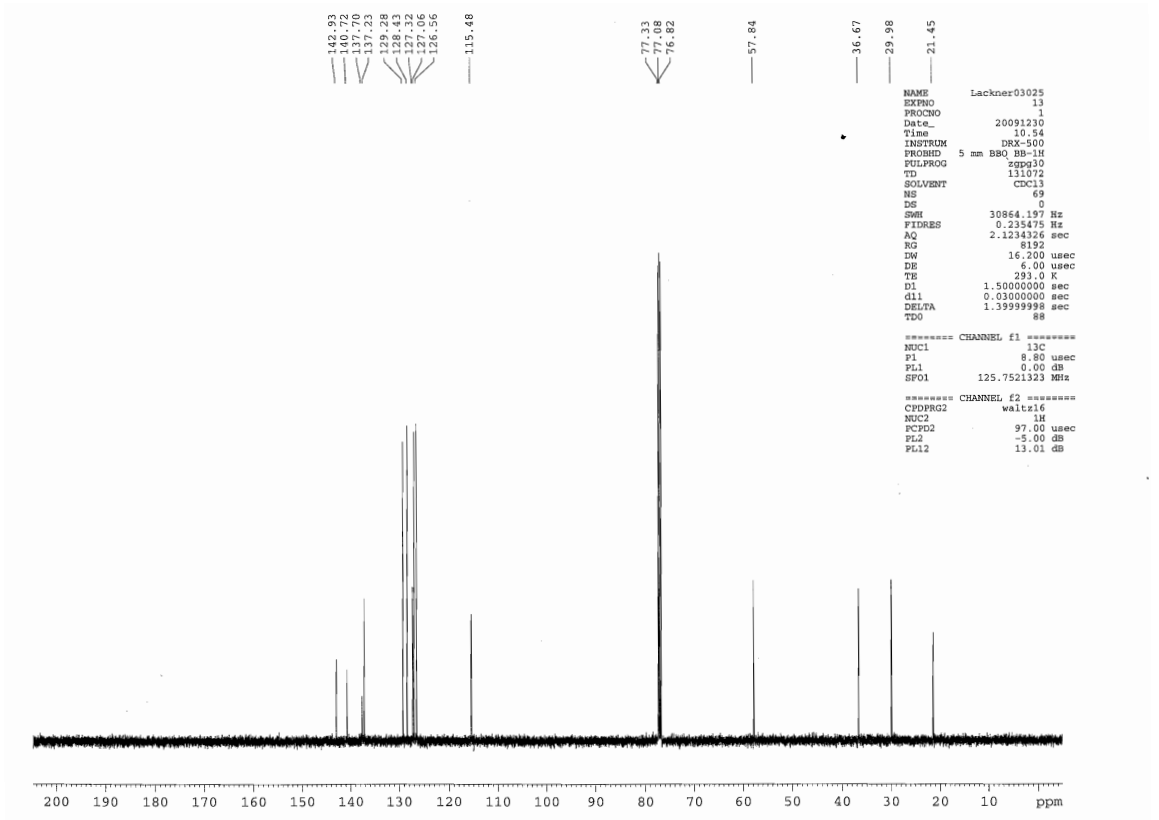
142.93
140.72
137.70
137.23
129.28
128.43
127.32
127.06
126.56
115.48
77.33
77.08
76.82
57.84
36.67
29.98
21.45
NAME Lackner03025
EXPNO 13
PROCNO 1
Date_ 20091230
Time 10.54
INSTRUM DRX-500
PROBHD 5 mm BBO BB-1H
PULPROG zgpg30
TD 131072
SOLVENT CDCl3
NS 69
DS 0
SWH 30864.197 Hz
FIDRES 0.235475 Hz
AQ 2.1234326 sec
RG 8192
DW 16.200 usec
DE 6.00 usec
TE 293.0 K
D1 1.50000000 sec
d11 0.03000000 sec
DELTA 1.39999998 sec
TD0 88
======== CHANNEL f1 ========
NUC1 13C
P1 8.80 usec
PL1 0.00 dB
SFO1 125.7521323 MHz
======== CHANNEL f2 ========
CPDPRG2 waltz16
NUC2 1H
PCPD2 97.00 usec
PL2 -5.00 dB
PL12 13.01 dB
200
190
180
170
160
150
140
130
120
110
100
90
80
70
60
50
40
30
20
10
ppm

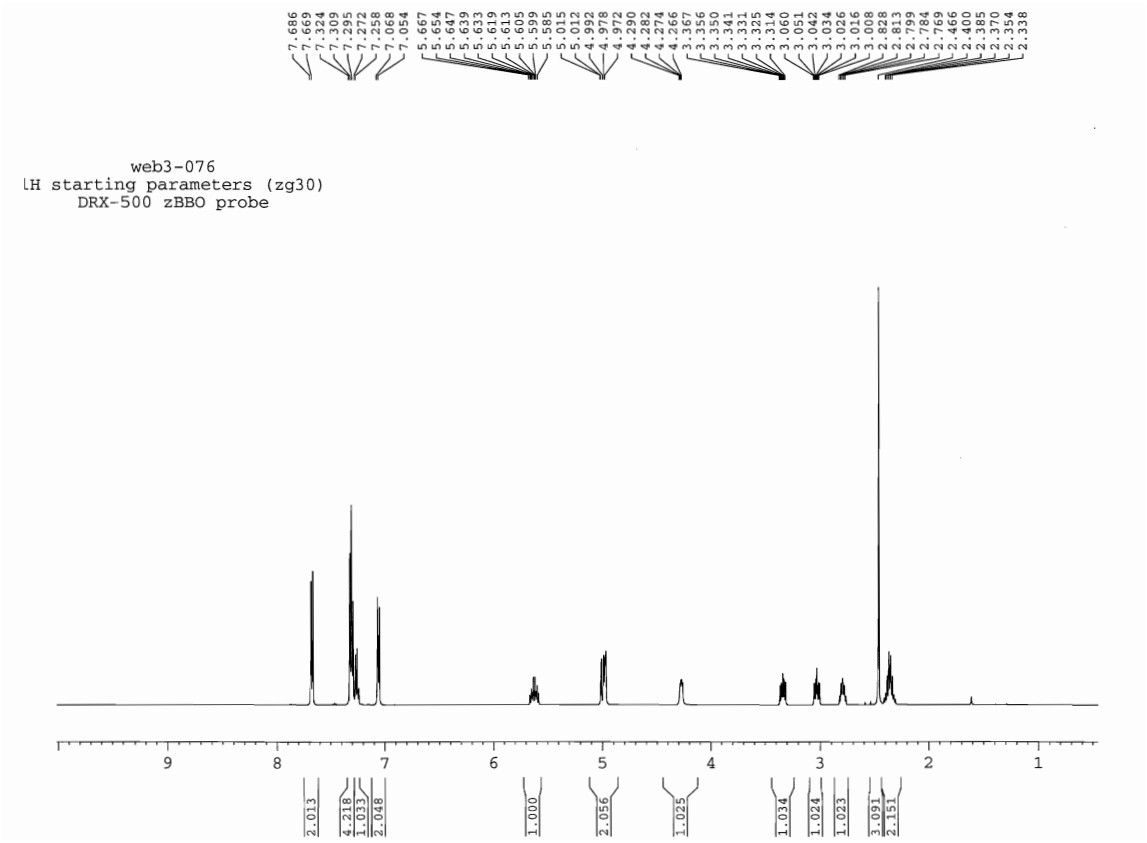
7.686
7.669
7.324
7.309
7.295
7.272
7.258
7.068
7.054
5.667
5.654
5.647
5.639
5.633
5.619
5.613
5.605
5.599
5.585
5.015
5.012
4.992
4.978
4.972
4.290
4.282
4.274
4.266
3.367
3.356
3.350
3.341
3.331
3.325
3.314
3.060
3.051
3.042
3.034
3.026
3.016
3.008
2.828
2.813
2.799
2.784
2.769
2.466
2.400
2.385
2.370
2.354
2.338
web3-076
1H starting parameters (zg30)
DRX-500 zBBO probe
9
8
7
6
5
4
3
2
1
2.013
4.218
1.033
2.048
1.000
2.056
1.025
1.034
1.024
1.023
3.091
2.151

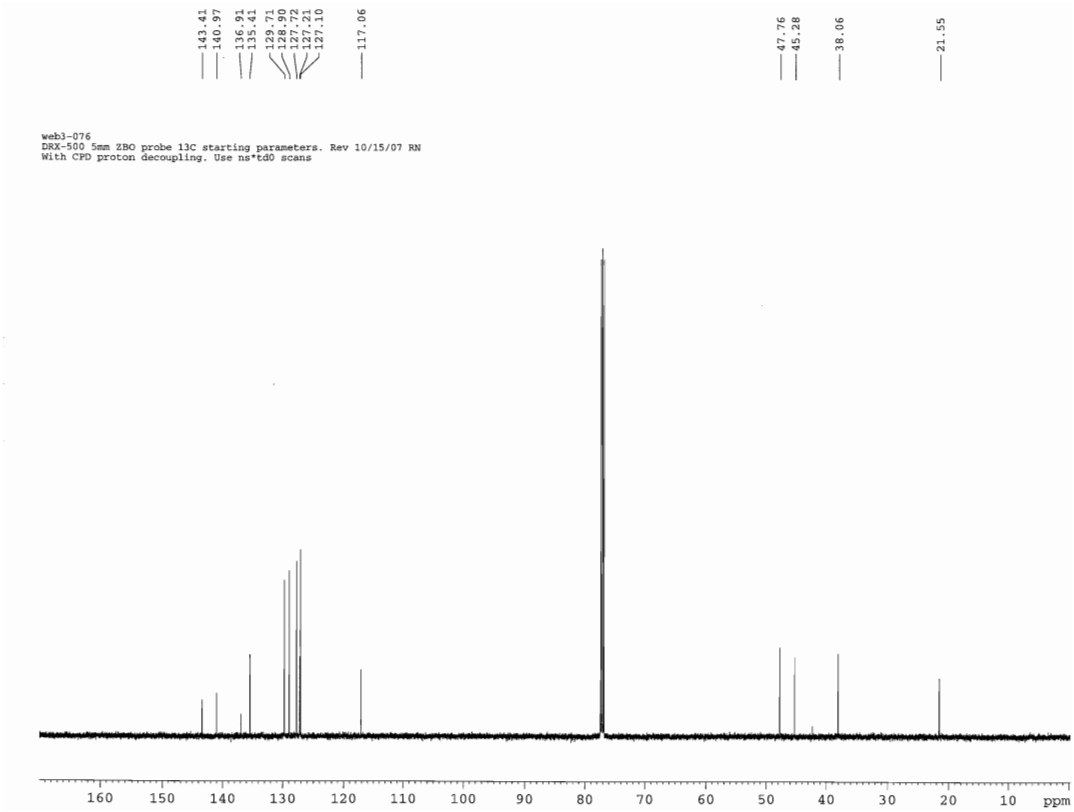
143.41
140.97
136.91
135.41
129.71
128.90
127.72
127.21
127.10
117.06
47.76
45.28
38.06
21.55
web3-076
DRX-500 5mm ZBO probe 13C starting parameters. Rev 10/15/07 RN
With CPD proton decoupling. Use ns*td0 scans
160
150
140
130
120
110
100
90
80
70
60
50
40
30
20
10
ppm

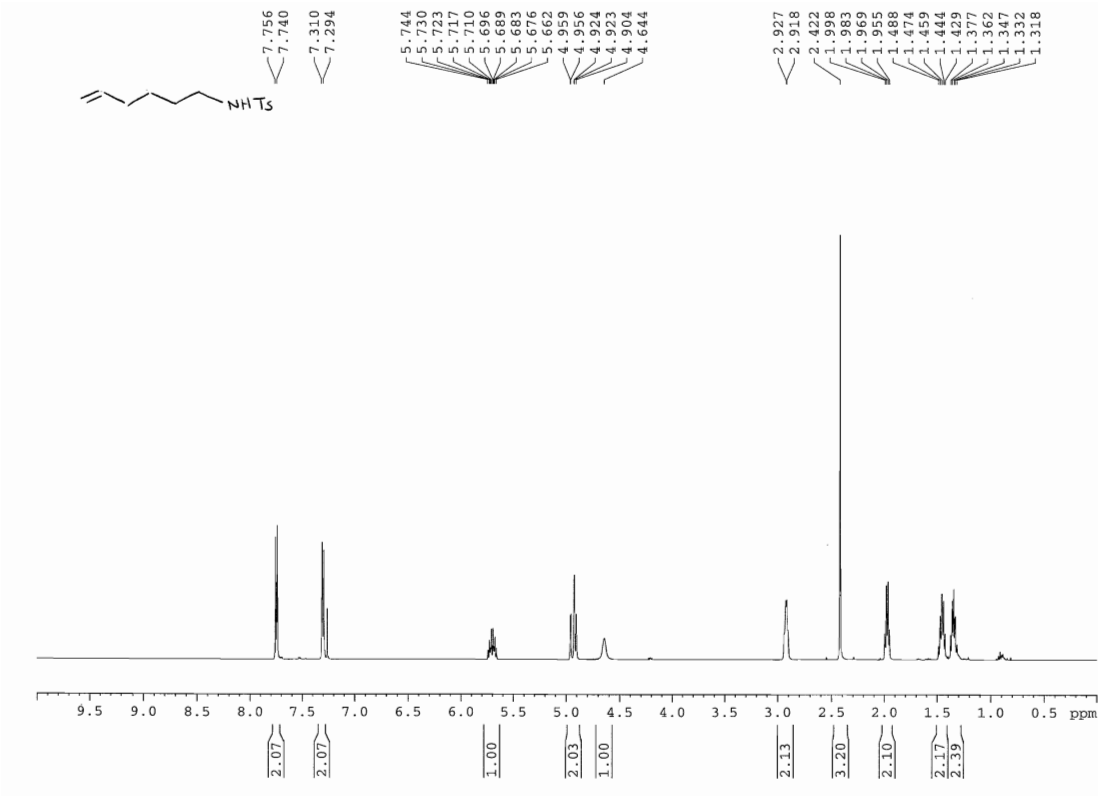
NHTs
7.756
7.740
7.310
7.294
5.744
5.730
5.723
5.717
5.710
5.696
5.689
5.683
5.676
5.662
4.959
4.956
4.924
4.923
4.904
4.644
2.927
2.918
2.422
1.998
1.983
1.969
1.955
1.488
1.474
1.459
1.444
1.429
1.377
1.362
1.347
1.332
1.318
9.5 9.0 8.5 8.0 7.5 7.0 6.5 6.0 5.5 5.0 4.5 4.0 3.5 3.0 2.5 2.0 1.5 1.0 0.5 ppm
2.07
2.07
1.00
2.03
1.00
2.13
3.20
2.10
2.17
2.39

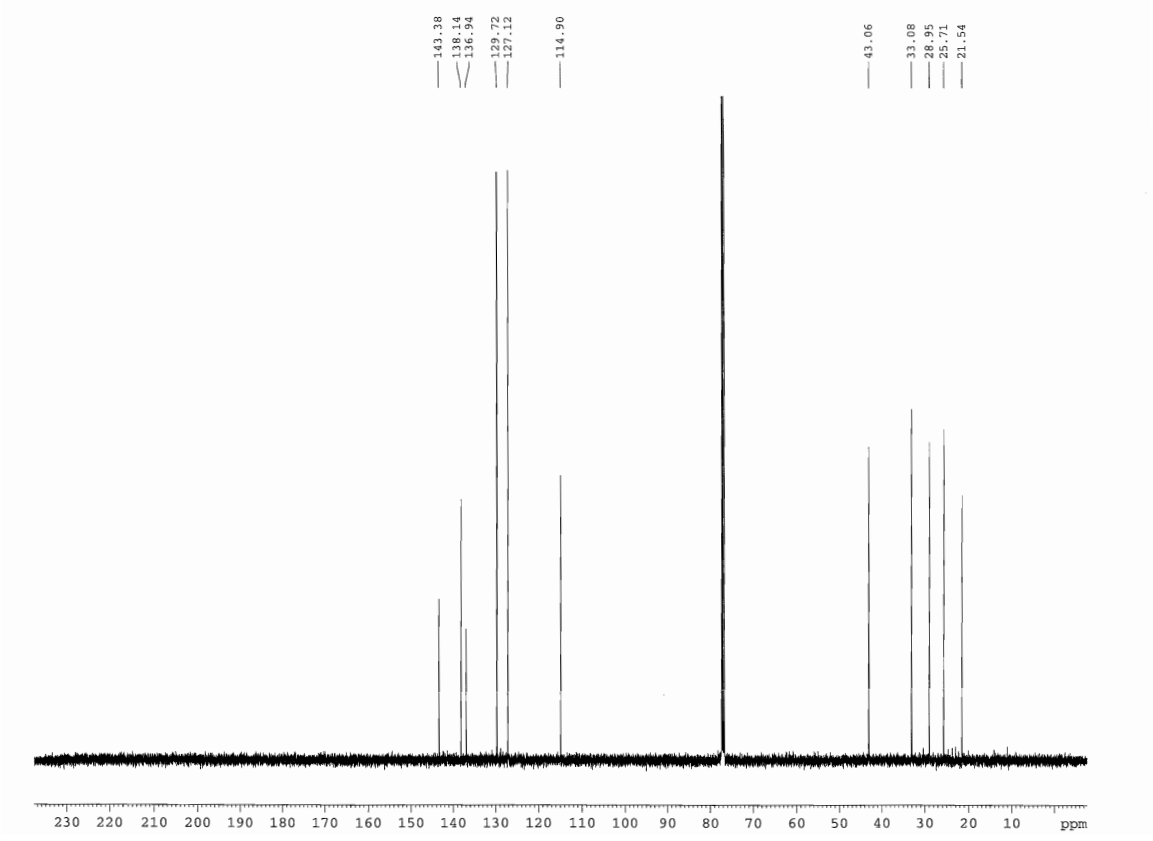
143.38
138.14
136.94
129.72
127.12
114.90
43.06
33.08
28.95
25.71
21.54
230 220 210 200 190 180 170 160 150 140 130 120 110 100 90 80 70 60 50 40 30 20 10 ppm

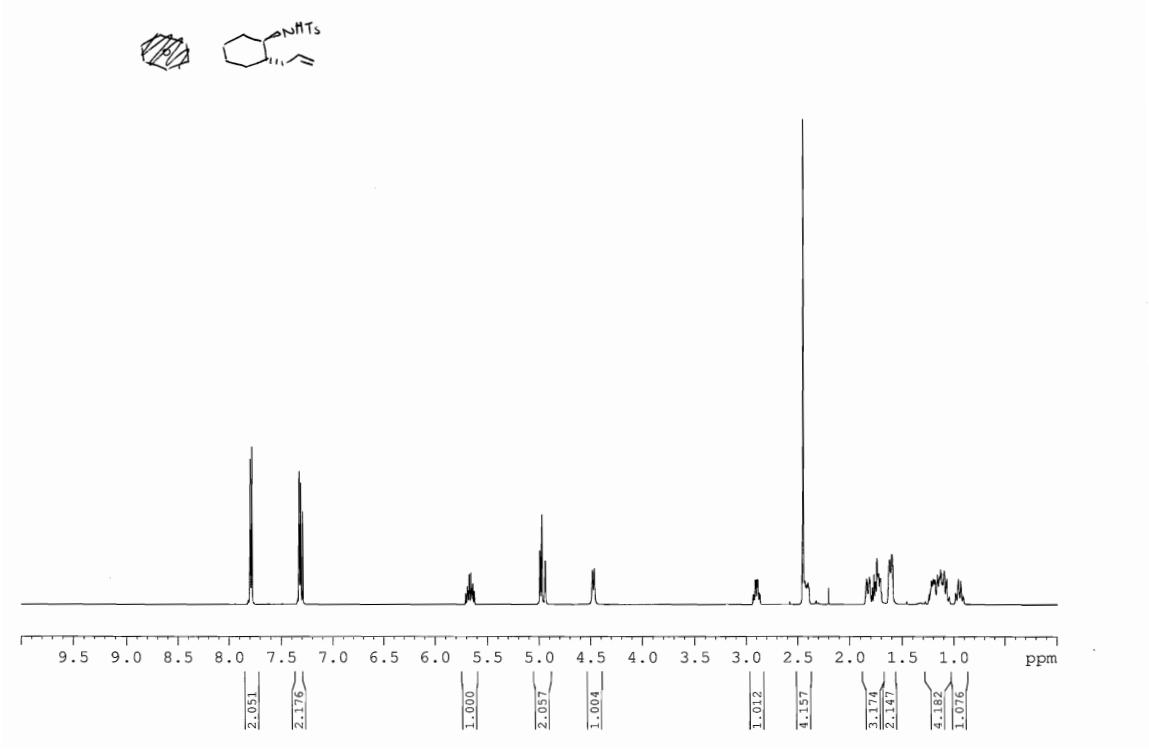
NHTs
9.5 9.0 8.5 8.0 7.5 7.0 6.5 6.0 5.5 5.0 4.5 4.0 3.5 3.0 2.5 2.0 1.5 1.0 ppm
2.051
2.176
1.000
2.057
1.004
1.012
4.157
3.174
2.147
4.182
1.076

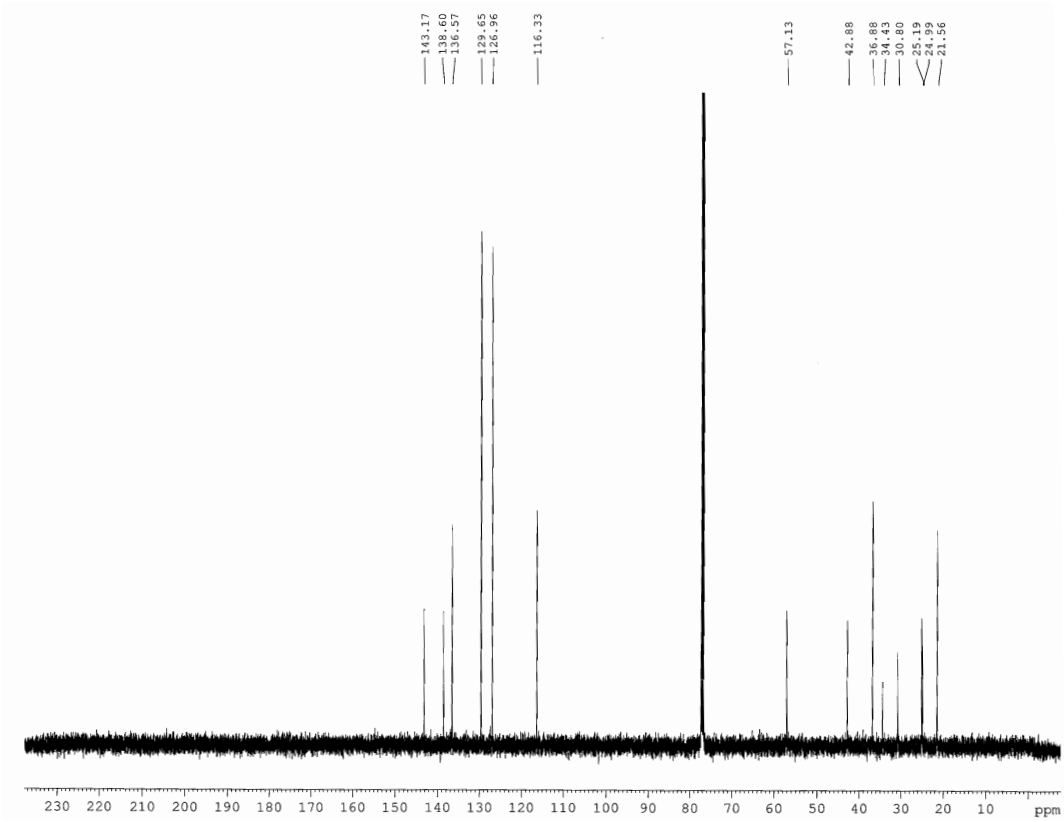
143.17
138.60
136.57
129.65
126.96
116.33
57.13
42.88
36.88
34.43
30.80
25.19
24.99
21.56
230 220 210 200 190 180 170 160 150 140 130 120 110 100 90 80 70 60 50 40 30 20 10 ppm

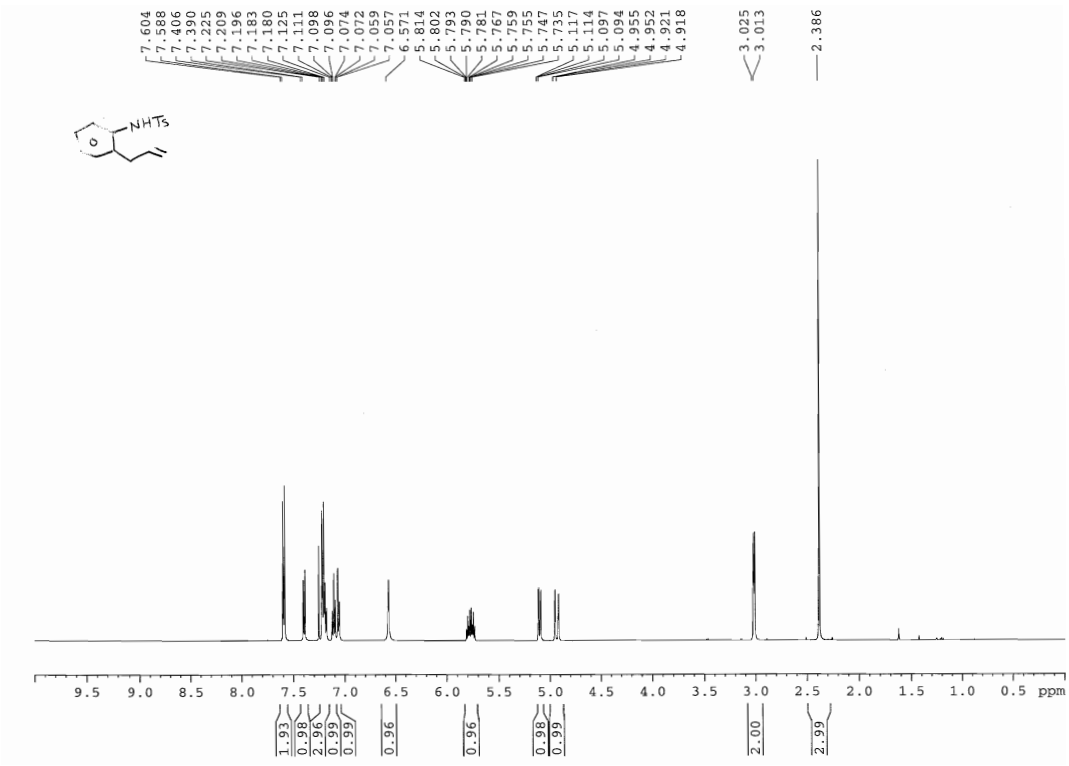
7.604
7.588
7.406
7.390
7.225
7.209
7.196
7.183
7.180
7.125
7.111
7.098
7.096
7.074
7.072
7.059
7.057
6.571
5.814
5.802
5.793
5.790
5.781
5.767
5.759
5.755
5.747
5.735
5.117
5.114
5.097
5.094
4.955
4.952
4.921
4.918
3.025
3.013
2.386
NHTs
O
9.5 9.0 8.5 8.0 7.5 7.0 6.5 6.0 5.5 5.0 4.5 4.0 3.5 3.0 2.5 2.0 1.5 1.0 0.5 ppm
1.93
0.98
2.96
0.99
0.99
0.96
0.96
0.98
0.99
2.00
2.99

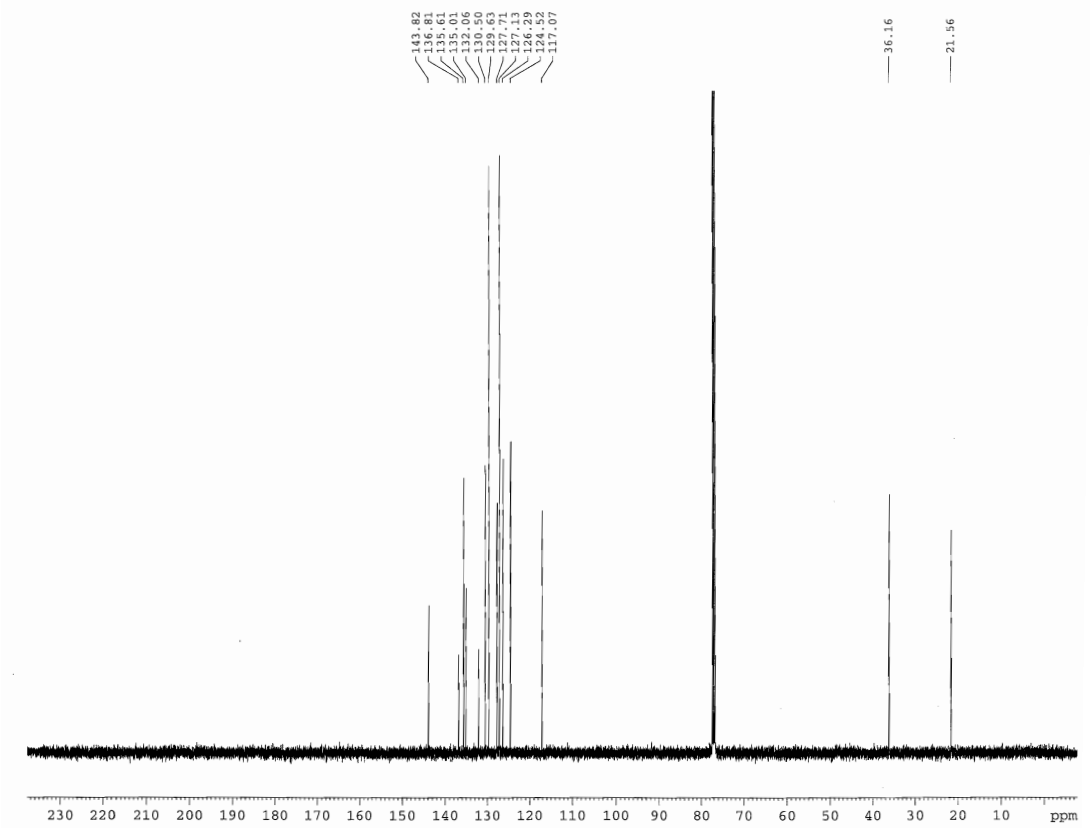
143.82
136.81
135.61
135.01
132.06
130.50
129.63
127.71
127.13
126.29
124.52
117.07
36.16
21.56
230 220 210 200 190 180 170 160 150 140 130 120 110 100 90 80 70 60 50 40 30 20 10 ppm

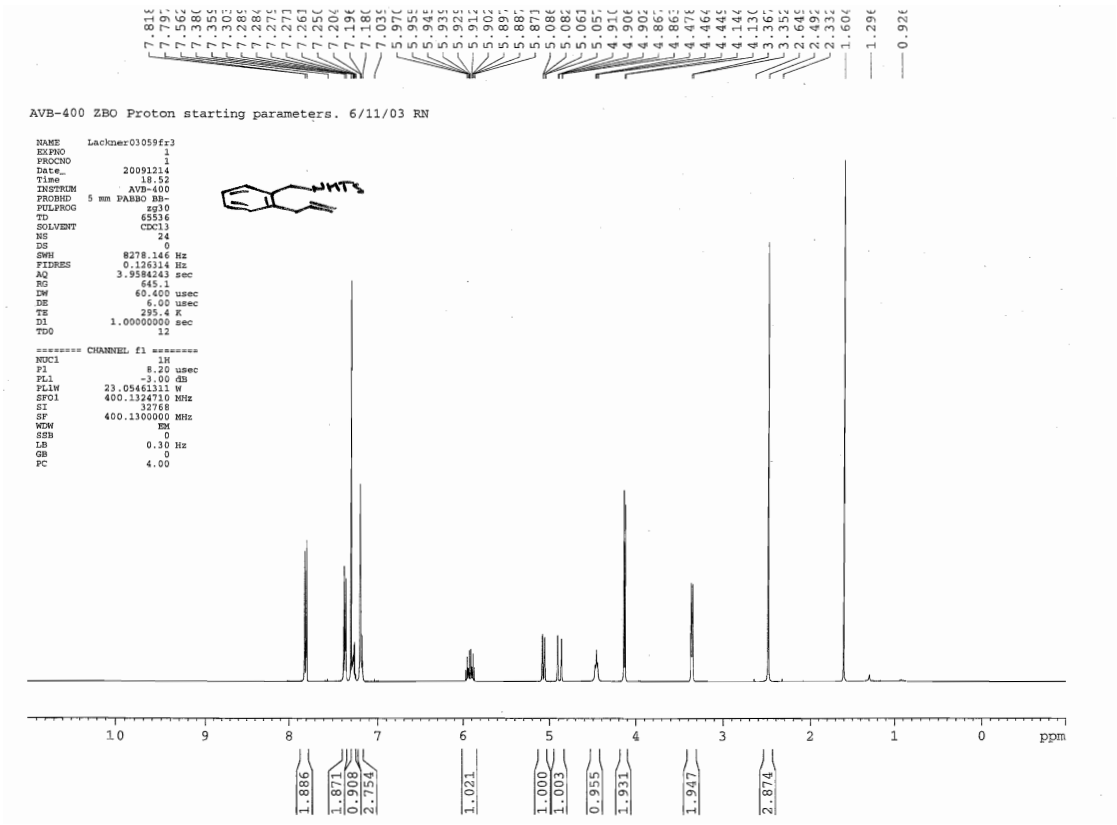
AVB-400 ZBO Proton starting parameters. 6/11/03 RN
NAME Lackner03059fr3
EXPNO 1
PROCNO 1
Date_ 20091214
Time 18.52
INSTRUM AVB-400
PROBHD 5 mm PABBO BB-
PULPROG zg30
TD 65536
SOLVENT CDCl3
NS 24
DS 0
SWH 8278.146 Hz
FIDRES 0.126314 Hz
AQ 3.9584243 sec
RG 645.1
DW 60.400 usec
DE 6.00 usec
TE 295.4 K
D1 1.00000000 sec
TD0 12
======== CHANNEL f1 ========
NUC1 1H
P1 8.20 usec
PL1 -3.00 dB
PL1W 23.05461311 W
SFO1 400.1324710 MHz
SI 32768
SF 400.1300000 MHz
WDW EM
SSB 0
LB 0.30 Hz
GB 0
PC 4.00
NHTs
10 9 8 7 6 5 4 3 2 1 0 ppm
1.886 1.871 0.908 2.754 1.021 1.000 1.003 0.955 1.931 1.947 2.874

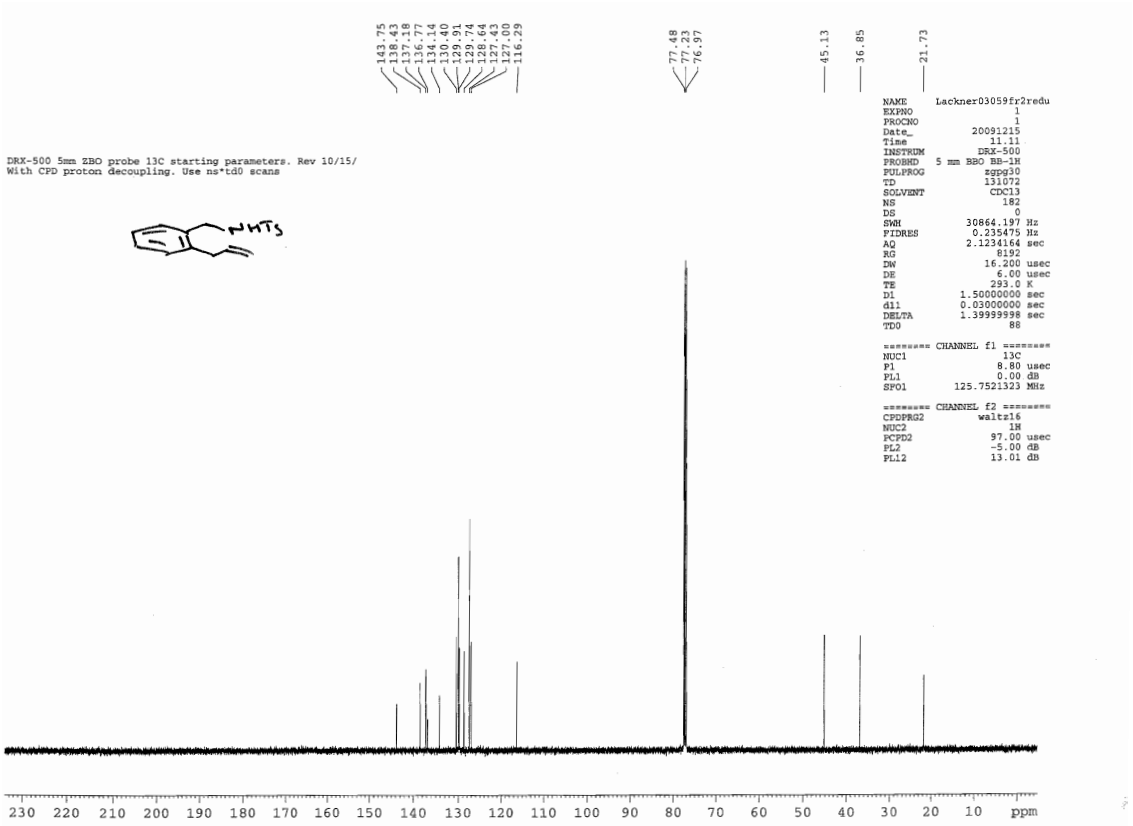
143.75
138.43
137.18
136.77
134.14
130.40
130.01
129.74
128.64
127.43
127.00
116.29
77.48
77.23
76.97
45.13
36.85
21.73
DRX-500 5mm ZBO probe 13C starting parameters. Rev 10/15/
With CPD proton decoupling. Use ns*td0 scans
NAME Lackner03059fr2redu
EXPNO 1
PROCNO 1
Date_ 20091215
Time 11.11
INSTRUM DRX-500
PROBHD 5 mm BBO BB-1H
PULPROG zgpg30
TD 131072
SOLVENT CDCl3
NS 182
DS 0
SWH 30864.197 Hz
FIDRES 0.235475 Hz
AQ 2.1234164 sec
RG 8192
DW 16.200 usec
DE 6.00 usec
TE 293.0 K
D1 1.50000000 sec
d11 0.03000000 sec
DELTA 1.39999998 sec
TD0 88
======== CHANNEL f1 ========
NUC1 13C
P1 8.80 usec
PL1 0.00 dB
SFO1 125.7521323 MHz
======== CHANNEL f2 ========
CPDPRG2 waltz16
NUC2 1H
PCPD2 97.00 usec
PL2 -5.00 dB
PL12 13.01 dB
NHTs
230 220 210 200 190 180 170 160 150 140 130 120 110 100 90 80 70 60 50 40 30 20 10 ppm

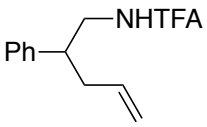
NHTFA
Ph

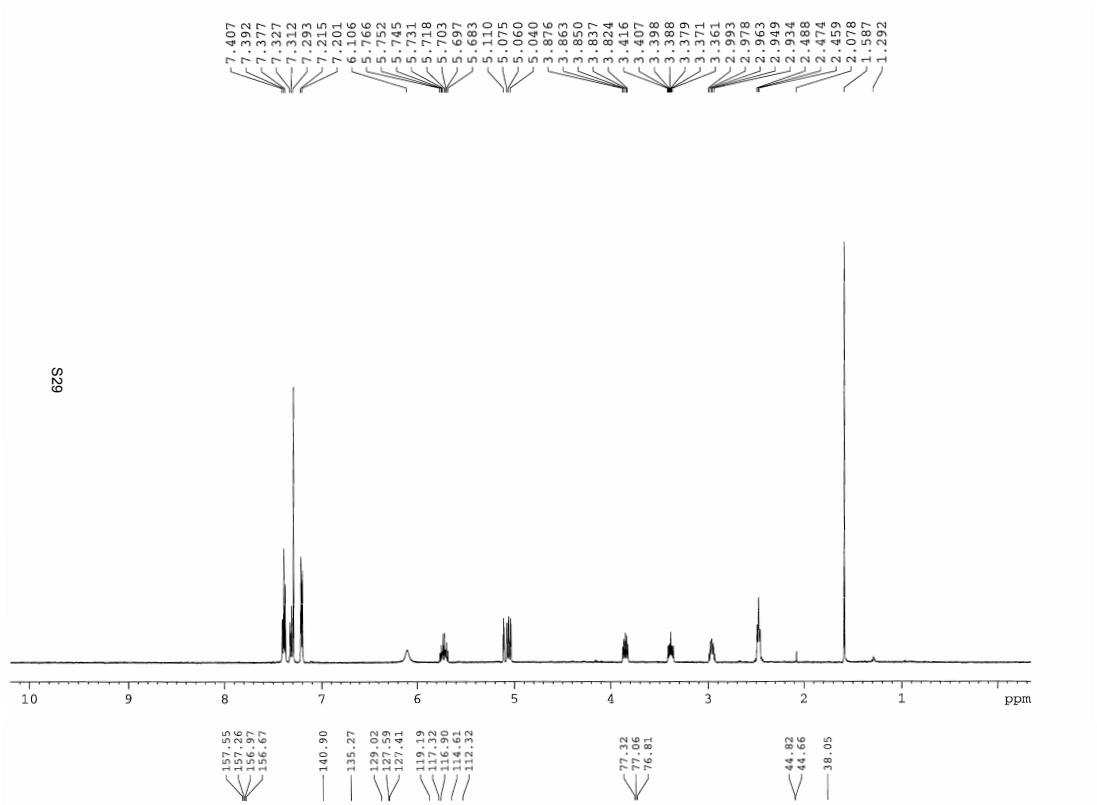
7.407
7.392
7.377
7.327
7.312
7.293
7.215
7.201
6.106
5.766
5.752
5.745
5.731
5.718
5.703
5.697
5.683
5.110
5.075
5.060
5.040
3.876
3.863
3.850
3.837
3.824
3.416
3.407
3.398
3.388
3.379
3.371
3.361
2.993
2.978
2.963
2.949
2.934
2.488
2.474
2.459
2.078
1.587
1.292
S29
10
9
8
7
6
5
4
3
2
1
ppm

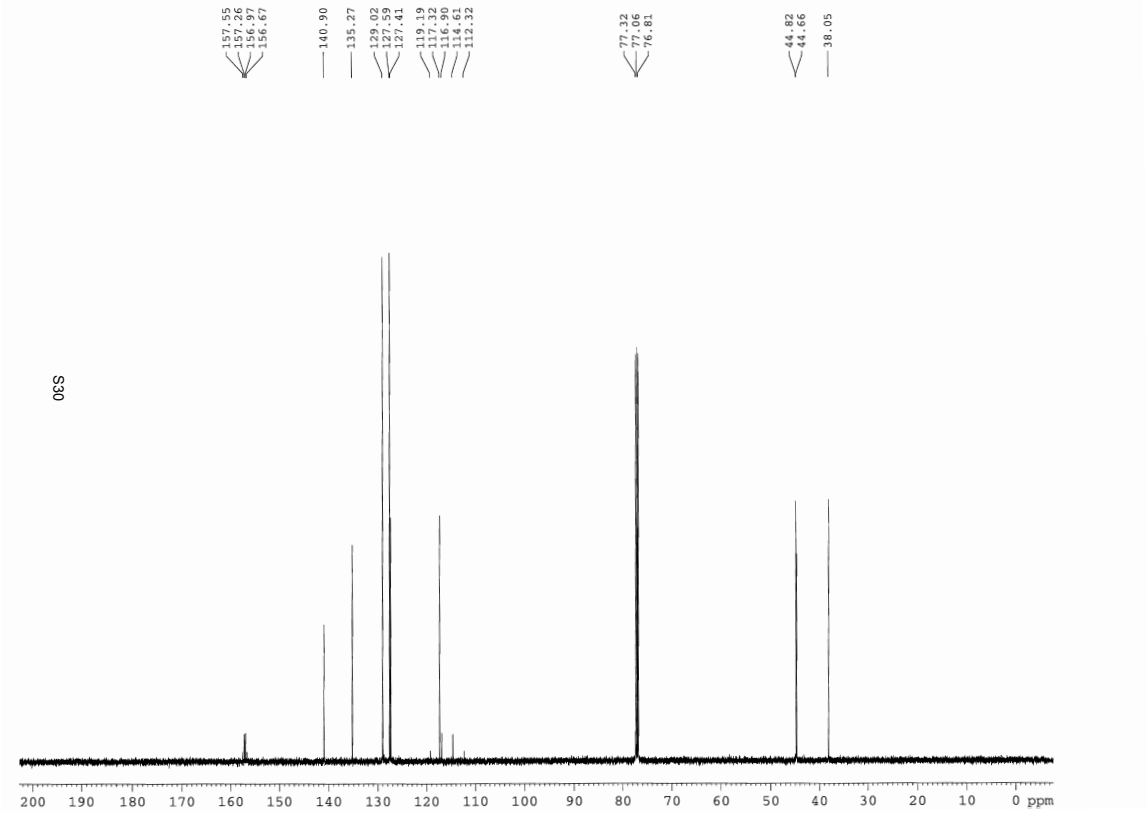
157.55
157.26
156.97
156.67
140.90
135.27
129.02
127.59
127.41
119.19
117.32
116.90
114.61
112.32
77.32
77.06
76.81
44.82
44.66
38.05
S30
200
190
180
170
160
150
140
130
120
110
100
90
80
70
60
50
40
30
20
10
0 ppm

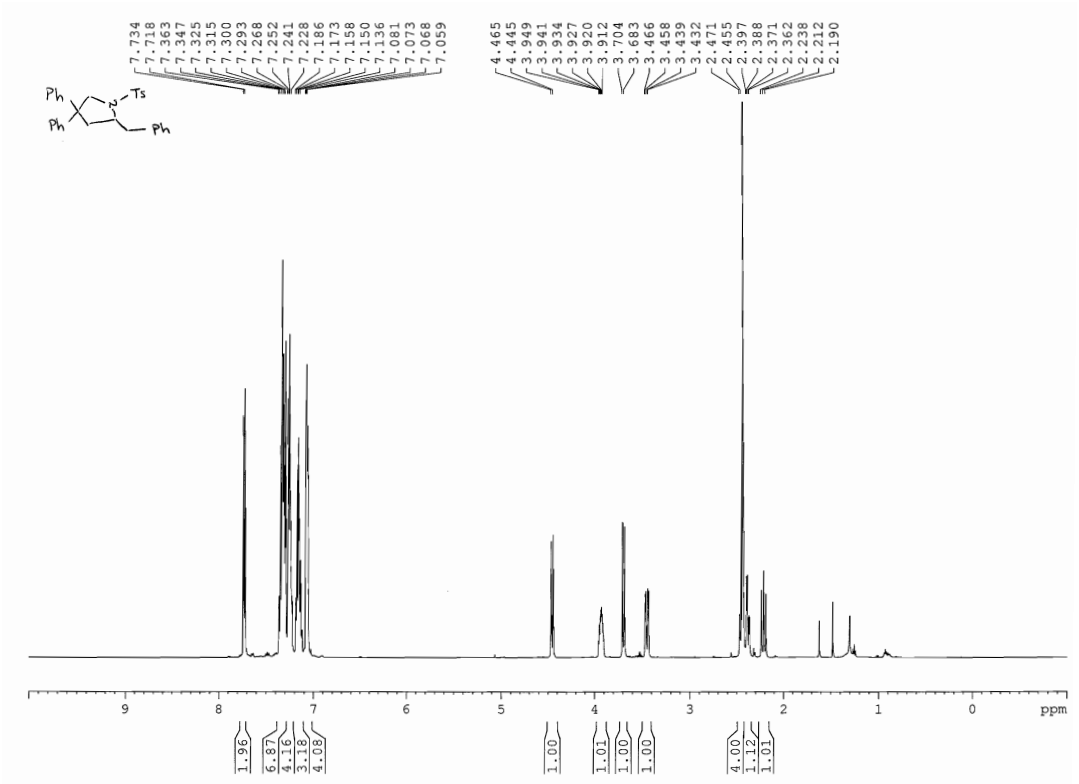
7.734
7.718
7.363
7.347
7.325
7.315
7.300
7.293
7.268
7.252
7.241
7.228
7.186
7.173
7.158
7.150
7.136
7.081
7.073
7.068
7.059
4.465
4.445
3.949
3.941
3.934
3.927
3.920
3.912
3.704
3.683
3.466
3.458
3.439
3.432
2.471
2.455
2.397
2.388
2.371
2.362
2.238
2.212
2.190
Ph
Ph
Ts
N
Ph
9
8
7
6
5
4
3
2
1
0
ppm
1.96
6.87
4.16
3.18
4.08
1.00
1.01
1.00
1.00
4.00
1.12
1.01

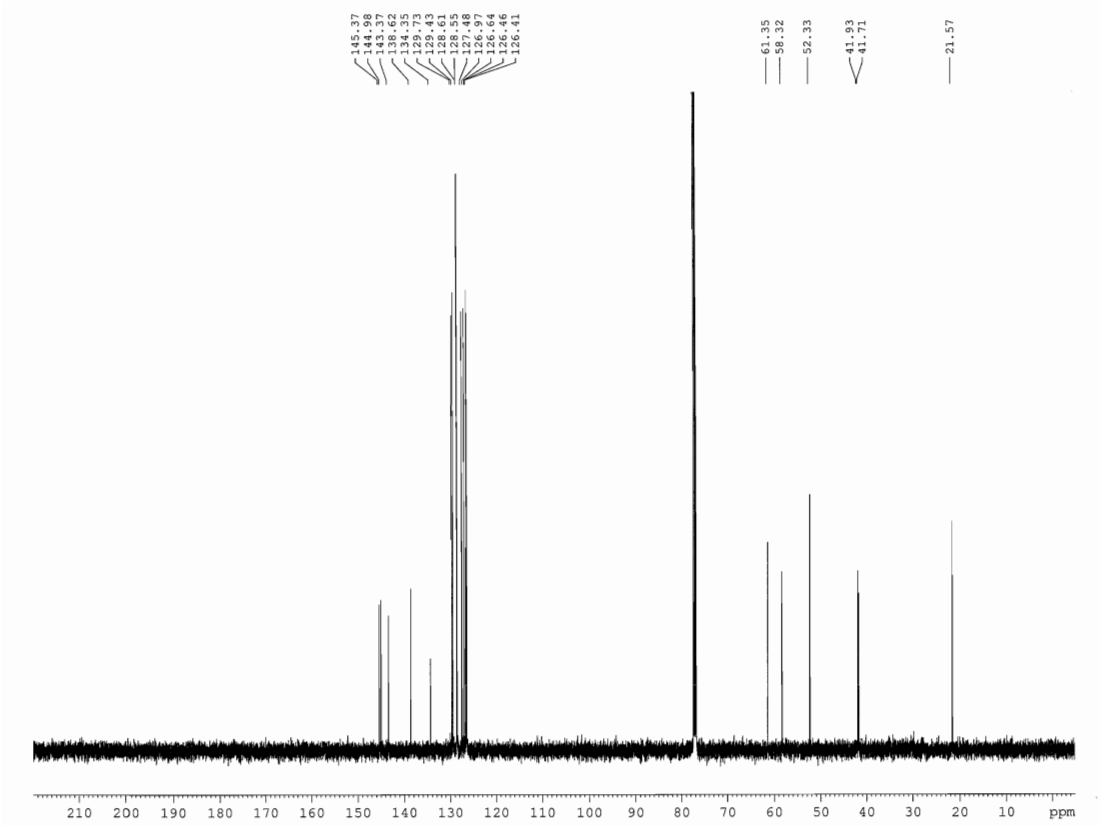
145.37
144.98
143.37
138.62
134.35
129.73
129.43
129.01
128.55
127.48
126.97
126.64
126.46
126.41
61.35
58.32
52.33
41.93
41.71
21.57
210
200
190
180
170
160
150
140
130
120
110
100
90
80
70
60
50
40
30
20
10
ppm

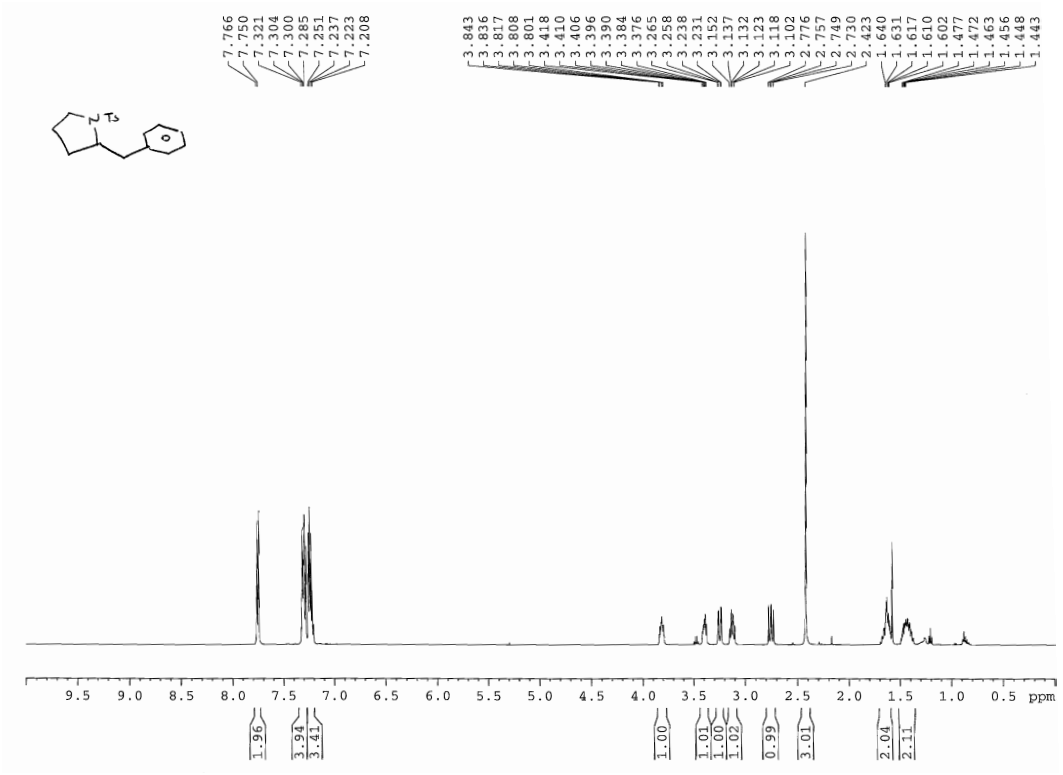
7.766
7.750
7.321
7.304
7.300
7.285
7.251
7.237
7.223
7.208
3.843
3.836
3.817
3.808
3.801
3.418
3.410
3.406
3.396
3.390
3.384
3.376
3.265
3.258
3.238
3.231
3.152
3.137
3.132
3.123
3.118
3.102
2.776
2.757
2.749
2.730
2.423
1.640
1.631
1.617
1.610
1.602
1.477
1.472
1.463
1.456
1.448
1.443
9.5 9.0 8.5 8.0 7.5 7.0 6.5 6.0 5.5 5.0 4.5 4.0 3.5 3.0 2.5 2.0 1.5 1.0 0.5 ppm
1.96
3.94
3.41
1.00
1.01
1.00
1.02
0.99
3.01
2.04
2.11

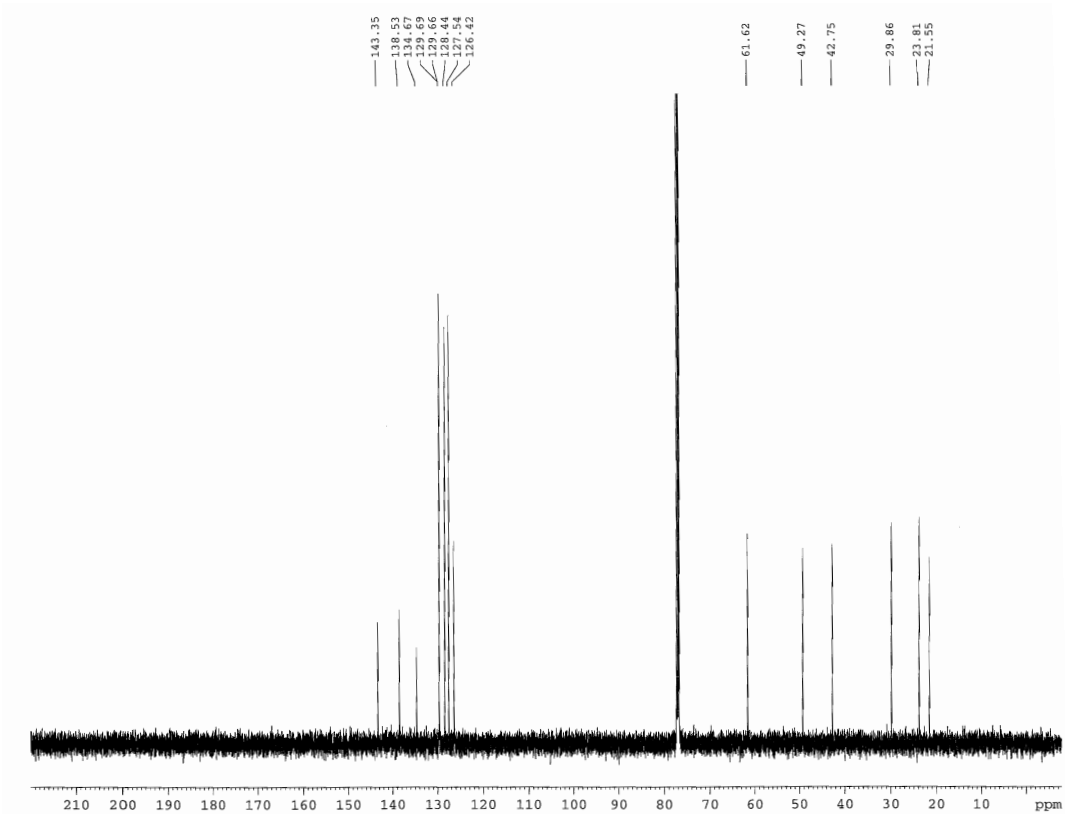
143.35
138.53
134.67
129.69
129.66
128.44
127.54
126.42
61.62
49.27
42.75
29.86
23.81
21.55
210 200 190 180 170 160 150 140 130 120 110 100 90 80 70 60 50 40 30 20 10 ppm

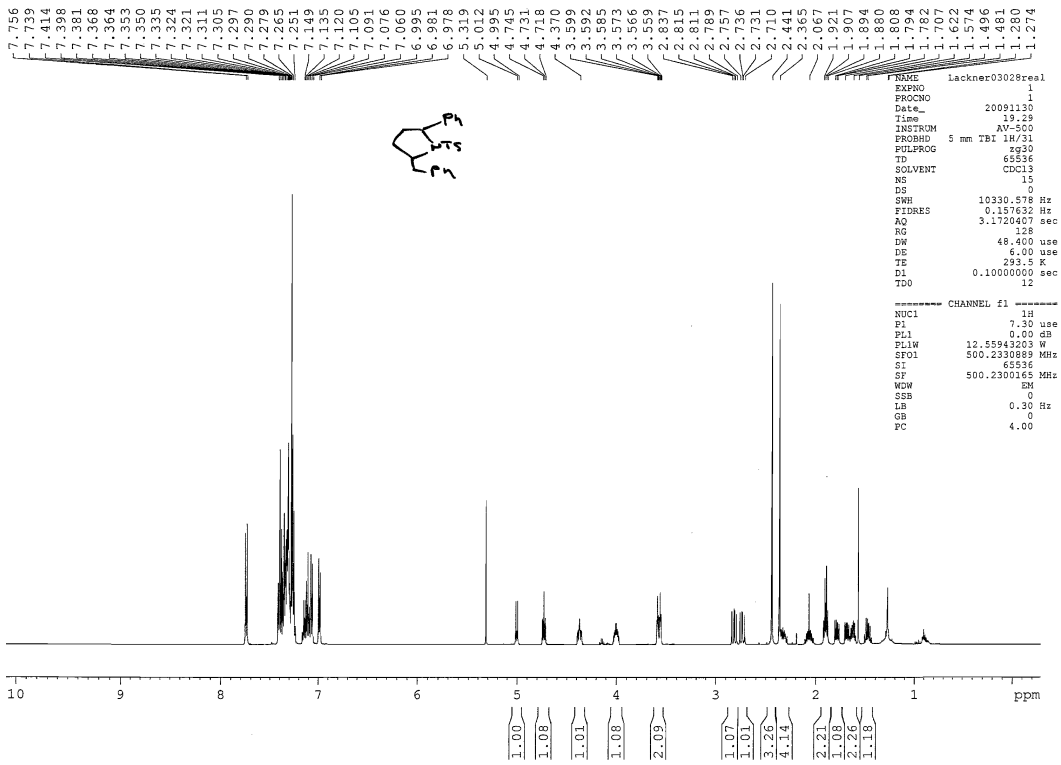
7.756 7.739 7.414 7.398 7.381 7.368 7.364 7.353 7.350 7.335 7.324 7.321 7.311 7.305 7.297 7.290 7.279 7.265 7.251 7.149 7.135 7.120 7.105 7.091 7.076 7.060 6.995 6.981 6.978 5.319 5.012 4.995 4.745 4.731 4.718 4.370 3.599 3.592 3.585 3.573 3.566 3.559 2.837 2.815 2.811 2.789 2.757 2.736 2.731 2.710 2.441 2.365 2.067 1.921 1.907 1.894 1.880 1.808 1.794 1.782 1.707 1.622 1.574 1.496 1.481 1.280 1.274
Ph
NTs
Ph
NAME Lackner03028real
EXPNO 1
PROCNO 1
Date_ 20091130
Time 19.29
INSTRUM AV-500
PROBHD 5 mm TBI 1H/31
PULPROG zg30
TD 65536
SOLVENT CDCl3
NS 15
DS 0
SWH 10330.578 Hz
FIDRES 0.157632 Hz
AQ 3.1720407 sec
RG 128
DW 48.400 use
DE 6.00 use
TE 293.5 K
D1 0.10000000 sec
TD0 12
======== CHANNEL f1 =======
NUC1 1H
P1 7.30 use
PL1 0.00 dB
PL1W 12.55943203 W
SFO1 500.2330889 MHz
SI 65536
SF 500.2300165 MHz
WDW EM
SSB 0
LB 0.30 Hz
GB 0
PC 4.00
10 9 8 7 6 5 4 3 2 1 ppm
1.00 1.08 1.01 1.08 2.09 1.07 1.01 3.26 4.14 2.21 1.08 2.26 1.18

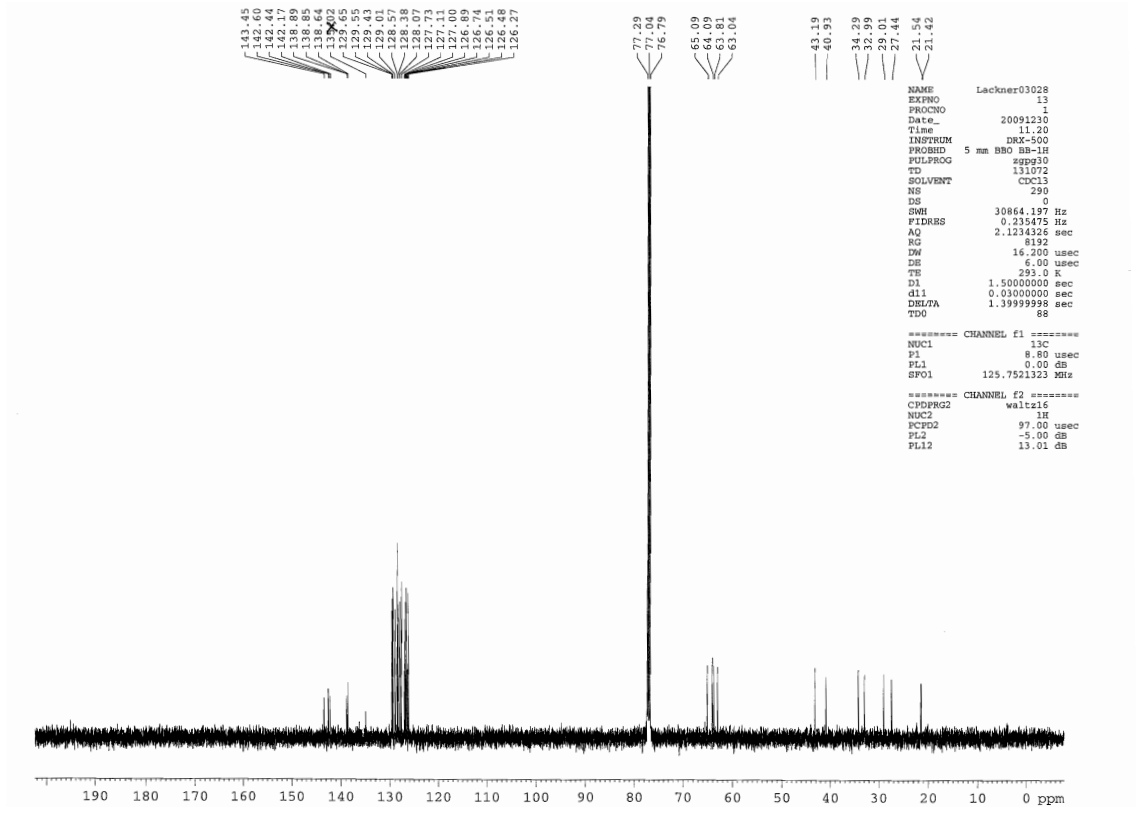
143.45 142.60 142.44 142.17 138.89 138.85 138.64 138.02 129.65 129.55 129.43 129.01 128.57 128.38 128.07 127.73 127.11 127.00 126.89 126.74 126.51 126.40 126.27
77.29 77.04 76.79
65.09 64.09 63.81 63.04
43.19 40.93
34.29 32.99 29.01 27.44
21.54 21.42
NAME Lackner03028
EXPNO 13
PROCNO 1
Date_ 20091230
Time 11.20
INSTRUM DRX-500
PROBHD 5 mm BBO BB-1H
PULPROG zgpg30
TD 131072
SOLVENT CDCl3
NS 290
DS 0
SWH 30864.197 Hz
FIDRES 0.235475 Hz
AQ 2.1234326 sec
RG 8192
DW 16.200 usec
DE 6.00 usec
TE 293.0 K
D1 1.50000000 sec
d11 0.03000000 sec
DELTA 1.39999998 sec
TD0 88
======== CHANNEL f1 ========
NUC1 13C
P1 8.80 usec
PL1 0.00 dB
SFO1 125.7521323 MHz
======== CHANNEL f2 ========
CPDPRG2 waltz16
NUC2 1H
PCPD2 97.00 usec
PL2 -5.00 dB
PL12 13.01 dB
190 180 170 160 150 140 130 120 110 100 90 80 70 60 50 40 30 20 10 0 ppm

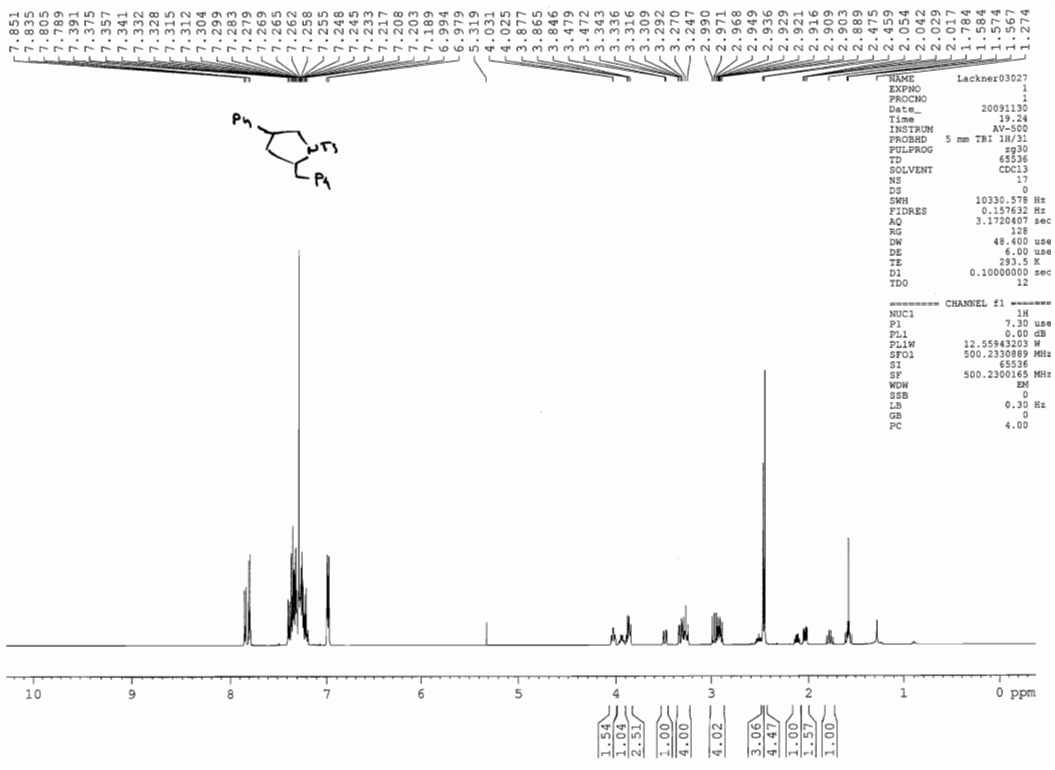

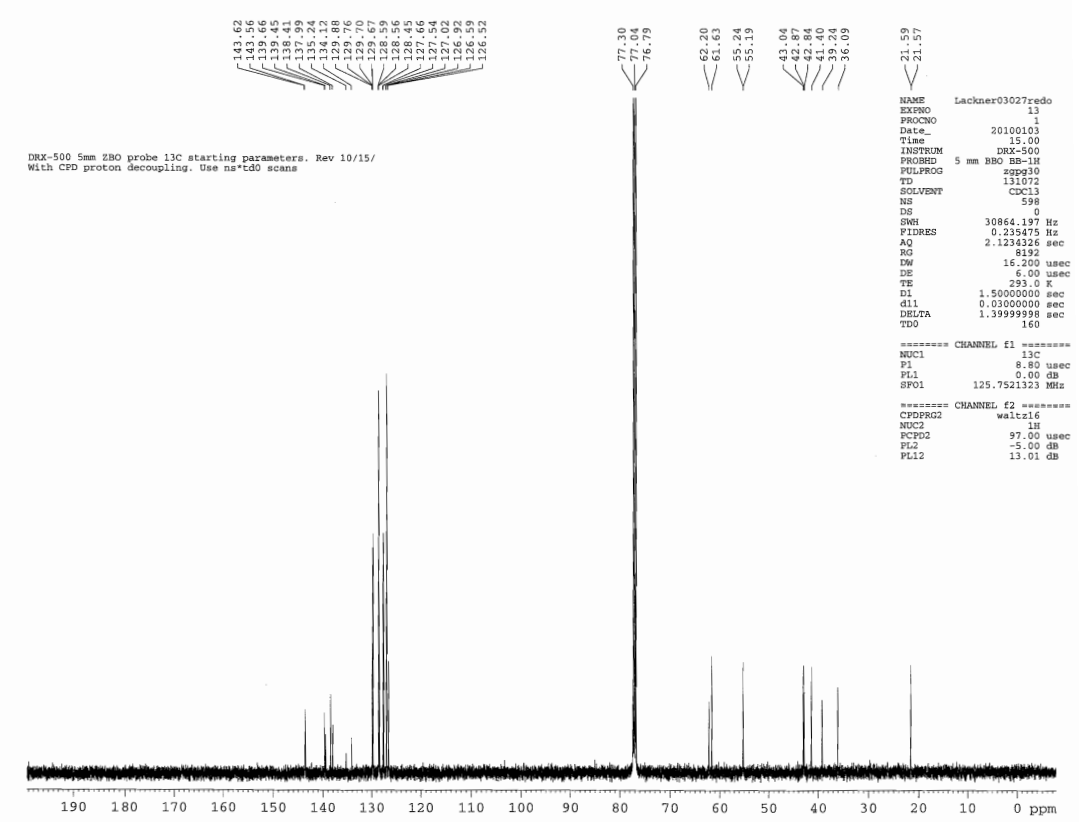
DRX-500 5mm ZBO probe 13C starting parameters. Rev 10/15/
With CPD proton decoupling. Use ns*td0 scans

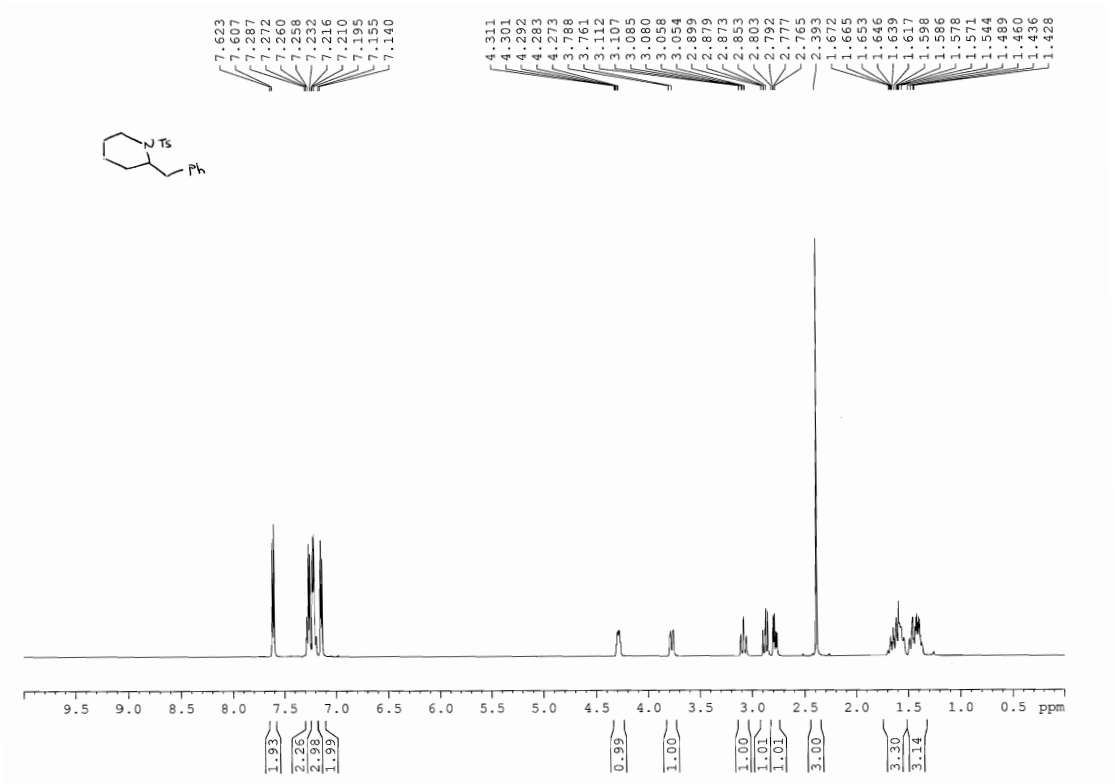
7.623
7.607
7.287
7.272
7.260
7.258
7.232
7.216
7.210
7.195
7.155
7.140
4.311
4.301
4.292
4.283
4.273
4.268
3.761
3.112
3.107
3.085
3.080
3.058
3.054
2.899
2.879
2.873
2.853
2.803
2.792
2.777
2.765
2.393
1.672
1.665
1.653
1.646
1.639
1.617
1.598
1.586
1.578
1.571
1.544
1.489
1.460
1.436
1.428
N Ts
Ph
9.5 9.0 8.5 8.0 7.5 7.0 6.5 6.0 5.5 5.0 4.5 4.0 3.5 3.0 2.5 2.0 1.5 1.0 0.5 ppm
1.93
2.26
2.98
1.99
0.99
1.00
1.00
1.01
1.01
3.00
3.30
3.14

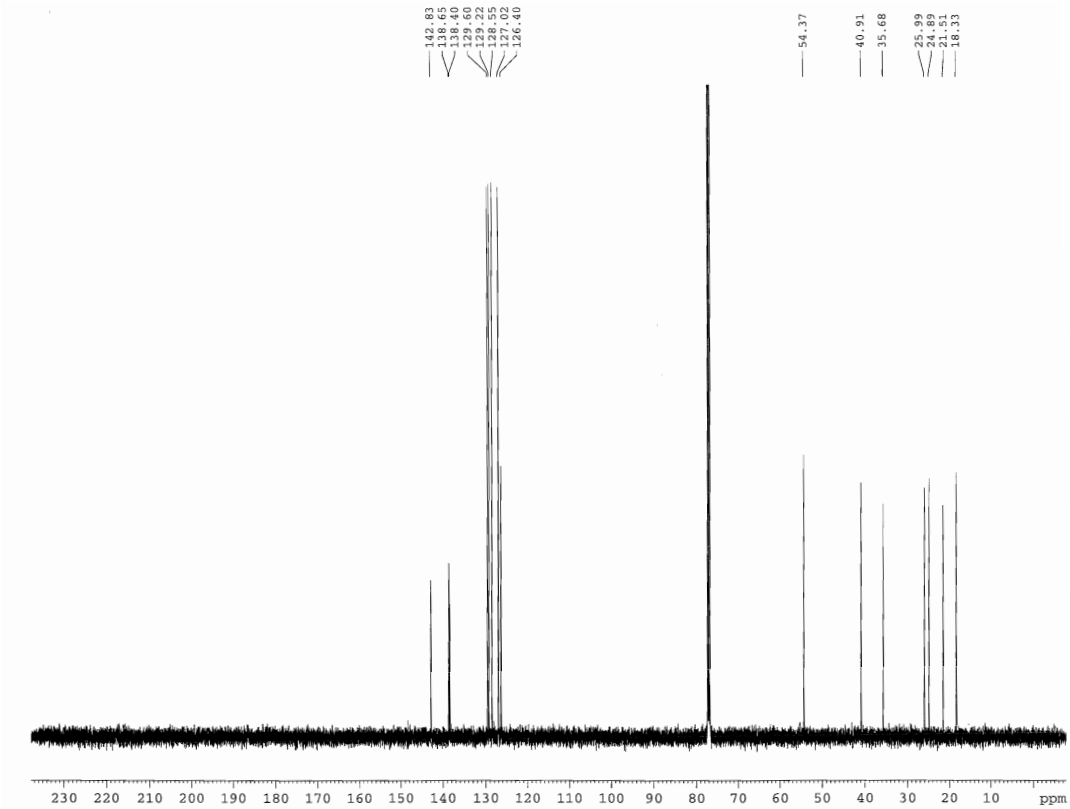
142.83
138.65
138.40
129.60
129.22
128.55
127.02
126.40
54.37
40.91
35.68
25.99
24.89
21.51
18.33
230 220 210 200 190 180 170 160 150 140 130 120 110 100 90 80 70 60 50 40 30 20 10 ppm

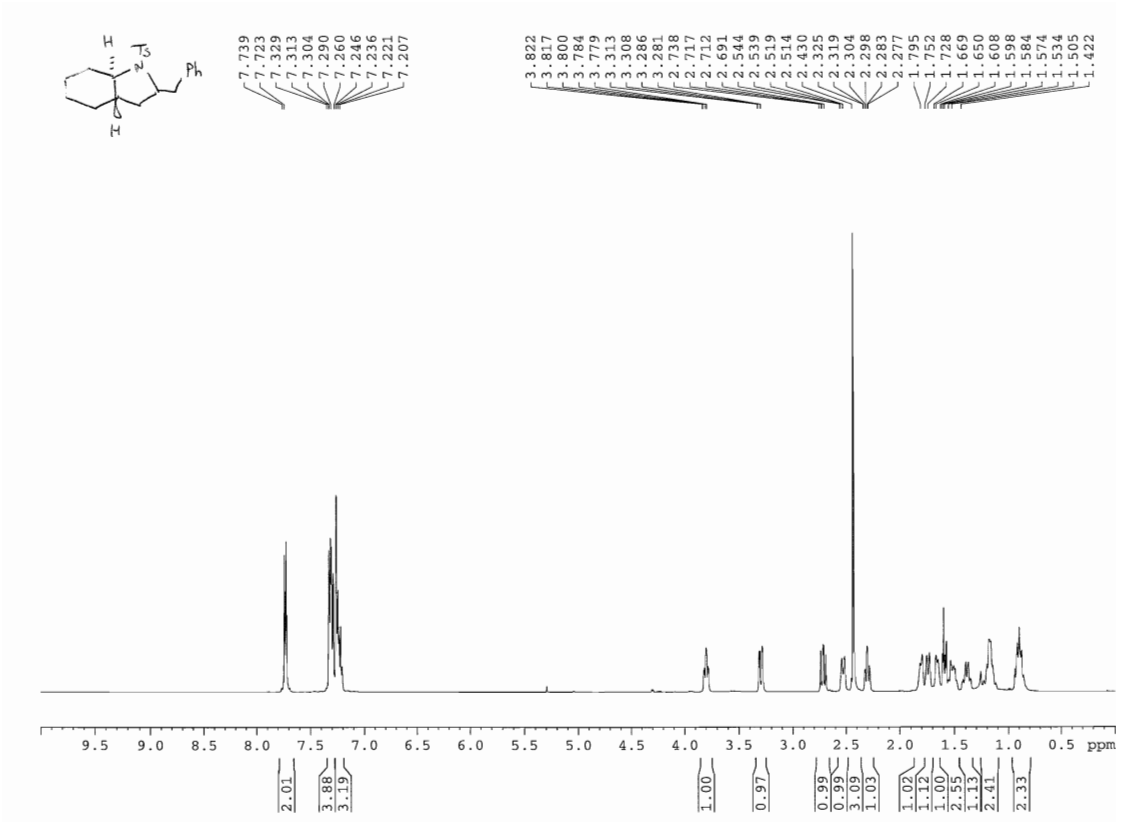
7.739
7.723
7.329
7.313
7.304
7.290
7.260
7.246
7.236
7.221
7.207
3.822
3.817
3.800
3.784
3.779
3.313
3.308
3.286
3.281
2.738
2.717
2.712
2.691
2.544
2.539
2.519
2.514
2.430
2.325
2.319
2.304
2.298
2.283
2.277
1.795
1.752
1.728
1.669
1.650
1.608
1.598
1.584
1.574
1.534
1.505
1.422
9.5 9.0 8.5 8.0 7.5 7.0 6.5 6.0 5.5 5.0 4.5 4.0 3.5 3.0 2.5 2.0 1.5 1.0 0.5 ppm
2.01
3.88
3.19
1.00
0.97
0.99
0.99
3.09
1.03
1.02
1.12
1.00
2.55
1.13
2.41
2.33

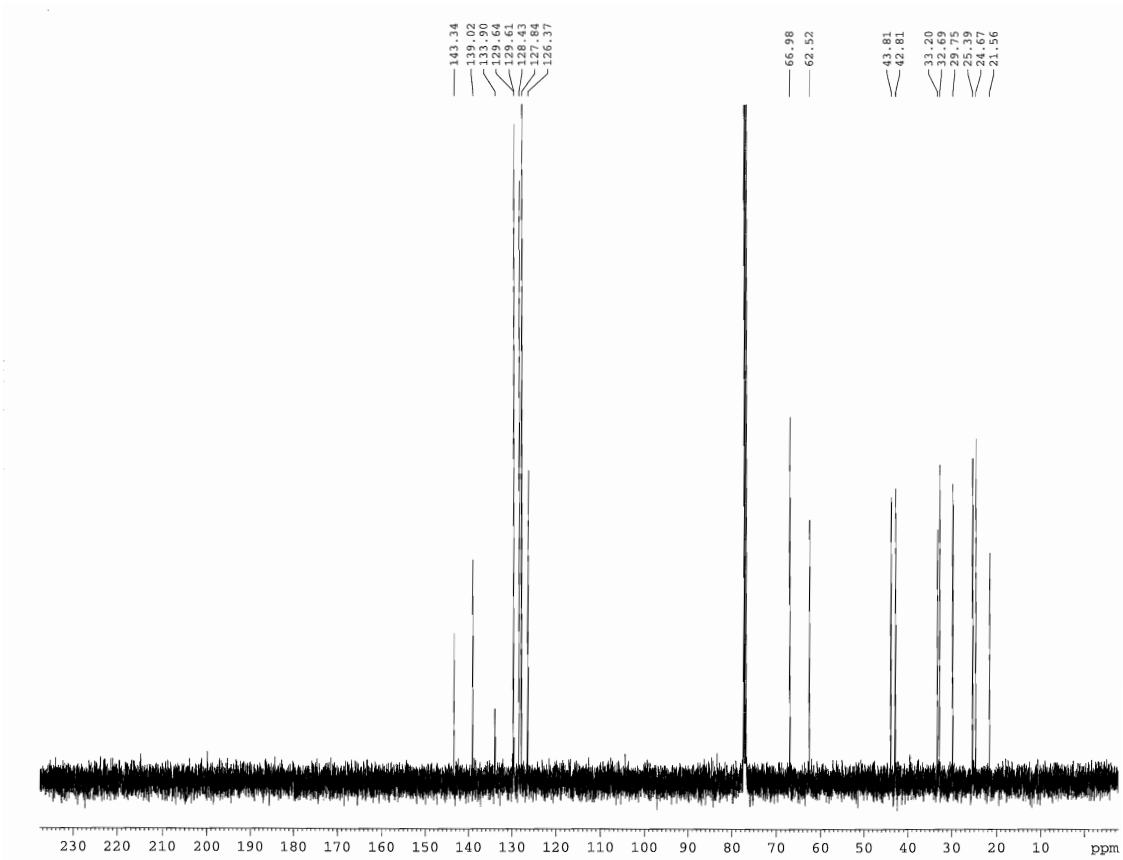
143.34
139.02
133.90
129.64
129.61
128.43
127.84
126.37
66.98
62.52
43.81
42.81
33.20
32.69
29.75
25.39
24.67
21.56
230 220 210 200 190 180 170 160 150 140 130 120 110 100 90 80 70 60 50 40 30 20 10 ppm

1.41

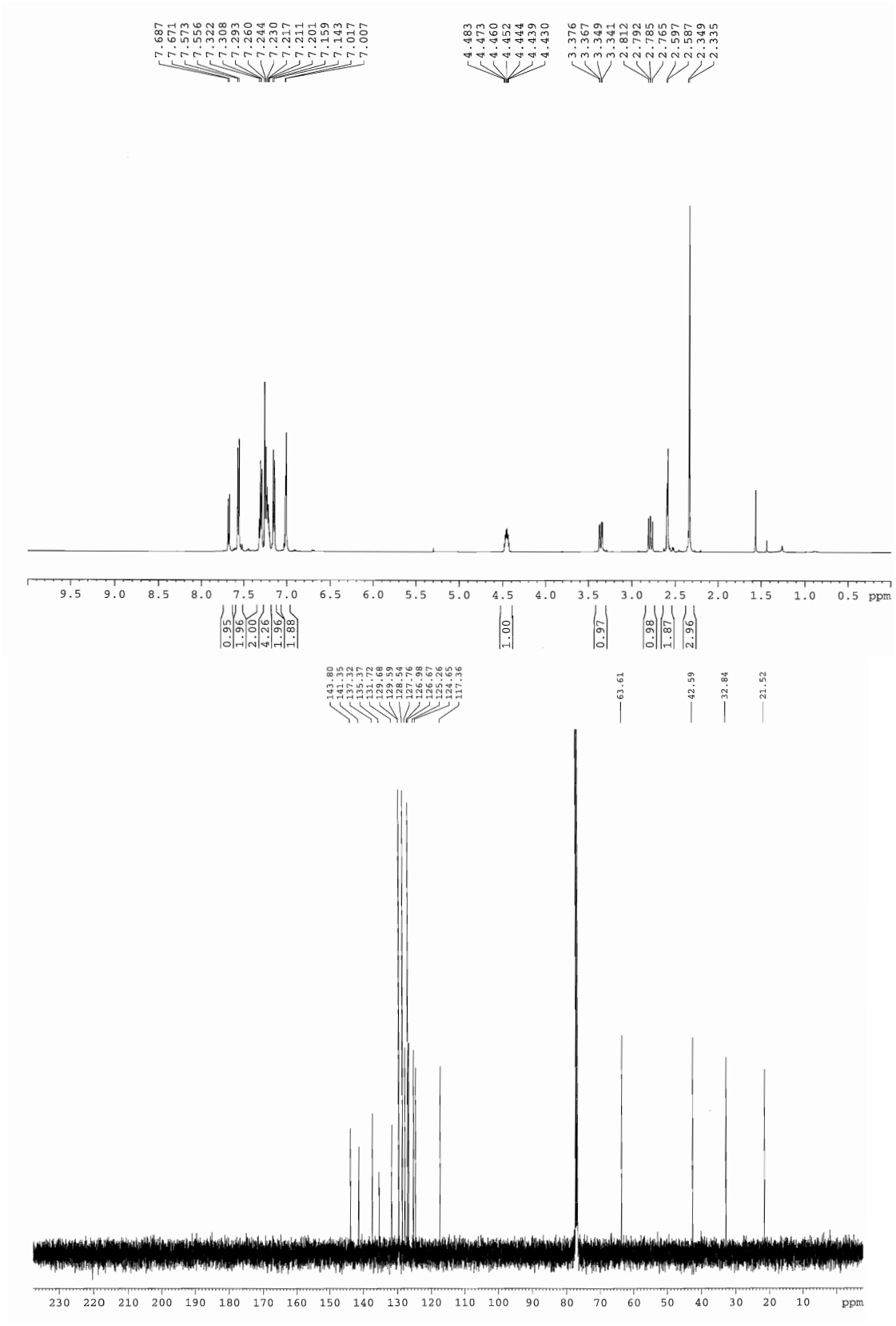
7.687
7.671
7.573
7.556
7.322
7.308
7.293
7.260
7.244
7.230
7.217
7.211
7.201
7.159
7.143
7.017
7.007
4.483
4.473
4.460
4.452
4.444
4.439
4.430
3.376
3.367
3.349
3.341
2.812
2.792
2.785
2.765
2.597
2.587
2.349
2.335
ppm
0.95
1.96
2.00
4.26
1.96
1.88
1.00
0.97
0.98
1.87
2.96
143.80
141.35
137.32
135.37
131.72
129.68
129.59
128.54
127.76
126.98
126.67
125.26
124.65
117.36
63.61
42.59
32.84
21.52
ppm

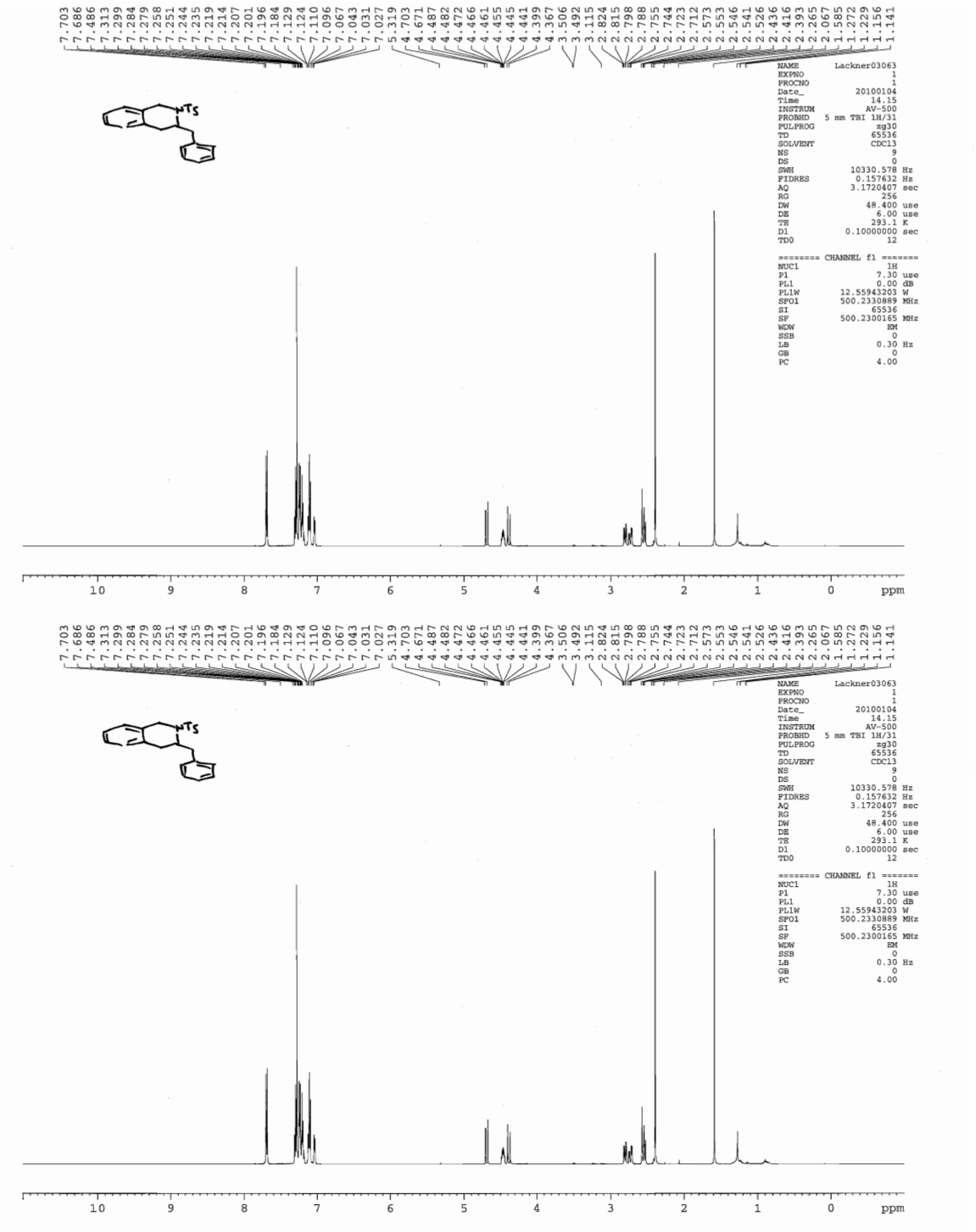
7.703 7.686 7.486 7.313 7.299 7.284 7.279 7.258 7.251 7.244 7.235 7.219 7.214 7.207 7.201 7.196 7.184 7.129 7.124 7.110 7.096 7.067 7.043 7.031 7.027 5.319 4.703 4.671 4.487 4.482 4.472 4.466 4.461 4.455 4.445 4.441 4.399 4.367 3.506 3.492 3.115 2.824 2.815 2.798 2.788 2.755 2.744 2.723 2.712 2.573 2.553 2.546 2.541 2.526 2.436 2.416 2.393 2.265 2.067 1.585 1.272 1.229 1.156 1.141
NTs
NAME Lackner03063
EXPNO 1
PROCNO 1
Date_ 20100104
Time 14.15
INSTRUM AV-500
PROBHD 5 mm TBI 1H/31
PULPROG zg30
TD 65536
SOLVENT CDCl3
NS 9
DS 0
SWH 10330.578 Hz
FIDRES 0.157632 Hz
AQ 3.1720407 sec
RG 256
DW 48.400 use
DE 6.00 use
TE 293.1 K
D1 0.10000000 sec
TD0 12
======== CHANNEL f1 ========
NUC1 1H
P1 7.30 use
PL1 0.00 dB
PL1W 12.55943203 W
SFO1 500.2330889 MHz
SI 65536
SF 500.2300165 MHz
WDW EM
SSB 0
LB 0.30 Hz
GB 0
PC 4.00
10 9 8 7 6 5 4 3 2 1 0 ppm
7.703 7.686 7.486 7.313 7.299 7.284 7.279 7.258 7.251 7.244 7.235 7.219 7.214 7.207 7.201 7.196 7.184 7.129 7.124 7.110 7.096 7.067 7.043 7.031 7.027 5.319 4.703 4.671 4.487 4.482 4.472 4.466 4.461 4.455 4.445 4.441 4.399 4.367 3.506 3.492 3.115 2.824 2.815 2.798 2.788 2.755 2.744 2.723 2.712 2.573 2.553 2.546 2.541 2.526 2.436 2.416 2.393 2.265 2.067 1.585 1.272 1.229 1.156 1.141
NTs
NAME Lackner03063
EXPNO 1
PROCNO 1
Date_ 20100104
Time 14.15
INSTRUM AV-500
PROBHD 5 mm TBI 1H/31
PULPROG zg30
TD 65536
SOLVENT CDCl3
NS 9
DS 0
SWH 10330.578 Hz
FIDRES 0.157632 Hz
AQ 3.1720407 sec
RG 256
DW 48.400 use
DE 6.00 use
TE 293.1 K
D1 0.10000000 sec
TD0 12
======== CHANNEL f1 ========
NUC1 1H
P1 7.30 use
PL1 0.00 dB
PL1W 12.55943203 W
SFO1 500.2330889 MHz
SI 65536
SF 500.2300165 MHz
WDW EM
SSB 0
LB 0.30 Hz
GB 0
PC 4.00
10 9 8 7 6 5 4 3 2 1 0 ppm

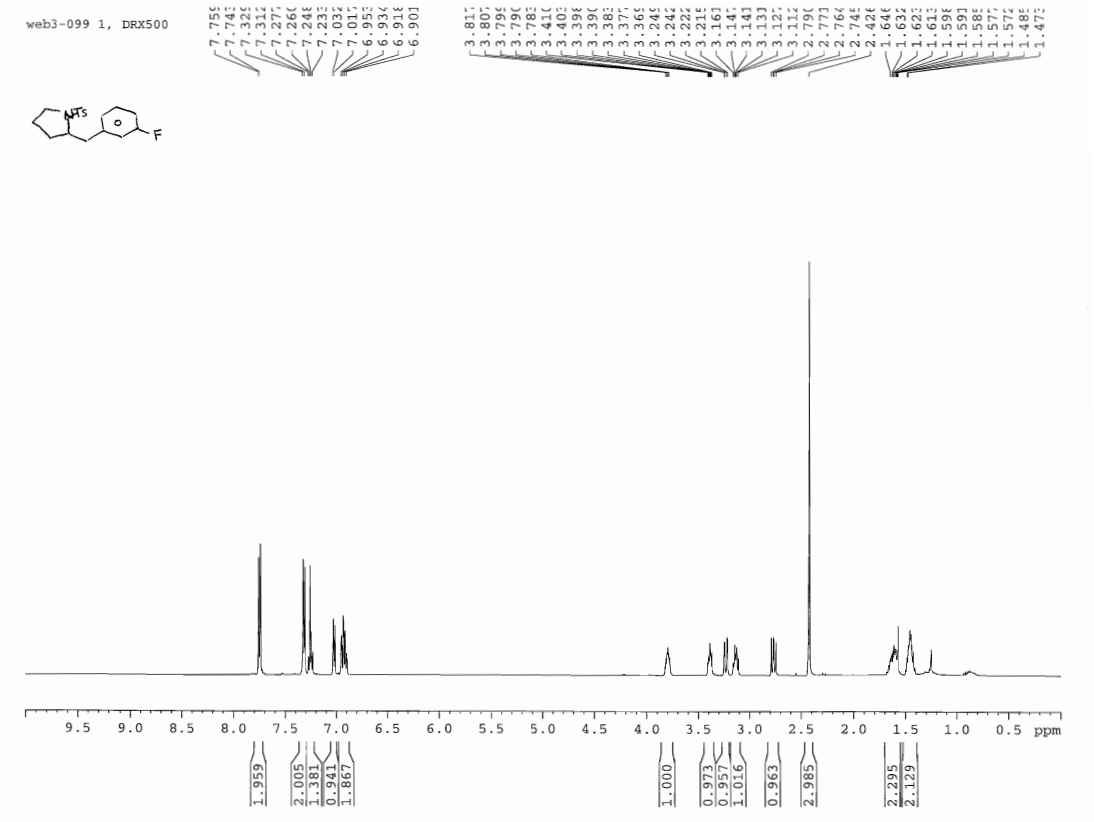
web3-099 1, DRX500
Ts
F
9.5 9.0 8.5 8.0 7.5 7.0 6.5 6.0 5.5 5.0 4.5 4.0 3.5 3.0 2.5 2.0 1.5 1.0 0.5 ppm
1.959
2.005
1.381
0.941
1.867
1.000
0.973
0.957
1.016
0.963
2.985
2.295
2.129

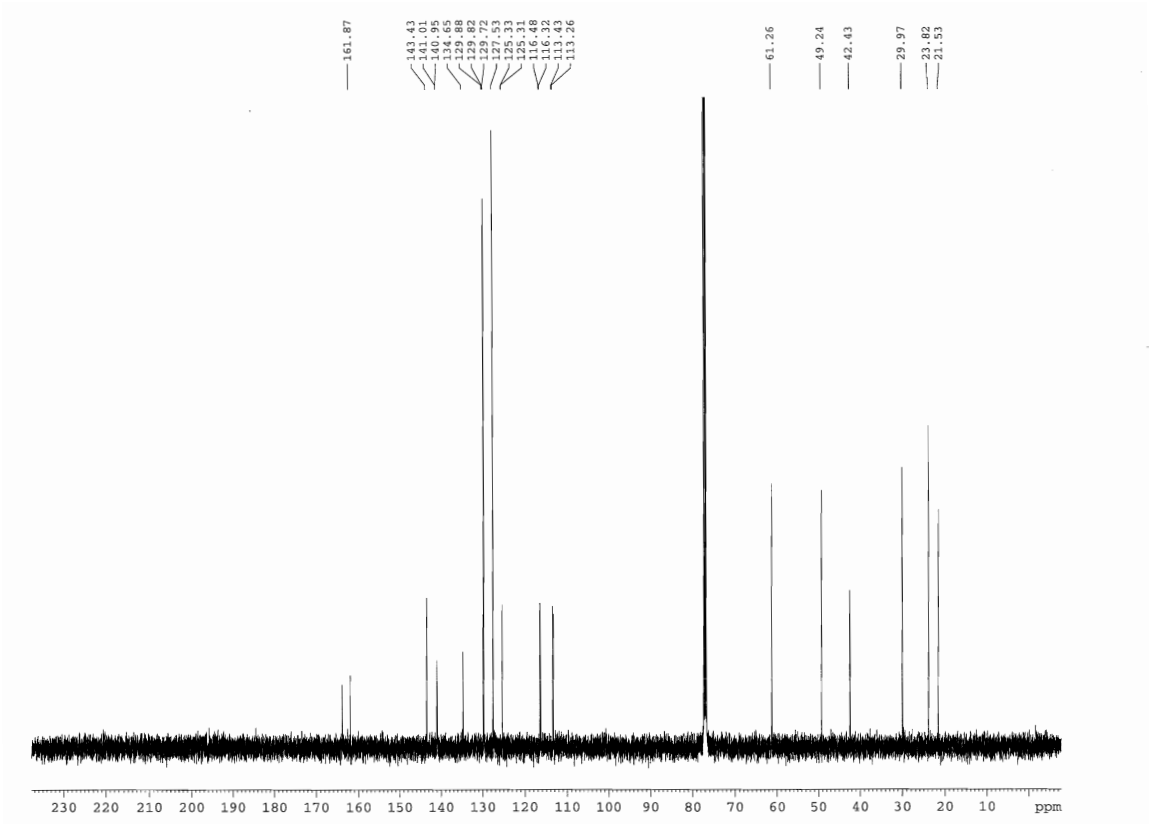
161.87
143.43
141.01
140.95
134.65
129.88
129.62
129.32
127.53
125.33
125.31
116.48
116.32
113.43
113.26
61.26
49.24
42.43
29.97
23.82
21.53
230 220 210 200 190 180 170 160 150 140 130 120 110 100 90 80 70 60 50 40 30 20 10 ppm

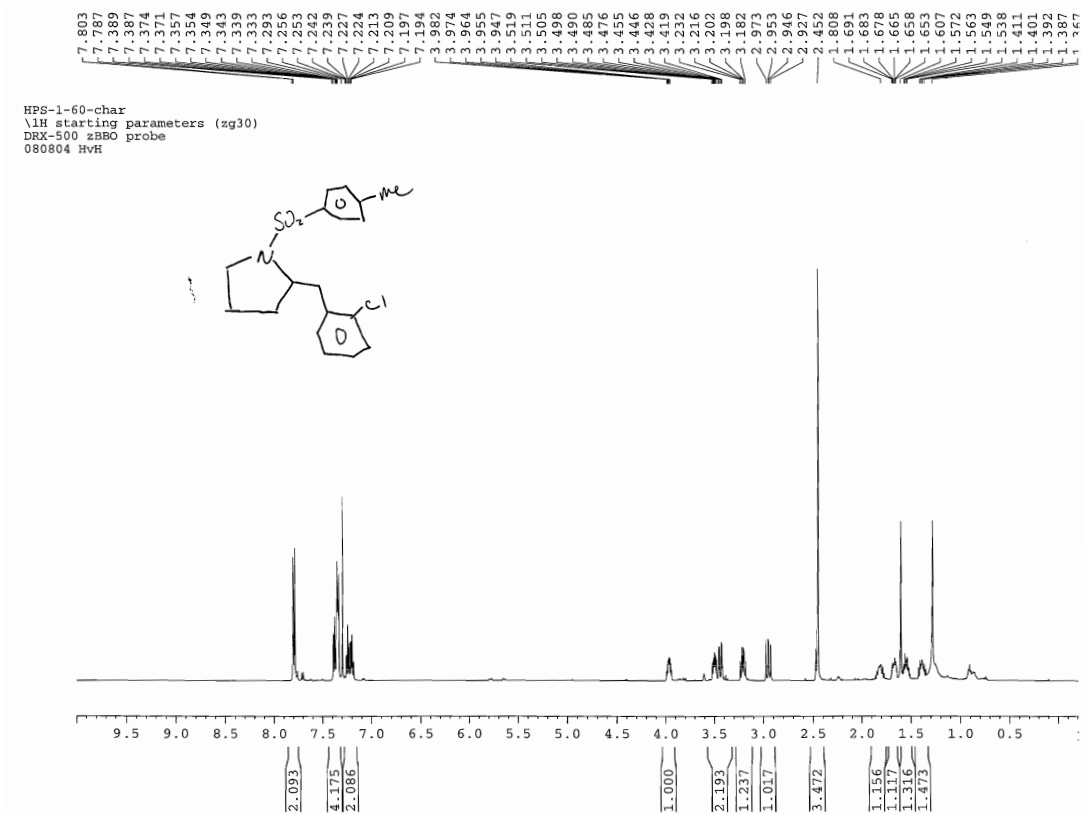
7.803 7.787 7.389 7.387 7.374 7.371 7.357 7.354 7.349 7.343 7.339 7.333 7.293 7.256 7.253 7.242 7.239 7.227 7.224 7.213 7.209 7.197 7.194 3.982 3.974 3.964 3.955 3.947 3.519 3.511 3.505 3.498 3.490 3.485 3.476 3.455 3.446 3.428 3.419 3.232 3.216 3.202 3.198 3.182 2.973 2.953 2.946 2.927 2.452 1.808 1.691 1.683 1.678 1.665 1.658 1.653 1.607 1.572 1.563 1.549 1.538 1.411 1.401 1.392 1.387
HPS-1-60-char
\1H starting parameters (zg30)
DRX-500 zBBO probe
080804 HvH
Me
SO2
N
Cl
O
9.5 9.0 8.5 8.0 7.5 7.0 6.5 6.0 5.5 5.0 4.5 4.0 3.5 3.0 2.5 2.0 1.5 1.0 0.5
2.093 4.175 2.086 1.000 2.193 1.237 1.017 3.472 1.156 1.117 1.316 1.473

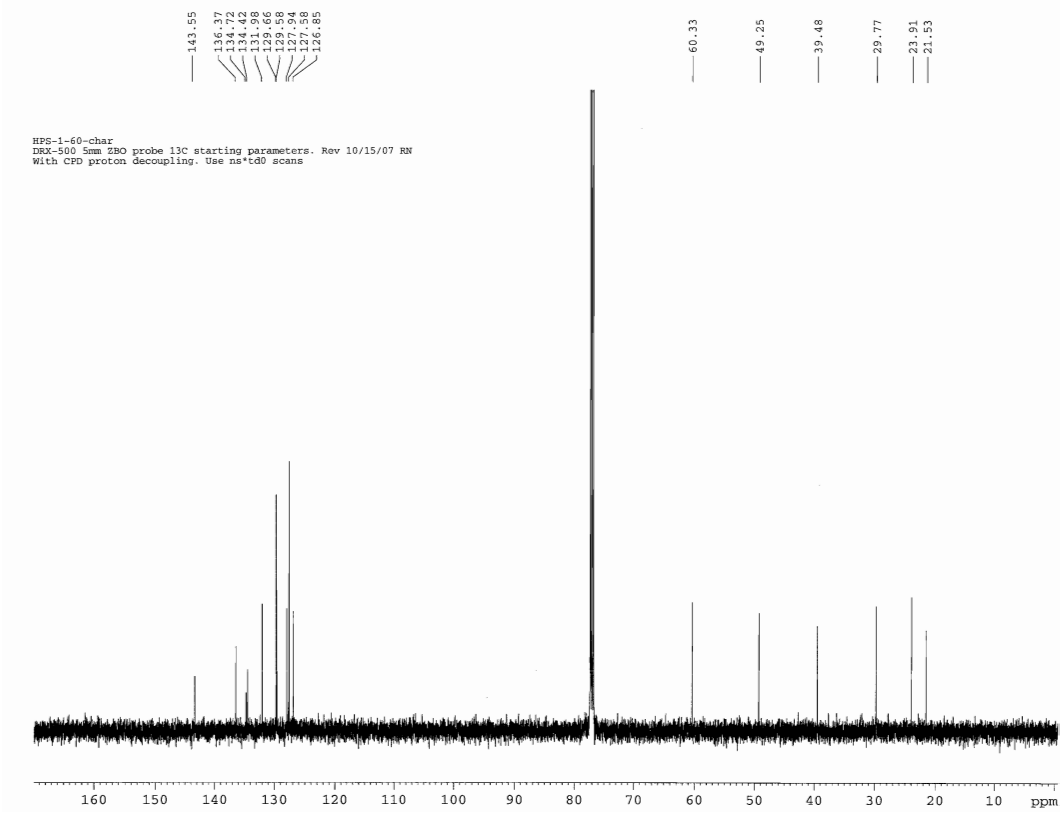
143.55 136.37 134.72 134.42 131.98 129.66 129.58 127.94 127.38 126.85 60.33 49.25 39.48 29.77 23.91 21.53
HPS-1-60-char
DRX-500 5mm ZBO probe 13C starting parameters. Rev 10/15/07 RN
With CPD proton decoupling. Use ns*td0 scans
160 150 140 130 120 110 100 90 80 70 60 50 40 30 20 10 ppm

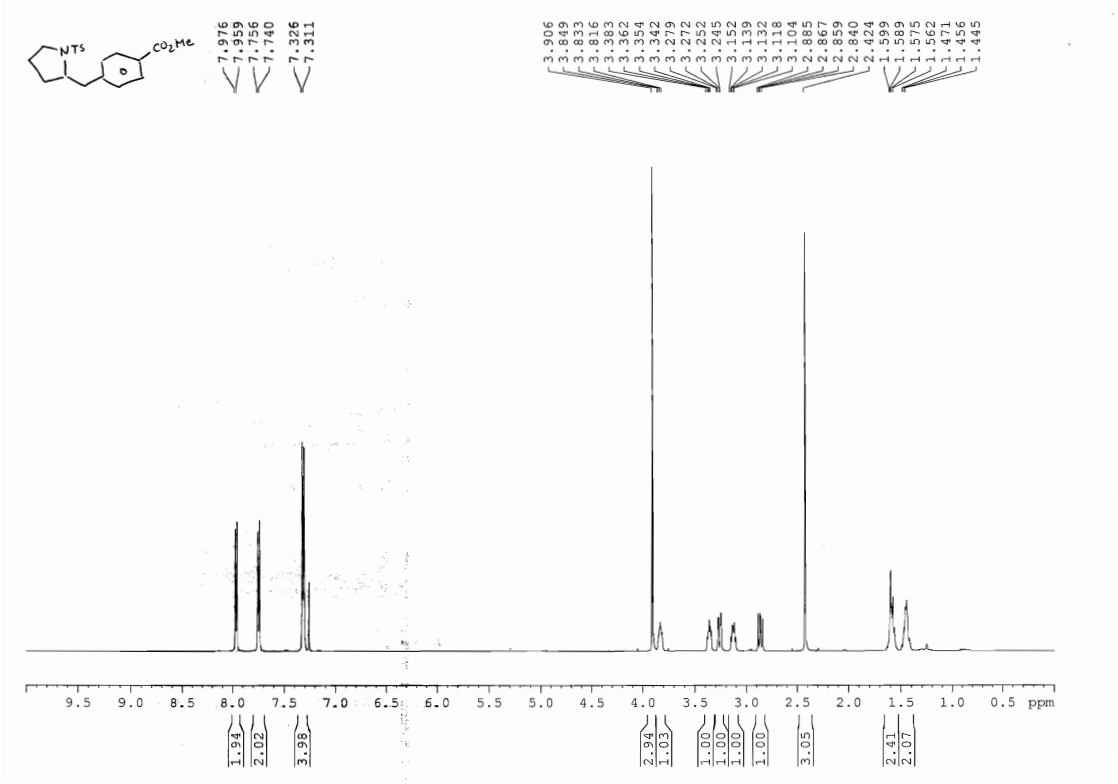
NTs
CO2Me
O
7.976
7.959
7.756
7.740
7.326
7.311
3.906
3.849
3.833
3.816
3.383
3.362
3.354
3.342
3.279
3.272
3.252
3.245
3.152
3.139
3.132
3.118
3.104
2.885
2.867
2.859
2.840
2.424
1.599
1.589
1.575
1.562
1.471
1.456
1.445
9.5 9.0 8.5 8.0 7.5 7.0 6.5 6.0 5.5 5.0 4.5 4.0 3.5 3.0 2.5 2.0 1.5 1.0 0.5 ppm
1.94
2.02
3.98
2.94
1.03
1.00
1.00
1.00
1.00
3.05
2.41
2.07

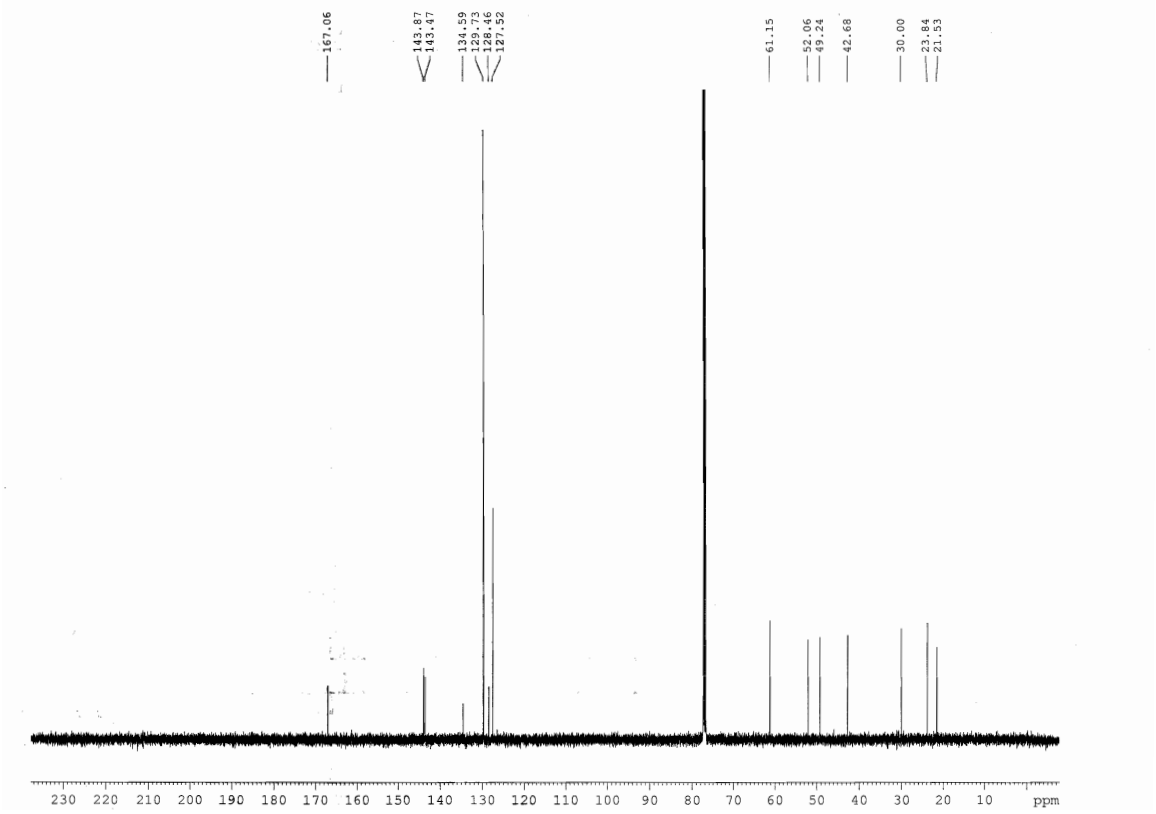
167.06
143.87
143.47
134.59
129.73
128.46
127.52
61.15
52.06
49.24
42.68
30.00
23.84
21.53
230 220 210 200 190 180 170 160 150 140 130 120 110 100 90 80 70 60 50 40 30 20 10 ppm

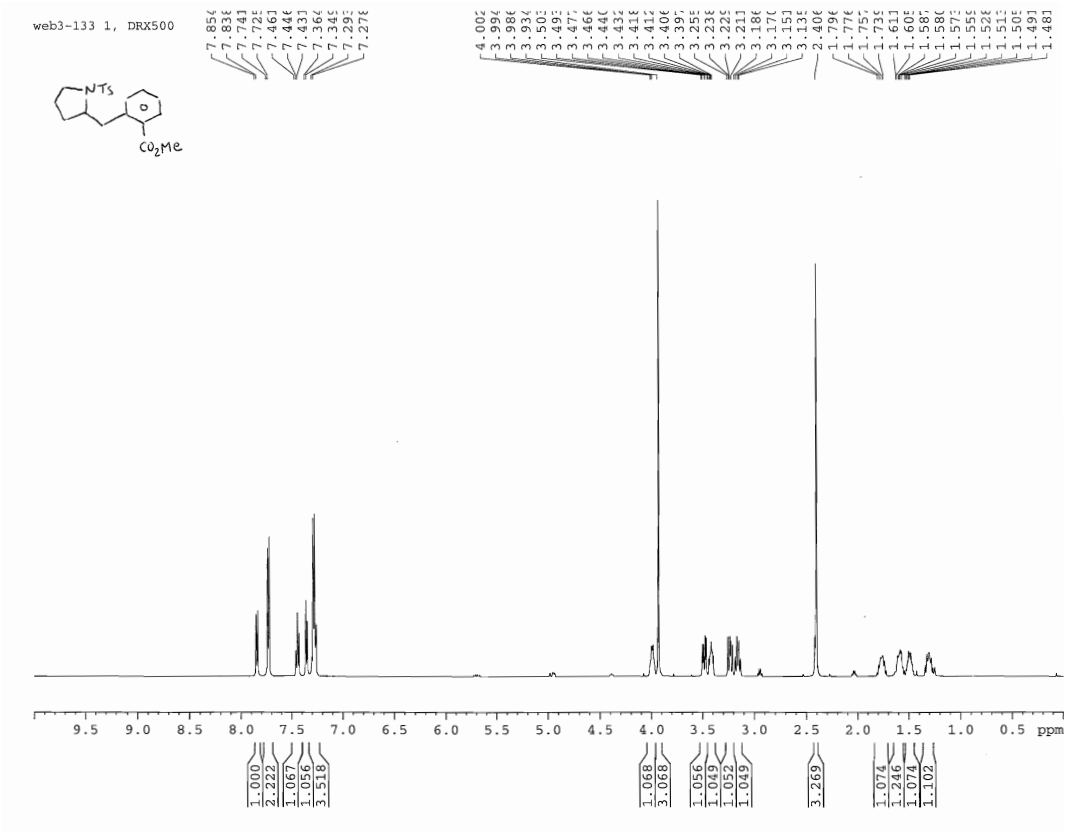
web3-133 1, DRX500
NTs
O
CO2Me
9.5 9.0 8.5 8.0 7.5 7.0 6.5 6.0 5.5 5.0 4.5 4.0 3.5 3.0 2.5 2.0 1.5 1.0 0.5 ppm
1.000
2.222
1.067
1.056
3.518
1.068
3.068
1.056
1.049
1.052
1.049
3.269
1.074
1.246
1.074
1.102

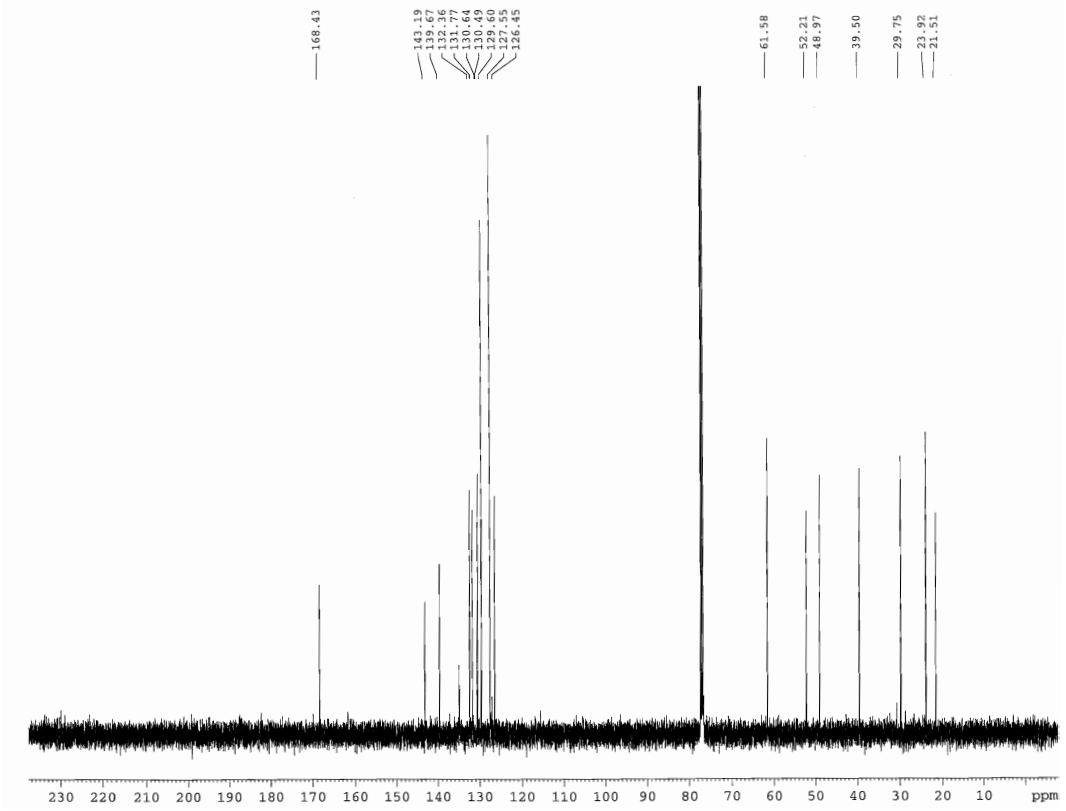
168.43
143.19
139.67
133.46
131.77
130.64
130.49
129.60
127.55
126.45
61.58
52.21
48.97
39.50
29.75
23.92
21.51
230 220 210 200 190 180 170 160 150 140 130 120 110 100 90 80 70 60 50 40 30 20 10 ppm

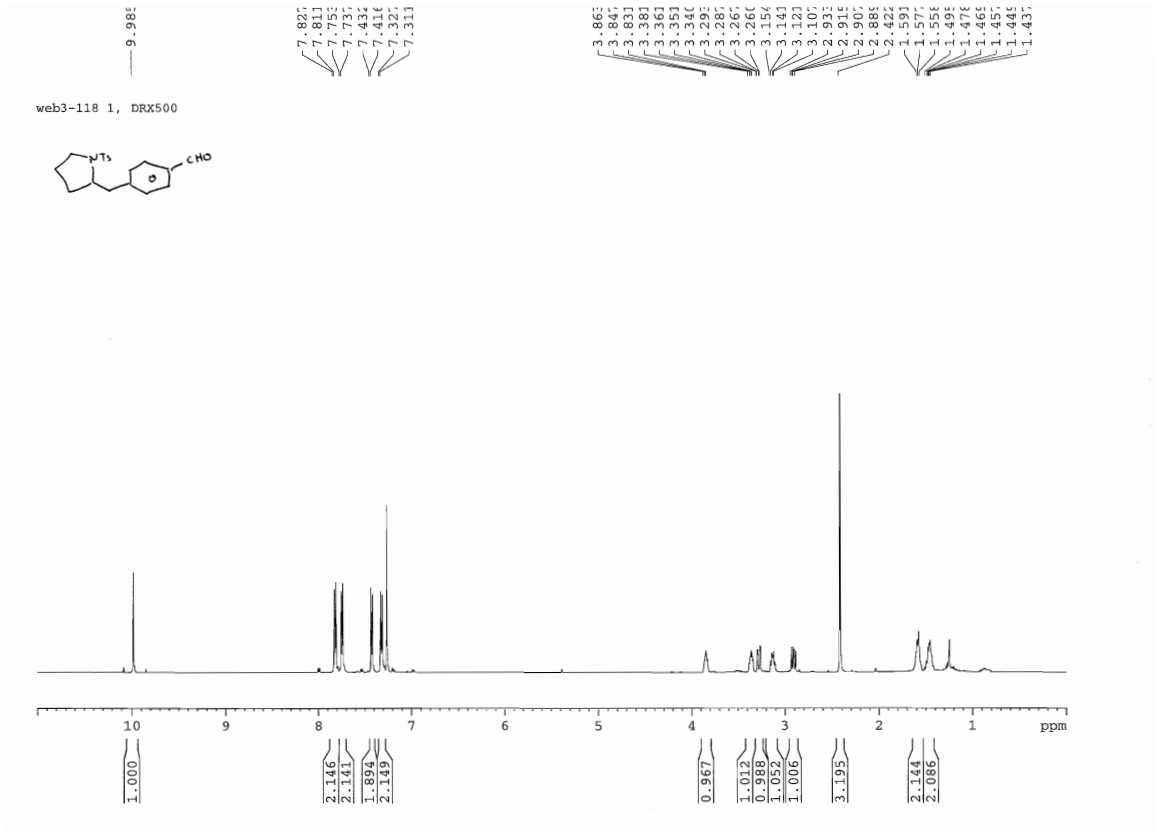
web3-118 1, DRX500
NTs
CHO
9.98
7.82
7.81
7.75
7.73
7.43
7.41
7.32
7.31
3.86
3.84
3.83
3.38
3.36
3.35
3.34
3.29
3.28
3.26
3.15
3.14
3.12
3.10
2.93
2.91
2.90
2.88
2.42
1.59
1.57
1.55
1.49
1.47
1.46
1.45
1.44
1.43
10
9
8
7
6
5
4
3
2
1
ppm
1.000
2.146
2.141
1.894
2.149
0.967
1.012
0.988
1.052
1.006
3.195
2.144
2.086

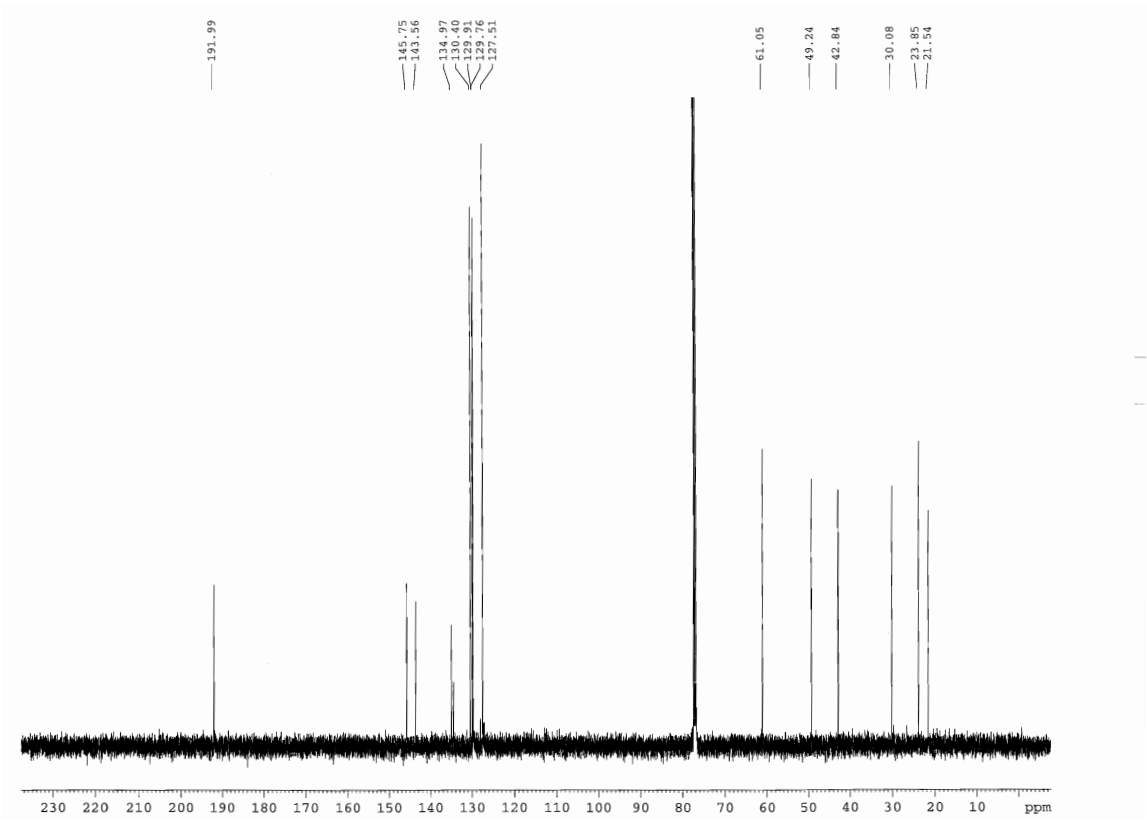
191.99
145.75
143.56
134.97
130.40
129.91
129.76
127.51
61.05
49.24
42.84
30.08
23.85
21.54
230
220
210
200
190
180
170
160
150
140
130
120
110
100
90
80
70
60
50
40
30
20
10
ppm

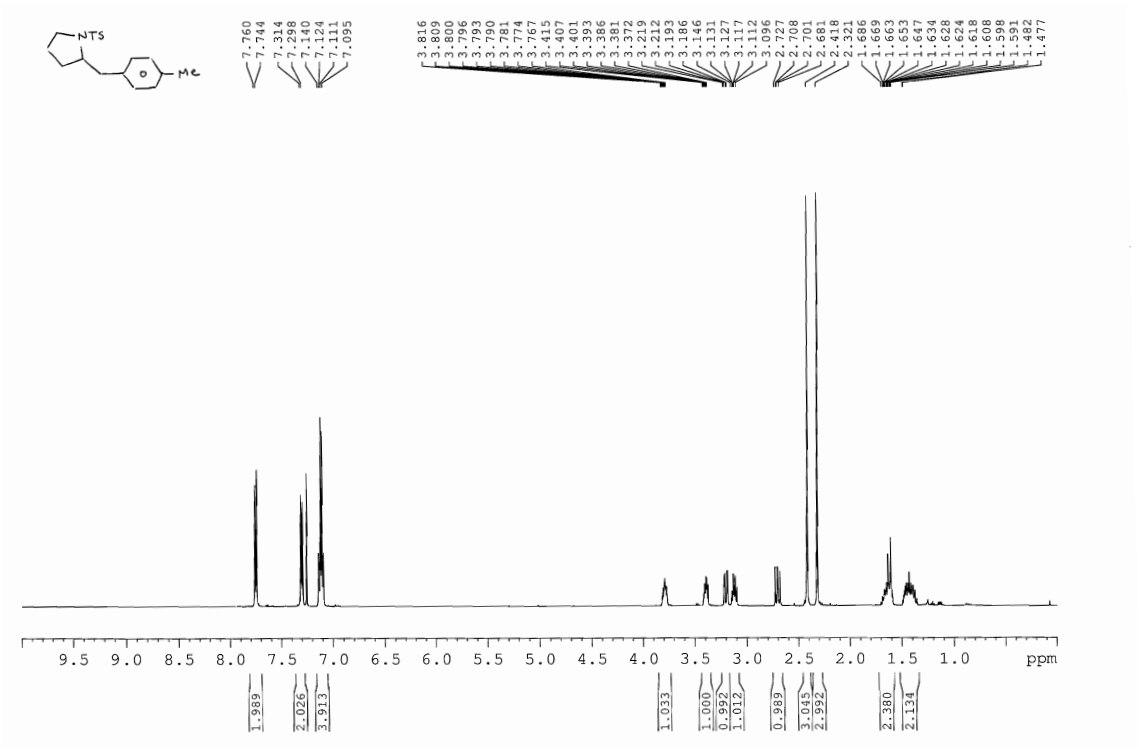
NTS
Me
O
7.760
7.744
7.314
7.298
7.140
7.124
7.111
7.095
3.816
3.809
3.800
3.796
3.793
3.790
3.781
3.774
3.767
3.415
3.407
3.401
3.393
3.386
3.381
3.372
3.219
3.212
3.193
3.186
3.146
3.131
3.127
3.117
3.112
3.096
2.727
2.708
2.701
2.681
2.668
2.321
2.686
1.669
1.663
1.653
1.647
1.634
1.628
1.624
1.618
1.608
1.598
1.591
1.482
1.477
9.5 9.0 8.5 8.0 7.5 7.0 6.5 6.0 5.5 5.0 4.5 4.0 3.5 3.0 2.5 2.0 1.5 1.0 ppm
1.989
2.026
3.913
1.033
1.000
0.992
1.012
0.989
3.045
2.992
2.380
2.134

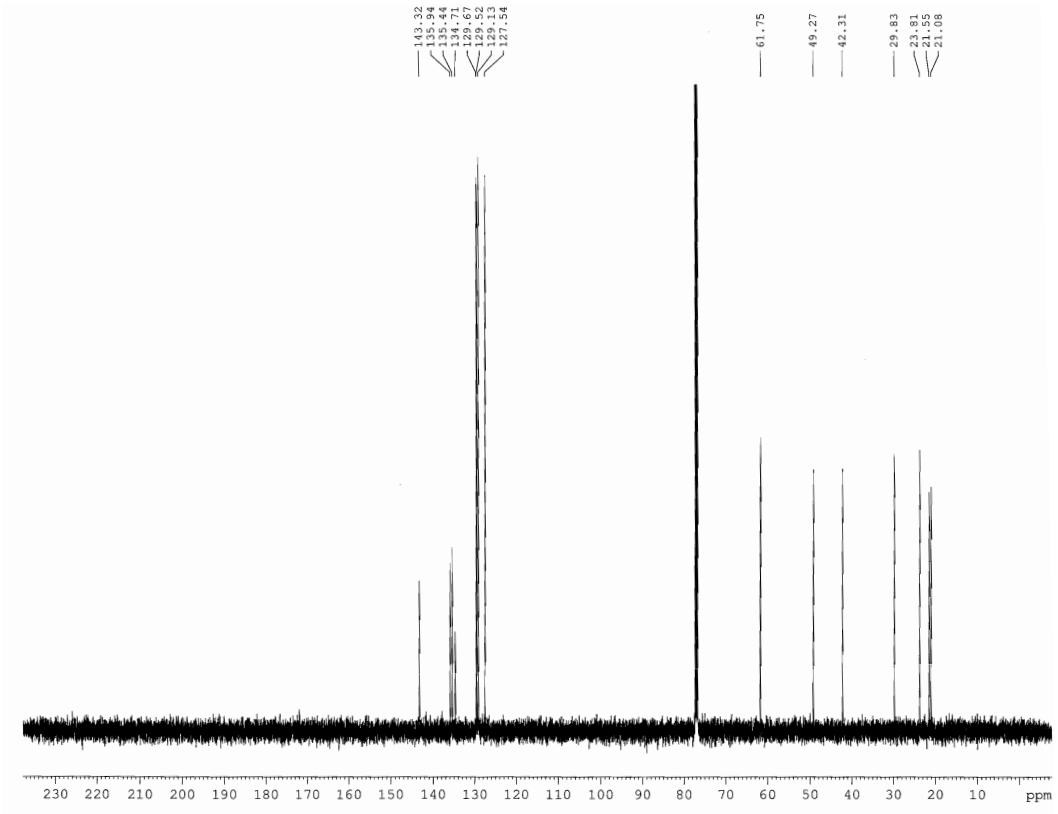
143.32
135.94
135.44
134.71
129.67
129.52
129.13
127.54
61.75
49.27
42.31
29.83
23.81
21.55
21.08
230 220 210 200 190 180 170 160 150 140 130 120 110 100 90 80 70 60 50 40 30 20 10 ppm

1.6a

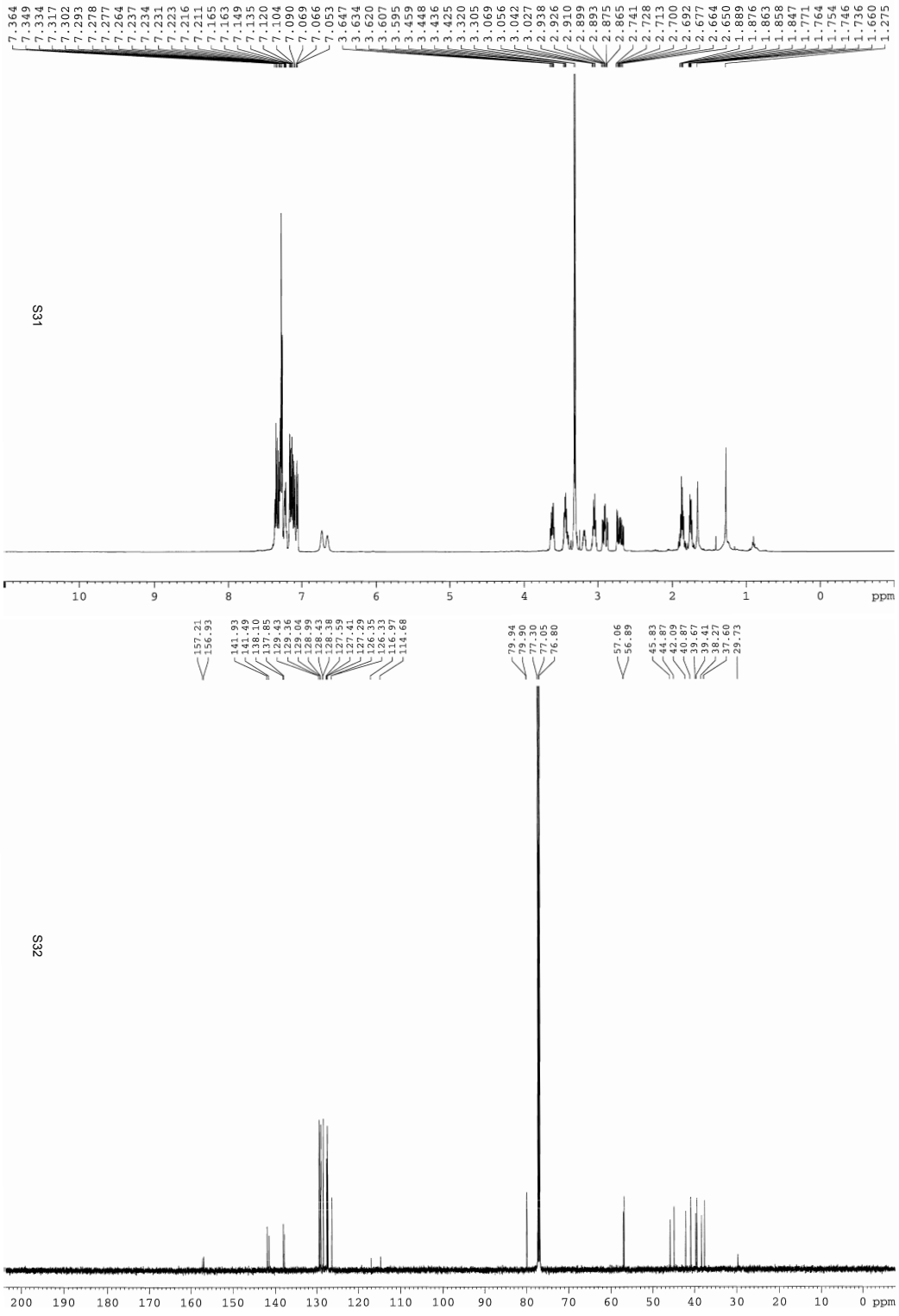
7.364
7.349
7.334
7.317
7.302
7.293
7.278
7.277
7.264
7.237
7.234
7.231
7.223
7.216
7.211
7.165
7.163
7.149
7.135
7.120
7.104
7.090
7.069
7.066
7.053
3.647
3.634
3.620
3.607
3.595
3.459
3.448
3.436
3.425
3.320
3.305
3.069
3.056
3.042
3.027
2.938
2.926
2.910
2.899
2.893
2.875
2.865
2.741
2.728
2.713
2.700
2.692
2.677
2.664
2.650
1.889
1.876
1.863
1.858
1.847
1.771
1.764
1.754
1.746
1.736
1.660
1.275
S31
10
9
8
7
6
5
4
3
2
1
0
ppm
157.21
156.93
141.93
141.49
138.10
137.85
129.43
129.36
128.94
128.87
128.43
128.38
127.59
127.41
127.29
126.35
126.33
116.97
114.68
79.94
79.90
77.30
77.05
76.80
57.06
56.89
45.83
44.87
42.09
40.87
39.67
39.41
38.27
37.60
29.73
S32
200
190
180
170
160
150
140
130
120
110
100
90
80
70
60
50
40
30
20
10
0 ppm

1.6b

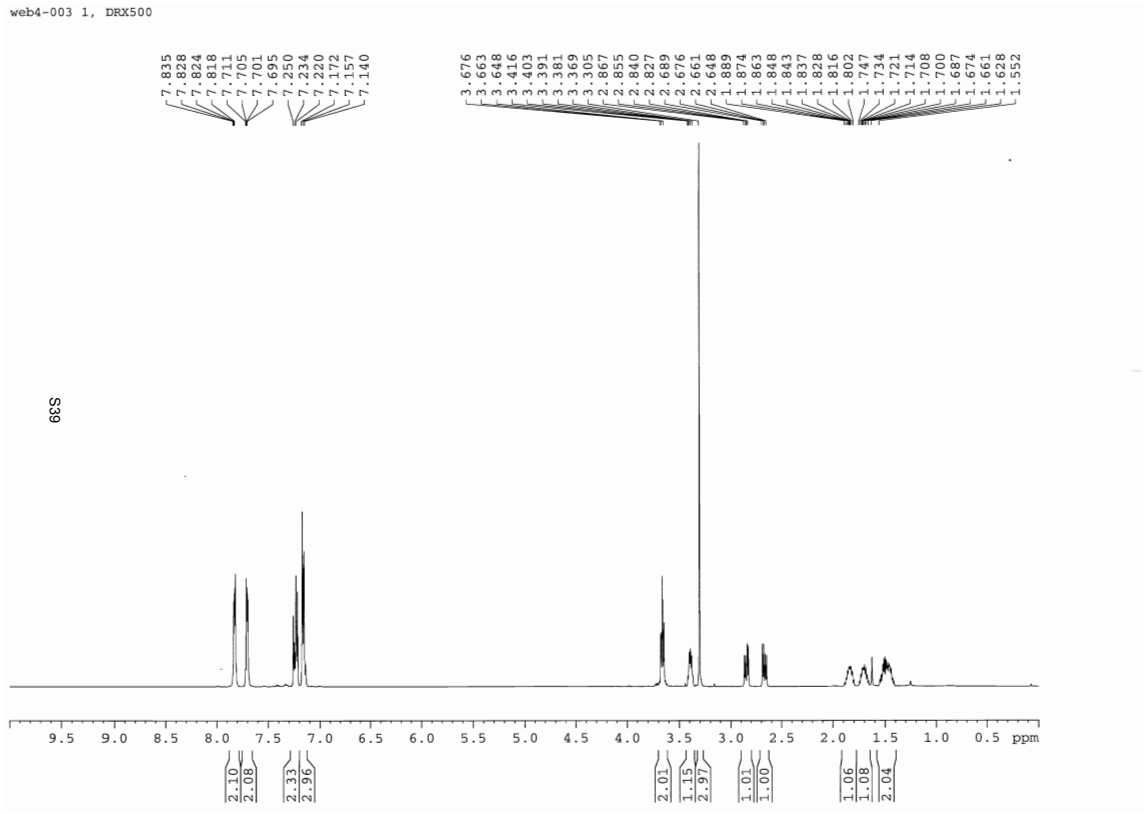
web4-003 1, DRX500
S39
7.835
7.828
7.824
7.818
7.711
7.705
7.701
7.695
7.250
7.234
7.220
7.172
7.157
7.140
3.676
3.663
3.648
3.416
3.403
3.391
3.381
3.369
3.305
2.867
2.855
2.840
2.827
2.689
2.676
2.661
2.648
1.889
1.874
1.863
1.848
1.843
1.837
1.828
1.816
1.802
1.747
1.734
1.721
1.714
1.708
1.700
1.687
1.674
1.661
1.628
1.552
9.5 9.0 8.5 8.0 7.5 7.0 6.5 6.0 5.5 5.0 4.5 4.0 3.5 3.0 2.5 2.0 1.5 1.0 0.5 ppm
2.10
2.08
2.33
2.96
2.01
1.15
2.97
1.01
1.00
1.06
1.08
2.04

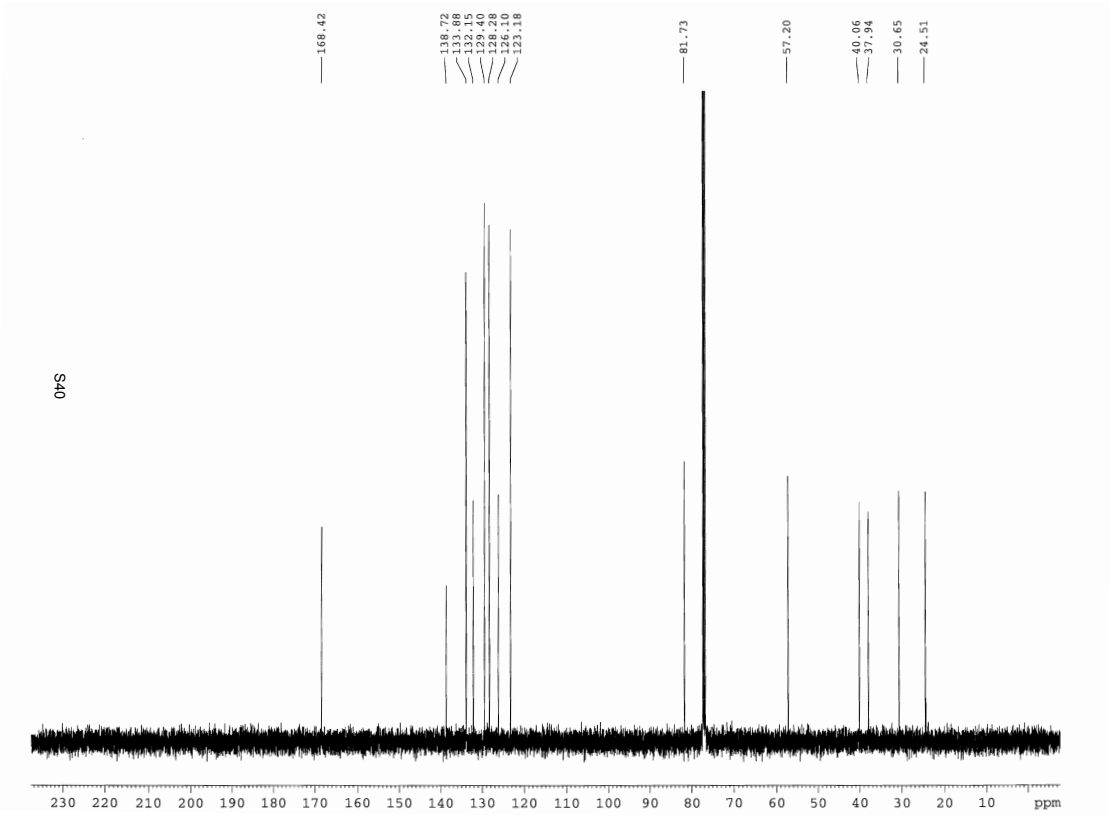
S40
168.42
138.72
133.88
132.15
130.40
128.28
126.10
123.18
81.73
57.20
40.06
37.94
30.65
24.51
230 220 210 200 190 180 170 160 150 140 130 120 110 100 90 80 70 60 50 40 30 20 10 ppm

1.6c

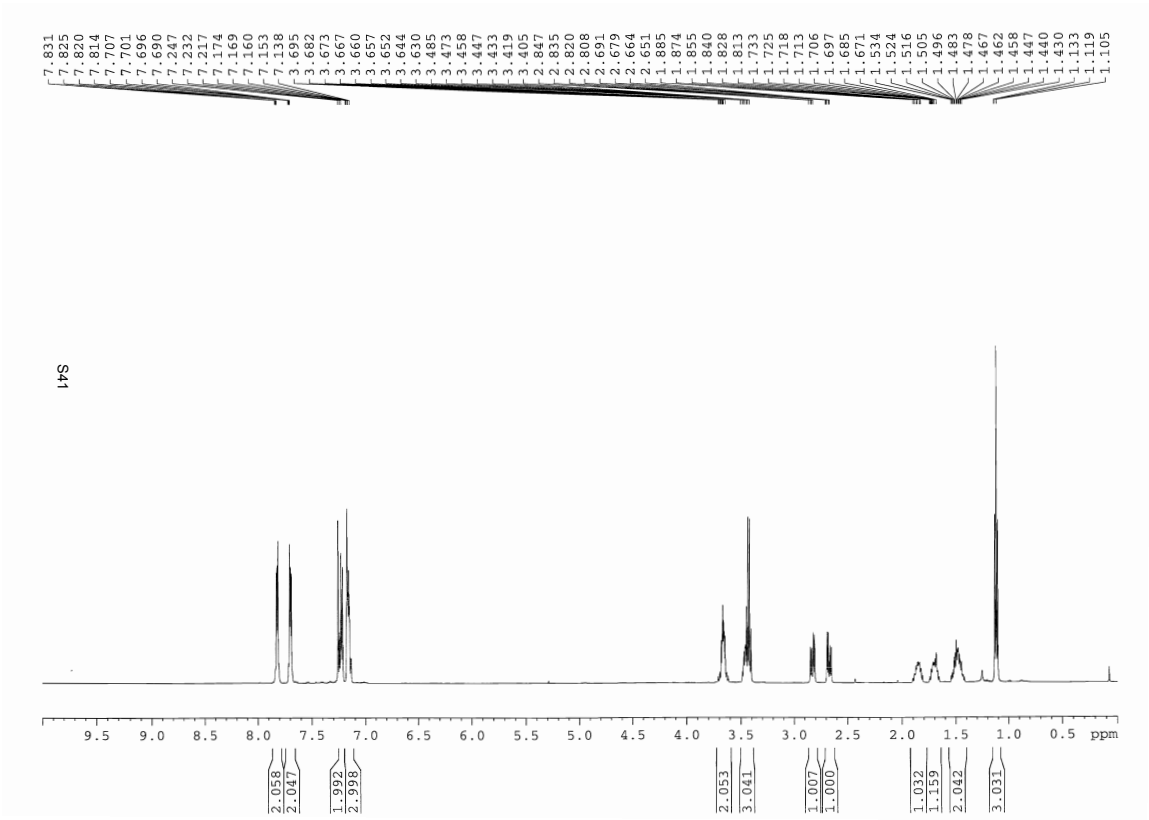
7.831
7.825
7.820
7.814
7.707
7.701
7.696
7.690
7.247
7.232
7.217
7.174
7.169
7.160
7.153
7.138
3.695
3.682
3.673
3.667
3.660
3.657
3.652
3.644
3.630
3.485
3.473
3.458
3.447
3.433
3.419
3.405
2.847
2.835
2.820
2.808
2.691
2.679
2.664
2.651
1.885
1.874
1.855
1.840
1.828
1.813
1.733
1.725
1.718
1.713
1.706
1.697
1.685
1.671
1.534
1.524
1.516
1.505
1.496
1.483
1.478
1.467
1.462
1.458
1.447
1.440
1.430
1.133
1.119
1.105
S41
9.5 9.0 8.5 8.0 7.5 7.0 6.5 6.0 5.5 5.0 4.5 4.0 3.5 3.0 2.5 2.0 1.5 1.0 0.5 ppm
2.058
2.047
1.992
2.998
2.053
3.041
1.007
1.000
1.032
1.159
2.042
3.031

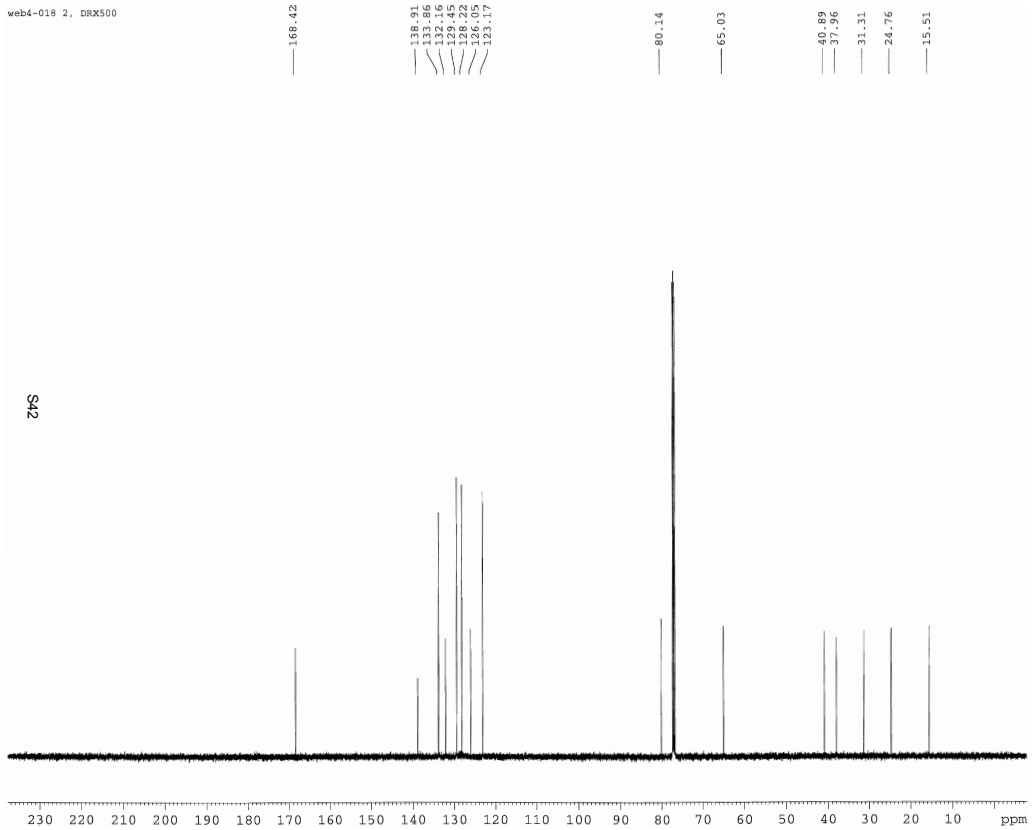
web4-018 2, DRX500
168.42
138.91
133.86
132.16
129.45
128.22
126.05
123.17
80.14
65.03
40.89
37.96
31.31
24.76
15.51
S42
230 220 210 200 190 180 170 160 150 140 130 120 110 100 90 80 70 60 50 40 30 20 10 ppm

1.6d

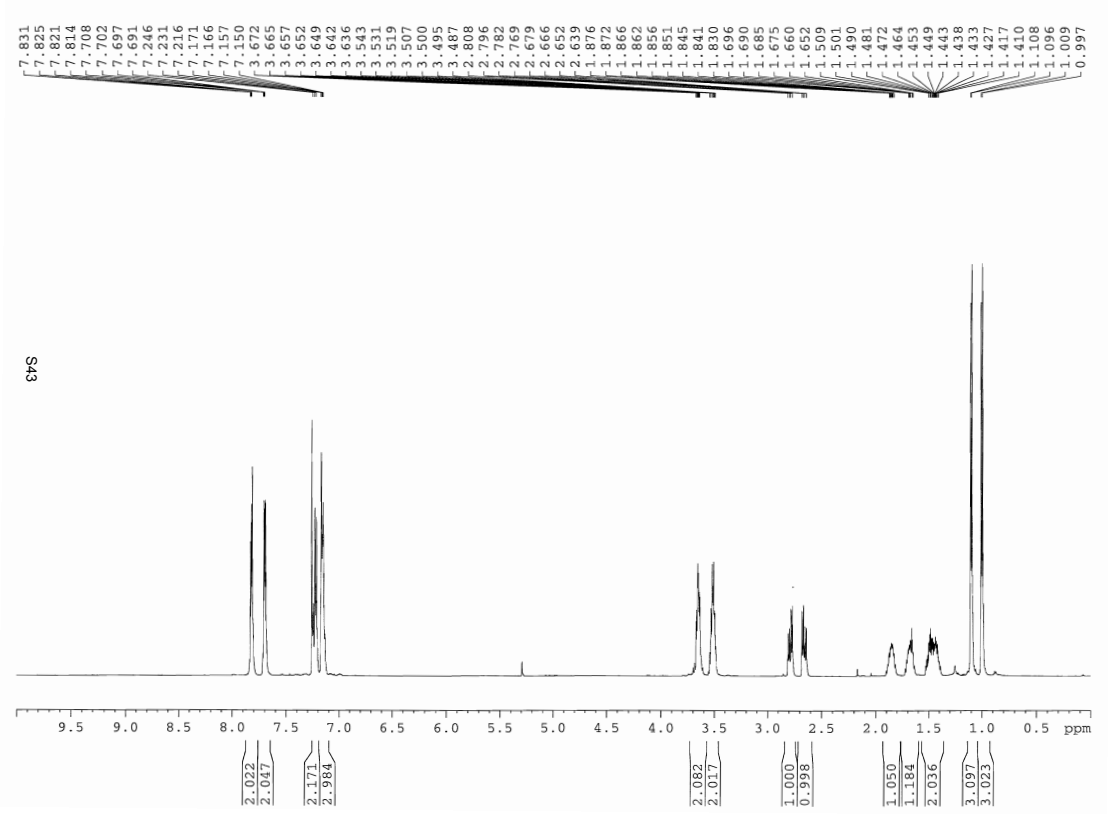

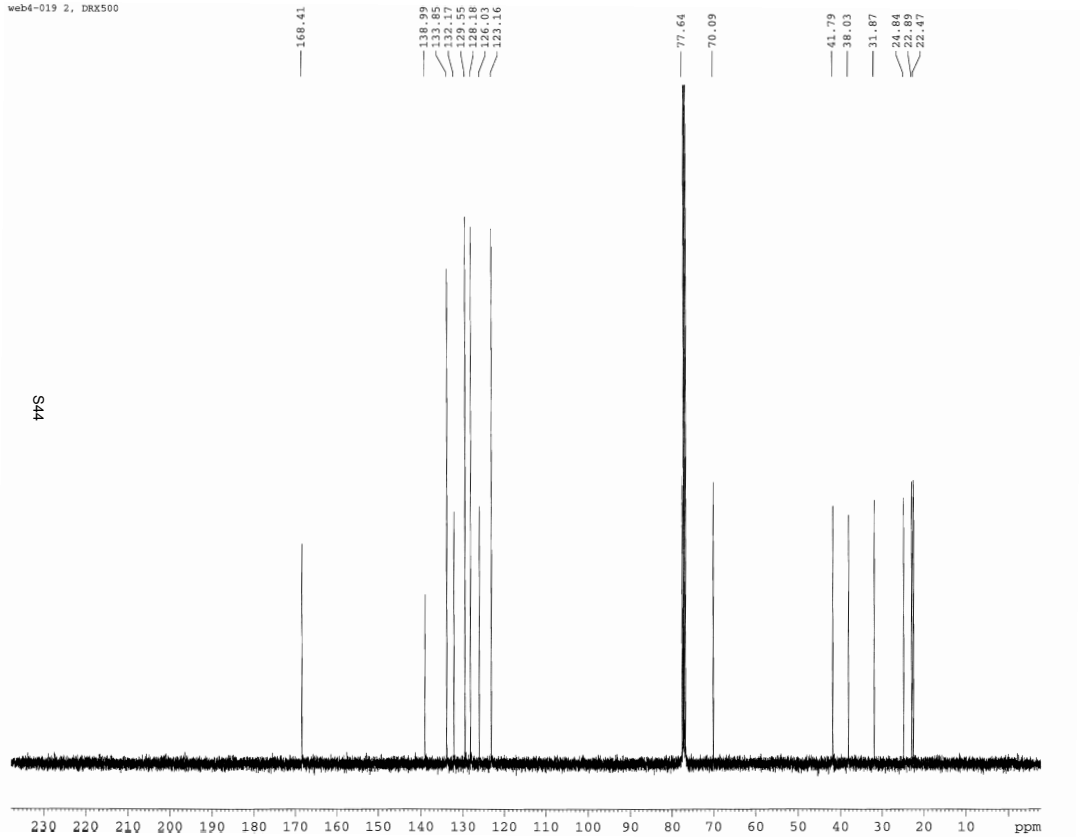

1.6e

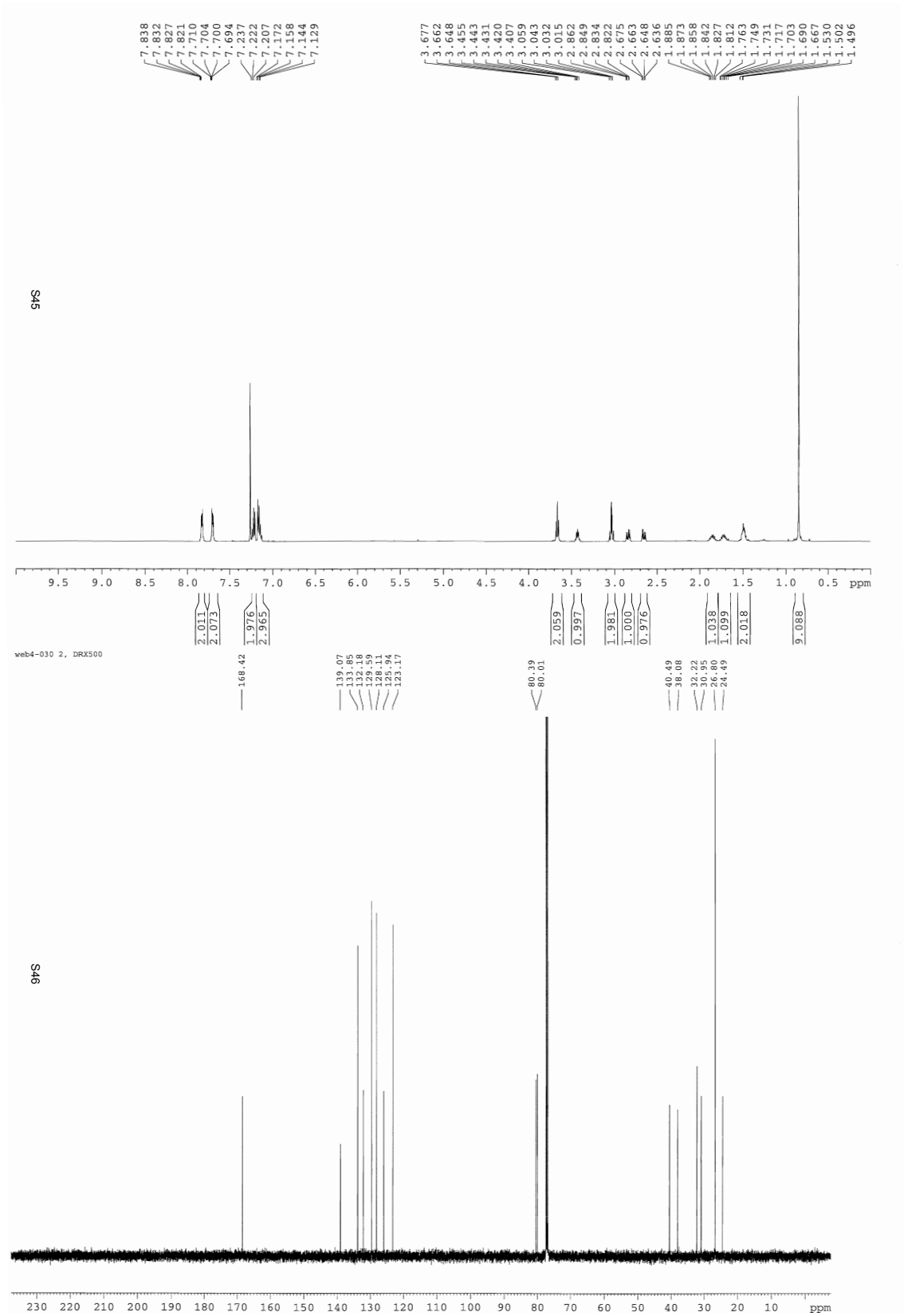
S45
7.838
7.832
7.827
7.821
7.710
7.704
7.700
7.694
7.237
7.222
7.207
7.172
7.158
7.144
7.129
3.677
3.662
3.648
3.455
3.443
3.431
3.420
3.407
3.059
3.043
3.032
3.015
2.862
2.849
2.834
2.822
2.675
2.663
2.648
2.636
1.885
1.873
1.858
1.842
1.827
1.812
1.763
1.749
1.731
1.717
1.703
1.690
1.667
1.530
1.502
1.496
ppm
2.011
2.073
1.976
2.965
2.059
0.997
1.981
1.000
0.976
1.038
1.099
2.018
9.088
web4-030 2, DRX500
168.42
139.07
133.85
132.18
129.59
128.11
125.94
123.17
80.39
80.01
40.49
38.08
32.22
30.95
26.80
24.49
S46
ppm

1.6f

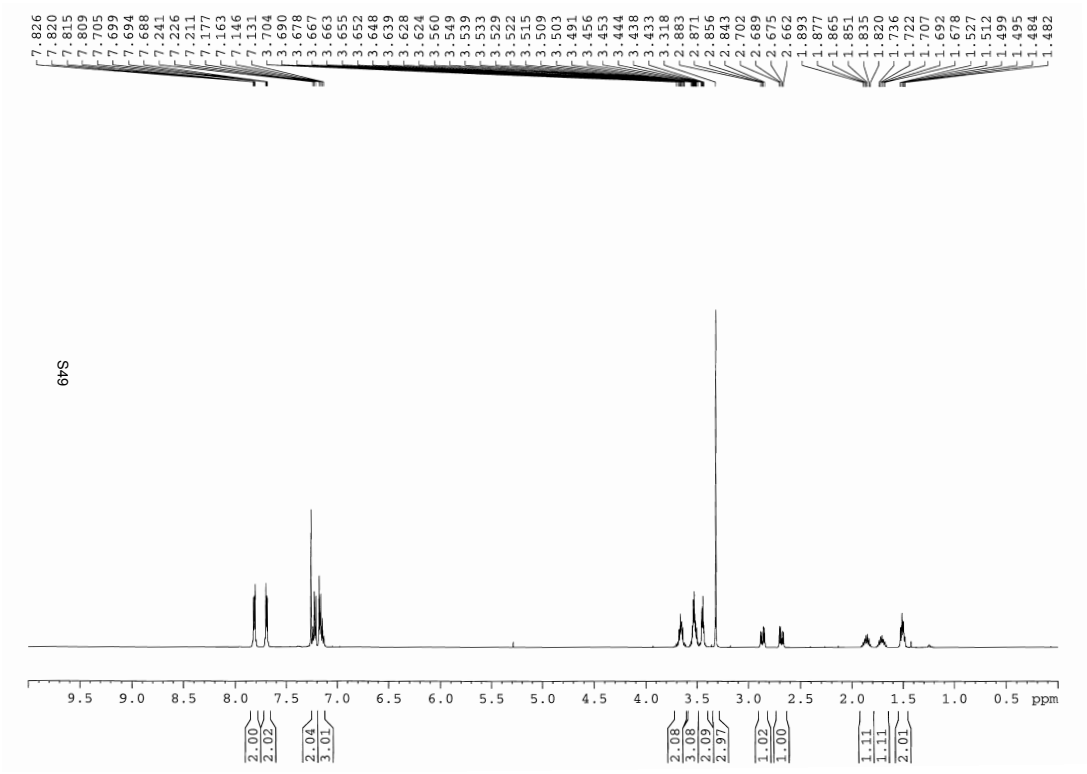
S49
9.5 9.0 8.5 8.0 7.5 7.0 6.5 6.0 5.5 5.0 4.5 4.0 3.5 3.0 2.5 2.0 1.5 1.0 0.5 ppm
2.00 2.02 2.04 3.01 2.08 3.08 2.09 2.97 1.02 1.00 1.11 1.11 2.01

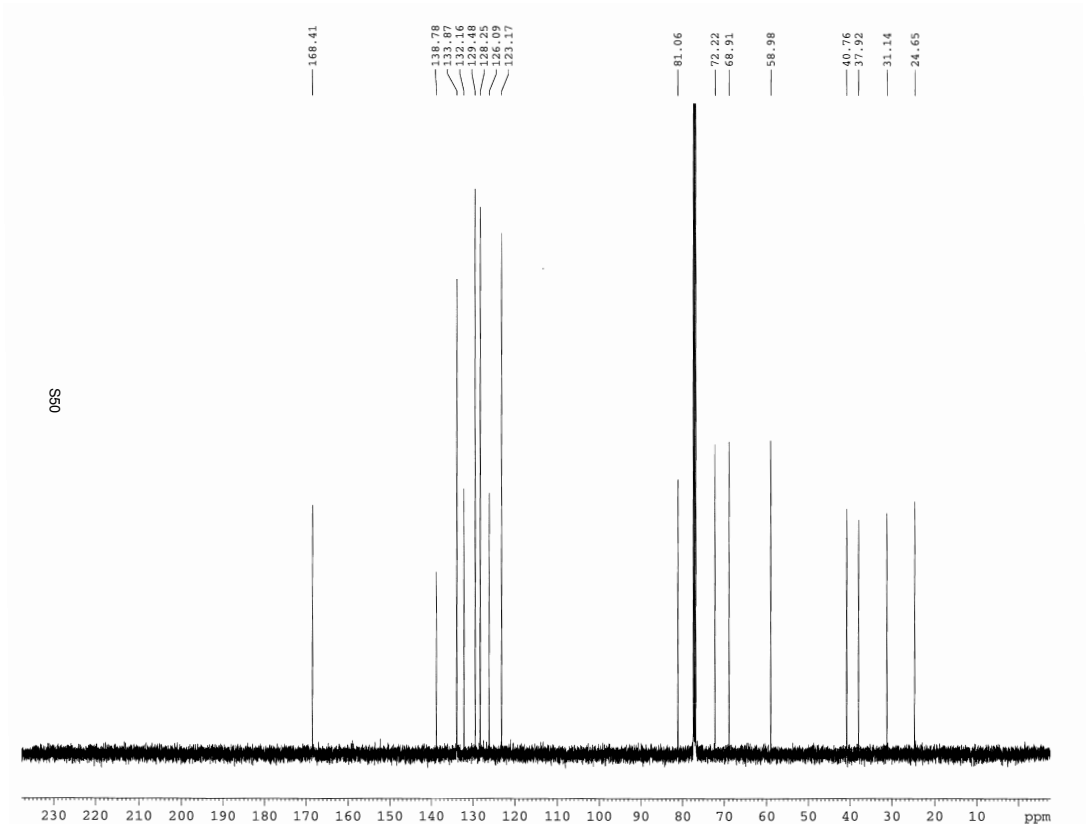
S50
168.41
138.78 133.87 132.16 129.48 128.25 126.09 123.17
81.06
72.22 68.91
58.98
40.76 37.92
31.14
24.65
230 220 210 200 190 180 170 160 150 140 130 120 110 100 90 80 70 60 50 40 30 20 10 ppm

1.6g

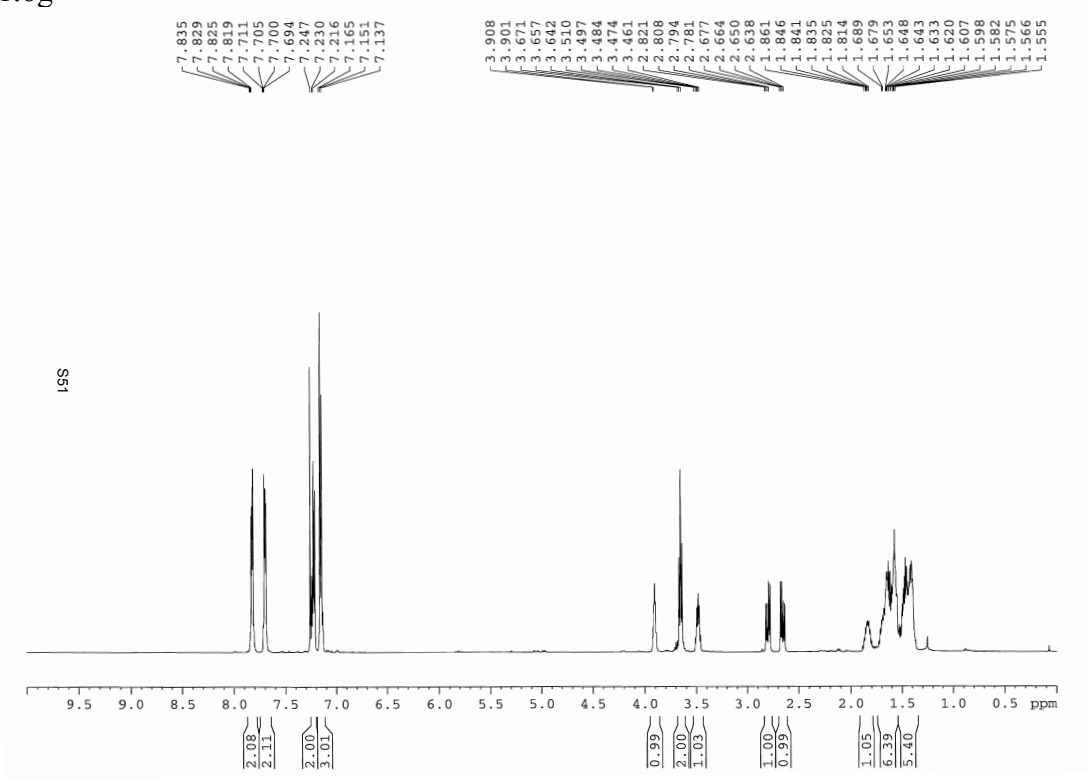
7.835
7.829
7.825
7.819
7.711
7.705
7.700
7.694
7.247
7.230
7.216
7.165
7.151
7.137
3.908
3.901
3.671
3.657
3.642
3.510
3.497
3.484
3.474
3.461
2.821
2.808
2.794
2.781
2.677
2.664
2.650
2.638
1.861
1.846
1.841
1.835
1.825
1.814
1.689
1.679
1.653
1.648
1.643
1.633
1.620
1.607
1.598
1.582
1.575
1.566
1.555
S51
9.5 9.0 8.5 8.0 7.5 7.0 6.5 6.0 5.5 5.0 4.5 4.0 3.5 3.0 2.5 2.0 1.5 1.0 0.5 ppm
2.08
2.11
2.00
3.01
0.99
2.00
1.03
1.00
0.99
1.05
6.39
5.40

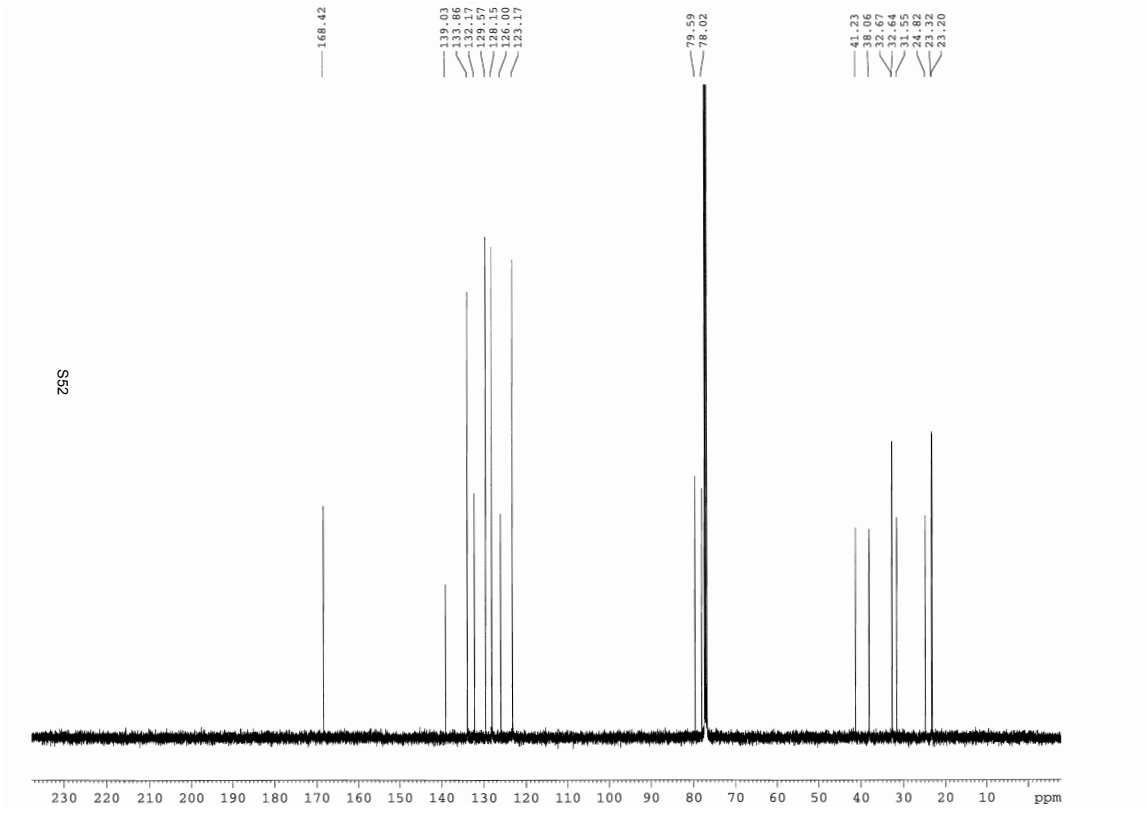
168.42
139.03
131.86
132.17
129.57
128.15
126.00
123.17
79.59
78.02
41.23
38.06
32.67
32.64
31.55
24.82
23.32
23.20
S52
230 220 210 200 190 180 170 160 150 140 130 120 110 100 90 80 70 60 50 40 30 20 10 ppm

1.6h

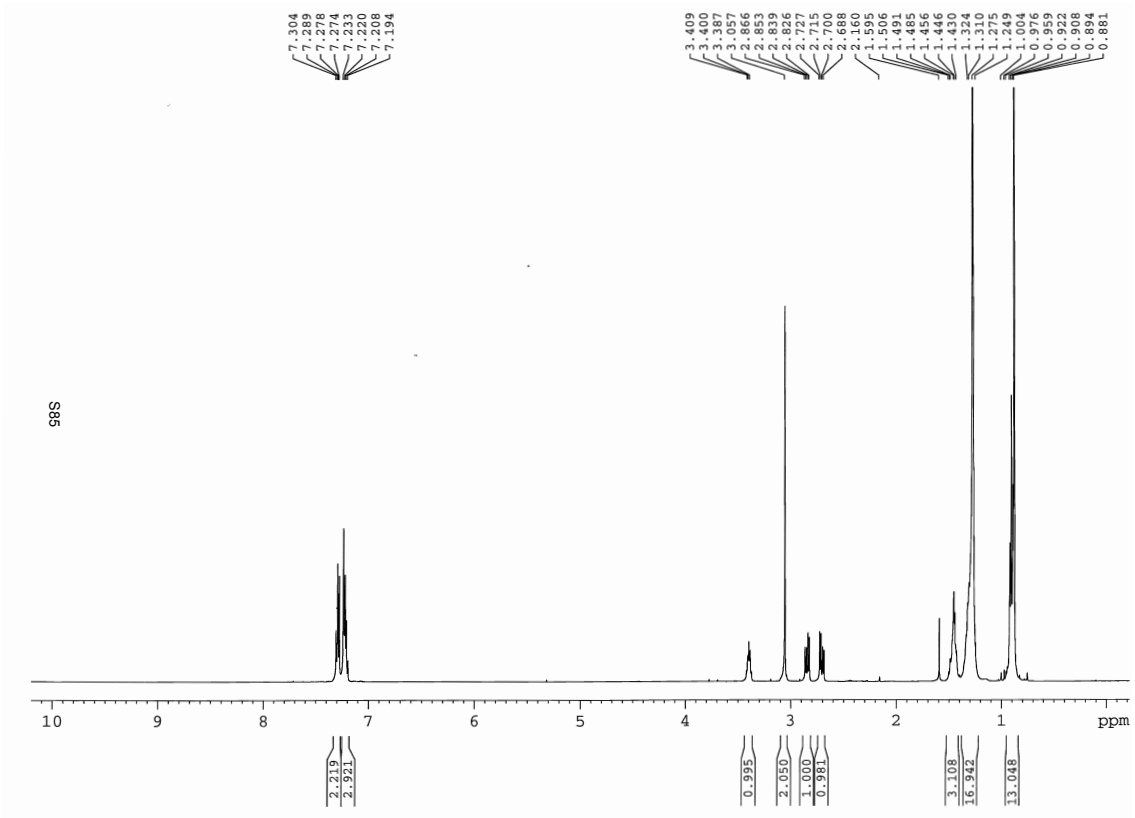
S85
7.304
7.289
7.278
7.274
7.233
7.220
7.208
7.194
3.409
3.400
3.387
3.057
2.866
2.853
2.839
2.826
2.727
2.715
2.700
2.688
2.160
1.595
1.596
1.481
1.465
1.446
1.430
1.324
1.310
1.275
1.249
1.004
0.976
0.959
0.922
0.908
0.894
0.881
10
9
8
7
6
5
4
3
2
1
ppm
2.219
2.921
0.995
2.050
1.000
0.981
3.108
16.942
13.048

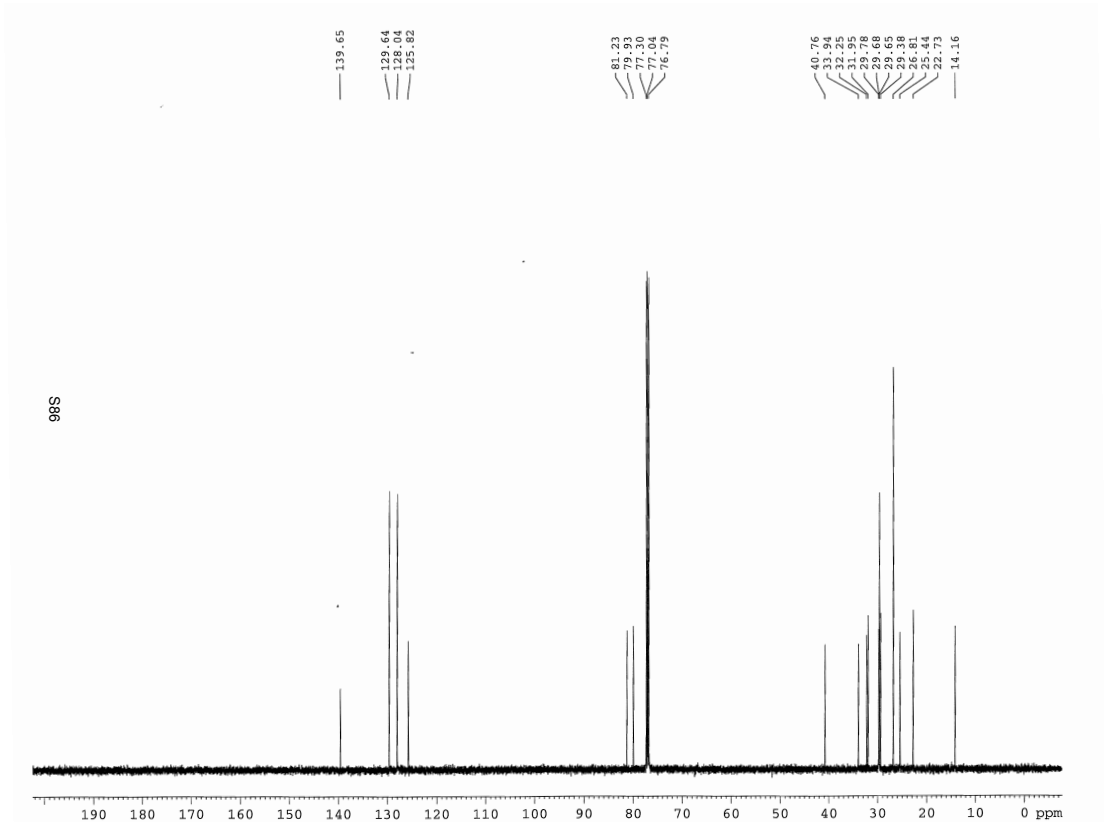
S86
139.65
129.64
128.04
125.82
81.23
79.93
77.30
77.04
76.79
40.76
33.94
32.25
31.95
29.78
29.68
29.65
29.38
26.81
25.44
22.73
14.16
190
180
170
160
150
140
130
120
110
100
90
80
70
60
50
40
30
20
10
0 ppm

1.6i

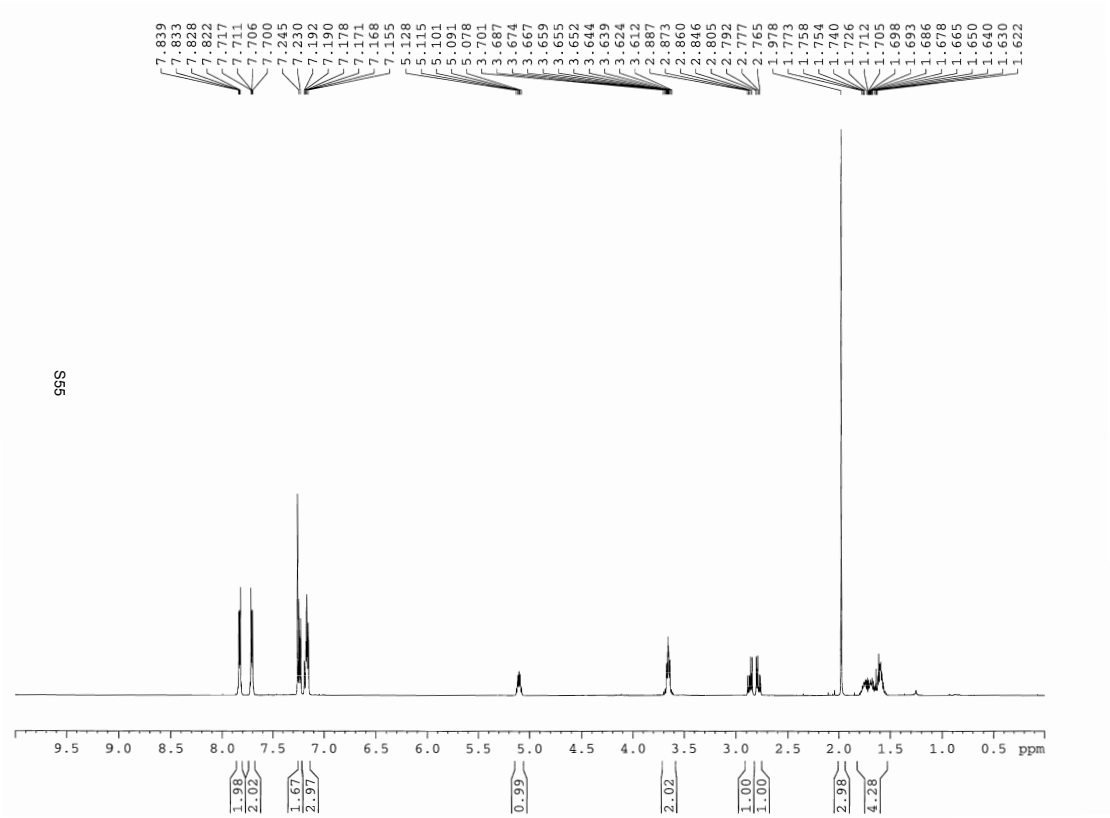
7.839
7.833
7.828
7.822
7.717
7.711
7.706
7.700
7.245
7.230
7.192
7.190
7.178
7.171
7.168
7.155
5.128
5.115
5.101
5.091
5.078
3.701
3.687
3.674
3.667
3.659
3.655
3.652
3.644
3.639
3.624
3.612
2.887
2.873
2.860
2.846
2.805
2.792
2.777
2.765
1.978
1.773
1.758
1.754
1.740
1.726
1.712
1.705
1.698
1.693
1.686
1.678
1.665
1.650
1.640
1.630
1.622
S55
9.5 9.0 8.5 8.0 7.5 7.0 6.5 6.0 5.5 5.0 4.5 4.0 3.5 3.0 2.5 2.0 1.5 1.0 0.5 ppm
1.98
2.02
1.67
2.97
0.99
2.02
1.00
1.00
2.98
4.28

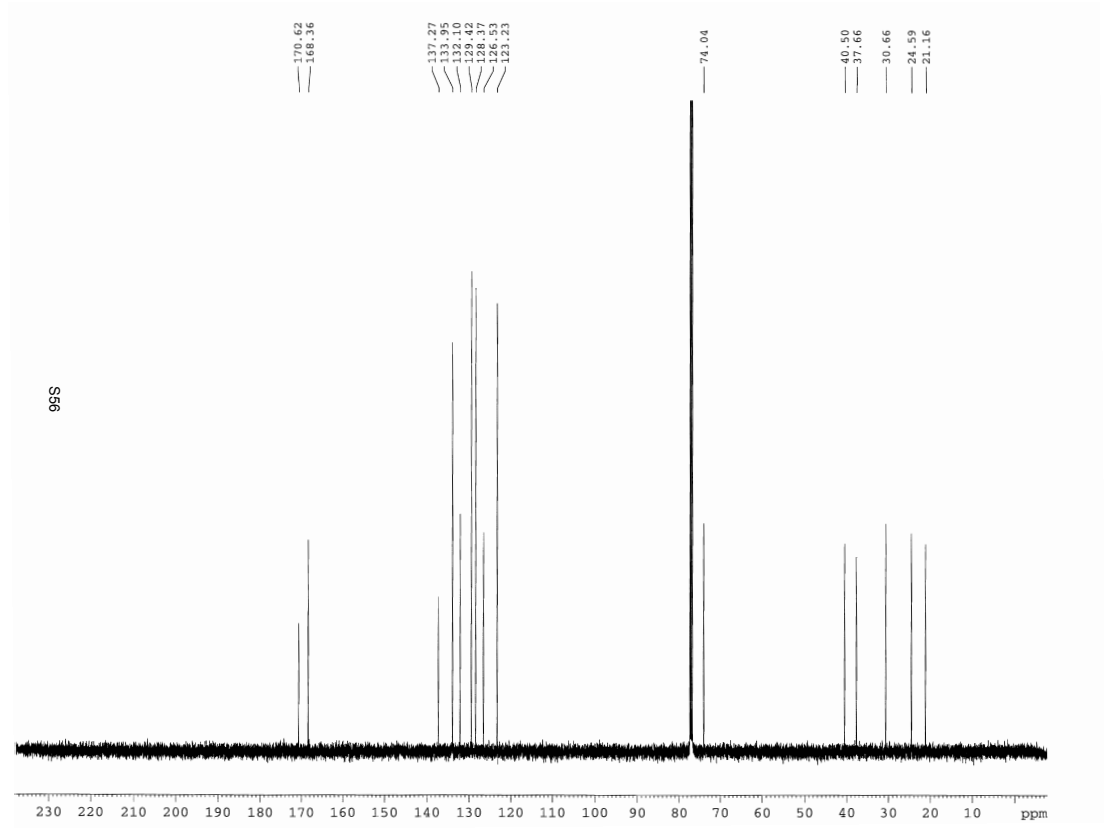
170.62
168.36
137.27
133.95
132.10
129.42
128.17
126.53
123.23
74.04
40.50
37.66
30.66
24.59
21.16
S56
230 220 210 200 190 180 170 160 150 140 130 120 110 100 90 80 70 60 50 40 30 20 10 ppm

1.6j

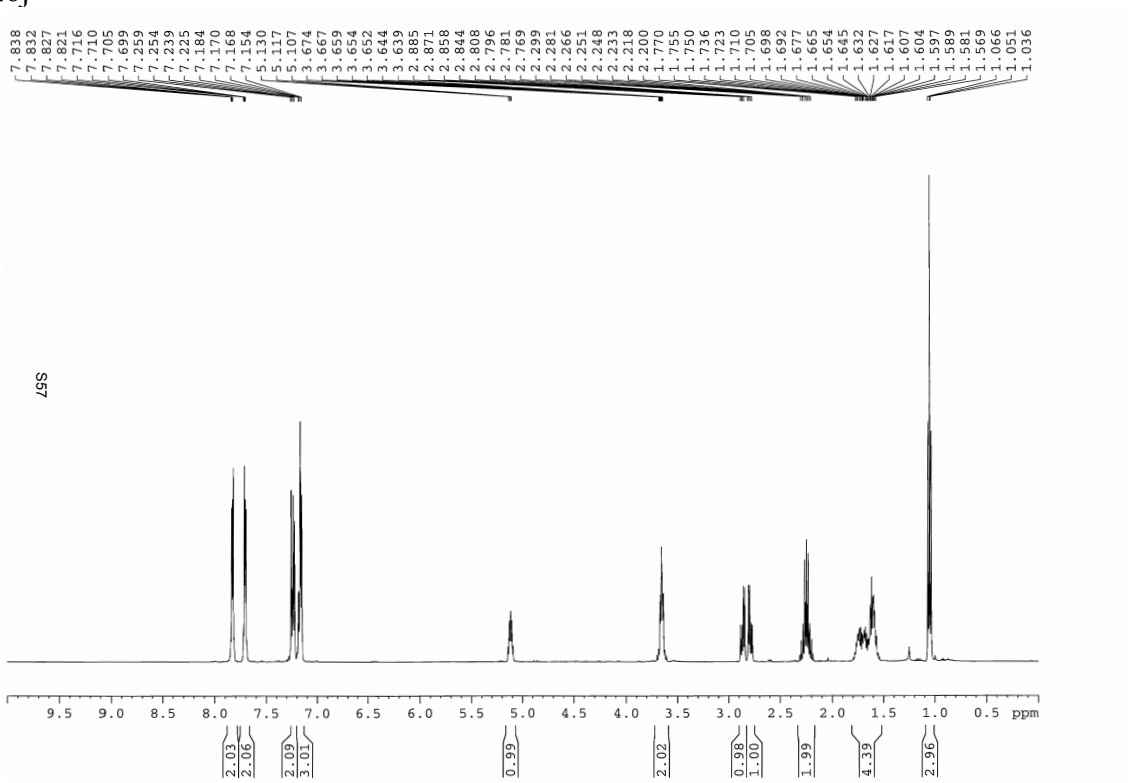
7.838
7.832
7.827
7.821
7.716
7.710
7.705
7.699
7.259
7.254
7.239
7.225
7.184
7.170
7.168
7.154
5.130
5.117
5.107
3.674
3.667
3.659
3.654
3.652
3.644
3.639
2.885
2.871
2.858
2.844
2.808
2.796
2.781
2.769
2.299
2.281
2.266
2.251
2.248
2.233
2.218
2.200
1.770
1.755
1.750
1.736
1.723
1.710
1.705
1.698
1.692
1.677
1.665
1.654
1.645
1.632
1.627
1.617
1.607
1.604
1.597
1.589
1.581
1.569
1.066
1.051
1.036
S57
9.5 9.0 8.5 8.0 7.5 7.0 6.5 6.0 5.5 5.0 4.5 4.0 3.5 3.0 2.5 2.0 1.5 1.0 0.5 ppm
2.03
2.06
2.09
3.01
0.99
2.02
0.98
1.00
1.99
4.39
2.96

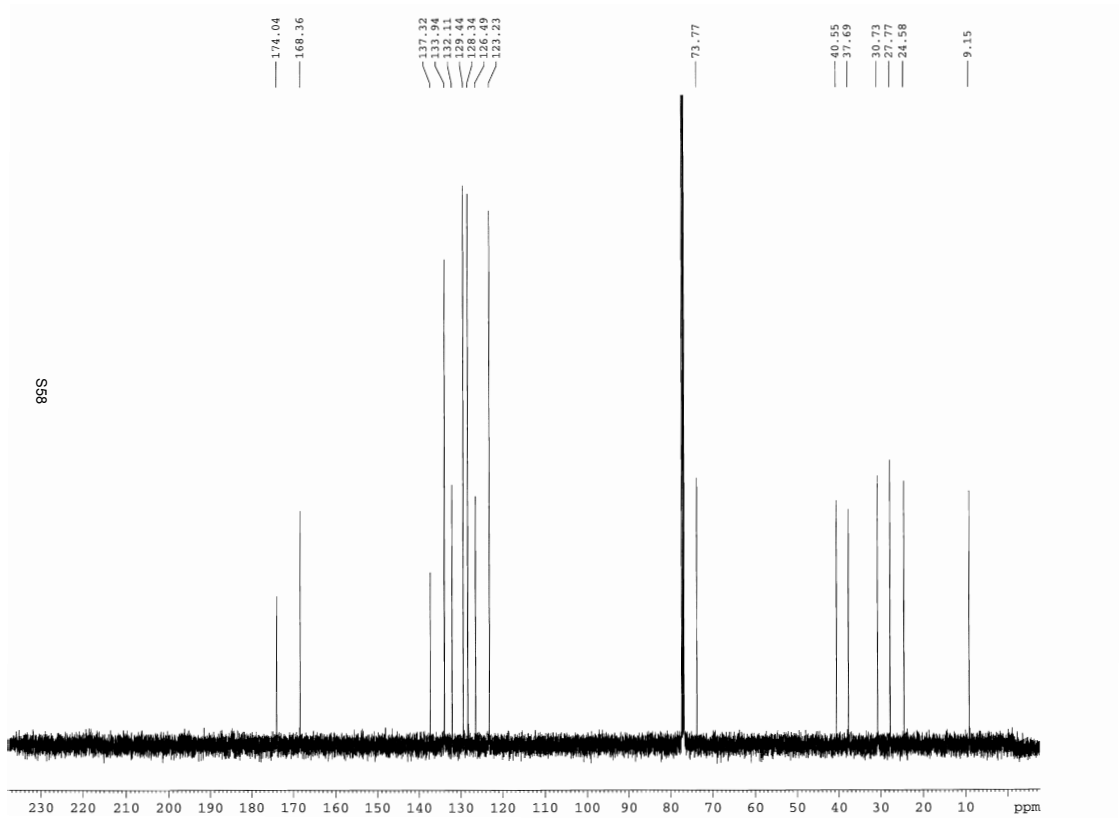
174.04
168.36
137.32
133.94
132.11
129.44
128.34
126.49
123.23
73.77
40.55
37.69
30.73
27.77
24.58
9.15
S58
230 220 210 200 190 180 170 160 150 140 130 120 110 100 90 80 70 60 50 40 30 20 10 ppm

1.6k

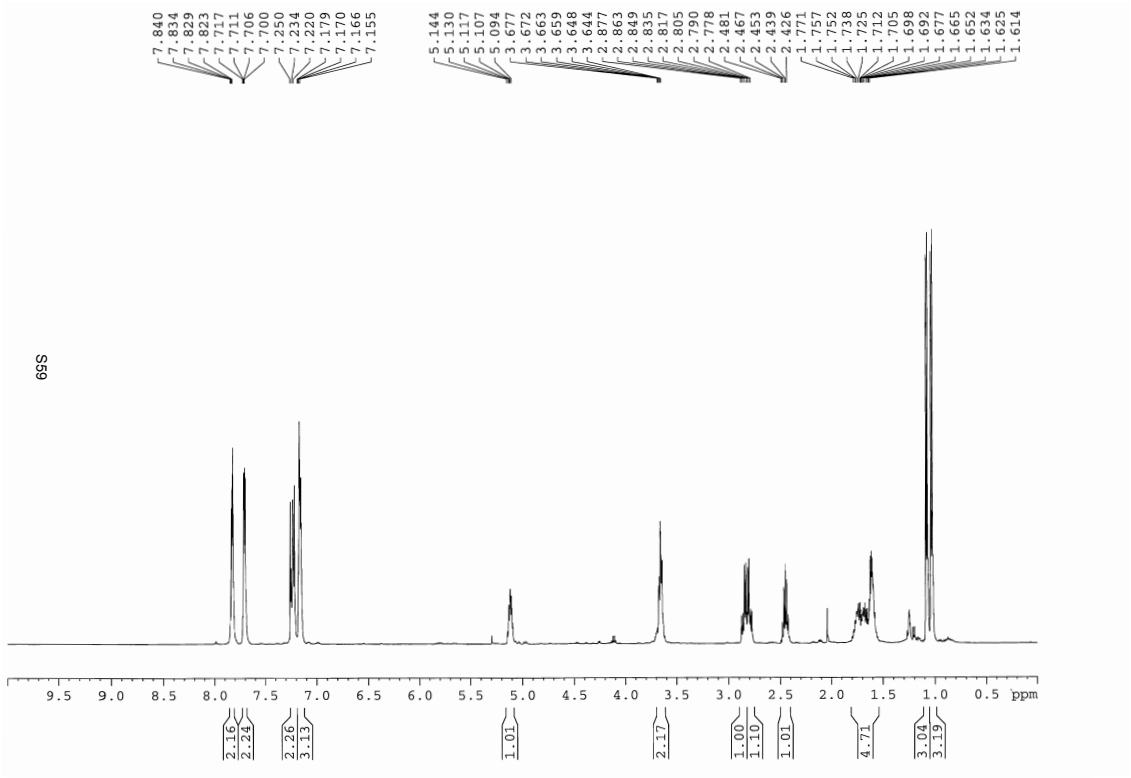
7.840
7.834
7.829
7.823
7.717
7.711
7.706
7.700
7.250
7.234
7.220
7.179
7.170
7.166
7.155
5.144
5.130
5.117
5.107
5.094
3.677
3.672
3.663
3.659
3.648
3.644
2.877
2.863
2.849
2.835
2.817
2.805
2.790
2.778
2.481
2.467
2.453
2.439
2.426
1.771
1.757
1.752
1.738
1.725
1.712
1.705
1.698
1.692
1.677
1.665
1.652
1.634
1.625
1.614
S59
9.5 9.0 8.5 8.0 7.5 7.0 6.5 6.0 5.5 5.0 4.5 4.0 3.5 3.0 2.5 2.0 1.5 1.0 0.5 ppm
2.16
2.24
2.26
3.13
1.01
2.17
1.00
1.10
1.01
4.71
3.04
3.19

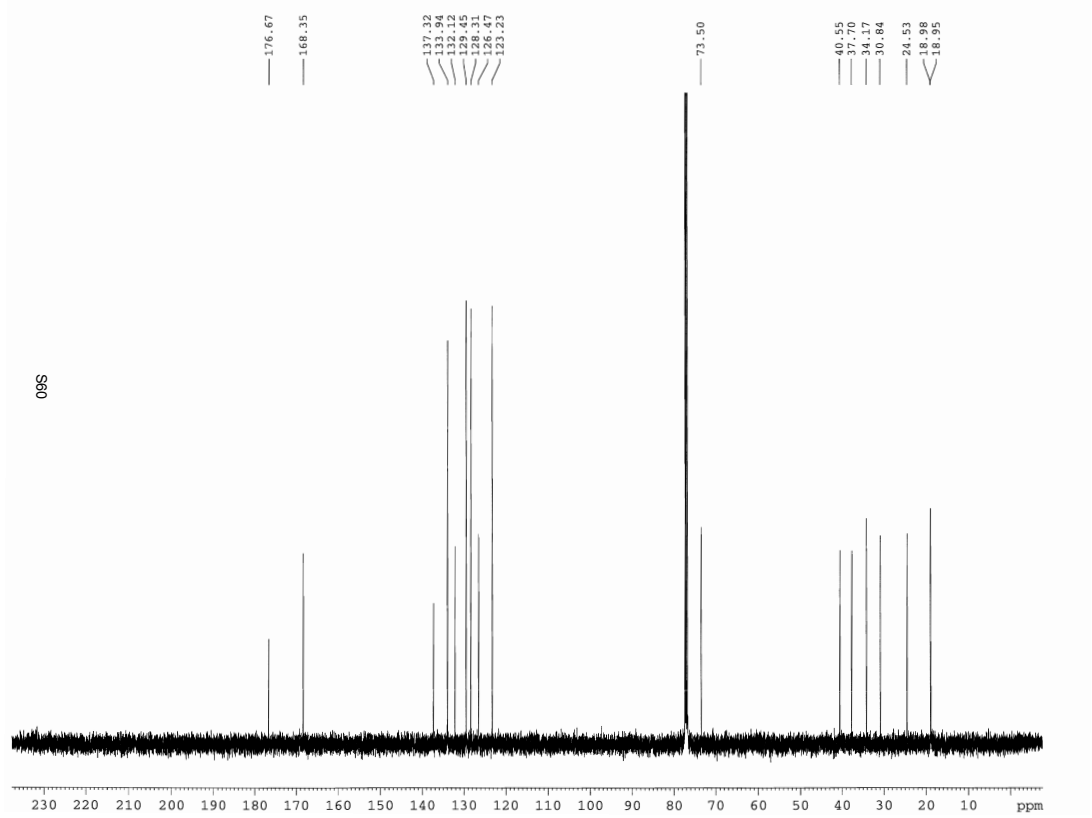
176.67
168.35
137.32
131.94
132.12
129.45
128.31
126.47
123.23
73.50
40.55
37.70
34.17
30.84
24.53
18.98
18.95
S60
230 220 210 200 190 180 170 160 150 140 130 120 110 100 90 80 70 60 50 40 30 20 10 ppm

1.6l

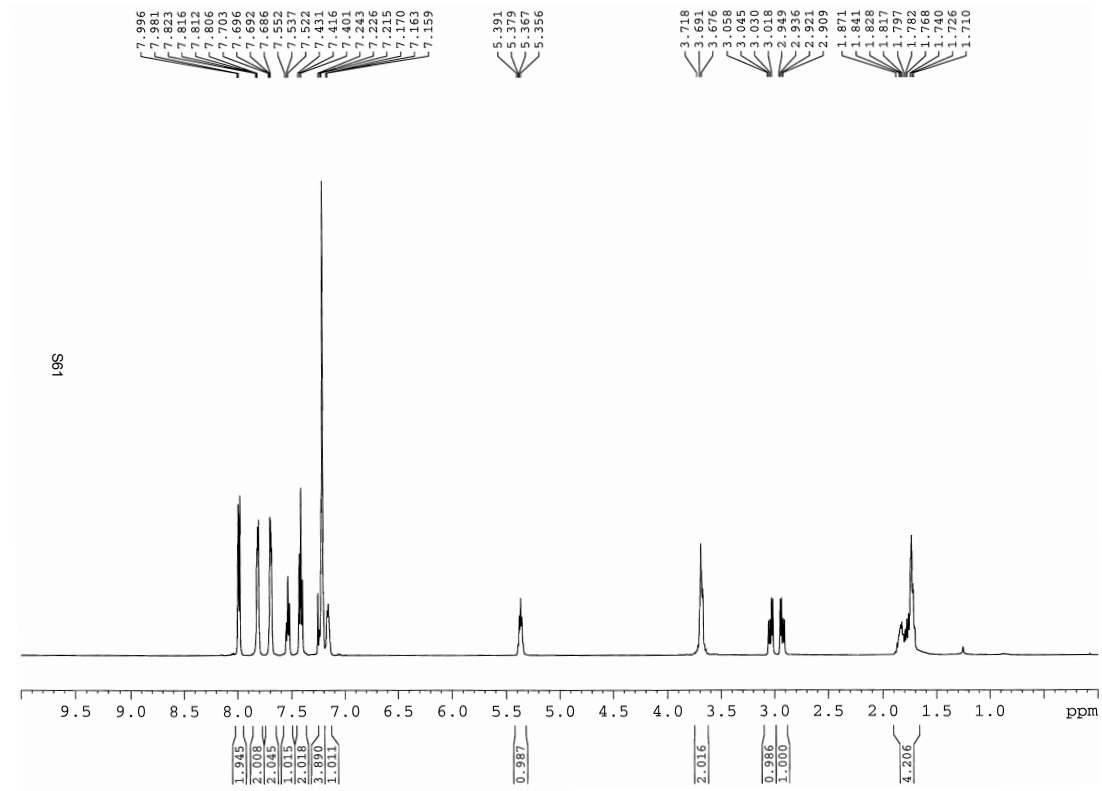
7.996
7.981
7.823
7.816
7.812
7.806
7.703
7.696
7.692
7.686
7.552
7.537
7.522
7.431
7.416
7.401
7.243
7.226
7.215
7.170
7.163
7.159
5.391
5.379
5.367
5.356
3.718
3.691
3.676
3.058
3.045
3.030
3.018
2.949
2.936
2.921
2.909
1.871
1.841
1.828
1.817
1.797
1.782
1.768
1.740
1.726
1.710
S61
9.5 9.0 8.5 8.0 7.5 7.0 6.5 6.0 5.5 5.0 4.5 4.0 3.5 3.0 2.5 2.0 1.5 1.0 ppm
1.945
2.008
2.045
1.015
2.018
3.890
1.011
0.987
2.016
0.986
1.000
4.206

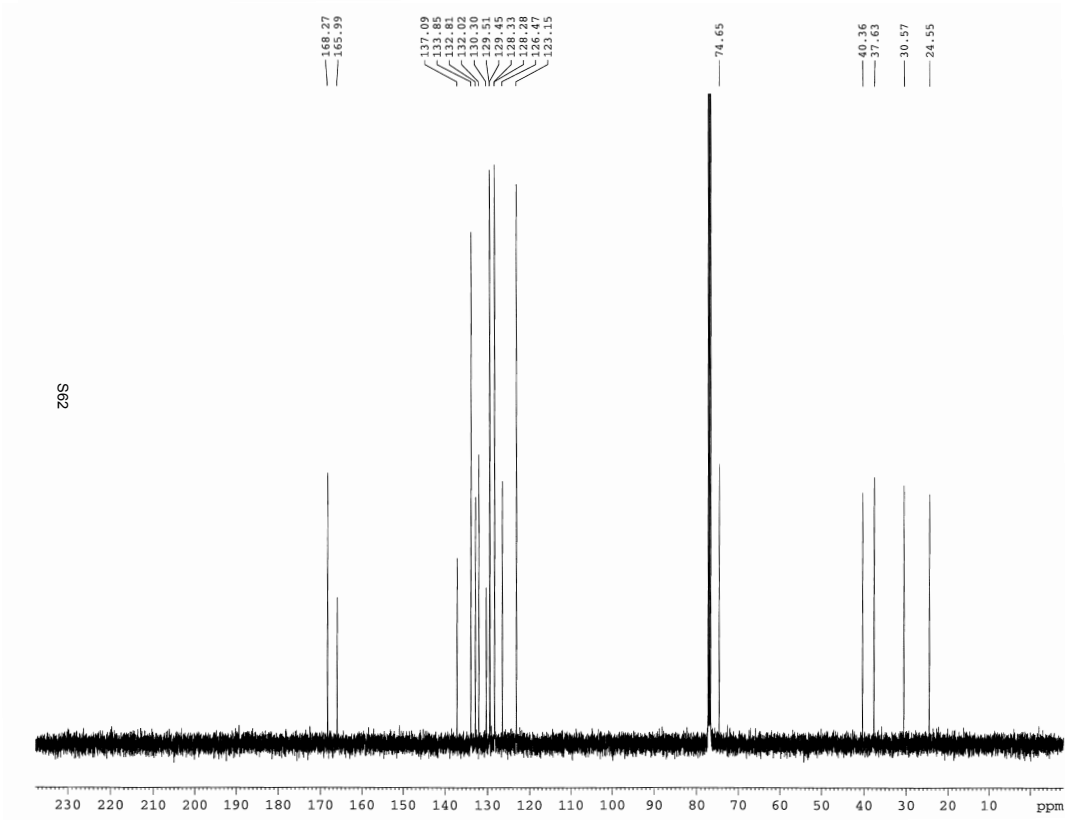
168.27
165.99
137.09
133.85
132.81
132.02
130.30
129.51
129.45
128.33
128.28
126.47
123.15
74.65
40.36
37.63
30.57
24.55
S62
230 220 210 200 190 180 170 160 150 140 130 120 110 100 90 80 70 60 50 40 30 20 10 ppm

1.6m

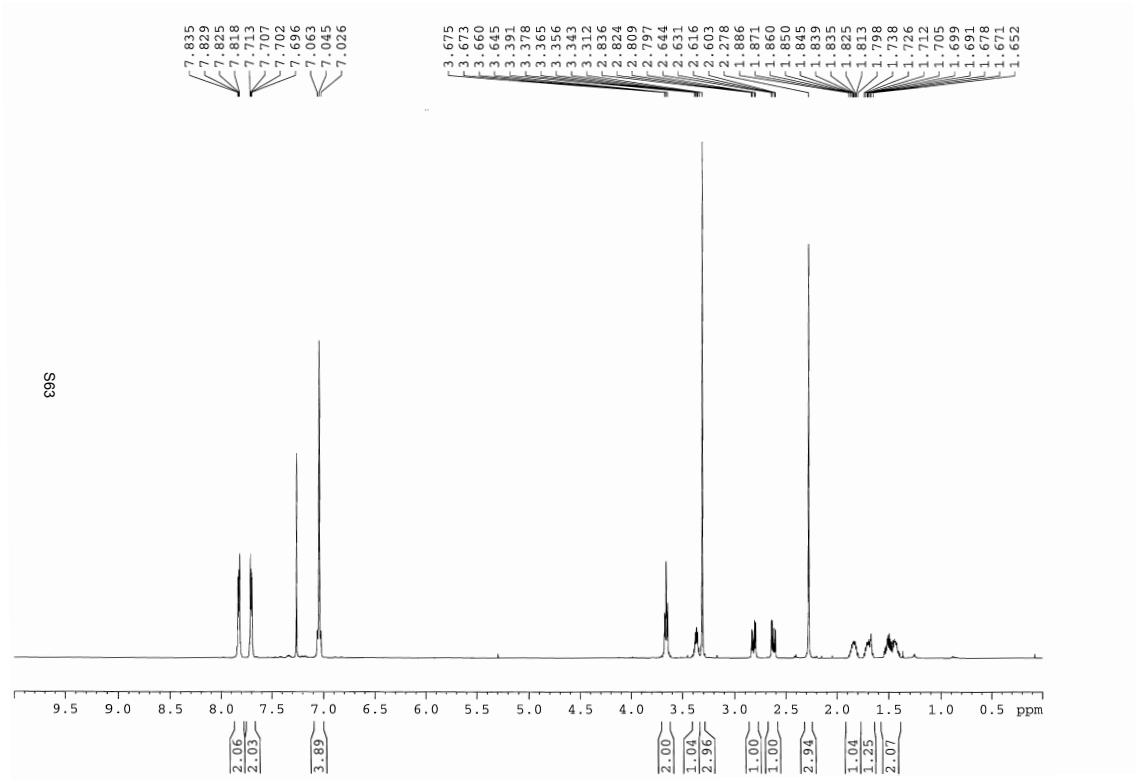
7.835
7.829
7.825
7.818
7.713
7.707
7.702
7.696
7.063
7.045
7.026
3.675
3.673
3.660
3.645
3.391
3.378
3.365
3.356
3.343
3.312
2.836
2.824
2.809
2.797
2.644
2.631
2.616
2.603
2.278
1.886
1.871
1.860
1.850
1.845
1.839
1.835
1.825
1.813
1.798
1.738
1.726
1.712
1.705
1.699
1.691
1.678
1.671
1.652
S63
9.5 9.0 8.5 8.0 7.5 7.0 6.5 6.0 5.5 5.0 4.5 4.0 3.5 3.0 2.5 2.0 1.5 1.0 0.5 ppm
2.06
2.03
3.89
2.00
1.04
2.96
1.00
1.00
2.94
1.04
1.25
2.07

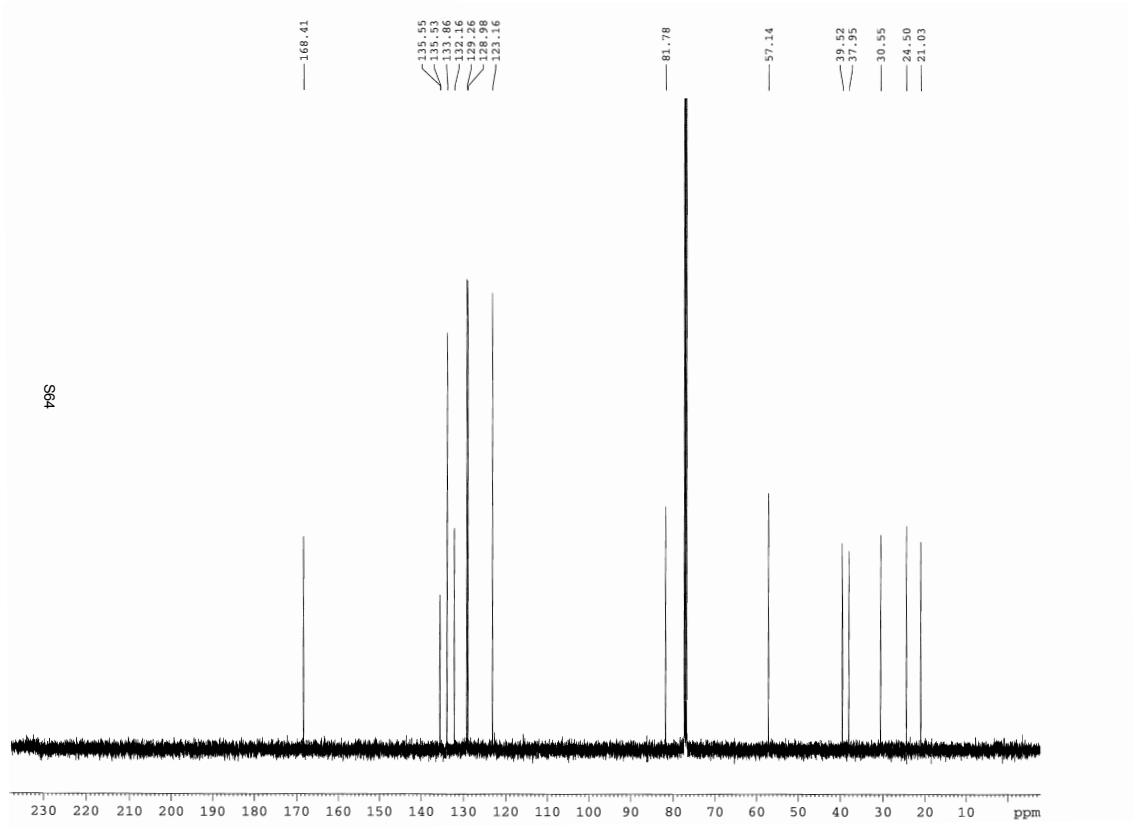
168.41
135.55
135.53
133.86
132.16
129.26
128.98
123.16
81.78
57.14
39.52
37.95
30.55
24.50
21.03
S64
230 220 210 200 190 180 170 160 150 140 130 120 110 100 90 80 70 60 50 40 30 20 10 ppm

1.6n

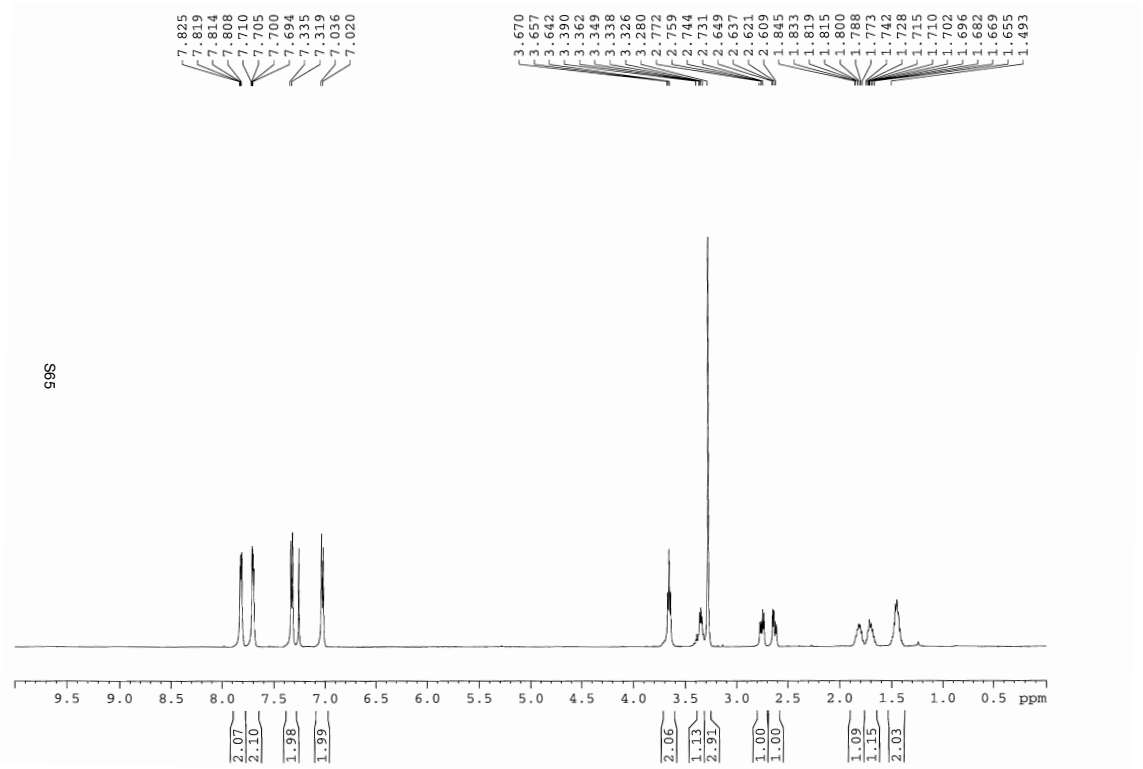
7.825
7.819
7.814
7.808
7.710
7.705
7.700
7.694
7.335
7.319
7.036
7.020
3.670
3.657
3.642
3.390
3.362
3.349
3.338
3.326
3.280
2.772
2.759
2.744
2.731
2.649
2.637
2.621
2.609
1.845
1.833
1.819
1.815
1.800
1.788
1.773
1.742
1.728
1.715
1.710
1.702
1.696
1.682
1.669
1.655
1.493
S65
9.5 9.0 8.5 8.0 7.5 7.0 6.5 6.0 5.5 5.0 4.5 4.0 3.5 3.0 2.5 2.0 1.5 1.0 0.5 ppm
2.07
2.10
1.98
1.99
2.06
1.13
2.91
1.00
1.00
1.09
1.15
2.03

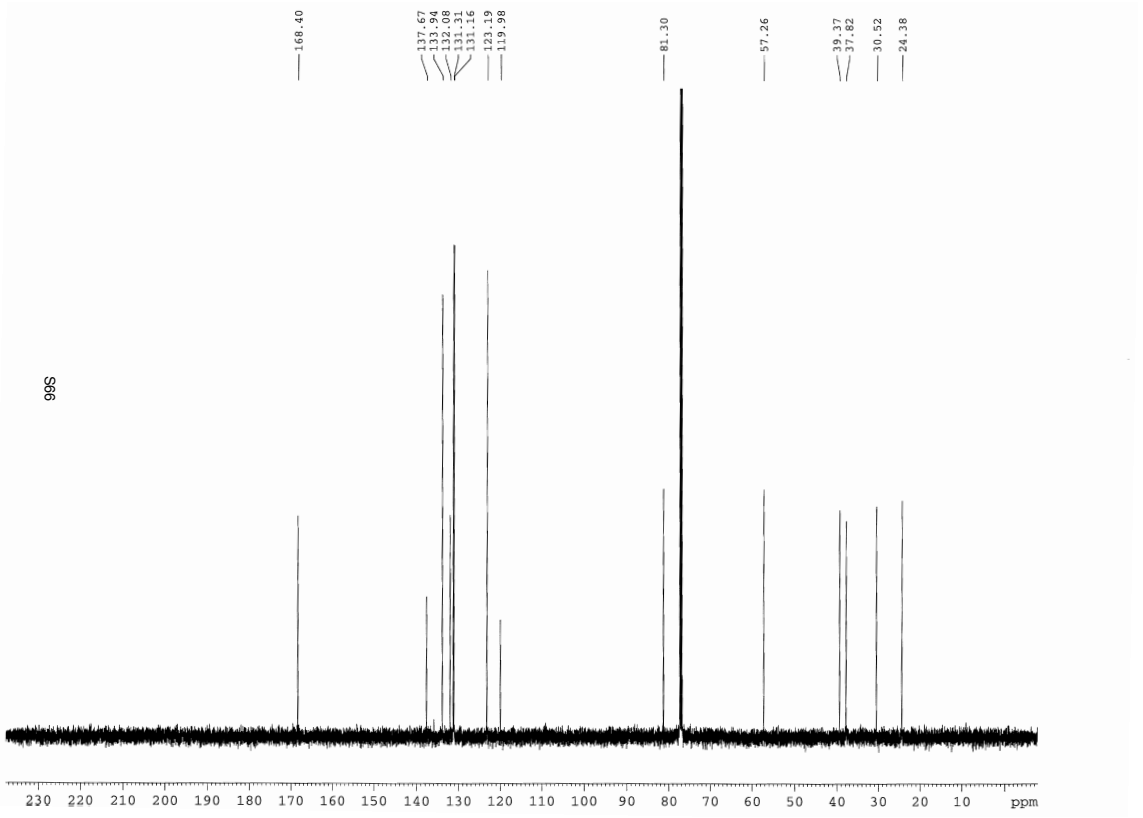
168.40
137.67
133.94
132.08
131.31
131.16
123.19
119.98
81.30
57.26
39.37
37.82
30.52
24.38
S66
230 220 210 200 190 180 170 160 150 140 130 120 110 100 90 80 70 60 50 40 30 20 10 ppm

1.6o

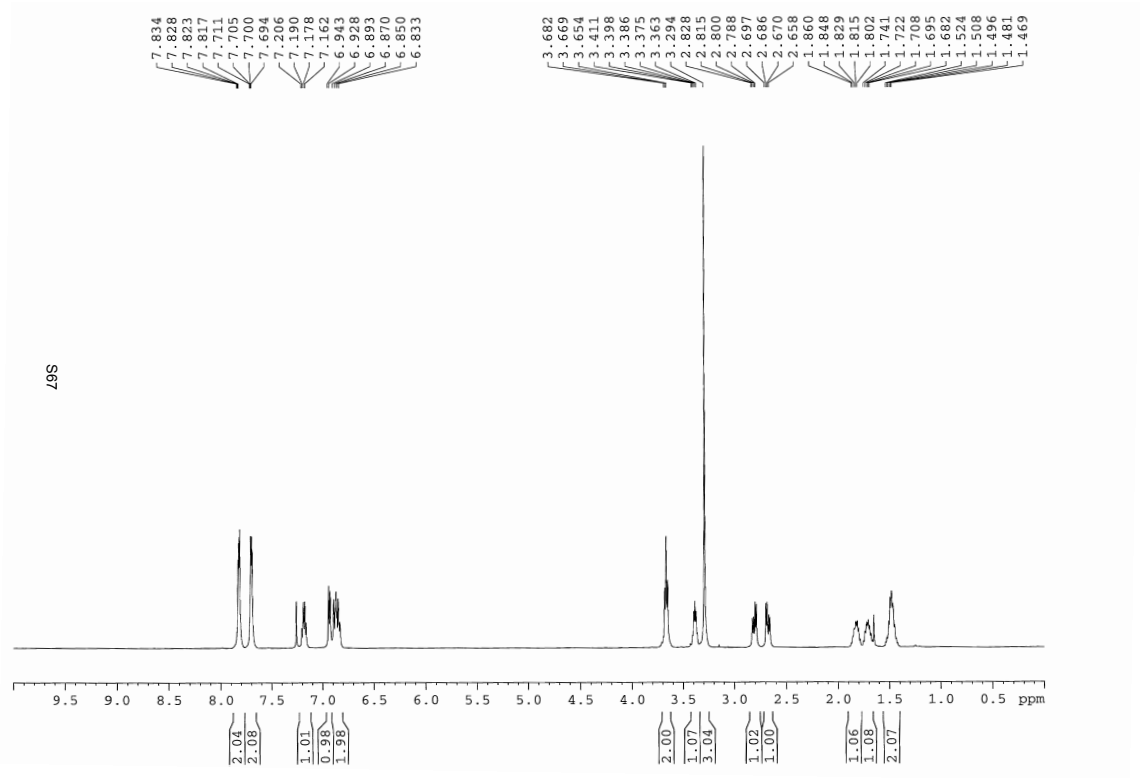
S67
7.834
7.828
7.823
7.817
7.711
7.705
7.700
7.694
7.206
7.190
7.178
7.162
6.943
6.928
6.893
6.870
6.850
6.833
3.682
3.669
3.654
3.411
3.398
3.386
3.375
3.363
3.294
2.828
2.815
2.800
2.788
2.697
2.686
2.670
2.658
1.860
1.848
1.829
1.815
1.802
1.741
1.722
1.708
1.695
1.682
1.524
1.508
1.496
1.481
1.469
9.5 9.0 8.5 8.0 7.5 7.0 6.5 6.0 5.5 5.0 4.5 4.0 3.5 3.0 2.5 2.0 1.5 1.0 0.5 ppm
2.04
2.08
1.01
0.98
1.98
2.00
1.07
3.04
1.02
1.00
1.06
1.08
2.07

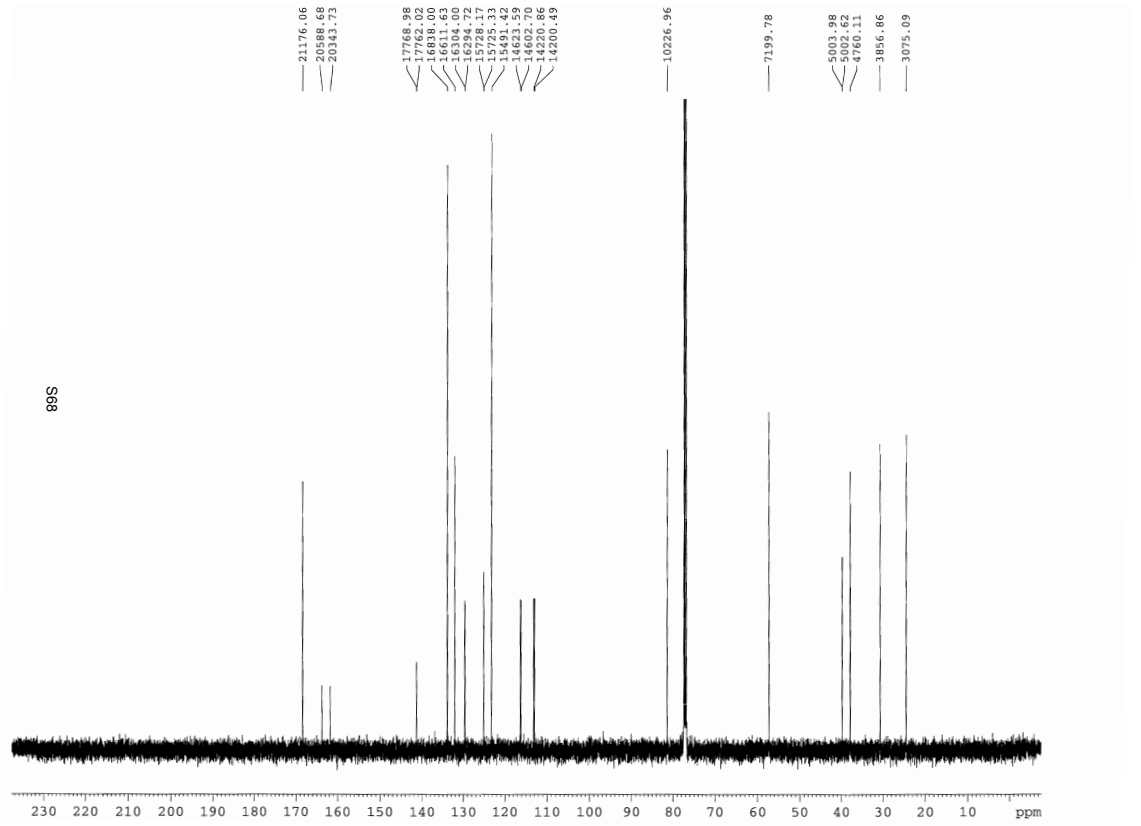
S68
21176.06
20588.68
20343.73
17768.98
17762.02
16811.00
16611.63
16304.00
16294.72
15728.17
15725.33
15491.42
14623.59
14621.70
14220.86
14200.49
10226.96
7199.78
5003.98
5002.62
4760.11
3856.86
3075.09
230 220 210 200 190 180 170 160 150 140 130 120 110 100 90 80 70 60 50 40 30 20 10 ppm

1.6p

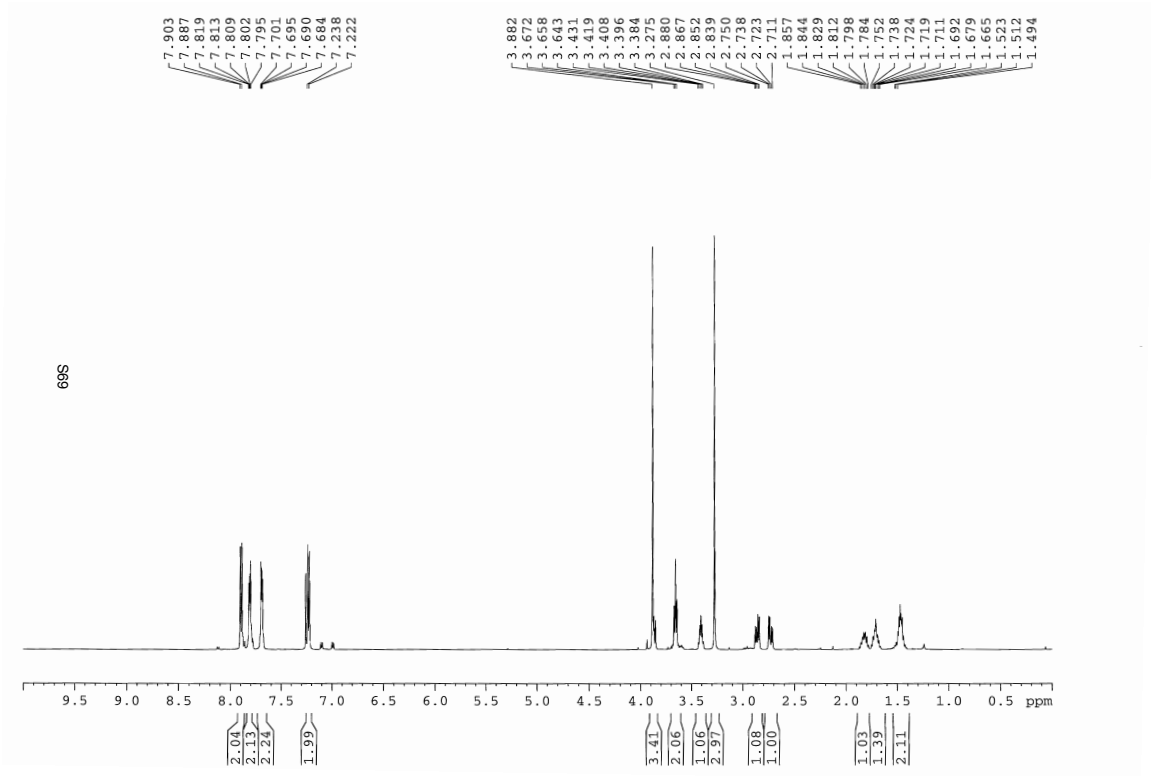
7.903
7.887
7.819
7.813
7.809
7.802
7.795
7.701
7.695
7.690
7.684
7.238
7.222
3.882
3.672
3.658
3.643
3.431
3.419
3.408
3.396
3.384
3.275
2.880
2.867
2.852
2.839
2.750
2.738
2.723
2.711
1.857
1.844
1.829
1.812
1.798
1.784
1.752
1.738
1.724
1.719
1.711
1.692
1.679
1.665
1.523
1.512
1.494
S69
9.5 9.0 8.5 8.0 7.5 7.0 6.5 6.0 5.5 5.0 4.5 4.0 3.5 3.0 2.5 2.0 1.5 1.0 0.5 ppm
2.04
2.13
2.24
1.99
3.41
2.06
1.06
2.97
1.08
1.00
1.03
1.39
2.11

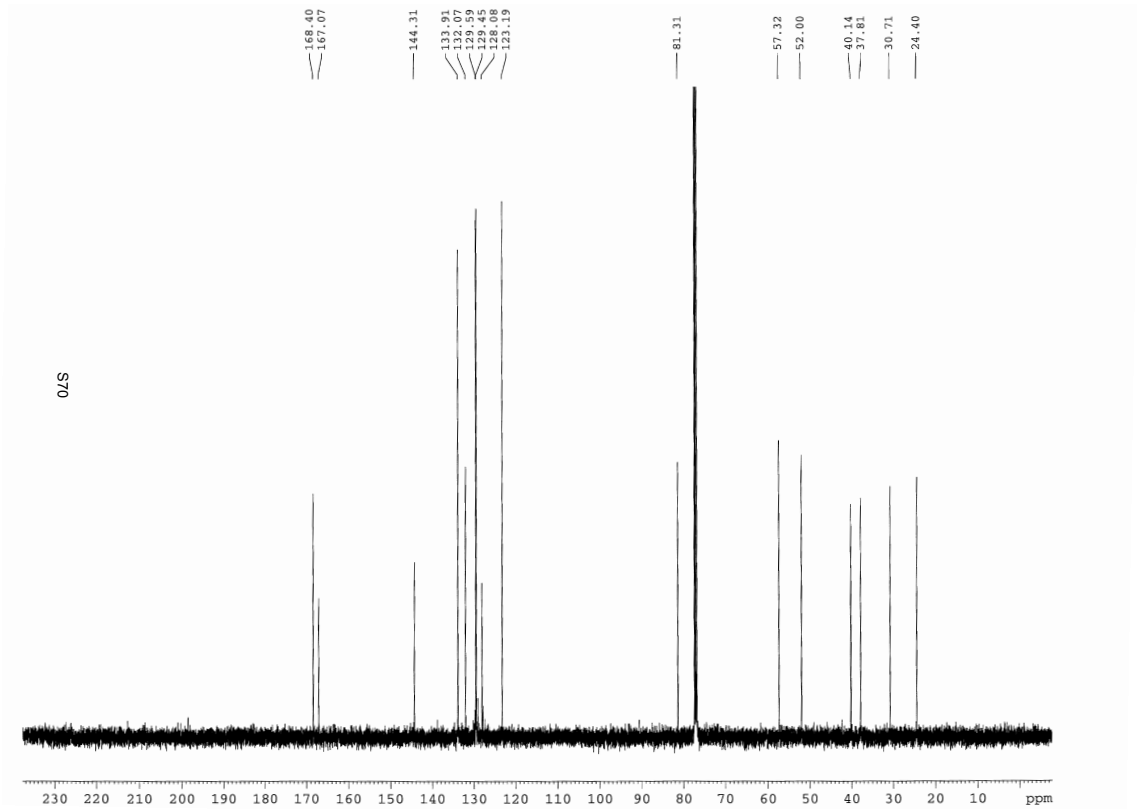
168.40
167.07
144.31
133.91
132.07
130.59
129.45
128.08
123.19
81.31
57.32
52.00
40.14
37.81
30.71
24.40
S70
230 220 210 200 190 180 170 160 150 140 130 120 110 100 90 80 70 60 50 40 30 20 10 ppm

1.6q

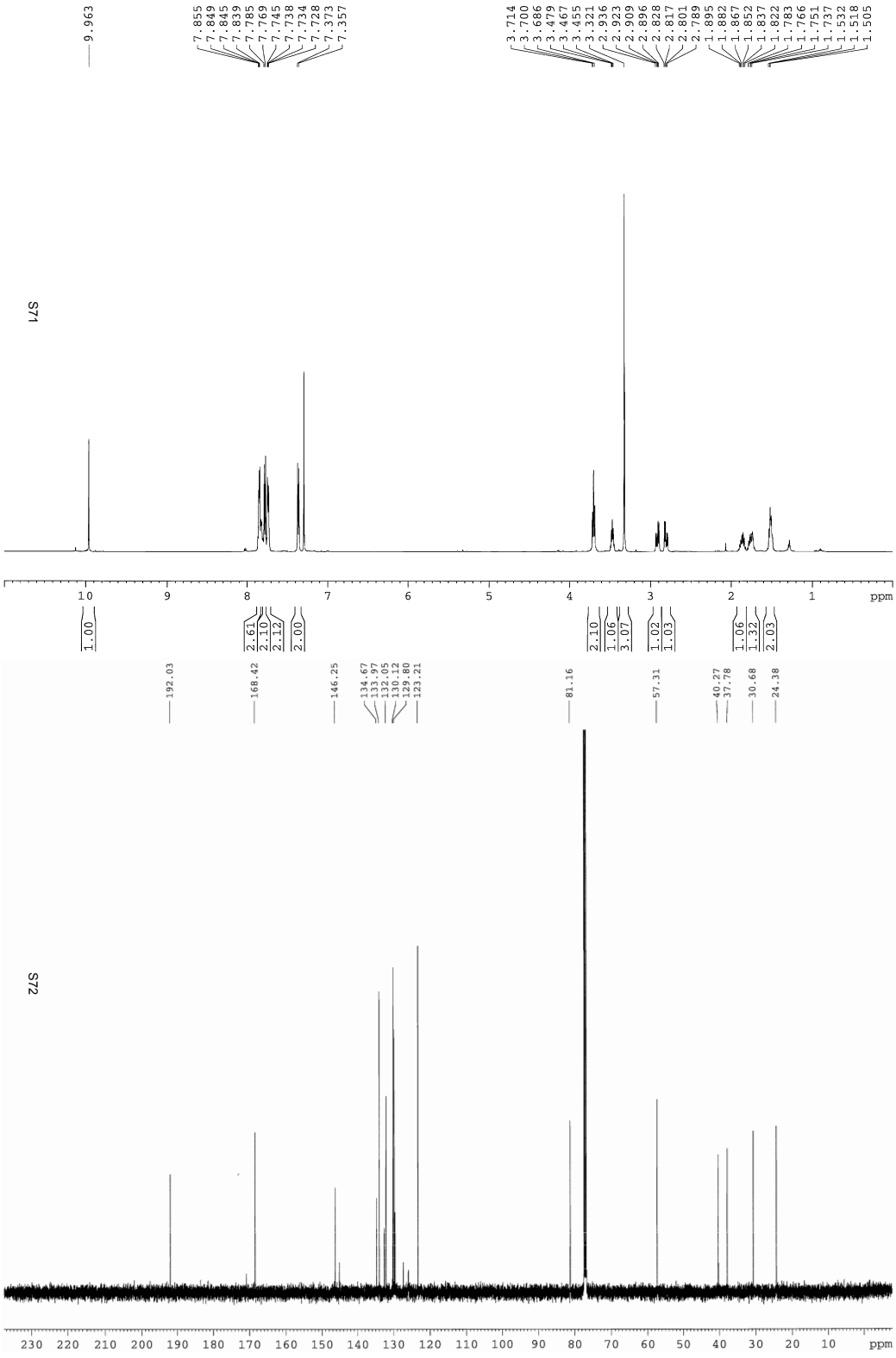
9.963
7.855
7.849
7.845
7.839
7.785
7.769
7.745
7.738
7.734
7.728
7.373
7.357
3.714
3.700
3.686
3.479
3.467
3.455
3.321
2.936
2.923
2.909
2.896
2.828
2.817
2.801
2.789
1.895
1.882
1.867
1.852
1.837
1.822
1.783
1.766
1.751
1.737
1.532
1.518
1.505
S71
ppm
1.00
2.61
2.10
2.12
2.00
2.10
1.06
3.07
1.02
1.03
1.06
1.32
2.03
192.03
168.42
146.25
134.67
133.97
132.05
130.12
129.80
123.21
81.16
57.31
40.27
37.78
30.68
24.38
S72
ppm

1.6r

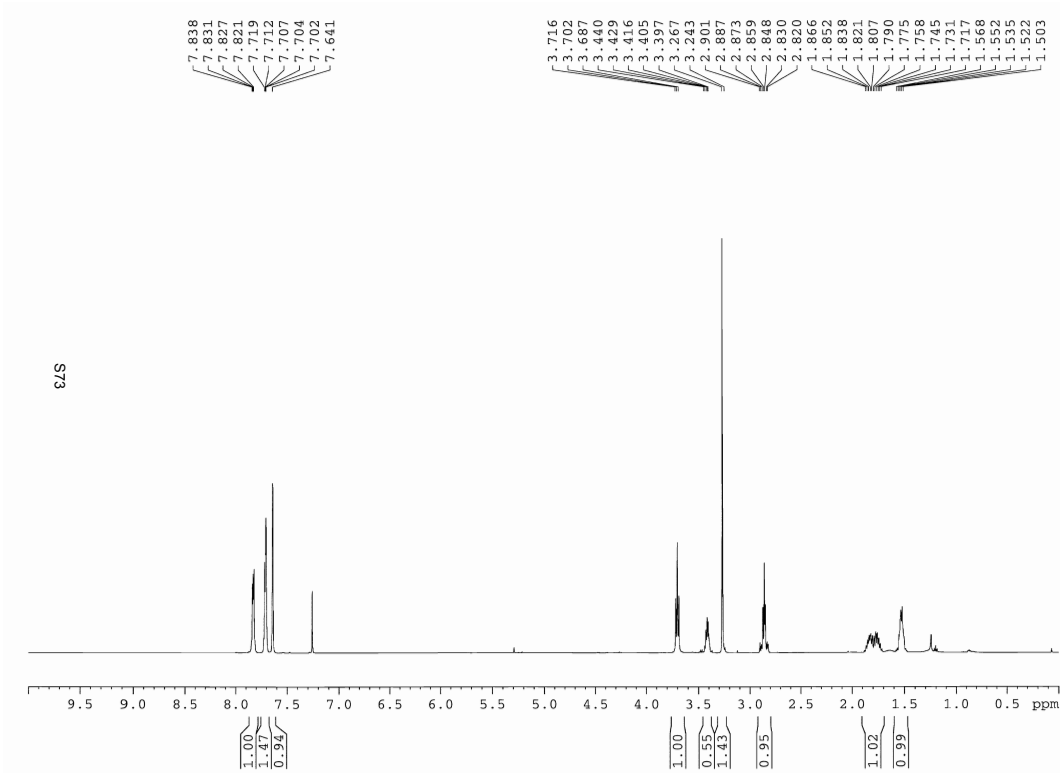
7.838
7.831
7.827
7.821
7.719
7.712
7.707
7.704
7.702
7.641
3.716
3.702
3.687
3.440
3.429
3.416
3.405
3.397
3.267
3.243
3.201
2.887
2.873
2.859
2.848
2.830
2.820
1.866
1.852
1.838
1.821
1.807
1.790
1.775
1.758
1.745
1.731
1.717
1.568
1.552
1.535
1.522
1.503
S73
9.5 9.0 8.5 8.0 7.5 7.0 6.5 6.0 5.5 5.0 4.5 4.0 3.5 3.0 2.5 2.0 1.5 1.0 0.5 ppm
1.00
1.47
0.94
1.00
0.55
1.43
0.95
1.02
0.99

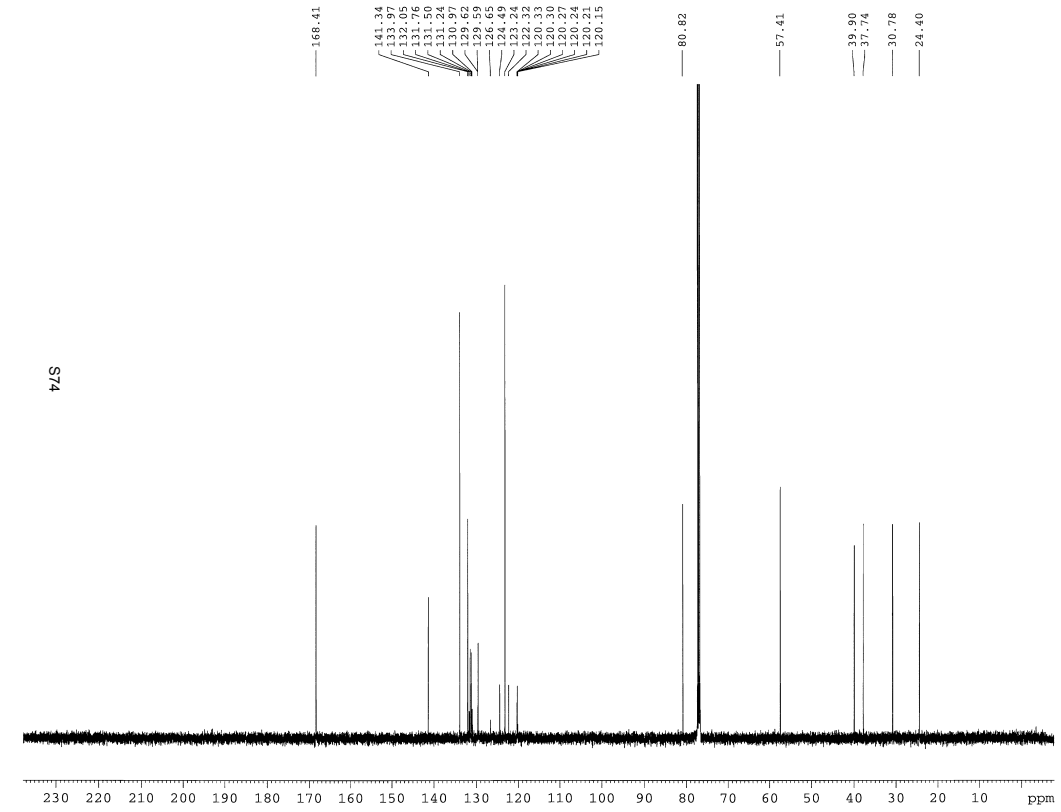
168.41
141.34
133.97
132.05
131.76
131.50
131.24
130.97
129.62
129.59
126.65
124.49
123.24
122.32
120.33
120.30
120.27
120.24
120.21
120.15
80.82
57.41
39.90
37.74
30.78
24.40
S74
230 220 210 200 190 180 170 160 150 140 130 120 110 100 90 80 70 60 50 40 30 20 10 ppm

1.6s

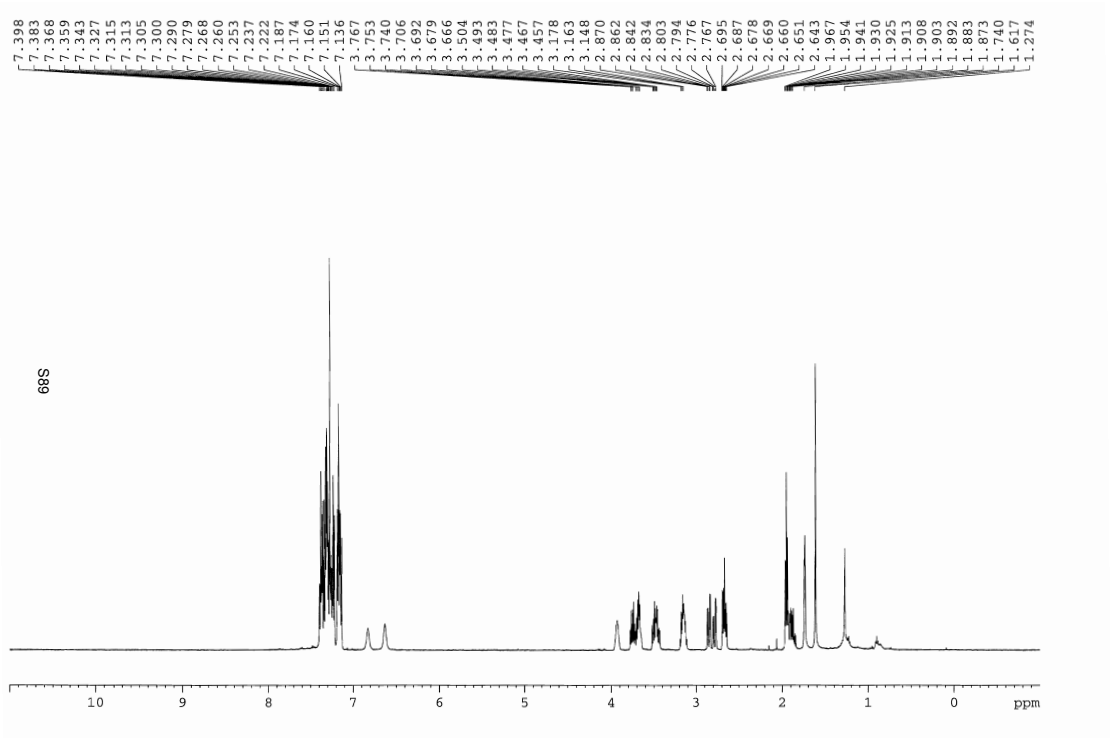
7.398
7.383
7.368
7.359
7.343
7.327
7.315
7.313
7.305
7.300
7.290
7.279
7.268
7.260
7.253
7.237
7.222
7.187
7.174
7.160
7.151
7.136
3.767
3.753
3.740
3.706
3.692
3.679
3.666
3.504
3.493
3.483
3.477
3.467
3.457
3.178
3.163
3.148
2.870
2.862
2.842
2.834
2.803
2.794
2.776
2.767
2.695
2.687
2.678
2.669
2.660
2.651
2.643
1.967
1.954
1.941
1.930
1.925
1.913
1.908
1.903
1.892
1.883
1.873
1.740
1.617
1.274
S89
10
9
8
7
6
5
4
3
2
1
0
ppm

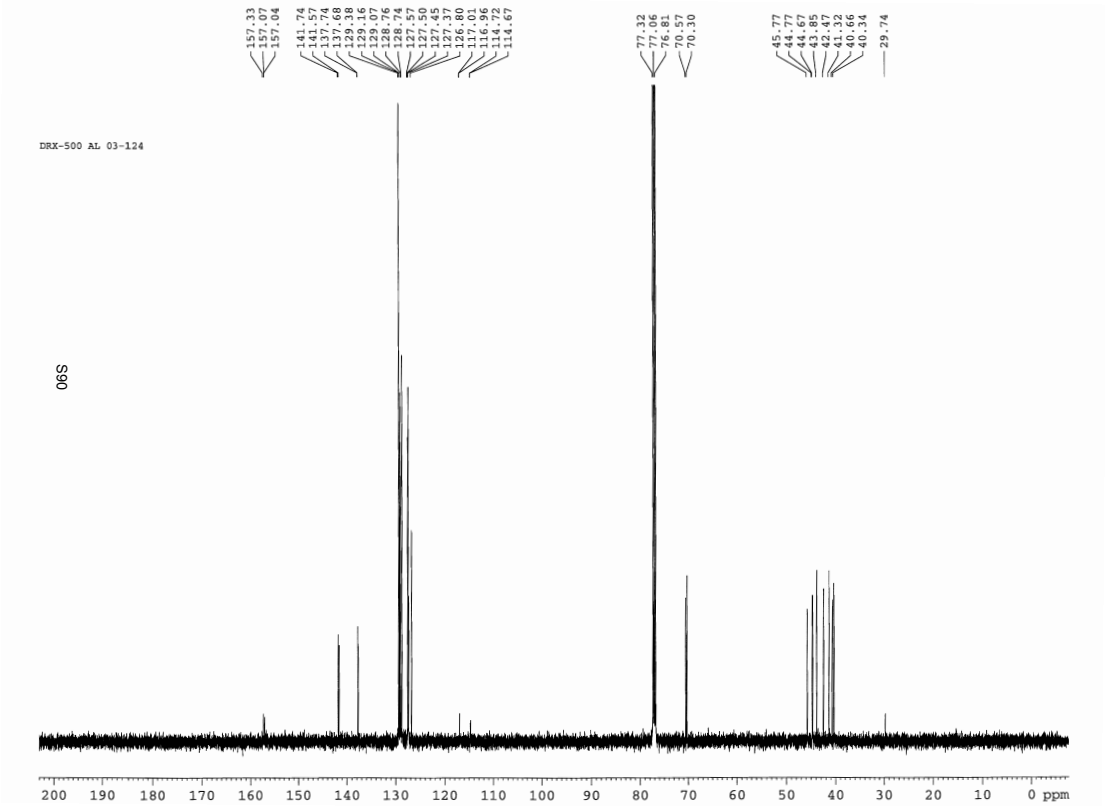
157.33
157.07
157.04
141.74
141.57
137.74
137.68
129.38
129.16
129.07
128.76
128.74
127.57
127.50
127.45
127.37
126.80
117.01
115.96
114.72
114.67
77.32
77.06
76.81
70.57
70.30
45.77
44.77
44.67
43.85
42.47
41.32
40.66
40.34
29.74
DRX-500 AL 03-124
S90
200
190
180
170
160
150
140
130
120
110
100
90
80
70
60
50
40
30
20
10
0 ppm

1.6t

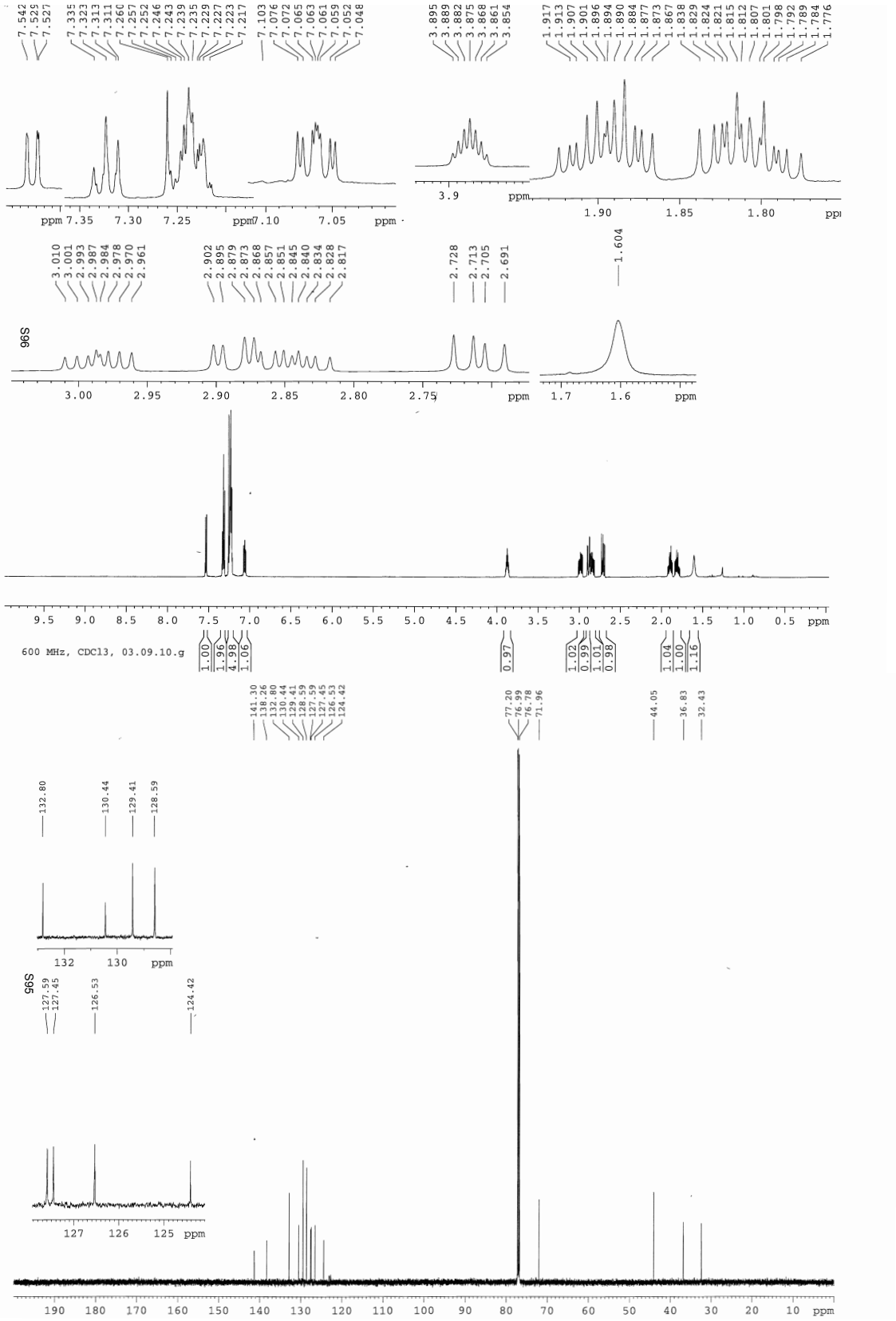

1.6u

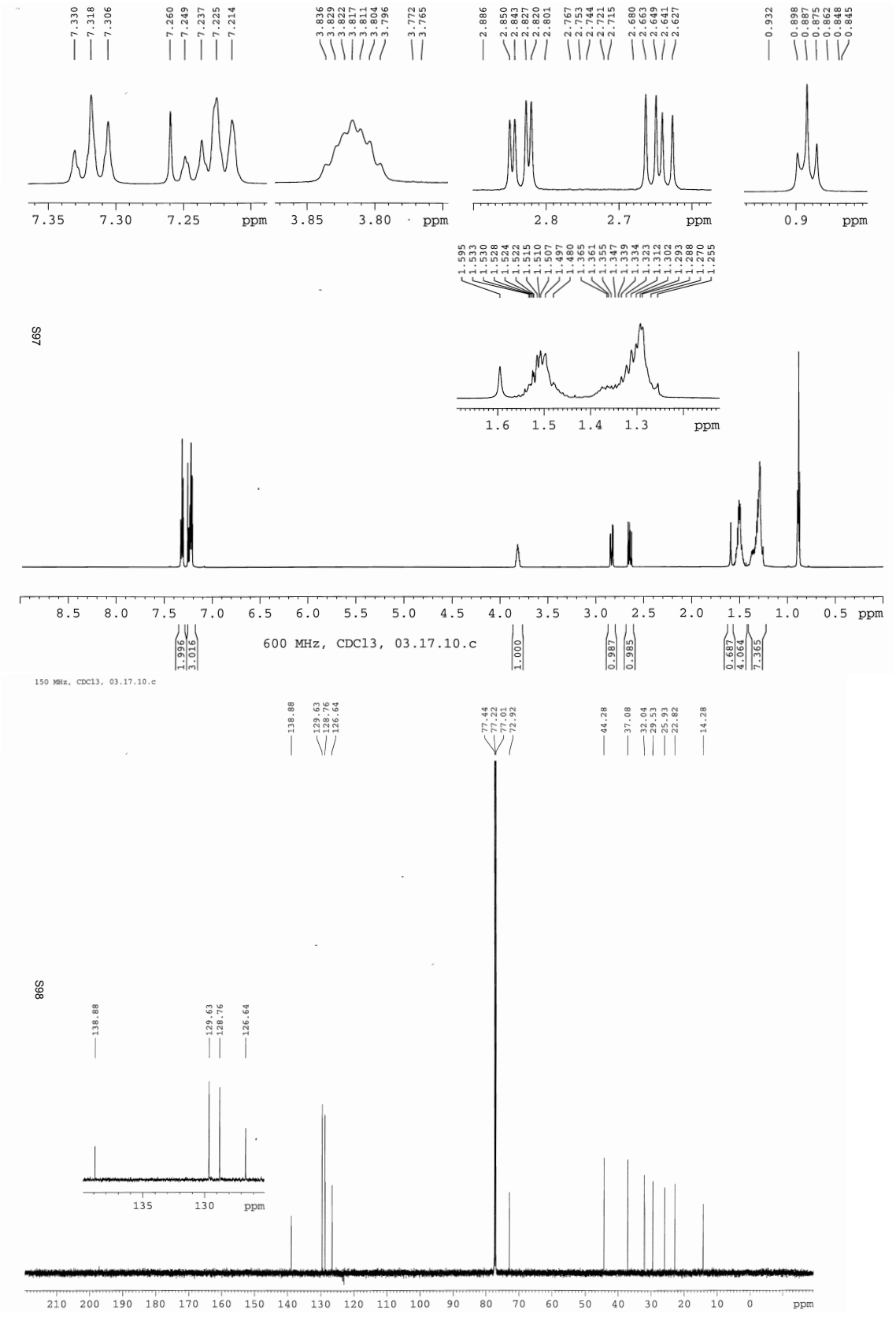

1.6v

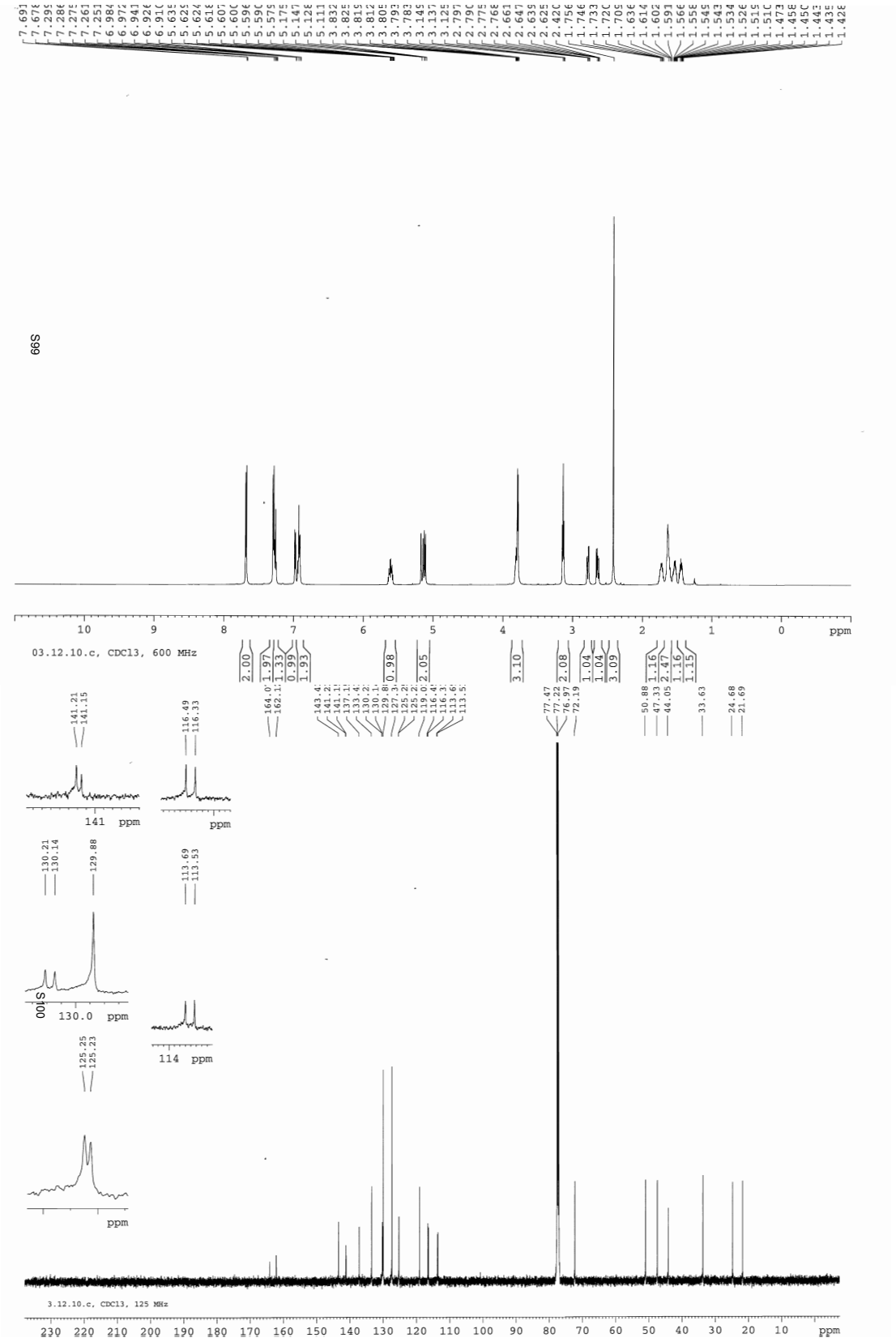

1.6w

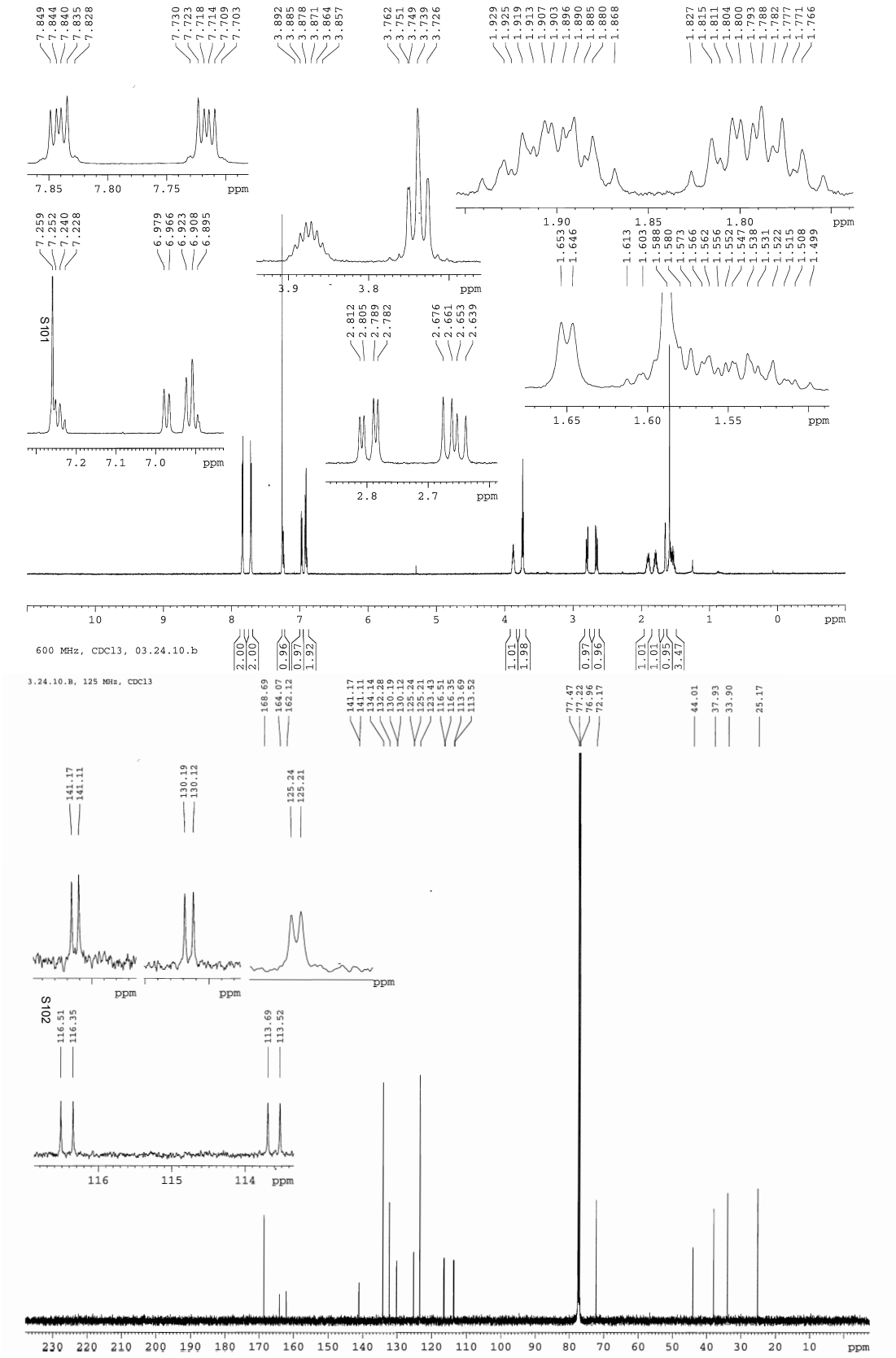

1.6x

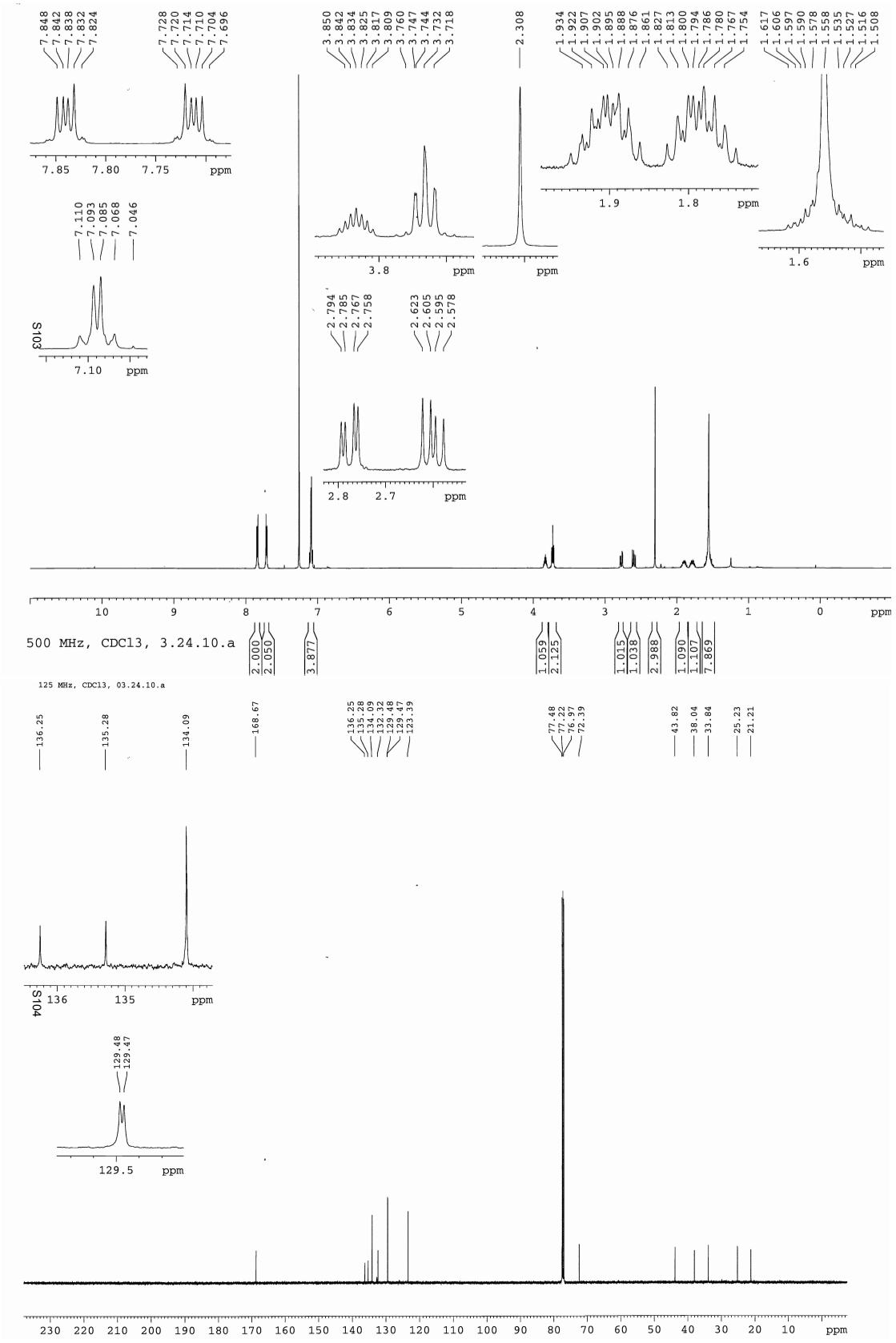

Chapter 2. Enantioselective electrophilic fluorination through chiral anion phase-transfer catalysis

The development of enantioselective fluorination reactions has the potential to be of significant value, as organofluorine compounds are highly utilized in the pharmaceutical industry. However, reports to date are generally restricted to either use of stoichiometric chiral fluorinating reagents, or chiral substrate activation, and as a result substrate scope has been limited. Here we present an alternative method using chiral anions as phase-transfer catalysts. In conjunction with an insoluble cationic fluorinating reagent, the phosphate is able to undergo counterion metathesis, thus ion pairing with the reagent. With appropriately lipophilic phosphates, the fluorinating reagent is rendered both soluble and chiral. High levels of enantioselectivity are observed as a result of the well-known enantioinduction of the BINOL-derived phosphate, and the suppression of nonselective background reaction through phase separation. The concept is demonstrated using the electrophilic fluorinating reagent Selectfluor to mediate enantioselective fluorocyclization of alkenes, a reaction class with very limited precedent.

Portions of this chapter are based on work done in collaboration with Vivek Rauniyar, Gregory Hamilton, and Ji Lee.

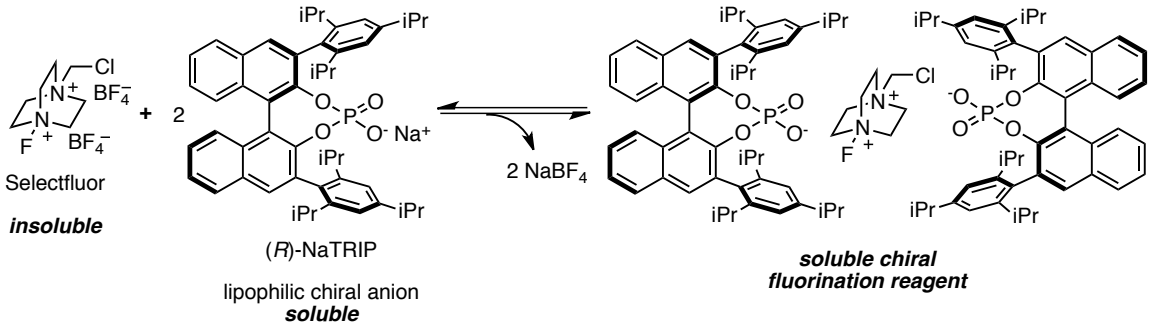

Introduction

The importance of fluorine-containing organic molecules in the pharmaceutical industry, among others, has grown dramatically in the past decades. While the first fluorine-containing drug was not developed until 1957, it is now estimated that as much as 20% of all pharmaceuticals contain at least one fluorine atom.[1] This is remarkable given that historically, the pharmaceutical community has turned to natural product for inspiration, but the number of total organofluorine natural products known (13) is nearly matched by the number of fluorine-containing molecules that are in the top 20 best-selling drugs (9).[2] This is in no small part due to the effect that the installation of fluorine can have on a molecule's chemical, and thus biological, properties, without greatly altering the molecule's size. Typical effects that fluorine can impart on a molecule include improved resistance to cytochrome P450 oxidation, higher bioavailability by raising logD, and strengthened protein-ligand interactions.[1] The development of methods for the facile installation of fluorine into organic compounds could therefore be of significant value.

While much of the recent effort in fluorination methodology has been in aryl fluorination through metal-catalyzed (or -mediated) cross-coupling,[3] fewer strides have been made toward the selective formation of alkyl-fluorides, particularly in an enantioselective fashion. The vast majority of the literature methods use electrophilic fluorine sources, and only specific reports that exemplify each of three general strategies will be presented here.[4] The complementary enantioselective nucleophilic fluorination, for which there are only very few recent examples, will not be discussed.[5] Perhaps because of the only recent advent of stable, safe electrophilic fluorinating reagents, such as Selectfluor, NFSI and N-fluoropyridinium tetrafluoroborate, the first enantioselective fluorination method was not reported until 2000. Togni and coworkers showed that a β-ketoester, in the presence of a chiral titanium catalyst, forms an active, chiral enolate nucleophile, which reacts with the Selectfluor to form an enantioenriched α-fluoro-β-ketoester (Scheme 1).[6]

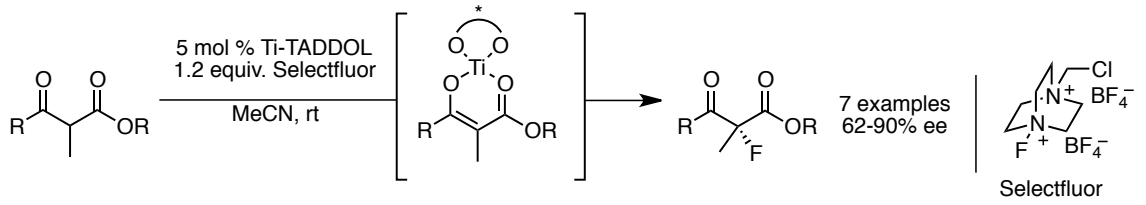

Scheme 1. Enantioselective fluorination through the generation of chiral enolates (ref. 6).

Since then, this concept has been expanded by, among others, Sodeoka, who has shown that chiral Pd-bisphosphine catalysts can form chiral enolate complexes with a variety of activated substrates.[7] Two other main strategies have been developed for enantioselective fluorination. MacMillan has demonstrated that, using a chiral amine as a covalent catalyst, ketones can undergo enantioselective α-fluorination by proceeding through an asymmetric nucleophilic enamine intermediate (Scheme 2).[8]

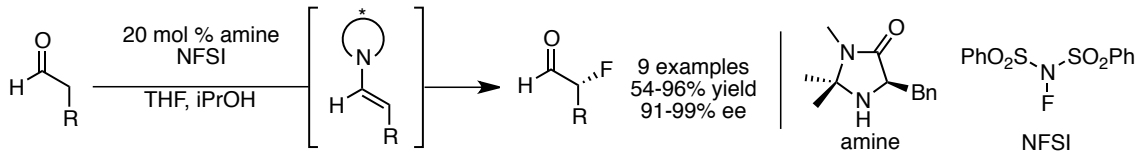

Scheme 2. Enantioselective fluorination using a chiral amine catalyst (ref. 8).

The use of stoichiometric chiral fluorinating reagents has also been developed, as demonstrated by the Shibata group. Reacting Selectfluor with a chinchona alkaloid, a chiral, cationic electrophilic fluorine source is generated. Reagents of this type have been shown to be effective in the enantioselective fluorination of substrates such as silyl enol ethers (Scheme 3).[9] These reagents are necessarily less reactive than the reaction's original fluorine source, Selectfluor.

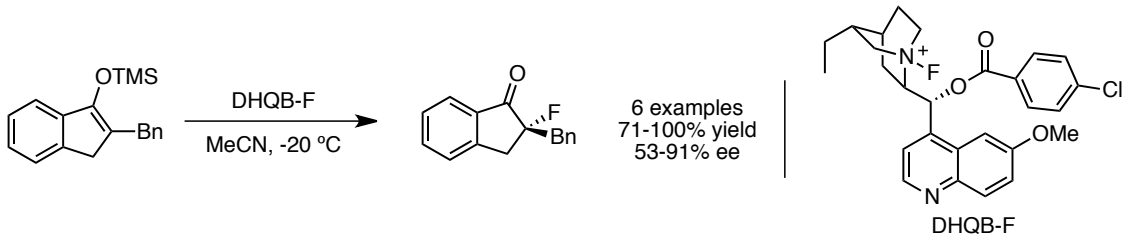

Scheme 3. Enantioselective fluorination using a chiral fluorination reagent (ref. 9).

Each of these strategies has proven quite effective, though they are not without their limitations. The reactions shown in Schemes 1 and 2, in which chiral Lewis acids and chiral amines are used respectively as catalysts, have necessary substrate limitations for the generation of the active nucleophile, while that in Scheme 3 uses as stoichiometric amount of chiral input. Though our group's experience in enantioselective fluorination was nonexistent, our familiarity with one common electrophilic fluorinating reagent, Selectfluor (see Chapter 1), as well as previous work within our labs toward the development of new modes of enantioselective catalysis, led us to consider enantioselective fluorination from a different perspective.

In 2008, a report from our group detailed the transformation of racemic trans-β-chloroamines to highly enantioenriched aminoalkoxides using a chiral phosphoric acid, alcohol nucleophiles, and a silver salt promotor .[10] Building on previous precedent,[11,12] the chiral phosphate (which was generated in situ from the phosphoric acid precatalyst), drives the enantioselective reaction in two different contexts. By reacting with Ag_2CO_3, which is otherwise insoluble in the reaction medium, it is used to solubilize one equivalent of Ag^+. The equivalent of Ag^+ abstracts the halide from the substrate to form a cationic *meso*-aziridinium intermediate. Ring opening of this intermediate by the alcohol nucleophile is directed by the ion paired chiral phosphate (Scheme 4).

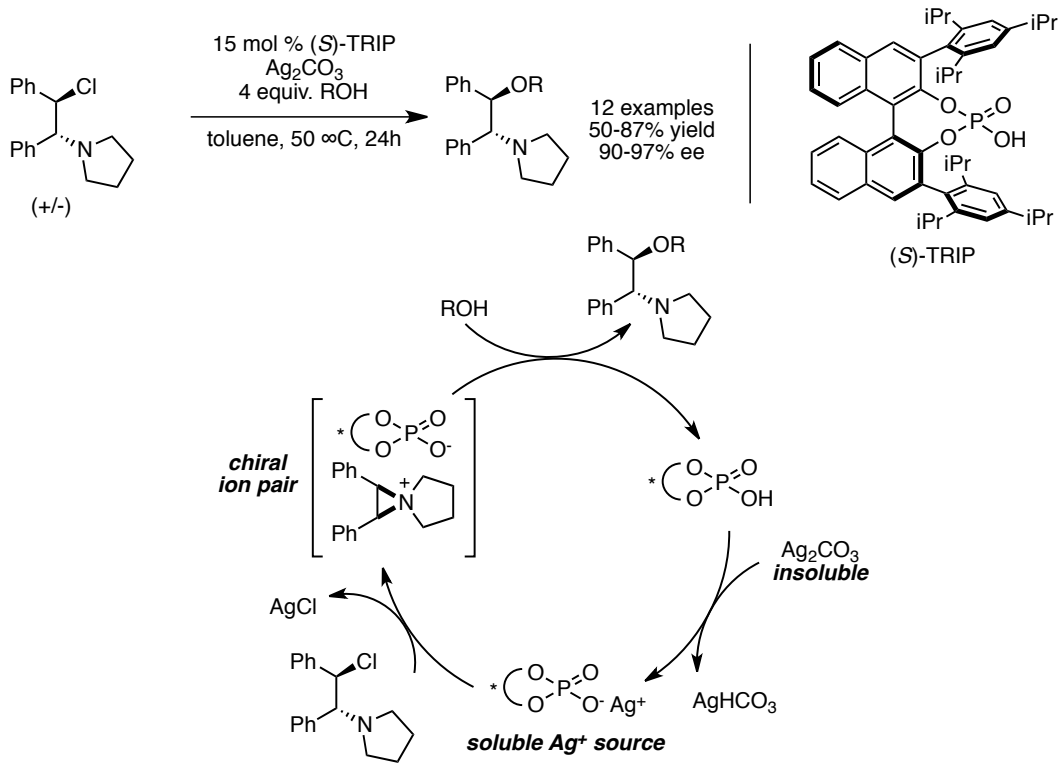

Scheme 4. Enantioselective azidirinium ring opening enabled by phase transfer (ref. 10).

The phosphate, then, has been utilized both as a phase-transfer catalyst, ensuring that the cationic silver salt is present in solution only when accompanied by the chiral anion and thus limiting nonselective background reaction. Then, upon abstraction of the halide, the phosphate again acts as an ion pair, directing the enantioselective addition of the nucleophile.

We imagined that the concept of using a lipophilic chiral phosphate anion as a solubilizing counterion could be applied using Selectfluor as a reagent toward enantioselective electrophilic fluorination. One of Selectfluor's defining characteristics (at least in our laboratories) is its insolubility in nonpolar organic solvents. We imagined a scenario in which Selectfluor, existing out of solution in a nonpolar solvent, undergoes counterion metathesis with the phosphate catalyst. The resulting ion pair (or ion triplet in the case of double counterion metathesis) would be rendered both chiral, and soluble on the basis of its lipophilicity. Thus the phosphate would be serving as a phase-transfer catalyst to generate catalytic amounts of a chiral fluorine source (Figure 1), and without the solubilizing ion pairing interaction, Selectfluor itself cannot mediate nonselective fluorination. Conceptually, this strategy might improve on previous enantioselective fluorination limitations: by rendering the fluorination reagent chiral (rather than the nucleophile, as in the case of lewis acid or amine catalysis), a wider substrate scope might be achieved. Using phase-separation, this could be accomplished using a catalytic amount of catalyst without concern for racemic background reaction.

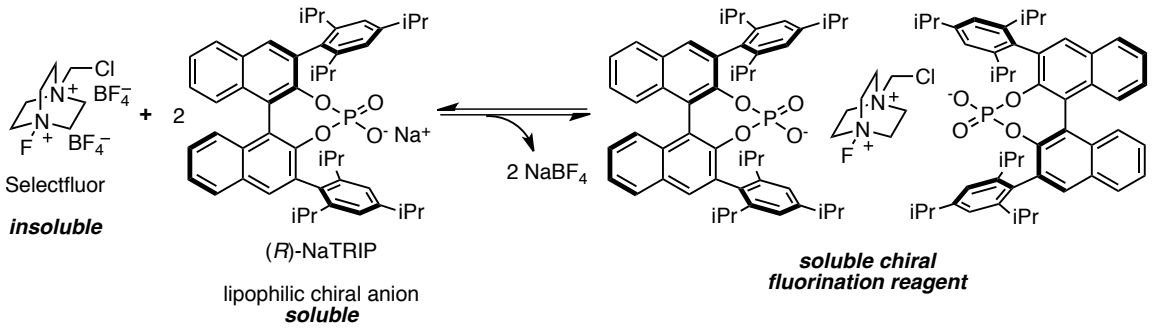

Figure 1. The conceptualized chiral anion phase transfer in nonpolar solvent.

We were interested in testing our concept on the same vinyl cyclopropanol substrate on which we had attempted gold-catalyzed oxidative coupling as discussed at the end of Chapter 1. Its reactivity toward Selectfluor had already been established and its structure offered no obvious means of implementing previously reported strategies for enantioselective fluorination.

Results and Discussion

The vinyl cyclopropanol substrate **2.1a** is a fairly reactive nucleophile. Over the course of weeks, when stored at -20 °C, acid-catalyzed ring expansion to the cyclobutanone product is observed, so in retrospect its direct reaction with a strong electrophile such as Selectfluor should not be a surprise. In acetonitrile, one of the few organic solvents in which Selectfluor displays solubility, the fluorinated cyclobutanone product **2.2a** is observed cleanly within one hour. In contrast, in nonpolar solvent, such as benzene, <10% conversion of starting material is observed, even after 14 h, indicating that in fact, when maintained out of bulk solution, reaction of the substrate with Selectfluor is insignificant (Scheme 5).

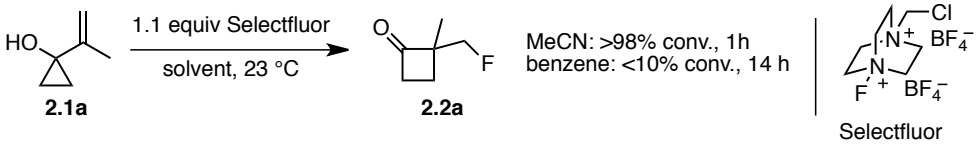

Scheme 5. Reactivity of vinyl cyclobutanol toward Selectfluor in polar and nonpolar solvents.

We were excited, then, to determine whether the inclusion of the lipophilic chiral phosphate (*R*)-NaTRIP would lead to conversion in benzene. In fact, the substrate was fully converted, and **2.2a** was observed; however, it was the minor product. The major species was the proteated (rather than fluorinated) cyclobutanone **2.3a** (Table 1, entry 1). Given the aforementioned acid sensitivity of **2.1a**, this should have been the expected result. Upon reaction of **2.1a** with Selectfluor, one equivalent of acid is produced. It is likely that the phosphate acts as the initial base, generating phosphoric acid. Not only can it no longer serve as a phase-transfer catalyst (it is neutral and cannot ion pair with the reagent), but it also catalyzes the non-fluorinative ring expansion of the substrate to yield **2.3**. Nevertheless, we were strongly encouraged that the minor fluorinated product was obtained in significantly enantioenriched form (65% ee). In order to regenerate the

phosphate catalyst, stoichiometric inorganic base additives were included in the reaction. Inorganic bases, which also generally have low solubility in organic solvents, were chosen as we theorized they would be less likely to interfere in ion pairing or the reaction course in general, while still regenerating the phosphate. $NaHCO_3$ did in fact lead to a major improvement in the ratio of fluorinated to proteated products; however, slight decreases in both conversion and enantioselectivity of **2.2a** were also observed (entry 2). The more strongly basic Na_2CO_3 again led to improved selectivity for the desired product, and levels of both conversion and enantiomeric excess were restored (entry 3).

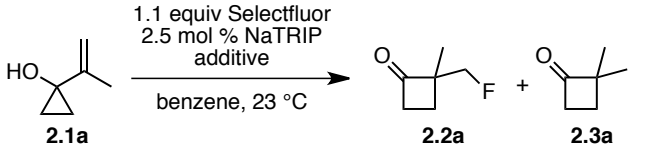

2.1a **2.2a** **2.3a**

entry	additive	conversion	ratio **2.2**:**2.3**	ee **2.3**
1	none	>98%	1:15	65%
2	1.1 equiv. $NaHCO_3$	91%	1:1	59%
3	1.1 equiv. Na_2CO_3	98%	4:1	65%

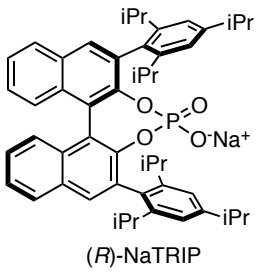

(*R*)-NaTRIP

Table 1. Initial enantioselective fluorination result and effect of base additives.

In switching reaction solvent to toluene, the acid-catalyzed pathway was fully suppressed (Table 2, entry 1). We also identified phenyl substituted substrate **2.1b** as a better candidate for optimization studies, as it gave the product both in moderate conversion and in moderate enantioenrichment (Table 2, entry 2).

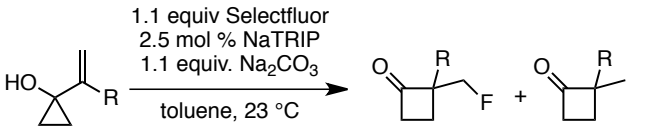

R = Me, **2.1a**
R = Ph, **2.1b**

R = Me, **2.2a**
R = Ph, **2.2b**

R = Me, **2.3a**
R = Ph, **2.3b**

entry	substrate	conversion	ratio **2.2**:**2.3**	ee **2.2**
1	**2.1a**	>98%	1:0	65%
2	**2.1b**	57%	1:0	33%

Table 2. Fluorination of vinyl cyclopropanol substrates in toluene.

Again, nonpolar solvents were screened (Table 3). Hydrocarbon solvents, as well as hydrocarbon-containing solvent mixtures (entries 2-4, 6-8), generally led to improved conversion, and ee as high as 58% were observed (entries 1, 7, 8). More exotic solvents, such as perfluorooctane (entry 9) and ethyl benzene (entry 12) were inferior, as was methyl tert-butyl ether (entry 10).

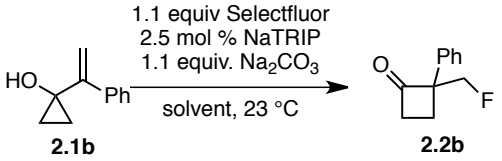

2.1b **2.2b**

entry	solvent	conv.	ee	entry	solvent	conv.	ee
1	1:1 tol/Et_2O	57%	58%	7	pet. ether	>98%	58%
2	1:1 tol/Hex	>98%	52%	8	pentane	>98%	58%
3	1:3 tol/Hex	>98%	54%	9	C_8F_{17}	26%	nd
4	hexanes	90%	56%	10	MTBE	15%	nd
5	C_6H_{12}	78%	53%	11	mesitylene	83%	51%
6	heptane	95%	56%	12	PhEt	9%	nd

Table 3. Solvent effects on the fluorination of substrate **2.1b**.

While these initial results proved quite promising, further work toward optimization of this class of substrates was unsuccessful, and a brief list of failed conditions is listed qualitatively here. A variety of 3,3′-disubstituted-BINOL-derived phosphates (as well as chiral sulfonates and bis-sulfonamides) were evaluated as phase-transfer catalysts, and all suffered from diminished conversion, enantioselectivity, or both. No other cationic electrophilic fluorinating reagent employed resulted in conversion under phase-transfer conditions. Protecting groups on the alcohol were explored and similarly led to no conversion. Temperature had little impact on enantioselectivity, but lowered reaction temperature led to lower conversion. After attempts to explore as many variables as possible, we began to wonder if perhaps the stereodifferentiating ability of the phosphate catalyst NaTRIP on our chosen substrates was simply too low for practical purposes. We could therefore consider two possible paths forward, either exploring significantly different catalyst classes or exploring different substrates. Based on the wealth of previously reported highly enantioselective transformations using BINOL-derived phosphoric acids[13] or phosphates[12a] as chiral information, we felt that instead altering the substrate would be more practical means toward a successful demonstration of enantioselective fluorination by chiral anion phase-transfer catalysis.

Another transformation that seemed appropriate to showcase the advantages of a phase-transfer strategy was the fluorocyclization of alkenes (Figure 3).[14] Though a report employing electrophilic fluorination reagents and cinchona alkaloids (in either stoichiometric or catalytic quantities), was published during the course of our investigations,[15] at the start of our exploration into the reaction no known enantioselective fluorocyclization was known. It also, perhaps not coincidentally, offered another substrate platform on which previous methods of catalytic enantioselective fluorination would be difficult to achieve (no carbonyl or β-ketoester for the generation of a chiral nucleophile).

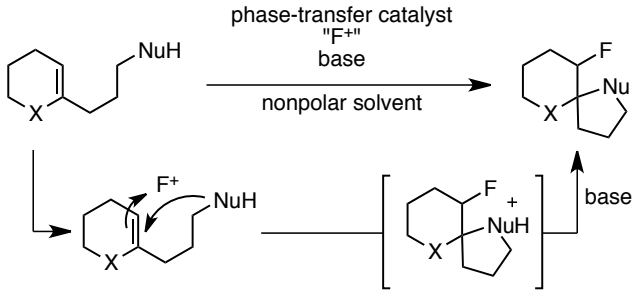

Figure 3. Proposed generalized fluorocyclization transformation.

Beginning our investigations on the activated dihydropyran substrate **2.4a**, we were pleased to find that in fact enantioselective fluorocyclization under phase-transfer conditions was possible (Table 4), and through a solvent screen, fluorobenzene was identified as a particularly effective reaction medium, as the fluorinated product was generated in high diastereo- and enantioselectivity (entry 5). By using the more lipophilic catalyst C_8-TRIP, which we hypothesized would be a more efficient catalyst due to increased solubility, diastereoselectivity and enantioselectivity were further improved (entry 6).

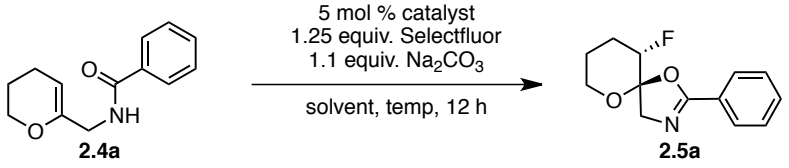

entry	catalyst	solvent	temp	% conv. (% yield)	dr	% ee
1	(*R*)-TRIP	heptane	57 °C	>98	1:1	15
2	(*R*)-TRIP	Et_2O	23 °C	>98	1.5:1	33
3	(*R*)-TRIP	MTBE	23 °C	>98	ND	64
4	(*R*)-TRIP	toluene	23 °C	>98	9:1	62
5	(*R*)-TRIP	C_6H_5F	23 °C	>98	9.3:1	70
6	(*R*)-C_8-TRIP	C_6H_5F	23 °C	>98 (<10%)	>25:1	87

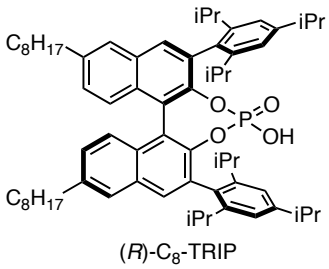

Table 4. Solvent effects and catalyst on the fluorocyclization of dihydropyranyl substrate **4a**.

However, as with the initial vinyl cyclopropanol substrate **2.1a**, inspection of the crude reaction mixture revealed that in fact **2.5a** was produced as the minor product. The major product was determined to be **2.3c**, the product of an acid-catalyzed dimerization (Figure 4).

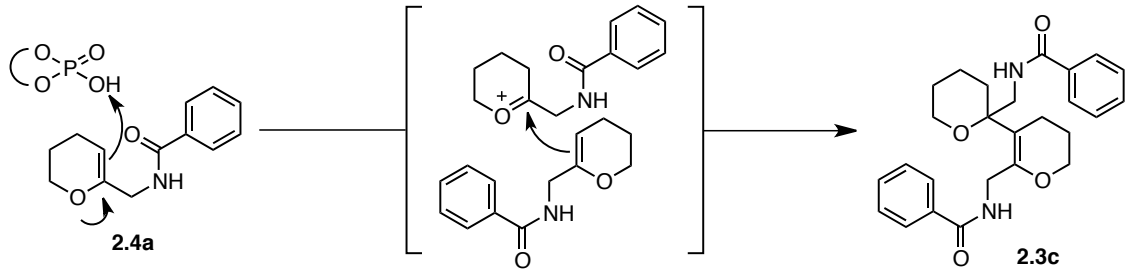

Figure 4. Acid-catalyzed dimerization pathway of substrate **4a**.

By employing a soluble organic base, Proton Sponge, instead of Na_2CO_3 to improve regeneration of the phosphate catalyst, chemoselectivity toward the fluorinated product was increased (Table 5, entry 1). This was accompanied by a deterioration in selectivity, but by lowering the reaction temperature to -20 ^oC, the fluorocyclized product **2.5a** was obtained in high yield, diastereoselectivity and enantioselectivity (entry 2).

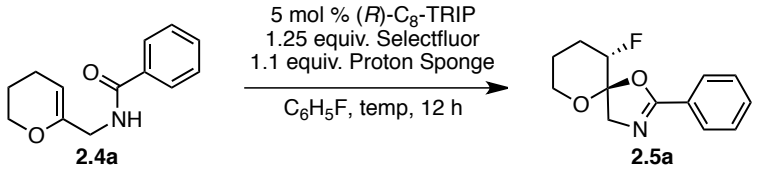

2.4a **2.5a**

entry	temp	% conv. (% yield)	dr	% ee
1	23 ^oC	>98 (62)	12:1	62
2	-20 ^oC	>98 (86)	>25:1	92

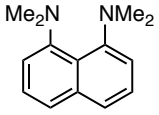

Proton Sponge

Table 5. The use of C_8-TRIP and Proton Sponge lead to improved yield and selectivity.

As previous employment of lowered reaction temperature had done little to affect enantioselectivity, we hypothesize that at this temperature, a competitive fluorination of the base Proton Sponge (eq 1), is shut down. As this would result in an achiral (and soluble) fluorine source, eliminating this pathway should lead to an improvement in observed enantioenrichment.

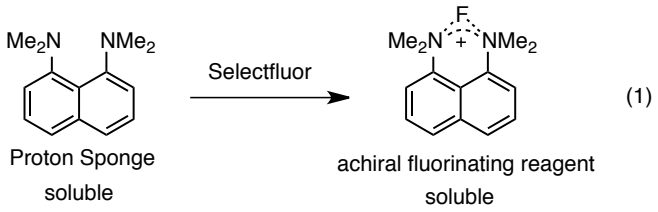

Proton Sponge
soluble

achiral fluorinating reagent
soluble

(1)

We were able to extend the protocol to dihydropyran substrates with a number of different benzamide derivatives (Table 6). Different functionality, both electron rich and electron poor, was tolerated, as was substitution at *para*-, *meta*- and *ortho*- positions. Diastereoselectivity and enantioselectivity were very high for *para*- substituted substrates (**2.5b-f**) and 2-naphthyl substrate **2.5g**, though selectivities were somewhat diminished in the cases of disubstituted benzamide **2.5h** and *ortho*-substituted benzamide **2.5i**.

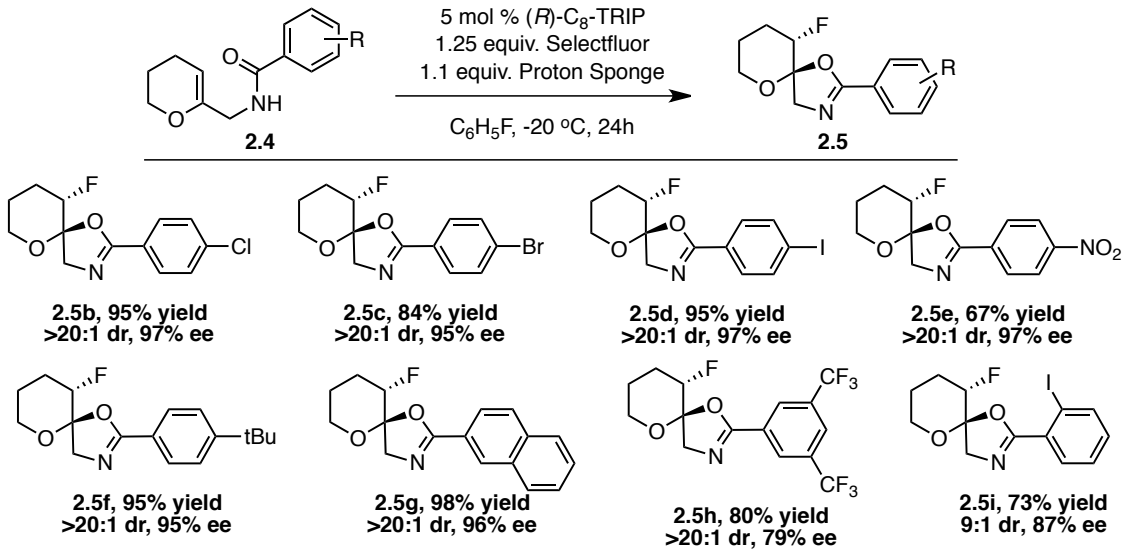

Table 6. Scope of dihydropyranyl substrates for the fluorocyclization reaction.

Less activated substrates were also amenable to enantioselective fluorocyclization under phase-transfer conditions. Dihydronaphthyl- and dihydrochromenyl-derived benzamides **2.6** were fluorinated in good yield and high selectivity (Table 7). In these cases, reactivity was improved by increasing catalyst loading, and by using hexanes as a cosolvent. Because these substrates are less acid sensitive, inorganic bases could again be employed, and thus no cryogenic temperatures were necessary.

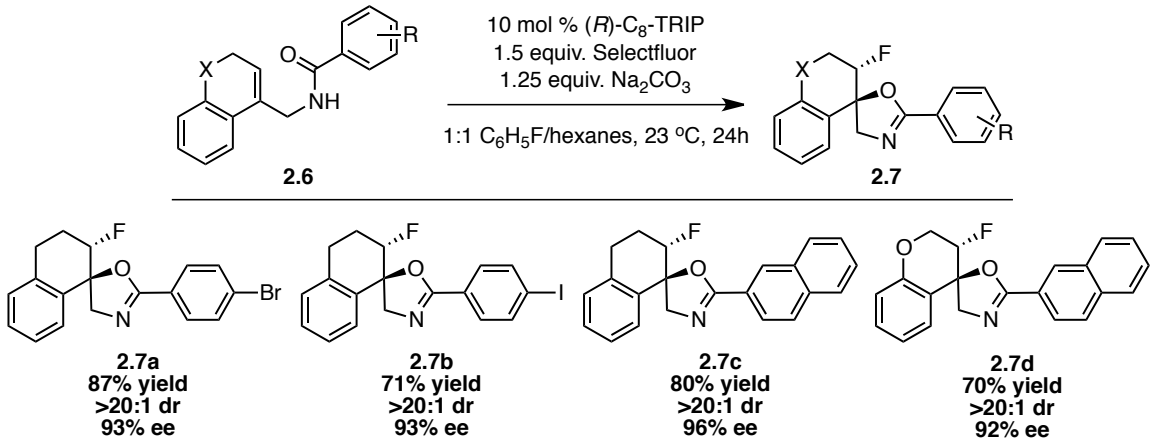

Table 7. Scope of dihydronaphthyl and dihydrochromenyl-derived substrates in the fluorocyclization reaction.

Even a simple, unactivated alkene underwent selective fluorocyclization. The disubstituted alkene substrate **2.8** yielded the fluorine-containing isoxazoline **2.9** after reaction at elevated temperature in good enantioenrichment (eq 2) using the phase-transfer TCYP instead of C_8-TRIP.

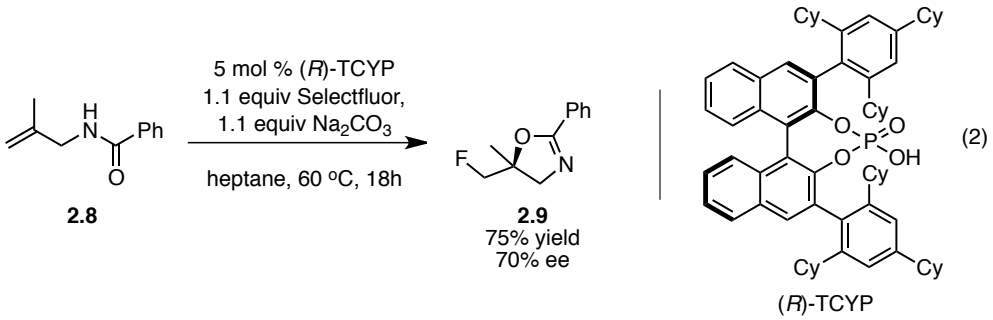

Electrophilic fluorination through chiral anion phase-transfer catalysis offers an unexpected advantage as well. The reactivity of the fluorinating reagent in nonpolar solvent, either as a result of tighter ion pairing or of lowered concentration of active reagent, is attenuated when compared to Selectfluor under homogeneous conditions. For sensitive substrates, in addition to the demonstrated enantioselectivity, this can mean significant improvements in chemoselectivity. In the case of benzothiophene substrate **2.10**, under homogeneous conditions, the substrate is fully converted to a complex mixture of products, including apparent sulfur oxidation and polymerization products, and no fluorocylization product was observed. In contrast, under phase-transfer conditions, enantioenriched product **2.11** was obtained in good yield (Scheme 6)

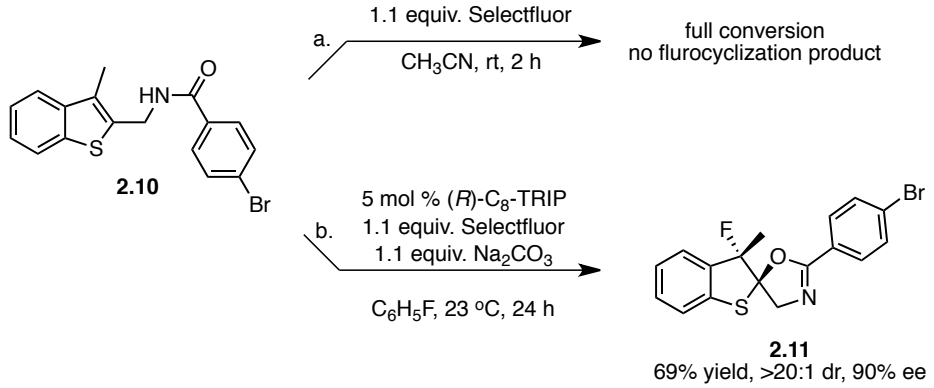

Scheme 6. Impact of phase-transfer conditions on chemoselectivity for sensitive substrates.

In considering the mechanism of the reaction, we were interested in discerning the precise nature of the active fluorinating species: specifically, whether one or both of the tetrafluoroborate counteranions of Selectfluor are exchanged for chiral phosphate anions. It also remained a possibility that the phosphate itself was being fluorinated, and acting as a covalent catalyst for fluorination. If more than one equivalent of the chiral catalyst is involved in the reaction transition state (as would be the case in a double counterion exchange but not in the cases of a single counterion exchange or covalent catalysis) a nonlinear relationship between enantioenrichment of the catalyst and enantioenrichment of the product can be observed (Figure 5).[16]

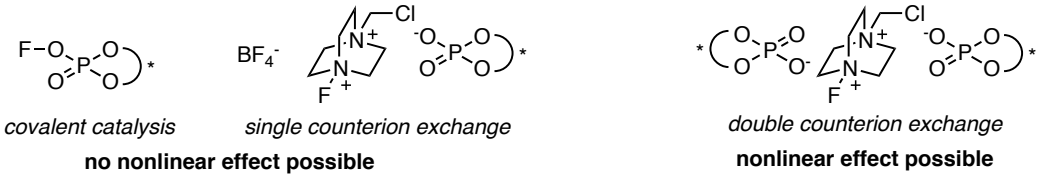

Figure 5. Possible different modes of activation.

This phenomenon is a result of the different types of complexes that can be formed involving two molecules of a chiral material. Homodimers, comprised of both (*R*) or both (*S*) enantiomers (Figure 6a and c), may form, or the heterodimer, comprised of one (*R*) enantiomer and one (*S*) enaniomer may form (Figure 6b). As the homodimers are enantiomeric, their reactivities toward an achiral substrate are kinetically equivalent. The heterodimer, however, is diastereotopic in relationship to these two cases and may therefore exhibit differing reactivity, and be either more reactive or less reactive than the homodimer. It is as a result of this heterodimer that a deviation from linearity between catalyst enantioenrichment and product enantioenrichment may be observed.

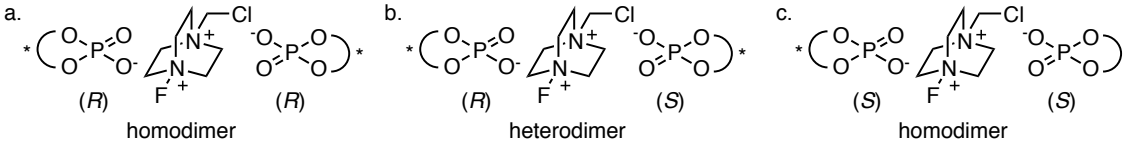

Figure 6. Possible dimers in the case of double counterion exchange.

When substrate **2.7a** was subjected to reaction conditions in the presence of TRIP catalyst of differing levels of enantioenrichment, a shallow but significant negative nonlinear effect was observed (Figure 7).

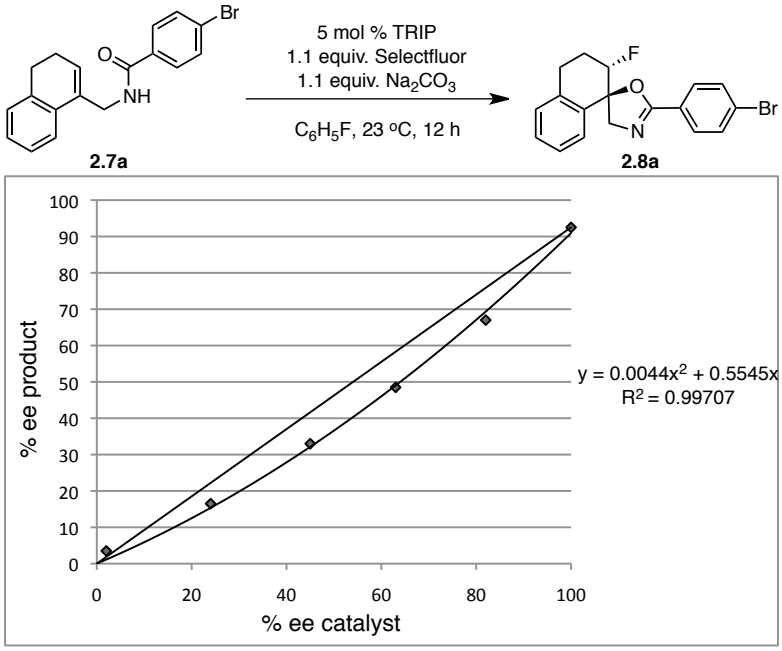

Figure 7. Observed nonlinear effect in chiral anion phase-transfer fluorocyclization.

The results of this experiment are in support of a double counterion exchange and would be in contrast to a covalent catalysis pathway. We therefore proposed the following catalytic cycle (Figure 8).

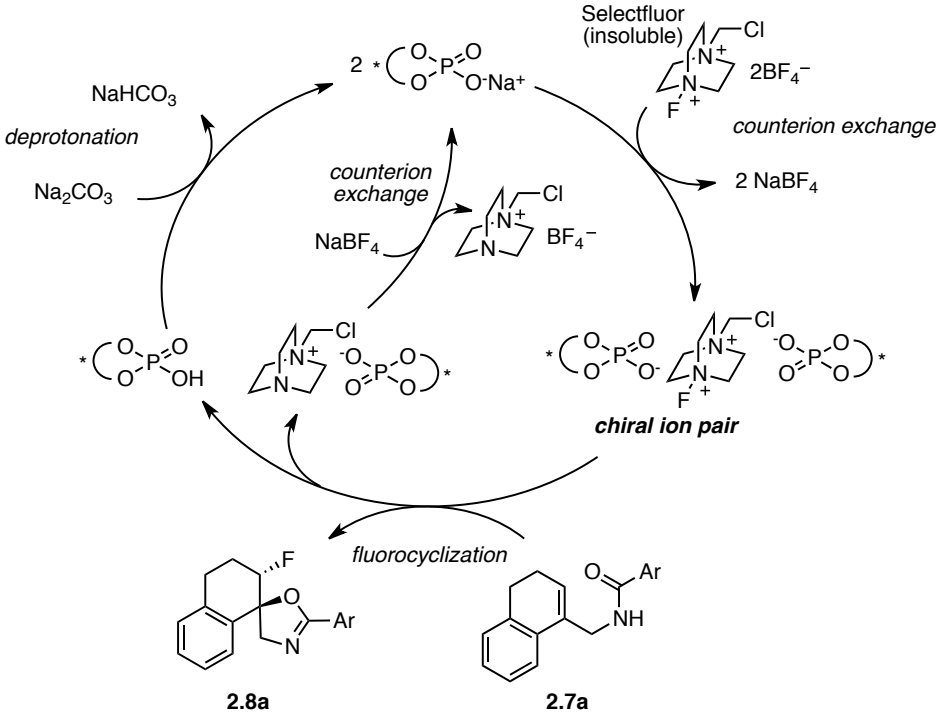

Figure 8. Proposed mechanism for chiral anion phase-transfer catalyzed fluorocyclization.

Two equivalents of the chiral phosphate, generated *in situ* by deprotonation, serve to solubilize the fluorinating reagent through counterion exchange. The chiral, soluble electrophilic fluorine source can then mediate asymmetric fluorination of the substrate, generating one equivalent of phosphoric acid and one equivalent of the defluorinated monocationic ion pair. The active phosphate can be generated from these intermediates by deprotonation and counterion exchange respectively.

The ability to replace Selectfluor with different cationic reagents for the enantioselective catalysis of different types of transformations would be an indication of the potential utility of the anionic phase transfer strategy. Toward this end, the commercially available oxidant 4-acetamido-2,2,6,6-tetramethyl-1-oxopiperidinium tetrafluoroborate, **2.14**, was employed for the enantioselective oxidation of *meso*-diols. Low levels of enanioinduction were observed in the oxidative desymmetrization of *meso*-hydrobenzoin, **2.12** (Table 8). And while hexanes proved to be the best solvent for enantioselectivity, the desired product **2.13** was observed in low yield (entry 4).

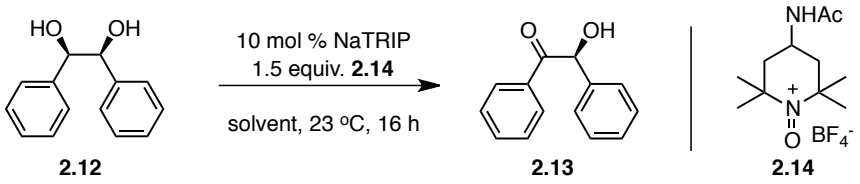

2.12 **2.13** **2.14**

entry	solvent	ee (conv.)
1	toluene	20%
2	Et_2O	13%
3	C_6H_5F	3%
4	hexanes	40%(<20%)

Table 8. Solvent effects on oxidative desymmetrization of *meso*-hydrobenzoin.

By switching to the less-substituted oxidant **2.15**, product enantioenrichment could be improved, however conversion remained low (Table 9, entry 1). Perhaps unsurprisingly, addition of stoichiometric inorganic base significantly improved conversion to oxidized product (entry 2).

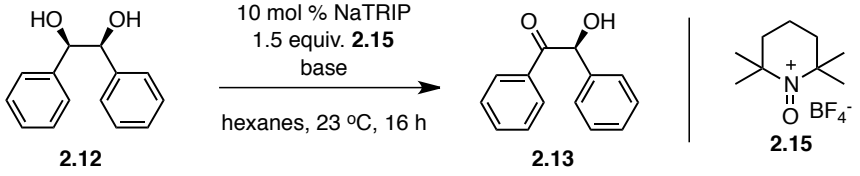

2.12 **2.13** **2.15**

entry	base	ee (conv.)
1	--	69% (9%)
2	1.5 equiv. Na_2CO_3	71% (50%)

Table 9. Employment of oxidant **2.15** and base improve enantioenrichment and conversion.

Again, numerous variables including the nature of the catalyst, catalyst loading, and the nature of the base were examined, with no further improvement in results. One major problem was the solubility of the substrate **2.12** as compared to the product **2.13**. The monoketone product has a higher degree of solubility in hexanes, and given that it still has an oxidizable alcohol moiety, overoxidation to the diketone was consistently observed. Furthermore, a more significant background reaction was observed, even in hexanes, indicating a "leaky" system (eq 3).

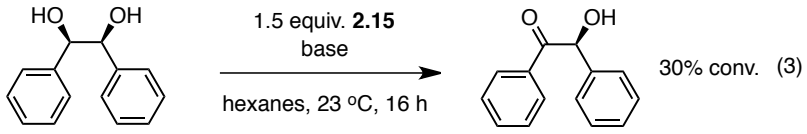

2.12 **2.13**

Owing to these inherent problems and the limited scope that the reaction would possess even if it were improved, we considered instead the oxidative kinetic resolution of chiral alcohols.[17] If one enantiomer could be oxidized preferentially over the other, the starting material can be reisolated in enantioenriched form. Initial investigations indicated that

simple alcohols were unsuitable substrates, being oxidized indiscriminately (Table 10).

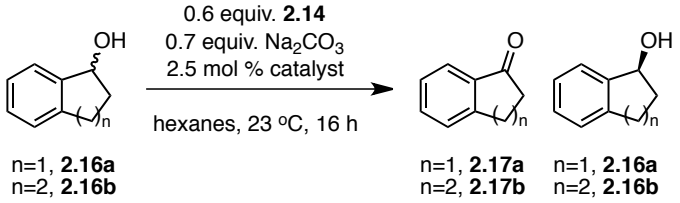

entry	substrate	conv. to **2.17**	ee **2.16**
1	**2.16a**	26%	0%
2	**2.16b**	25%	0%

Table 10. Nonselective oxidation of simple alcohol substrates.

It occurred to us that better selectivity may have been achieved with the *meso*-diols because the nonoxidized alcohol was acting as a directing group, a feature missing in substrates **2.16a** and **2.16b**. When substrate **2.16c**, which contains a proximal benzamide that might interact with the phosphate catalyst through hydrogen bonding, was subjected to the same reaction conditions, enantioenriched starting alcohol was indeed reisolated, and the selectivity factor (the preference for reaction of one enantiomer over the other) when toluene was employed as solvent was a respectable 11.3 (Table 11, entry 2).

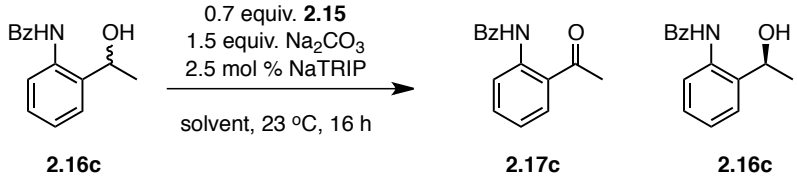

entry	solvent	conv. to **2.17c**	ee **2.16c** (*s*)
1	9:1 hex/tol	55%	30% (2.2)
2	toluene	31%	35% (11.3)

Table 11. Enantioselective oxidation of benzyl alcohols with a benzamide directing group.

While these results were certainly encouraging, the limitation of a simple kinetic resolution, in which 50% of the starting material is discarded (the oxidized product **2.17c**), made us again rethink our strategy. Considerations of how that material might be recycled led us into the project discussed in Chapter 3, the single-operation deracemization of chiral substrates by purely chemical means.

Conclusions

The physical properties of the dicationic electrophilic fluorinating reagent Selectfluor drastically limit its availability for reaction in nonpolar solvents. Typically this would be a drawback in achieving desired reactivity. However, this insolubility is integral to obtaining highly enantioenriched fluorinated compounds through chiral anion phase-transfer catalysis. This constitutes a new strategy for enantioselective fluorination and further work in our laboratories has begun to exploit this mode of catalysis toward the enantioselective synthesis of more complex fluorine-containing products.

Experimental Details

General Information: Unless otherwise noted, all commercial reagents were used without further purification. Selecfluor (Sigma Aldrich) was dried with heating under high vacuum for 15 minutes prior to use. Small scale reactions were run in 25mm test tubes fitted with a rubber septum. Dichloromethane, toluene, ether, toluene and triethylamine were purified by passage through an activated alumina column under argon. Thin-layer chromatography analysis of reaction mixtures was performed using Merck silica gel 60 F254 TLC plates, and visualized under UV or by staining with ceric ammonium molybdate or $KMnO_4$. Flash column chromatography was carried out on Merck Silica Gel 60 Å, 230 X 400 mesh. Nuclear magnetic resonance (NMR) spectra were recorded using Bruker DRX-500, AVQ-400 and AV-300 spectrometers. ^{1}H and ^{13}C chemical shifts are reported in ppm downfield of tetramethylsilane and referenced to residual solvent peak ($CHCl_3$; $\delta_H = 7.26$ and $\delta_C = 77.0$, CH_3OH; $\delta_H = 3.31$ and $\delta_H = 49.2$). Multiplicities are reported using the following abbreviations: s = singlet, d = doublet, t = triplet, q = quartet, m = multiplet, br = broad resonance. Diastereomeric ratios were determined by integration of ^{19}F NMR spectra of crude product prior to purification. Mass spectral data were obtained from the Micro-Mass/Analytical Facility operated by the College of Chemistry, University of California, Berkeley. Enantiomeric excesses were determined on a Shimadzu VP Series Chiral HPLC. The synthesis of the phosphoric acid TCYP has been previously described.[18]

Catalyst Synthesis

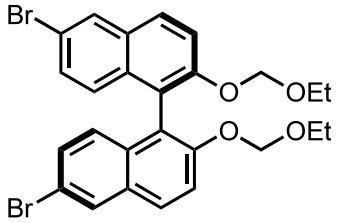

(*R,R*)-6,6'-dibromo-2,2'-bis(ethoxymethoxy)-1,1'-binaphthalene (S2.1): To a suspension of NaH (60 wt%, 2.5 equiv, 50 mmol) in THF 100 mL at 0 ºC was added a solution of (*R*)- 6,6'-dibromo-[1,1'-binaphthalene]-2,2'-diol[19] (20 mmol) in THF 20 mL. The resulting solution was stirred for 1 h at 0ºC and after the elapsed time, EOM-Cl (60 mmol) was added in one portion. The resulting solution was stirred for 1 h while gradually warming the reaction temperature to ambient. After the elapsed time, water was carefully added and the reaction mixture was extracted with EtOAc and washed with brine and dried over anhydrous $MgSO_4$, filtered and concentrated *in vacuo*. The crude material was dissolved in minimal amount of CH_2Cl_2 and precipitated by addition of

MeOH. The precipitate was filtered and dried under high vacuum for 1 h to afford the title compound in 16.6 mmol (83% yield as a white crystalline powder). ^{1}H-NMR (400 MHz, $CDCl_3$) δ (ppm) 8.04 (d, J = 2 Hz, 2H), 7.86 (d, J = 9.2 Hz, 2H), 7.64 (d, J = 9.2 Hz, 2H), 7.30 (dd, J = 2.0, 9.2 Hz, 2H), 7.00 (d, J = 9.2 Hz, 2H), 5.14 (d, J = 7.2 Hz, 2H), 5.04 (d, J = 7.2 Hz, 2H), 3.47-3.35 (m, 4H), 1.06 (t, J = 7.2 Hz, 6H); ^{13}C-NMR δ (100.6 MHz, $CDCl_3$) δ (ppm) 153.1, 132.3, 130.7, 129.8, 129.6, 128.6, 127.1, 120.5, 118.1, 117.8, 93.6, 64.1, 14.9; HRMS Calcd. For $C_{26}H_{24}{}^{79}Br_2O_4Na$: 580.9934; found: 580.9947.

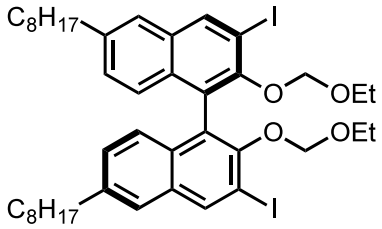

(*R,R*)-2,2'-bis(ethoxymethoxy)-3,3'-diiodo-6,6'-dioctyl-1,1'-binaphthalene (S2.2): Into a flame-dried 3-neck round bottom flask equipped with a magnetic stir bar and a reflux condenser was added $NiCl_2$(dppp) 540 mg (10 mol%) and (*R*)-6,6'-dibromo-2,2'-bis(ethoxymethoxy)-1,1'-binaphthalene (5.56 g, 1.0 equiv). The flask was evacuated and purged with nitrogen. Anhydrous Et_2O (35 ml) was added and the reaction mixture was cooled to 0ºC. To the suspension was drop-wise added *n*-octylmagnesium bromide (24.8 mL, 2.0 M in Et_2O, 5.0 equiv) over the course of 10 min. The reaction mixture was gradually warmed to room temperature and stirred for 30 min, upon which TLC indicated complete consumption of the starting material. The reaction mixture was carefully poured over frozen 1*N* HCl (50 mL) and the mixture was extracted with Et_2O. The combined organic extracts were dried over anhydrous magnesium sulfate and filtered through a small pad of silica. The filtrate was concentrated *in vacuo* and transferred to a flame dried 500 mL flask equipped with a magnetic stir bar. To the crude product was added anhydrous THF (100 mL) and the solution was cooled to –78 ºC. After 10 min, *n*-BuLi (14.0 mL, 2.5 M in hexanes, 3.5 equiv) was added drop-wise over 10 min. The solution was kept at –78 ºC for 30 min and then warmed to 0 ºC and stirred for 1.5 h at this temperature upon which fine light-brown precipitate was observed. After the elapsed time the reaction mixture was cooled to –78 ºC and iodine 9.48 g (3.75 equiv) was added in one portion. The reaction mixture was stirred for 10 min and then warmed to room temperature over 40 min. The reaction mixture was quenched with satd. Na_2SO_3 and extracted with EtOAc. The organic layer was washed with water and brine and dried over anhydrous $MgSO_4$, filtered and concentrated *in vacuo.* The residue was subjected to purification by flash chromatography (0-10% Et_2O gradient) to obtain the desired product 6.54 g (75% overall yield). ^{1}H-NMR (400 MHz, $CDCl_3$) δ (ppm) 8.45 (s, 2H), 7.53 (s, 2H), 7.14 (d, J = 8.8 Hz, 2H), 7.08 (d, J = 8.4 Hz, 2H), 4.86 (d, J = 5.6 Hz, 2H), 4.70 (d, J = 5.6 Hz, 2H), 3.03-3.10 (m, 2H), 2.71 (t, J = 7.6 Hz, 4H), 2.69-2.62 (m, 2H), 1.63 (q, J

= 6.8 Hz, 4 H), 1.44-1.25 (m, 20H), 0.87 (t, *J* = 6.4 Hz, 6H), 0.65 (d, *J* = 7.2 Hz, 6H). ^{13}C-NMR δ (ppm) 151.4, 140.5, 139.3, 132.4, 132.1, 128.8, 126.3, 126.0, 125.1, 98.0, 92.4, 69.9, 35.8, 31.8, 31.1, 29.4, 29.3, 29.2, 22.6, 14.4, 14.1). HMRS Calcd. For $C_{42}H_{56}O_4{}^{127}I_2Na$: 901.2160; found 901.2172.

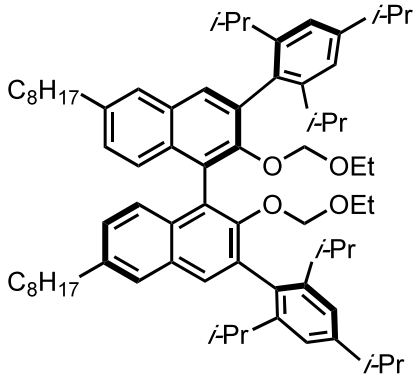

(*R*,*R*)-2,2'-bis(ethoxymethoxy)-6,6'-dioctyl-3,3'-bis(2,4,6-triisopropylphenyl)-1,1'-binaphthalene (S2.3): Into a flame-dried 3-neck round-bottom flask equipped with a reflux condenser and a magnetic stir bar was charged magnesium metal (496 mg, 20.4 mmol) and a small crystal of iodine. THF 1 ml was added and the mixture was heated until the color of iodine disappeared. To thus activated magnesium was added 1,3,5-triisopropylbromobenzene 5.5 g (19.4 mmol) in THF 25 mL. The resulting mixture was heated at reflux for 3 h and cooled to room temperature. On the side, into a flame dried round bottom flask equipped with a stir bar was charged (*R*)- 2,2'-bis(ethoxymethoxy)-3,3'-diiodo-6,6'-dioctyl-1,1'-binaphthalene 2.84 g (3.24 mmol) and $NiCl_2(PPh_3)_2$ 211 mg (0.32 mmol) and the mixture was suspended in anhydrous Et_2O (10 mL). To the solution at room temperature was added drop-wise the Grignard prepared above. The reaction mixture was stirred for 45 min and carefully poured over ice-cold 1*N* HCl. The mixture was extracted with CH_2Cl_2 and washed with brine and dried over anhydrous $MgSO_4$, filtered and concentrated *in vacuo*. The product was purified by flash chromatography (0-20% CH_2Cl_2/hexanes) to afford 1.83 g of the desired product (55% yield). ^{1}H-NMR (300 MHz, $CDCl_3$) δ (ppm) 7.72 (s, 2H), 7.67 (s, 2H), 7.39 (d, *J* = 8.7 Hz, 2 H), 7.22 (dd, *J* = 1.5, 8.4 Hz, 2H), 7.18-7.14 (m, 4H), 4.32 (d, *J* = 5.1 Hz, 2H), 4.29 (d, *J* = 5.1 Hz, 2H), 3.08-2.87 (m, 6H), 2.80 (apt, *J* = 7.5 Hz, 4H), 2.61-2.42 (m, 4H), 1.83-1.72 (m, 4H), 1.38-1.21 (m, 44H), 1.05 (d, *J* = 6.6 Hz, 6H), 0.96-0.92 (m, 6H), 0.56 (t, *J* = 7.2 Hz, 6H);). ^{13}C NMR (75.5 MHz, $CDCl_3$) δ (ppm) 151.7, 148.1, 147.6, 146.7, 140.7, 134.2, 133.5, 133.3, 132.1, 130.5, 130.3, 127.7, 126.1, 125.9, 121.3, 120.7, 120.4, 96.4, 63.5, 36.0, 34.4, 31.9, 31.4, 30.9, 30.8, 29.6, 29.5, 29.3, 26.0, 25.2, 24.1, 23.3, 23.2, 22.7, 14.5, 14.1; HRMS Calcd. for $C_{72}H_{102}O_4Na$: 1053.7670, found: 1053.7690.

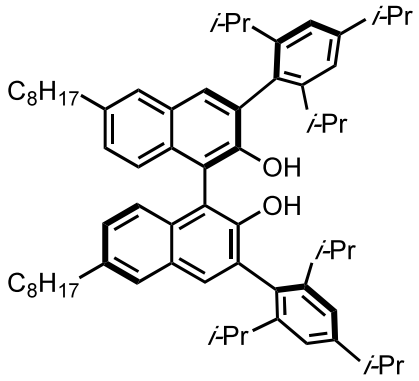

(*R,R*)-6,6'-dioctyl-3,3'-bis(2,4,6-triisopropylphenyl)-[1,1'-binaphthalene]-2,2'-diol (S2.4) : 1.5 g of **S2.3** was dissolved in Dioxane 50 mL. Conc HCl (5 mL) was added and the solution was heated to 70 ºC and stirred at this temperature for 1 h upon which TLC indicated complete consumption of the acetal. The solvent was evaporated *in vacuo*, and the residue was dissolved in CH_2Cl_2 and washed with Satd. $NaHCO_3$ and then water and then brine. The organic layer was then dried over anhydrous $MgSO_4$ and filtered and concentrated *in vacuo*. The residue was purified by flash chromatography (CH_2Cl_2/hexane 0-20% gradient) to obtain 968 mg of the bisphenol adduct in 72% yield. ^{1}H-NMR (300 MHz, $CDCl_3$) δ (ppm) 7.78 (s, 2H), 7.72 (s, 2H), 7.33-7.21 (m, 8H), 4.96 (s, 2H), 3.10-2.92 (m, 4H), 2.85-2.75 (m, 6H), 1.99-1.77 (m, 4H), 1.42-1.04 (m, 56H), 0.96-0.94 (m, 6H); ^{13}C-NMR (75.5 MHz, $CDCl_3$) δ (ppm) 150.0, 148.9, 147.7, 147.6, 138.4, 131.8, 130.8, 130.2, 129.2, 128.9, 128.2, 126.6, 124.5, 121.1, 112.9, 36.0, 34.3, 31.9, 31.5, 30.8, 29.6, 29.5, 29.3, 25.3, 24.34, 24.3, 24.1, 24.0, 23.9, 23.7, 22.7, 12.1; HRMS Calcd. for: [M-H] $C_{66}H_{89}O_2$: 913.6868, found: 913.6857.

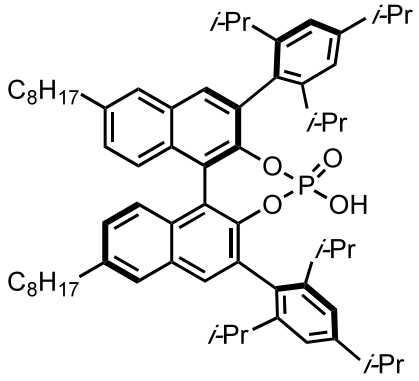

(*R,R*)-4-hydroxy-9,14-dioctyl-2,6-bis(2,4,6-triisopropylphenyl)dinaphtho[2,1-*d*:1',2'-*f*][1,3,2]dioxaphosphepine 4-oxide ((*R*)-C$_8$-TRIP): Bisphenol **S2.4**, 968 mg (1.06 mmol) was suspended in anhydrous pyridine 3 mL and to the mixture was added $POCl_3$ (194 µL, 2.12 mmol). The resultant was heated at 95 ºC for 16 h. The resulting solution was cooled to rt and water 3 mL was added. This mixture was then heated at 105 ºC for 5 h and then cooled to rt. The reaction mixture was diluted with CH_2Cl_2 and washed three times with 3*N* HCl and then dried over anhydrous $MgSO_4$, filtered and concentrated *in vacuo*. The crude material was purified by flash chromatography (0-5% MeOH/ CH_2Cl_2). The fractions containing the desired product were combined and the solvent

evaporated. The residue was then dissolved in anhydrous Et_2O and treated with anhydrous HCl (5 mL, 2.0 M in Et_2O) and stirred at room temperature for 30 min. The resulting ethereal solution was filtered through celite and the solvent evaporated *in vacuo*, and the residue was dried until a constant mass of 931 mg (90% yield). ^{1}H-NMR (400 MHz, $CDCl_3$) δ (ppm) 7.71 (s, 2H), 7.63 (s, 2H), 7.25 (d, J = 8.8 Hz, 2H), 7.20 (d, J = 8.0 Hz, 2H), 2.88-2.76 (m, 6H), 2.58 (sept, J = 6.8 Hz, 2 H), 2.52 (sept, J = 6.8 Hz, 2H), 1.77-1.69 (m, 4H), 1.45-1.30 (m, 20 H), 1.23 (dd, J = 6.8, 0.8 Hz, 12H), 1.05-0.96 (m, 12H), 0.91-0.88 (m, 12 H), 0.50 (d, J = 6Hz, 6H); ^{13}C-NMR δ (100.6 MHz, $CDCl_3$) δ (ppm) 148.1, 147.6, 147.0, 145.4, 145.3, 140.3, 132.3, 132.3, 131.1, 130.7, 127.5, 127.5, 126.4, 121.8, 121.2, 120.2, 36.1, 36.0, 34.7. 34.1, 32.0, 31.7, 31.4, 31.0, 30.7, 29.6, 29.55, 29.3, 26.4, 25.3, 25.0, 24.13, 24.11, 23.8, 23.7, 22.7, 11.5; HRMS Calcd. for : [M-H] $C_{66}H_{88}O_4P$: 975.6426; found: 974.6416.

Substrate Synthesis

Preparation of dihydropyranyl amine (S2.5):

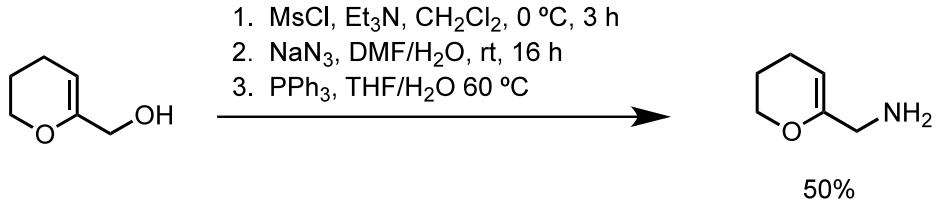

50%

(3,4-Dihydro-2*H*-pyran-6-yl)methanol (4.6 g, 40.4 mmol, 1.0 equiv) was dissolved in CH_2Cl_2 (125 mL) and cooled to 0 ºC. To above was added Et_3N (8.43 mL, 60.5 mmol, 1.5 equiv) followed by drop-wise addition of methanesulfonylchloride (3.75 mL, 1.2 equiv). The resulting mixture was stirred at 0 ºC for 2 h after which Et_3N (3.94 mL, 0.7 equiv) and methanesulfonylchloride (1.56 mL, 0.5 equiv) were added. The mixture was stirred for additional 1 h at 0 ºC. After the elapsed time, water was added and the product was extracted with CH_2Cl_2, washed with brine and dried over anhydrous $MgSO_4$, filtered and concentrated *in vacuo*. To thus obtained crude mesylate was added DMF (75 mL) and water (7.5 mL). The above solution was subsequently treated with NaN_3 (3.15 g, 48.4 mmol, 1.2 equiv) and the mixture was allowed to stir at rt for 16 h. After the elapsed time, the mixture was extracted with EtOAc and the combined organic extract was washed (3X) with water and brine, dried over anhydrous $MgSO_4$, filtered and concentrated *in vacuo*, to approximately 75 ml volume. To the resulting solution was added PPh_3 (9.7 g, 37 mmol), THF (100 mL) and water (10 mL). The resulting mixture was heated at 60 ºC for 2h. The product was extracted with EtOAc, and the organic layer was washed with water and brine and dried over anhydrous $MgSO_4$, filtered and concentrated *in vacuo.* The crude product was purified by bulb-to-bulb distillation (85 ºC, 0.1 mm Hg) to afford 2.3 g of the desired amine (50% yield). ^{1}H-NMR (300 MHz, $CDCl_3$) δ (ppm) 4.59 (t, J = 3.6 Hz, 1H), 3.97 (apt, J = 5.4 Hz, 2H), 3.10 (s, 2H), 2.00-1.95 (m, 2H), 1.80-1.73 (m, 2H); ^{13}C-NMR δ (100.6 MHz, $CDCl_3$) δ (ppm) 154.9, 95.3, 66.2, 45.0, 22.3, 19.9. HRMS (ESI) calcd *m/z* for C $_6H_{12}ON$ [M+H]: 114.0913; found: 114.0915.

General procedure for the preparation of dihydropyranyl amides (2.4a-i):

To a 0.1 M CH_2Cl_2 solution of (3,4-Dihydro-2*H*-pyran-6-yl) methanamine **S2.5** (1.0 equiv) at 0 ºC was added Et_3N (2.0 equiv) and the appropriate acid chloride (1.1 equiv). The reaction mixture was warmed to room temperature and stirred for 30 min after which water was added. The mixture was extracted with CH_2Cl_2, washed with brine and dried over anhydrous $MgSO_4$, filtered and concentrated *in vacuo*. The residue was purified by flash chromatography using Et_3N treated silica gel (10-20% EtOAc containing 1% Et_3N). The fractions containing the product were combined and evaporated to yield the desired product as crystalline white solids. (**Note**: Thus obtained products were immediately used for the fluorocyclization reactions. Over time, impurities arising from dimerization of the substrates (acid-catalyzed process) begin to appear.

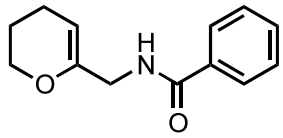

***N*-((3,4-Dihydro-2*H*-pyran-6-yl)methyl)benzamide (2.4a)**: Prepared according to general procedure above. Flash chromatography (10-20% EtOAc/hexanes containing 1% Et_3N) afforded the desired product as crystalline white solid (55% yield). ^{1}H-NMR (400 MHz, $CDCl_3$) δ (ppm) 7.77 (d, J = 7.6 Hz, 2H), 7.49-7.46 (m, 1H), 7.42-7.39 (m, 2H), 6.49 (m, 1H), 4.6 (t, J = 3.6 Hz, 1H), 4.02-3.97 (m, 4 H), 2.05-1.97 (m, 2H), 1.83-1.77 (m, 2H); ^{13}C-NMR δ (100.6 MHz, $CDCl_3$) δ (ppm) 167.2, 149.9, 134.5, 131.3, 128.4, 126.9, 97.9, 66.3, 42.7, 22.1, 19.9; HRMS calcd *m/z* for [M+H] $C_{13}H_{16}O_2N$: 218.1176; found: 218.1177

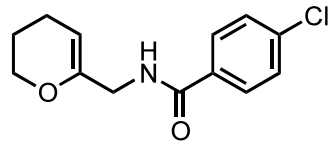

4-Chloro-*N*-((3,4-dihydro-2*H*-pyran-6-yl)methyl)benzamide (2.4b): Prepared according to general procedure above. Flash chromatography (10-20% EtOAc containing 1% Et_3N) afforded the desired product as crystalline white solid (60% yield)^{1}H-NMR (400 MHz, $CDCl_3$) δ (ppm) 7.71 (d, J = 8.4 Hz, 2H), 7.36 (d, J = 8.4 Hz, 2H), 6.55 (m, 1H) 4.75 (t, J = 3.6 Hz, 1H), 3.99 (appt, J = 5.2 Hz, 2H), 3.97 (d, J = 10 Hz, 2H), 2.02-1.98 (m, 2H), 1.82-1.76 (m, 2H); ^{13}C-NMR δ (100.6 MHz, $CDCl_3$) δ (ppm) 166.1, 149.8, 137.5, 132.8, 128.6, 128.4, 98.0, 66.4, 42.8, 22.1, 19.9; HRMS calcd *m/z* for [M+H] $C_{13}H_{15}O_2N^{35}Cl$: 252.0786; found: 252.0787.

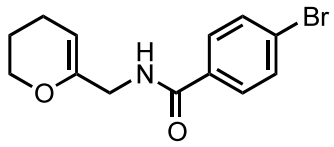

4-Bromo-*N*-((3,4-dihydro-2*H*-pyran-6-yl)methyl)benzamide (2.4c): Prepared according to general procedure above. Flash chromatography (10-20% EtOAc containing 1% Et_3N) afforded the desired product as crystalline white solid (52% yield)^{1}H-NMR (400 MHz, $CDCl_3$) δ (ppm) 7.63 (d, *J* = 8.4 Hz, 2H), 7.47 (d, *J* = 8.8 Hz, 2H), 6.82 (m, 1H), 4.70 (t, *J* = 3.6 Hz, 1H), 3.95 (appt, *J* = 4.8 Hz, 2H), 3.91 (d, *J* = 5.2 Hz, 2H), 1.99-1.92 (m, 2H), 1.78-1.72 (m, 2H); ^{13}C-NMR δ (100.6 MHz, $CDCl_3$) δ (ppm) 166.3, 149.7, 133.1, 131.4, 128.6, 125.8, 97.7, 66.2, 42.6, 22.0, 19.8; HRMS calcd *m/z* for [M+H] $C_{13}H_{15}O_2N^{79}Br$: 296.0281; found: 296.0283.

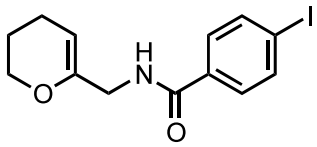

***N*-((3,4-Dihydro-2*H*-pyran-6-yl)methyl)-4-iodobenzamide (2.4d)**: Prepared according to general procedure above. Flash chromatography (10-20% EtOAc containing 1% Et_3N) afforded the desired product as crystalline white solid (65% yield). ^{1}H-NMR (400 MHz, $CDCl_3$) δ (ppm) 7.75 (d, *J* = 8.4 Hz, 2H), 7.50 (d, *J* = 8.4 Hz, 2H), 6.44 (m, 1H), 4.76 (t, *J* = 3.6 Hz, 1H), 4.01 (appt, *J* = 5.2 Hz, 2H), 3.96 (d, *J* = 5.6 Hz, 2H), 2.03-1.99 (m, 2H), 1.83-1.77 (m, 2H); ^{13}C-NMR δ (100.6 MHz, $CDCl_3$) δ (ppm) 166.4, 149.7, 137.3, 133.9, 128.6, 98.3, 98.2, 66.4, 42.9, 22.1, 19.9; HRMS calcd *m/z* for for [M+H] $C_{13}H_{15}O_2N^{127}I$: 344.0142; found: 344.0141.

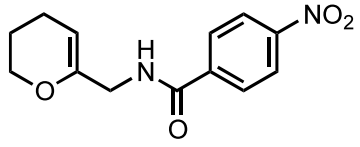

***N*-((3,4-Dihydro-2*H*-pyran-6-yl)methyl)-4-nitrobenzamide (2.4e)**: Prepared according to general procedure above. Flash chromatography (10-30% EtOAc containing 1% Et_3N) afforded the desired product as crystalline white solid (45% yield): ^{1}H-NMR (400 MHz, $CDCl_3$) δ (ppm) 8.24 (d, *J* = 8.8 Hz, 2H), 7.94 (d, *J* = 8.8 Hz, 2H), 6.67 (m, 1H), 4.78 (t, *J* = 3.6 Hz, 1H), 4.02-3.97 (m, 4H), 2.04-1.98 (m, 2H), 1.83-1.77 (m, 2H); ^{13}C-NMR δ (100.6 MHz, $CDCl_3$) δ (ppm) 165.2, 149.4, 149.3, 140.0, 128.2, 123.7, 98.5, 66.4, 43.1, 22.0, 19.9; HRMS calcd *m/z* for [M+H] $C_{13}H_{15}O_4N_2$: 263.1026; found: 263.1028.

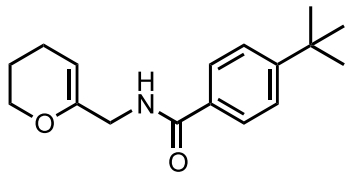

4-(*Tert*-butyl)-*N*-((3,4-dihydro-2*H*-pyran-6-yl)methyl)benzamide (2.4f): Prepared according to general procedure above. Flash chromatography (10-20% EtOAc containing 1% Et_3N) afforded the desired product as crystalline white solid (70% yield). ^{1}H-NMR (400 MHz, $CDCl_3$) δ (ppm) 7.72 (d, *J* = 8.4 Hz, 2H), 7.43 (d, *J* = 8.4 Hz, 2H), 6.40 (m, 1H), 4.77 (t, *J* = 3.6 Hz, 1H), 4.12-3.98 (m, 4H), 2.05-1.98(m, 2H), 1.83-1.77 (m, 2H), 1.32 (s, 9H); ^{13}C-NMR δ (100.6 MHz, $CDCl_3$) δ (ppm) 167.1, 154.7, 150.1, 131.5, 126.9, 126.7, 125.3, 97.5, 66.2, 42.5, 34.7, 31.0, 22.1, 19.8, 18.4; HRMS calcd *m/z* for [M+H] $C_{17}H_{24}O_2N$: 274.1802; found: 274.1802.

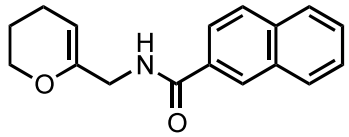

***N*-((3,4-Dihydro-2*H*-pyran-6-yl)methyl)-2-naphthamide (2.4g)**: Prepared according to general procedure above. Flash chromatography (10-20% EtOAc containing 1% Et_3N) afforded the desired product as crystalline white solid (55% yield). ^{1}H-NMR (400 MHz, $CDCl_3$) δ (ppm) 8.30 (s, 1H), 7.90-7.84 (m, 4H), 7.56-7.64 (m, 2H), 6.66 (m, 1H), 4.81 (t, *J* = 3.6 Hz, 1H), 4.06-4.02 (m, 4H), 2.05-2.01 (m, 2H), 1.84-1.71 (m, 2H); ^{13}C-NMR δ (100.6 MHz, $CDCl_3$) δ (ppm) 167.3, 150.0, 134.6, 132.5, 131.7, 128.9, 128.3, 127.7, 127.5, 127.4, 126.6, 123.6, 98.0, 66.4, 42.9, 22.1, 19.9; HRMS calcd *m/z* for [M+H] $C_{17}H_{18}O_2N$: 268.1332; found: 268.1332.

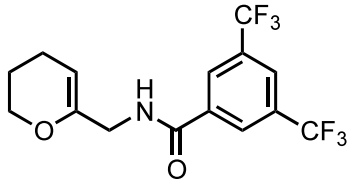

***N*-((3,4-Dihydro-2*H*-pyran-6-yl)methyl)-3,5-dimethoxybenzamide (2.4h)**: Prepared according to general procedure above. Flash chromatography (5-10% EtOAc containing 1% Et_3N) afforded the desired product as crystalline white solid (80% yield) ^{1}H-NMR (400 MHz, $CDCl_3$) δ (ppm) 8.23 (s, 2H), 8.00 (s, 1H), 6.54 (m, 1H), 4.82 (t, *J* = 3.6 Hz,

1H), 4.06-4.02 (m, 4H0, 2.05-2.04 (m, 2H), 1.86-1.82 (m, 2H); ^{13}C-NMR δ (100.6 MHz, $CDCl_3$) δ (ppm) 164.3, 149.3, 136.6, 132.1 (q, J_{C-F} = 45.3 Hz), 127.4, 126.9, 124.8 122.3 (q, J_{C-F} = 272.6 Hz), 98.8, 66.5, 43.3, 22.1, 19.9; HRMS calcd *m/z* for [M+H] $C_{17}H_{24}O_2N$: 274.1802; found: 274.1802

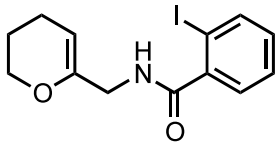

***N*-((3,4-Dihydro-2*H*-pyran-6-yl)methyl)-2-iodobenzamide (2.4i)**: Prepared according to general procedure above. Flash chromatography (10-20% EtOAc containing 1% Et_3N) afforded the desired product as crystalline white solid (72% yield). ^{1}H-NMR (400 MHz, $CDCl_3$) δ (ppm) 7.85 (d, *J* = 8.0 Hz, 1H), 7.41-7.35 (m, 2H), 7.09 (ddd, *J* = 8.0, 8.0, 1.6 Hz), 6.05 (m, 1H), 4.83 (t, *J* = 3.6 Hz, 1H), 4.02 (apt, *J* = 4.8 Hz, 2H), 3.98 (d, *J* = 5.6 Hz, 2H), 2.06-2.00 (m, 2H), 1.84-1.73 (m, 2H); ^{13}C-NMR δ (100.6 MHz, $CDCl_3$) δ (ppm) 169.0, 149.5, 142.2, 139.8, 131.0, 128.3, 128.1, 98.3, 92.4, 66.3, 42.8, 22.1, 19.9; HRMS calcd *m/z* for [M+H] $C_{17}H_{24}O_2N$: 274.1802; found: 274.1802.

Synthetic scheme for synthesis of dihydropyranyl and chromenyl substrates:

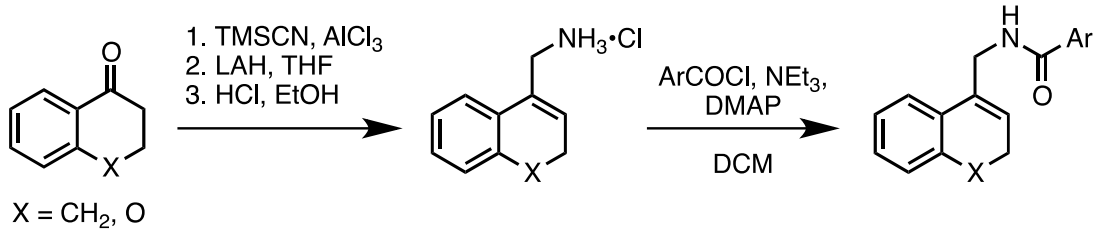

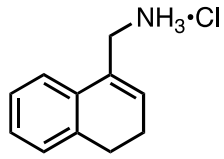

(3,4-Dihydronaphthalen-1-yl)methanammonium chloride (**S2.6a**): Prepared according to the methods of Trivedi et al.[20] To alpha-tetralone (1.97 ml, 16.2 mmol) and $AlCl_3$ (3 mg, 0.02 mmol) in an oven dried 100 ml round bottom flask under N_2 was added TMSCN (1.4 ml, 17.8 mmol). The reaction mixture was warmed to 35 ºC and stirred for 20 h. To the reaction mixture was added 30 ml THF, and it was then cooled to 0 ºC. LAH (740 mg, 19.4 mmol) was added portionwise and warmed to 23 ºC. The reaction mixture was stirred under N_2 for 3h. The reaction was quenched by the addition of $NaSO_4 \cdot 10H_2O$.

After stirring 1h the heterogeneous mixture became white in color. The reaction mixture was filtered, washing with Et_2O (2 x 15ml). The filtrate was concentrated and redissolved in EtOH (100 ml). 10 ml conc. HCl was added and the reaction mixture was heated to 60 ºC and stirred for 16 h. The reaction mixture was concentrated to dryness by rotary evaporation and the resulting solid was washed with Et_2O and dichloromethane. The resulting colorless crystalline solid was dried under high vacuum to give **S2.6a** (1.1 g, 35% yield). ^{1}H NMR: (400 MHz, CD_3OD) δ 7.25-7.24 (m, 2H), 7.21-7.19 (m, 2H), 6.24 (t, J = 4.4 Hz, 1H), 3.98 (s, 2H), 2.79 (t, J = 8.0 Hz, 2H), 2.40-2.30 (m, 2H); ^{13}C NMR: (125 MHz, CD_3OD) δ 137.9, 133.1, 131.6, 131.4, 129.2, 129.2, 128.1, 123.2, 41.7, 28.7, 24.1; HRMS (ESI) exact mass for M-H of free amine ($C_{11}H_{14}N$) calcd *m/z* 160.1121 found 160.1122.

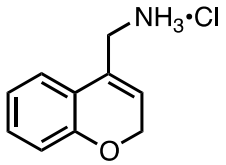

(2*H*-Chromen-4-yl)methanammonium chloride (S2.6b): Prepared analogously to **S2.6a**. To 4-chromanone (1.61 g, 10.9 mmol) and $AlCl_3$ (3 mg, 0.02 mmol) in an oven dried 100 ml round bottom flask under N_2 was added TMSCN (940 ul, 11.9 mmol). The reaction mixture was warmed to 35 ºC and stirred for 20 h. To the reaction mixture was added 30 ml THF, and it was then cooled to 0 ºC. LAH (494 mg, 13.0 mmol) was added portionwise and warmed to 23 ºC. The reaction mixture was stirred under N_2 for 3h. The reaction was quenched by the addition of $NaSO_4 \cdot 10H_2O$. After stirring 1h the heterogeneous mxture became white in color. The reaction mixture was filtered, washing with Et_2O (2 x 15ml). The filtrate was concentrated and redissolved in EtOH (100 ml). 10 ml conc. HCl were added and the reaction mixture was heated to 60 ºC and stirred for 16 h. The reaction mixture was concentrated to dryness by rotary evaporation and the resulting solid was washed with Et_2O and dichloromethane. The resulting colorless crystalline solid was dried under high vacuum to give **S2.6b** (610 mg, 29% yield). ^{1}H NMR (400 MHz, CD_3OD) δ 7.22-7.17 (m, 2H), 6.96 (t, J = 7.6 Hz, 1H), 6.82 (d, J = 7.6 Hz, 1H), 5.97 (t, J = 3.6 Hz, 1H), 4.77 (d, J = 3.6 Hz, 2H), 2.96 (s, 2H); ^{13}C NMR (125 MHz, CD_3OD) δ 154.3, 129.8, 127.5, 122.5, 122.2, 121.4, 120.5, 116.0, 64.5, 38.7; HRMS (ESI) exact mass for M-H of free amine ($C_{10}H_{12}ON$) calcd *m/z* 162.0913 found 162.0914.

General procedure for synthesis of dihydronaphthyl and chromenyl substrates: In a 20 ml scintillation vial containing **S2.6a** or **S2.6b** (98 mg, 0.5 mmol) in dichloromethane (5 ml) was added NEt_3 (280 ul, 2.0 mmol). The reaction mixture became homogeneous, and the substituted benzoyl chloride (0.75 mmol) was added followed by DMAP (6 mg, 0.05 mmol). The reaction mxiture was stirred at 23 ºC for 3h. The reaction was quenched by the addition of saturated aqueous NH_4Cl (15 ml). The aqueous phase was extracted with dichloromethane (3 x 15 ml) and the combined organic phases were dried with

$MgSO_4$, filtered and concentrated by rotory evaporation. Purification by flash column chromatography afforded the substituted benzamide substrate.

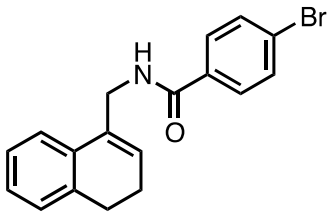

4-Bromo-*N*-((3,4-dihydronaphthalen-1-yl)methyl)benzamide (**2.6a**): Prepared according to the above general procedure on a 1.0 mmol scale. Flash column chromatography on silica eluting with 13:4:3 hexanes/dichloromethane/ethyl acetate) afforded **2.6a** (280 mg, 82% yield) as a colorless crystalline solid. ^{1}H NMR: (500 MHz, $CDCl_3$) δ 7.64 (d, J = 8.5 Hz, 2H), 7.55 (d, J = 8.5 Hz, 2H), 7.30 (t, J = 3.5 Hz, 1H), 7.25-7.20 (m, 3H), 6.23 (br s, 1H), 6.14 (t, J = 4.5 Hz, 1H), 4.50 (d, J = 5 Hz, 2H), 2.82 (t, J = 8.0 Hz, 2H), 2.48-2.34 (m, 2H); ^{13}C NMR: (125 MHz, $CDCl_3$) δ 166.4, 136.5, 133.3, 132.9, 132.8, 131.8, 128.7, 128.6, 127.9, 127.5, 126.8, 126.2, 122.6, 42.6, 27.9, 23.1; HRMS (ESI) exact mass for MH^+ ($C_{18}H_{17}NOBr$) calcd *m/z* 342.0488 found 342.0491.

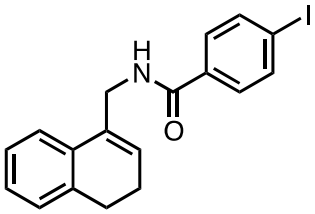

4-Iodo-*N*-((3,4-dihydronaphthalen-1-yl)methyl)benzamide (2.6b): Prepared according to the above general procedure on a 0.5 mmol scale. Flash column chromatography on silica eluting with 13:4:3 hexanes/dichloromethane/ethyl acetate) afforded **2.6b** (94 mg, 48% yield) as a colorless crystalline solid. ^{1}H NMR: (500 MHz, $CDCl_3$) δ 7.76 (d, J = 8.5 Hz, 2H), 7.49 (d, J = 8.5 Hz, 2H), 7.30-7.26 (m, 1H), 7.23-7.19 (m, 3H), 6.24 (br s, 1H), 6.14 (t, J = 4.0 Hz, 1H), 4.49 (d, J = 5.0 Hz, 2H), 2.82 (t, J = 8.0 Hz, 2H), 2.38-2.34 (m, 2H); ^{13}C NMR: (125 MHz, $CDCl_3$) δ 166.6, 137.8, 136.5, 133.9, 132.9, 132.8, 128.6, 128.6, 127.9, 127.5, 126.8, 122.6, 98.4, 42.5, 27.9, 23.1; HRMS (ESI) exact mass for M-H ($C_{18}H_{17}NOI$) calcd *m/z* 390.0349 found 390.0354.

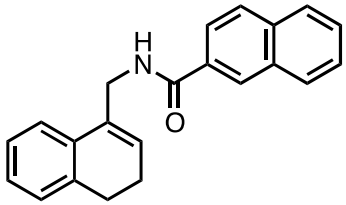

***N*-((3,4-Dihydronaphthalen-1-yl)methyl)-2-naphthamide (2.6c)**: Prepared according to the above general procedure on a 0.5 mmol scale. Flash column chromatography on silica eluting with 13:4:3 hexanes/dichloromethane/ethyl acetate) afforded **2.6c** (124 mg, 79% yield) as a colorless crystalline solid. ^{1}H NMR: (500 MHz, $CDCl_3$) δ 8.30 (s, 1H), 7.94-7.84 (m, 4H), 7.60-7.54 (m, 2H), 7.39 (d, J = 5.0 Hz, 1H), 7.26-7.25 (m, 1H), 6.33 (br s, 1H), 6.19 (t, J = 4 Hz, 1H), 4.58 (d, J = 4 Hz, 2H), 2.87 (t, J = 8 Hz, 2H), 2.41-2.37 (m, 2H); ^{13}C NMR: (125 MHz, $CDCl_3$) δ 167.4, 136.5, 134.8, 133.1, 133.0, 132.6, 131.7, 128.9, 128.6, 128.5, 127.9, 127.8, 127.7, 127.4, 127.4, 126.8, 126.8, 123.6, 122.8, 42.6, 28.0, 23.1; HRMS (ESI) exact mass for M-H ($C_{22}H_{20}NO$) calcd *m/z* 314.1539 found 314.1542.

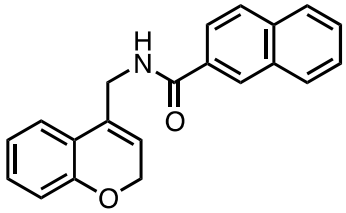

***N*-((2*H*-Chromen-4-yl)methyl)-2-naphthamide (2.6d)**: Prepared according to the above general procedure on a 1.0 mmol scale. Flash column chromatography on silica eluting with 13:4:3 hexanes/dichloromethane/ethyl acetate) afforded **2.6d** (144 mg, 91% yield) as a colorless crystalline solid. ^{1}H NMR (500 MHz, $CDCl_3$) δ 8.32 (s, 1H), 7.90-7.85 (m, 4H), 7.60-7.53 (m, 2H), 7.25 (dd, J = 8.0 Hz, 1.5 Hz, 1H), 7.18 (td, J = 8.0 Hz, 1.5 Hz, 1H), 6.93 (t, J = 8.0 Hz, 1H), 6.87 (d, J = 8.0 Hz, 1H), 6.63 (br s, 1H), 5.83 (t, J = 3.5 Hz, 1H), 4.80 (d, J = 3.5 Hz, 2H), 4.51 (d, J = 4.5 Hz, 2H); ^{13}C NMR (125 MHz, $CDCl_3$), δ 167.6, 154.3, 134.8, 132.6, 131.4, 130.9, 129.6, 129.0, 128.6, 127.8, 127.5, 126.8, 123.6, 123.3, 121.7, 121.6, 120.1, 116.2, 65.3, 40.9; HRMS (ESI) exact mass for M-H ($C_{21}H_{18}NO_2$) calcd *m/z* 316.1332 found 316.1334.

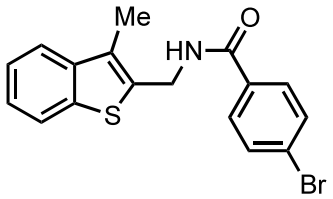

4-Bromo-N-((3-methylbenzo[b]thiophen-2-yl)methyl)benzamide (2.10): Prepared from the corresponding amine and 4-bromobenzoyl chloride according to the general procedure above. Flash chromatography (5-10% EtOAc/hexanes) afforded the desired compound as a crystalline white solid in 60% yield. ^{1}H-NMR (400 MHz, $CDCl_3$) δ (ppm) 7.75 (d, *J*= 7.6 Hz, 1H), 7.63 (d, *J* = 7.6 Hz, 1H), 7.61 (d, *J* = 7.6 Hz, 2H), 7.48 (d, *J* = 8.4 Hz, 2H), 7.39-7.36 (m, 1H), 7.34-7.30 (m, 1H), 6.75 (m, 1H), 4.80 (d, *J* = 5.2 Hz, 2H), 2.38 (s, 3H); ^{13}C-NMR δ (100.6 MHz, $CDCl_3$) δ (ppm) 166.3, 140.4, 138.5, 134.2, 132.7, 131.7, 129.4, 128.6, 126.3, 124.5, 124.1, 122.3, 121.8, 37.4, 11.6; HRMS calcd *m/z* for [M+H] $C_{17}H_{15}ON^{79}Br^{32}S$: 360.0052; found: 360.0057.

Fluorocyclization procedures

General procedure for the fluorocyclization of dihydropyran-derived benzamides: To a 30 mL test-tube equipped with a stir-bar and rubber septa was added the benzamide substrate (**2.4a-i**) (0.5 mmol, 1.0 equiv), Proton Sponge (1.1 equiv) and chiral phosphoric acid ((*R*)-C_8-TRIP) (5 mol%). To the heterogeneous mixture was added fluorobenzene (5.0 mL). The resulting solution was cooled to –20 ºC and maintained at this temperature for 10 minutes. After the elapsed time, Selectfluor (1.25 equiv) was added in one portion. The tube was capped with a rubber septum and the mixture was stirred at –20 ºC for 24 h. After the elapsed time, the reaction mixture was quenched by addition of saturated aqueous $Na_2S_2O_3$. The reaction mixture was extracted with CH_2Cl_2 and the combined organic extract was washed with brine and dried over anhydrous $MgSO_4$, filtered and concentrated *in vacuo*. The diastereoselectivity of the reaction was determined from thus obtained crude products by ^{19}F-NMR. Thus obtained crude product was loaded onto silica-gel and purified by flash chromatography (5-10% EtOAc/hexanes) to afford the desired products. Absolute stereochemistry was determined by X-ray crystallography of **2.5c**, all other products assigned by analogy.

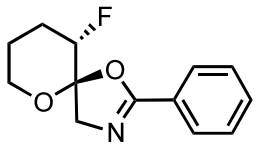

(5*R*,10*S*)-10-Fluoro-2-phenyl-1,6-dioxa-3-azaspiro[4.5]dec-2-ene (2.5a): Prepared according to the general procedure outlined above and obtained as an off-white solid (92.0 mg, 86% yield). ^{1}H-NMR (400 MHz, $CDCl_3$) δ (ppm) 7.95-7.93 (m, 2H), 7.50-7.46 (m, 1H), 7.43-7.35 (m, 2H), 4.59 (dt, $J_{H\text{-}F}$ = 47.2 Hz, $J_{H–H}$ = 2.8 Hz 1H), 4.11 (d, *J* = 15.6 Hz, 1H), 4.05 (m, 1H), 3.92 (d, *J* = 16.4 Hz, 1H), 3.83-3.81 (dd, *J* = 11.2, 4.4 Hz, 1H), 2.22-2.06 (m, 3H), 1.54-1.57 (m, 1H); ^{13}C-NMR (100.6 MHz, $CDCl_3$) δ (ppm) 161.9, 131.5, 128.3, 128.0, 127.5, 105.3 (d, $J_{C–F}$ = 28.2 Hz), 86.8 (d, $J_{C–F}$ = 175.0 Hz), 63.4 (d, $J_{C–F}$ = 129.7 Hz), 25.3 (d, $J_{C–F}$ = 21.1 Hz), 18.6;); ^{19}F-NMR (376.4 MHz) δ (ppm) –192.44 - –192.72 (m); HRMS (ESI) Calcd. for [M+H] $C_{13}H_{15}O_2NF$: 236.1081; found: 236.1081. HPLC (ChiralPak IC column) 95:05 (hexane/*i*PrOH) 1mL/min; T_{major} (9.0 min), T_{minor} (10.3 min); 92% *ee.*

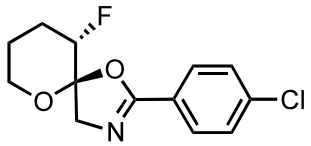

(5*R*,10*S*)-2-(4-Chlorophenyl)-10-fluoro-1,6-dioxa-3-azaspiro[4.5]dec-2-ene (2.5b): Prepared according to the general procedure outlined above and obtained as a colorless solid (130.0 mg, 97% yield)^{1}H-NMR (400 MHz, $CDCl_3$) δ (ppm) 7.85 (d, J = 8.4 Hz, 2H), 7.37 (d, J = 8.4 Hz, 2H), 4.57 (dt, J = 2.8 Hz, $J_{H–F}$ = 47.6 Hz, 1H), 4.09 (d, J = 16.4, 1H), 4.01 (dt, J = 12.0, 2.0 Hz, 1H), 3.90 (d, J = 16.4 Hz, 1H), 3.85-3.81 (m, 1H), 2.18-2.00 (m, 3H), 1.54-1.47(m, 1H); ^{13}C-NMR (100.6 MHz, $CDCl_3$) δ (ppm) 161.1, 137.6, 129.3, 128.6, 125.9, 105.6 (d, $J_{C–F}$ = 28.2 Hz), 86.7 (d, $J_{C–F}$ = 175.0 Hz), 63.4 (d, $J_{C–F}$ = 122.7 Hz), 25.2 (d, $J_{C–F}$ = 20.1 Hz), 18.6; ^{19}F-NMR (376.4 MHz) δ (ppm) –192.36 - –192.64 (m); HRMS (ESI) Calcd. for [M+H] $C_{13}H_{14}O_2N^{35}ClF$: 270.0692; found: 70.0693. HPLC (ChiralPak IC column) 98:02 (hexane/*i*PrOH) 1mL/min; T_{major} (9.6 min), T_{minor} (10.4 min); 95% *ee.*

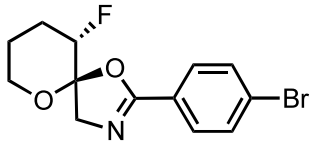

(5*R*,10*S*)-2-(4-Bromophenyl)-10-fluoro-1,6-dioxa-3-azaspiro[4.5]dec-2-ene (2.5c): Prepared according to the general procedure outlined above and obtained as an off-white solid (130.2 mg, 83.6% yield)^{1}H-NMR (400 MHz, $CDCl_3$) δ (ppm) 7.78 (dt, J = 8.4 Hz, $J_{H–F}$ = 2.4 Hz, 2H), 7.53 (dt, J = 8.4 Hz, $J_{H–F}$ = 2.4 Hz, 2H), 4.57 (dt, J = 2.8 Hz, $J_{H–F}$ = 44.8 Hz, 1H), 4.08 (dd, J = 16.4, $J_{H–F}$ = 0.8 Hz, 1H), 4.01 (dt, J = 12.8, 2.8 Hz, 1H), 3.85-3.81 (m, 1H), 2.17-2.00 (m, 3H), 1.53-1.47 (m, 1H); ^{13}C-NMR (100.6 MHz, $CDCl_3$) δ (ppm) 161.1, 131.6, 129.5, 126.4, 126.1, 105.6 (d, $J_{C–F}$ = 28.2 Hz), 86.7 (d, $J_{C–F}$ = 175.3 Hz), 63.4 (d, $J_{C–F}$ = 126.0 Hz), 25.2 (d, $J_{C–F}$ = 21.2 Hz), 18.6; ^{19}F-NMR (376.4 MHz) δ (ppm) –192.35 - –192.63 (m); HRMS (ESI) Calcd. for [M+H] $C_{13}H_{14}O_2N^{79}BrF$: 314.0186; found: 314.0188. HPLC (ChiralPak IC column) 95:05 (hexane/*i*PrOH) 1mL/min; T_{major} (10.1 min), T_{minor} (11.0 min); 92% *ee.* ORTEP visualization of crystal structure shown below.

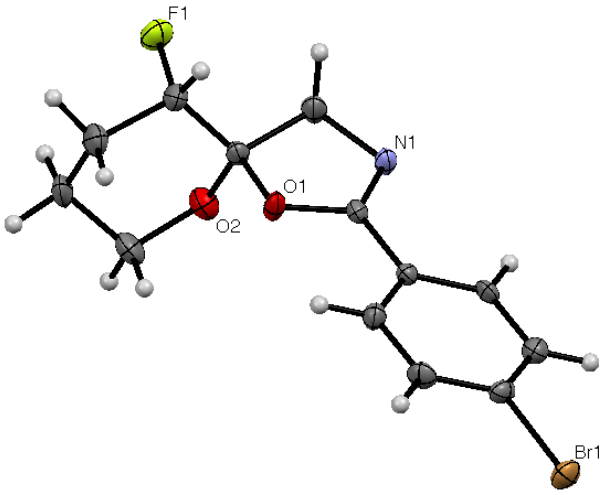

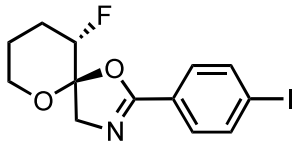

(5*R*,10*S*)-10-Fluoro-2-(4-iodophenyl)-1,6-dioxa-3-azaspiro[4.5]dec-2-ene (2.5d): Prepared according to the general procedure outlined above and obtained as a faint yellow solid (170.3 mg, 95% yield)^{1}H-NMR (400 MHz, $CDCl_3$) δ (ppm) 7.74 (d, J = 8.4 Hz, 2H), 7.62 (d, J = 8.4 Hz, 2H), 4.56 (dt, J = 2.8 Hz, J_{H-F} = 47.2 Hz, 1H), 4.07 (d, J = 16.4, 1H), 4.00 (dt, J = 12.4, 2.4 Hz, 1H), 3.87 (d, J = 16.8 Hz, 1H), 3.84-3.80 (m, 1H), 2.17-2.00 (m, 3H), 1.53-1.45 (m, 1H); ^{13}C-NMR (100.6 MHz, $CDCl_3$) δ (ppm) 161.2, 137.5, 129.5, 126.9, 105.5 (d, J_{C-F} = 28.2 Hz), 98.5, 86.7 (d, J_{C-F} = 174.0 Hz), 63.4 (d, J_{C-F} = 125.8 Hz), 25.2 (d, J_{C-F} = 20.1 Hz), 18.5; ^{19}F-NMR (376.4 MHz) δ (ppm) –192.31 - –192.59 (m); HRMS (ESI) Calcd. for [M+H] $C_{13}H_{14}O_2N^{127}IF$: 362.0048; found: 362.0044. HPLC (ChiralPak IC colum) 98:02 (hexane/*i*PrOH) 1mL/min; T_{major} (11.1 min), T_{minor} (10.4 min); 97% *ee.*

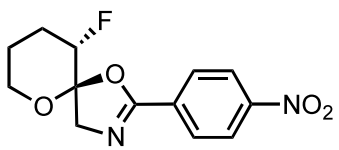

(5*R*,10*S*)-10-Fluoro-2-(4-nitrophenyl)-1,6-dioxa-3-azaspiro[4.5]dec-2-ene (2.5e): Prepared according to the general procedure outlined above and obtained as a colorless solid (94.0 mg, 67% yield)^{1}H-NMR (400 MHz, $CDCl_3$) δ (ppm) 8.25 (d, J = 8.8 Hz, 2H), 8.09 (d, J = 8.4 Hz, 2H), 4.61 (dt, J = 2.8 Hz, J_{H-F} = 47.2 Hz, 1H), 4.14 (d, J = 16.8, 1H), 4.02 (dt, J = 12.4, 2.4 Hz, 1H), 3.94 (d, J = 16.8 Hz, 1H), 3.87-3.83 (m, 1H), 2.25-2.03 (m, 3H), 1.58-1.49 (m, 1H); ^{13}C-NMR (100.6 MHz, $CDCl_3$) δ (ppm) 160.1, 149.5, 133.2, 129.0, 123.5, 106.2 (d, J_{C-F} = 28.1 Hz), 86.6 (d, J_{C-F} = 175.0 Hz), 63.9 (d, J_{C-F} = 127.8 Hz), 25.2 (d, J_{C-F} = 20.1 Hz), 18.5; ^{19}F-NMR (376.4 MHz) δ (ppm) –192.31 - –192.59 (m); HRMS (ESI) Calcd. for [M+H] $C_{13}H_{14}O_4N_2F$: 281.0932; found: 281.0932. HPLC (ChiralPak IC column) 95:05 (hexane/*i*PrOH) 1mL/min; T_{major} (17.4 min), T_{minor} (20.2 min); 97% *ee.*

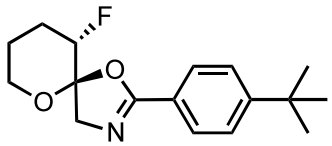

(5*R*,10*S*)-2-(4-(*Tert*-butyl)phenyl)-10-fluoro-1,6-dioxa-3-azaspiro[4.5]dec-2-ene (2.5f): Prepared according to the general procedure outlined above and obtained as a colorless solid (137.3 mg, 94.8% yield) ^{1}H-NMR (400 MHz, $CDCl_3$) δ (ppm) 7.87 (d, J = 8.4 Hz, 2H), 7.43 (d, J = 8.4 Hz, 2H), 4.57 (d, J_{H-F} = 47.2 Hz, 1H), 4.10 (d, J = 16.4, 1H), 4.04 (dt, J = 11.0, 2.0 Hz, 1H), 3.91 (d, J = 16.0 Hz, 1H), 3.83-3.81 (m, 1H), 2.21-2.01 (m, 3H), 1.51-1.48 (m, 1H), 1.33 (s, 9H); ^{13}C-NMR (100.6 MHz, $CDCl_3$) δ (ppm) 162.0, 155.0, 127.8, 125.3, 124.6, 105.2 (d, J_{C-F} = 28.2 Hz), 86.9 (d, J_{C-F} = 175.0 Hz), 63.0 (d, J_{C-F} = 130.0 Hz), 34.9, 31.0. 25.3 (d, J_{C-F} = 20.1 Hz), 18.5; ^{19}F-NMR (376.4 MHz) δ (ppm) –192.40 - –192.68 (m); HRMS (ESI) Calcd. for [M+H] $C_{17}H_{23}O_2NF$: 292.1707; found: 292.1706. HPLC (Chiralpak IC column) 98:02 (hexane/*i*PrOH) 1mL/min; T_{major} (14.7 min), T_{minor} (17.9 min); 95% *ee.*

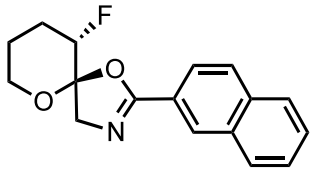

(5*R*,10*S*)-10-Fluoro-2-(naphthalen-2-yl)-1,6-dioxa-3-azaspiro[4.5]dec-2-ene (2.5g): Prepared according to the general procedure outlined above and obtained as a faint yellow solid (132.0 mg, 94% yield)^{1}H-NMR (400 MHz, $CDCl_3$) δ (ppm) 8.42 (s, 1H), 8.03 (dd, J = 8.4, 1.2 Hz, 1H), 7.92 (d, J = 7.6 Hz, 1H), 7.88-7.85 (m, 2H), 7.57-7.51 (m, 2H), 4.65 (d, J_{H-F} = 46.8 Hz), 4.18 (d, J = 16.4 Hz, 1H), 4.12 (d, J=11.2 Hz, 1H), 3.99 (d, J = 16.4 Hz, 1H), 3.90-3.86 (m, 1H), 2.32-2.04 (m, 3H), 1.57-1.52 (m, 1H); ^{13}C-NMR (100.6 MHz, $CDCl_3$) δ (ppm) 162.1, 134.7, 132.5, 128.8, 128.5, 128.2, 127.8, 127.6,

126.6, 124.8, 124.5, 105.5 (d, $J_{C–F}$ = 28.2 Hz), 86.9 (d, $J_{C–F}$ = 175.0 Hz), 63.5 (d, $J_{C–F}$ = 131.8 Hz), 25.3 (d, $J_{C–F}$ = 21.1 Hz), 18.7; ^{19}F-NMR (376.4 MHz) δ (ppm) –192.30 - –192.57 (m); HRMS (ESI) Calcd. for [M+H] $C_{17}H_{17}O_2NF$: 286.1238; found: 286.1236. HPLC (ChiralPak IC column) 95:05 (hexane/*i*PrOH) 1mL/min; T_{major} (11.4 min), T_{minor} (13.2 min); 96% *ee.*

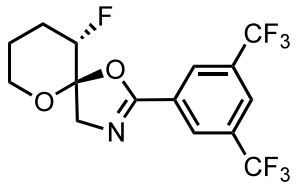

(5*R*,10*S*)-2-(3,5-Bis(trifluoromethyl)phenyl)-10-fluoro-1,6-dioxa-3-azaspiro[4.5]dec-2-ene (2.5h): Prepared according to the general procedure outlined above and obtained as a faint-yellow solid (123.8 mg, 80% yield, 0.4 mmol scale). ^{1}H-NMR (400 MHz, $CDCl_3$) δ (ppm) 8.73 (s, 2H), 7.98 (s, 1H), 4.61 (dt, *J* = 2.8 Hz, J_{H-F} = 46.4 Hz, 1H), 4.15 (d, *J* = 16.8 Hz, 1H), 4.05 (dt, *J* = 10.8, 2.0 Hz, 1H), 3.95 (d, *J* = 16.8 Hz, 1H), 3.88-3.85 (m, 1H), 2.25-2.03 (m, 3H), 1.57-1.54 (m, 1H); ^{13}C-NMR (100.6 MHz, $CDCl_3$) δ (ppm) 159.5, 132.1 (q, J_{C-F} = 33.2 Hz), 129.8, 128.1, 124.8, 122.9 (q, J_{C-F} = 272.6 Hz), 106.6 1 (d, J_{C-F} = 28.2 Hz), 86.6 (d, J_{C-F} = 175.0 Hz), 63.6 (d, J_{C-F} = 102.6 Hz), 25.2 (d, J_{C-F} = 21.1 Hz), 18.5; ^{19}F-NMR (376.4 MHz) δ (ppm) –62.29 (s), –192.28—192.55 (m); HRMS (ESI) Calcd. for [M+H] $C_{15}H_{12}F_7NO_2$: found: HPLC (ChiralPak IC column) 99.9:0.01 (hexane/*i*PrOH) 1mL/min; T_{major} (12.9 min), T_{minor} (16.0 min); 79% *ee.*

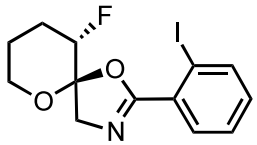

(5*R*,10*S*)-10-Fluoro-2-(2-iodophenyl)-1,6-dioxa-3-azaspiro[4.5]dec-2-ene (2.5i): Prepared according to the general procedure outlined above and obtained as a faint-yellow solid (131.8 mg, 73% yield, 0.5 mmol scale). ^{1}H-NMR (400 MHz, $CDCl_3$) δ (ppm) 7.93 (d, *J* = 8.0 Hz, 1H), 7.68 (d, J = 7.6 Hz, 1H), 7.38 (t, *J* = 7.6 Hz, 1H), 7.13 (d, *J* = 8.0 Hz, 1H), 4.64 (d, $J_{H–F}$ = 47.2 Hz, 1H), 4.14 (d, *J* = 16.4, 1H), 4.07 (d, *J* = 10.0 Hz, 1H), 3.92 (d, J = 16.4 Hz, 1H), 3.88-3.84 (m, 1H), 2.21-2.03 (m, 3H), 1.52-1.47 (m, 1H), 1.33 (s, 9H); ^{13}C-NMR (100.6 MHz, $CDCl_3$) δ (ppm) 162.0, 140.6, 133.0, 131.8, 131.1, 127.8, 106.2 (d, $J_{C–F}$ = 28.2 Hz), 94.0, 86.5 (d, $J_{C–F}$ = 175.0 Hz), 63.6 (d, $J_{C–F}$ = 97.6 Hz), 25.1 (d, $J_{C–F}$ = 20.1 Hz), 18.5; ^{19}F-NMR (376.4 MHz) δ (ppm) –193.03 - –193.30 (m); HRMS (ESI) Calcd. for [M+H] $C_{17}H_{23}O_2NF$: 292.1707; found: 292.1706. HPLC (ChiralPakIC column) 95:05 (hexane/*i*PrOH) 1mL/min; T_{major} (11.2 min), T_{minor} (12.5 min); 89% *ee.*

General procedure for the asymmetric fluorocyclization of substrates 2.7a-d: In a 25 mm test tube that had been oven dried and cooled under an atmosphere of N_2 was added

alkene substrate (0.15 mmol), catalyst (*R*)-C_8-TRIP (0.015 mmol), powdered anhydrous Na_2CO_3 (0.19 mmol) and a 1:1 hexanes/fluorobenzene solvent mixture (10 ml total). Selectfluor (0.23 mmol) was added last, a 24/40 septum was affixed to the test tube and the reaction mixture was stirred vigorously under N_2 at 23 ºC for 24 hours. The reaction was quenched by the addition of saturated aqueous $Na_2S_2O_3$ (15 mL) and stirring of the consequent biphasic mixture for 10 min. The reaction mixture was transferred to a separatory funnel and the organic phase was diluted with dichloromethane (30 ml). The organic phase was collected and the aqueous phase was extracted with dichloromethane (3 x 15 ml). The combined organic phases were dried with $MgSO_4$, filtered and concentrated. Crude product was analyzed by ^1H and ^{19}F NMR to determine diastereoselectivity. The crude product was then purified by flash column chromatography on silica gel, eluting with hexanes/ethyl acetate to afford the desired fluorocyclization product. Enantiopurity was determined by HPLC analysis.

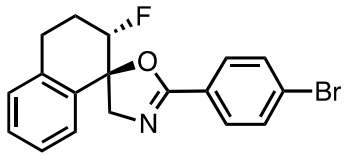

(1*R*,2*S*)-2'-(4-Bromophenyl)-2-fluoro-3,4-dihydro-2*H*,4'*H*-spiro[naphthalene-1,5'-oxazole] (2.7a): Prepared according to the general procedure on a 0.15 mmol scale (52 mg). Purification by flash column chromatography on silica gel, eluting with 7:1 hexanes/ethyl acetate afforded **6a** as a colorless crystalline solid (47 mg, 87% yield). ^1H NMR (500 MHz, $CDCl_3$) δ 7.91 (d, J = 8.5 Hz, 2H), 7.60 (d, J = 8.5 Hz, 2H), 7.36-7.33 (m, 1H), 7.31-7.27 (m, 2H), 7.18-7.17 (m, 1H), 5.09 (ddd, $J_{H\text{-}F}$ = 50 Hz, $J_{H\text{-}H}$ = 11 Hz, 3.5 Hz, 1H), 4.56 (d, J = 15 Hz, 1H), 4.07 (dd, J = 15.5 Hz, 3.0 Hz, 1H), 3.08-2.97 (m, 2H), 2.41-2.32 (m, 1H), 2.20-2.11 (m, 1H); ^{13}C NMR (125 MHz, $CDCl_3$) δ 162.8, 137.4 (d, $J_{C\text{-}F}$ = 4 Hz), 134.8 (d, $J_{C\text{-}F}$ = 1 Hz), 131.7, 129.9, 128.5, 128.3, 127.5, 126.5 (d, $J_{C\text{-}F}$ = 2 Hz), 126.4, 126.3, 92.1 (d, $J_{C\text{-}F}$ = 180 Hz), 86.9 (d, $J_{C\text{-}F}$ = 20 Hz), 64.2 (d, $J_{C\text{-}F}$ = 6 Hz, 26.5 (d, $J_{C\text{-}F}$ = 10 Hz), 26.1 (d, $J_{C\text{-}F}$ = 19 Hz); ^{19}F NMR (376 MHz, $CDCl_3$) δ -192.45 (dd, $J_{H\text{-}F}$ = 49 Hz, 19 Hz); HRMS (ESI) exact mass for M-H ($C_{18}H_{16}NOBrF$) calcd *m/z* 360.0394 found 360.0398. HPLC (Chiralpak IA column, 95:5 hexanes/isopropanol, 1 mL/min) t_r = 12.7 min (major), 14.1 min (minor); 93% ee.

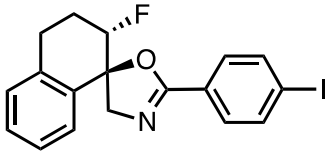

(1*R*,2*S*)-2'-(4-Iodophenyl)-2-fluoro-3,4-dihydro-2*H*,4'*H*-spiro[naphthalene-1,5'-oxazole] (2.7b): Prepared according to the general procedure on a 0.15 mmol scale (58 mg). Purification by flash column chromatography on silica gel, eluting with 7:1 hexanes/ethyl acetate afforded **6b** as a colorless solid (44 mg, 71% yield). ^1H NMR (500

MHz, $CDCl_3$) δ 7.82 (d, J = 8.5 Hz, 2H), 7.76 (d, J = 8.5 Hz, 2H), 7.35-7.33 (m, 1H), 7.31-7.25 (m, 2H), 7.18-7.17 (m, 1H), 5.08 (ddd, $J_{H\text{-}F}$ = 50.0 Hz, $J_{H\text{-}H}$ = 11.0 Hz, 3.5 Hz, 1H), 4.57 (d, J = 15.5 Hz, 1H), 4.06 (dd, J = 15.0 Hz, 3.0 Hz, 1H), 3.07-2.97 (m, 2H), 2.41-2.32 (m, 1H), 2.20-2.11 (m, 1H); ^{13}C NMR (125 MHz, $CDCl_3$) δ 162.3, 137.7, 137.4 (d, $J_{C\text{-}F}$ = 4 Hz), 134.8 (d, $J_{C\text{-}F}$ = 1 Hz), 129.9, 128.5, 128.3, 127.5, 12.0, 126.5 (d, $J_{C\text{-}F}$ = 1Hz), 98.5, 92.1 (d, $J_{C\text{-}F}$ = 181 Hz), 86.8 (d, $J_{C\text{-}F}$ = 21 Hz), 64.2 (d, $J_{C\text{-}F}$ = 6 Hz), 26.5 (d, $J_{C\text{-}F}$ = 11 Hz), 26.1 (d, $J_{C\text{-}F}$ = 19 Hz); HRMS (ESI) exact mass for M-H ($C_{18}H_{16}NOIF$) calcd *m/z* 408.0255 found 408.0258. HPLC (Chirlpak IA column, 95:5 hexanes/isopropanol, 1 mL/min; t_r = 14.7 min (major), 16.3 min (minor); 93% ee.

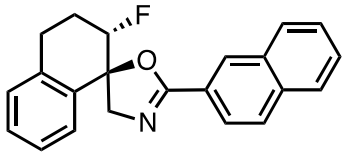

(1*R*,2*S*)-2-Fluoro-2'-(naphthalen-2-yl)-3,4-dihydro-2*H*,4'*H*-spiro[naphthalene-1,5'-oxazole] (2.7c): Prepared according to the general procedure on a 0.14 mmol scale (43 mg). Purification by flash column chromatography on silica gel, eluting with 7:1 hexanes/ethyl acetate afforded **6c** as a colorless solid (28 mg, 62% yield). ^{1}H NMR (500 MHz, $CDCl_3$) δ 8.54 (s, 1H), 8.16 (dd, J = 8.5 Hz, 1.5 Hz, 1H), 7.94-7.90 (m, 3H), 7.61-7.54 (m, 2H), 7.45-7.43 (m, 1H), 7.32-7.28 (m, 2H), 2.70-7.10 (m, 1H), 5.17 (ddd, $J_{H\text{-}F}$ = 50 Hz, $J_{H\text{-}H}$ = 11 Hz, 3.5 Hz, 1H), 4.66 (d, J = 15.5 Hz, 1H), 4.16 (dd, J = 15.0 Hz, 2.5 Hz, 1H), 3.11-3.01 (m, 2H), 2.45-2.38 (m, 1H), 2.25-2.20 (m, 1H); ^{13}C NMR (125 MHz, $CDCl_3$) δ 163.7, 137.7 (d, $J_{C\text{-}F}$ = 5 Hz), 134.8 (d, $J_{C\text{-}F}$ = 1 Hz), 134.8, 132.7, 128.9, 128.4, 128.3, 1282, 127.8, 127.6, 127.5, 126.6 (d, $J_{C\text{-}F}$ = 2 Hz), 126.6, 124.9, 124.8, 92.6 (d, $J_{C\text{-}F}$ = 181 Hz), 86.5 (d, $J_{C\text{-}F}$ = 21 Hz), 64.3 (d, $J_{C\text{-}F}$ = 6 Hz), 26.5 (d, $J_{C\text{-}F}$ = 11 Hz), 26.2 (d, $J_{C\text{-}F}$ = 20 Hz); ^{19}F NMR (376 MHz, $CDCl_3$) δ -192.375 (dd, $J_{H\text{-}F}$ = 49 Hz, 19 Hz); HRMS (ESI) exact mass for MH^+ ($C_{22}H_{19}FNO$) calcd *m/z* 332.1445 found 332.1444. HPLC (Chirlpak IA column, 95:5 hexanes/isopropanol, 1 ml/min; t_r = 15.4 min (major), 17.4 min (minor); 96% ee.

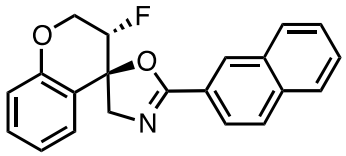

(3*S*,4*R*)-3-Fluoro-2'-(naphthalen-2-yl)-4'*H*-spiro[chroman-4,5'-oxazole] (**2.7d**): Prepared according to the general procedure on a 0.15 mmol scale (47 mg). Purification by flash column chromatography on silica gel, eluting with 6:1 hexanes/ethyl acetate afforded **6d** as a colorless solid (35 mg, 70% yield). ^{1}H NMR (500 MHz, $CDCl_3$) δ 8.45 (s, 1H), 8.10 (d, J = 8.5 Hz, 1H), 7.93-7.8 (m, 3H), 7.61-7.54 (m, 2H), 7.46 (d, J = 8.0 Hz, 1H), 3.42 (t J = 8.0 Hz, 1H), 7.07 (d, J = 8.0 Hz, 1H), 7.01 (d, J = 8.5 Hz, 1H), 5.00 (dd, $J_{H\text{-}F}$ = 45.0 Hz, $J_{H\text{-}H}$ = 3.0 Hz, 1H), 4.64 (d, J = 16.0 Hz, 1H), 4.54-4.46 (m, 2H),

4.46 (d, J = 15.5 Hz, 1H); ^{13}C NMR (125 MHz, $CDCl_3$) δ 162.7, 153.5, 134.9, 132.6, 130.7, 129.0, 128.9, 128.3, 128.0, 127.9, 127.8, 126.7, 124.7, 124.4, 122.3, 121.3, 117.2, 86.6 (d, $J_{C\text{-}F}$ = 183 Hz), 80.1 (d, $J_{C\text{-}F}$ = 26 Hz), 64.6, (d, $J_{C\text{-}F}$ = 21 Hz), 63.0 (d, $J_{C\text{-}F}$ = 4 Hz); ^{19}F NMR (376 MHz, $CDCl_3$) δ 200.70 (ddd, J = 49 Hz, 30 Hz, 11 Hz); HRMS (ESI) exact mass for M-H ($C_{21}H_{17}FNO_2$) calcd *m/z* 334.1238 found 334.1241. HPLC (Chiralpak IA column, 95:5 hexanes/isopropanol, 1 ml/min; t_r = 12.2 min (major), 15.2 min (minor); 92% ee.

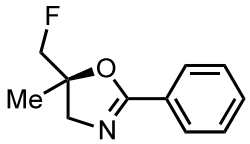

(*R*)-5-(Fluoromethyl)-5-methyl-2-phenyl-4,5-dihydrooxazole (2.9) : *N*-(2-methylallyl)benzamide[21] (17.8 mg, 0.1 mmol. 1.0 equiv), Selectfluor (42.0 mg, 0.12 mmol, 1.2 equiv), Na_2CO_3 (11.6 mg, 0.11 mmol, 1.1 equiv) and phosphoric acid ((*R*)-TCYP) (5.0 mg, 0.005 mmol, 5 mol%) were charged into a 1-dram vial and anhydrous heptane 2.0 ml was charged. The heterogeneous mixture was heated at 60 ºC for 24 h after which it was filtered through a cotton-plug. The filtrate was directly loaded onto silica gel. The product was eluted with 10-30% EtOAc/hexanes gradient. Evaporation of fractions containing the product yielded 14.7 mg of the desired product as a glassy solid (75% yield). ^{1}H-NMR (400 MHz, $CDCl_3$) δ (ppm) 7.93 (d, J = 7.2 Hz, 2H), 7.50-7.46 (m, 1H), 7.43-7.39 (m, 2H), 4.48 (dd, $J_{H–F}$ = 47.6 Hz, $J_{H–H}$ = 10.0 Hz, 1H), 4.37 (dd, $J_{H–F}$ = 47.6 Hz, $J_{H–H}$ = 10.0 Hz, 1H), 4.01 (d, J = 15.2 Hz, 1H), 3.76 (dd, J = 14.8, 2.4 Hz, 1H), 1.51 (d, $J_{H\text{-}F}$ = 1.6 Hz, 3H); ^{13}C-NMR δ (100.6 MHz, $CDCl_3$) δ (ppm) 166.3, 131.4, 128.3, 128.1, 127.6, 85.9 (d, $J_{C–F}$ = 179.1 Hz), 83.9 (d, $J_{C–F}$ = 19.1 Hz), 62.2 (d, $J_{C–F}$ = 3.02 Hz), 21.7 (d, $J_{C–F}$ = 4.0 Hz); ^{19}F-NMR (376.4 MHz) δ (ppm) –225.61 (t, $J_{H–F}$ = 48.9 Hz); HRMS (EI) Calcd. for $C_{12}H_{12}ON^{19}F$: 193.0903; found: 193.0908.

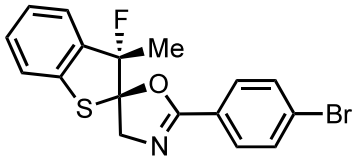

(2*S*,3*S*)-2'-(4-Bromophenyl)-3-fluoro-3-methyl-3*H*,4'*H*-spiro[benzo[*b*]thiophene-2,5'-oxazole] **(2.11)**: Prepared according to the general procedure for the asymmetric fluorination outlined in the dihydropyran series except that Proton Sponge® was replaced with anhydrous Na_2CO_3 and that the reaction was run at room temperature. Flash chromatography yielded the desired product as a colorless solid (76 mg, 69% yield, 0.30 mmol scale). ^{1}H-NMR (400 MHz, $CDCl_3$) δ (ppm) 7.75 (d, J = 8.4 Hz, 2H), 7.53 (d, J = 8.4 Hz, 2H), 7.44-7.38 (m, 2H), 7.30 (d, J = 8.0 Hz, 1H), 7.26-7.23 (m, 1H), 4.69 (d, J = 17.2 Hz, 1H), 4.39 (d, J = 17.6 Hz, 1H), 1.79 (d, $J_{H\text{-}F}$ = 20.8 Hz, 3H); ^{13}C-NMR (100.6 MHz, $CDCl_3$) δ (ppm) 162.0, 141.0 (d, $J_{C–F}$ = 5.0 Hz), 136.5 (d, $J_{C–F}$ = 19.1 Hz), 131.7, 131.5 (d, $J_{C–F}$ = 4.0 Hz), 129.7, 126.6, 125.7, 125.6 (d, $J_{C–F}$ = 3.0 Hz)m 125.2 (d, $J_{C–F}$ = 2.0 Hz), 122.9 (d, $J_{C–F}$ = 3.0 Hz), 105.6 (d, $J_{C–F}$ = 35.2 Hz), 103.1 ((d, $J_{C–F}$ = 178.1 Hz),

17.0 (d, J_{C-F} = 26.1 Hz); ^{19}F-NMR (376.4 MHz) δ (ppm) –135.82 (q, J_{H-F} = 18.8 Hz); HRMS (ESI) Calcd. for [M+H] $C_{17}H_{14}ON^{79}BrF^{32}S$: 377.9958; found: 377.9968. HPLC (ChiralPak IC column) 99:01 (hexane/*i*PrOH) 1mL/min; T_{major} (10.8 min), T_{minor} (12.1 min); 97% *ee.*

Nonlinear effect study

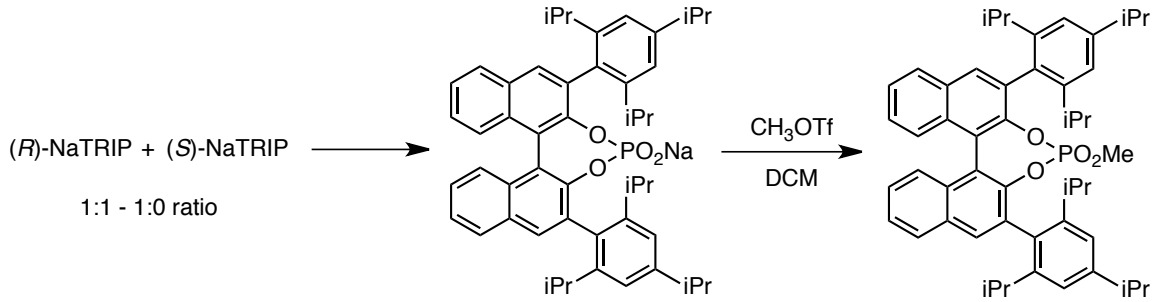

S2.7(i-vi)

Preparation of enantioenriched phosphate catalysts

(*R*)- and (*S*)-NaTRIP (citation) were combined in in ratios of app roximately 1:1, 3:2, 7:3, 4:1, 9:1 and 1:0 on a total scale of 0.025 mmol.The combined chiral phosphate salts were dissolved in 10 ml C_6H_5F. In order to determine the optical purity of each catalyst mixture, 1 ml aliquots were removed, concentrated, redeposited in dichloromethane, and an excess of CH_3OTf was added to generate the phosphate methyl esters for HPLC analysis. The reaction mixtures were stirred 1h, at which point TLC indicated conversion of starting material. The reaction mixtures were concentrated, taken up inHPLC hexanes, filtered through Wattman paper filters and analyzed by HPLC (Whelk column, 99.9:0.01 hexanes/isopropanol, 1 ml/min) t_r = 5.9 min (minor), 8.8 min (major). The observed enantioenrichents are listed below:

S2.7i: >99%

S2.7ii: 82%

S2.7iii: 63%

S2.7iv: 45%

S2.7v: 24%

S2.7vi: 2%

Assessment of effect of enantiopurity of catalyst on enantiopurity of product

Each reaction was run in duplicate and the plotted data is an average of the two results. To **2.7a** (8.6 mg, 0.025 mmol), Na_2CO_3 (2.9 mg, 0.0275 mmol), and catalyst **S2.7(i-vi)** in 1 mL C_6H_5F was added Selectfluor (9.7 mg, 0.0275 mmol). The reaction mxiture was stirred at 23 ºC for 12 h. The reaction mixture was filtered through cotton, washing with Et_2O, and concentrated. The crude filtrate was dissolved in EtOAc, filtered through through a Wattman paper filter and submitted directly for HPLC analysis (Chiralpak IC column, 99:01 hexanes/isopropanol, 1 ml/min) t_r = 18.7 min (minor), 19.7 (major). The enantiopurities are presented below as a function of the catalyst enantiopurity. One result (catalyst **S2.7iv**, run 2) has been discarded as a result of HPLC data compromised by spectral artifacts.

Catalyst	**% *ee* (Catalyst)**	**% *ee* (Product)**
S2.7i	>99	93
S2.7i	>99	93
S2.7ii	82	67
S2.7ii	82	67
S2.7iii	63	48
S2.7iii	63	48
S2.7iv	45	45
S2.7iv	45	xx
S2.7v	24	16
S2.7v	24	16
S2.7vi	2	4
S2.7vi	2	3

Notes and references

1. Müller, K. Faeh, C. Diedrich, F. *Science*, **2007**, *317*, 181-1886.
2. O'Hagan, D.; Harper, D. B.; *J. Fluorine Chem.* **1999**, *100*, 127-133.
3. Furuya, T.; Kamlet, A. S.; Ritter, T. *Nature*, **2011**, *473*, 470-477.
4. For a recent review on enantioselective fluorination see: Lectard, S.; Hamashima, Y.; Sodeoka, M. *Adv. Synth. Catal.* **2010**, *352*, 2708-2732.
5. (a) Kalow, J. A.; Doyle, A. G. *J. Am. Chem. Soc.,* **2010**, *132*, 3268-3269. (b) Katcher, M. H.; Doyle, A. G. *J. Am. Chem. Soc.,* **2010**, *132*, 17402-17404.
6. Hintermann, L.; Togni, A. *Angew. Chem. Int. Ed.* **2000**, *39*, 43594362.
7. Hamashima, Y.; Yagi, K.; Takano, H.; Tamas, L.; Sodeoka, M. *J. Am. Chem. Soc.*, **2002**, *124*, 14530-14531.
8. Beeson, T. D.; MacMillan, D. W. C. *J. Am. Chem. Soc.*, **2005**, *127*, 8826-8828.
9. Shibata, N.; Suzuki, E.; Asahi, T.; Shiro, M. *J. Am. Chem. Soc.* **2001**, *123*, 7001-7009.
10. Hamilton, G. L.; Kanai, T.; Toste, F. D. *J. Am. Chem. Soc.*, **2008**, *130*, 14984-14986.
11. Hamilton, G. L.; Kang, E. J.; Mba, M.; Toste, F. D. *Science* **2007**, *317*, 496-499.
12. For recent reviews on the use of chiral anions in enantioselective synthesis see: (a) Phipps, R. J.; Hamilton, G. L.; Toste, F. D. *Nature Chem.* **2012**, *4*, 603-614. (b) Brak, K.; Jacobsen, E. N. *Angew. Chem. Int. Ed.* **2013**, *52*, 534-561. (c) Mahlau, M.; List, B. *Angew. Chem. Int. Ed.* **2013**, *52*, 518-533.
13. Rueping, M.; Nachtsheim, B. J.; Ieawsuwan, W.; Atodiresei, I. *Angew. Chem. Int. Ed.* **2011**, *50*, 6706-6720.
14. Wilkinson, S. C.; Salmon, R.; Gouverneur, V. *Future Med. Chem.* **2009**, *1*, 847-863.
15. Lozano, O.; Blessley, G.; Martinez del Campo, T.; Thompson, A. L; Giuffredi, G. T.; Bettati, M.; Walker, M; Borman, R.; Gouverneur, V. *Angew. Chem. Int. Ed.* **2011**, *50*, 8105-8109.
16. Girard, C.; Kagan, H. B. *Angew. Chem. Int. Ed.* **1998**, *37*, 2922-2959.
17. Schultz, M. J.; Sigman, M. S. *Tetrahedron*, **2006**, *62*, 8227-8241.
18. Rauniyar,V.; Wang, J. Z.; Burks, H.; Toste, F. D. *J. Am. Chem. Soc.* **2011**, *133*, 8486-8489.
19. Rueping, M.; Sugiono, E.; Steck, A.; Theissmann, T. *Adv. Synth. Catal.* **2010**, *352 (2+3)*, 281-287.
20. Trivedi, B. K.; Blankley, C. J.; Bristol, J. A.; Hamilton, H. W.; Patt, W. C.; Kramer, W. J.; Johnson, S. A.; Bruns, R. F.; Cohen, D. M.; Ryan, M. J. *J. Med. Chem.* **1991**, *34*, 1043-1049.
21. Samii, Z. K. M.; Ashmawy, M. A. I.; Mellor, J. M. *J. Chem. Soc., Perk. Trans. I.* **1988**. 2517.

NMR and HPLC spectra

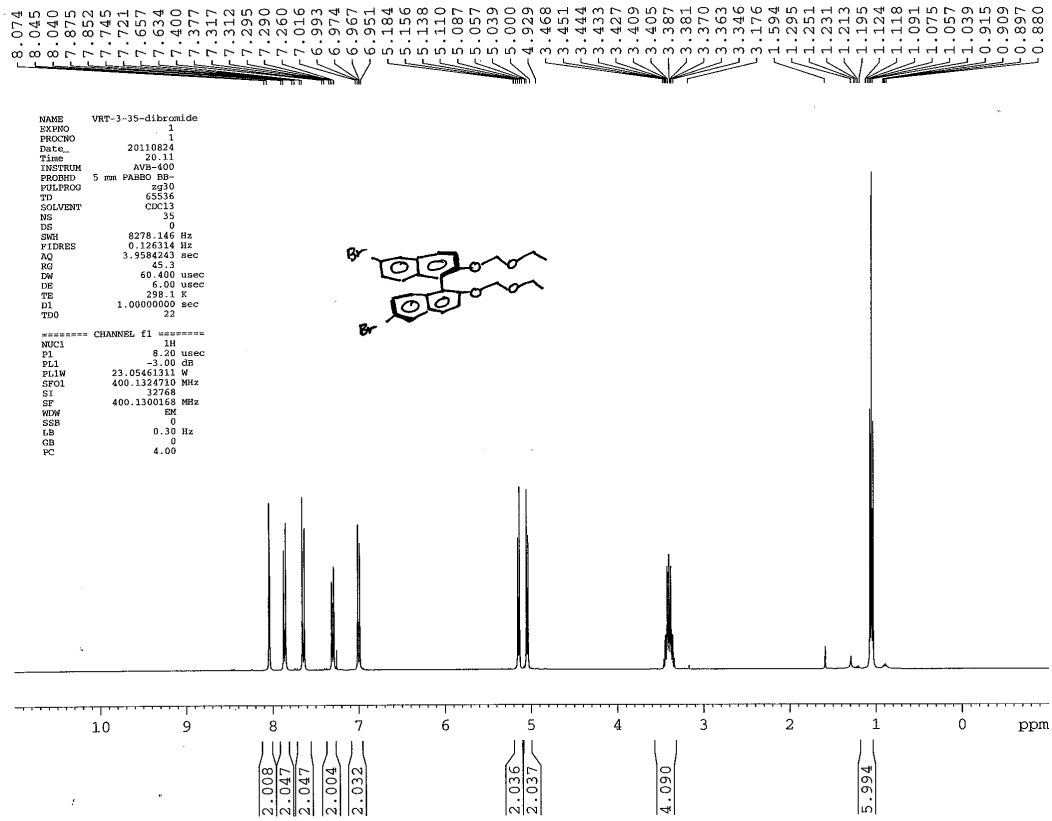

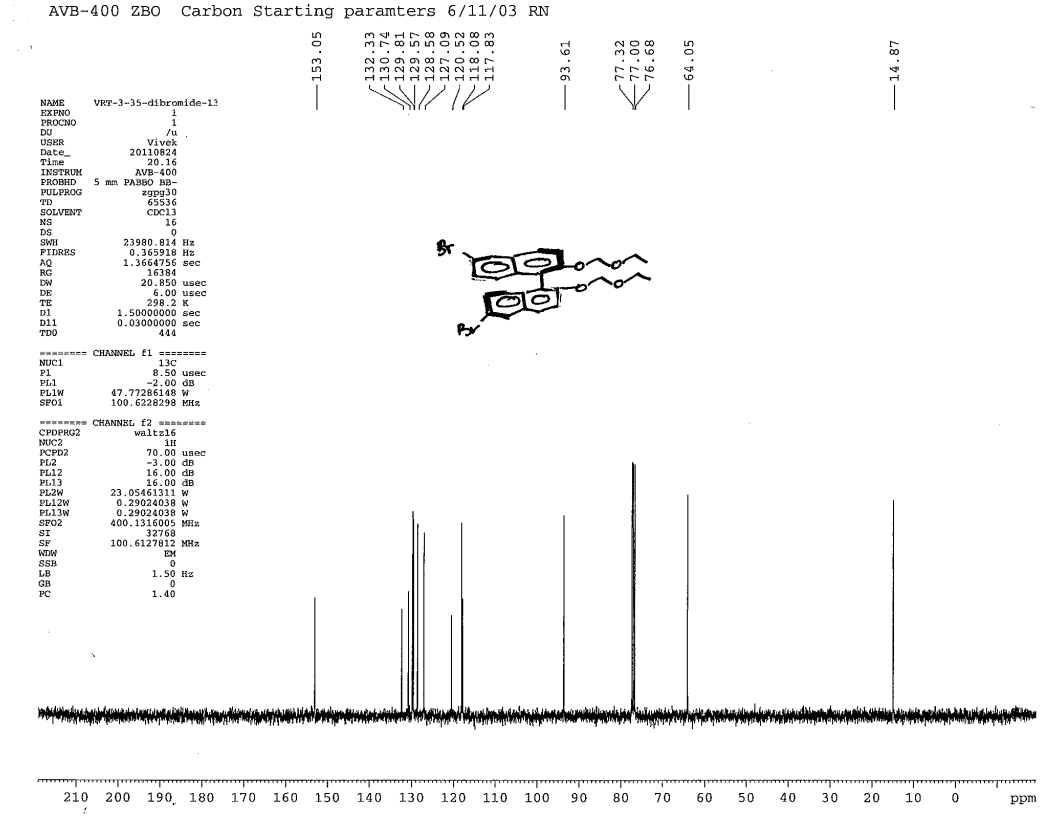

AVQ-400 QNP Proton starting parameters. 7/16/03. Revised 7/22/03 RN

NAME	VRT-3-35-iodide-1H
EXPNO	1
PROCNO	1
Date_	20110529
Time	12.47
INSTRUM	AVQ-400
PROBHD	5 mm QNP 1H/13
PULPROG	zg30
TD	65536
SOLVENT	CDCl3
NS	20
DS	0
SWH	8012.820 Hz
FIDRES	0.122266 Hz
AQ	4.0895586 sec
RG	16
DW	62.400 usec
DE	6.00 usec
TE	292.5 K
D1	1.00000000 sec
TD0	22
======== CHANNEL f1 ========	
NUC1	1H
P1	12.80 usec
PL1	0.00 dB
PL1W	9.54516888 W
SFO1	400.1324700 MHz
SI	65536
SF	400.1300172 MHz
WDW	EM
SSB	0
LB	0.30 Hz
GB	0
PC	4.00

8.453 7.609 7.590 7.526 7.464 7.445 7.426 7.348 7.260 7.151 7.129 7.087 7.066 5.298 4.869 4.855 4.708 4.694 3.766 3.750 3.735 3.101 3.083 3.065 3.060 3.042 3.025 2.727 2.708 2.688 2.677 2.659 2.654 2.636 2.619 1.871 1.863 1.855 1.847 1.839 1.667 1.650 1.632 1.613 1.582 1.435 1.312 1.296 1.275 1.260 1.190 1.173 1.133 1.118

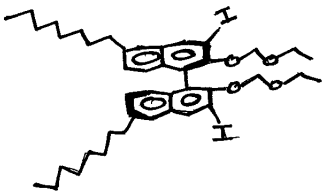

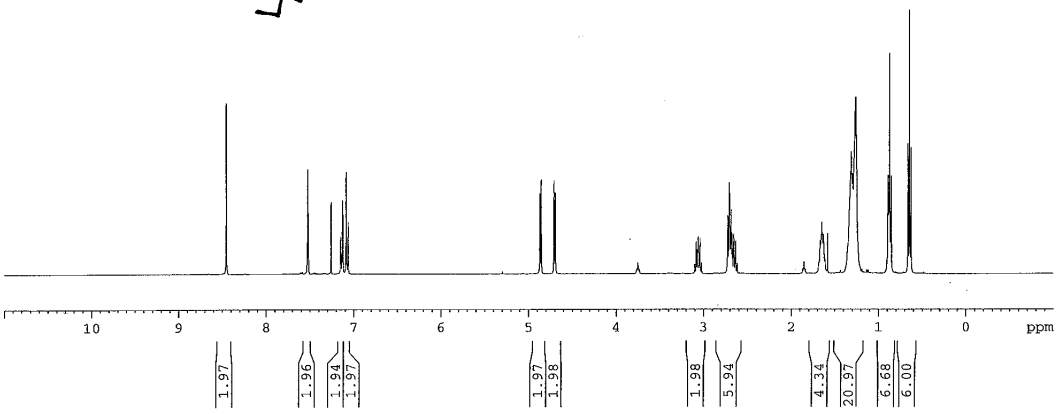

AVQ-400 QNP Carbon Starting parameters 7/16/03 revised 7/22/03 RN

151.38 140.46 139.32 132.41 132.14 128.77 128.33 126.04 125.06 98.04 92.44 77.32 77.00 76.68 64.94 35.77 31.84 31.07 29.43 29.30 29.23 22.64 14.38 14.09

NAME	VRT-3-35-iodide-13C
EXPNO	1
PROCNO	1
Date_	20110529
Time	12.52
INSTRUM	AVQ-400
PROBHD	5 mm QNP 1H/13
PULPROG	zgpg30
TD	65536
SOLVENT	CDCl3
NS	112
DS	0
SWH	24038.461 Hz
FIDRES	0.366798 Hz
AQ	1.3632196 sec
RG	16384
DW	20.800 usec
DE	6.00 usec
TE	292.5 K
D1	2.00000000 sec
D11	0.03000000 sec
TD0	4444
======== CHANNEL f1 ========	
NUC1	13C
P1	8.50 usec
PL1	-2.00 dB
PL1W	47.77286148 W
SFO1	100.6228298 MHz
======== CHANNEL f2 ========	
CPDPRG2	waltz16
NUC2	1H
PCPD2	70.00 usec
PL2	0.00 dB
PL12	15.00 dB
PL13	17.00 dB
PL2W	9.54516888 W
PL12W	0.30184472 W
PL13W	0.19045115 W
SFO2	400.1316000 MHz
SI	32768
SF	100.6127758 MHz
WDW	EM
SSB	0
LB	1.50 Hz
GB	0
PC	1.40

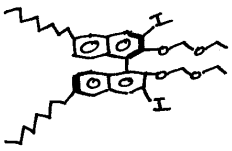

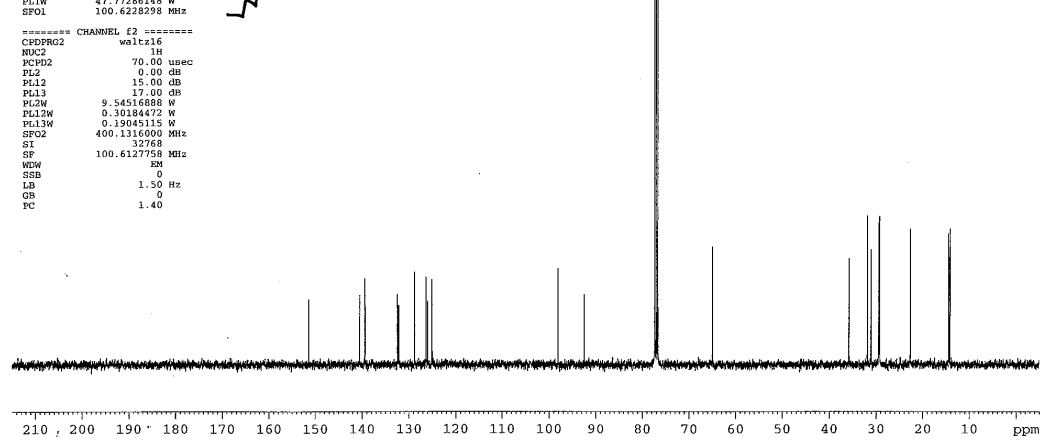

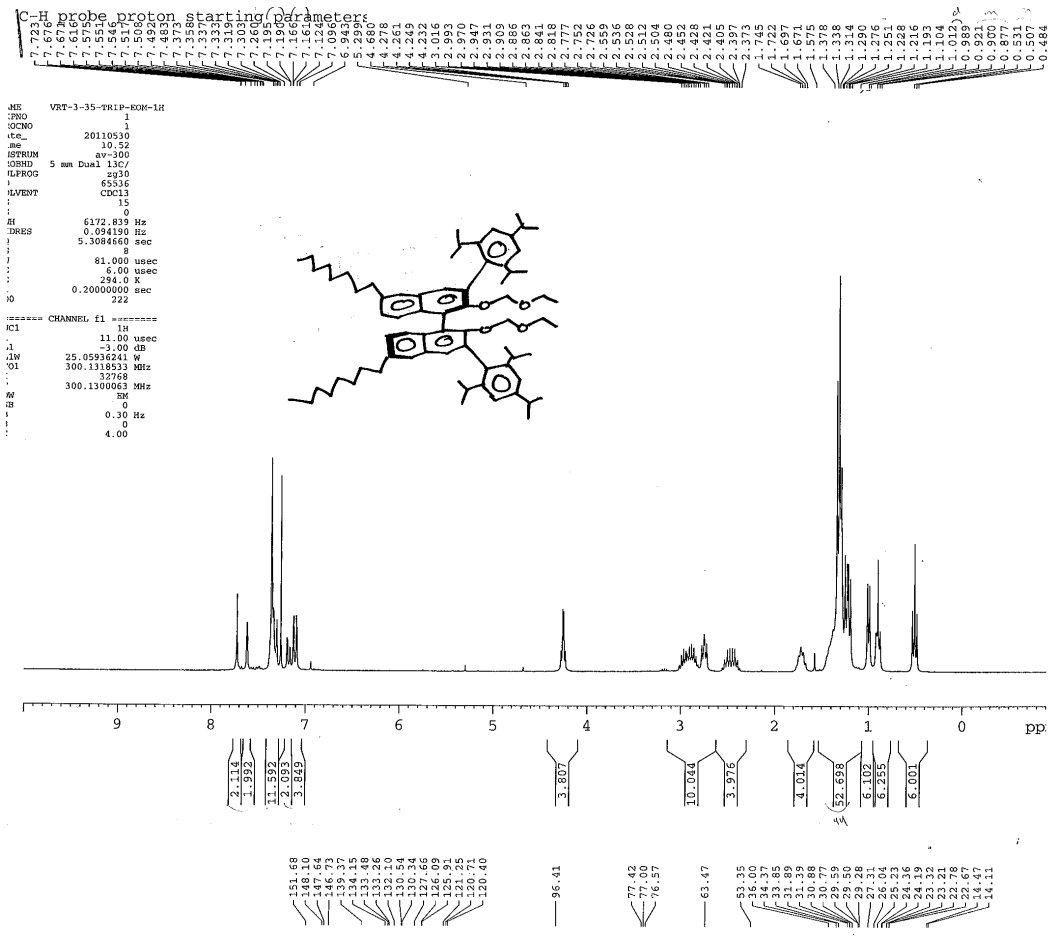

AV-300 Dual C-H probe Carbon starting parameters 7/23/03

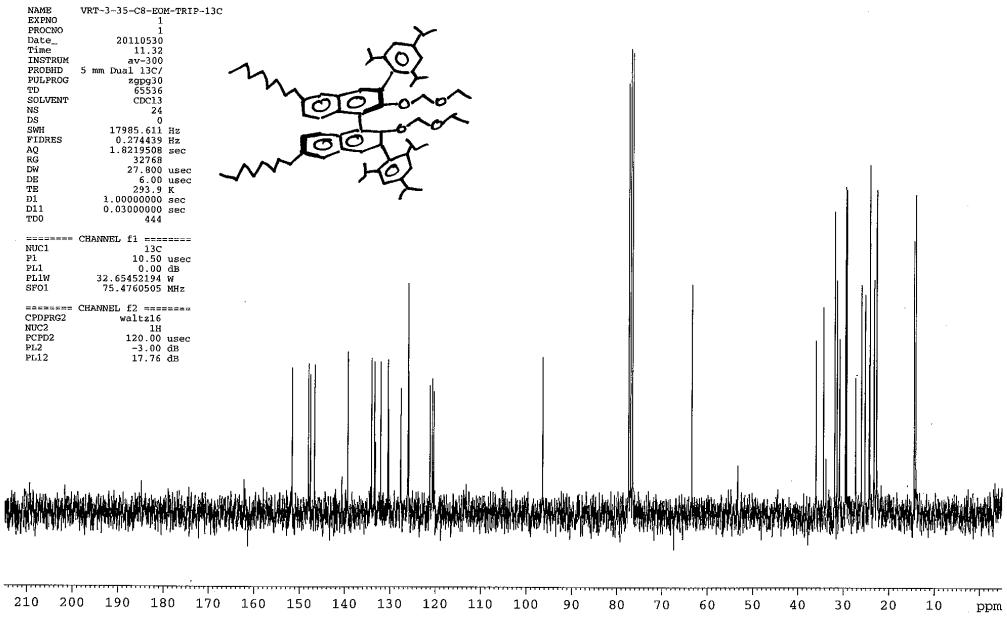

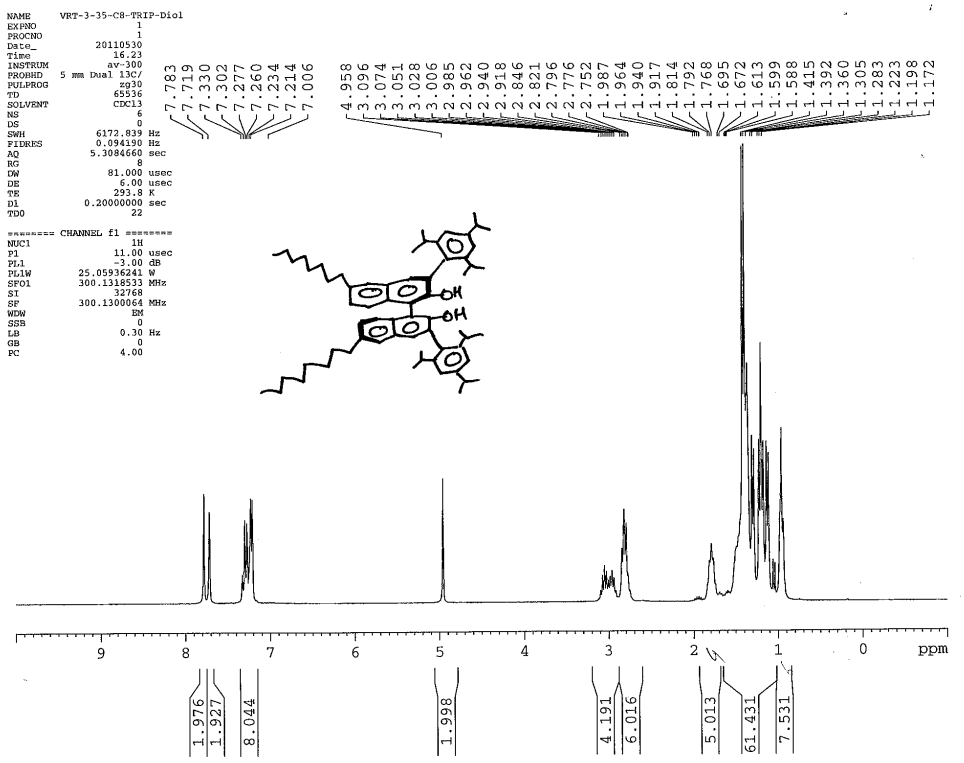
NAME VRT-3-35-C8-TRIP-Diol
EXPNO 1
PROCNO 1
Date_ 20110530
Time 16.23
INSTRUM av-300
PROBHD 5 mm Dual 13C/
PULPROG zg30
TD 65536
SOLVENT CDCl3
NS 6
DS 0
SWH 6172.839 Hz
FIDRES 0.094190 Hz
AQ 5.3084660 sec
RG 8
DW 81.000 usec
DE 6.00 usec
TE 293.8 K
D1 0.20000000 sec
TD0 22
======== CHANNEL f1 ========
NUC1 1H
P1 11.00 usec
PL1 -3.00 dB
PL1W 25.05936241 W
SFO1 300.1318533 MHz
SI 32768
SF 300.1300064 MHz
WDW EM
SSB 0
LB 0.30 Hz
GB 0
PC 4.00
7.783
7.719
7.330
7.302
7.277
7.260
7.234
7.214
7.006
4.958
3.096
3.074
3.051
3.028
3.006
2.985
2.962
2.940
2.918
2.846
2.821
2.796
2.776
2.752
1.987
1.964
1.940
1.917
1.814
1.792
1.768
1.695
1.672
1.613
1.599
1.588
1.415
1.392
1.360
1.305
1.283
1.223
1.198
1.172
OH
OH
9
8
7
6
5
4
3
2
1
0
ppm
1.976
1.927
8.044
1.998
4.191
6.016
5.013
61.431
7.531

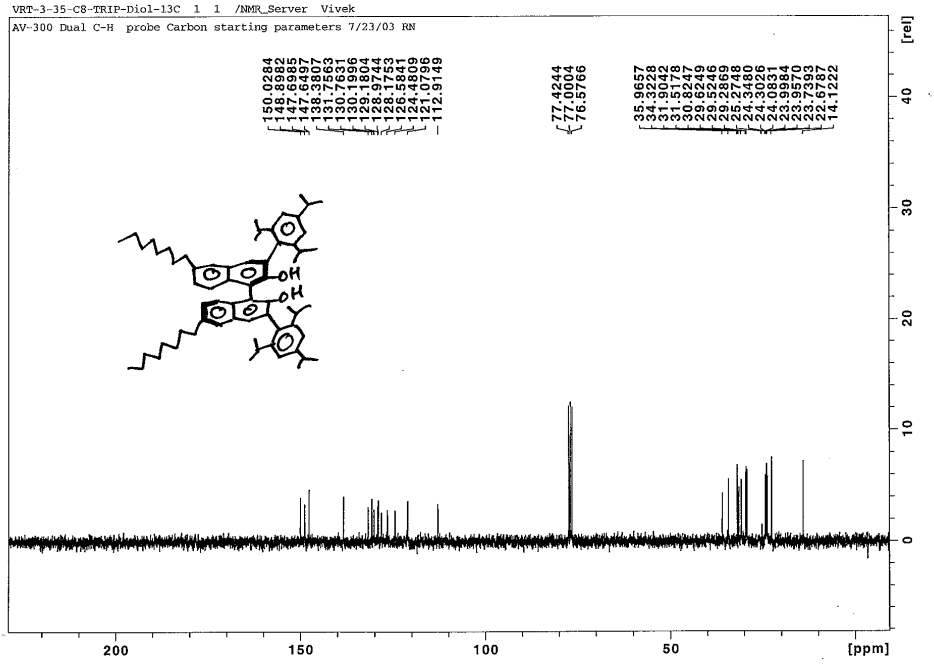
VRT-3-35-C8-TRIP-Diol-13C 1 1 /NMR_Server Vivek
AV-300 Dual C-H probe Carbon starting parameters 7/23/03 RN
150.0284
148.8882
147.6985
147.6497
138.3807
131.7563
130.7831
130.1996
130.1004
128.9744
128.1753
126.5841
124.4809
121.0796
112.9149
77.4244
77.0004
76.5766
35.9657
34.3228
31.9042
31.5173
30.8247
30.6446
29.5246
29.2869
25.2748
24.3480
24.3026
24.0831
23.9844
23.9570
23.7393
22.6787
14.1222
OH
OH
[rel]
40
30
20
10
0
200
150
100
50
[ppm]

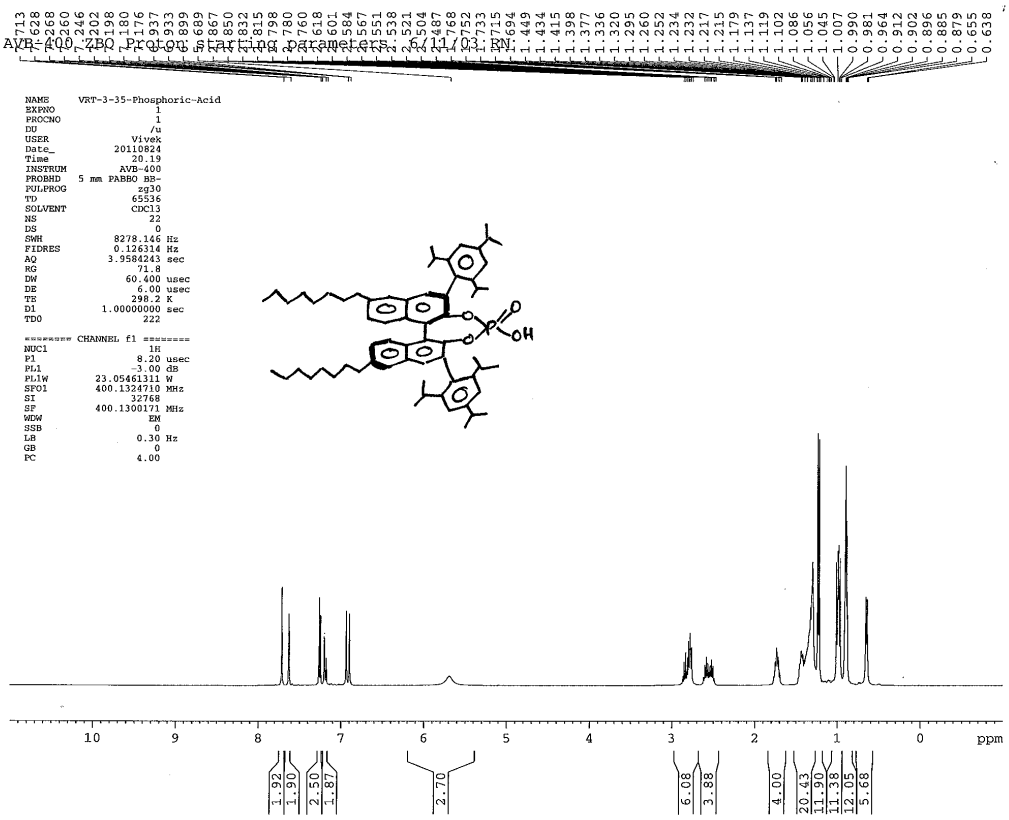
AVB-400 ZBO Proton Starting parameters 6/11/03 RN
NAME VRT-3-35-Phosphoric-Acid
EXPNO 1
PROCNO 1
DU /u
USER Vivek
Date_ 20110824
Time 20.19
INSTRUM AVB-400
PROBHD 5 mm PABBO BB-
PULPROG zg30
TD 65536
SOLVENT CDCl3
NS 22
DS 0
SWH 8278.146 Hz
FIDRES 0.126314 Hz
AQ 3.9584243 sec
RG 71.8
DW 60.400 usec
DE 6.00 usec
TE 298.2 K
D1 1.00000000 sec
TD0 222
======== CHANNEL f1 ========
NUC1 1H
P1 8.20 usec
PL1 -3.00 dB
PL1W 23.05461311 W
SFO1 400.1324710 MHz
SI 32768
SF 400.1300171 MHz
WDW EM
SSB 0
LB 0.30 Hz
GB 0
PC 4.00
OH
10 9 8 7 6 5 4 3 2 1 0 ppm
1.92 1.90 2.50 1.87 2.70 6.08 3.88 4.00 20.43 11.90 11.38 12.05 5.68

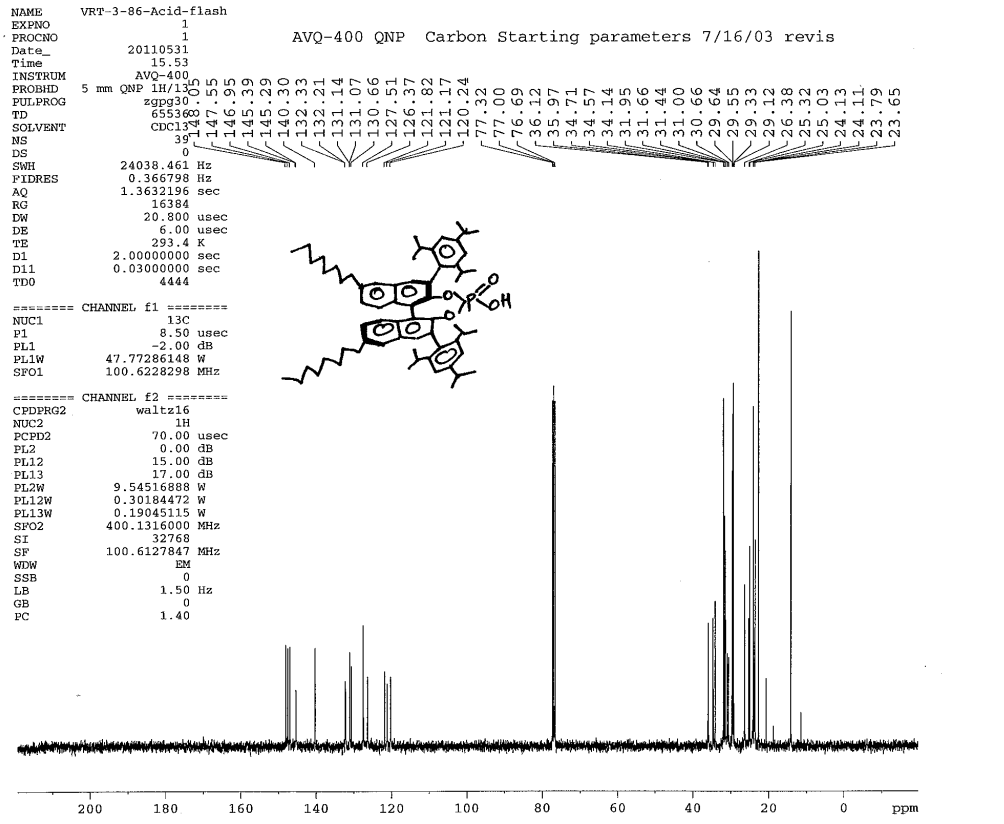
NAME VRT-3-86-Acid-flash
EXPNO 1
PROCNO 1
Date_ 20110531
Time 15.53
INSTRUM AVQ-400
PROBHD 5 mm QNP 1H/13
PULPROG zgpg30
TD 65536
SOLVENT CDCl3
NS 39
DS 0
SWH 24038.461 Hz
FIDRES 0.366798 Hz
AQ 1.3632196 sec
RG 16384
DW 20.800 usec
DE 6.00 usec
TE 293.4 K
D1 2.00000000 sec
D11 0.03000000 sec
TD0 4444
======== CHANNEL f1 ========
NUC1 13C
P1 8.50 usec
PL1 -2.00 dB
PL1W 47.77286148 W
SFO1 100.6228298 MHz
======== CHANNEL f2 ========
CPDPRG2 waltz16
NUC2 1H
PCPD2 70.00 usec
PL2 0.00 dB
PL12 15.00 dB
PL13 17.00 dB
PL2W 9.54516888 W
PL12W 0.30184472 W
PL13W 0.19045115 W
SFO2 400.1316000 MHz
SI 32768
SF 100.6127847 MHz
WDW EM
SSB 0
LB 1.50 Hz
GB 0
PC 1.40
AVQ-400 QNP Carbon Starting parameters 7/16/03 revis
148.05 147.55 146.95 145.39 145.29 140.30 132.33 132.21 131.14 131.07 130.66 127.51 126.37 121.82 121.17 120.24 77.32 77.00 76.69 36.12 35.97 34.71 34.57 34.14 31.95 31.66 31.44 31.00 30.66 29.64 29.55 29.33 29.12 26.38 25.32 25.03 24.13 24.11 23.79 23.65
OH
200 180 160 140 120 100 80 60 40 20 0 ppm

AVQ-400 QNP 31P Starting parameters. Trimethyl phosph

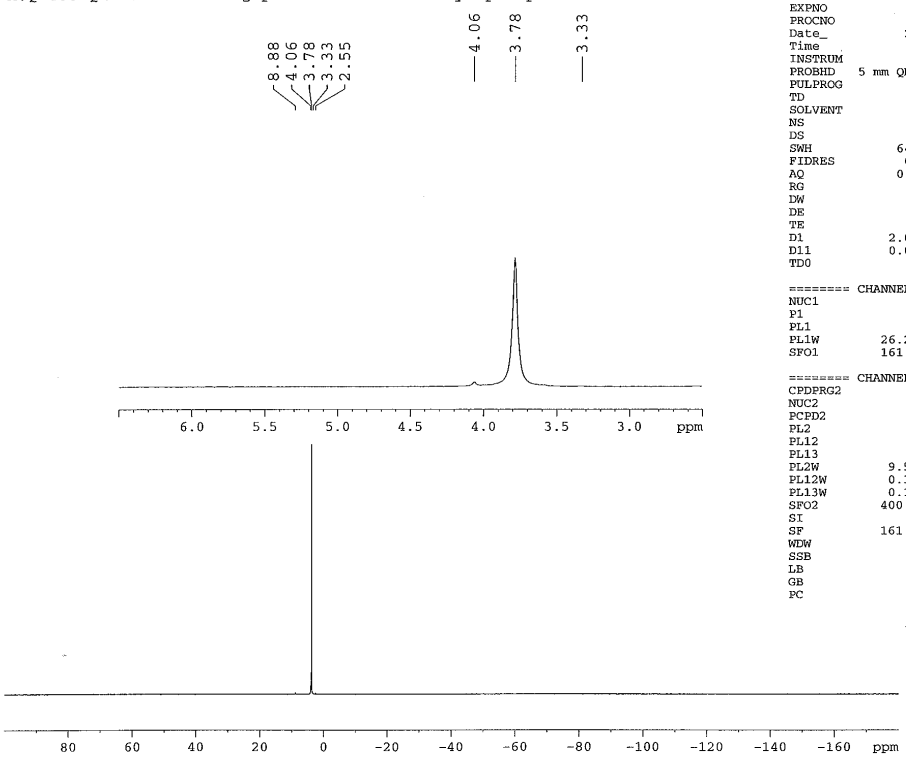

NAME	VRT-3-86-Acid-flash
EXPNO	1
PROCNO	1
Date_	20110531
Time	15.52
INSTRUM	AVQ-400
PROBHD	5 mm QNP 1H/13
PULPROG	zgpg30
TD	65536
SOLVENT	CDCl3
NS	11
DS	0
SWH	64724.918 Hz
FIDRES	0.987624 Hz
AQ	0.5063233 sec
RG	8192
DW	7.725 usec
DE	6.00 usec
TE	293.3 K
D1	2.00000000 sec
D11	0.03000000 sec
TD0	44
======== CHANNEL f1 ========	
NUC1	31P
P1	7.70 usec
PL1	-2.00 dB
PL1W	26.27507401 W
SFO1	161.9674750 MHz
======== CHANNEL f2 ========	
CPDPRG2	waltz16
NUC2	1H
PCPD2	70.00 usec
PL2	0.00 dB
PL12	15.00 dB
PL13	17.00 dB
PL2W	9.54516888 W
PL12W	0.30184472 W
PL13W	0.19045115 W
SFO2	400.1316005 MHz
SI	65536
SF	161.9755989 MHz
WDW	EM
SSB	0
LB	1.00 Hz
GB	0
PC	1.40

AVQ-400 QNP Proton starting parameters. 7/16/

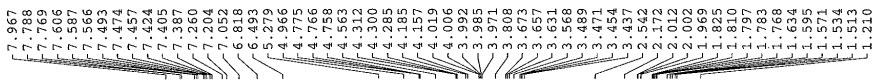


```
NAME        VRT-3-Phenyl-Substrate
EXPNO                1
PROCNO               1
Date_         20110813
Time             12.22
INSTRUM        AVQ-400
PROBHD   5 mm QNP 1H/13
PULPROG           zg30
TD               65536
SOLVENT           CDCl3
NS                  22
DS                   0
SWH           8012.820 Hz
FIDRES        0.122266 Hz
AQ            4.0895586 sec
RG                 114
DW              62.400 usec
DE               6.00 usec
TE              293.9 K
D1            1.00000000 sec
TD0                 22

======== CHANNEL f1 ========
NUC1                1H
P1               12.80 usec
PL1               0.00 dB
PL1W        9.54516888 W
SFO1       400.1324700 MHz
SI               65536
SF         400.1300174 MHz
WDW                EM
SSB                 0
LB               0.30 Hz
GB                  0
PC               4.00
```

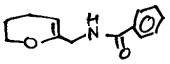

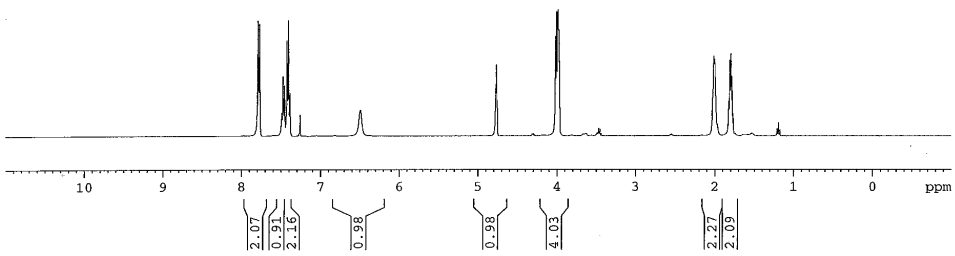

JP Carbon Starting parameters 7/16/03 revised 7

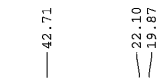


```
NAME        VRT-3-Phenyl-Substrat
EXPNO                1
PROCNO               1
Date_         20110813
Time             12.28
INSTRUM        AVQ-400
PROBHD   5 mm QNP 1H/13
PULPROG         zgpg30
TD               65536
SOLVENT           CDCl3
NS                  16
DS                   0
SWH          24038.461 Hz
FIDRES        0.366798 Hz
AQ            1.3632196 sec
RG                16384
DW              20.800 usec
DE               6.00 usec
TE              293.9 K
D1            2.00000000 sec
D11           0.03000000 sec
TD0                444

======== CHANNEL f1 ========
NUC1               13C
P1                8.50 usec
PL1              -2.00 dB
PL1W       47.77286148 W
SFO1      100.6228298 MHz

======== CHANNEL f2 ========
CPDPRG2         waltz16
NUC2                1H
PCPD2           70.00 usec
PL2               0.00 dB
PL12             15.00 dB
PL13             17.00 dB
PL2W        9.54516888 W
PL12W       0.30184472 W
PL13W       0.19045115 W
SFO2       400.1316000 MHz
SI               32768
SF         100.6127802 MHz
WDW                EM
SSB                 0
LB               1.50 Hz
GB                  0
PC               1.40
```

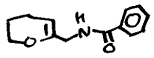

AVQ-400 QNP Proton starting parameters. 7/16/

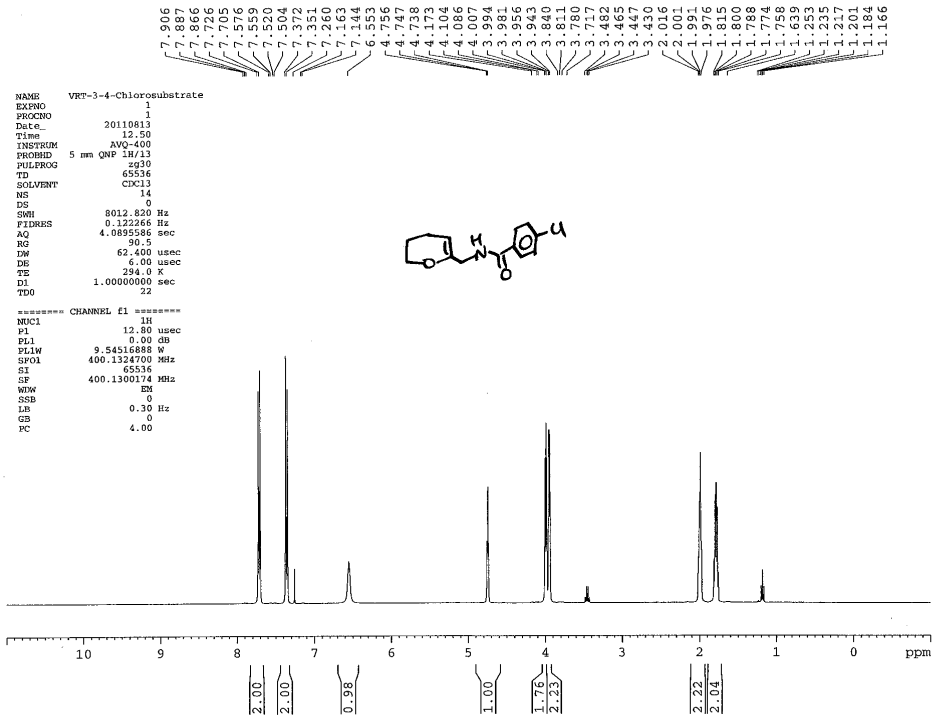

JP Carbon Starting parameters 7/16/03 revised 7

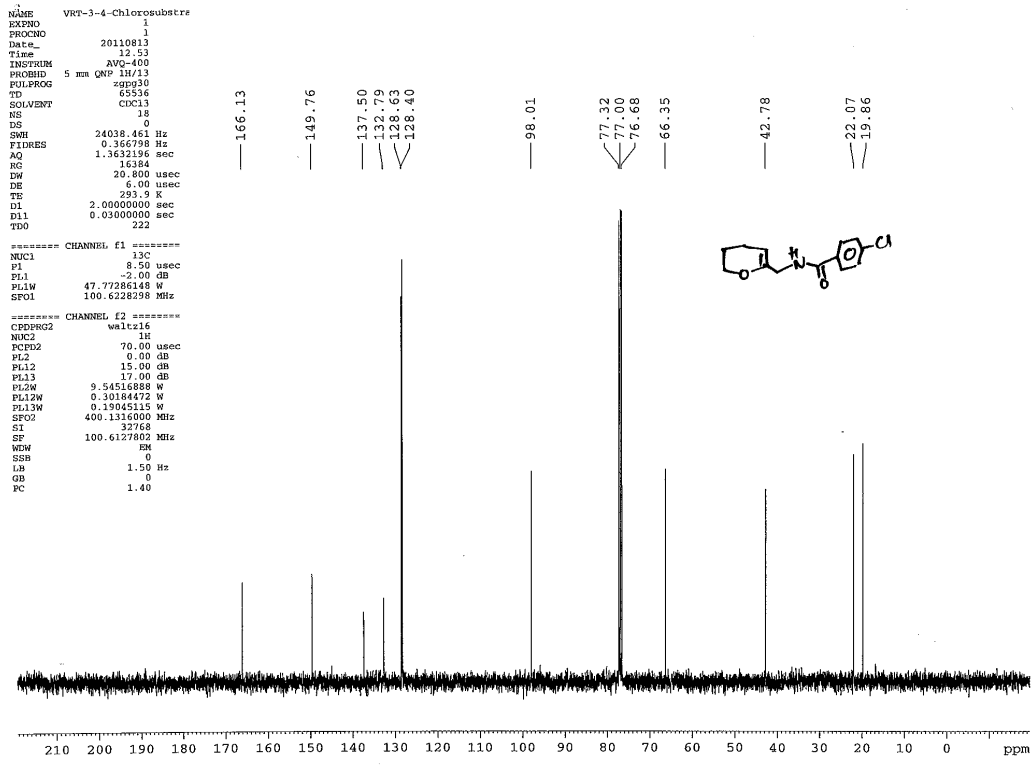

AVQ-400 QNP Proton starting parameters. 7/16/

7.845 7.828 7.787 7.765 7.696 7.646 7.625 7.487 7.465 7.443 7.422 7.275 7.260 6.821 5.254 4.706 4.697 4.688 4.404 4.144 4.131 4.119 4.090 4.077 4.013 3.964 3.952 3.939 3.917 3.904 3.843 3.802 3.780 3.767 3.754 3.740 3.726 3.676 3.636 3.592 3.578 3.458 3.440 3.423 3.405 2.308 2.119 1.959 1.949 1.775 1.760 1.747 1.733 1.718 1.597 1.586 1.571 1.493 1.217 1.175 1.158 1.140 0.837

NAME	VRT-3-4-Bromo-Substrate
EXPNO	1
PROCNO	1
Date_	20110817
Time	20.11
INSTRUM	AVQ-400
PROBHD	5 mm QNP 1H/13
PULPROG	zg30
TD	65536
SOLVENT	CDCl3
NS	12
DS	0
SWH	8012.820 Hz
FIDRES	0.122266 Hz
AQ	4.0895586 sec
RG	45.3
DW	62.400 usec
DE	6.00 usec
TE	294.0 K
D1	1.00000000 sec
TD0	22
======== CHANNEL f1 ========	
NUC1	1H
P1	12.80 usec
PL1	0.00 dB
PL1W	9.54516888 W
SFO1	400.1324700 MHz
SI	65536
SF	400.1300174 MHz
WDW	EM
SSB	0
LB	0.30 Hz
GB	0
PC	4.00

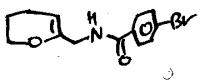

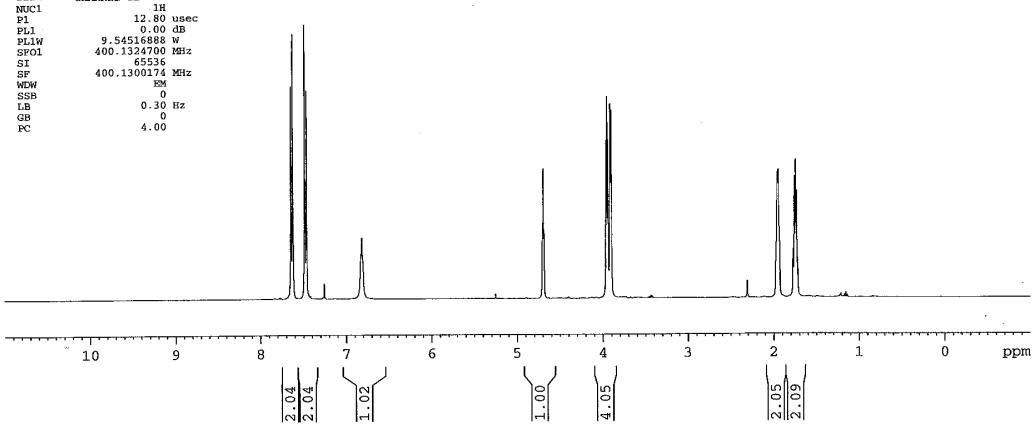

NP Carbon Starting parameters 7/16/03 revised

166.25 149.74 133.14 131.44 128.59 125.84 97.68 77.32 77.00 76.68 66.20 42.60 21.98 19.77

NAME	VRT-3-4-Bromo-Substra
EXPNO	1
PROCNO	1
Date_	20110817
Time	20.14
INSTRUM	AVQ-400
PROBHD	5 mm QNP 1H/13
PULPROG	zgpg30
TD	65536
SOLVENT	CDCl3
NS	15
DS	0
SWH	24038.461 Hz
FIDRES	0.366798 Hz
AQ	1.3632196 sec
RG	16384
DW	20.800 usec
DE	6.00 usec
TE	294.0 K
D1	2.00000000 sec
D11	0.03000000 sec
TD0	3333
======== CHANNEL f1 ========	
NUC1	13C
P1	8.50 usec
PL1	-2.00 dB
PL1W	47.77286148 W
SFO1	100.6228298 MHz
======== CHANNEL f2 ========	
CPDPRG2	waltz16
NUC2	1H
PCPD2	70.00 usec
PL2	0.00 dB
PL12	15.00 dB
PL13	17.00 dB
PL2W	9.54516888 W
PL12W	0.30184472 W
PL13W	0.19045115 W
SFO2	400.1316000 MHz
SI	32768
SF	100.6127883 MHz
WDW	EM
SSB	0
LB	1.50 Hz
GB	0
PC	1.40

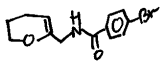

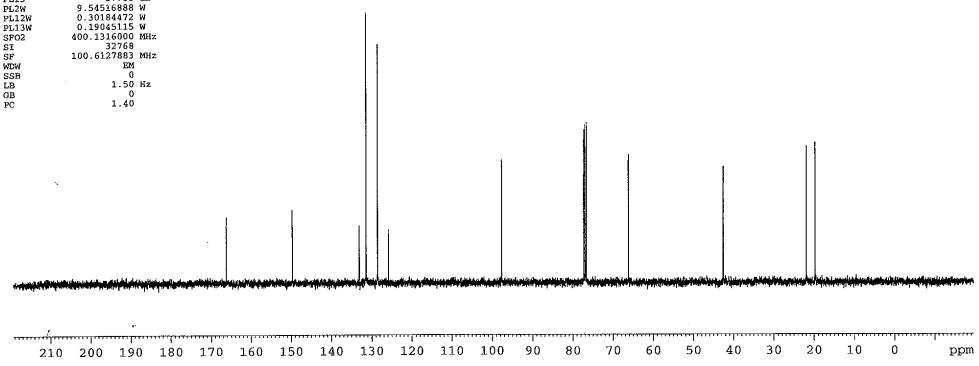

AVQ-400 QNP Proton starting parameters. 7/16/

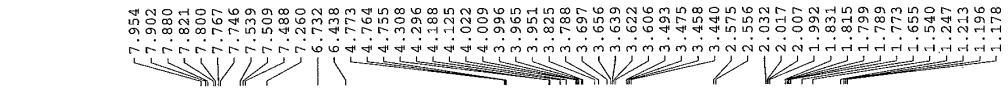


```
NAME        VRT-3-4-Iodo-Substrate
EXPNO                            1
PROCNO                           1
Date_                     20110813
Time                         13.02
INSTRUM                    AVQ-400
PROBHD   5 mm QNP 1H/13
PULPROG                      zg30
TD                          65536
SOLVENT                     CDCl3
NS                             22
DS                              0
SWH                     8012.820 Hz
FIDRES                  0.122266 Hz
AQ                      4.0895586 sec
RG                            181
DW                       62.400 usec
DE                        6.00 usec
TE                        293.9 K
D1                   1.00000000 sec
TD0                            22

======== CHANNEL f1 ========
NUC1                           1H
P1                        12.80 usec
PL1                        0.00 dB
PL1W                9.54516888 W
SFO1              400.1324700 MHz
SI                         65536
SF                400.1300176 MHz
WDW                           EM
SSB                            0
LB                        0.30 Hz
GB                             0
PC                         4.00
```

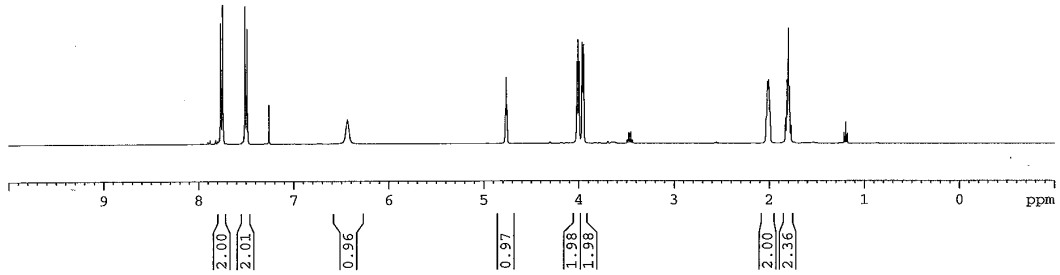

JP Carbon Starting parameters 7/16/03 revised 7

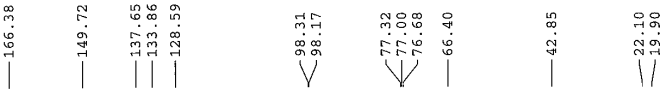


```
NAME        VRT-3-4-Iodo-Substrat
EXPNO                            1
PROCNO                           1
Date_                     20110813
Time                         13.07
INSTRUM                    AVQ-400
PROBHD   5 mm QNP 1H/13
PULPROG                   zgpg30
TD                          65536
SOLVENT                     CDCl3
NS                             26
DS                              0
SWH                    24038.461 Hz
FIDRES                  0.366798 Hz
AQ                      1.3632196 sec
RG                          16384
DW                       20.800 usec
DE                        6.00 usec
TE                        293.9 K
D1                   2.00000000 sec
D11                  0.03000000 sec
TD0                          2222

======== CHANNEL f1 ========
NUC1                          13C
P1                         8.50 usec
PL1                       -2.00 dB
PL1W               47.77286148 W
SFO1              100.6228298 MHz

======== CHANNEL f2 ========
CPDPRG2                 waltz16
NUC2                           1H
PCPD2                     70.00 usec
PL2                        0.00 dB
PL12                      15.00 dB
PL13                      17.00 dB
PL2W                9.54516888 W
PL12W               0.30184472 W
PL13W               0.19045115 W
SFO2              400.1316000 MHz
SI                         32768
SF                100.6127774 MHz
WDW                           EM
SSB                            0
LB                        1.50 Hz
GB                             0
PC                         1.40
```

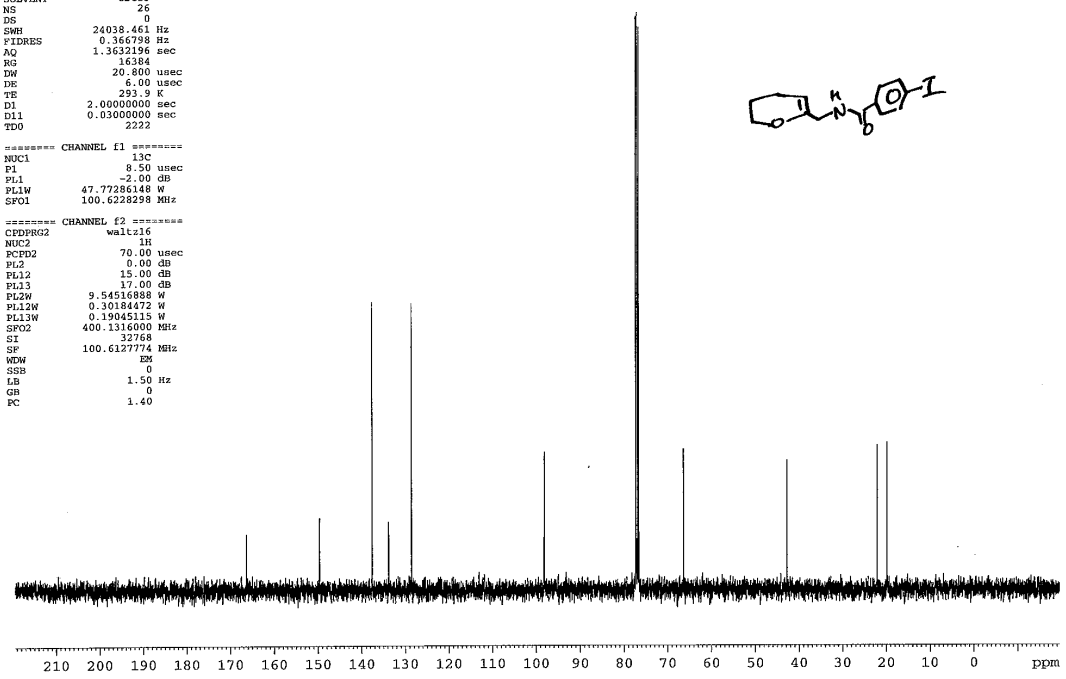

AVQ-400 QNP Proton starting parameters. 7/16/

8.450 8.259 8.237 8.158 7.986 7.954 7.932 7.745 7.260 7.176 6.937 6.670 4.787 4.778 4.769 4.342 4.330 4.184 4.119 4.101 4.083 4.065 4.017 4.005 3.990 3.973 3.900 3.808 3.667 3.651 3.633 3.617 3.596 3.522 3.507 3.487 3.473 3.464 3.446 2.592 2.574 2.555 2.014 2.004 1.990 1.903 1.826 1.812 1.798 1.785 1.769 1.737 1.619 1.600 1.580 1.562

NAME	VRT-3-Nitro-Substrate
EXPNO	1
PROCNO	1
Date_	20110813
Time	12.31
INSTRUM	AVQ-400
PROBHD	5 mm QNP 1H/13
PULPROG	zg30
TD	65536
SOLVENT	CDCl3
NS	22
DS	0
SWH	8012.820 Hz
FIDRES	0.122266 Hz
AQ	4.0895586 sec
RG	128
DW	62.400 usec
DE	6.00 usec
TE	293.9 K
D1	1.00000000 sec
TD0	222

======== CHANNEL f1 ========

NUC1	1H
P1	12.80 usec
PL1	0.00 dB
PL1W	9.54516888 W
SFO1	400.1324700 MHz
SI	65536
SF	400.1300177 MHz
WDW	EM
SSB	0
LB	0.30 Hz
GB	0
PC	4.00

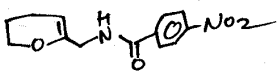

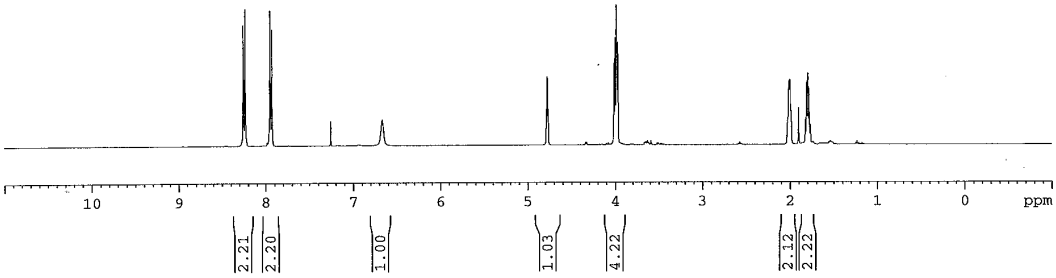

JP Carbon Starting parameters 7/16/03 revised 7

NAME	VRT-3-Nitro-Substrate
EXPNO	1
PROCNO	1
Date_	20110813
Time	12.36
INSTRUM	AVQ-400
PROBHD	5 mm QNP 1H/13
PULPROG	xgpg30
TD	65536
SOLVENT	CDCl3
NS	20
DS	0
SWH	24038.461 Hz
FIDRES	0.366798 Hz
AQ	1.3632196 sec
RG	16384
DW	20.800 usec
DE	6.00 usec
TE	293.9 K
D1	2.00000000 sec
D11	0.03000000 sec
TD0	444

======== CHANNEL f1 ========

NUC1	13C
P1	8.50 usec
PL1	-2.00 dB
PL1W	47.77286148 W
SFO1	100.6228298 MHz

======== CHANNEL f2 ========

CPDPRG2	waltz16
NUC2	1H
PCPD2	70.00 usec
PL2	0.00 dB
PL12	15.00 dB
PL13	17.00 dB
PL2W	9.54516888 W
PL12W	0.30184472 W
PL13W	0.19045115 W
SFO2	400.1316000 MHz
SI	32768
SF	100.6127796 MHz
WDW	EM
SSB	0
LB	1.50 Hz
GB	0
PC	1.40

165.17 149.43 149.33 140.02 128.18 123.66 98.53 77.31 77.00 76.68 66.43 43.07 22.02 19.86

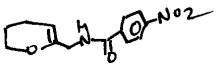

AVQ-400 QNP Proton starting parameters. 7/16/

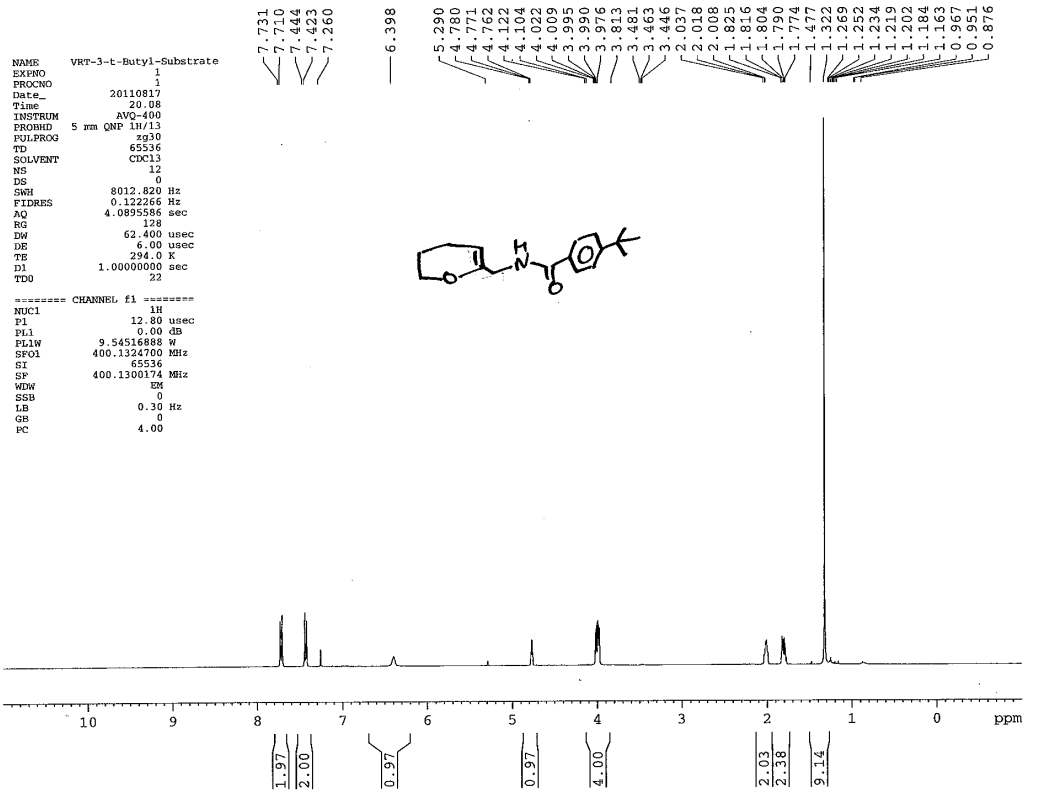


```
NAME        VRT-3-t-Butyl-Substrate
EXPNO                             1
PROCNO                            1
Date_                      20110817
Time                          20.08
INSTRUM                    AVQ-400
PROBHD   5 mm QNP 1H/13
PULPROG                       zg30
TD                           65536
SOLVENT                      CDCl3
NS                              12
DS                               0
SWH                     8012.820 Hz
FIDRES                     0.122266 Hz
AQ                      4.0895586 sec
RG                             128
DW                         62.400 usec
DE                          6.00 usec
TE                          294.0 K
D1                     1.00000000 sec
TD0                             22

======== CHANNEL f1 ========
NUC1                            1H
P1                         12.80 usec
PL1                         0.00 dB
PL1W                    9.54516888 W
SFO1                  400.1324700 MHz
SI                           65536
SF                    400.1300174 MHz
WDW                             EM
SSB                              0
LB                          0.30 Hz
GB                               0
PC                          4.00
```

VP Carbon Starting parameters 7/16/03 revised 7

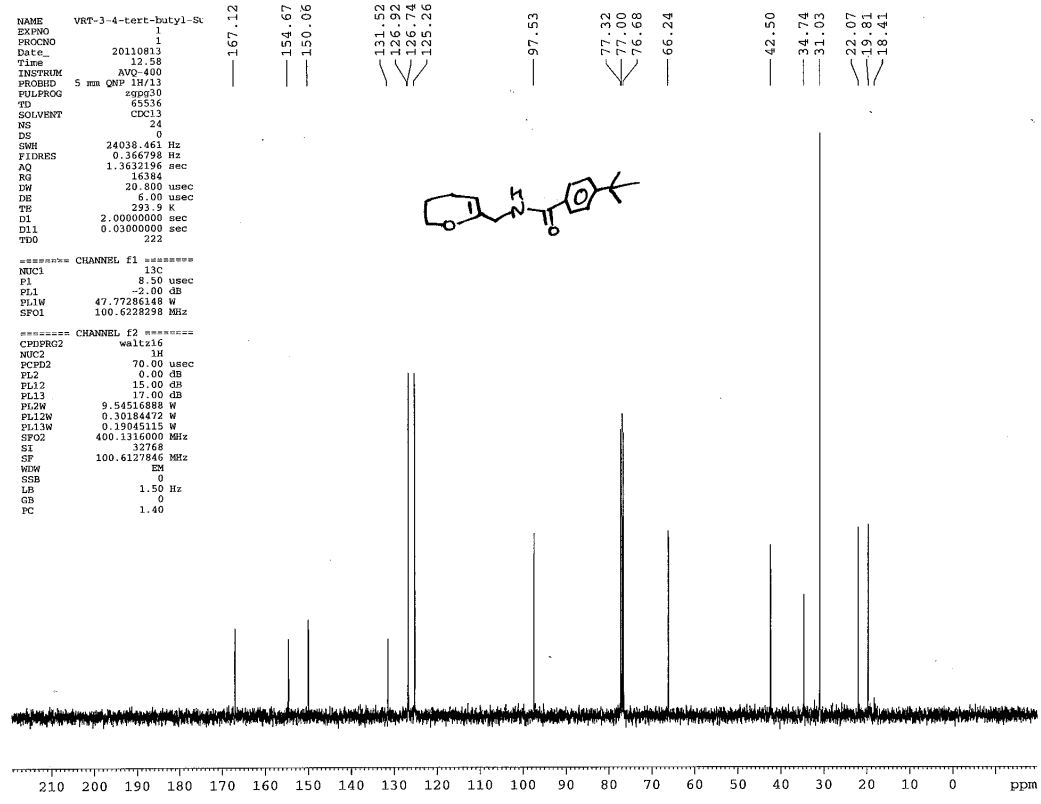


```
NAME        VRT-3-4-tert-butyl-Su
EXPNO                             1
PROCNO                            1
Date_                      20110813
Time                          12.58
INSTRUM                    AVQ-400
PROBHD   5 mm QNP 1H/13
PULPROG                    zgpg30
TD                           65536
SOLVENT                      CDCl3
NS                              24
DS                               0
SWH                    24038.461 Hz
FIDRES                     0.366798 Hz
AQ                      1.3632196 sec
RG                           16384
DW                         20.800 usec
DE                          6.00 usec
TE                          293.9 K
D1                     2.00000000 sec
D11                    0.03000000 sec
TD0                            222

======== CHANNEL f1 ========
NUC1                           13C
P1                          8.50 usec
PL1                        -2.00 dB
PL1W                   47.77286148 W
SFO1                  100.6228298 MHz

======== CHANNEL f2 ========
CPDPRG2                   waltz16
NUC2                            1H
PCPD2                      70.00 usec
PL2                         0.00 dB
PL12                       15.00 dB
PL13                       17.00 dB
PL2W                    9.54516888 W
PL12W                   0.30184472 W
PL13W                   0.19045115 W
SFO2                  400.1316000 MHz
SI                           32768
SF                    100.6127846 MHz
WDW                             EM
SSB                              0
LB                          1.50 Hz
GB                               0
PC                          1.40
```

AVQ-400 QNP Proton starting parameters. 7/16/

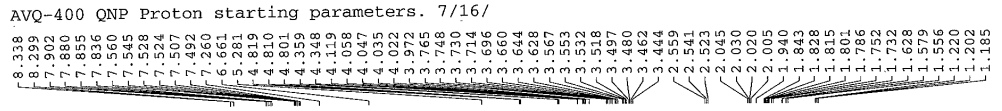


```
NAME        VRT-3-2-Naphtyl-Substrate
EXPNO                   1
PROCNO                  1
Date_            20110813
Time                12.39
INSTRUM           AVQ-400
PROBHD   5 mm QNP 1H/13
PULPROG               zg30
TD                   65536
SOLVENT               CDCl3
NS                       20
DS                        0
SWH              8012.820 Hz
FIDRES           0.122266 Hz
AQ               4.0895586 sec
RG                      114
DW                 62.400 usec
DE                  6.00 usec
TE                 293.9 K
D1              1.00000000 sec
TD0                     222

======== CHANNEL f1 ========
NUC1                    1H
P1                 12.80 usec
PL1                 0.00 dB
PL1W          9.54516888 W
SFO1        400.1324700 MHz
SI                   65536
SF          400.1300175 MHz
WDW                     EM
SSB                      0
LB                  0.30 Hz
GB                       0
PC                  4.00
```

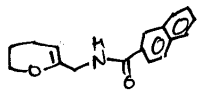

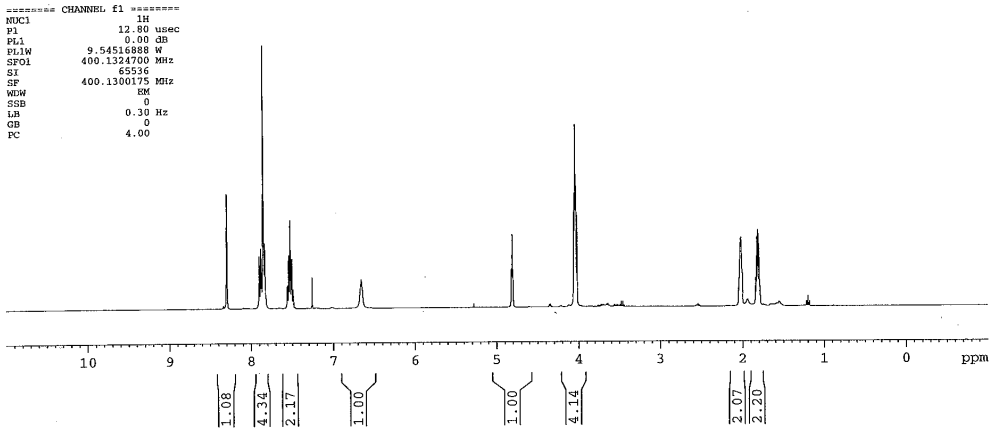

JP Carbon Starting parameters 7/16/03 revised 7

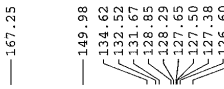


```
NAME        VRT-3-2-Naphtyl-Subst
EXPNO                   1
PROCNO                  1
Date_            20110813
Time                12.44
INSTRUM           AVQ-400
PROBHD   5 mm QNP 1H/13
PULPROG            zgpg30
TD                   65536
SOLVENT               CDCl3
NS                       40
DS                        0
SWH             24038.461 Hz
FIDRES           0.366798 Hz
AQ               1.3632196 sec
RG                   16384
DW                 20.800 usec
DE                  6.00 usec
TE                 293.9 K
D1              2.00000000 sec
D11             0.03000000 sec
TD0                     444

======== CHANNEL f1 ========
NUC1                   13C
P1                  8.50 usec
PL1                -2.00 dB
PL1W         47.77286148 W
SFO1        100.6228298 MHz

======== CHANNEL f2 ========
CPDPRG2            waltz16
NUC2                    1H
PCPD2              70.00 usec
PL2                 0.00 dB
PL12               15.00 dB
PL13               17.00 dB
PL2W          9.54516888 W
PL12W         0.30184472 W
PL13W         0.19045115 W
SFO2        400.1316000 MHz
SI                   32768
SF          100.6127802 MHz
WDW                     EM
SSB                      0
LB                  1.50 Hz
GB                       0
PC                  1.40
```

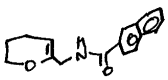

AVQ-400 QNP Proton starting parameters. 7/16/

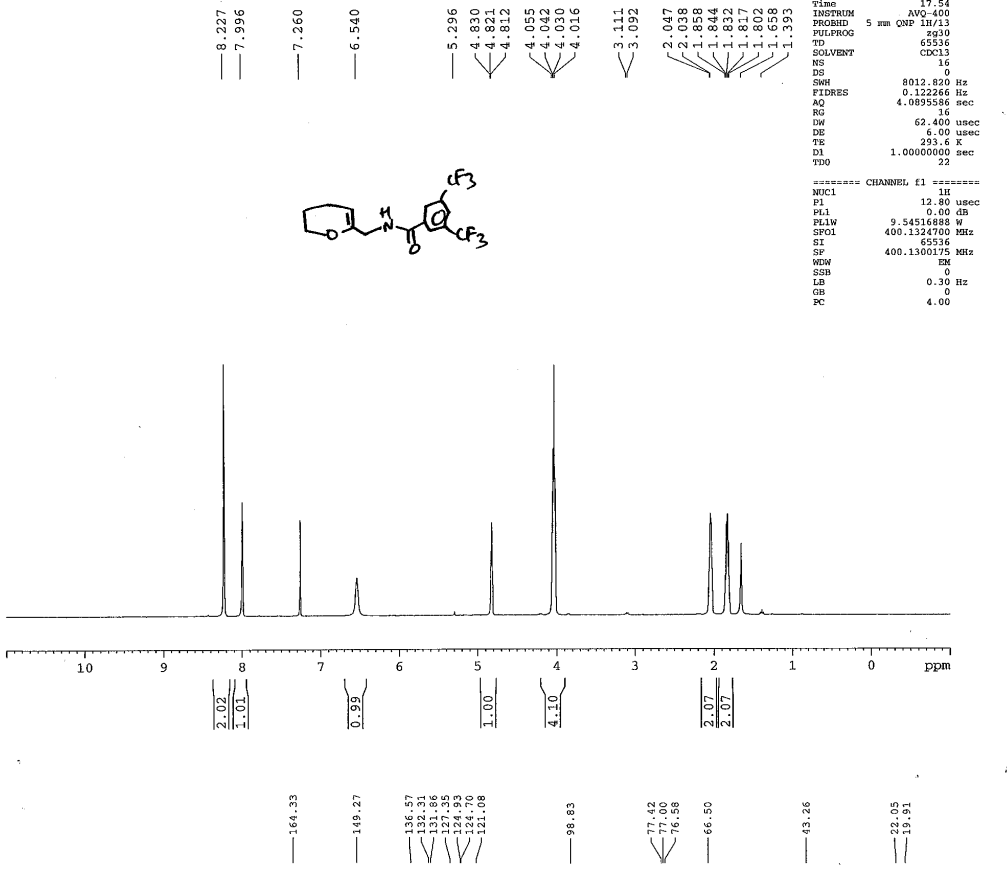

NAME	VRT-3-5-bis-CF3-SM
EXPNO	1
PROCNO	1
Date_	20110905
Time	17.54
INSTRUM	AVQ-400
PROBHD	5 mm QNP 1H/13
PULPROG	zg30
TD	65536
SOLVENT	CDCl3
NS	16
DS	0
SWH	8012.820 Hz
FIDRES	0.122266 Hz
AQ	4.0895586 sec
RG	16
DW	62.400 usec
DE	6.00 usec
TE	293.6 K
D1	1.00000000 sec
TD0	22
======== CHANNEL f1 ========	
NUC1	1H
P1	12.80 usec
PL1	0.00 dB
PL1W	9.54516888 W
SFO1	400.1324700 MHz
SI	65536
SF	400.1300175 MHz
WDW	EM
SSB	0
LB	0.30 Hz
GB	0
PC	4.00

AV-300 Dual C-H probe Carbon starting parameters 7/23/03

NAME	3-5-bistrilfuoromethyl-subst
EXPNO	1
PROCNO	1
Date_	20110827
Time	19.32
INSTRUM	av-300
PROBHD	5 mm Dual 13C/
PULPROG	xgpg30
TD	65536
SOLVENT	CDCl3
NS	197
DS	0
SWH	17985.611 Hz
FIDRES	0.274439 Hz
AQ	1.8219508 sec
RG	32768
DW	27.800 usec
DE	6.00 usec
TE	295.3 K
D1	1.00000000 sec
D11	0.03000000 sec
TD0	444
======== CHANNEL f1 ========	
NUC1	13C
P1	10.50 usec
PL1	0.00 dB
PL1W	32.65452194 W
SFO1	75.4760505 MHz
======== CHANNEL f2 ========	
CPDPRG2	waltz16
NUC2	1H
PCPD2	120.00 usec
PL2	-3.00 dB
PL12	17.76 dB

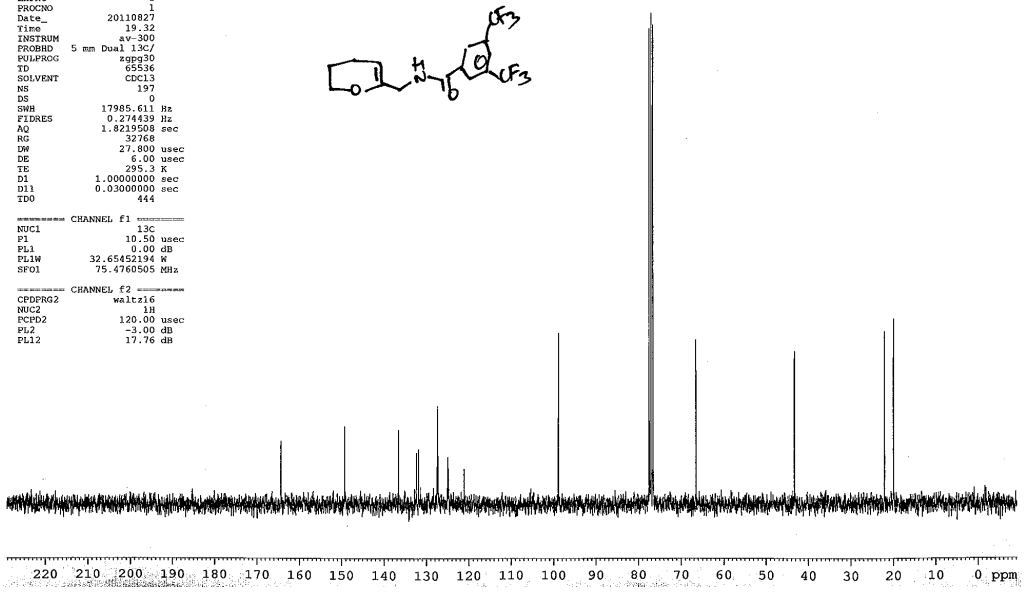

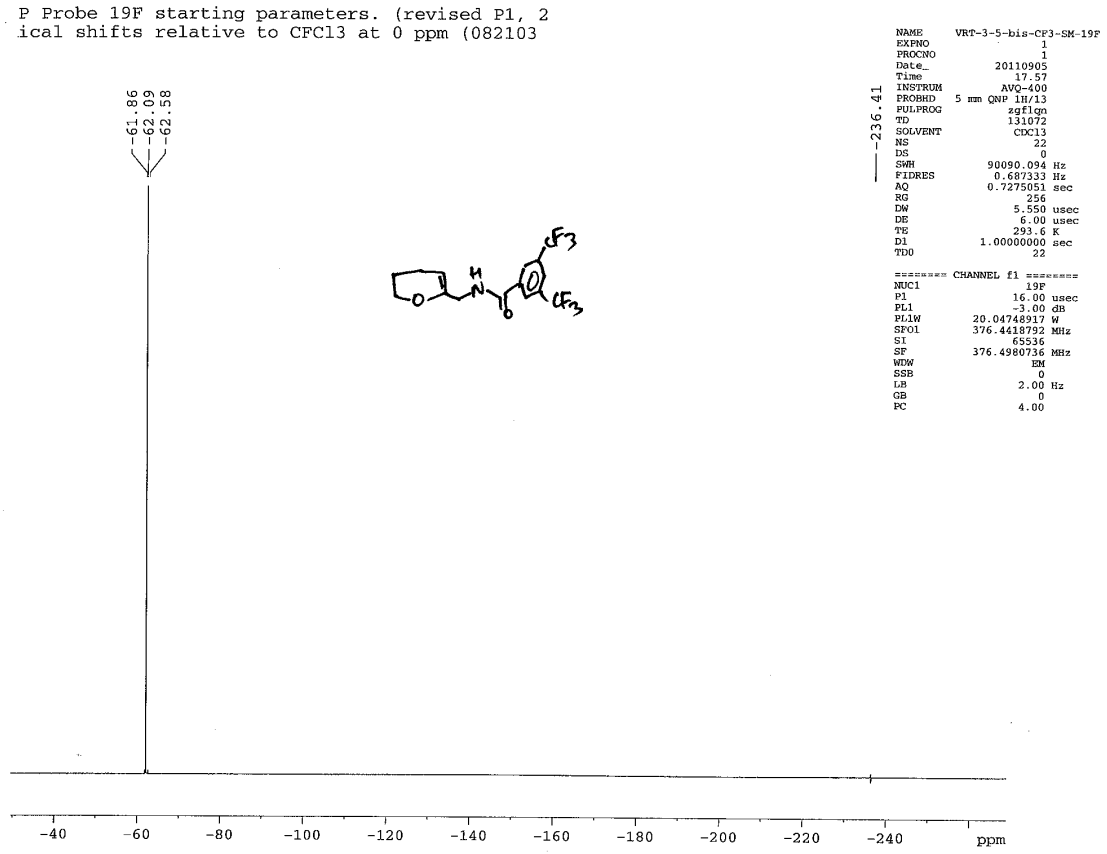
P Probe 19F starting parameters. (revised P1, 2
ical shifts relative to CFCl3 at 0 ppm (082103
-61.86
-62.09
-62.58
-236.41
NAME VRT-3-5-bis-CF3-SM-19F
EXPNO 1
PROCNO 1
Date_ 20110905
Time 17.57
INSTRUM AVQ-400
PROBHD 5 mm QNP 1H/13
PULPROG zgflqn
TD 131072
SOLVENT CDCl3
NS 22
DS 0
SWH 90090.094 Hz
FIDRES 0.687333 Hz
AQ 0.7275051 sec
RG 256
DW 5.550 usec
DE 6.00 usec
TE 293.6 K
D1 1.00000000 sec
TD0 22
======== CHANNEL f1 ========
NUC1 19F
P1 16.00 usec
PL1 -3.00 dB
PL1W 20.04748917 W
SFO1 376.4418792 MHz
SI 65536
SF 376.4980736 MHz
WDW EM
SSB 0
LB 2.00 Hz
GB 0
PC 4.00
-40
-60
-80
-100
-120
-140
-160
-180
-200
-220
-240
ppm

AVQ-400 QNP Proton starting parameters. 7/16/

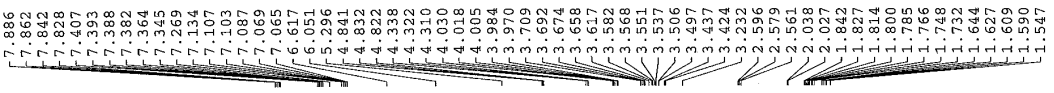


```
NAME        VRT-3-195-2-Ioo-Substrate
EXPNO                   1
PROCNO                  1
Date_            20110823
Time                19.45
INSTRUM          AVQ-400
PROBHD   5 mm QNP 1H/13
PULPROG              zg30
TD                  65536
SOLVENT             CDCl3
NS                     12
DS                      0
SWH           8012.820 Hz
FIDRES        0.122266 Hz
AQ            4.0895586 sec
RG                    181
DW              62.400 usec
DE                6.00 usec
TE                294.9 K
D1           1.00000000 sec
TD0                    22

======== CHANNEL f1 ========
NUC1                   1H
P1                12.80 usec
PL1                0.00 dB
PL1W         9.54516888 W
SFO1        400.1324700 MHz
SI                  65536
SF          400.1300142 MHz
WDW                    EM
SSB                     0
LB                 0.30 Hz
GB                      0
PC                   4.00
```

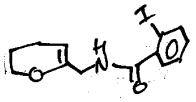

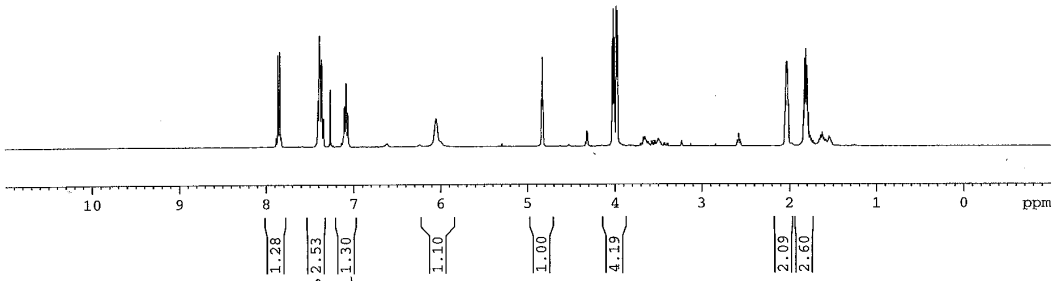

JP Carbon Starting parameters 7/16/03 revised 7


```
NAME        VRT-3-195-2-Ioo-Subst
EXPNO                   1
PROCNO                  1
Date_            20110823
Time                19.50
INSTRUM          AVQ-400
PROBHD   5 mm QNP 1H/13
PULPROG          zgpg30
TD                  65536
SOLVENT             CDCl3
NS                     24
DS                      0
SWH          24038.461 Hz
FIDRES        0.366798 Hz
AQ            1.3632196 sec
RG                  16384
DW              20.800 usec
DE                6.00 usec
TE                294.9 K
D1           2.00000000 sec
D11          0.03000000 sec
TD0                  2222

======== CHANNEL f1 ========
NUC1                  13C
P1                 8.50 usec
PL1               -2.00 dB
PL1W        47.77286148 W
SFO1       100.6228298 MHz

======== CHANNEL f2 ========
CPDPRG2          waltz16
NUC2                   1H
PCPD2             70.00 usec
PL2                0.00 dB
PL12              15.00 dB
PL13              17.00 dB
PL2W         9.54516888 W
PL12W        0.30184472 W
PL13W        0.19045115 W
SFO2        400.1316000 MHz
SI                  32768
SF          100.6127781 MHz
WDW                    EM
SSB                     0
LB                 1.50 Hz
GB                      0
PC                   1.40
```

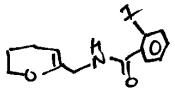

AVQ-400 AL 07-174 precipitate in MeOD 8/11/11

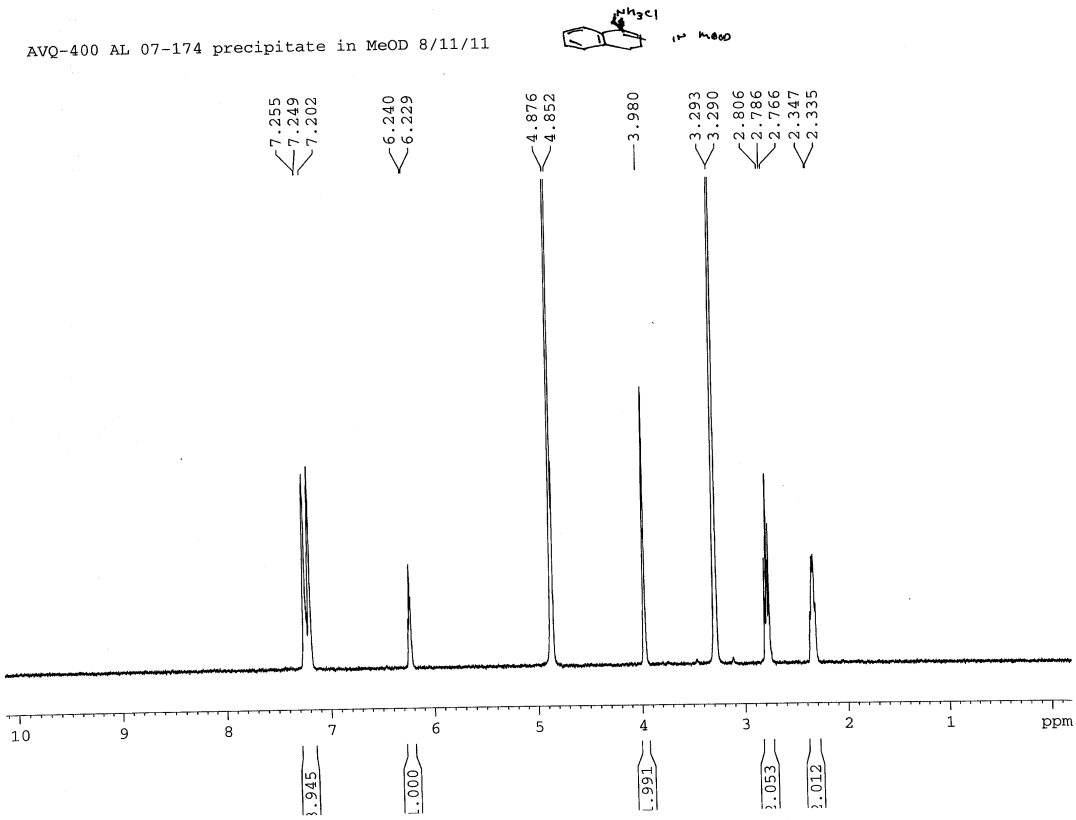

DRX-500 AL 07-174 precipitate in MeOD 8/11/11

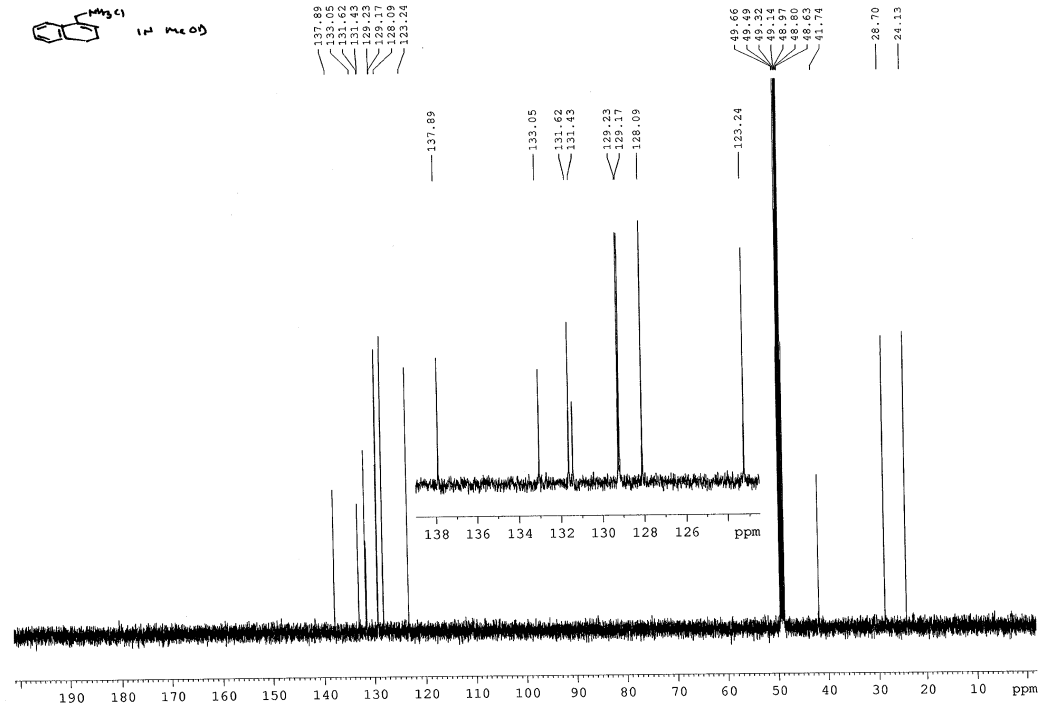

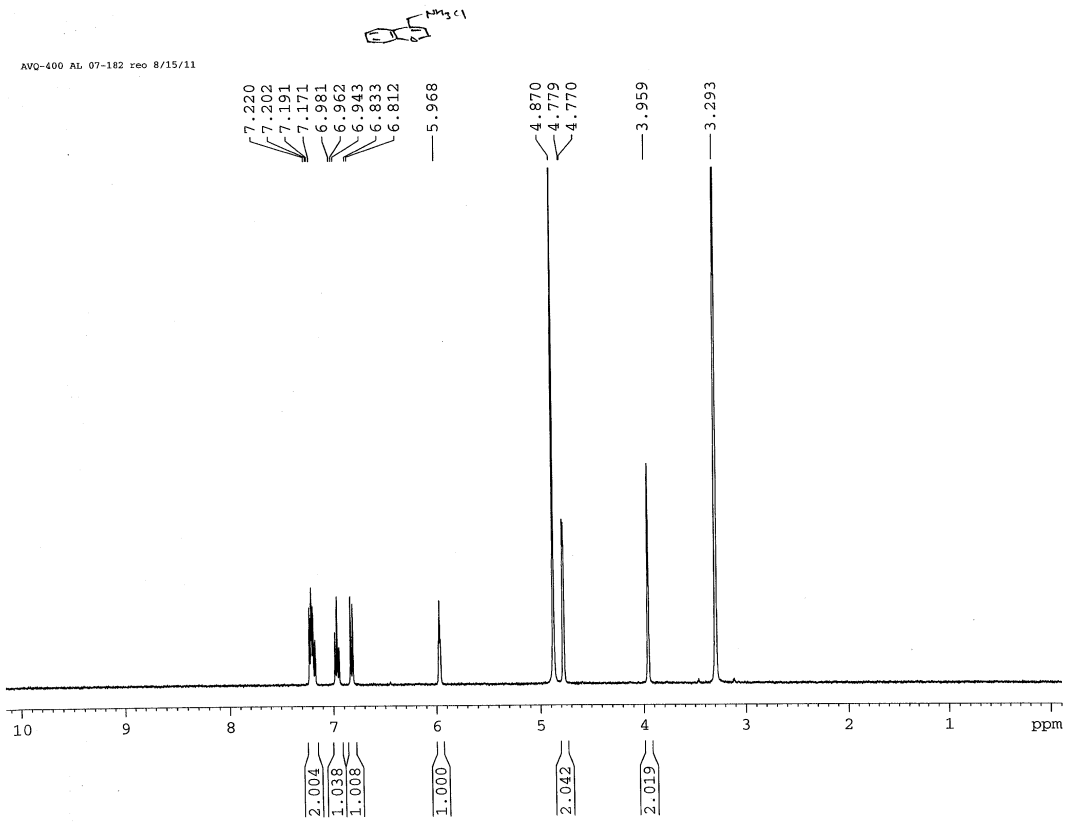
AVQ-400 AL 07-182 reo 8/15/11
7.220
7.202
7.191
7.171
6.981
6.962
6.943
6.833
6.812
5.968
4.870
4.779
4.770
3.959
3.293
10
9
8
7
6
5
4
3
2
1
ppm
2.004
1.038
1.008
1.000
2.042
2.019

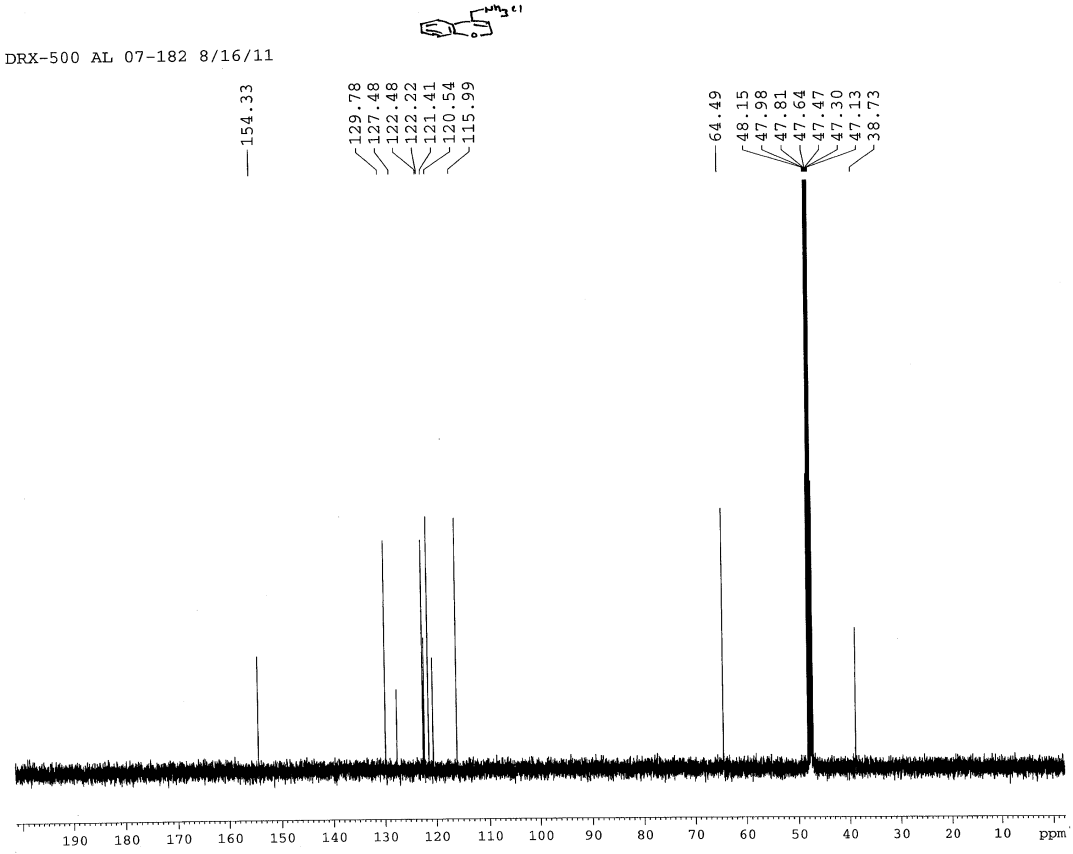
DRX-500 AL 07-182 8/16/11
154.33
129.78
127.48
122.48
122.22
121.41
120.54
115.99
64.49
48.15
47.98
47.81
47.64
47.47
47.30
47.13
38.73
190
180
170
160
150
140
130
120
110
100
90
80
70
60
50
40
30
20
10
ppm

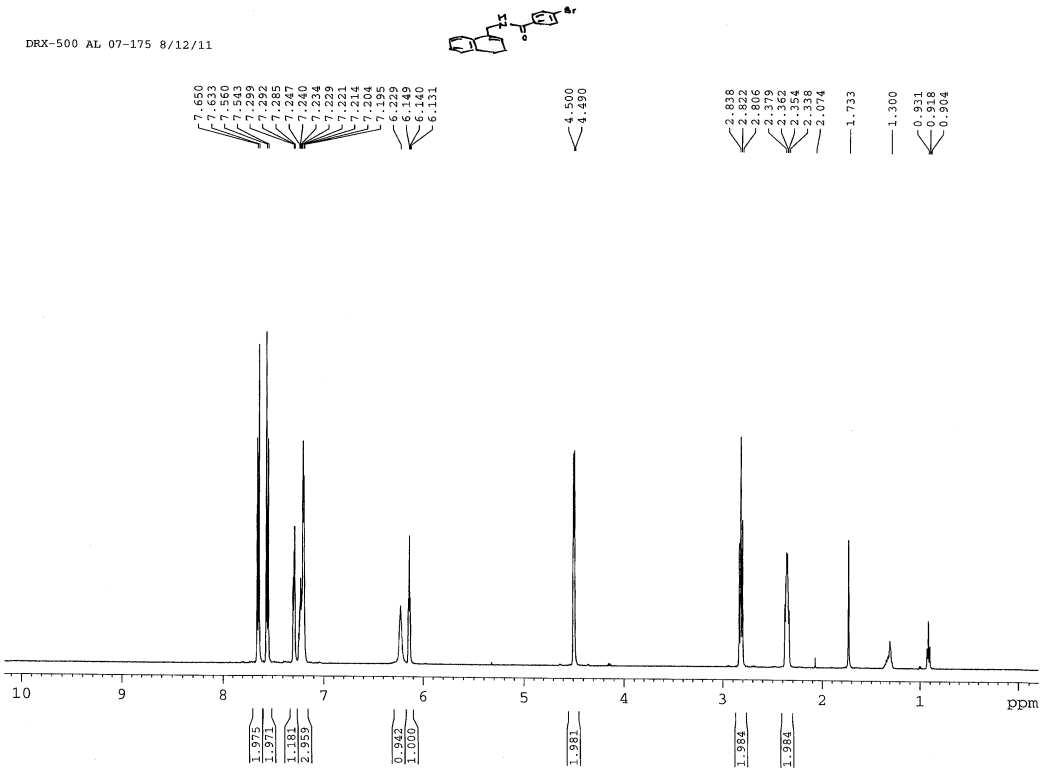
DRX-500 AL 07-175 8/12/11
7.650
7.633
7.560
7.543
7.299
7.282
7.265
7.247
7.240
7.234
7.229
7.221
7.214
7.204
7.195
6.229
6.149
6.140
6.131
4.500
4.490
2.838
2.822
2.806
2.379
2.362
2.354
2.338
2.074
1.733
1.300
0.931
0.918
0.904
1.975
1.971
1.181
2.953
0.942
1.000
1.981
1.984
1.984
ppm

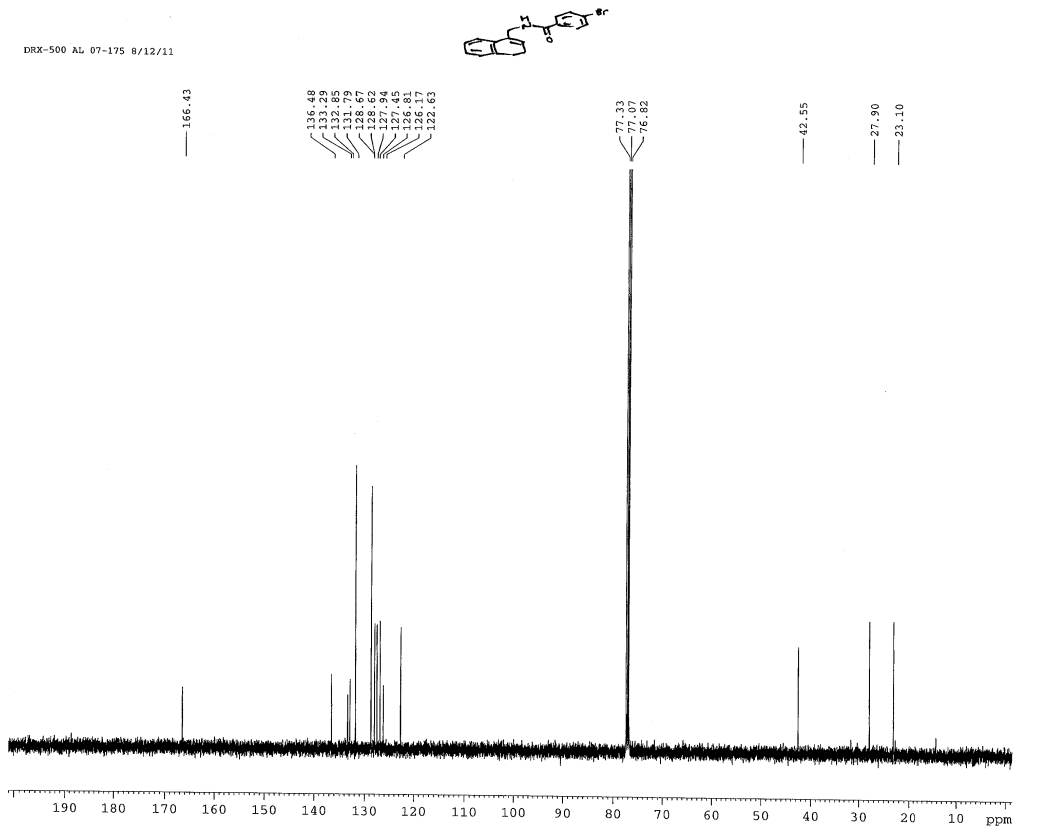
DRX-500 AL 07-175 8/12/11
166.43
136.48
133.29
132.85
131.79
128.67
128.62
127.94
127.45
126.81
126.17
122.63
77.33
77.07
76.82
42.55
27.90
23.10
ppm

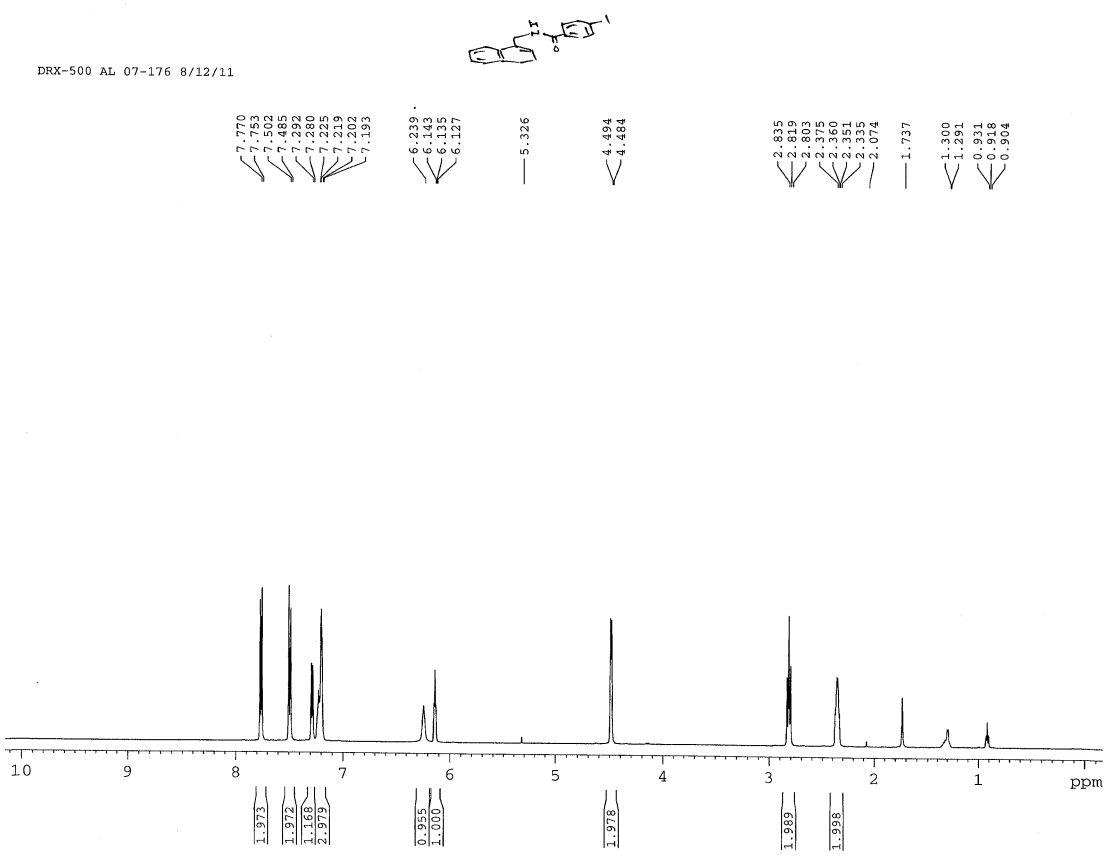
DRX-500 AL 07-176 8/12/11
7.770
7.753
7.502
7.485
7.292
7.280
7.225
7.219
7.202
7.193
6.239
6.143
6.135
6.127
5.326
4.494
4.484
2.835
2.819
2.803
2.375
2.360
2.351
2.335
2.074
1.737
1.300
1.291
0.931
0.918
0.904
10
9
8
7
6
5
4
3
2
1
ppm
1.973
1.972
1.168
2.979
0.955
1.000
1.978
1.989
1.998

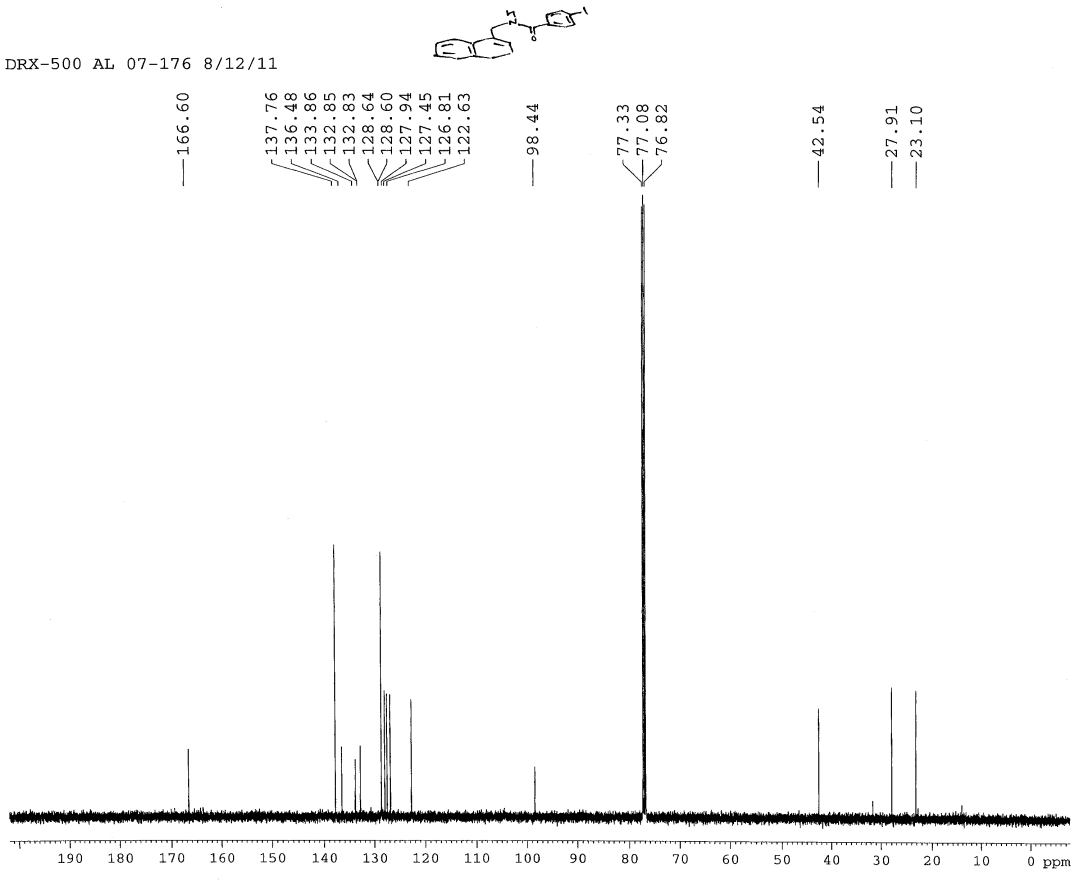
DRX-500 AL 07-176 8/12/11
166.60
137.76
136.48
133.86
132.85
132.83
128.64
128.60
127.94
127.45
126.81
122.63
98.44
77.33
77.08
76.82
42.54
27.91
23.10
190 180 170 160 150 140 130 120 110 100 90 80 70 60 50 40 30 20 10 0 ppm

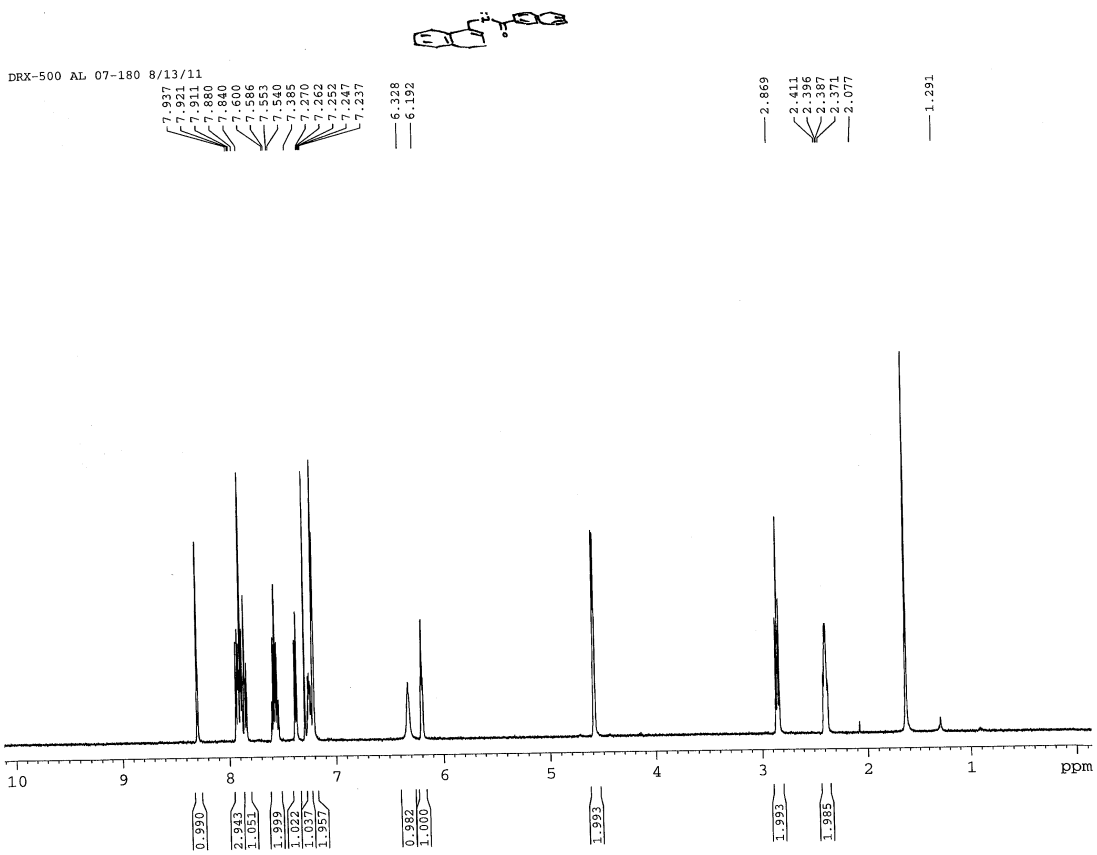
DRX-500 AL 07-180 8/13/11
7.937
7.921
7.911
7.880
7.840
7.600
7.586
7.553
7.540
7.385
7.270
7.262
7.252
7.247
7.237
6.328
6.192
2.869
2.411
2.396
2.387
2.371
2.077
1.291
ppm
0.990
2.943
1.051
1.999
1.022
1.037
1.957
0.982
1.000
1.993
1.993
1.985

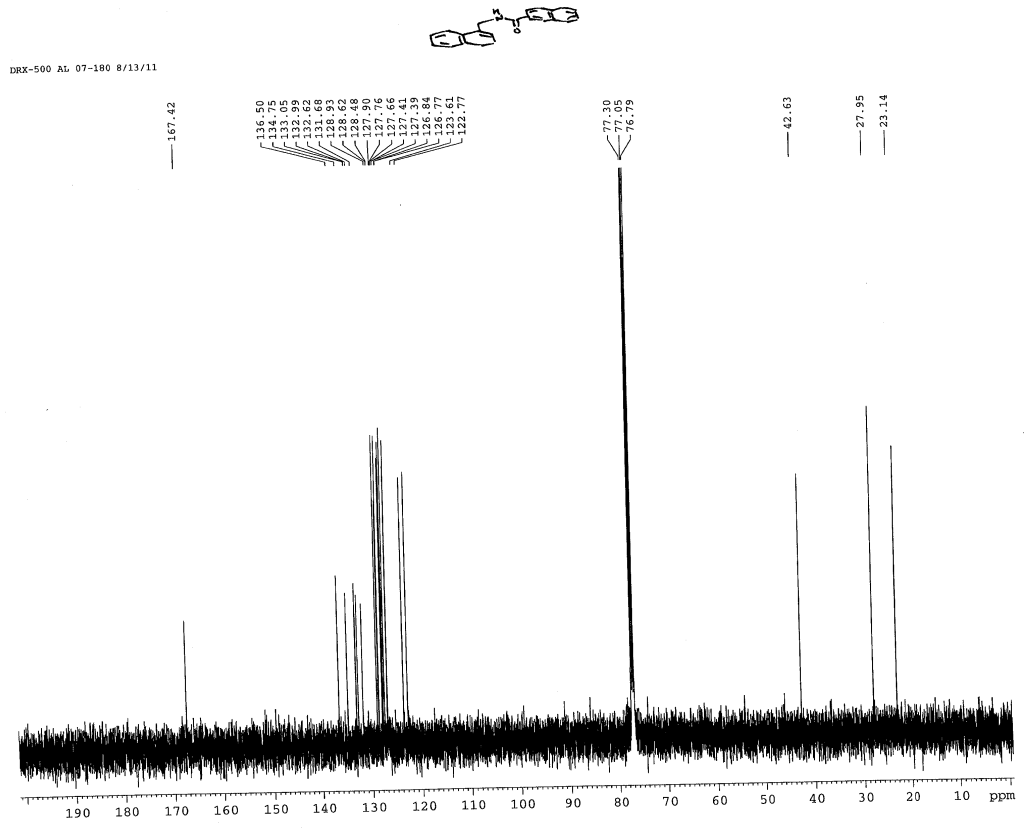
DRX-500 AL 07-180 8/13/11
167.42
136.50
134.75
133.95
133.39
132.62
131.68
128.93
128.62
128.48
127.90
127.76
127.66
127.41
127.39
126.84
126.77
123.67
122.77
77.30
77.05
76.79
42.63
27.95
23.14
ppm

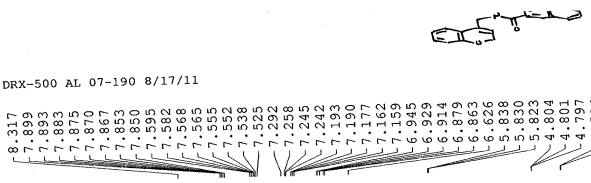
DRX-500 AL 07-190 8/17/11
8.317
7.899
7.893
7.883
7.875
7.870
7.867
7.853
7.850
7.595
7.582
7.568
7.565
7.555
7.552
7.538
7.525
7.292
7.258
7.245
7.242
7.193
7.190
7.177
7.162
7.159
6.945
6.929
6.914
6.879
6.863
6.626
5.838
5.830
5.823
4.804
4.801
4.797
4.514
4.505
1.805

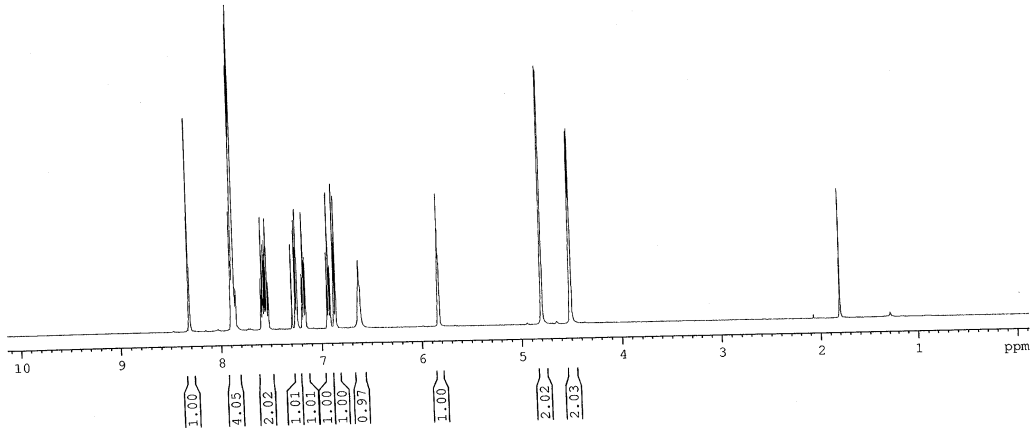
10
9
8
7
6
5
4
3
2
1
ppm
1.00
4.05
2.02
1.01
1.01
1.00
1.00
0.97
1.00
2.02
2.03

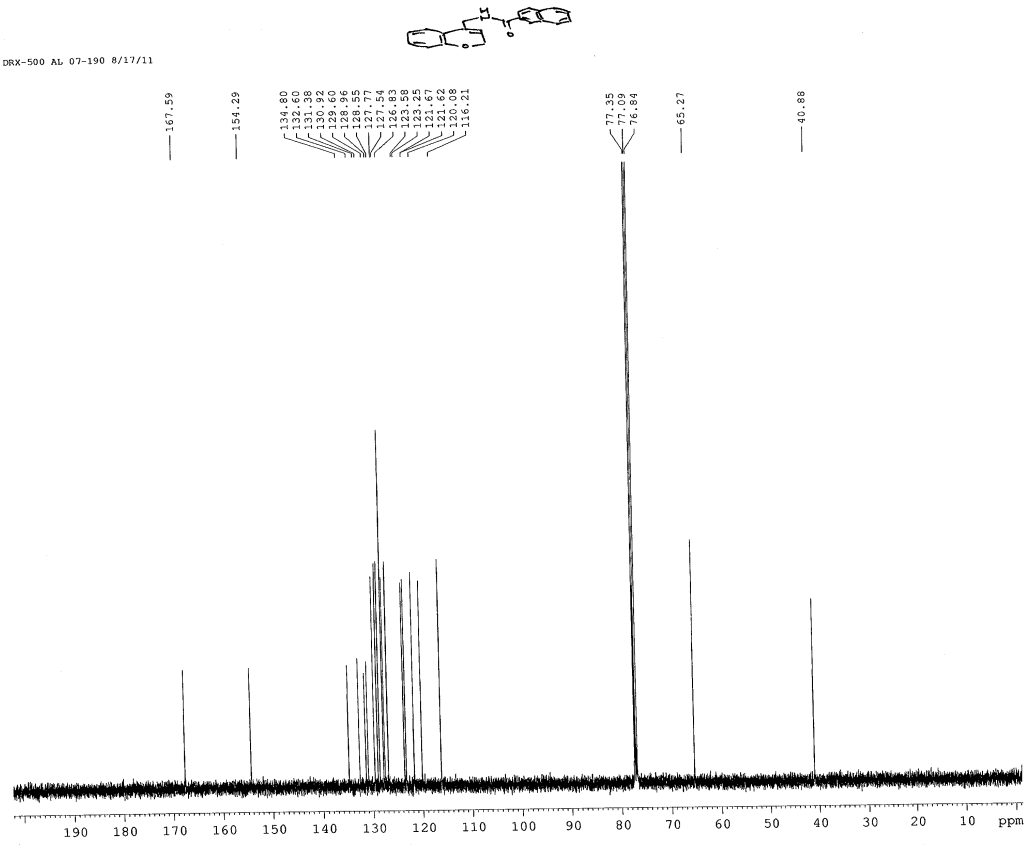
DRX-500 AL 07-190 8/17/11
167.59
154.29
134.80
132.60
131.38
130.92
129.60
128.96
128.55
127.77
127.54
126.83
123.58
123.25
121.67
121.62
120.08
116.21
77.35
77.09
76.84
65.27
40.88
190
180
170
160
150
140
130
120
110
100
90
80
70
60
50
40
30
20
10
ppm

AVQ-400 QNP Proton starting parameters. 7/16/

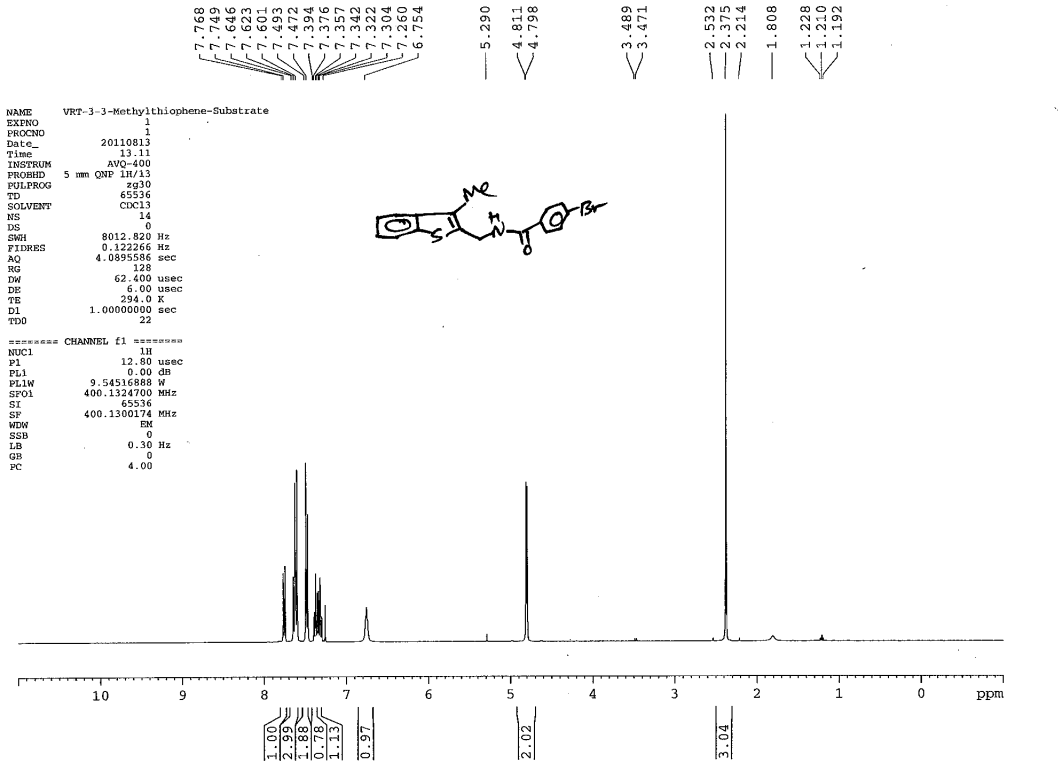

JP Carbon Starting parameters 7/16/03 revised 7

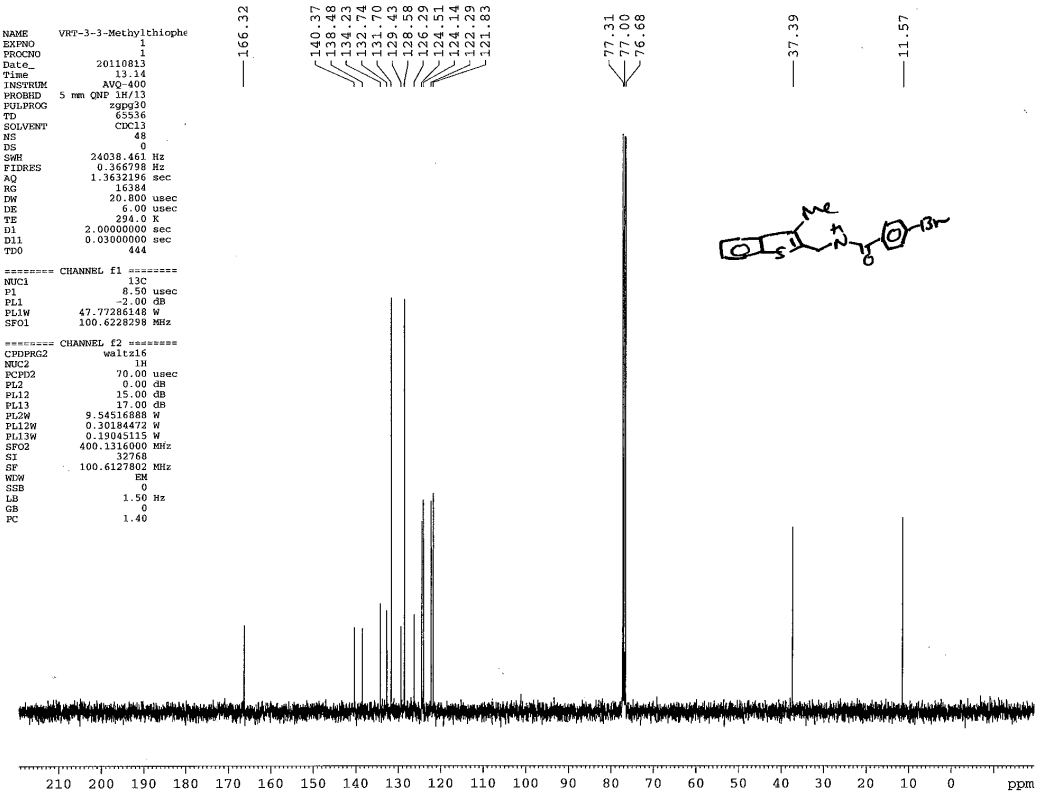

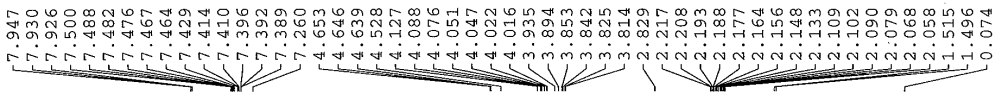


```
NAME      VRT-3-96-Phenyl-Substrate-1H
EXPNO               1
PROCNO              1
Date_        20110607
Time             9.04
INSTRUM       AVQ-400
PROBHD   5 mm QNP 1H/13
PULPROG          zg30
TD              65536
SOLVENT         CDCl3
NS                 44
DS                  0
SWH          8012.820 Hz
FIDRES       0.122266 Hz
AQ           4.0895586 sec
RG                 16
DW              62.400 usec
DE               6.00 usec
TE              293.5 K
D1           1.00000000 sec
TD0                22

======== CHANNEL f1 ========
NUC1               1H
P1              12.80 usec
PL1              0.00 dB
PL1W       9.54516888 W
SFO1     400.1324700 MHz
SI             65536
SF       400.1300174 MHz
WDW               EM
SSB                0
LB              0.30 Hz
GB                 0
PC             150.00
```

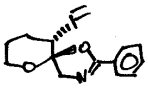

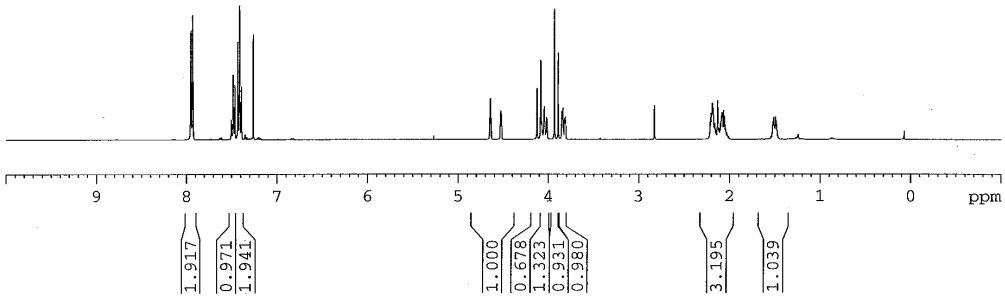

AVQ-400 QNP Carbon Starting parameters 7/16/03 revised 7/22/03 RN

```
NAME      VRT-3-96-Phenyl-Subst
EXPNO               1
PROCNO              1
Date_        20110607
Time             9.13
INSTRUM       AVQ-400
PROBHD   5 mm QNP 1H/13
PULPROG       zgpg30
TD              65536
SOLVENT         CDCl3
NS                133
DS                  0
SWH         24038.461 Hz
FIDRES       0.366798 Hz
AQ           1.3632196 sec
RG              16384
DW              20.800 usec
DE               6.00 usec
TE              293.5 K
D1           2.00000000 sec
D11          0.03000000 sec
TD0               444

======== CHANNEL f1 ========
NUC1               13C
P1               8.50 usec
PL1             -2.00 dB
PL1W      47.77286148 W
SFO1     100.6228298 MHz

======== CHANNEL f2 ========
CPDPRG2        waltz16
NUC2               1H
PCPD2           70.00 usec
PL2              0.00 dB
PL12            15.00 dB
PL13            17.00 dB
PL2W       9.54516888 W
PL12W      0.30184472 W
PL13W      0.19045115 W
SFO2     400.1316000 MHz
SI             32768
SF       100.6127806 MHz
WDW               EM
SSB                0
LB              1.50 Hz
GB                 0
PC              1.40
```

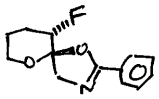

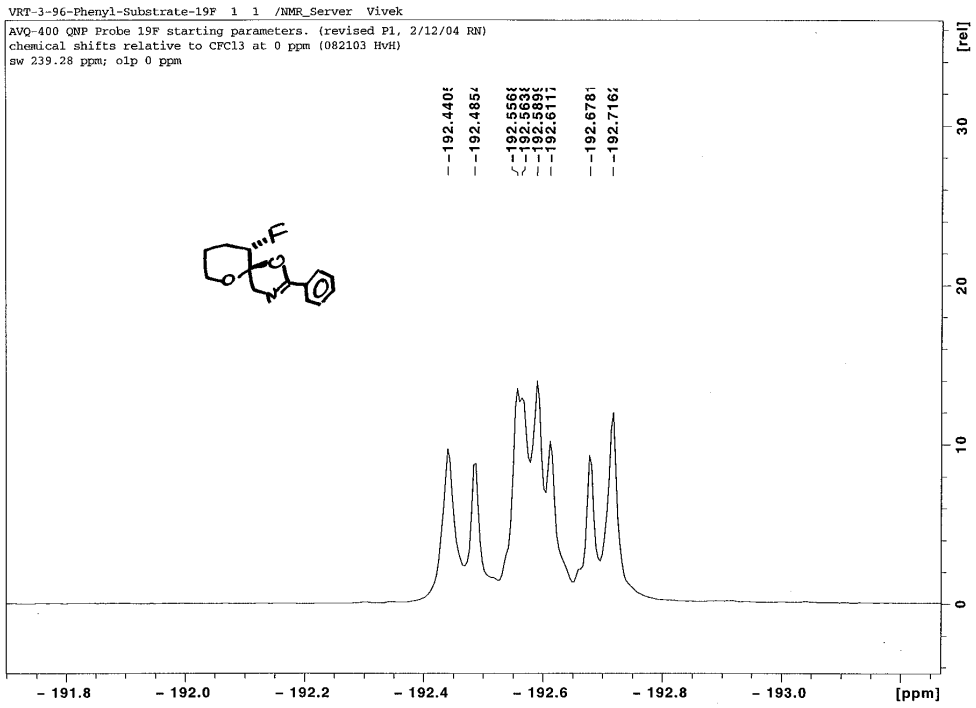
VRT-3-96-Phenyl-Substrate-19F 1 1 /NMR_Server Vivek
AVQ-400 QNP Probe 19F starting parameters. (revised P1, 2/12/04 RN)
chemical shifts relative to CFCl3 at 0 ppm (082103 HvH)
sw 239.28 ppm; o1p 0 ppm
-192.4405
-192.4854
-192.5564
-192.5631
-192.5895
-192.6111
-192.6781
-192.7164
F
[rel]
30
20
10
0
- 191.8
- 192.0
- 192.2
- 192.4
- 192.6
- 192.8
- 193.0
[ppm]

AVQ-400 QNP Proton starting parameters. 7/16/

8.595 8.049 7.865 7.844 7.639 7.586 7.382 7.361 7.260 7.196 7.176 7.157 6.852 6.833 6.817 6.798 5.269 4.633 4.514 4.108 4.067 4.047 4.041 4.017 4.011 3.987 3.957 3.914 3.873 3.845 3.835 3.817 3.811 3.728 3.688 3.462 3.444 2.823 2.181 2.169 2.154 2.133 2.126 2.118 2.107 2.088 2.077 2.064 2.040 2.034 2.019 2.002 1.536 1.513 1.506 1.488 1.484 1.456 1.233 1.202 1.184 1.167 0.910

NAME	VRT-3-105C-Chloro-Product-1H
EXPNO	2
PROCNO	1
Date_	20110813
Time	16.33
INSTRUM	AVQ-400
PROBHD	5 mm QNP 1H/13
PULPROG	zg30
TD	65536
SOLVENT	CDCl3
NS	24
DS	0
SWH	8012.820 Hz
FIDRES	0.122266 Hz
AQ	4.0895586 sec
RG	71.8
DW	62.400 usec
DE	6.00 usec
TE	294.0 K
D1	1.00000000 sec
TD0	222
======== CHANNEL f1 ========	
NUC1	1H
P1	12.80 usec
PL1	0.00 dB
PL1W	9.54516888 W
SFO1	400.1324700 MHz
SI	65536
SF	400.1300175 MHz
WDW	EM
SSB	0
LB	0.30 Hz
GB	0
PC	4.00

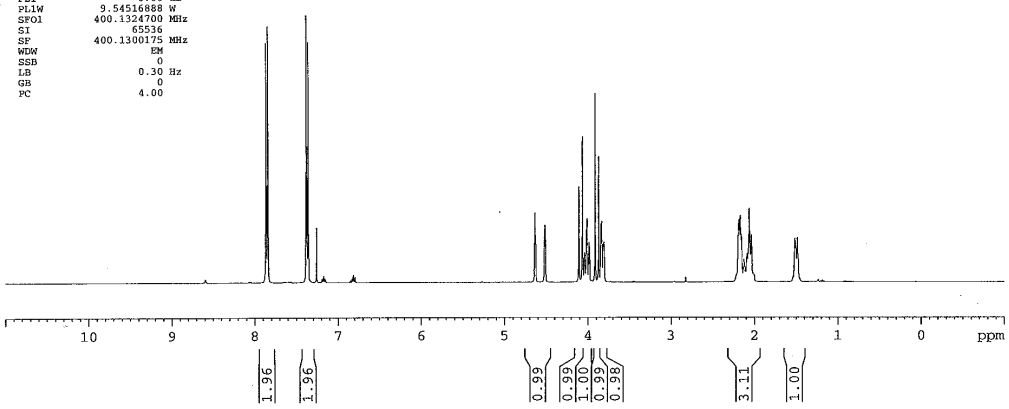

JP Carbon Starting parameters 7/16/03 revised 7

161.05 137.64 129.34 128.62 125.94 105.74 105.46 87.57 85.83 77.32 77.00 76.68 63.99 62.77 25.33 25.13 18.55

NAME	VRT-3-105C-Chloro-Prc
EXPNO	2
PROCNO	1
Date_	20110813
Time	16.37
INSTRUM	AVQ-400
PROBHD	5 mm QNP 1H/13
PULPROG	zgpg30
TD	65536
SOLVENT	CDCl3
NS	14
DS	0
SWH	24038.461 Hz
FIDRES	0.366798 Hz
AQ	1.3632196 sec
RG	16384
DW	20.800 usec
DE	6.00 usec
TE	294.0 K
D1	2.00000000 sec
D11	0.03000000 sec
TD0	222
======== CHANNEL f1 ========	
NUC1	13C
P1	8.50 usec
PL1	-2.00 dB
PL1W	47.77286148 W
SFO1	100.6228298 MHz
======== CHANNEL f2 ========	
CPDPRG2	waltz16
NUC2	1H
PCPD2	70.00 usec
PL2	0.00 dB
PL12	15.00 dB
PL13	17.00 dB
PL2W	9.54516888 W
PL12W	0.30184472 W
PL13W	0.19045115 W
SFO2	400.1316000 MHz
SI	32768
SF	100.6127810 MHz
WDW	EM
SSB	0
LB	1.50 Hz
GB	0
PC	1.40

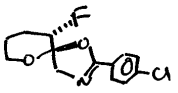

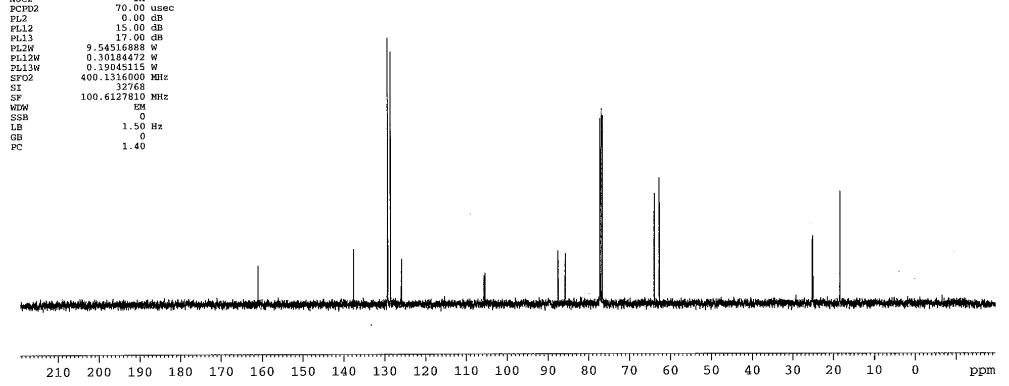

P Probe 19F starting parameters. (revised P1, 2
ical shifts relative to CFCl3 at 0 ppm (082103

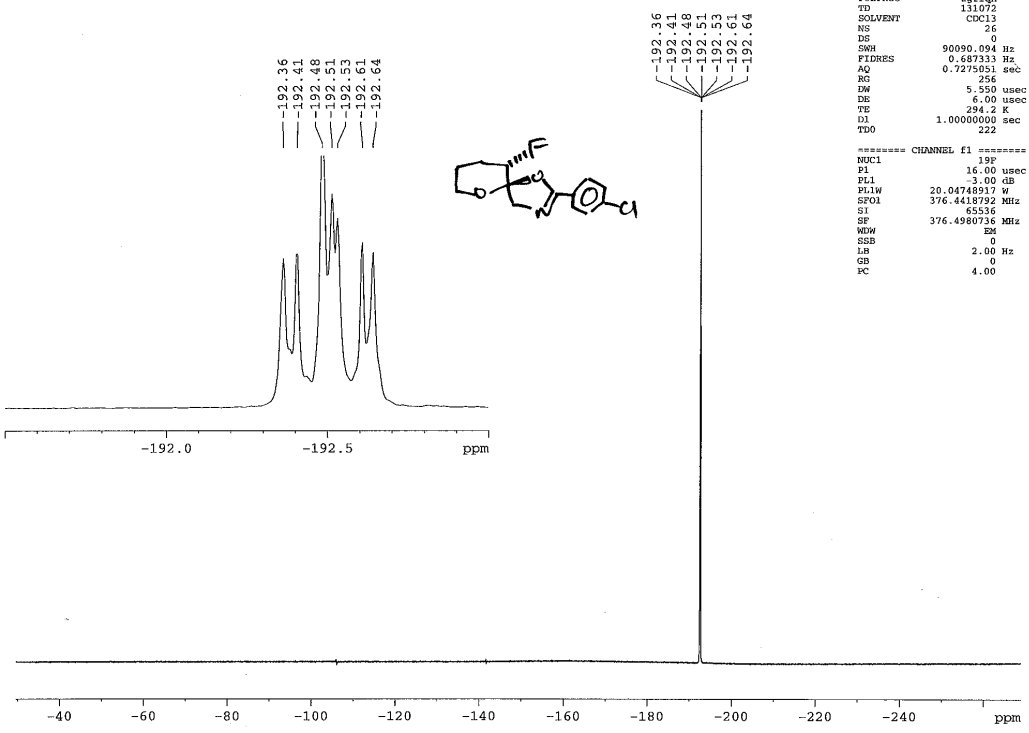

NAME	VRT-3-105C-Chloro-Prc
EXPNO	2
PROCNO	1
Date_	20110813
Time	16.39
INSTRUM	AVQ-400
PROBHD	5 mm QNP 1H/13
PULPROG	zgflqn
TD	131072
SOLVENT	CDCl3
NS	26
DS	0
SWH	90090.094 Hz
FIDRES	0.687333 Hz
AQ	0.7275051 sec
RG	256
DW	5.550 usec
DE	6.00 usec
TE	294.2 K
D1	1.00000000 sec
TD0	222
======== CHANNEL f1 ========	
NUC1	19F
P1	16.00 usec
PL1	-3.00 dB
PL1W	20.04748917 W
SFO1	376.4418792 MHz
SI	65536
SF	376.4980736 MHz
WDW	EM
SSB	0
LB	2.00 Hz
GB	0
PC	4.00

AVQ-400 QNP Proton starting parameters. 7/16/03. Revi

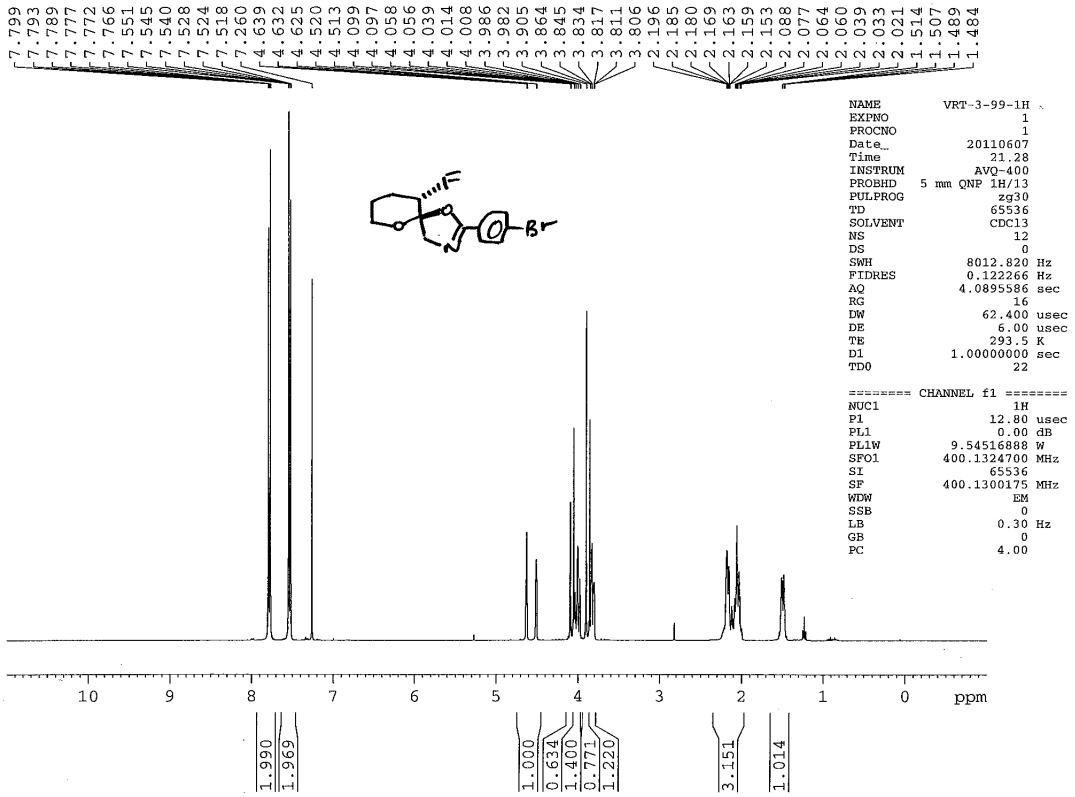

NAME	VRT-3-99-1H
EXPNO	1
PROCNO	1
Date_	20110607
Time	21.28
INSTRUM	AVQ-400
PROBHD	5 mm QNP 1H/13
PULPROG	zg30
TD	65536
SOLVENT	CDCl3
NS	12
DS	0
SWH	8012.820 Hz
FIDRES	0.122266 Hz
AQ	4.0895586 sec
RG	16
DW	62.400 usec
DE	6.00 usec
TE	293.5 K
D1	1.00000000 sec
TD0	22
========= CHANNEL f1 ========	
NUC1	1H
P1	12.80 usec
PL1	0.00 dB
PL1W	9.54516888 W
SFO1	400.1324700 MHz
SI	65536
SF	400.1300175 MHz
WDW	EM
SSB	0
LB	0.30 Hz
GB	0
PC	4.00

AVQ-400 QNP Carbon Starting parameters 7/16/03 revised 7/22/03 RN

NAME	VRT-3-99-13C
EXPNO	1
PROCNO	1
Date_	20110607
Time	21.29
INSTRUM	AVQ-400
PROBHD	5 mm QNP 1H/13
PULPROG	zgpg30
TD	65536
SOLVENT	CDCl3
NS	40
DS	0
SWH	24038.461 Hz
FIDRES	0.366798 Hz
AQ	1.3632196 sec
RG	16384
DW	20.800 usec
DE	6.00 usec
TE	293.6 K
D1	2.00000000 sec
D11	0.03000000 sec
TD0	4444
========= CHANNEL f1 ========	
NUC1	13C
P1	8.50 usec
PL1	-2.00 dB
PL1W	47.77286148 W
SFO1	100.6228298 MHz
========= CHANNEL f2 ========	
CPDPRG2	waltz16
NUC2	1H
PCPD2	70.00 usec
PL2	0.00 dB
PL12	15.00 dB
PL13	17.00 dB
PL2W	9.54516888 W
PL12W	0.30184472 W
PL13W	0.19045115 W
SFO2	400.1316000 MHz
SI	32768
SF	100.6127806 MHz
WDW	EM
SSB	0
LB	1.50 Hz
GB	0
PC	1.40

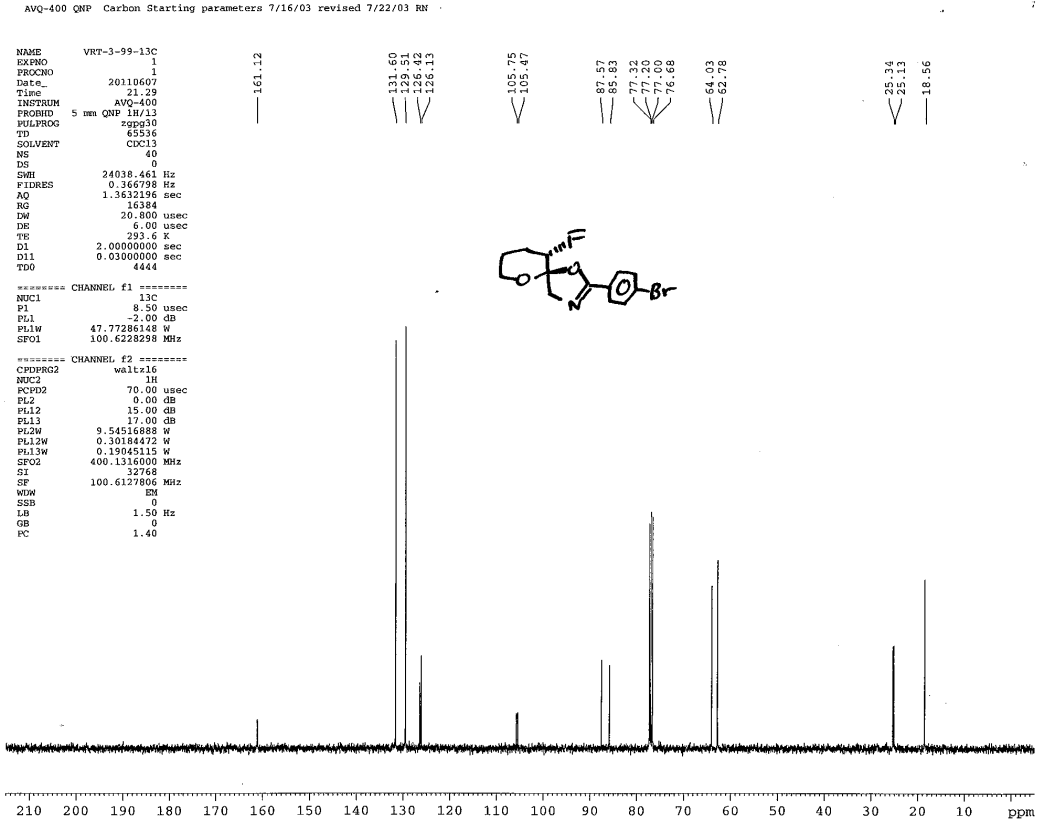

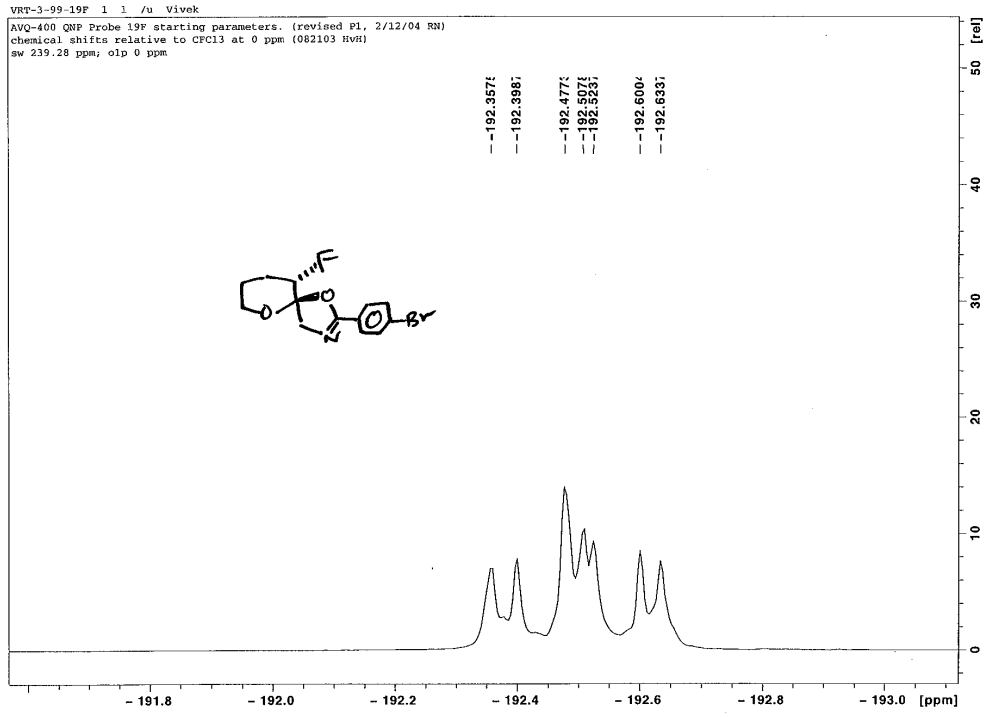
VRT-3-99-19F 1 1 /u Vivek
AVQ-400 QNP Probe 19F starting parameters. (revised P1, 2/12/04 RN)
chemical shifts relative to CFCl3 at 0 ppm (082103 HvH)
sw 239.28 ppm; olp 0 ppm
-192.357
-192.398
-192.477
-192.507
-192.523
-192.600
-192.633
[rel]
50
40
30
20
10
0
-191.8
-192.0
-192.2
-192.4
-192.6
-192.8
-193.0
[ppm]

AVQ-400 QNP Proton starting parameters. 7/16/

7.956 7.938 7.840 7.823 7.752 7.731 7.689 7.637 7.616 7.537 7.519 7.432 7.411 7.260 7.170 6.808 6.788 5.266 4.624 4.506 4.264 4.222 4.088 4.047 4.035 4.028 4.004 3.998 3.974 3.895 3.853 3.835 3.825 3.807 3.801 3.710 3.668 3.473 3.455 3.437 3.420 2.818 2.177 2.160 2.153 2.144 2.116 2.108 2.097 2.078 2.067 2.054 2.030 2.024 2.006 1.992 1.528 1.505 1.498 1.480 1.476 1.449 1.229 1.196 1.179 1.161

NAME	VRT-3-101B-iodo-1H
EXPNO	1
PROCNO	1
Date_	20110813
Time	15.34
INSTRUM	AVQ-400
PROBHD	5 mm QNP 1H/13
PULPROG	zg30
TD	65536
SOLVENT	CDCl3
NS	13
DS	0
SWH	8012.820 Hz
FIDRES	0.122266 Hz
AQ	4.0895586 sec
RG	16
DW	62.400 usec
DE	6.00 usec
TE	294.0 K
D1	1.00000000 sec
TD0	22
======== CHANNEL f1 ========	
NUC1	1H
P1	12.80 usec
PL1	0.00 dB
PL1W	9.54516888 W
SFO1	400.1324700 MHz
SI	65536
SF	400.1300174 MHz
WDW	EM
SSB	0
LB	0.30 Hz
GB	0
PC	4.00

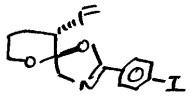

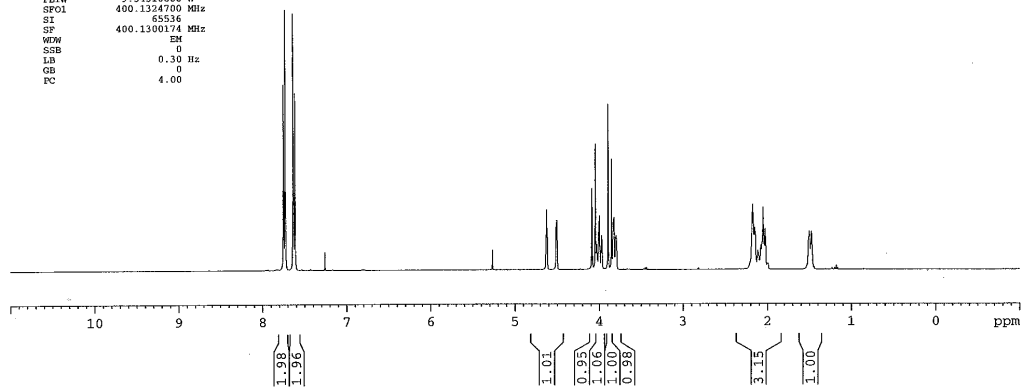

JP Carbon Starting parameters 7/16/03 revised

NAME	VRT-3-101B-iodo-13C
EXPNO	1
PROCNO	1
Date_	20110813
Time	15.38
INSTRUM	AVQ-400
PROBHD	5 mm QNP 1H/13
PULPROG	zgpg30
TD	65536
SOLVENT	CDCl3
NS	28
DS	0
SWH	24038.461 Hz
FIDRES	0.366798 Hz
AQ	1.3632196 sec
RG	16384
DW	20.800 usec
DE	6.00 usec
TE	294.0 K
D1	2.00000000 sec
D11	0.03000000 sec
TD0	222
======== CHANNEL f1 ========	
NUC1	13C
P1	8.50 usec
PL1	-2.00 dB
PL1W	47.77286148 W
SFO1	100.6228298 MHz
======== CHANNEL f2 ========	
CPDPRG2	waltz16
NUC2	1H
PCPD2	70.00 usec
PL2	0.00 dB
PL12	15.00 dB
PL13	17.00 dB
PL2W	9.54516888 W
PL12W	0.30184472 W
PL13W	0.19045115 W
SFO2	400.1316000 MHz
SI	32768
SF	100.6127846 MHz
WDW	EM
SSB	0
LB	1.50 Hz
GB	0
PC	1.40

161.24 137.53 129.45 126.92 105.68 105.40 98.46 87.52 85.79 77.31 77.00 76.68 63.99 62.74 25.30 25.10 18.53

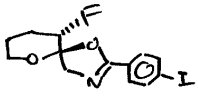

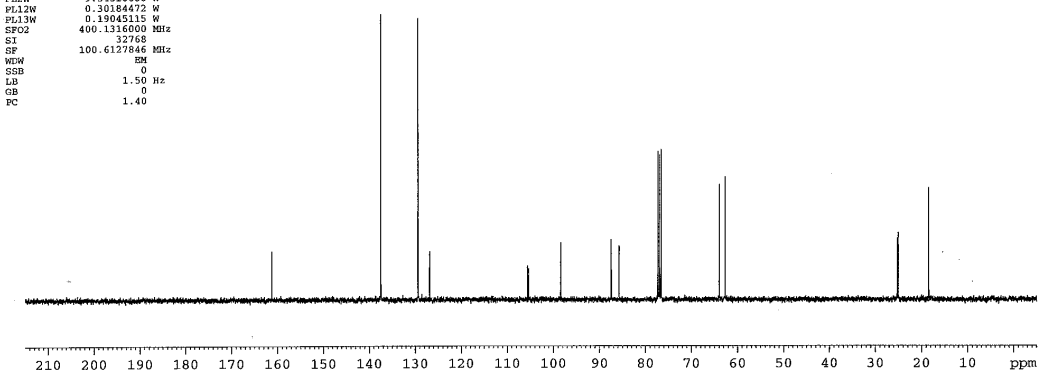

P Probe 19F starting parameters. (revised P1, 2
ical shifts relative to CFCl3 at 0 ppm (082103

NAME	VRT-3-101B-iodo-19F
EXPNO	1
PROCNO	1
Date_	20110813
Time	15.41
INSTRUM	AVQ-400
PROBHD	5 mm QNP 1H/13
PULPROG	zgflqn
TD	131072
SOLVENT	CDCl3
NS	28
DS	0
SWH	90090.094 Hz
FIDRES	0.687333 Hz
AQ	0.7275051 sec
RG	256
DW	5.550 usec
DE	6.00 usec
TE	294.2 K
D1	1.00000000 sec
TD0	222
======== CHANNEL f1 ========	
NUC1	19F
P1	16.00 usec
PL1	-3.00 dB
PL1W	20.04748917 W
SFO1	376.4418792 MHz
SI	65536
SF	376.4980736 MHz
WDW	EM
SSB	0
LB	2.00 Hz
GB	0
PC	4.00

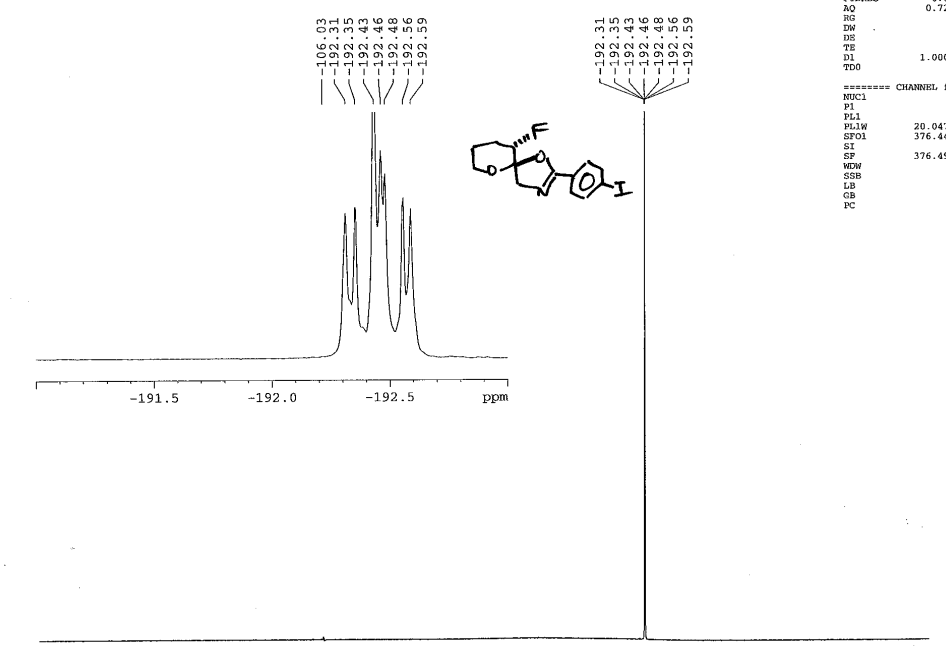

AVQ-400 QNP Proton starting parameters. 7/16/

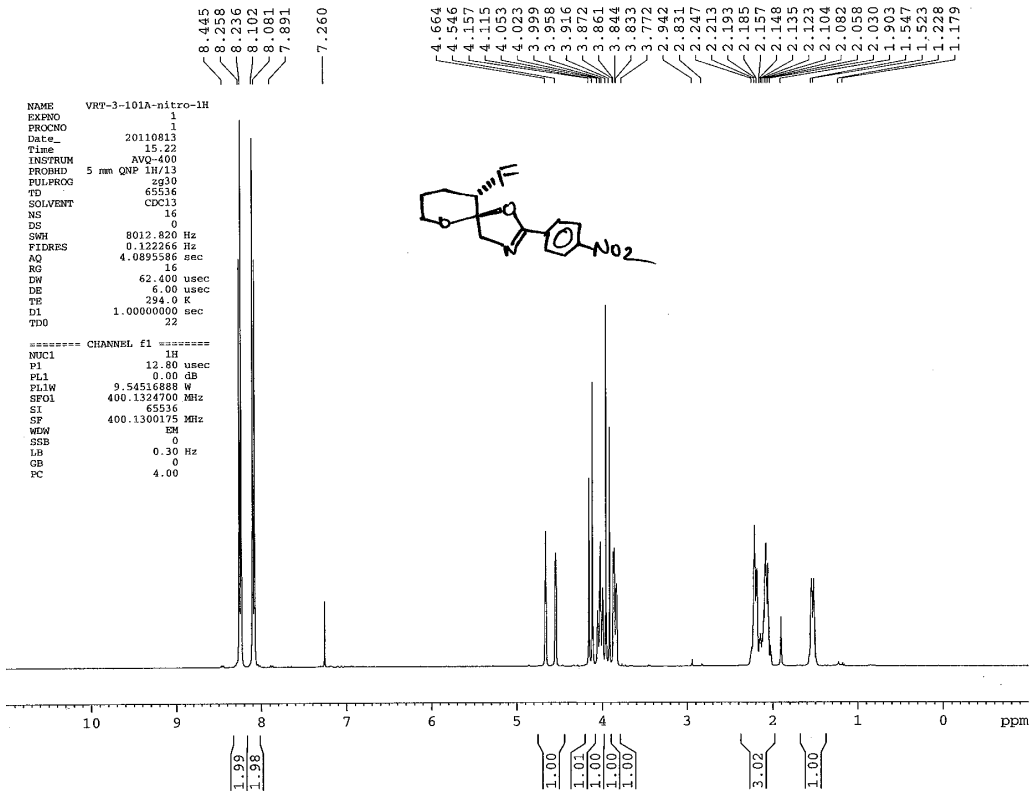


```
NAME        VRT-3-101A-nitro-1H
EXPNO                         1
PROCNO                        1
Date_                  20110813
Time                      15.22
INSTRUM                AVQ-400
PROBHD    5 mm QNP 1H/13
PULPROG                  zg30
TD                      65536
SOLVENT                 CDCl3
NS                         16
DS                          0
SWH                 8012.820 Hz
FIDRES              0.122266 Hz
AQ                  4.0895586 sec
RG                         16
DW                     62.400 usec
DE                      6.00 usec
TE                     294.0 K
D1                  1.00000000 sec
TD0                        22

======== CHANNEL f1 ========
NUC1                       1H
P1                      12.80 usec
PL1                      0.00 dB
PL1W                9.54516888 W
SFO1               400.1324700 MHz
SI                       65536
SF                 400.1300175 MHz
WDW                         EM
SSB                          0
LB                        0.30 Hz
GB                           0
PC                        4.00
```

NP Carbon Starting parameters 7/16/03 revised 7

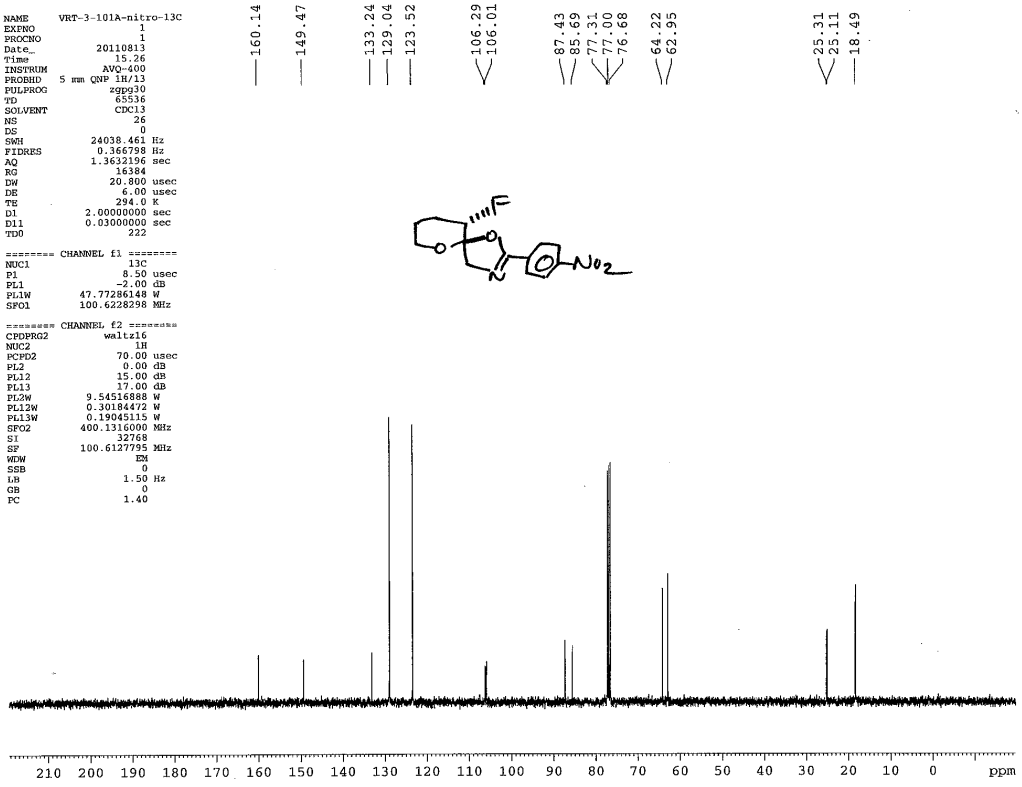


```
NAME        VRT-3-101A-nitro-13C
EXPNO                         1
PROCNO                        1
Date_                  20110813
Time                      15.26
INSTRUM                AVQ-400
PROBHD    5 mm QNP 1H/13
PULPROG                zgpg30
TD                      65536
SOLVENT                 CDCl3
NS                         26
DS                          0
SWH                24038.461 Hz
FIDRES              0.366798 Hz
AQ                  1.3632196 sec
RG                      16384
DW                     20.800 usec
DE                      6.00 usec
TE                     294.0 K
D1                  2.00000000 sec
D11                 0.03000000 sec
TD0                       222

======== CHANNEL f1 ========
NUC1                      13C
P1                       8.50 usec
PL1                     -2.00 dB
PL1W               47.77286148 W
SFO1               100.6228298 MHz

======== CHANNEL f2 ========
CPDPRG2                waltz16
NUC2                       1H
PCPD2                   70.00 usec
PL2                      0.00 dB
PL12                    15.00 dB
PL13                    17.00 dB
PL2W                9.54516888 W
PL12W               0.30184472 W
PL13W               0.19045115 W
SFO2               400.1316000 MHz
SI                       32768
SF                 100.6127795 MHz
WDW                         EM
SSB                          0
LB                        1.50 Hz
GB                           0
PC                        1.40
```

P Probe 19F starting parameters. (revised P1, 2
ical shifts relative to CFCl3 at 0 ppm (082103

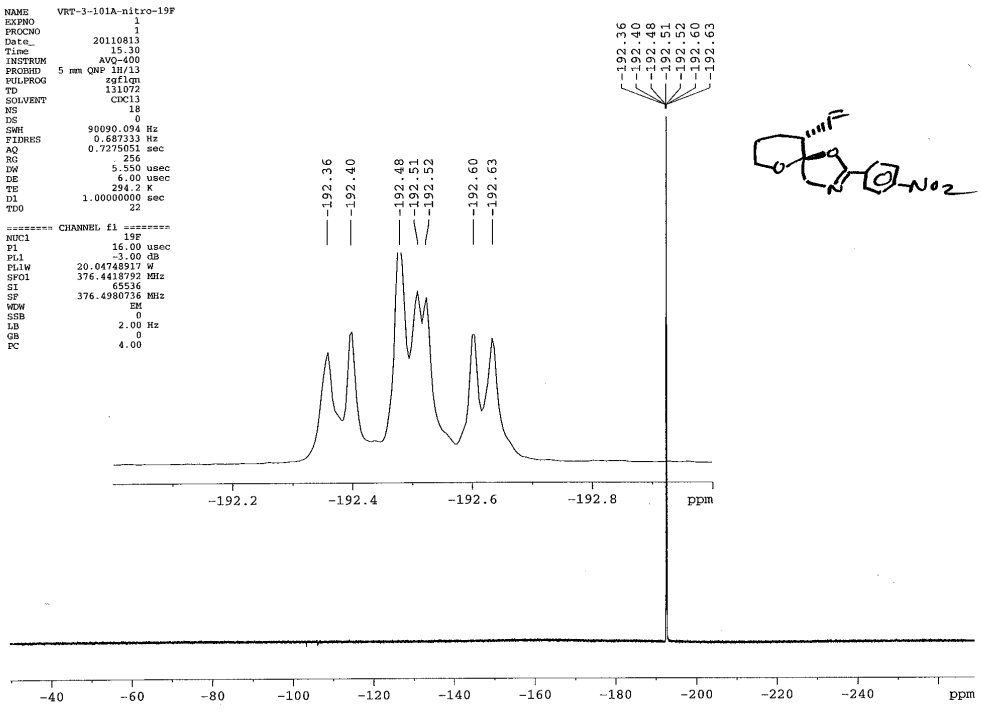

AVQ-400 QNP Proton starting parameters. 7/16/

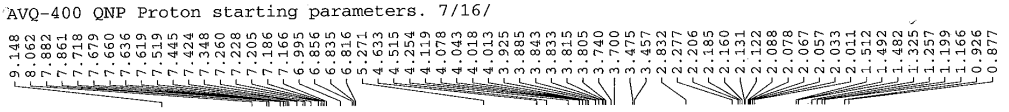


```
NAME        VRT-3-105B-tert-butyl-1H
EXPNO                1
PROCNO               1
Date_         20110813
Time             15.09
INSTRUM        AVQ-400
PROBHD   5 mm QNP 1H/13
PULPROG            zg30
TD                65536
SOLVENT           CDCl3
NS                   24
DS                    0
SWH           8012.820 Hz
FIDRES        0.122266 Hz
AQ            4.0895586 sec
RG                 40.3
DW               62.400 usec
DE                6.00 usec
TE               293.9 K
D1            1.00000000 sec
TD0                  22

======== CHANNEL f1 ========
NUC1                 1H
P1                12.80 usec
PL1                0.00 dB
PL1W         9.54516888 W
SFO1        400.1324700 MHz
SI                65536
SF          400.1300176 MHz
WDW                  EM
SSB                   0
LB                 0.30 Hz
GB                    0
PC                 4.00
```

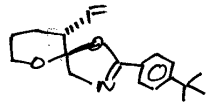

JP Carbon Starting parameters 7/16/03 revised 7

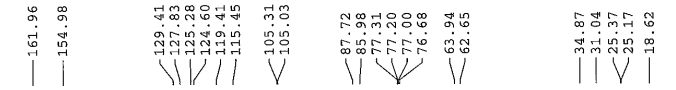


```
NAME        VRT-3-105B-tert-butyl
EXPNO                1
PROCNO               1
Date_         20110813
Time             15.17
INSTRUM        AVQ-400
PROBHD   5 mm QNP 1H/13
PULPROG          zgpg30
TD                65536
SOLVENT           CDCl3
NS                   50
DS                    0
SWH          24038.461 Hz
FIDRES        0.366798 Hz
AQ            1.3632196 sec
RG                16384
DW               20.800 usec
DE                6.00 usec
TE               293.9 K
D1            2.00000000 sec
D11           0.03000000 sec
TD0                 222

======== CHANNEL f1 ========
NUC1                13C
P1                8.50 usec
PL1               -2.00 dB
PL1W        47.77286148 W
SFO1       100.6228298 MHz

======== CHANNEL f2 ========
CPDPRG2         waltz16
NUC2                 1H
PCPD2            70.00 usec
PL2                0.00 dB
PL12              15.00 dB
PL13              17.00 dB
PL2W         9.54516888 W
PL12W        0.30184472 W
PL13W        0.19045115 W
SFO2       400.1316000 MHz
SI                32768
SF         100.6127817 MHz
WDW                  EM
SSB                   0
LB                 1.50 Hz
GB                    0
PC                 1.40
```

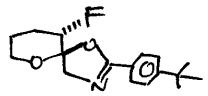

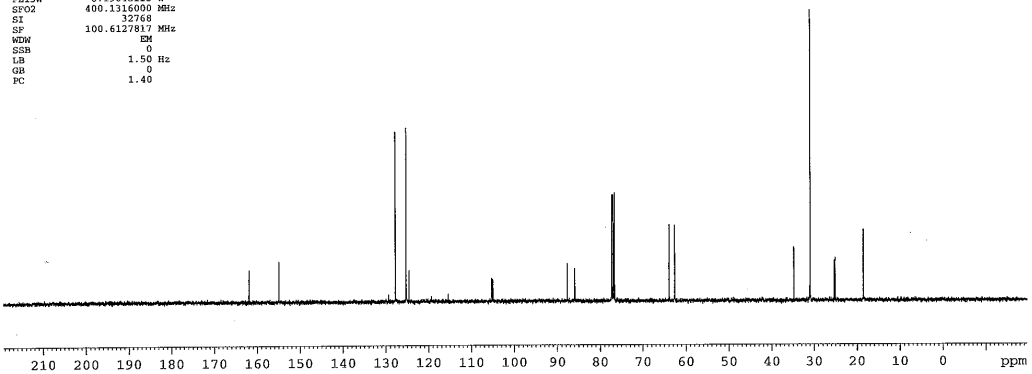

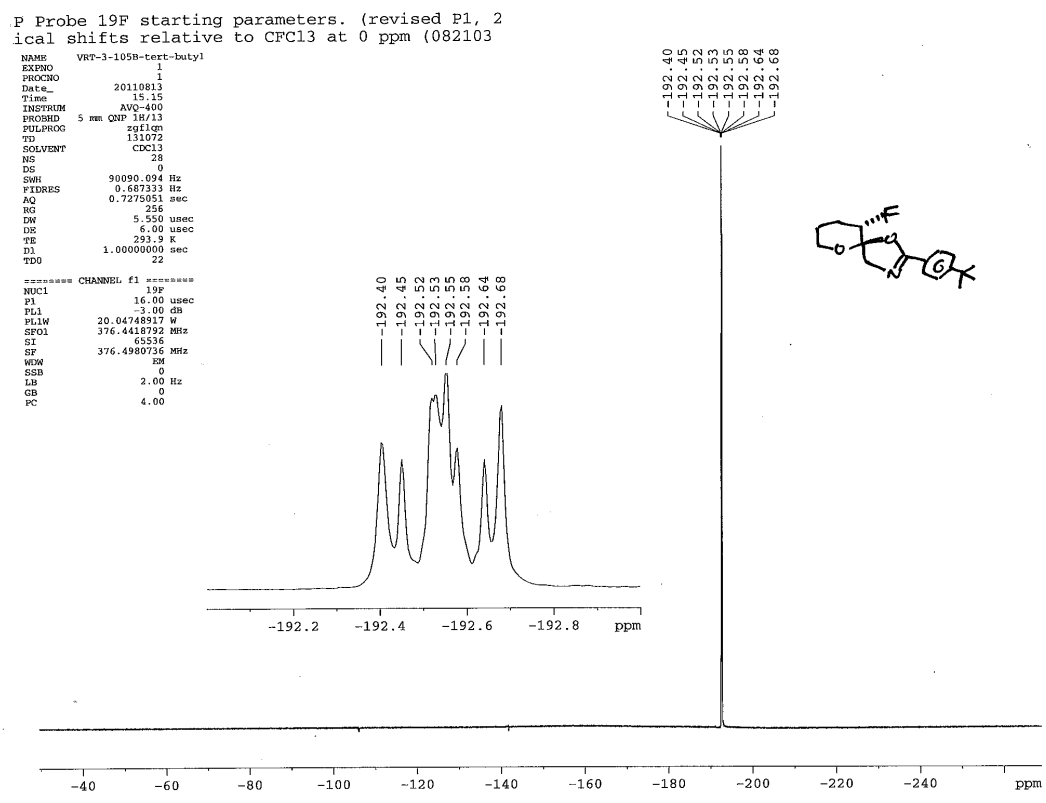
P Probe 19F starting parameters. (revised P1, 2
ical shifts relative to CFC13 at 0 ppm (082103
NAME VRT-3-105B-tert-butyl
EXPNO 1
PROCNO 1
Date_ 20110813
Time 15.15
INSTRUM AVQ-400
PROBHD 5 mm QNP 1H/13
PULPROG zgflqn
TD 131072
SOLVENT CDC13
NS 28
DS 0
SWH 90090.094 Hz
FIDRES 0.687333 Hz
AQ 0.7275051 sec
RG 256
DW 5.550 usec
DE 6.00 usec
TE 293.9 K
D1 1.00000000 sec
TD0 22
======== CHANNEL f1 ========
NUC1 19F
P1 16.00 usec
PL1 -3.00 dB
PL1W 20.04748917 W
SFO1 376.4418792 MHz
SI 65536
SF 376.4980736 MHz
WDW EM
SSB 0
LB 2.00 Hz
GB 0
PC 4.00
-192.40
-192.45
-192.52
-192.53
-192.55
-192.58
-192.64
-192.68
-192.2
-192.4
-192.6
-192.8
ppm
-40
-60
-80
-100
-120
-140
-160
-180
-200
-220
-240
ppm

AVQ-400 QNP Proton starting parameters. 7/16/

8.421 8.047 8.044 8.026 8.023 7.931 7.912 7.884 7.863 7.851 7.574 7.561 7.557 7.543 7.537 7.528 7.525 7.511 7.259 5.281 4.712 4.595 4.205 4.164 4.136 4.108 4.011 3.970 3.901 3.894 3.872 3.861 3.500 3.482 3.465 3.447 2.327 2.296 2.286 2.280 2.256 2.214 2.208 2.177 2.170 2.156 2.147 2.136 2.119 2.101 2.089 2.070 2.058 2.041 1.911 1.573 1.543 1.260 1.226 1.208 1.191 0.885 0.867

```
NAME        VRT-3-2-Naphtyl-adduct-1H
EXPNO                1
PROCNO               1
Date_         20110817
Time             12.12
INSTRUM        AVQ-400
PROBHD   5 mm QNP 1H/13
PULPROG          zg30
TD              65536
SOLVENT          CDCl3
NS                  16
DS                   0
SWH           8012.820 Hz
FIDRES        0.122266 Hz
AQ           4.0895586 sec
RG                90.5
DW              62.400 usec
DE               6.00 usec
TE              293.9 K
D1           1.00000000 sec
TD0                 22

======== CHANNEL f1 ========
NUC1                1H
P1               12.80 usec
PL1               0.00 dB
PL1W        9.54516888 W
SFO1       400.1324700 MHz
SI               65536
SF         400.1300176 MHz
WDW                 EM
SSB                  0
LB               0.30 Hz
GB                   0
PC                4.00
```

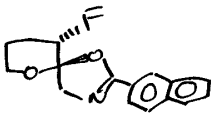

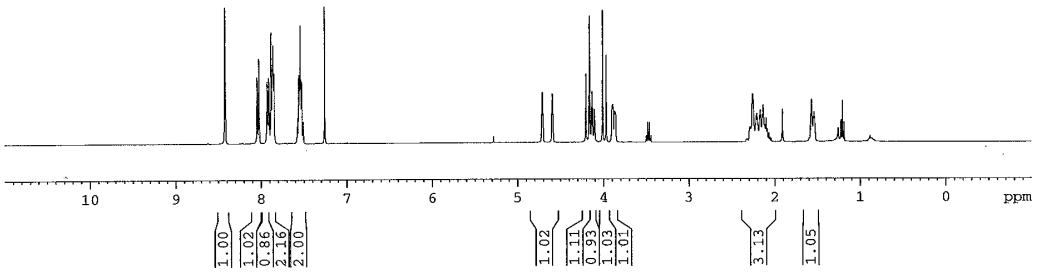

JP Carbon Starting parameters 7/16/03 revised 7

162.11 134.70 132.54 128.77 128.54 128.20 127.77 127.60 126.60 124.80 124.48 105.64 105.36 87.78 86.04 77.31 77.20 76.99 76.68 64.13 62.82 25.45 25.24 18.68 15.22

```
NAME        VRT-3-2-Naphtyl-adduc
EXPNO                1
PROCNO               1
Date_         20110817
Time             12.15
INSTRUM        AVQ-400
PROBHD   5 mm QNP 1H/13
PULPROG         zgpg30
TD              65536
SOLVENT          CDCl3
NS                  59
DS                   0
SWH          24038.461 Hz
FIDRES        0.366798 Hz
AQ           1.3632196 sec
RG               16384
DW              20.800 usec
DE               6.00 usec
TE              293.9 K
D1           2.00000000 sec
D11          0.03000000 sec
TD0                 222

======== CHANNEL f1 ========
NUC1                13C
P1                8.50 usec
PL1              -2.00 dB
PL1W        47.77286148 W
SFO1       100.6228298 MHz

======== CHANNEL f2 ========
CPDPRG2         waltz16
NUC2                1H
PCPD2            70.00 usec
PL2               0.00 dB
PL12             15.00 dB
PL13             17.00 dB
PL2W        9.54516888 W
PL12W       0.30184472 W
PL13W       0.19045115 W
SFO2       400.1316000 MHz
SI               32768
SF         100.6127794 MHz
WDW                 EM
SSB                  0
LB               1.50 Hz
GB                   0
PC                1.40
```

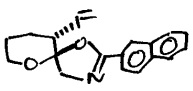

P Probe 19F starting parameters. (revised P1, 2
ical shifts relative to CFCl3 at 0 ppm (082103

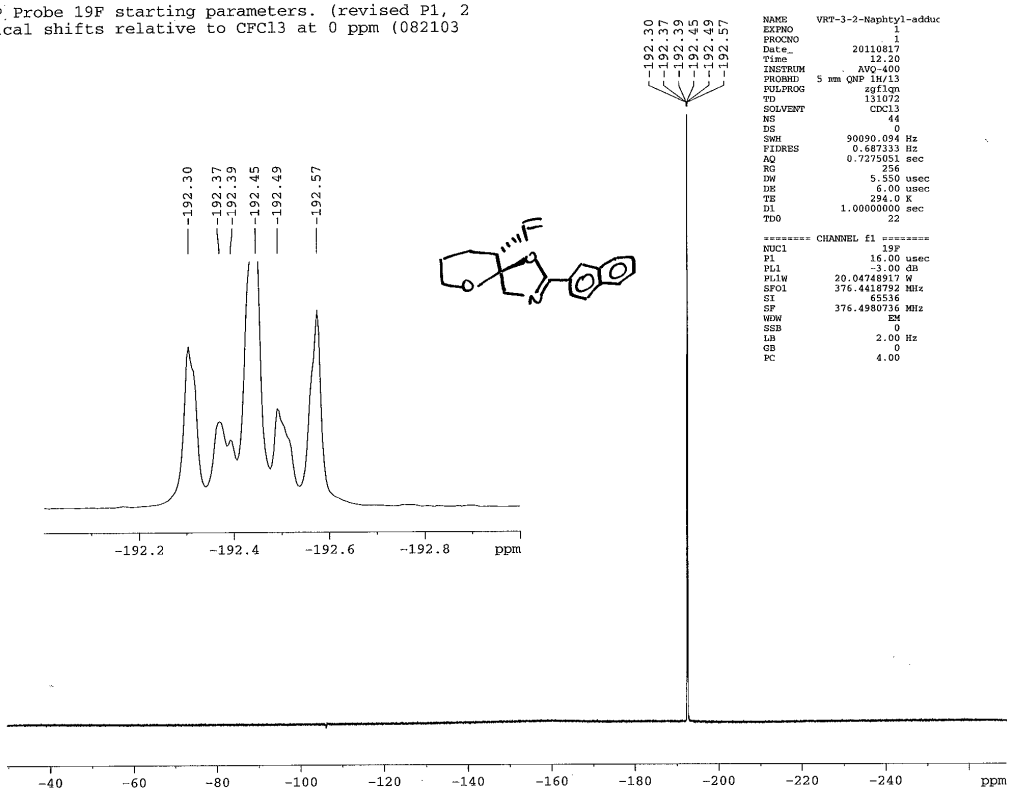

NAME	VRT-3-2-Naphtyl-adduc
EXPNO	1
PROCNO	1
Date_	20110817
Time	12.20
INSTRUM	AVQ-400
PROBHD	5 mm QNP 1H/13
PULPROG	zgflqn
TD	131072
SOLVENT	CDCl3
NS	44
DS	0
SWH	90090.094 Hz
FIDRES	0.687333 Hz
AQ	0.7275051 sec
RG	256
DW	5.550 usec
DE	6.00 usec
TE	294.0 K
D1	1.00000000 sec
TD0	22
========	CHANNEL f1 ========
NUC1	19F
P1	16.00 usec
PL1	-3.00 dB
PL1W	20.04748917 W
SFO1	376.4418792 MHz
SI	65536
SF	376.4980736 MHz
WDW	EM
SSB	0
LB	2.00 Hz
GB	0
PC	4.00

AVQ-400 QNP Proton starting parameters. 7/16/

8.580 8.491 8.372 8.161 7.980 7.260 7.194 7.167 7.155 7.145 5.281 4.736 4.677 4.670 4.664 4.554 4.174 4.132 4.076 4.049 4.022 4.017 3.975 3.933 3.884 3.876 3.858 3.848 3.118 2.974 2.252 2.244 2.236 2.228 2.212 2.205 2.171 2.158 2.153 2.142 2.120 2.100 2.094 2.075 2.064 2.045 2.029 1.811 1.573 1.550 1.543 1.394 1.271 1.242 0.950 0.935 0.918 0.899 0.877 0.861 0.843 0.833 0.072

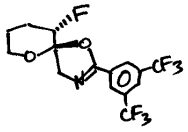

NAME	VRT-3-198B-Flash-1H
EXPNO	1
PROCNO	1
Date_	20110906
Time	16.02
INSTRUM	AVQ-400
PROBHD	5 mm QNP 1H/13
PULPROG	zg30
TD	65536
SOLVENT	CDCl3
NS	14
DS	0
SWH	8012.820 Hz
FIDRES	0.122266 Hz
AQ	4.0895586 sec
RG	16
DW	62.400 usec
DE	6.00 usec
TE	294.2 K
D1	1.00000000 sec
TD0	222

======== CHANNEL f1 ========

NUC1	1H
P1	12.80 usec
PL1	0.00 dB
PL1W	9.54516888 W
SFO1	400.1324700 MHz
SI	65536
SF	400.1300175 MHz
WDW	EM
SSB	0
LB	0.30 Hz
GB	0
PC	4.00

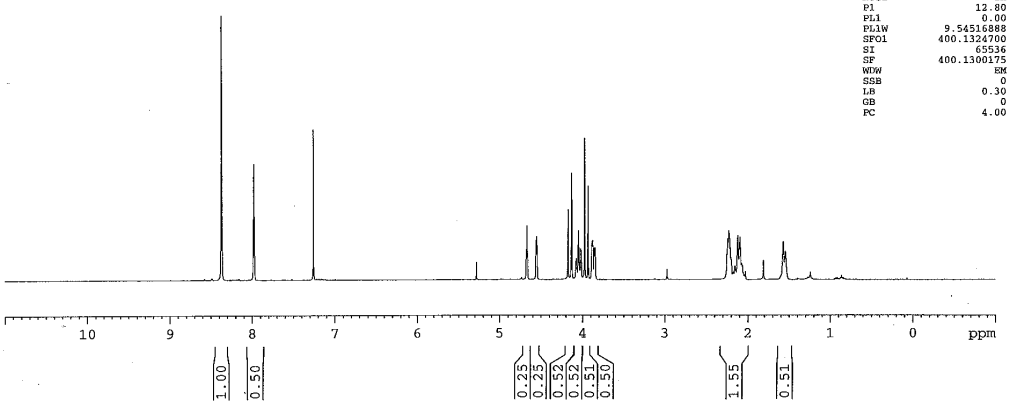

JP Carbon Starting parameters 7/16/03 revised

159.53 132.56 132.22 131.89 131.55 129.82 128.14 126.96 124.83 124.79 124.25 121.54 118.83 106.72 106.44 87.43 85.69 77.31 77.20 76.99 76.68 64.09 63.07 25.35 25.14 18.50

NAME	VRT-3-198B-Flash-13C
EXPNO	1
PROCNO	1
Date_	20110906
Time	16.05
INSTRUM	AVQ-400
PROBHD	5 mm QNP 1H/13
PULPROG	zgpg30
TD	65536
SOLVENT	CDCl3
NS	40
DS	0
SWH	24038.461 Hz
FIDRES	0.366798 Hz
AQ	1.3632196 sec
RG	16384
DW	20.800 usec
DE	6.00 usec
TE	294.3 K
D1	2.00000000 sec
D11	0.03000000 sec
TD0	444

======== CHANNEL f1 ========

NUC1	13C
P1	8.50 usec
PL1	-2.00 dB
PL1W	47.77286148 W
SFO1	100.6228298 MHz

======== CHANNEL f2 ========

CPDPRG2	waltz16
NUC2	1H
PCPD2	70.00 usec
PL2	0.00 dB
PL12	15.00 dB
PL13	17.00 dB
PL2W	9.54516888 W
PL12W	0.30184472 W
PL13W	0.19045115 W
SFO2	400.1316000 MHz
SI	32768
SF	100.6127723 MHz
WDW	EM
SSB	0
LB	1.50 Hz
GB	0
PC	1.40

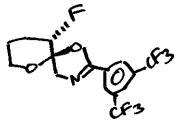

P Probe 19F starting parameters. (revised P1, 2
ical shifts relative to CFC13 at 0 ppm (082103

NAME	VRT-3-198B-Flash-19F
EXPNO	1
PROCNO	1
Date_	20110906
Time	15.59
INSTRUM	AVQ-400
PROBHD	5 mm QNP 1H/13
PULPROG	zgflqn
TD	131072
SOLVENT	CDC13
NS	62
DS	0
SWH	90090.094 Hz
FIDRES	0.687333 Hz
AQ	0.7275051 sec
RG	256
DW	5.550 usec
DE	6.00 usec
TE	294.2 K
D1	1.00000000 sec
TD0	222
======== CHANNEL f1 ========	
NUC1	19F
P1	16.00 usec
PL1	-3.00 dB
PL1W	20.04748917 W
SFO1	376.4418792 MHz
SI	65536
SF	376.4980736 MHz
WDW	EM
SSB	0
LB	2.00 Hz
GB	0
PC	4.00

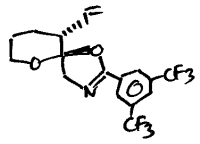

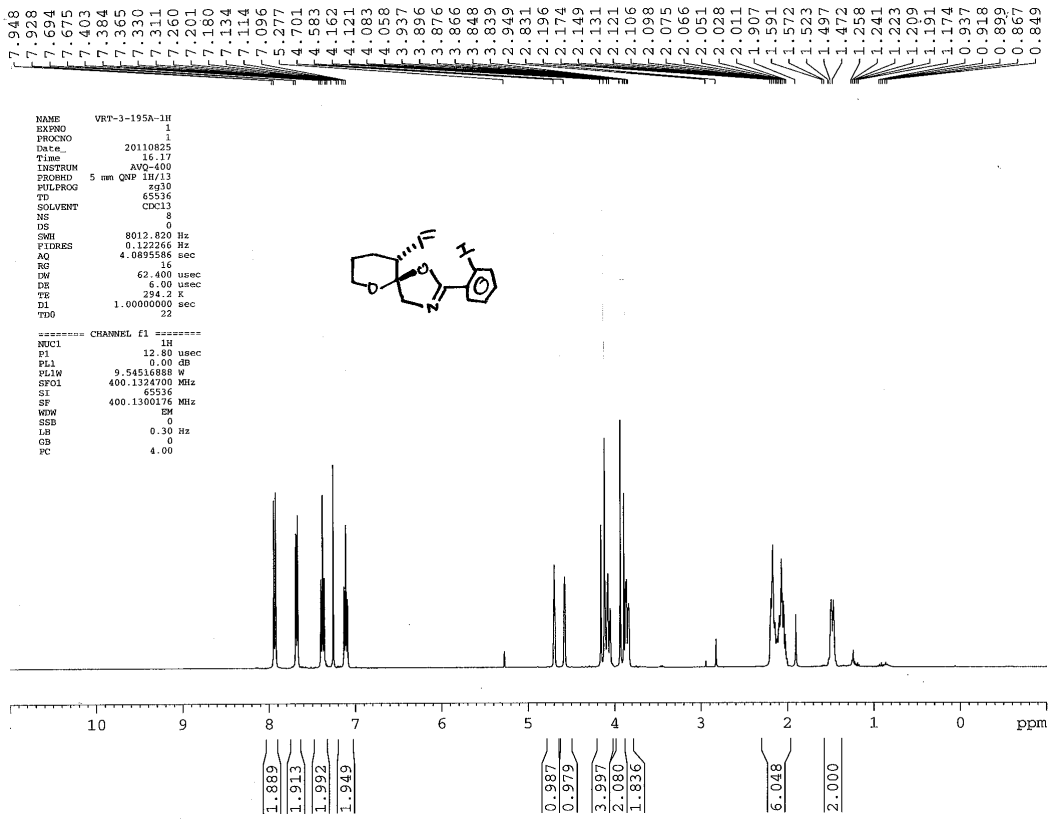
7.948 7.928 7.694 7.675 7.403 7.384 7.365 7.330 7.311 7.260 7.201 7.180 7.134 7.114 7.096 5.277 4.701 4.583 4.162 4.121 4.083 4.058 3.937 3.896 3.876 3.866 3.848 3.839 2.949 2.831 2.196 2.174 2.149 2.131 2.121 2.106 2.098 2.075 2.066 2.051 2.028 2.011 1.907 1.591 1.572 1.523 1.497 1.472 1.258 1.241 1.223 1.209 1.191 1.174 0.937 0.918 0.899 0.867 0.849
NAME VRT-3-195A-1H
EXPNO 1
PROCNO 1
Date_ 20110825
Time 16.17
INSTRUM AVQ-400
PROBHD 5 mm QNP 1H/13
PULPROG zg30
TD 65536
SOLVENT CDCl3
NS 8
DS 0
SWH 8012.820 Hz
FIDRES 0.122266 Hz
AQ 4.0895586 sec
RG 16
DW 62.400 usec
DE 6.00 usec
TE 294.2 K
D1 1.00000000 sec
TD0 22
======== CHANNEL f1 ========
NUC1 1H
P1 12.80 usec
PL1 0.00 dB
PL1W 9.54516888 W
SFO1 400.1324700 MHz
SI 65536
SF 400.1300176 MHz
WDW EM
SSB 0
LB 0.30 Hz
GB 0
PC 4.00
10 9 8 7 6 5 4 3 2 1 0 ppm
1.889 1.913 1.992 1.949 0.987 0.979 3.997 2.080 1.836 6.048 2.000
NAME VRT-3-195A-13C
EXPNO 1
PROCNO 1
Date_ 20110825
Time 16.18
INSTRUM AVQ-400
PROBHD 5 mm QNP 1H/13
PULPROG zgpg30
TD 65536
SOLVENT CDCl3
NS 36
DS 0
SWH 24038.461 Hz
FIDRES 0.366798 Hz
AQ 1.3632196 sec
RG 16384
DW 20.800 usec
DE 6.00 usec
TE 294.2 K
D1 2.00000000 sec
D11 0.03000000 sec
TD0 222
======== CHANNEL f1 ========
NUC1 13C
P1 8.50 usec
PL1 -2.00 dB
PL1W 47.77286148 W
SFO1 100.6228298 MHz
======== CHANNEL f2 ========
CPDPRG2 waltz16
NUC2 1H
PCPD2 70.00 usec
PL2 0.00 dB
PL12 15.00 dB
PL13 17.00 dB
PL2W 9.54516888 W
PL12W 0.30184472 W
PL13W 0.19045115 W
SFO2 400.1316000 MHz
SI 32768
SF 100.6127821 MHz
WDW EM
SSB 0
LB 1.50 Hz
GB 0
PC 1.40
162.03 140.58 133.01 131.80 131.10 127.81 106.16 105.88 94.03 87.41 85.67 77.31 77.20 77.00 76.68 64.10 63.13 25.15 24.95 18.44
210 200 190 180 170 160 150 140 130 120 110 100 90 80 70 60 50 40 30 20 10 ppm

P Probe 19F starting parameters. (revised P1, 2
ical shifts relative to CFCl3 at 0 ppm (082103

NAME	VRT-3-195A-19F
EXPNO	1
PROCNO	1
Date_	20110825
Time	16.15
INSTRUM	AVQ-400
PROBHD	5 mm QNP 1H/13
PULPROG	zgflqn
TD	131072
SOLVENT	CDCl3
NS	14
DS	0
SWH	90090.094 Hz
FIDRES	0.687333 Hz
AQ	0.7275051 sec
RG	256
DW	5.550 usec
DE	6.00 usec
TE	294.2 K
D1	1.00000000 sec
TD0	22
======== CHANNEL f1 ========	
NUC1	19F
P1	16.00 usec
PL1	-3.00 dB
PL1W	20.04748917 W
SFO1	376.4418792 MHz
SI	65536
SF	376.4980736 MHz
WDW	EM
SSB	0
LB	2.00 Hz
GB	0
PC	4.00

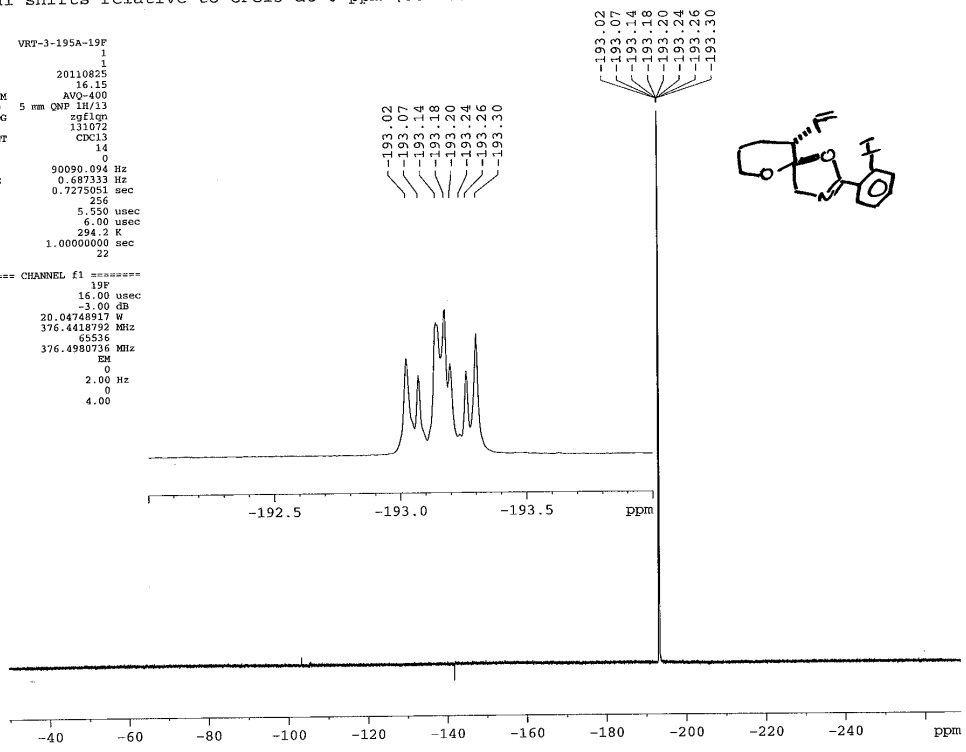

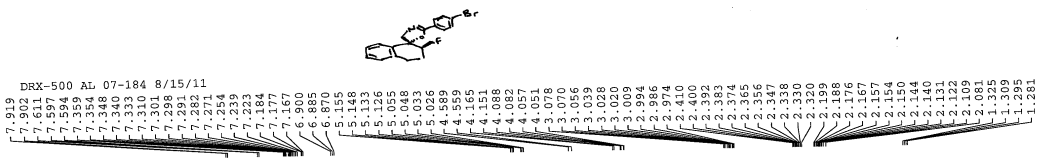
DRX-500 AL 07-184 8/15/11
7.919
7.902
7.611
7.597
7.594
7.359
7.354
7.348
7.340
7.313
7.310
7.301
7.298
7.291
7.282
7.271
7.254
7.239
7.223
7.184
7.177
7.167
6.900
6.885
6.870
5.155
5.148
5.133
5.126
5.055
5.048
5.033
5.026
4.589
4.559
4.165
4.151
4.088
4.082
4.057
4.051
4.078
4.070
4.056
3.039
3.028
3.020
3.009
2.994
2.986
2.974
2.410
2.400
2.392
2.383
2.374
2.365
2.356
2.347
2.338
2.330
2.320
2.199
2.188
2.176
2.167
2.157
2.154
2.150
2.144
2.140
2.131
2.122
2.109
2.081
1.325
1.309
1.295
1.281

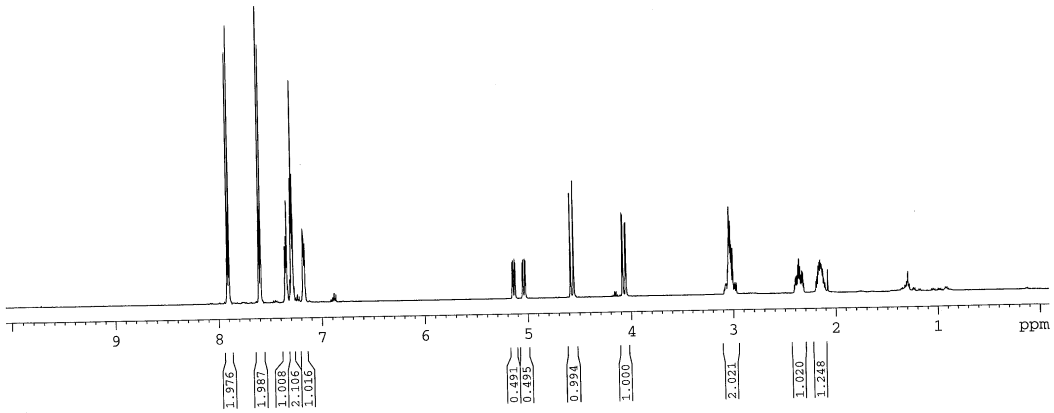
9
8
7
6
5
4
3
2
1
ppm
1.976
1.987
1.008
2.106
1.016
0.491
0.495
0.994
1.000
2.021
1.020
1.248

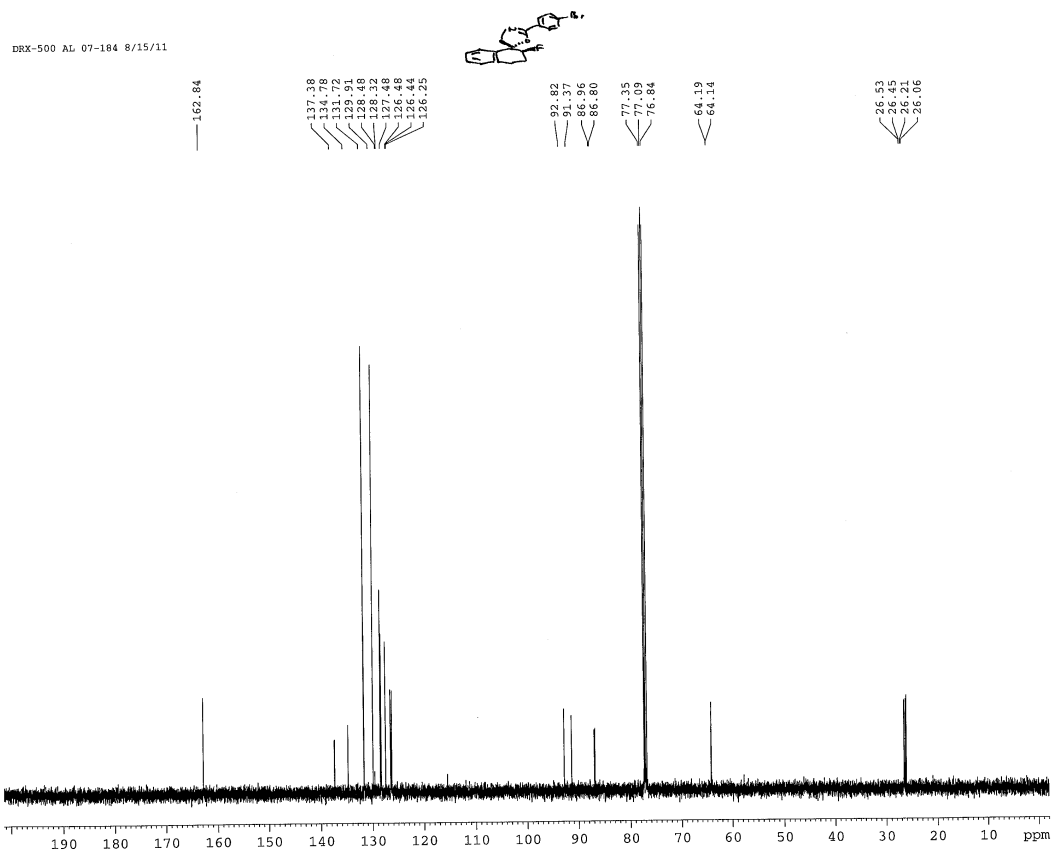
DRX-500 AL 07-184 8/15/11
162.84
137.38
134.78
131.72
129.91
128.48
128.32
127.48
126.48
126.44
126.25
92.82
91.37
86.96
86.80
77.35
77.09
76.84
64.19
64.14
26.53
26.45
26.21
26.06
190
180
170
160
150
140
130
120
110
100
90
80
70
60
50
40
30
20
10
ppm

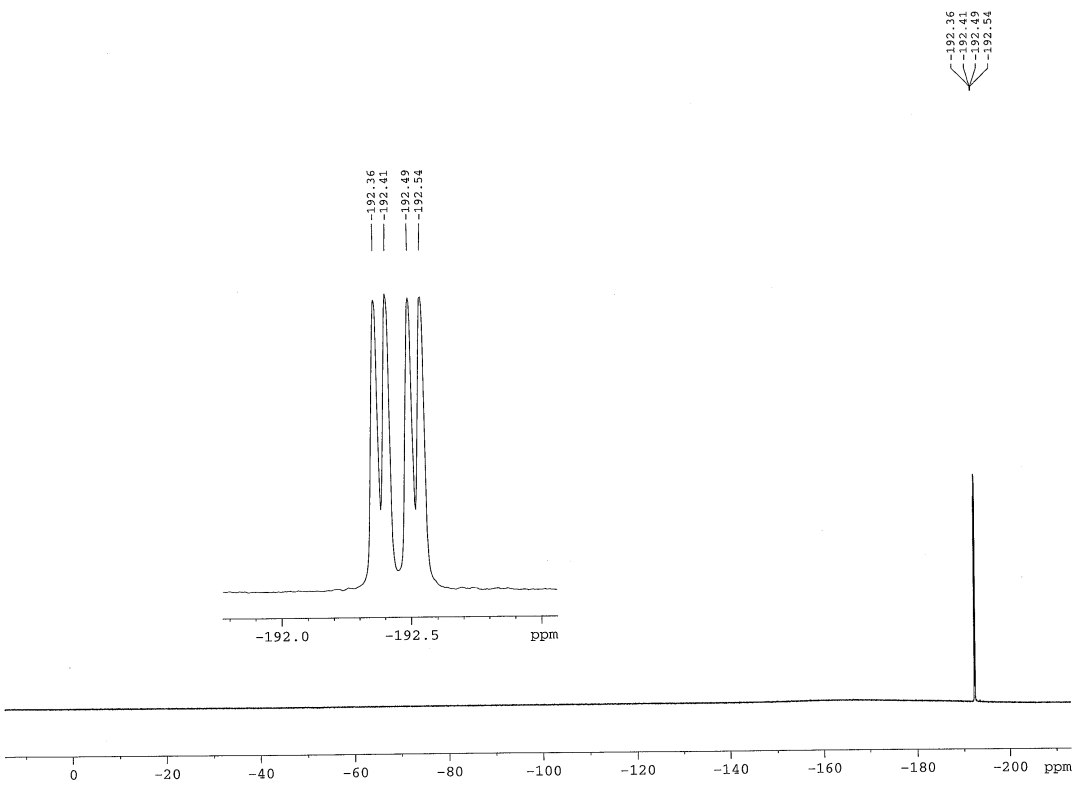
AVQ-400 AL 07-184 19F in CDCl3 8/15/11
-192.36
-192.41
-192.49
-192.54
-192.36
-192.41
-192.49
-192.54
-192.0
-192.5
ppm
0
-20
-40
-60
-80
-100
-120
-140
-160
-180
-200
ppm

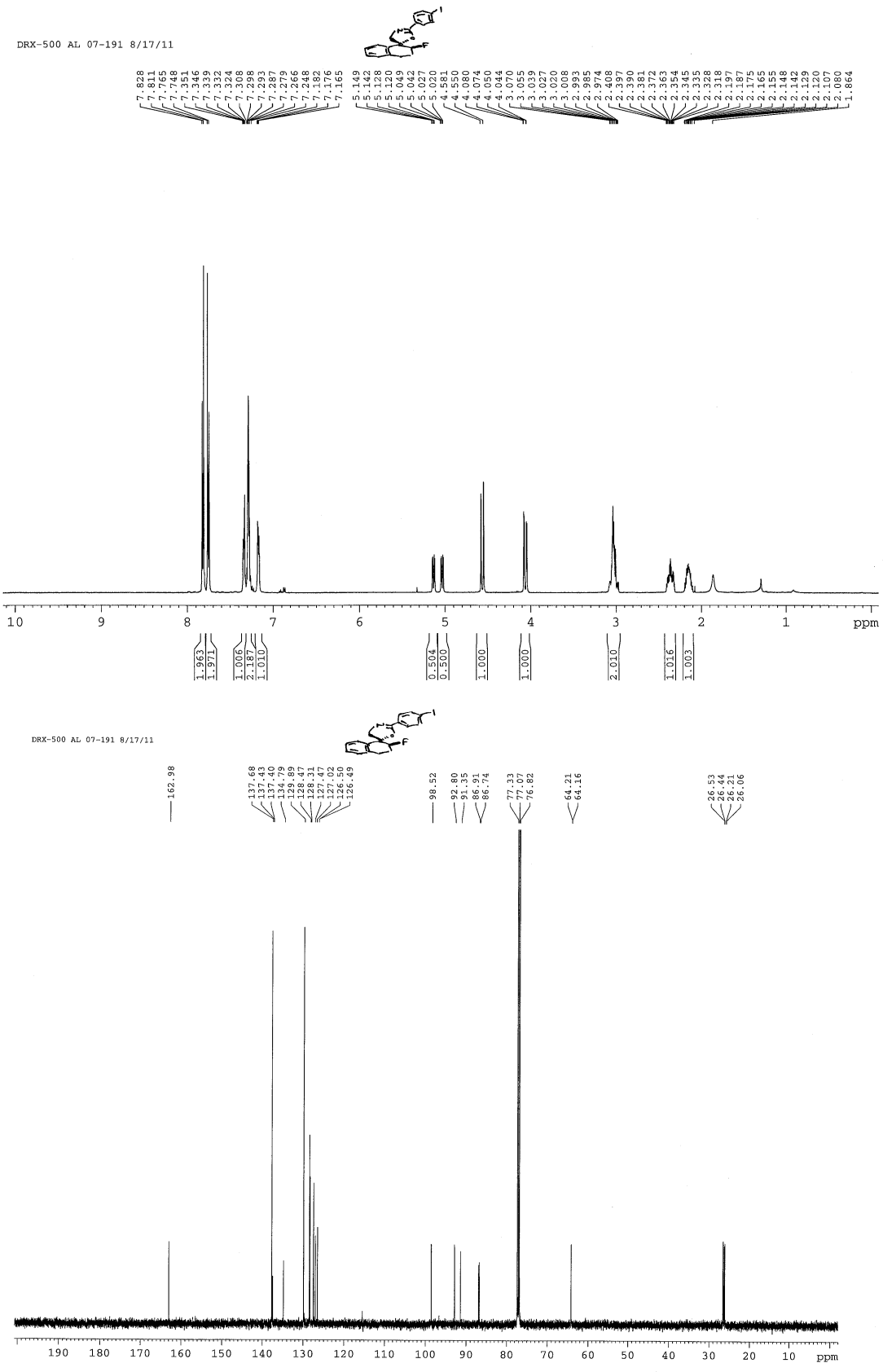
DRX-500 AL 07-191 8/17/11
7.828
7.811
7.765
7.748
7.351
7.346
7.339
7.332
7.324
7.308
7.298
7.293
7.287
7.279
7.266
7.248
7.182
7.176
7.165
5.149
5.142
5.128
5.120
5.049
5.042
5.027
5.020
4.581
4.550
4.080
4.074
4.050
4.044
3.070
3.055
3.039
3.027
3.020
3.008
2.993
2.985
2.974
2.408
2.397
2.390
2.381
2.372
2.363
2.354
2.345
2.335
2.328
2.318
2.197
2.187
2.175
2.165
2.155
2.148
2.142
2.129
2.120
2.107
2.080
1.864
10
9
8
7
6
5
4
3
2
1
ppm
1.963
1.971
1.006
2.187
1.010
0.504
0.500
1.000
1.000
2.010
1.016
1.003
DRX-500 AL 07-191 8/17/11
162.98
137.68
137.43
137.40
134.79
134.69
128.47
128.31
127.47
127.02
126.50
126.49
98.52
92.80
91.35
86.91
86.74
77.33
77.07
76.82
64.21
64.16
26.53
26.44
26.21
26.06
190
180
170
160
150
140
130
120
110
100
90
80
70
60
50
40
30
20
10
ppm

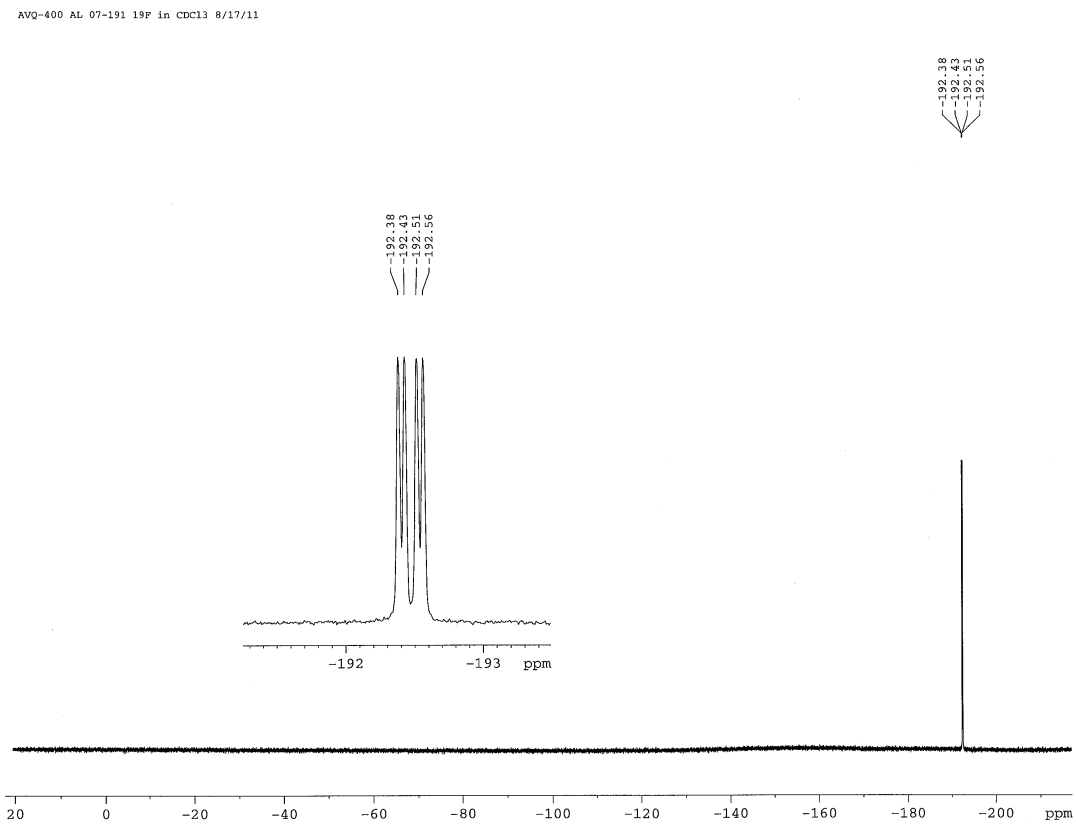
AVQ-400 AL 07-191 19F in CDCl3 8/17/11
-192.38
-192.43
-192.51
-192.56
-192.38
-192.43
-192.51
-192.56
-192
-193
ppm
20
0
-20
-40
-60
-80
-100
-120
-140
-160
-180
-200
ppm

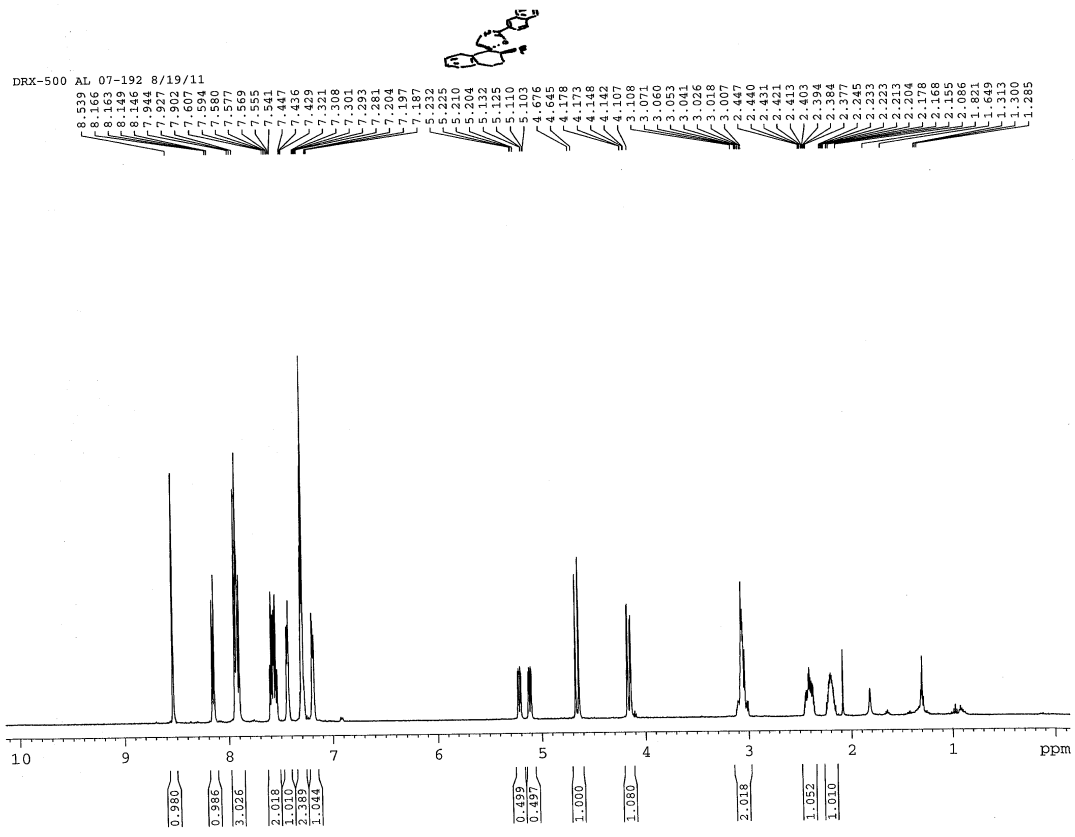
DRX-500 AL 07-192 8/19/11
8.539
8.166
8.163
8.149
8.146
7.944
7.927
7.902
7.607
7.594
7.580
7.577
7.569
7.555
7.541
7.447
7.436
7.429
7.321
7.308
7.301
7.293
7.281
7.204
7.197
7.187
5.232
5.225
5.210
5.204
5.132
5.125
5.110
5.103
4.676
4.645
4.173
4.148
4.142
4.107
3.108
3.071
3.060
3.053
3.041
3.026
3.018
3.007
2.447
2.440
2.431
2.421
2.413
2.403
2.394
2.384
2.377
2.245
2.233
2.223
2.213
2.204
2.178
2.168
2.155
2.086
1.821
1.649
1.313
1.300
1.285
10
9
8
7
6
5
4
3
2
1
ppm
0.980
0.986
3.026
2.018
1.010
2.389
1.044
0.499
0.497
1.000
1.080
2.018
1.052
1.010

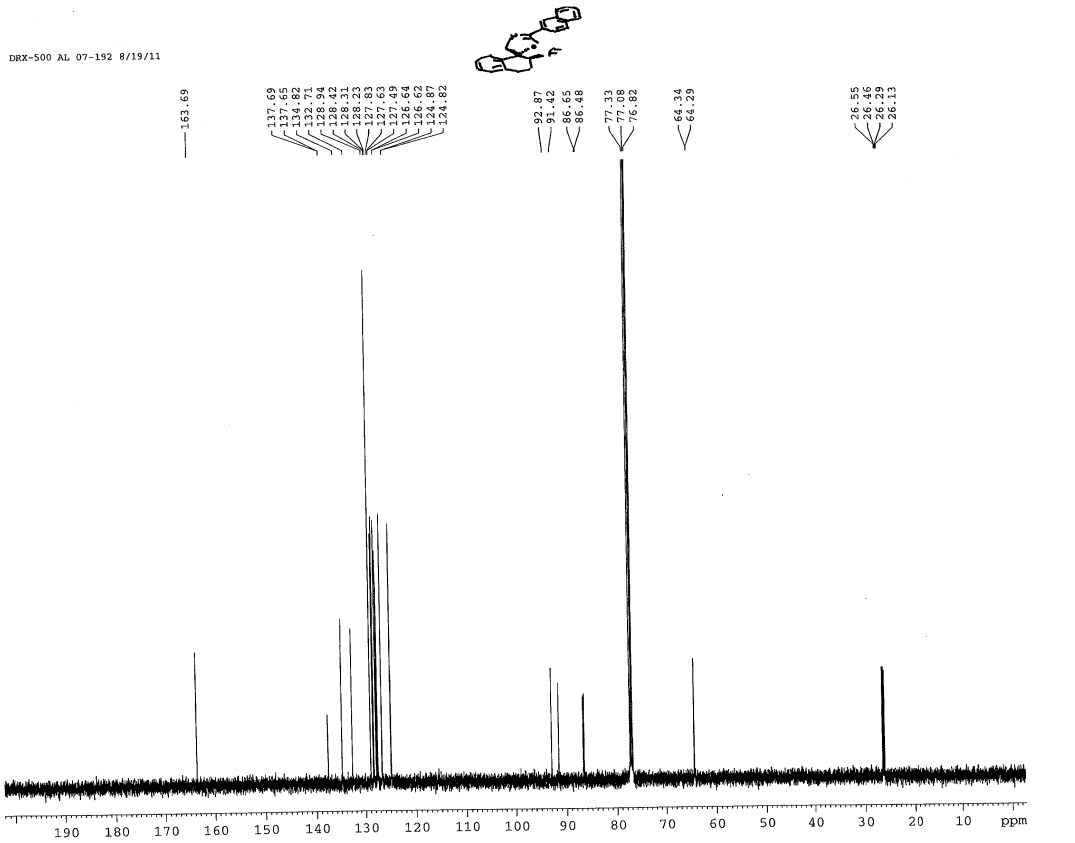
DRX-500 AL 07-192 8/19/11
163.69
137.69
137.65
134.82
132.71
128.94
128.42
128.31
128.23
127.83
127.63
127.49
126.64
126.62
124.87
124.82
92.87
91.42
86.65
86.48
77.33
77.08
76.82
64.34
64.29
26.55
26.46
26.29
26.13
190
180
170
160
150
140
130
120
110
100
90
80
70
60
50
40
30
20
10
ppm

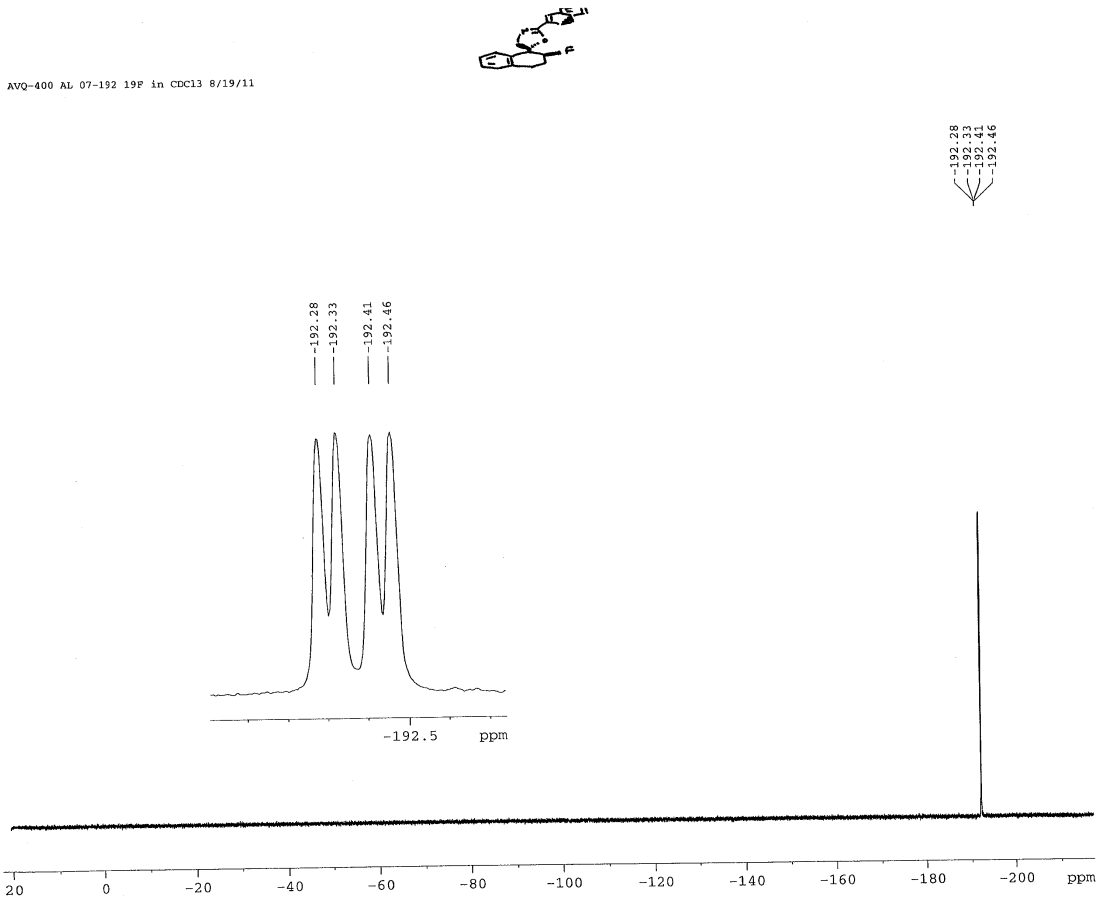
AVQ-400 AL 07-192 19F in CDCl3 8/19/11
-192.28
-192.33
-192.41
-192.46
-192.28
-192.33
-192.41
-192.46
-192.5
ppm
20
0
-20
-40
-60
-80
-100
-120
-140
-160
-180
-200
ppm

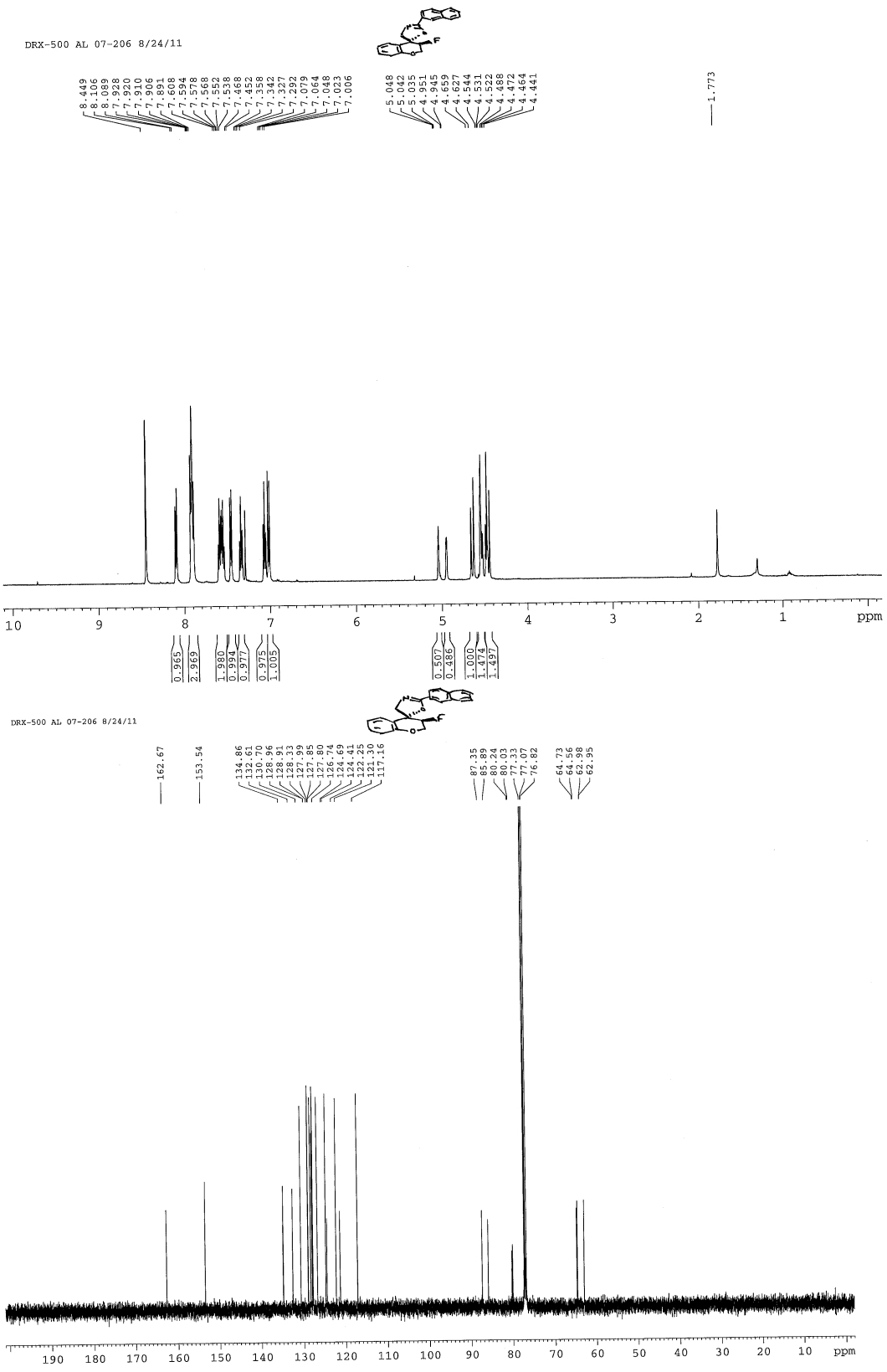
DRX-500 AL 07-206 8/24/11
8.449
8.106
8.098
7.928
7.920
7.910
7.906
7.891
7.608
7.594
7.578
7.568
7.552
7.538
7.468
7.452
7.358
7.342
7.327
7.292
7.079
7.064
7.048
7.023
7.006
5.048
5.042
5.035
4.951
4.945
4.659
4.627
4.544
4.531
4.522
4.488
4.472
4.464
4.441
1.773
10
9
8
7
6
5
4
3
2
1
ppm
0.965
2.969
1.980
0.994
0.977
0.975
1.005
0.507
0.486
1.000
1.774
1.497
DRX-500 AL 07-206 8/24/11
162.67
153.54
134.86
132.61
130.70
128.96
128.91
128.33
127.99
127.85
127.80
126.74
124.69
124.41
122.25
121.30
117.16
87.35
85.89
80.24
80.03
77.33
77.07
76.82
64.73
64.56
62.98
62.95
190
180
170
160
150
140
130
120
110
100
90
80
70
60
50
40
30
20
10
ppm

AVQ-400 AL 07-206 19F in CDCl3 8/24/11

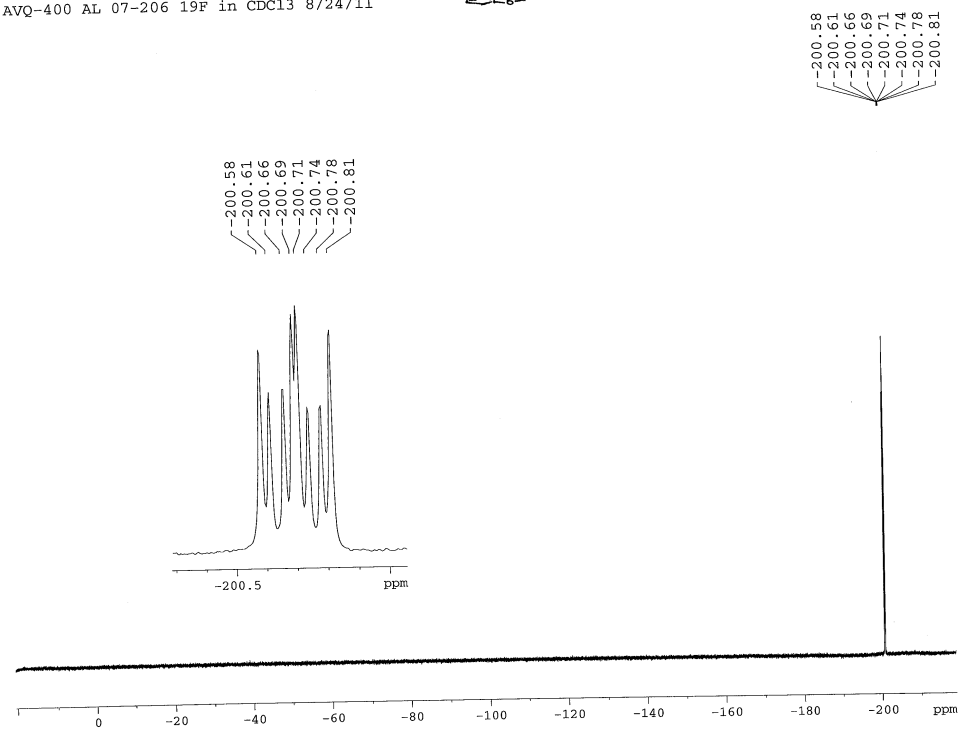

AVQ-400 QNP Proton starting parameters. 7/16/

```
NAME          VRT-3-189-Chiral-1
EXPNO                  1
PROCNO                 1
Date_           20110821
Time              10.11
INSTRUM          AVQ-400
PROBHD   5 mm QNP 1H/13
PULPROG             zg30
TD                 65536
SOLVENT            CDCl3
NS                    18
DS                     0
SWH            8012.820 Hz
FIDRES            0.122266 Hz
AQ             4.0895586 sec
RG                 456.1
DW                62.400 usec
DE                 6.00 usec
TE                293.7 K
D1             1.00000000 sec
TD0                   22

======== CHANNEL f1 ========
NUC1                  1H
P1                 12.80 usec
PL1                0.00 dB
PL1W          9.54516888 W
SFO1        400.1324700 MHz
SI                 65536
SF          400.1300180 MHz
WDW                   EM
SSB                    0
LB                 0.30 Hz
GB                     0
PC                 4.00
```

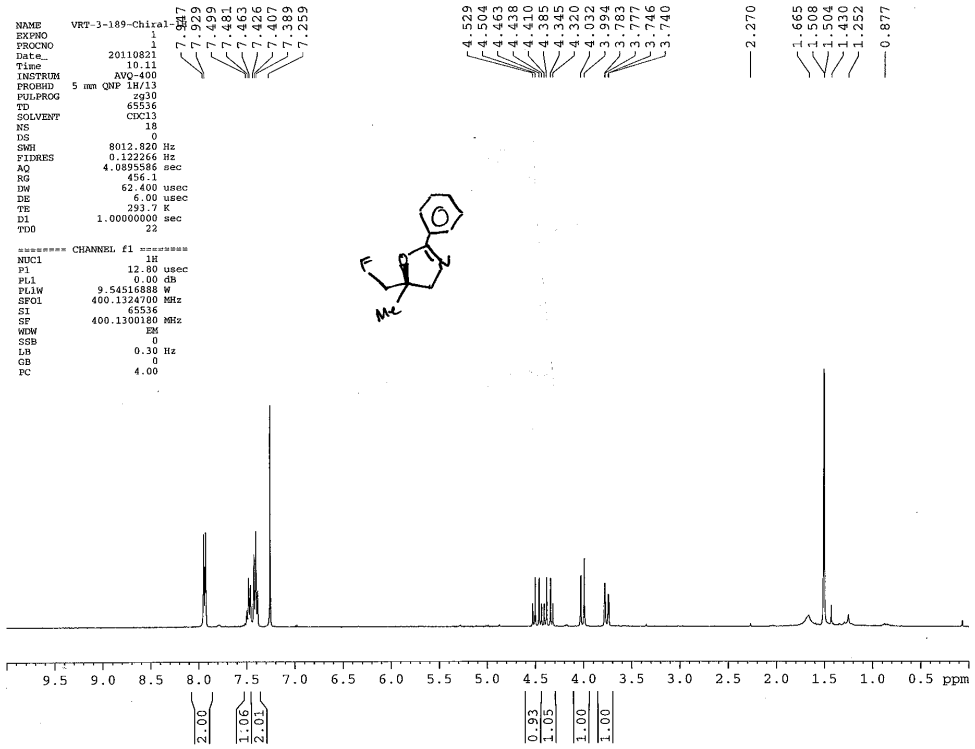

QP Carbon Starting parameters 7/16/03 revised 7

```
NAME          VRT-3-189-Carbon
EXPNO                  1
PROCNO                 1
Date_           20110820
Time              20.53
INSTRUM          AVQ-400
PROBHD   5 mm QNP 1H/13
PULPROG           zgpg30
TD                 65536
SOLVENT            CDCl3
NS                    34
DS                     0
SWH           24038.461 Hz
FIDRES            0.366798 Hz
AQ             1.3632196 sec
RG                 16384
DW                20.800 usec
DE                 6.00 usec
TE                293.5 K
D1             2.00000000 sec
D11            0.03000000 sec
TD0                  222

======== CHANNEL f1 ========
NUC1                  13C
P1                 8.50 usec
PL1               -2.00 dB
PL1W          47.77286148 W
SFO1        100.6228298 MHz

======== CHANNEL f2 ========
CPDPRG2           waltz16
NUC2                  1H
PCPD2              70.00 usec
PL2                0.00 dB
PL12              15.00 dB
PL13              17.00 dB
PL2W          9.54516888 W
PL12W         0.30184472 W
PL13W         0.19045115 W
SFO2        400.1316000 MHz
SI                 32768
SF          100.6127769 MHz
WDW                   EM
SSB                    0
LB                 1.50 Hz
GB                     0
PC                 1.40
```

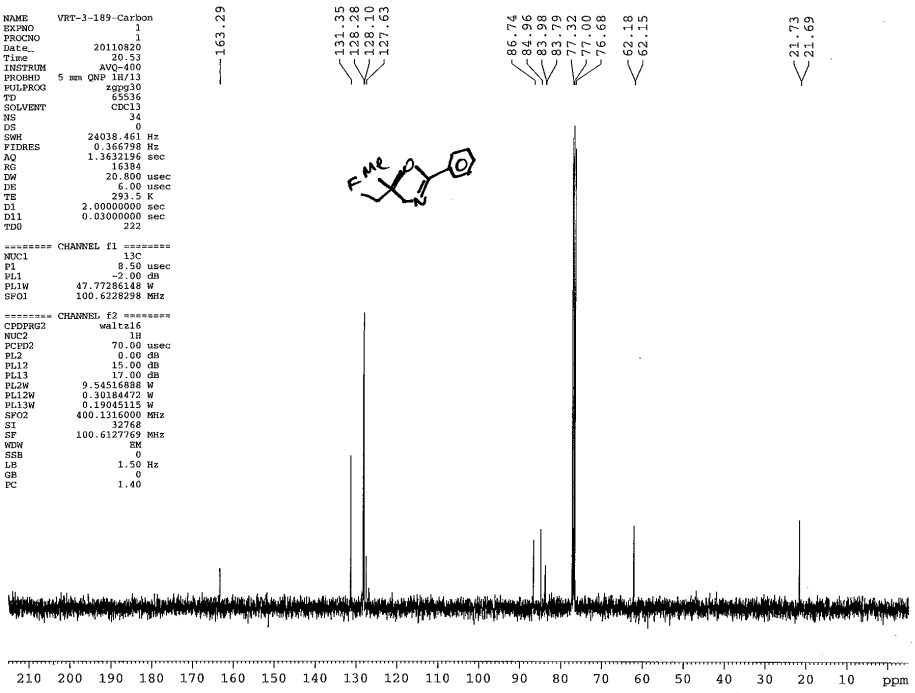

P Probe 19F starting parameters. (revised P1, 2
ical shifts relative to CFCl3 at 0 ppm (082103

```
NAME      VRT-3-189-Chiral-19F
EXPNO                        1
PROCNO                       1
Date_                 20110821
Time                     10.16
INSTRUM                AVQ-400
PROBHD   5 mm QNP 1H/13
PULPROG                 zgflqn
TD                      131072
SOLVENT                  CDCl3
NS                           28
DS                            0
SWH                  90090.094 Hz
FIDRES                0.687333 Hz
AQ                    0.7275051 sec
RG                          256
DW                      5.550 usec
DE                      6.00 usec
TE                      293.6 K
D1                    1.00000000 sec
TD0                         222

======== CHANNEL f1 ========
NUC1                        19F
P1                      16.00 usec
PL1                     -3.00 dB
PL1W                20.04748917 W
SFO1                376.4381143 MHz
SI                        65536
SF                  376.4980736 MHz
WDW                          EM
SSB                           0
LB                      2.00 Hz
GB                            0
PC                      4.00
```

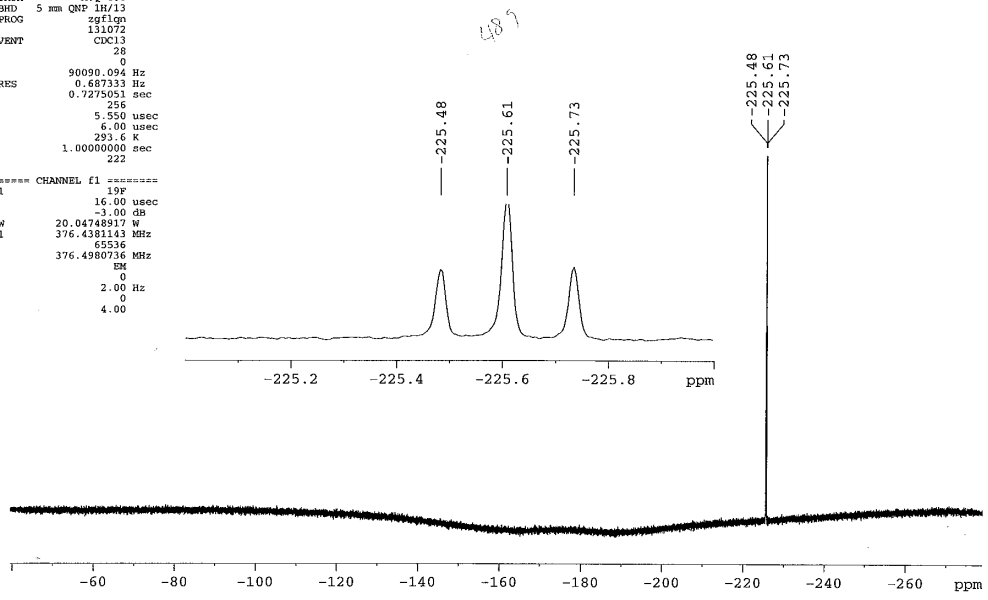

AVQ-400 QNP Proton starting parameters. 7/16/

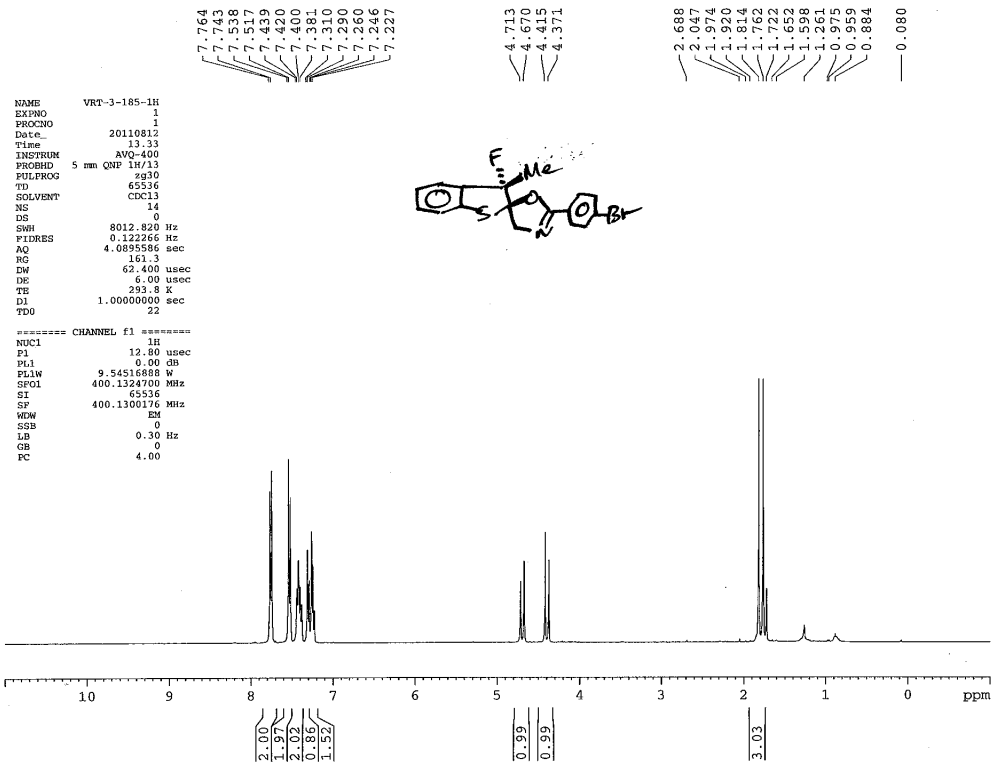

JP Carbon Starting parameters 7/16/03 revised 7

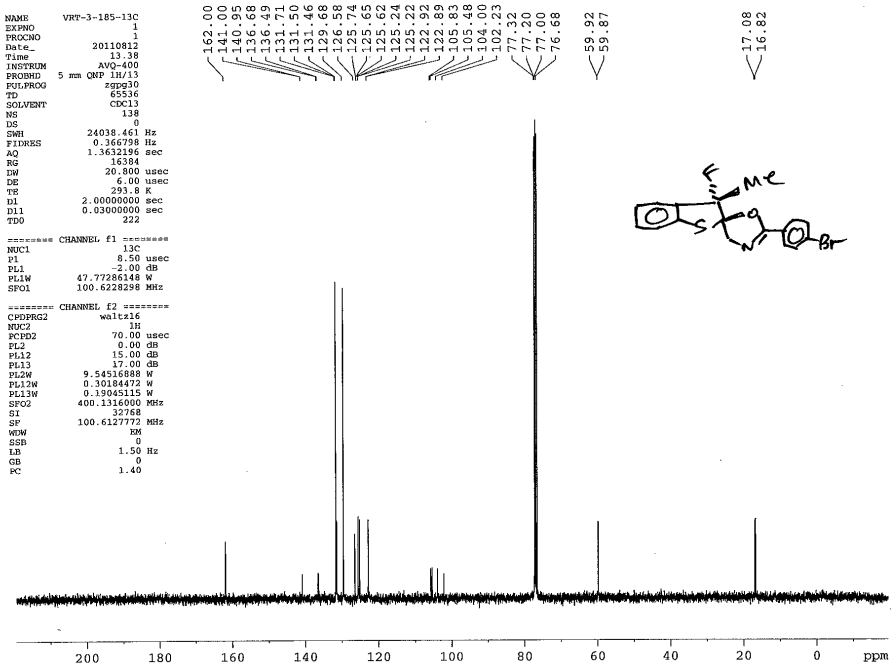

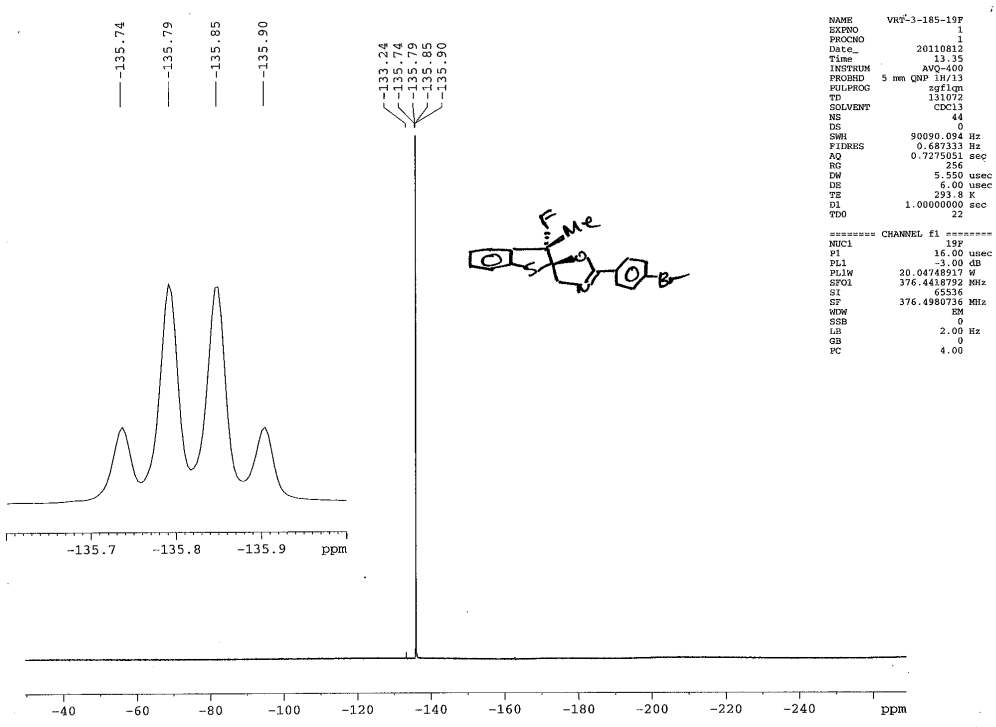

NAME	VRT-3-185-19F
EXPNO	1
PROCNO	1
Date_	20110812
Time	13.35
INSTRUM	AVQ-400
PROBHD	5 mm QNP 1H/13
PULPROG	zgflqn
TD	131072
SOLVENT	CDCl3
NS	44
DS	0
SWH	90090.094 Hz
FIDRES	0.687333 Hz
AQ	0.7275051 sec
RG	256
DW	5.550 usec
DE	6.00 usec
TE	293.8 K
D1	1.00000000 sec
TD0	22
======== CHANNEL f1 ========	
NUC1	19F
P1	16.00 usec
PL1	-3.00 dB
PL1W	20.04748917 W
SFO1	376.4418792 MHz
SI	65536
SF	376.4980736 MHz
WDW	EM
SSB	0
LB	2.00 Hz
GB	0
PC	4.00

HPLC data for fluorocyclization products

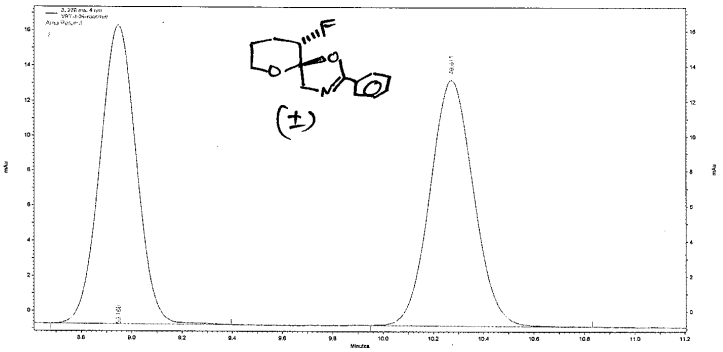

Results

Pk #	Retention Time	Area Percent	Lambda Max
1	8.948	50.189	205
2	10.272	49.811	205

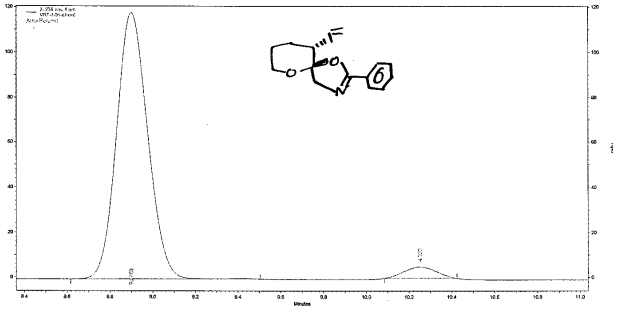

3: 278 nm, 4 nm
Results

Pk #	Retention Time	Area Percent	Lambda Max
1	8.900	95.768	206
2	10.252	4.232	205

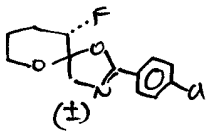

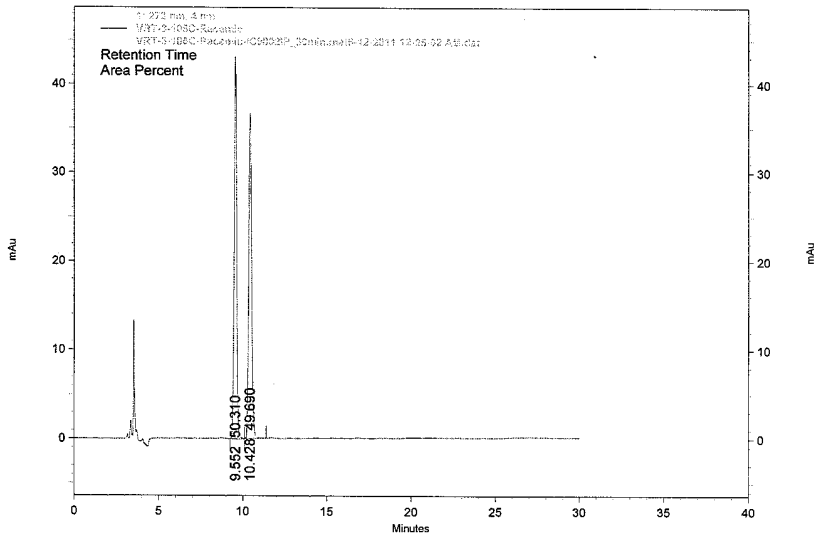

1: 273 nm, 4 nm
Results

Pk #	Retention Time	Area Percent	Lambda Max
1	9.552	50.310	205
2	10.428	49.690	205

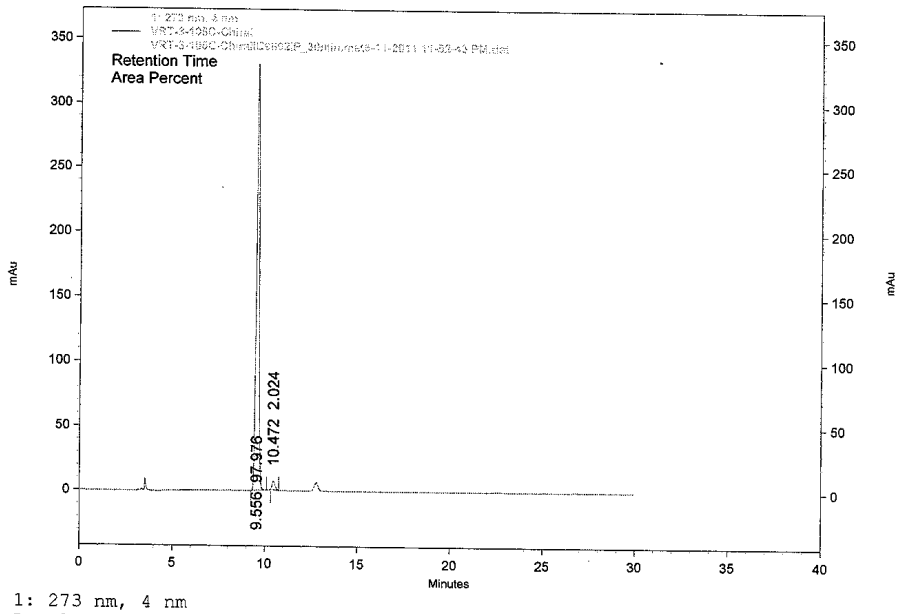

1: 273 nm, 4 nm
Results

Pk #	Retention Time	Area Percent	Lambda Max
1	9.556	97.976	198
2	10.472	2.024	205

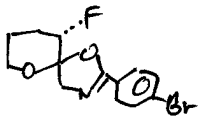

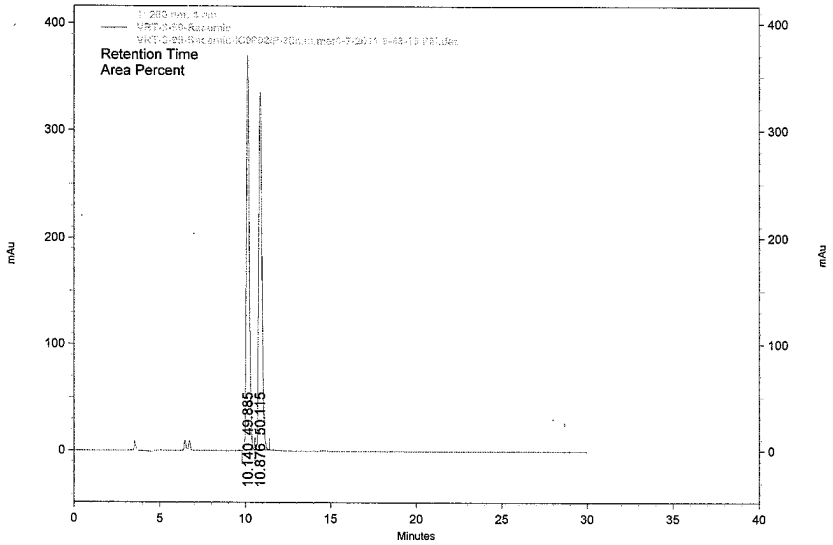

1: 280 nm, 4 nm
Results

Pk #	Retention Time	Area Percent	Lambda Max
1	10.140	49.885	210
2	10.876	50.115	210

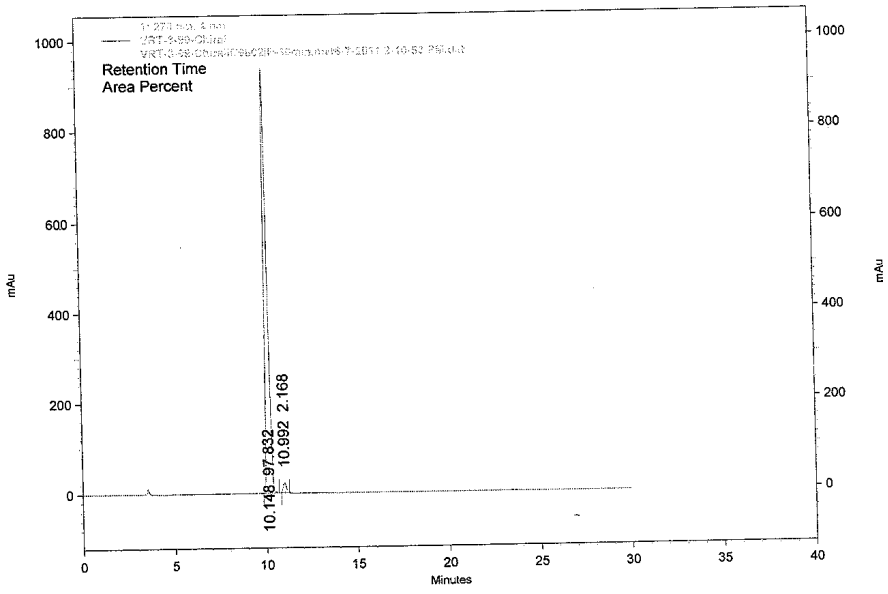

1: 270 nm, 4 nm
Results

Pk #	Retention Time	Area Percent	Lambda Max
1	10.148	97.832	209
2	10.992	2.168	249

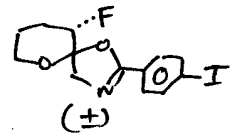

(±)

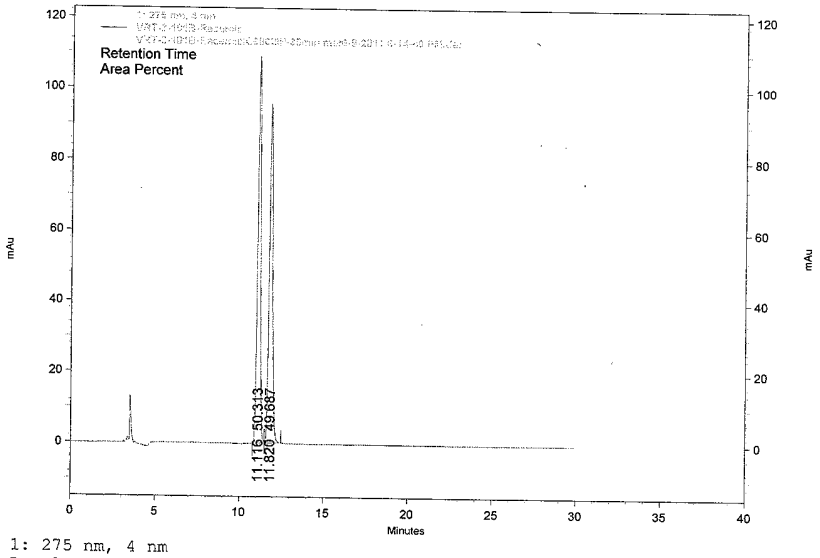

1: 275 nm, 4 nm
Results

Pk #	Retention Time	Area Percent	Lambda Max
1	11.116	50.313	258
2	11.820	49.687	258

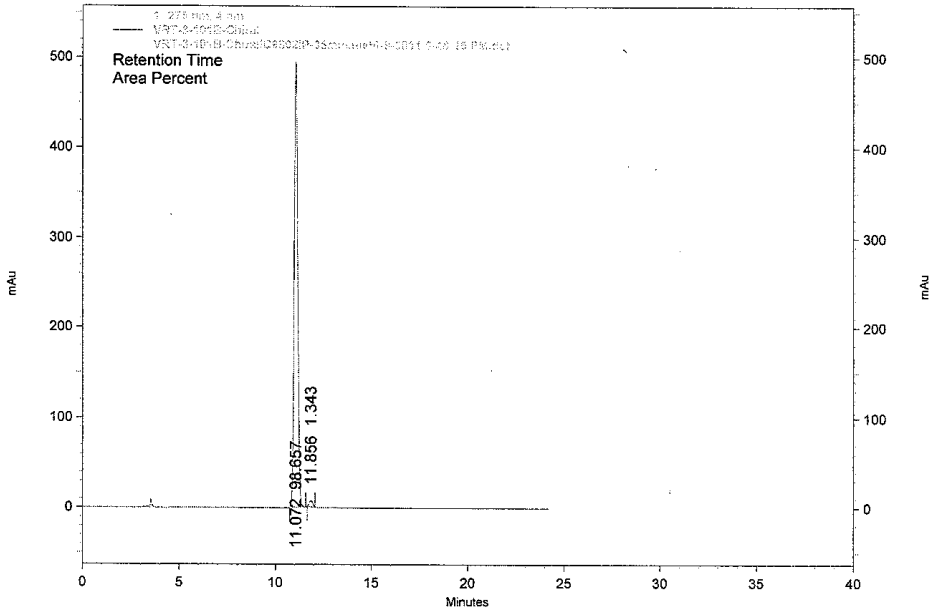

1: 275 nm, 4 nm
Results

Pk #	Retention Time	Area Percent	Lambda Max
1	11.072	98.657	191
2	11.856	1.343	258

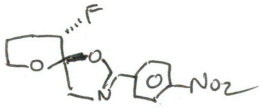

C:\EZStart\Projects\Default\Data\glh\VRT-152G_IA995005Et_50min.met3-18-2010 10-51-12 PM.dat

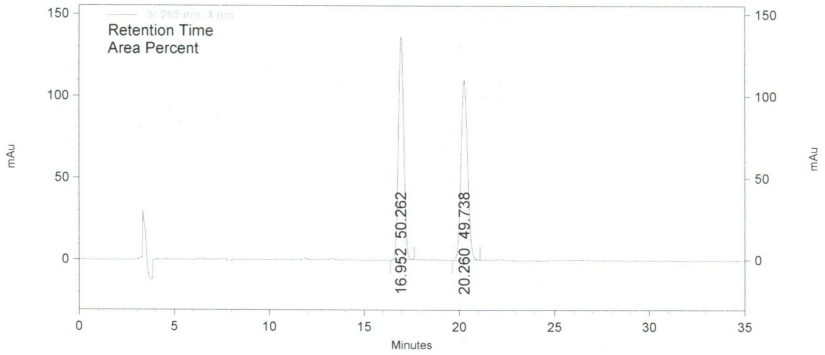

3: 265 nm, 4 nm

Results

Pk #	Retention Time	Area Percent	Lambda Max
1	16.952	50.262	276
2	20.260	49.738	276

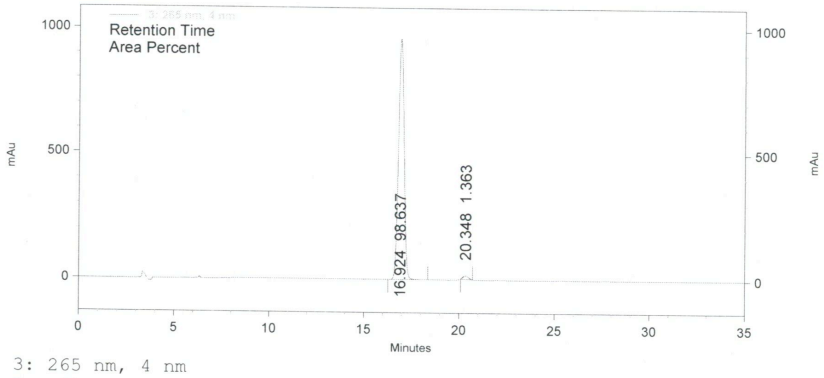

3: 265 nm, 4 nm

Results

Pk #	Retention Time	Area Percent	Lambda Max
1	16.924	98.637	198
2	20.348	1.363	274

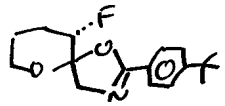

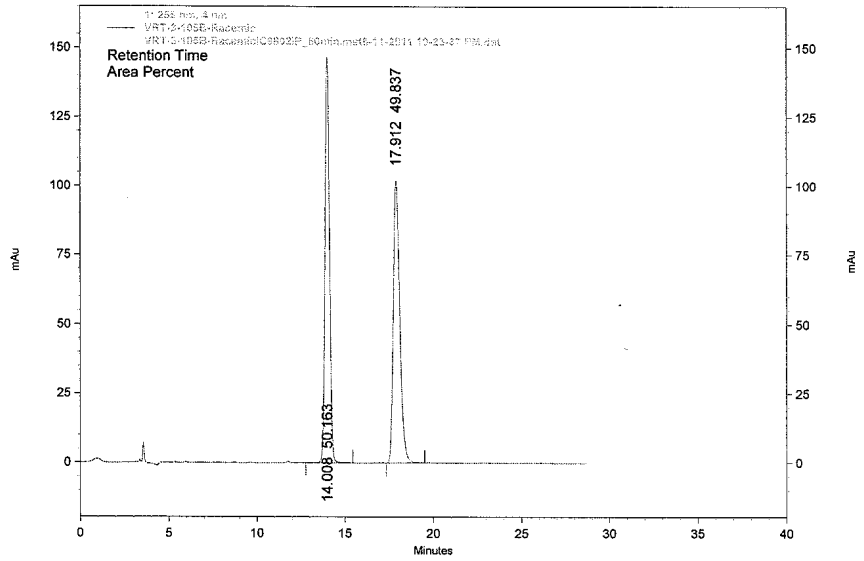

1: 255 nm, 4 nm
Results

Pk #	Retention Time	Area Percent	Lambda Max
1	14.008	50.163	205
2	17.912	49.837	205

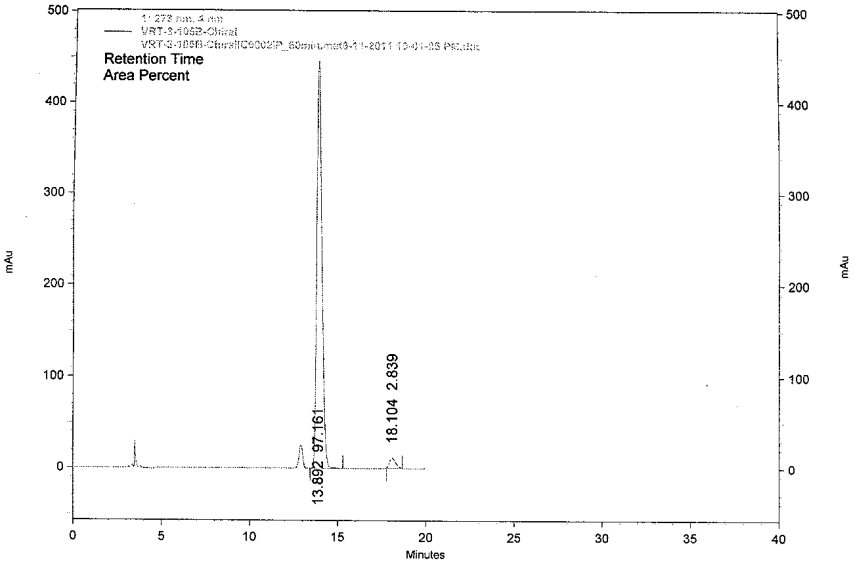

1: 273 nm, 4 nm
Results

Pk #	Retention Time	Area Percent	Lambda Max
1	13.892	97.161	208
2	18.104	2.839	205

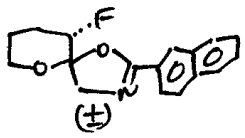

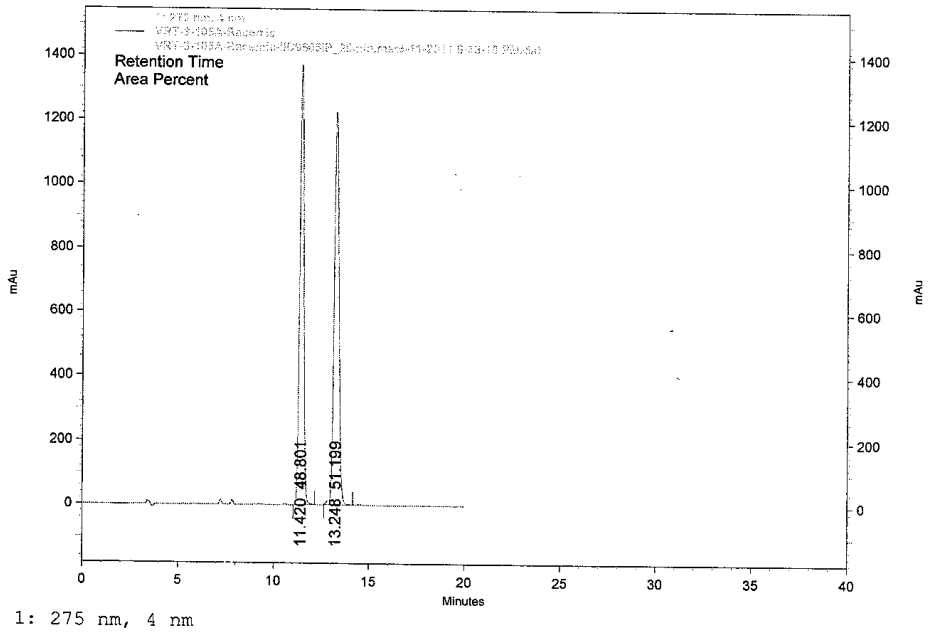

1: 275 nm, 4 nm
Results

Pk #	Retention Time	Area Percent	Lambda Max
1	11.420	48.801	224
2	13.248	51.199	224

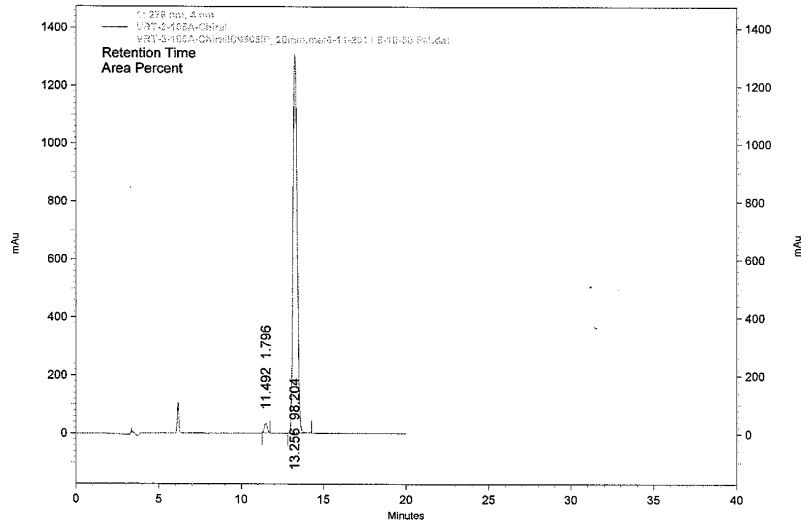

1: 276 nm, 4 nm
Results

Pk #	Retention Time	Area Percent	Lambda Max
1	11.492	1.796	236
2	13.256	98.204	224

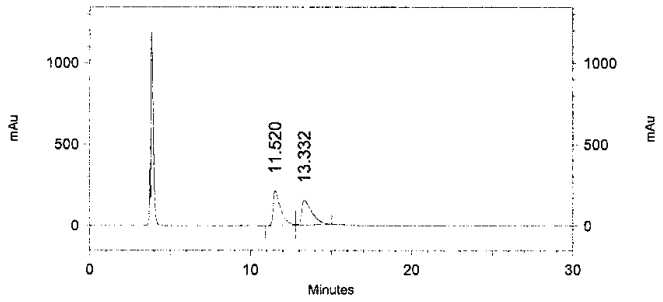

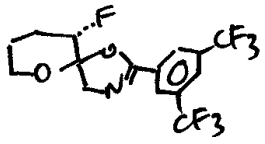

1: 210 nm, 4 nm Results

Retention Time	Area	Area Percent	Lambda Max
11.520	6788814	50.362	194
13.332	6691098	49.638	194

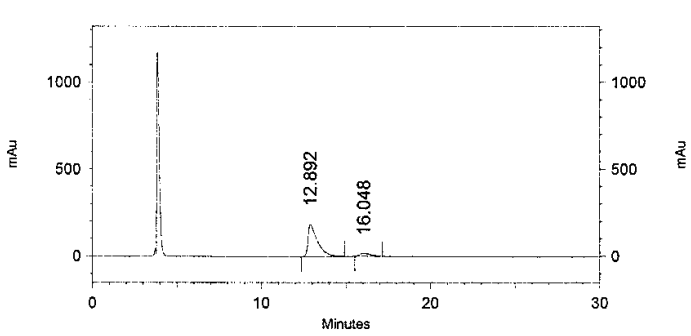

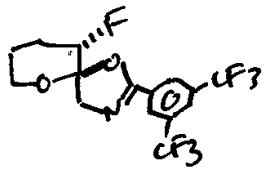

1: 210 nm, 4 nm Results

Retention Time	Area	Area Percent	Lambda Max
12.892	7151142	90.470	196
16.048	753316	9.530	211

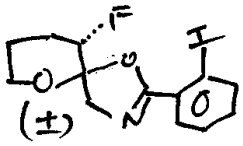

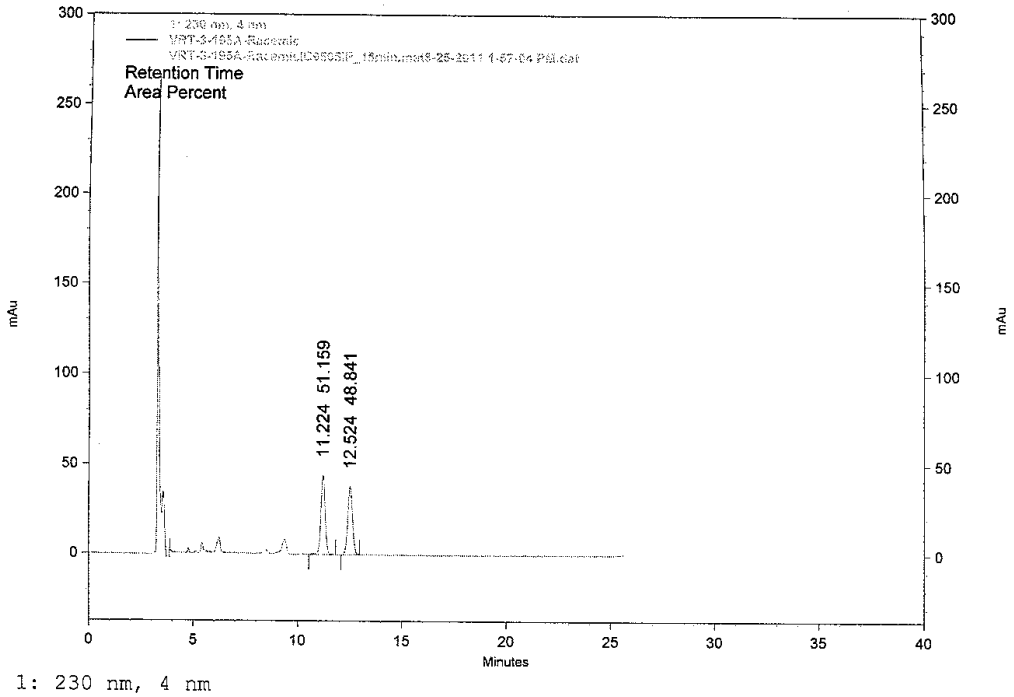

1: 230 nm, 4 nm
Results

Pk #	Retention Time	Area Percent	Lambda Max
1	11.224	51.159	483
2	12.524	48.841	483

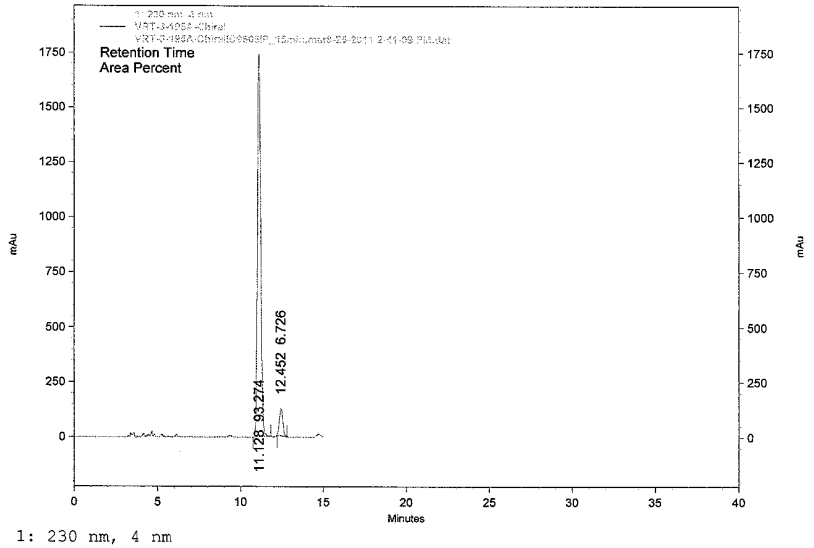

1: 230 nm, 4 nm
Results

Pk #	Retention Time	Area Percent	Lambda Max
1	11.128	93.274	212
2	12.452	6.726	375

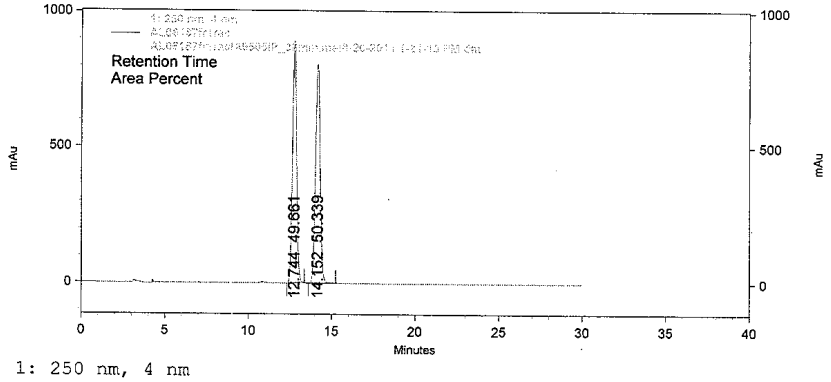

1: 250 nm, 4 nm
Results

Pk #	Retention Time	Area Percent	Lambda Max
1	12.744	49.661	196
2	14.152	50.339	195

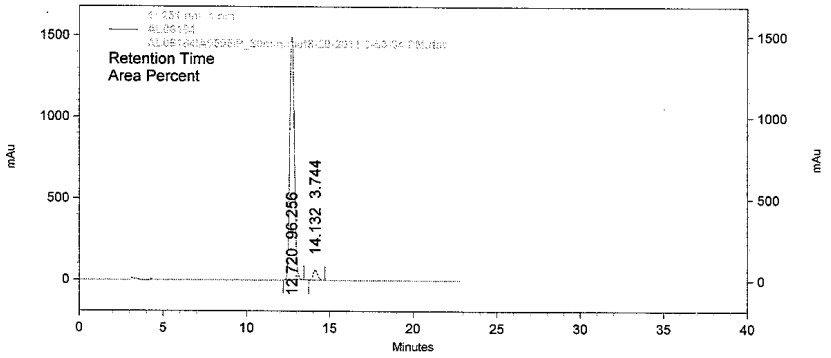

1: 251 nm, 4 nm
Results

Pk #	Retention Time	Area Percent	Lambda Max
1	12.720	96.256	208
2	14.132	3.744	205

C:\EZStart\Projects\Default\Data\glh\VRT-152G_IA995005Et_50min.met3-18-2010 10-51-12 PM.dat

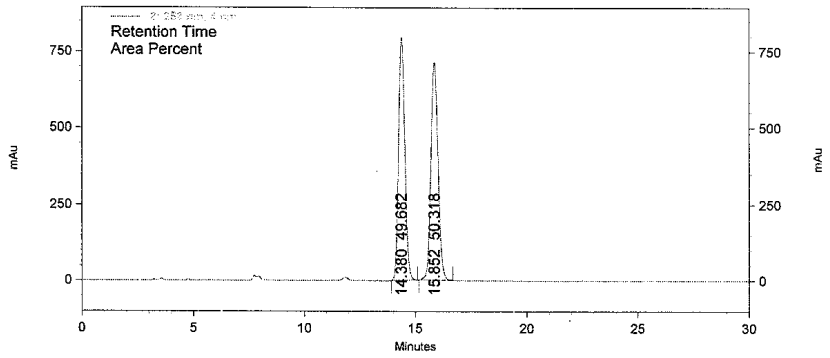

2: 258 nm, 4 nm AL07185A FR1 RACEMIC 95:05 IPA IA
Results

Pk #	Retention Time	Area Percent	Lambda Max
1	14.380	49.682	195
2	15.852	50.318	193

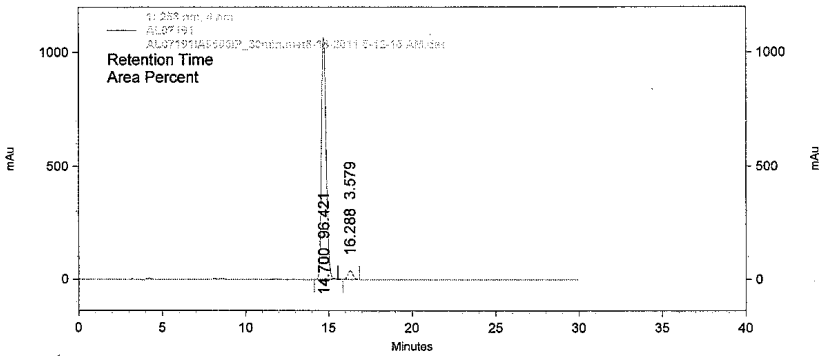

1: 258 nm, 4 nm
Results

Pk #	Retention Time	Area Percent	Lambda Max
1	14.700	96.421	199
2	16.288	3.579	204

C:\EZStart\Projects\Default\Data\glh\VRT-152G_IA995005Et_50min.met3-18-2010 10-51-12 PM.dat

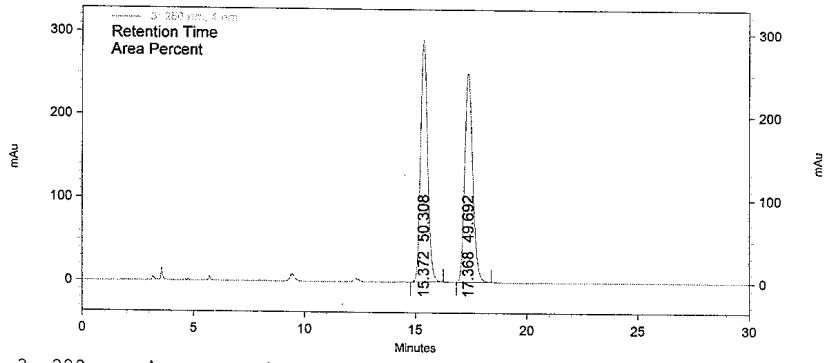

3: 280 nm, 4 nm AL 07186A FRI RACEMIC 95:05 IPA 1A

Results

Pk #	Retention Time	Area Percent	Lambda Max
1	15.372	50.308	197
2	17.368	49.692	192

AL07192

C:\EZStart\Projects\Default\Data\Aaron\AL07192IA9505IP_30min.met8-19-2011 8-22-10 AM.dat

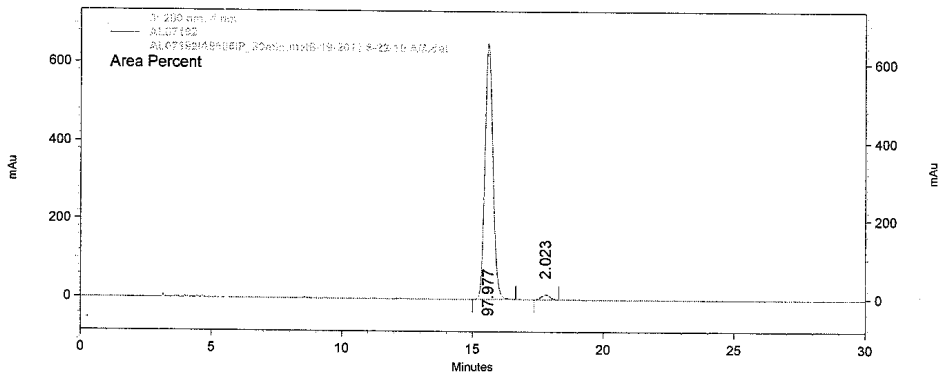

C:\EZStart\Projects\Default\Data\glh\VRT-152G_IA995005Et_50min.met3-18-2010 10-51-12 PM.dat

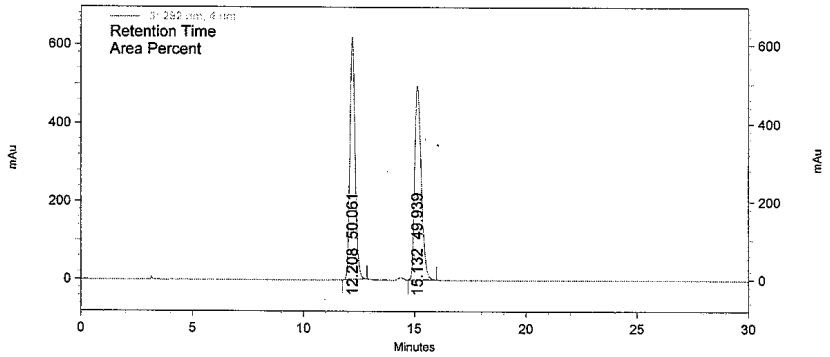

3: 292 nm, 4 nm
Results

Pk #	Retention Time	Area Percent	Lambda Max
1	12.208	50.061	206
2	15.132	49.939	224

C:\EZStart\Projects\Default\Data\glh\VRT-152G_IA995005Et_50min.met3-18-2010 10-51-12 PM.dat

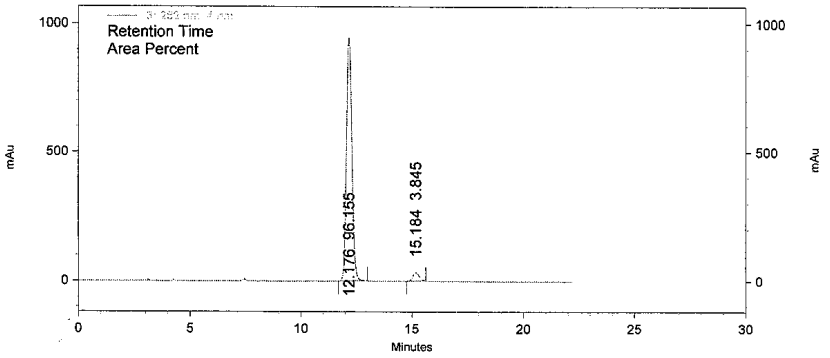

3: 292 nm, 4 nm
Results

Pk #	Retention Time	Area Percent	Lambda Max
1	12.176	96.155	224
2	15.184	3.845	236

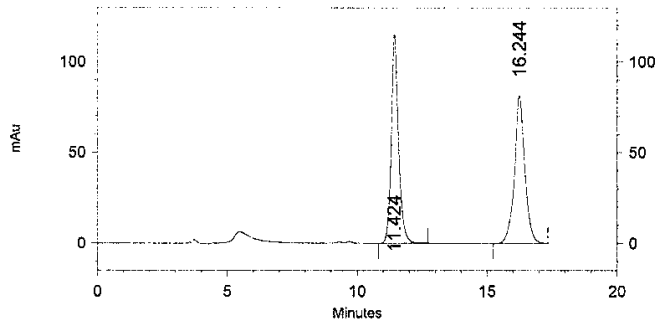

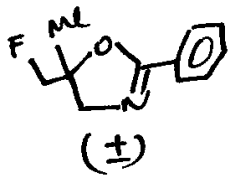

2: 254 nm, 4 nm Results

Retention Time	Area	Area Percent	Lambda Max
11.424	2224470	49.642	205
16.244	2256565	50.358	205

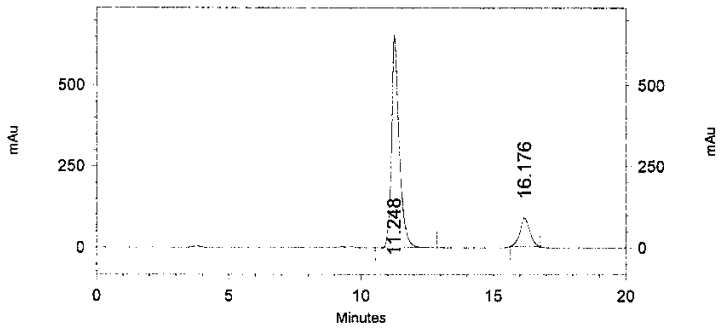

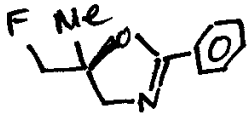

2: 254 nm, 4 nm Results

Retention Time	Area	Area Percent	Lambda Max
11.248	13206348	85.092	206
16.176	2313755	14.908	205

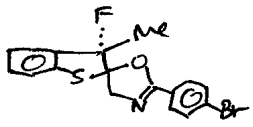

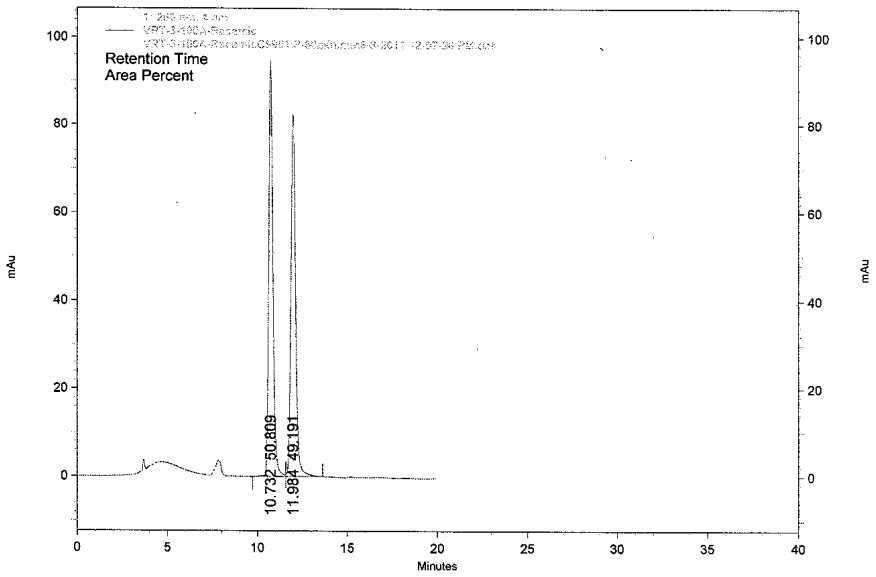

1: 260 nm, 4 nm
Results

Pk #	Retention Time	Area Percent	Lambda Max
1	10.732	50.809	204
2	11.984	49.191	204

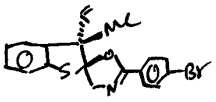

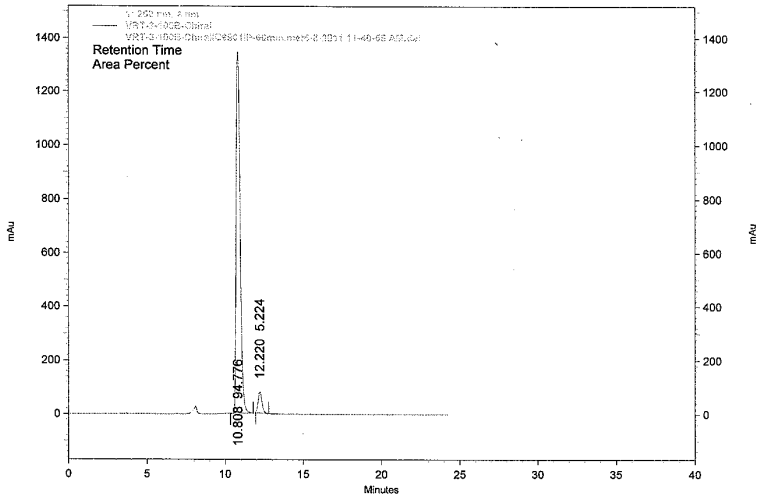

1: 260 nm, 4 nm
Results

Pk #	Retention Time	Area Percent	Lambda Max
1	10.808	94.776	205
2	12.220	5.224	205

Chapter 3. Single-operation chemically catalyzed deracemization of racemic 3H indolines enabled by phase separation

The deracemization of chiral substrates is typically accomplished through an enantioselective oxidation-reduction process. Because of the strong kinetic preference for the reaction of oxidant with terminal reductant rather than the desired reaction with substrate, achieving such a resolution through chemical means has proven elusive. Here we report a phase-separation strategy for the deracemization of chiral amines, in which a triphasic system is employed to minimize the quenching of reagents necessary for conversion of racemate. Partitioning of the cationic oxidant into an aqueous phase and employment of a lowly soluble reductant are key to the success of this single-operation protocol.

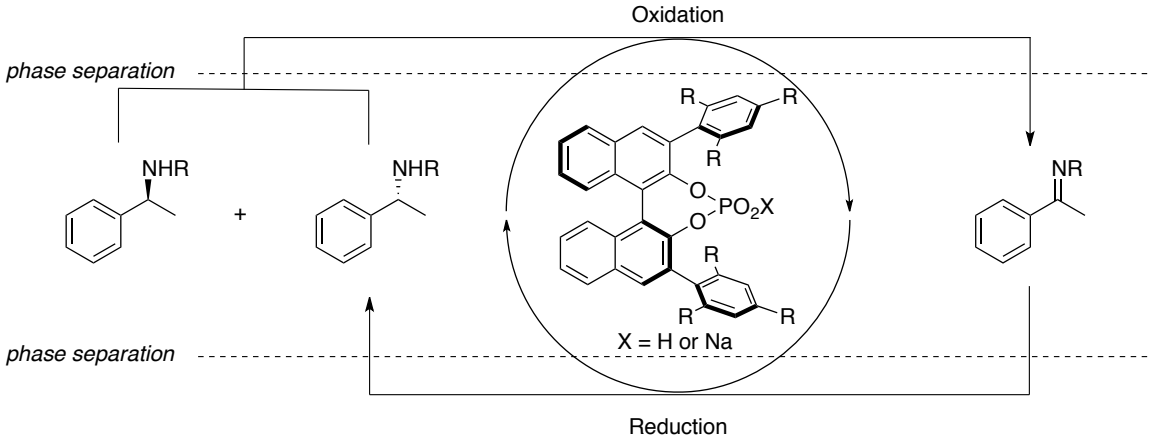

Introduction

The development of chiral anion phase-transfer catalysis in our labs has enabled us to consider reactivity, and, importantly, the suppression of unwanted reactivity, from a new perspective. In the case of enantioselective fluorination, high enantioselectivity is achievable because of the suppression of racemic background reaction, as discussed in Chapter 2. Insolubility, which is frequently viewed as a practical problem in synthetic chemistry because it can prevent the *desired* reactivity, can in this case be used to our advantage. By employing an insoluble reagent, no reaction occurs until the solubilizing chiral anion increases its availability through ion pairing. Phase separation, in this case, is integral to achieving the desired reactivity.

We wondered if we could use this concept to minimize, instead of a racemic background reaction, the reaction of two different reagents. This could allow for the inclusion of reactive reagents that otherwise would be incompatible into one reaction mixture, and perhaps enable dynamic processes that might not otherwise be possible. Specifically, we were intrigued by the possibility of a single-operation deracemization driven by an oxidation-reduction cycle. But before considering how phase-separation might enable this transformation, the principles and challenges of deracemization must be briefly presented.

For the purposes of this discussion, deracemization refers to a resolution, not a transformation, in which one enantiomer of a racemic mixture is dynamically converted to the other, resulting in the recovery of enantioenriched starting material. The reader is pointed to an enlightening discussion of the terminology associated with dynamic resolutions and transformations for further disambiguation.[1] The relevant point here is that the term deracemization has frequently been used regarding the transformation of a racemic mixture, frequently through an achiral intermediate, to an enantioenriched product of different chemical structure. This is more appropriately termed "dynamic kinetic transformation," whereas deracemization indicates a process in which a racemic starting material is converted to the enantioenriched form *of the same chemical structure* (Scheme 1). Deracemization holds significant appeal, as enantioenriched material can be obtained directly from the racemate, and maximum yields of up to 100% can be achieved, in contrast to chiral resolution, in which enantioenriched material is achieved by removing, rather than converting, the other enantiomer.[2]

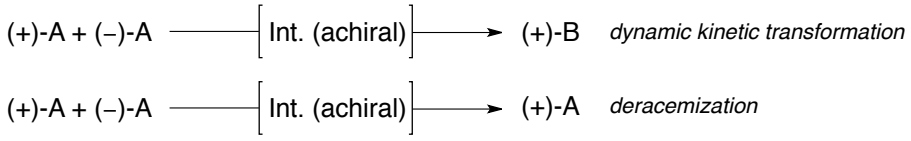

Scheme 1. Representations of dynamic kinetic transformation and deracemization.

While dynamic kinetic transformation and deracemization share some conceptual similarities, a reaction in which substrate and product share the same chemical structure forces added considerations. In particular, the principle of microscopic reversibility shapes the potential approaches to deracemization. When one enantiomer is converted to another in a *single* catalyzed process (Figure 1a), the starting material (one enantiomer)

and the product (the other) must necessarily be in equilibrium since they must interconvert for enantioenrichment to be achieved. The principle of microscopic reversibility dictates that the reverse reaction must also follow the same reaction pathway, and due to the thermodynamically equivalent nature of the two enantiomers, no net production of one enantiomer over the other can be achieved. The racemate, therefore, will inevitably be returned.[3]

Deracemization is still possible, but it requires that the forward reaction and the reverse reaction be decoupled: two different transformations proceeding through distinct mechanistic pathways must be employed (Figure 1b, and Scheme 1b). Perhaps the simplest conceptual approach to this is through a reaction pathway in which the stereocenter is destroyed, and then selectively reformed to return enantioenriched starting material (in analogy to the dynamic kinetic transformation example – in Figure 1b, a dynamic kinetic transformation would differ only in the conversion of the intermediate to a different product B). This is classically accomplished through oxidation and reduction chemistry, and in fact much work in the field adopts this general strategy.

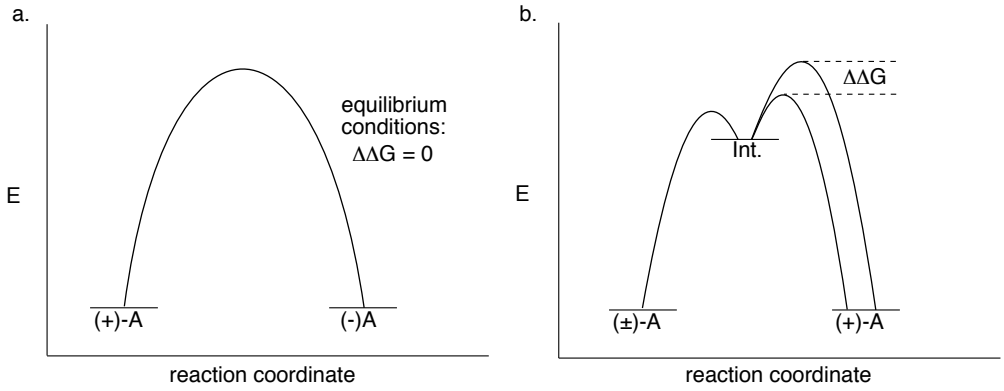

Figure 1. Energy diagrams of (a) single- and (b) two-step deracemization pathways.

Methods for enantioselective oxidation of chiral substrates, as well as enantioselective reduction of prochiral substrates are prevalent in the literature.[4] The identification, then, of an appropriate system in which a chiral substrate is readily oxidized to an achiral intermediate, and then reduced back to its starting form in a selective fashion seems relatively straightforward. It is the necessary presence of two reagents of opposing reactivity, an oxidant and a reductant, that poses the most significant practical challenge.

It is difficult to conceive of a way to force an oxidant to react with a substrate instead of a necessarily more reactive reductant. As the oxidant and reductant (in conjunction with a chiral catalyst) provide the means for deracemization, keeping them from reacting with each other is necessary for an effective procedure, and it is here that we believed phase separation might be useful: simply by keeping oxidant and reductant in separate phases, their direct reaction might be minimized (Figure 2). We hoped to employ a triphasic system[5] in which the oxidant and reductant exist largely as bulk solids out of the reaction mixture containing the substrate (solid-organic-solid phase separation). Alternatively, one reagent could be partitioned into an aqueous phase if it has appropriately high water solubility (aqueous-organic-solid phase separation).

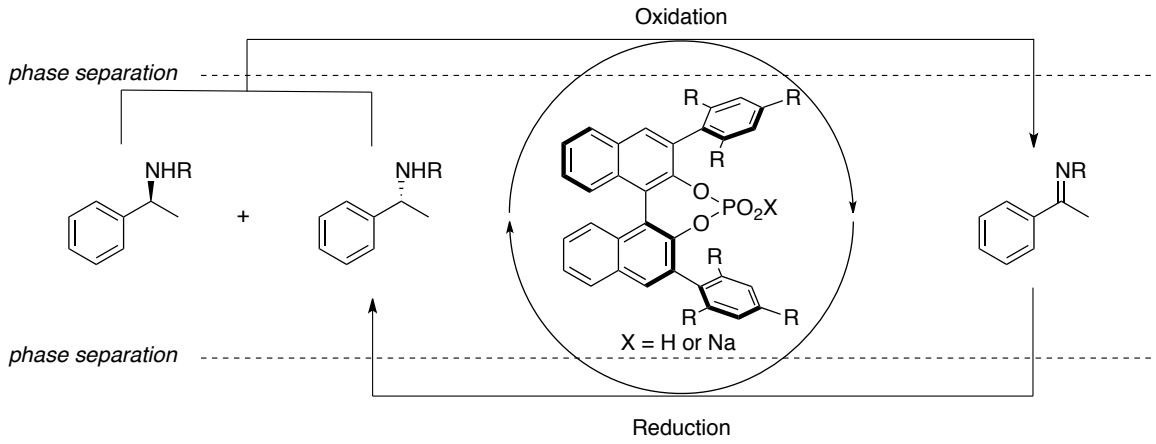

Figure 2. General concept for phase-separation deracemization.

We were also encouraged by precedents indicating that a single chiral input might catalyze both the oxidation and reduction steps. Chiral phosphoric acids have been shown to catalyze the enantioselective reduction of various imine substrates by activating them toward hydride delivery from Hantzsch esters.[6] And as discussed in Chapter 2, the conjugate base phosphates can promote enantioselective oxidation through phase-transfer catalysis using an oxopiperidinium salt, which was our entry point to considering deracemization. We also considered that other cationic reagents with demonstrated utility in chiral anion phase-transfer catalysis, such as Selectfluor, might be able to effect oxidation. We envisioned a catalytic cycle as shown in Figure 2, in which a chiral phosphate acts first as a phase-transfer catalyst for the oxidation of a chiral amine, and subsequently, as its conjugate acid, as an activator of the consequent imine intermediate for reduction by the Hantzsch ester. Both Hantzsch esters and the oxopiperidinium salt display limited solubility in organic solvents, and we were confident this would allow us to test our hypotheses.

Results and Discussion

Though presented in the introduction as an easy step in the progression toward deracemization, identification of a suitable reaction platform was a lengthy process, and is discussed briefly in the first paragraphs. As deracemization would combine two chemical reactions, and it was likely that many other variables would need to be considered, it made sense to start with a system in which at least one reaction is well-precedented in order to have a base from which to begin optimization. N-aryl benzylimines such as **3.1** were the first and among the most developed substrates for chiral acid-catalyzed reduction,[7] and the procedure was readily reproducible in our hands using ethyl Hantzsch ester **3.2a** and chiral phosphoric acid **3.3a**, (*S*)-TRIP (Scheme 2). Thus their chiral reduced form, N-arylbenzylamines, seemed a logical starting point for reaction development.

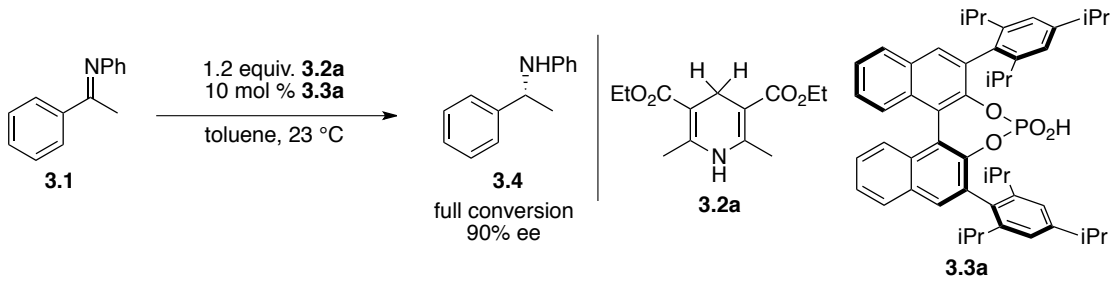

Scheme 2. Precedented enantioselective reduction of benzylimines.

Among the cationic oxidants employed in attempts to oxidize N-arylbenzylamines bearing different substitution to their imine forms were tritylium terafluoroborate **3.5**, oxopiperidinium tetrafluoroborate **3.6**, Selectfluor, **3.7**, and brominating reagent **3.8** developed within our labs.[8] The vast majority of conditions and substrates employed were unsuccessful, and are only briefly discussed here as a negative result. The only instances in which reactivity was observed employed **3.7** or **3.8** as an oxidant, and underwent either undesired electrophilic aromatic substitution on the aniline moiety (Table 1) or N-halogenation with α proton elimination to give **3.10** (Scheme 3).

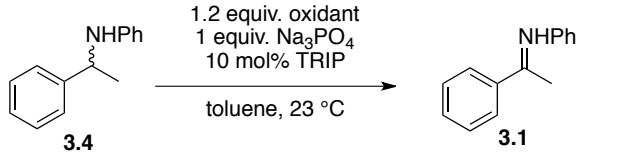

entry	oxidant	yield
1	**3.5**	0%
2	**3.6**	0%
3	**3.7**	0%[a]
4	**3.8**	0%[a]

[a] Electrophilic aromatic halogenation product observed.

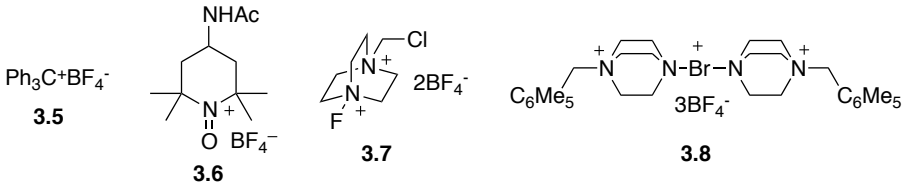

Table 1. Oxidants employed in the attempted oxidation of N-aryl benzylamines.

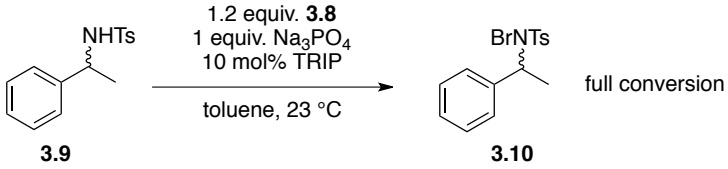

Scheme 3. N-halogenation of N-tosyl benzylamines.

Attempts at oxidation of phenyl glyoxylate derivatives, which we thought may favor β elimination instead of α elimination, resulting in the imine, did in fact show 30% conversion to desired product (Scheme 4), but only under homogeneous conditions. In any event, having significantly modified the substrate from the originally reported

conditions, we were unable to effect enantioselective reduction on the resulting imine **3.12**.

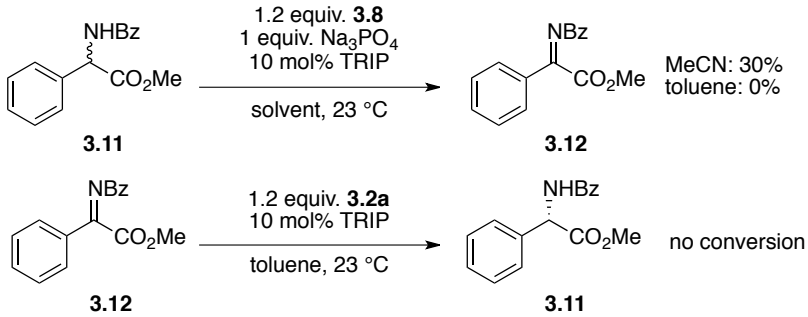

Scheme 4. Attempted oxidation and reduction of phenylglyoxylate derived substrates.

As it seemed that the likelihood of success with benzylamine substrates was continuing to diminish, we approached the problem from the opposite direction, attempting to develop appropriate reductive conditions for a substrate that can be easily accessed through mild oxidative conditions. Tetrahydroisoquinolines occupy a special place in the literature as a readily oxidizable scaffold with biological relevance and as such have become a common substrate in, among other methodologies, cross-dehydrogenative coupling.[9] As such, we felt we could readily establish oxidative conditions and spend our efforts on reducing the consequent 3,4-dihydroisoquinoline.

We first examined 1-methyl tetrahydroisoquinoline, **3.13**, and indeed under phase-transfer conditions in the presence of Selectfluor, full conversion to the dihydroisoquinoline **3.14** was observed in a crude ^{1}H NMR experiment. However we were unable to effect reduction of **3.14** under chiral acid catalysis conditions (Scheme 5).

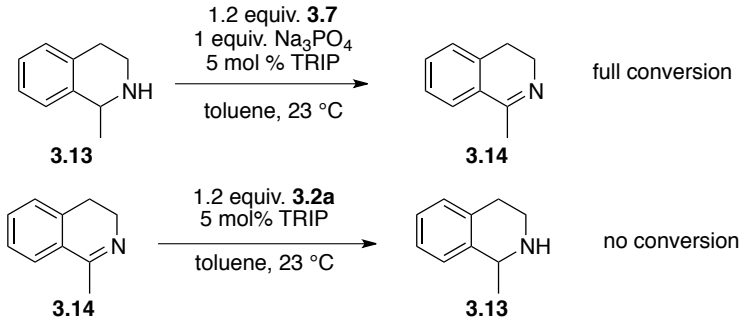

Scheme 5. Dihydroisoquinoline substrate does not undergo acid-catalyzed reduction.

We rationalized that by forcing oxidation of an N-substituted tetrahydroisoquinoline to result in a cationic dihydroisoquinolinium rather than neutral dihydroisoquinoline, reduction would become a more kinetically accessible process. Only on N-methyl substrate **3.15** was oxidation still cleanly achieved, and only under homogeneous conditions. Even so, the enantioselective reduction of the N-methyl dihydroisoquinolinium **3.16** was not achieved (Scheme 6). The tetrahydroisoquinoline scaffold was thereafter explored no further.

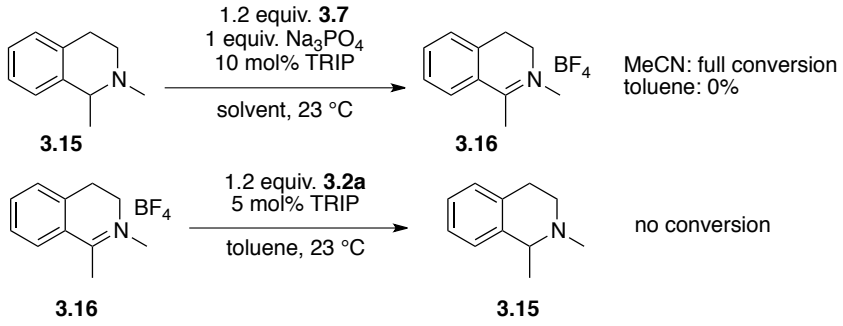

Scheme 6. N-Me dihydroisoquinolinium substrate also does not undergo reduction.

After further perusal of the literature, a different class of substrates, 3H indolines, whose oxidized form readily undergoes chiral acid-catalyzed reduction, was identified.[10] In this case we were very pleased to show that the reduced form 3H indoline was cleanly oxidized to the indole form by oxopiperidinium **3.6** under basic phase-transfer conditions (though when the reaction is not run to completion, virtually no chiral resolution is achieved), and in the same reaction solvent, the 3H indole was reduced in very high enantioselectivity to the 3H indoline (Scheme 7). Furthermore, the solubility of both the reductant and the oxidant in the reaction solvent, toluene, was fairly low (7.8 mM and 0.1 mM respectively).

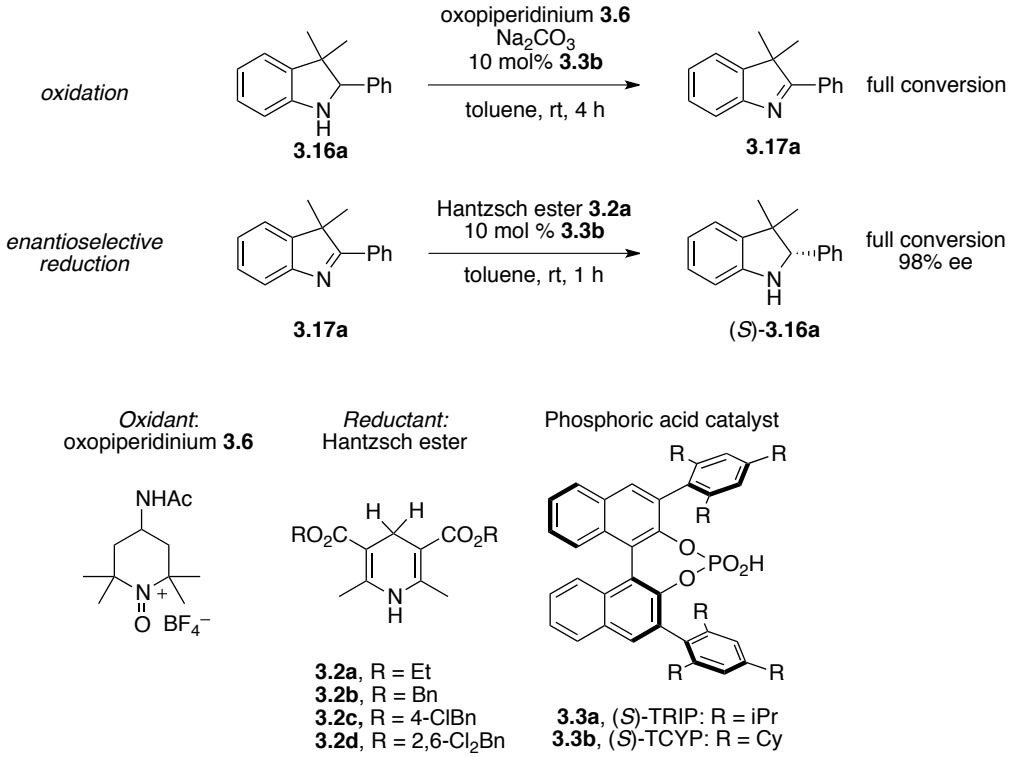

Scheme 7. Identification of 3H indolines as feasible substrates.

Before attempting method development, we realized that analysis of a deracemization reaction, in which the starting material and the product are of the same structure, would

be difficult since conversion of starting material cannot be quantified. Our solution was to instead use the deuterated analog **3.17a**-D, and to use deuterium erosion, which occurs by oxidation and subsequent hydride delivery from the Hantzsch ester, as an indicator of conversion. Given the high enantioselectivity of the reduction, we were confident that conversion of the deuterated substrate and enantiomeric excess would track closely.

To evaluate the feasibility of solid-organic-solid phase-separation, two equivalents of reductant and oxidant were added to substrate in the presence of 10 mol % **3.3b** in toluene under phase-transfer (basic) conditions. The indoline was reisolated as the racemate with no detectable deuterium erosion (Table 2, entry 1). The consumption of oxidant, which can be followed qualititatively by the dissipation of its bright yellow color, appeared faster than in the presence of substrate alone, and we believe that the oxidant was consumed completely by reaction with reductant rather than substrate (nearly two full equivalents of oxidized Hantzch ester was observed in the crude ^{1}H NMR spectrum). Since basic conditions may impede the enantioselective reduction of any oxidized intermediate, we also ran the reaction under nonbasic conditions (entry 2), though again no deuterium erosion was observed.

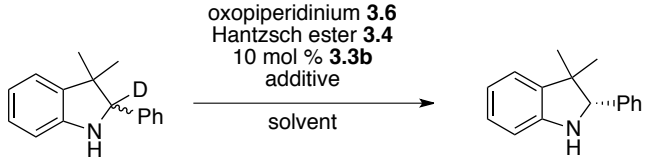

(±)-**3.17a**-D (*S*)-**3.17a**

entry	Hantzsh ester (equiv.)[a]	solvent	additive (equiv.)	%ee	%D erosion
1	**3.2a** (2.0)	$PhCH_3$	Na_2CO_3 (2.0)	0%	0%
2	**3.2a** (2.0)	$PhCH_3$	--	0%	0%
3	**3.2a** (2.0)	1:1 $PhCH_3/H_2O$	--	4%	5%
4	**3.2a** (2.0)	9:1:10 Hex/Et_2O/H_2O	--	67%	68%
5	**3.2a** (2.0)	9:1:10 Hex/Et_2O/H_2O	Na_2CO_3 (2.0)	42%	57%
6	**3.2a** (2.0)	9:1:10 Hex/Et_2O/H_2O	HCl (1.0)	81%	84%
7	**3.2b** (2.0)	9:1:10 Hex/Et_2O/H_2O	HCl (1.0)	56%	56%
8	**3.2c** (2.0)	9:1:10 Hex/Et_2O/H_2O	HCl (1.0)	92%	97%
9	**3.2c** (1.5)	9:1:10 Hex/Et_2O/H_2O	HCl (1.0)	91%	94%
10	**3.2d** (1.5)	9:1:10 Hex/Et_2O/H_2O	HCl (1.0)	92%	96%
11[b]	**3.2d** (1.5)	9:1:10 Hex/Et_2O/H_2O	HCl (1.0)	94%	98%
12[b,c]	**3.2d** (1.5)	9:1:10 Hex/Et_2O/H_2O	HCl (1.0)	94%	97%

[a] Equimolar amount of oxopiperidinium used; [b] (*S*)-TRIP, **3.3a**, used as catalyst instead of (*S*)-TCYP; [c] Reaction run in stepwise fashion; [d] proteated substrate used

Table 2. Optimization of reaction conditions for deracemization of 3H indolines.

Given the high water solubility of the oxammonium salt (~70 mM),[11] we rationalized that aqueous-organic-solid phase-separation might more effectively partition oxidant and reductant. Indeed, when the oxidant was added as an aqueous solution,[12] 5% deuterium erosion was observed, along with 4% ee (entry 3), indicating that a small fraction of the substrate had been oxidized and subsequently reduced enantioselectively. Switching the organic phase to a 9:1 hexanes/diethyl ether mixture resulted in a significant improvement in both conversion and enantioenrichment (entry 4). This result is in line

with our phase-separation hypothesis, as both oxopiperidinium **3.6** (0.07 mM) and Hantzsch ester **3.2a** (0.4 mM) have lower solubility in the less polar organic mixture. Under the analogous basic conditions, though comparable conversion was observed, the indoline was isolated with a significantly deteriorated enantioenrichment (entry 5). Conversely, we found that one equivalent of strong acid led to improved results in the presence of an aqueous phase (entry 6). This phenomenon has also been observed in a previously reported chiral phosphoric acid-catalyzed reduction methodologies,[13] and we believe it is at least in part due to the improved ability to free the phosphoric acid from ion pairing with the pyridine generated from consumption of reductant. That the reaction proceeds more favorably in the absence of base, and in fact is promoted by more acidic conditions strongly implies that the catalyst does not act as an anionic phase-transfer catalyst, as originally envisioned.

By altering the solubility properties of the Hantzsch ester reductant, we hoped to further eliminate reagent quenching and thus improve enantioenrichment of the isolated product. While benzyl Hantzsch ester **3.2b** gave worse results compared to the ethyl analog (entry 7), use of 4-Cl-Bn Hantzsch ester **3.2c** improved conversion of deuterated substrate, also reflected in the product enantioenrichment (entries 8). Furthermore, oxidant and reductant stoichiometry could be lowered from 2.0 to 1.5 equivalents without compromising enantioenrichment (entry 9). 2,6-Cl_2-Bn Hantzsch ester **3.2d** (which has a measured solubility of 0.08 mM in 9:1 hexanes/diethyl ether) gave comparable conversion (entry 10), and its highly crystalline nature makes it easier to handle than **3.2c**. Use of the chiral phosphoric acid TRIP (**3.3a**) in place of TCYP (**3.3b**) as catalyst led to a further increase in enantioselectivity (entry 11). Under these conditions, the enantioenrichment matched that of a stepwise oxidation-reduction sequence (entry 12). Absolute stereochemistry of the product was confirmed through X-ray crystallography of the hydrochloride salt, and is in agreement with the literature assignment.[10]

The proteated isotopologue **3.17a** was deracemized to the same degree as **3.17a**-D (Figure 3), and 3H indolines of various substitution patterns were subjected to the same one-step deracemization (a slight excess of reductant is used to ensure full reduction), and compared to their stepwise oxidation-reduction to determine efficacy. Spirocyclic products were obtained in good yields and high enantiomeric excesses (**3.17b** and **3.17c**). Substitution around the indoline arene was well tolerated, as in the cases of benzoindoline **3.17d** and 5-bromoindoline **3.17e**. Substrates with 2-aryl functionality were subjected to reaction conditions and isolated in good to high enantiomeric excess, including para- (**3.17f**, **3.17j**, **3.17k**), meta- (**3.17g**, **3.17h**, **3.17i**), and ortho- (**3.17h**) substituted 2-arylindolines. Electron rich arenes (**3.17f**, **3.17g**) were well tolerated, though in the case of substrate **3.17f**, the enantioselectivity of the reduction is slightly diminished. Electron poor substrates (**3.17e**, **3.17h**, **3.17i**, **3.17j**, **3.17k**) were also isolated in high enantiomeric excess, however in these cases a higher loading of oxidant (1.75 equivalents) and reductant (1.80 equivalents) was needed for full deracemization.[14]

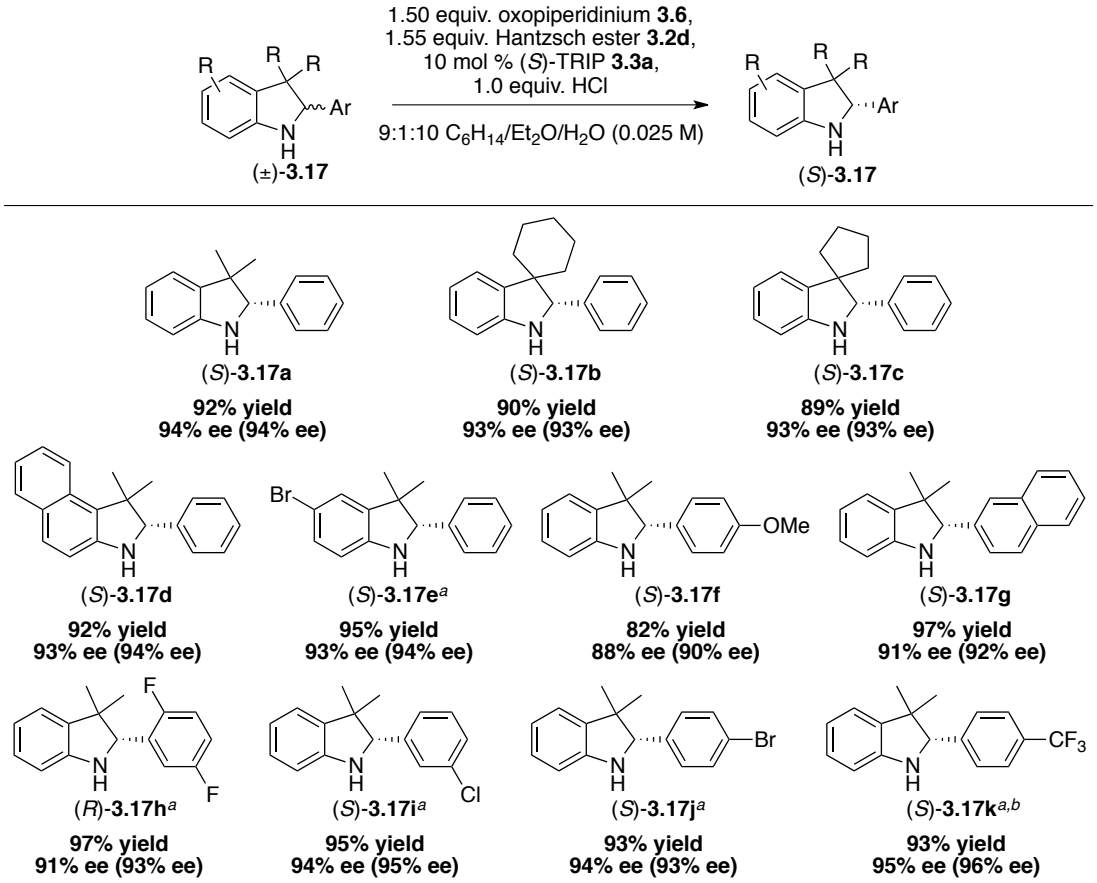

[a] 1.75 equiv. oxopiperidinium, 1.80 equiv. Hantzsch ester **4**; [b] (*S*)-TCYP **3.3b** used as catalyst.

Figure 3. Scope of deracemization of 3H indolines.

We were also able to show that highly enantioenriched material could be converted to the opposite enantiomer under the same reaction conditions as were used for racemic starting material. When (*S*)-**3.17a** (93% ee) was submitted to reaction conditions, the antipode (*R*)-**3.17a** was isolated in high yield and ee (Scheme 9, 98% and 94% respectively).

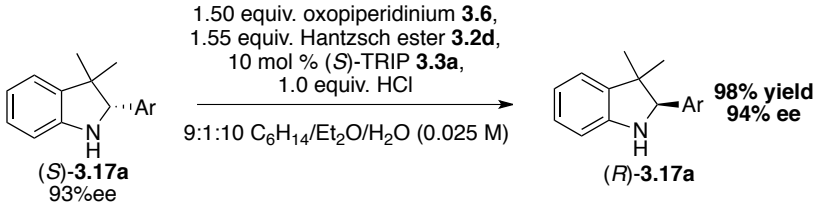

Scheme 9. Inversion of highly enantioenriched starting material under reaction conditions.

At the time of the writing of this text, representative examples of two other classes of substrates, substituted benzoxazines and substituted tetrahydroquinolines, had been deracemized following the same procedure. In these cases, the single-operation procedure resulted in 5-10% lower enantioenrichment than achieved through the stepwise procedure. These substrates will require further optimization of reaction conditions (as

well as full characterization), though their (pending) successful deracemization suggests a certain generality to the procedure.

Conclusions

The development of a single-operation deracemization enabled by a three-phase system demonstrates the ability of phase-separation to suppress undesired reactivity: it has allowed us to develop a reaction for which there was no purely chemical methodology. That it has been used to enable what would be a minor or fully inaccessible reaction pathway under more typical reaction conditions (cf Table 2, entries 1, 2), demonstrates its efficacy as a strategy. We hope that this strategy will prove amenable to a wide scope of chiral substrates, and that it can be extended to cascade reactions beyond deracemization protocols.

Experimental Details

General: Unless otherwise noted, all commercial reagents were used without further purification. 4-acetamido-2,2,6,6-tetramethyl-1-oxopiperidinium tetrafluoroborate was reprecipitated from MeCN/Et_2O prior to use. Small scale reactions were run in scintillation vials with screw caps. Dichloromethane, toluene, ether, toluene and triethylamine were purified by passage through an activated alumina column under argon. Thin-layer chromatography analysis of reaction mixtures was performed using Merck silica gel 60 F254 TLC plates, and visualized under UV or by staining with ceric ammonium molybdate or $KMnO_4$. Flash column chromatography was carried out on Merck Silica Gel 60 Å, 230 X 400 mesh. Nuclear magnetic resonance (NMR) spectra were recorded using Bruker DRX-500, AVQ-400 and AV-300 spectrometers. ^1H and ^{13}C chemical shifts are reported in ppm downfield of tetramethylsilane and referenced to residual solvent peak ($CHCl_3$; $\delta_H = 7.26$ and $\delta_C = 77.0$, CH_3OH; $\delta_H = 3.31$ and $\delta_H = 49.2$). Multiplicities are reported using the following abbreviations: s = singlet, d = doublet, t = triplet, q = quartet, m = multiplet, br = broad resonance. Mass spectral data were obtained from the Micro-Mass/Analytical Facility operated by the College of Chemistry, University of California, Berkeley. Enantiomeric excesses were determined on a Shimadzu VP Series Chiral HPLC.

Synthesis of reagents and substrates.

3.2a,[15] **3.2b**,[15] **3.3a**,[16] **3.3b**,[17] **3.1**,[18] **3.4**,[19] **3.9**,[20] **3.11**,[21] **3.12**,[22] **3.13**,[23] **3.14**,[24] were prepared according to the literature.

Procedures for the synthesis of Hantzsch esters have not been optimized for yield.

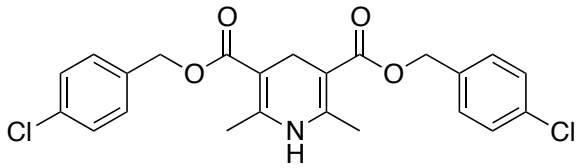

Bis(4-chlorobenzyl)-2,6-dimethyl-1,4-dihydropyridine-3,5-dicarboxylate 3.2c: 4-chlorobenzyl alcohol (2.85 g, 20 mmol) was added to ethyl acetoacetate (3.0 ml, 24 mmol) in toluene (0.4 M) and the reaction mixture was heated to reflux in an open flask for 24 h. Following transesterification, the excess ethyl acetoacetate was removed by distillation under high vacuum (60 ^oC, 1 torr). The crude 4-chlorobenzyl acetoacetate was added to ammonium acetate (770 mg, 10 mmol) and paraformaldehyde (300 mg, 10 mmol) in ethanol (0.2 M) and heated to reflux for 16 h. A pale yellow precipitate formed through the course of the reaction, and the crude mixture was allowed to cool to room temperature and filtered through filter paper. The precipitate was washed with ethanol and diethyl ether, and purified by layered recrystallization from DCM and hexanes. Pale yellow needles. Yield: 77% (3.4g, 7.7 mmol).

^1H NMR (500 MHz, $CDCl_3$) δ 7.38-7.29 (m, 8H), 5.23 (s, 1H), 5.14 (s, 4H), 3.37 (s, 2H), 2.22 (s, 6H).

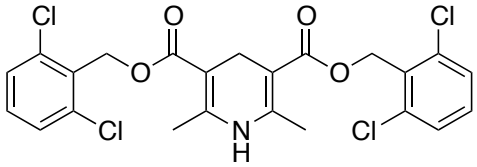

Bis(2,6-dichlorobenzyl)-2,6-dimethyl-1,4-dihydropyridine-3,5-dicarboxylate 3.2d: 2,6-dichlorobenzyl alcohol (3.5 g, 20 mmol) was added to ethyl acetoacetate (5.0 ml, 40 mmol) in toluene (0.4 M) and the reaction mixture was heated to reflux in an open flask for 48 h. Following transesterification, the excess ethyl acetoacetate was removed by distillation under high vacuum (60 ^{o}C, 1 torr). The crude 2,6-dichlorobenzyl acetoacetate was added to ammonium acetate (770 mg, 10 mmol) and paraformaldehyde (300 mg, 10 mmol) in 1:1 ethanol/1,2-dichloroethane (0.2 M) and heated to reflux for 24 h. A bright yellow precipitate formed through the course of the reaction, and the crude mixture was allowed to cool to room temperature and concentrated. The crude product was deposited into diethyl ether and filtered through filter paper. The precipitate was washed with ethanol and diethyl ether. The precipitate was recrystallized from hot 1,2-dichloroethane. Hot filtration through celite was necessary to ensure a homogeneous solution for recrystallization. Only the first crop was kept. Bright yellow crystalline solid. Yield: 30% (1.56 g, 3.0 mmol)

^{1}H NMR (300 MHz, $CDCl_3$) δ 7.31-7.17 (m, 6H), 5.46 (s, 4H), 512 (s, 1H), 3.22 (s, 2H), 2.14 (s, 6H).

General procedures A and B for the synthesis of 3H indoline substrates (±)-**3.17**.

Procedures for the synthesis of substrates have not been optimized for yield.

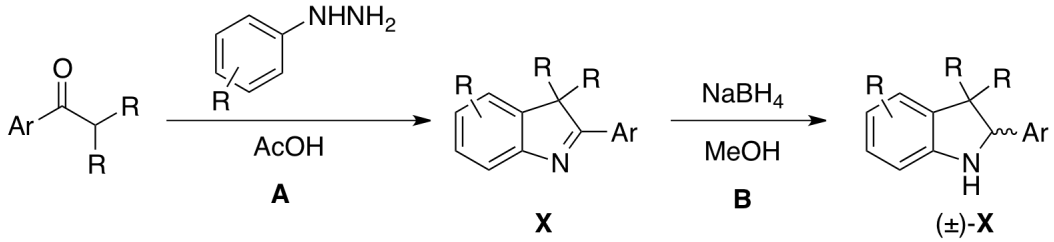

General procedure A: To a 4 dram vial was added the appropriate ketone and arylhydrazine. 5 ml glacial acetic acid was added and the reaction mixture was heated to 120 ^{o}C and stirred 16 h. The reaction mixture was poured onto saturated aqueous Na_2CO_3 and the crude product was extracted with DCM (3 x 20 ml). The combined organic layers were dried with $MgSO_4$, filtered, concentrated and purified by flash column chromatography on SiO_2 to give indicated 3H indole intermediate **S3.1**.

General procedure B: In a 100 ml round bottom flask, the appropriate 3H indole **S3.1** was dissolved in MeOH (0.2 M) and the reaction mixture was cooled to 0 ^{o}C. $NaBH_4$ was added and the reaction mixture was allowed to warm to room temperatue and stirred 5 h. The reaction mixture was concentrated by rotory evaporation under reduced pressure partitioned between DCM and water (20 ml each). The organic layer was removed and the aqueous layer extracted with DCM (2 x 20 ml). The combined organic layers were

dried w $MgSO_4$, filtered, concentrated and purified by flash column chromatography on SiO_2 to give the racemic 3H indoline product (±)-**3.17**.

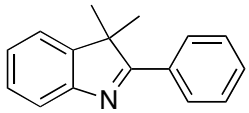

3,3-Dimethyl-2-phenyl-3*H*-indole, S3.1a: Prepared according to general procedure A from isopropyl phenyl ketone (1510 ul, 10 mmol) and phenylhydrazine (960 ul, 10 mmol). Eluent: 9:1 hexanes/ethyl acetate. Isolated yield: 70% (1.54 g, 7.0 mmol), yellow oil.

^{1}H NMR (500 MHz, $CDCl_3$) δ 8.12 (m, 2H), 7.68 (d, J = 7.5 Hz, 1H), 7.48-7.45 (m, 3H), 7.36-7.32 (m, 2H), 7.27-7.26 (m, 1H), 1.58 (s, 6H); ^{13}C NMR (125 MHz, $CDCl_3$) δ 183.4, 153.2, 147.7, 133.4, 130.7, 128.8, 128.5, 127.9, 126.0, 121.1, 121.0, 53.7, 24.9; HRMS (ESI) exact mass for MH^+ ($C_{16}H_{16}N$) calcd *m/z* 222.1277 found 222.1275.

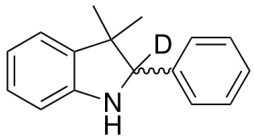

(±)-**3.17a**-D: To 3H indole **S3.1a** (221 mg, 1.0 mmol) in DCM (0.1 M) was added 4,4-dideuterio-2,6-dimethyl-3,5-dicarboethoxy-l,4-dihydropyridine (doi: 10.1002/anie.201007571) (306 mg, 1.2 mmol) and p-toluenesulfonic acid monohydrate (0.1 mmol, 19 mg). The reaction mixture was stirred at room temperature for 3 h, at which point TLC indicated full conversion. The reaction mixture was concentrated and purified directly by flash column chromatography on SiO_2 (9:1 hexanes/diethyl ether). Isolated yield: 95% (213 mg, 0.95 mmol), colorless powder, >98% deuterium incorporation.

^{1}H NMR (500 MHz, $CDCl_3$) δ 7.48 (d, J = 7.5 Hz, 2H), 7.39-7.31 (m, 3H), 7.12-7.07 (m, 2H), 6.81 (t, J = 7.5 Hz, 1H), 6.75 (d, J = 7.5 Hz, 1H), 4.09 (br s, 1H), 1.45 (s, 3H), 0.76 (s, 3H); ^{2}H NMR (77 MHz, $CHCl_3$) δ 4.58 vs $CDCl_3$ reference; ^{13}C NMR (125 MHz, $CDCl_3$) δ 149.5, 140.1, 138.2, 128.3, 127.7, 127.6, 127.6, 122.7, 119.1, 109.3, 74.7 (br), 45.4, 26.7, 24.7 ; HRMS (ESI) exact mass for MH^+ ($C_{16}H_{17}DN$) calcd *m/z* 225.1497 found 225.1497.

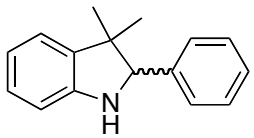

3,3-Dimethyl-2-phenylindoline, (±)-**3.17a**: Prepared according to general procedure B from 3H indole **S3.1a** (443 mg, 2.0 mmol) and $NaBH_4$ (380 mg, 10 mmol). Eluent: 9:1 hexanes/diethyl ether. Isolated yield: 79% (353 mg, 1.6 mmol), colorless powder.

^{1}H NMR (500 MHz, $CDCl_3$) δ 7.48 (d, J = 7.5 Hz, 2H), 7.47-7.31 (m, 3H), 7.12-7.07 (m, 2H), 6.82 (t, J = 7.5 Hz, 1H), 6.76 (d, J = 7.5 Hz, 1H), 4.63 (s, 1H), 4.15 (br s, 1H), 1.46

(s, 3H), 0.76 (s, 3H); ^{13}C NMR (125 MHz, $CDCl_3$) δ 149.5, 140.1, 138.2, 128.3, 127.7, 127.6, 127.6, 122.7, 119.1, 109.3, 74.7, 45.5, 26.7, 24.7; HRMS (ESI) exact mass for MH^+ ($C_{16}H_{18}N$) calcd *m/z* 224.1434 found 224.1432.

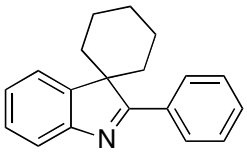

2'-Phenylspiro[cyclohexane-1,3'-indole], S3.1b: Prepared according to general procedure A from cyclohexyl phenyl ketone (941 mg, 5 mmol) and phenylhydrazine (490 ul, 5 mmol). Eluent: 9:1 hexanes/ethyl acetate. Isolated yield: 62% (810 mg, 3.1 mmol), yellow oil. ^{1}H NMR (400 MHz, $CDCl_3$) δ 8.06 (m, 2H), 7.84 (d, *J* = 7.2 Hz, 1H), 7.74 (d, *J* = 8.0 Hz, 1H), 7.50-7.48 (m, 3H), 7.40 (t, *J* = 7.6 Hz, 1H), 7.24 (d, *J* = 7.2 Hz, 1H), 2,30 (td, *J* = 13.6 Hz, 4.4 Hz, 2H), 2.08-1.98 (m, 3H), 1.87-1.84 (m, 2H), 1.55-1.44 (m, 3H); ^{13}C NMR (125 MHz, $CDCl_3$) δ 184.0, 153.8, 146.2, 134.0, 130.0, 128.6, 128.4, 127.7, 124.9, 124.4, 121.3, 58.5, 31.2, 25.2, 21.8; HRMS (ESI) exact mass for MH^+ ($C_{19}H_{20}N$) calcd *m/z* 262.1590 found 262.1589.

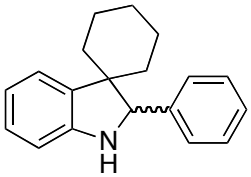

2'-Phenylspiro[cyclohexane-1,3'-indoline], (±)-**3.17b**: Prepared according to general procedure B from **S3.1b** (392 mg, 1.5 mmol) and $NaBH_4$ (170, 4.5 mmol). Eluent: 16:1 hexanes/ethyl acetate. Isolated yield: 91% (360 mg, 1.4 mmol), pale yellow oil.

^{1}H NMR (500 MHz, $CDCl_3$) δ 7.35-7.28 (m, 6H), 7.12 (t, *J* = 7.5 Hz, 1H), 6.83-6.78 (m, 1H), 6.75-6.71 (m, 1H), 4.61 (s, 1H), 1.87 (d, *J* = 10 Hz, 2H), 1.72 (d, *J* = 10 Hz), 1.65-1.40 (m, 4H), 1.22-1.18 (m, 2H); ^{13}C NMR (125 MHz, $CDCl_3$) δ 150.3, 141.4, 137.3, 128.3, 128.1, 127.8, 127.6, 124.5, 118.6, 108.9, 73.2, 49.3, 37.5, 32.0, 25.9, 23.2, 22.3; HRMS (ESI) exact mass for MH^+ ($C_{18}H_{22}N$) calcd *m/z* 264.1747 found 264.1745.

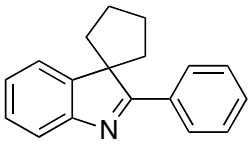

2'-Phenylspiro[cyclopentane-1,3'-indole], S3.1c: Prepared according to general procedure A from cyclopentyl phenyl ketone (doi: 10.1016/S0040-4020(03)01091-3) (490 mg, 2.8 mmol) and phenylhydrazine (550 µl, 5.6 mmol). Eluent: 9:1 hexanes/diethyl ether. Isolated yield: 69% (480 mg, 1.9 mmol), colorless oil.
^{1}H NMR (300 MHz, $CDCl_3$) δ 8.12-8.05 (m, 2H) 7.68 (d, *J* = 7.5 Hz, 1H), 7.48 (m, 3H), 7.41-7.32 (m, 2H), 7.22 (d, *J* = 4.0 Hz, 1H); ^{13}C NMR (125 MHz, $CDCl_3$) δ 182.7, 153.0, 150.3, 132.8, 130.5, 128.6, 128.3, 127.4, 125.9, 121.0, 120.7, 63.3, 36.9, 27.6; HRMS (ESI) exact mass for MH^+ ($C_{18}H_{18}N$) calcd *m/z* 248.1434 found 248.1432.

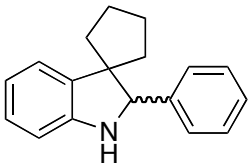

2'-Phenylspiro[cyclopentane-1,3'-indoline], (±)-**3.17c**: Prepared according to general procedure B from **S3.1c** (250 mg, 1.0 mmol) and $NaBH_4$ (190, 5.0 mmol). Eluent: 19:1 hexanes/ethyl acetate. Isolated yield: 55% (135 mg, 0.55 mmol), pale yellow oil.

^{1}H NMR (500 MHz, $CDCl_3$) δ 7.40-7.30 (m, 5H), 7.10 (t, J = 7.5 Hz, 2H), 6.82 (t, J = 7.5 Hz, 1H), 6.75-6.80 (m, 1H), 4.68 (s, 1H), 2.04 (t, J = 7.0 Hz, 2H), 1.90-1.80 (m, 1H), 1.75-1.60 (m, 2H), 1.47 (t, J = 7.0 Hz, 2H), 1.30-1.22 (m, 1H); ^{13}C NMR (125 MHz, $CDCl_3$) δ 150.0, 141.3, 128.2, 128.4, 127.8, 127.5, 123.0, 119.2, 108.9, 73.9, 57.4, 39.7, 35.07, 24.8, 24.7; HRMS (ESI) exact mass for MH^+ ($C_{18}H_{20}N$) calcd *m/z* 250.1590 found 250.1589.

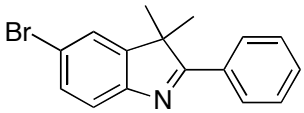

5-Bromo-3,3-dimethyl-2-phenyl-3*H*-indole, S3.1d: Prepared according to general procedure A from isopropyl phenyl ketone (1510 µl, 10 mmol) and p-bromophenylhydrazine hydrochloride (2.24 g, 10 mmol). Eluent: 19:1 hexanes/ethyl acetate. Isolated yield: 48% (1.43 g, 4.8 mmol), tan crystalline solid.

^{1}H NMR (500 MHz, $CDCl_3$) δ 8.15 (m, 2H), 7.57 (d, J = 8.5 Hz) 7.53-7.49 (m, 5H), 1.62 (s, 6H); ^{13}C NMR (125 MHz, $CDCl_3$) δ 183.7, 152.2, 149.9, 133.0, 131.6, 131.4, 128.9, 128.5, 124.7, 122.4, 119.7, 54.2, 24.8; HRMS (ESI) exact mass for MH^+ ($C_{16}H_{15}N^{79}Br$) calcd *m/z* 300.0382 found 300.0380.

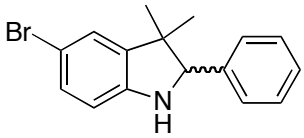

5-Bromo-3,3-dimethyl-2-phenylindoline, (±)-**3.17d**: Prepared according to general procedure B from **S3.1d** (300 mg, 1.0 mmol) and $NaBH_4$ (190, 5.0 mmol). Eluent: 19:1 hexanes/ethyl acetate. Isolated yield: 91% (275 mg, 0.91 mmol), pale tan powder.

^{1}H NMR (500 MHz, $CDCl_3$) δ 7.44 (d, J = 7.0 Hz, 2H), 7.39-7.32 (m, 3H), 7.18 (dd, J = 8.5 Hz, 2.0 Hz, 1H), 7.14 (d, J = 2.0 Hz, 1H), 6.62 (d, J = 8.0 Hz, 1H), 4.62 (s, 1H), 1.48 (s, 3H), 0.75 (s, 3H); ^{13}C NMR (125 MHz, $CDCl_3$) δ 148.5, 140.7, 139.5, 130.2, 128.4, 127.9, 127.5, 125.9, 110.7, 110.7, 74.9, 45.8, 26.7, 24.6,; HRMS (ESI) exact mass for MH^+ ($C_{16}H_{17}N^{79}Br$) calcd *m/z* 302.0539 found 302.0539.

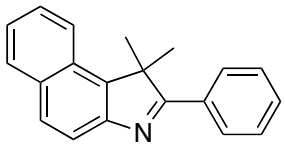

1,1-Dimethyl-2-phenyl-1*H*-benzo[*e*]indole, S3.1e: Prepared according to general procedure A from isopropylphenyl ketone (750 µl, 5 mmol) and 2-naphthylhydrazine hydrochloride (900 mg, 5 mmol). Eluent: 19:1 hexanes/ethyl acetate. Isolated yield: 40% (540 mg, 2.0 mmol), colorless solid.

^{1}H NMR (300 MHz, $CDCl_3$) δ 8.23-8.20 (m, 2H), 8.13 (d, J = 8.4 Hz, 1H), 7.98 (d, J = 8.1 Hz, 1H), 7.95-7.90 (m, 2H), 7.61-7.45 (m, 5H), 1.84 (s, 6H); ^{13}C NMR (125 MHz, $CDCl_3$) δ 185.3, 150.3, 140.6, 133.1, 132.8, 130.5, 129.9, 129.2, 128.7, 128.3, 128.1, 126.4, 124.7, 122.8, 120.6, 55.4, 24.2; HRMS (ESI) exact mass for MH^+ ($C_{20}H_{18}N$) calcd *m/z* 272.1434 found 272.1434.

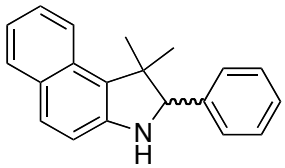

1,1-Dimethyl-2-phenyl-2,3-dihydro-1*H*-benzo[*e*]indole, (±)-**3.17e**: Prepared according to general procedure B from **S3.1e** (270 mg, 1.0 mmol) and $NaBH_4$ (190, 5.0 mmol). Eluent: 24:1 hexanes/diethyl ether. Isolated yield: 66% (180 mg, 0.66 mmol), pale yellow oil.

^{1}H NMR (400 MHz, $CDCl_3$) δ 7.96 (d, J = 8.8 Hz, 1H), 7.78 (d, J = 8.0 Hz, 1H), 7.65 (d, J = 8.8 Hz, 1H), 7.54 (d, J = 7.2 Hz, 2H), 7.39-7.34 (m, 4H), 7.20 (t, J = 8.0 Hz, 1H), 7.02 (d, J = 8.4 Hz, 1H), 4.73 (s, 1H), 4.30 (br s, 1H), 1.77 (s, 3H), 1.00 (s, 3H); ^{13}C NMR (125 MHz, $CDCl_3$) δ 147.3, 129.8, 131.2, 129.8, 129.7, 129.1, 128.3, 128.2, 127.8, 126.7, 126.3, 121.7, 121.7, 113.0, 75.3, 47.3, 27.6, 23.2; HRMS (ESI) exact mass for MH^+ ($C_{20}H_{20}N$) calcd *m/z* 274.1590 found 274.1594.

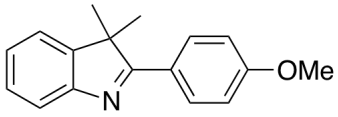

2-(4-Methoxyphenyl)-3,3-dimethyl-3*H*-indole, S3.1f: Prepared according to general procedure A from isopropyl 4-methoxyphenyl ketone (doi: 10.1021/ol7015065) (660 mg, 3.7 mmol) and phenylhydrazine (360 µl, 3.7 mmol). Eluent: 7:1 hexanes/ethyl acetate. Isolated yield: 76% (710 mg, 2.82 mmol), colorless powder.
^{1}H NMR (500 MHz, $CDCl_3$) δ 8.15-8.20 (m, 2H), 7.68 (app s, 1H), 7.39-7.35 (m, 2H), 7.26 (d, J = 7.5 Hz, 1H), 7.03 (d, J = 8.0 Hz, 2H), 3.91 (s, 3H), 1.62 (s, 6H); ^{13}C NMR (125 MHz, $CDCl_3$) δ 182.8, 161.7, 153.4, 147.6, 130.2, 127.9, 126.0, 125.5, 121.0, 120.6, 114.1, 55.5, 53.4, 25.2; HRMS (ESI) exact mass for MH^+ ($C_{17}H_{18}NO$) calcd *m/z* 252.1383 found 252.1381.

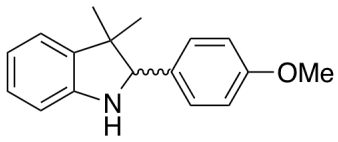

2-(4-Methoxyphenyl)-3,3-dimethylindoline, (±)-**3.17f**: Prepared according to general procedure B from **S3.1f** (250 mg, 1.0 mmol) and $NaBH_4$ (190, 5.0 mmol). Eluent: 19:1 hexanes/ethyl acetate. Isolated yield: 75% (190 mg, 0.75 mmol), pale tan powder.

^{1}H NMR (400 MHz, $CDCl_3$) δ 7.42 (d, *J* = 8.8 Hz, 2H), 7.15-7.09 (m, 2H), 6.96-6.93 (m, 2H), 6.83 (td, *J* = 7.2 Hz, 0.8 Hz, 1H), 6.76 (d, *J* = 7.6 Hz, 1H), 4.60 (s, 1H), 4.14 (br s, 1H), 3.87 (s, 3H), 1.45 (s, 3H), 0.79 (s, 3H); ^{13}C NMR (125 MHz, $CDCl_3$) δ 159,2, 149.5, 138.3, 132.0, 128.6, 127.5, 122.7, 119.0, 113.6, 109.3, 74.2, 55.4, 45.4, 26.5, 24.6; HRMS (ESI) exact mass for MH^+ ($C_{17}H_{20}NO$) calcd *m/z* 254.1539 found 254.1537.

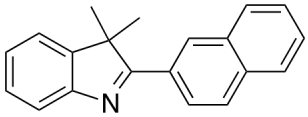

3,3-Dimethyl-2-(naphthalen-2-yl)-3*H*-indole, S3.1g: Prepared according to general procedure A from isopropyl 2-naphthyl ketone (doi: 10.1021/ol7015065) (410 mg, 2.1 mmol) and phenylhydrazine (210 µl, 2.1 mmol). Eluent: 19:1 hexanes/ethyl acetate. Isolated yield: 67% (380 mg, 1.4 mmol), colorless crystalline solid.
^{1}H NMR (500 MHz, $CDCl_3$) δ 8.56 (s, 1H), 8.41 (d, *J*, = 9.0 Hz, 1H), 8.02-7.99 (m, 1H), 7.97 (d, *J* = 9.0 Hz, 1H), 7.92-7.90 (m, 1H), 7.77 (d, *J* = 7.5 Hz, 1H), 7.60-7.55 (m, 2H), 7.42-7.40 (m, 2H), 7.33 (t, *J* = 7.0 Hz, 1H); ^{13}C NMR (125 MHz, $CDCl_3$) δ 183.2, 153.3, 147.9, 134.5, 133.1, 130.8, 129.2, 128.7, 128.5, 128.0, 127.9, 127.6, 126.7, 126.1, 125.7, 121.1, 121.1, 53.8, 25.3; HRMS (ESI) exact mass for MH^+ ($C_{20}H_{18}N$) calcd *m/z* 272.1434 found 272.1432.

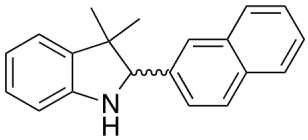

3,3-Dimethyl-2-(naphthalen-2-yl)indoline, (±)-3.17g: Prepared according to general procedure B from **S3.1g** (270 mg, 1.0 mmol) and $NaBH_4$ (190, 5.0 mmol). Eluent: 19:1 hexanes/ethyl acetate. Isolated yield: 76% (210 mg, 0.76 mmol), colorless crystalline solid.

^{1}H NMR (500 MHz, $CDCl_3$) δ 7.96 (s, 1H), 7.88-7.86 (m, 2H), 7.85 (d, *J* = 8.5 Hz, 1H), 7.60 (d, *J* = 8.5 Hz, 1H), 7.53-7.48 (m, 2H), 7.13 (d, *J* = 7.5 Hz, 1H), 7.11 (d, *J* = 7.5 Hz, 1H), 6.85 (t, *J* = 7.5 Hz, 1H), 6.80 (d, *J* = 8.0 Hz, 1H), 4.81 (s, 1H), 1.52 (s, 3H), 0.79 (s, 3H).; ^{13}C NMR (125 MHz, $CDCl_3$) δ 149.4, 138.3, 137.7, 133.4, 133.3, 128.1, 127.9, 127.8, 127.7, 126.3, 126.3, 126.0, 125.9, 122.7, 119.3, 109.5, 74.8, 45.8, 26.9, 24.9; HRMS (ESI) exact mass for MH^+ ($C_{20}H_{20}N$) calcd *m/z* 274.1590 found 274.1588.

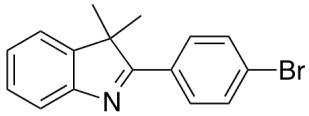

2-(4-Bromophenyl)-3,3-dimethyl-3*H*-indole, S3.1h: Prepared according to general procedure A from isopropyl 4-bromophenyl ketone (doi:http://dx.doi.org/10.1016/S0040-4020(00)01097-8) (630 mg, 2.8 mmol) and phenylhydrazine (550 µl, 5.6 mmol). Eluent: 19:1 hexanes/ethyl acetate. Isolated yield: 56% (470 mg, 1.6 mmol), colorless crystalline solid.
^{1}H NMR (400 MHz, $CDCl_3$) δ 8.03 (d, *J* = 8.8 Hz, 2H), 7.70 (d, *J* = 7.6 Hz, 1H), 7.63 (d, *J* = 8.8 Hz, 2H), 7.40-7.28 (m, 3H), 1.58 (s, 6H); ^{13}C NMR (125 MHz, $CDCl_3$) δ 182.1, 152.9, 147.5, 132.1, 131.9, 129.8, 127.9, 126.2, 125.2, 121.0, 121.0, 53.5, 24.7; HRMS (ESI) exact mass for MH^+ ($C_{16}H_{15}N^{79}Br$) calcd *m/z* 300.0382 found 300.0382.

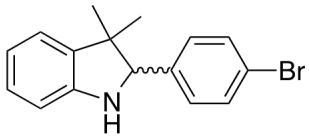

2-(4-Bromophenyl)-3,3-dimethylindoline, (±)-**3.17h**: Prepared according to general procedure B from **S3.1h** (300 mg, 1.0 mmol) and $NaBH_4$ (190, 5.0 mmol). Eluent: 19:1 hexanes/ethyl acetate. Isolated yield: 85% (255 mg, 0.85 mmol), colorless crystalline solid.

^{1}H NMR (500 MHz, $CDCl_3$) δ 7.50 (d, *J* = 8.0 Hz, 2H), 7.37 (d, *J* = 8.0 Hz, 2H), 7.13-7.07 (m, 2H), 6.88-6.82 (m, 1H), 6.79-6.75 (m, 1H), 4.69 (s, 1H), 1.44 (s, 3H), 0.75 (s, 3H); ^{13}C NMR (125 MHz, $CDCl_3$) δ 149.2, 139.1, 138.0, 131.4, 129.3, 127.7, 122.7, 121.4, 119.4, 109.5, 74.0, 45.5, 26.5, 24.7; HRMS (ESI) exact mass for MH^+ ($C_{16}H_{17}N^{79}Br$) calcd *m/z* 302.0539 found 302.0540.

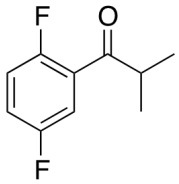

1-(2,5-Difluorophenyl)-2-methylpropan-1-one, **S3.2i**: To an oven-dried 250 ml round bottom flask under N_2 was added 2,5-difluorobenzaldehyde (1100 ul, 10 mmol) and THF (0.1 M). The reaction mixture was cooled to 0 ^{o}C and iPrMgCl•LiCl (9.2 ml of a 1.3 M solution in THF, 12 mmol) was added by syringe over 2 min. The reaction mixture was allowed to warm to room temperature and after 15 min, the reaction was quenched by addition of sat aq NH_4Cl. Crude product was extracted with Et_2O (2 x 50 ml). Combined organics were dried with $MgSO_4$, filtered, and concentrated under high vacuum. To the crude alcohol was added DCM (0.1 M) and DMSO (1.6 ml, 22 mmol) and the reaction mixture was cooled under N_2 to -78 ^{o}C, Oxalyl chloride (940 ul, 11 mmol) was added dropwise, and the reaction mixture stirred for 1 h. NEt_3 (7 ml, 50 mmol) was added and the reaction mixture was allowed to warm to room temp. The reaction was quenched by addition of H_2O (50 ml). The organic phase was removed, and the aqueous phase was

extracted with DCM (2 x 50 ml). The combined organics were dried with $MgSO_4$, filtered, and concentrated. The crude product was purified by flash column chromatography on SiO_2 (9:1 hexanes/ethyl acetate). Yield: 19% (1.9 mmol, 350 mg), yellow powder.

^{1}H NMR (300 MHz, $CDCl_3$) δ 7.49-7.43 (m, 1H), 7.20-7.06 (m, 2H), 3.38 (septet, J = 6.9 Hz, 1H), 1.19 (d, J = 6.9 Hz, 6H); ^{13}C NMR (125 MHz, $CDCl_3$) δ 202.1 (d, $J_{3C\text{-}F}$ = 6 Hz), 159.3 (d, $J_{1C\text{-}F}$ = 200 Hz), 156.8 (d, $J_{1C\text{-}F}$ = 204 Hz), 127.0 (dd, $J_{2C\text{-}F}$ = 21 Hz, $J_{3C\text{-}F}$ = 8 Hz), 120.8 (dd, $J_{2C\text{-}F}$ = 19 Hz, $J_{3C\text{-}F}$ = 11 Hz), 118.2 (dd, $J_{2C\text{-}F}$ = 35 Hz, $J_{3C\text{-}F}$ = 10 Hz), 117.0 (dd, $J_{2C\text{-}F}$ = 31 Hz, $J_{3C\text{-}F}$ = 4 Hz), 40.3, (d, J = 4 Hz), 18.5; ^{19}F NMR (376 MHz, $CDCl_3$) δ -116.3 (m). -116.9 (m);

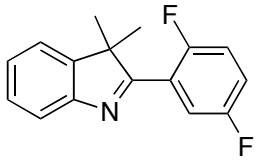

2-(2,5-Difluorophenyl)-3,3-dimethyl-3*H*-indole, **S3.1i**: Prepared according to general procedure A from 1-(2,5-difluorophenyl)-2-methylpropan-1-one (**S3.2i**) (240 mg, 1.3 mmol) and phenylhydrazine (260 µl, 2.6 mmol). Eluent: 19:1 hexanes/ethyl acetate. Isolated yield: 79% (265 mg, 1.0 mmol), pale tan solid.

^{1}H NMR (500 MHz, $CDCl_3$) δ 7.72 (d, J = 7.5 Hz, 1H), 7.42-7.32 (m, 4H), 7.19-7.16 (m, 2H), 1.47 (s, 6H); ^{13}C NMR (125 MHz, $CDCl_3$) δ 181.5, 158.5 (d, $J_{1C\text{-}F}$ = 242 Hz), 156.5 (d, $J_{1C\text{-}F}$ = 265 Hz), 153.1, 146.3, 128.0, 126.7, 124.0 (dd, $J_{2C\text{-}F}$ = 18 Hz, $J_{3C\text{-}F}$ = 9 Hz), 121.5, 121.5, 118.1 (dd, $J_{2C\text{-}F}$ = 24 Hz, $J_{3C\text{-}F}$ = 9 Hz), 117.8 (dd, $J_{2C\text{-}F}$ = 26 Hz, $J_{3C\text{-}F}$ = 9 Hz), 117.1 (dd, $J_{2C\text{-}F}$ = 25 Hz, $J_{3C\text{-}F}$ = 4 Hz), 55.6, 23.0 (d, J = 4 Hz); ^{19}F NMR (376 MHz, $CDCl_3$) δ -115.6 (m). -117.8 (m); HRMS (ESI) exact mass for MH^+ ($C_{16}H_{14}NF_2$) calcd *m/z* 258.1089 found 258.1089.

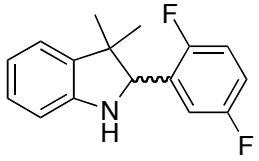

2-(2,5-Difluorophenyl)-3,3-dimethylindoline, (±)-**3.17i**: Prepared according to general procedure B from **S3.1i** (265 mg, 1.0 mmol) and $NaBH_4$ (190, 5.0 mmol). Eluent: 24:1 hexanes/diethyl ether. Isolated yield: 89% (230 mg, 0.89 mmol), colorless crystalline solid.

^{1}H NMR (300 MHz, $CDCl_3$) δ 7.43-7.37 (m, 1H), 7.11-6.89 (m, 4H), 6.80 (t, J = 7.2 Hz, 1H), 6.72 (d, J = 7.8 Hz, 1H), 4.98 (s, 1H), 3.98 (br s, 1H), 1.46 (d, J = 2.1 Hz, 3H), 0.83 (s, 3H); ^{13}C NMR (125 MHz, $CDCl_3$) δ 158.8 (d, $J_{1C\text{-}F}$ = 242 Hz), 156.6 (d, $J_{1C\text{-}F}$ = 240 Hz), 148.9,137.5, 129.7 (dd, $J_{2C\text{-}F}$ = 16 Hz, $J_{3C\text{-}F}$ = 7 Hz), 127.6, 122.5, 119.4, 116.2 (dd, $J_{2C\text{-}F}$ = 25 Hz, d, $J_{3C\text{-}F}$ = 9 Hz), 115.7 (dd, $J_{2C\text{-}F}$ = 25 Hz, d, $J_{3C\text{-}F}$ = 5 Hz), 115.0 (dd, $J_{2C\text{-}F}$ = 24 Hz, d, $J_{3C\text{-}F}$ = 9 Hz), 109.3, 66.7, 46.0, 27.6 (d, $J_{C\text{-}F}$ = 3 Hz), 24.8; ^{19}F NMR (376 MHz, $CDCl_3$) δ -117.9 (br s), -122.1 (br s) ; HRMS (ESI) exact mass for MH^+ ($C_{16}H_{16}NF_2$) calcd *m/z* 260.1245 found 260.1247.

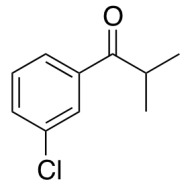

1-(3-Chlorophenyl)-2-methylpropan-1-one, S3.2j: To an oven-dried 250 ml round bottom flask under N_2 was added 3-chlorobenzaldehyde (1100 ul, 10 mmol) and THF (0.1 M). The reaction mixture was cooled to 0 ^oC and iPrMgCl•LiCl (9.2 ml of a 1.3 M solution in THF, 12 mmol) was added by syringe over 2 min. The reaction mixture was allowed to warm to room temperature and after 15 min, the reaction was quenched by addition of sat aq NH_4Cl. Crude product was extracted with Et_2O (2 x 50 ml). Combied organics were dried with $MgSO_4$, filtered, and concentrated under high vacuum. To the crude alcohol was added DCM (0.1 M) and DMSO (1.6 ml, 22 mmol) and the reaction mixture was cooled under N_2 to -78 ^oC, Oxalyl chloride (940 ul, 11 mmol) was added dropwise, and the reaction mixture stirred for 1 h. NEt_3 (7 ml, 50 mmol) was added and the reaction mixture was allowed to warm to room temp. The reaction was quenched by addition of H_2O (50 ml). The organic phase was removed, and the aqueous phase was extracted with DCM (2 x 50 ml). The combined organics were dried with $MgSO_4$, filtered, and concentrated. The crude product was purified by flash column chromatography on SiO_2 (9:1 hexanes/ethyl acetate). Yield: 24% (2.4 mmol, 450 mg), yellow powder.

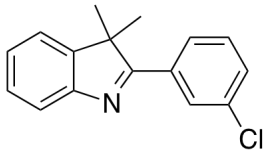

2-(3-Chlorophenyl)-3,3-dimethyl-3*H*-indole, S3.1j: Prepared according to general procedure A 1-(3-chlorophenyl)-2-methylpropan-1-one (**S3.2j**) (445 mg, 2.4 mmol) and phenylhydrazine (600 µl, 6.1 mmol). Eluent: 6:1 hexanes/ethyl acetate. Isolated yield: 64% (390 mg, 1.5 mmol), orange oil.

^1H NMR (300 MHz, $CDCl_3$) d 8.18 (s, 1H), 8.02 (d, J = 7.5 Hz, 1H), 7.72 (d, J = 7.5 Hz, 1H), 7.49-7.31 (m, 5H), 1.61 (s, 6H); ^{13}C NMR (125 MHz, $CDCl_3$) d 181.8, 152.8, 147.5, 135.1, 134.8, 130.5, 129.9, 128.3, 127.9, 126.3, 126.3, 121.2, 121.0, 53.6, 24.6; HRMS (ESI) exact mass for MH^+ ($C_{16}H_{15}N^{35}Cl$) calcd *m/z* 256.0888 found 257.0889.

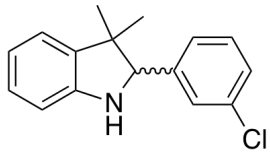

2-(3-Chlorophenyl)-3,3-dimethylindoline, (±)-**3.17j**: Prepared according to general procedure B from **S3.1j** (255 mg, 1.0 mmol) and $NaBH_4$ (190, 5.0 mmol). Eluent: 19:1 hexanes/ethyl acetate. Isolated yield: 85% (220 mg, 0.85 mmol), colorless crystalline solid.

^{1}H NMR (500 MHz, $CDCl_3$) δ 7.51 (s, 1H), 7.35-734 (m, 1H), 7.31-7.30 (m, 2H), 7.11 (t, J = 7.5 Hz, 1H), 7.07 (d, J = 7.0 Hz, 1H), 6.82 (t, J = 7.5 Hz, 1H), 6.75 (d, J = 7.5 Hz, 1H), 4.60 (s, 1H), 4.09 (s, 1H), 1.46 (s, 3H), 0.75 (s, 3H); ^{13}C NMR (125 MHz, $CDCl_3$) δ 149.1, 142.4, 137.9, 134.3, 129.6, 127.8, 127.7, 127.7, 125.8, 122.7, 119.4, 109.4, 74.1, 45.7, 26.6, 24.8; HRMS (ESI) exact mass for MH^+ ($C_{16}H_{17}N^{35}Cl$) calcd *m/z* 302.0539 found 302.0540.

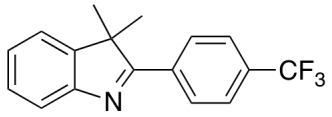

3,3-Dimethyl-2-(4-(trifluoromethyl)phenyl)-3*H*-indole, S3.1k: Prepared according to general procedure A from isopropyl 4-trifluoromethylphenyl ketone (doi:10.1021/ja300503k) (390 mg, 1.8 mmol) and phenylhydrazine (360 µl, 3.6 mmol). Eluent: 19:1 hexanes/ethyl acetate. Isolated yield: 88% (460 mg, 1.6 mmol), yellow crystalline solid.
^{1}H NMR (400 MHz, $CDCl_3$) δ 8.26 (d, J = 8.4 Hz, 2H), 7.77-7.72 (m, 3H), 7.42-7.31 (m, 3H), 1.61 (s, 3H); ^{13}C NMR (125 MHz, $CDCl_3$) δ 181.7, 152.8, 147.5, 136.5, 132.0 (q, $J_{C\text{-}F}$ = 33 Hz), 128.5, 128.0, 126.6, 125.5 (q, $J_{C\text{-}F}$ = 4 Hz), 124.0 (q, $J_{C\text{-}F}$ = 271 Hz), 121.4, 121.1, 53.7, 24.5; ^{19}F NMR (376 MHz, $CDCl_3$) δ -62.1 (s) ; HRMS (ESI) exact mass for MH^+ ($C_{17}H_{15}NF_3$) calcd *m/z* 290.1151 found 290.1149.

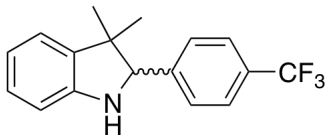

3,3-Dimethyl-2-(4-(trifluoromethyl)phenyl)indoline, (±)-**3.17k**: Prepared according to general procedure B from **S3.1k** (290 mg, 1.0 mmol) and $NaBH_4$ (190, 5.0 mmol). Eluent: 19:1 hexanes/ethyl acetate. Isolated yield: 79% (230 mg, 0.79 mmol), colorless crystalline solid.

^{1}H NMR (500 MHz, $CDCl_3$) δ 7.66-7.61 (m, 4H), 7.15-7.09 (m, 2H), 6.90-6.85 (m, 1H), 6.83-6.79 (m, 1H), 5.70 (s, 1H), 1.48 (s, 3H), 0.75 (s, 3H); ^{13}C NMR (125 MHz, $CDCl_3$) δ 149.1, 144.3, 137.8, 129.9 (q, $J_{C\text{-}F}$ = 33 Hz), 127.9, 127.8, 125.2 (q, $J_{C\text{-}F}$ = 4 Hz), 124.4 (q, $J_{C\text{-}F}$ = 271 Hz), 119.5, 109.6, 74.2, 45.8, 26.6, 24.8; ^{19}F NMR (376 MHz, $CDCl_3$) δ -62.0 (s); HRMS (ESI) exact mass for MH^+ ($C_{18}H_{14}NF_6$) calcd *m/z* 292.1308 found 292.1308.

Deracemization procedures

General procedure C: Deracemization of 3H indolines (±)-**3.17**.

(*S*)-TRIP **3.3a** (3.8 mg, 0.0050 mmol), (±)-**3.17** (0.050 mmol) and the indicated equivalency of Hantzsch ester **3.2d** were deposited as solids in a 1 dram vial with a stir bar. 1.0 ml of a mixture of 9:1 hexanes/diethyl ether was added. To this heterogeneous mixture was added 1.0 ml of an aqueous solution containing the indicated equivalency of oxopiperidinium **3.6** and HCl (0.050 mmol). The reaction mixture was vigorously stirred (800 rpm) for the indicated period of time, at which point the aqueous layer had lost its yellow color (indicating consumption of oxidant) and TLC showed only the presence of 3H indoline (indicating reduction of 3H indole intermediate). The reaction was quenched by addition of 1 ml of a 1:1 mixture of sat. aq. Na_2CO_3/sat. aq. Na_2SO_3. The aqueous phase was extracted with DCM (3 x 4 ml). The combined organics were concentrated and purified directly by flash column chromatography on SiO_2 to give (*S*)-**3.17**. Isolated yield was determined after removal of solvents under high vacuum, with 1H NMR indicating >95% purity.

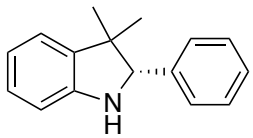

(*S*)-**3.17a**. The reaction was run according to general procedure C employing 1.50 equiv. **3.2d** and 1.55 equiv. **3.6**. Reaction time: 24 h. Isolated yield: 94% (10.3 mg). HPLC: Chiralpak IB column 95:5 hexanes/isopropanol, 1ml/min; t_r = 6.2 min (minor), 12.8 min (major); 94% ee.

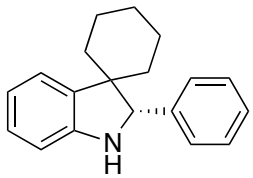

(*S*)-**3.17b**. The reaction was run according to general procedure C employing 1.50 equiv. **3.2d** and 1.55 equiv. **3.6**. Reaction time: 40 h. Isolated yield: 90% (11.8 mg). HPLC: Chiralpak IB column 95:5 hexanes/isopropanol, 1ml/min; t_r = 6.0 min (minor), 8.6 min (major); 93% ee.

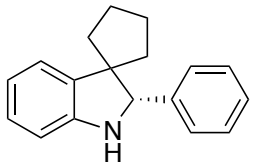

(*S*)-**3.17c**. The reaction was run according to general procedure C employing 1.50 equiv. **3.2d** and 1.55 equiv. **3.6**. Reaction time: 40 h. Isolated yield: 89% (11.1 mg). HPLC: Chiralpak IB column 95:5 hexanes/isopropanol, 1ml/min; t_r = 6.6 min (minor), 10.5 min (major); 93% ee.

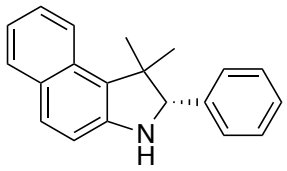

(*S*)-**3.17d**. The reaction was run according to general procedure C employing 1.50 equiv. **3.2d** and 1.55 equiv. **3.6**. Reaction time: 24 h. Isolated yield: 93% (12.6 mg). HPLC: Chiralpak IB column 95:5 hexanes/isopropanol, 1ml/min; t_r = 8.0 min (minor), 15.1 min (major); 93% ee.

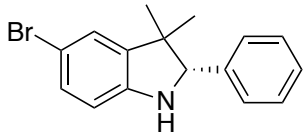

(*S*)-**3.17e**. The reaction was run according to general procedure C employing 1.75 equiv. **3.2d** and 1.80 equiv. **3.6**. Reaction time: 40 h. Isolated yield: 95% (14.3 mg). HPLC: Chiralpak IB column 90:10 hexanes/isopropanol, 1ml/min; t_r = 6.8 min (minor), 19.5 min (major); 93% ee.

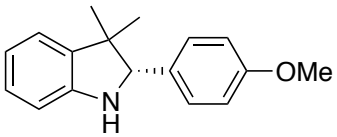

(*S*)-**3.17f**. The reaction was run according to general procedure C employing 1.50 equiv. **3.2d** and 1.55 equiv. **3.6**. Reaction time: 24 h. Isolated yield: 82% (10.4 mg). HPLC: Chiralpak IB column 95:5 hexanes/isopropanol, 1ml/min; t_r = 6.2 min (minor), 9.5 min (major); 88% ee.

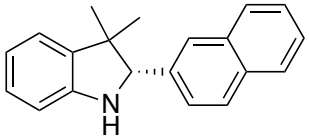

(*S*)-**3.17g**. The reaction was run according to general procedure C employing 1.50 equiv. **3.2d** and 1.55 equiv. **3.6**. Reaction time: 40 h. Isolated yield: 97% (13.3 mg). HPLC: Chiralpak IB column 95:5 hexanes/isopropanol, 1ml/min; t_r = 6.8 min (minor), 15.2 min (major); 91% ee.

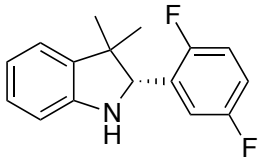

(*S*)-**3.17h**. The reaction was run according to general procedure C employing 1.75 equiv. **3.2d** and 1.80 equiv. **3.6**. Reaction time: 40 h. Isolated yield: 97% (12.6 mg). HPLC:

Chiralpak IB column 95:5 hexanes/isopropanol, 1ml/min; t_r = 5.0 min (minor), 6.3 min (major); 91% ee.

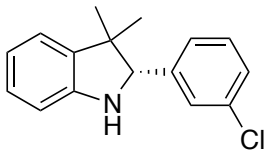

(*S*)-**3.17i**. The reaction was run according to general procedure C employing 1.75 equiv. **3.2d** and 1.80 equiv. **3.6**. Reaction time: 40 h. Isolated yield: 95% (12.2 mg). HPLC: Chiralpak IB column 95:5 hexanes/isopropanol, 1ml/min; t_r = 6.7 min (minor), 13.9 min (major); 94% ee.

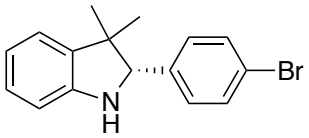

(*S*)-**3.17j**. The reaction was run according to general procedure C employing 1.75 equiv. **3.2d** and 1.80 equiv. **3.6**. Reaction time: 60 h. Isolated yield: 93% (14.1 mg). HPLC: Chiralpak IB column 90:10 hexanes/isopropanol, 1ml/min; t_r = 6.4 min (minor), 12.9 min (major); 94%.

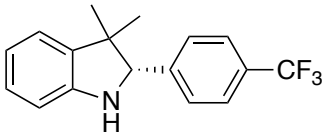

(*S*)-**3.17k**. The reaction was run according to general procedure C employing (*R*)-TCYP as catalyst, 1.75 equiv. **3.2d** and 1.80 equiv. **3.6**. Reaction time: 48 h. Isolated yield: 93% (13.5 mg). HPLC: Chiralpak IB column 95:5 hexanes/isopropanol, 1ml/min; t_r = 6.8 min (minor), 13.9 min (major); 95% ee.

Inversion of (*S*)-**3.17a**.

The reaction was run according to general procedure C employing 1.55 equivalents of **3.2d** and 1.50 equivalents of oxopiperidinium **3.6**, and (*R*)-TRIP as catalyst using (*S*)-**3.17a** (93% ee) as starting material. Reaction time: 24 h. Isolated yield: 98% (11.0 mg). Chiralpak IB column 95:5 hexanes/isopropanol, 1ml/min; t_r = 6.1 min (major), 13.2 min (minor); 94% ee.

Notes and references

1. Faber, K. *Chem. Eur. J.* **2001**, *7*, 5004-5010.
2. Keith, J. M.; Larrow, J. F.; Jacobsen, E. N. *Adv. Synth. Catal.* **2001**, *343*, 5-26.
3. (a) Blackmond, D. G.; Matar, O. K. *J. Phys. Chem. B*, **2008**, *112*, 5098-5104. (b) Blackmond, D. G. *Angew. Chem. Int. Ed.* **2009**, *48*, 2648-2654.
4. (a) P. Walsh, M. Kozlowski, *Fundamentals of Asymmetric Catalysis* (Univ. Science Books, 2008). (b) I. Ojima, Ed., *Catalytic Asymmetric Synthesis* (Wiley-VCH, New York, ed. 2, 2000). (c) Pellissier, H. *Adv. Synth. Catal.* **2011**, *353*, 1613-1666. (d) T. C. Nugent, Ed., *Chiral Amine Synthesis* (Wiley-VCH, Weinheim, 2010). (e) P. G. Andersson, I. J. Munslow, Eds., *Modern Reduction Methods* (Wiley-VCH, Weinheim, 2008).
5. (a) Cohen, B. J.; Kraus, M. A.; Patchornik, A.; *J. Am. Chem. Soc.* **1977**, *99*, 4164-4166. (b) Davies, I. W.; Matty, L.; Hughes, D. L. Reider, P. J. *J. Am. Chem. Soc.* **2001**, *123*, 10139-10140.
6. (a) Wang, Z.; Jiang, Z. *Asian J. Chem.* **2010**, *22*, 4141-4149. (b) Rueping, M.; Sugiono, E.; Schoepke, F. R. *Synlett* **2010**, *6*, 852-865.
7. Rueping, M.; Sugiono, E.; Azap, C.; Theissmann, T.; Bolte, M. *Org. Lett.* **2005**, *7*, 3781-3783.
8. Wang, Y.-M.; Wu, J.; Hoong, C.; Rauniyar, V.; Toste, F. D. *J. Am. Chem. Soc.* **2012**, *134*, 12928-12931.
9. C.-J. Li. *Acc. Chem. Res.* **2009**, *42*, 335-344.
10. Rueping, M.; Brinkmann, C.; Antonchick, A. P.; Atodiresei, I. *Org. Lett.* **2010**, *12*, 4604-4607.
11. Bobbitt, J. M. *J. Org. Chem.* **1998**, *63*, 9367-9374.
12. Rueping, M.; Theissmann, T. *Chem. Sci.* **2010**, *1*, 473-476.
13. Li, G.; Antilla, J.C. *Org. Lett.* **2009**, *11*, 1075-1078.
14. Qiu, J. C.; Pradhan, P. P.; Blanck, N. B.; Bobbitt, J. M.; Bailey, W. F. *Org. Lett.* **2012**, *14*, 350-353.
15. Roomi, M. W. *J. Med. Chem.* **1975**, *18*, 457-460.
16. Klussmann, M.; Ratjen, L.; Hoffmann, S.; Wakchaure, V.; Goddard, R.; List, B. *Synlett* **2010**, *14*, 2189-2192.
17. Rauniyar, V.; Wang, Z. J.; Burks, H. E.; Toste, F. D. *J. Am. Chem. Soc.* **2011**, *133*, 8486-8489.
18. Barluenga, J.; Jiménez-Aquino, A.; Aznar, F.; Valdés, C. *J. Am. Chem. Soc.* **2009**, *131*, 4031-4041.
19. Kotsuki, H.; Yoshimura, N.; Kadota, I.; Ushio, Y.; Ochi, M. *Synthesis*, **1990**, 401-403.
20. Alonso, E.; Ramón, D. J.; Yus, M. *Tetrahedron* **1997**, *53*, 14355-14368.
21. Ginzel, K.-D.; Brungs, P.; Steckhan, E. *Tetrahedron* **1989**, *45*, 1691-1701.
22. Koeppen, J.; Matthies, D.; Schweim, H. *Liebigs Ann. Chem.* **1985**, *12*, 2383-2389.
23. Wu, J.; Wang, C.; Tang, W.; Pettman, A.; Xiao, J. *Chem. Eur. J.* **2012**, *18*, 9525-9529.
24. Pechacek, J.; Vaclavik, J.; Prech, J.; Sot, P.; Januscak, J.; Vilhanova, B.; Vavrik, J.; Kuzma, M.; Kacer, P. *Tetrahedron: Asymmetry* **2013**, *24*, 233-239.

NMR and HPLC Spectra

3.2c

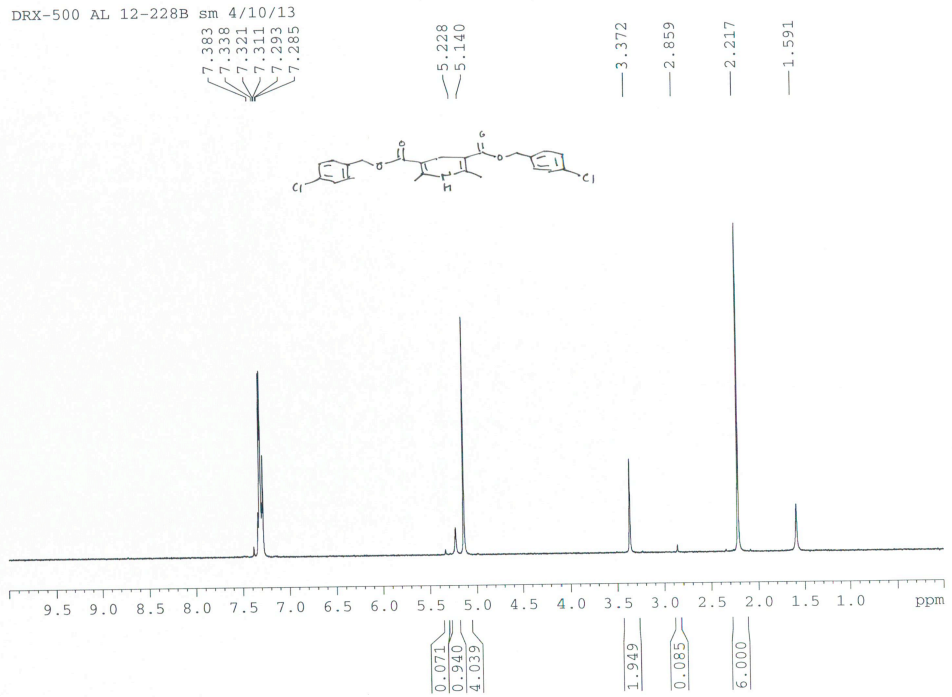

3.2d

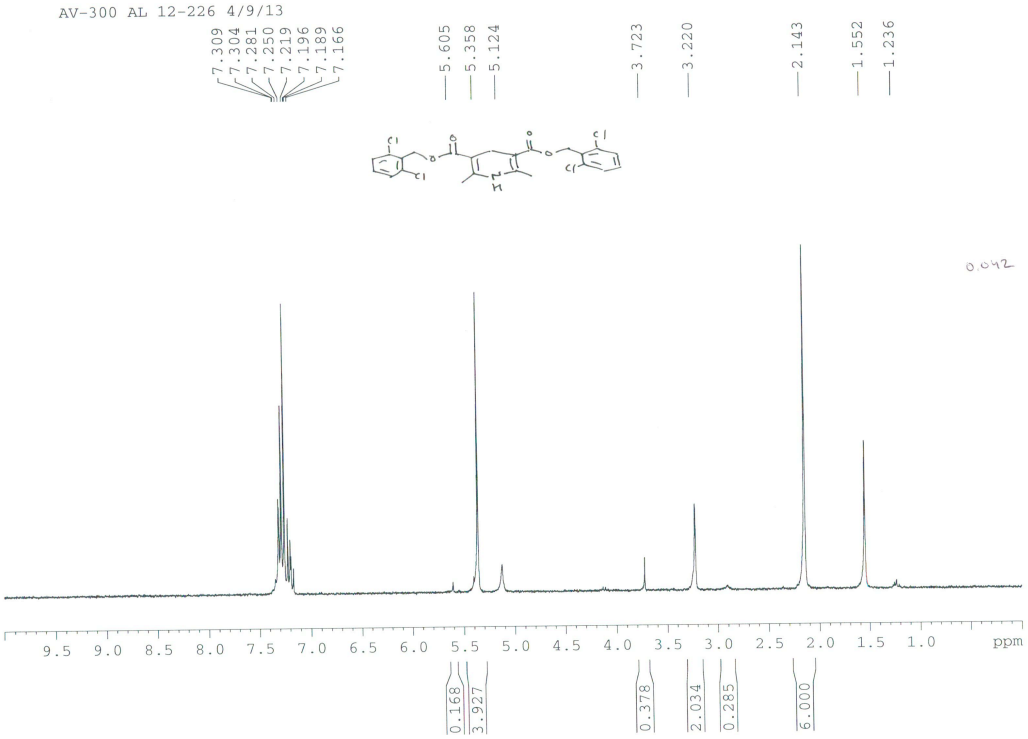

S3.1a

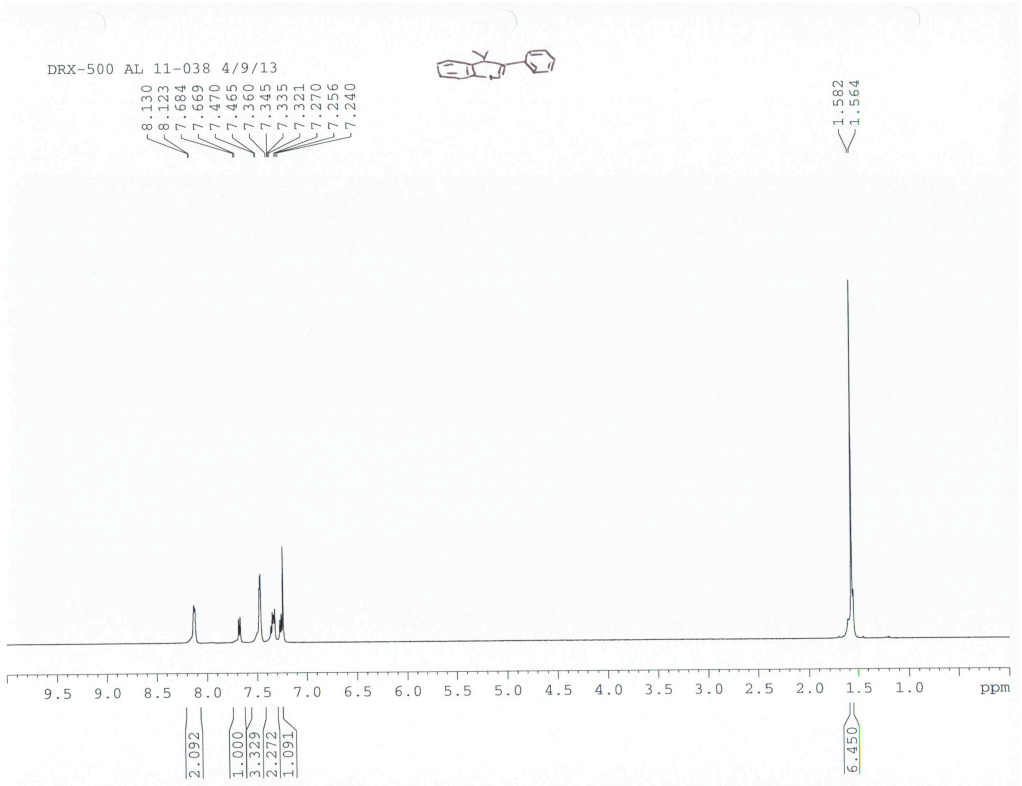
DRX-500 AL 11-038 4/9/13
8.130
8.123
7.684
7.669
7.470
7.465
7.360
7.345
7.335
7.321
7.270
7.256
7.240
1.582
1.564
9.5 9.0 8.5 8.0 7.5 7.0 6.5 6.0 5.5 5.0 4.5 4.0 3.5 3.0 2.5 2.0 1.5 1.0 ppm
2.092
1.000
3.329
2.272
1.091
6.450

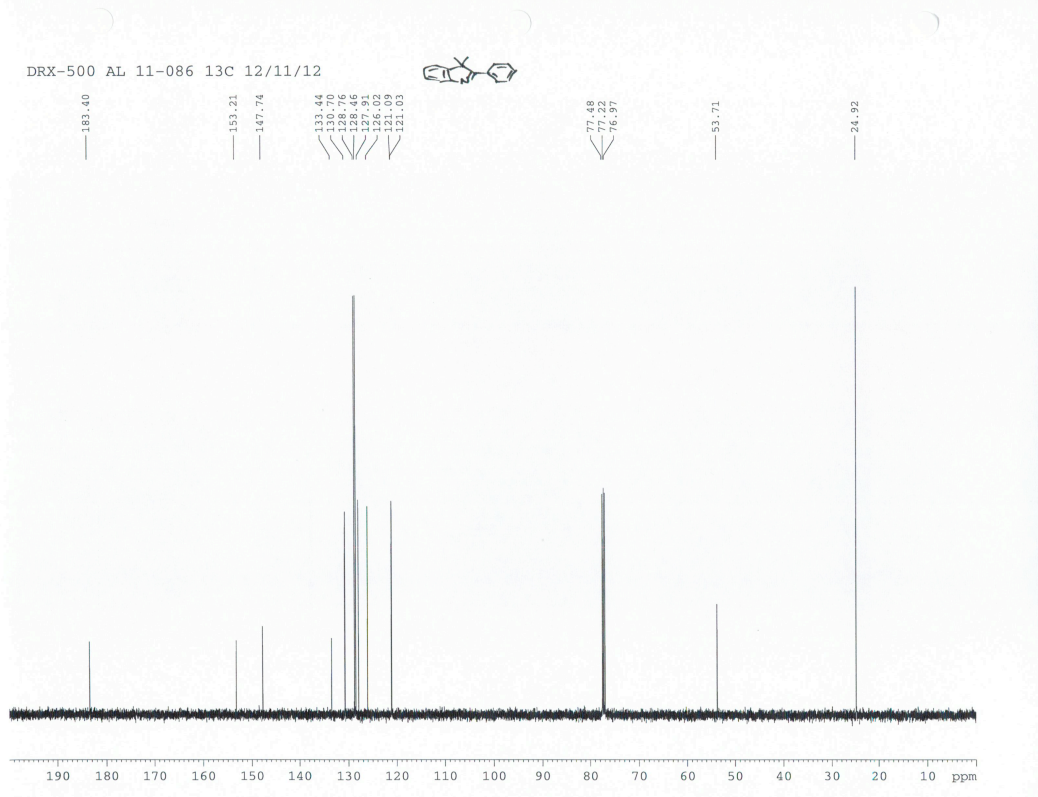
DRX-500 AL 11-086 13C 12/11/12
183.40
153.21
147.74
133.44
130.70
128.76
128.46
127.31
126.02
121.09
121.03
77.48
77.22
76.97
53.71
24.92
190 180 170 160 150 140 130 120 110 100 90 80 70 60 50 40 30 20 10 ppm

S3.1b

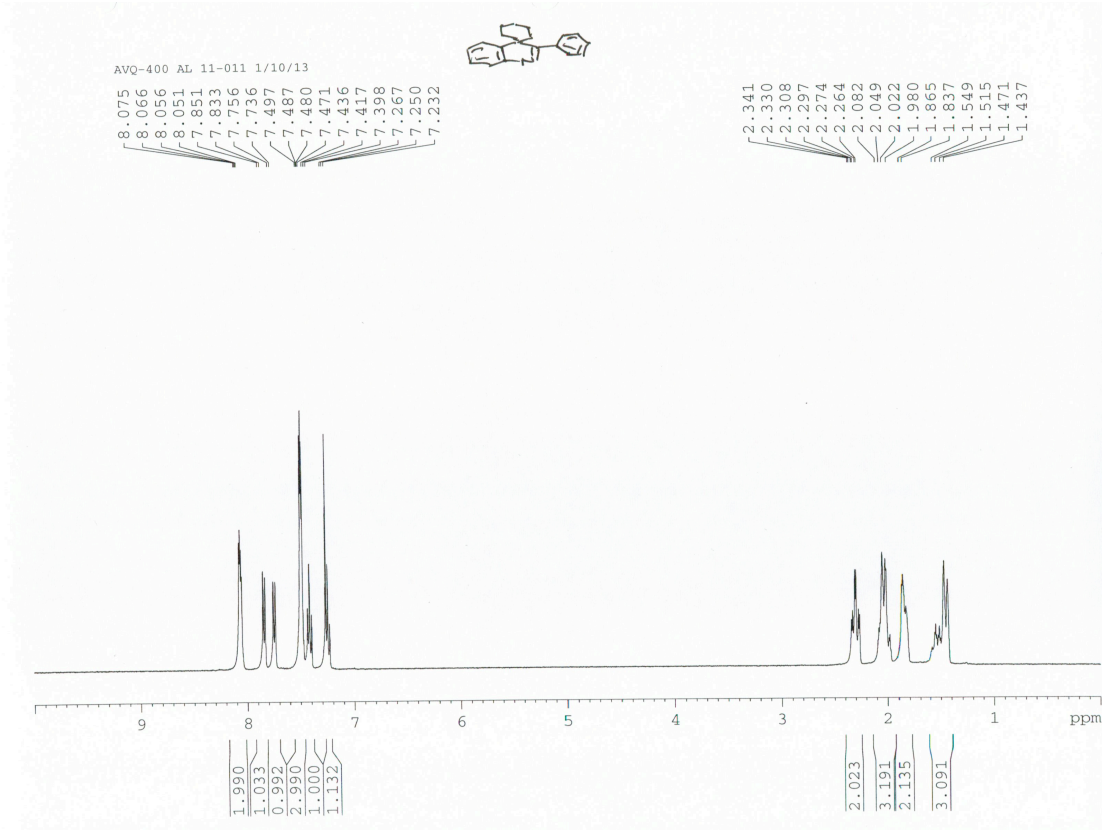
AVQ-400 AL 11-011 1/10/13
8.075
8.066
8.056
8.051
7.851
7.833
7.756
7.736
7.497
7.487
7.480
7.471
7.436
7.417
7.398
7.267
7.250
7.232
2.341
2.330
2.308
2.297
2.274
2.264
2.082
2.049
2.022
1.980
1.865
1.837
1.549
1.515
1.471
1.437
9
8
7
6
5
4
3
2
1
ppm
1.990
1.033
0.992
2.990
1.000
1.132
2.023
3.191
2.135
3.091

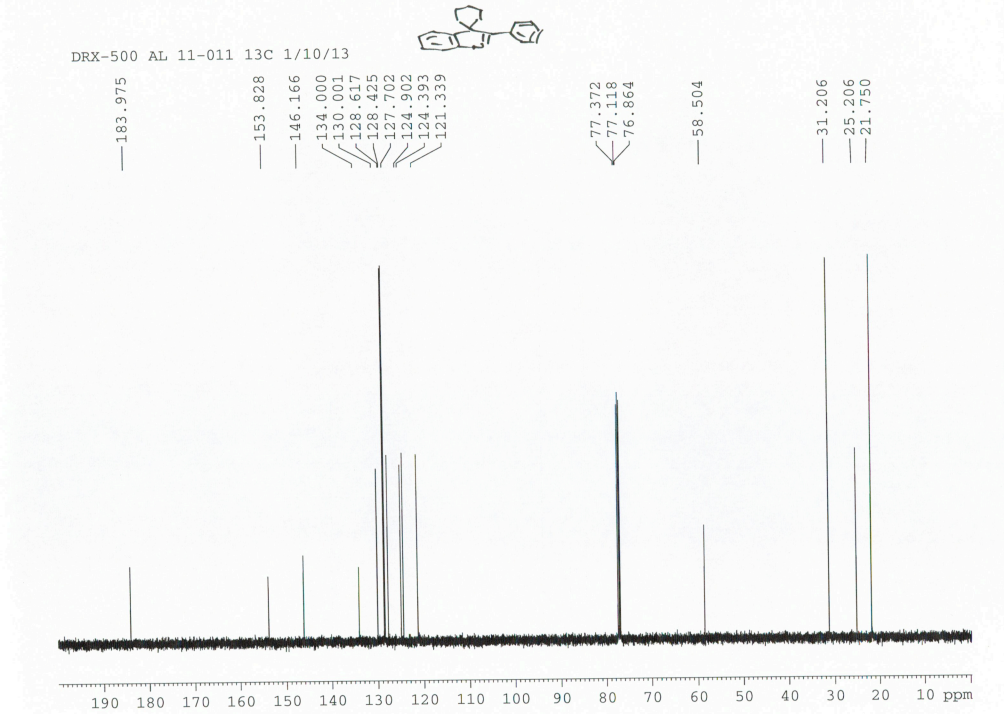
DRX-500 AL 11-011 13C 1/10/13
183.975
153.828
146.166
134.000
130.001
128.617
128.425
127.702
124.902
124.393
121.339
77.372
77.118
76.864
58.504
31.206
25.206
21.750
190 180 170 160 150 140 130 120 110 100 90 80 70 60 50 40 30 20 10 ppm

S3.1c

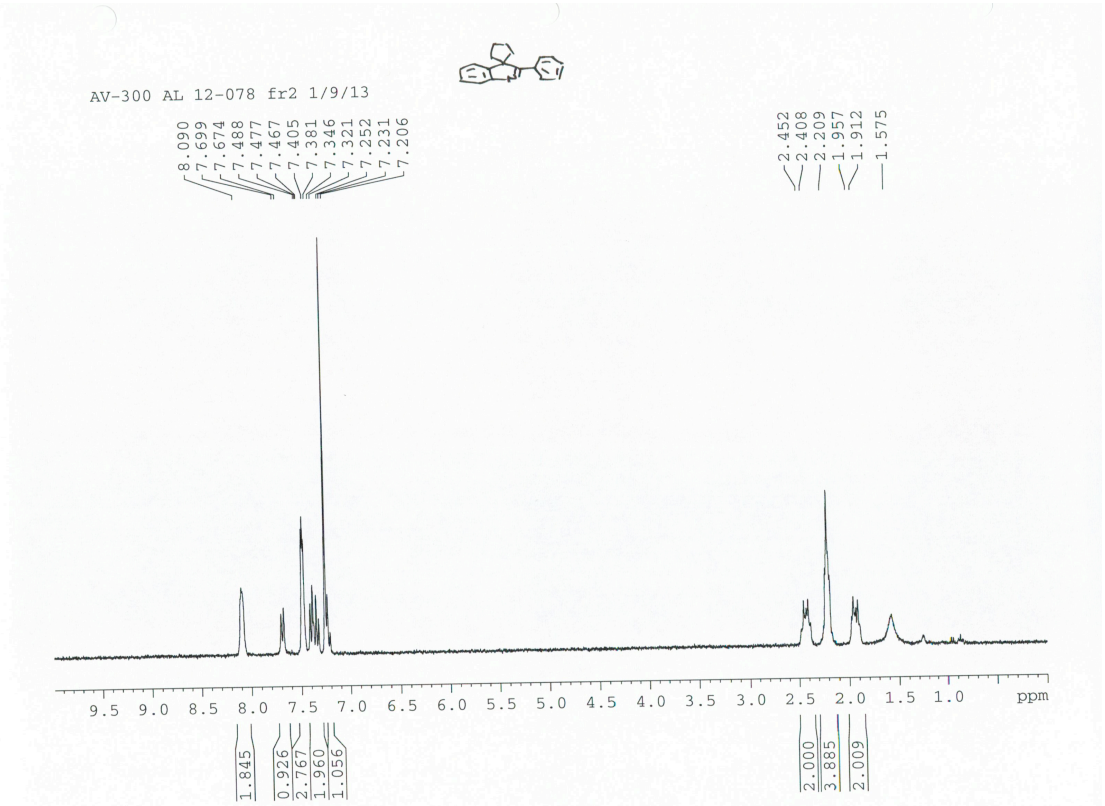
AV-300 AL 12-078 fr2 1/9/13
8.090
7.699
7.674
7.488
7.477
7.467
7.405
7.381
7.346
7.321
7.252
7.231
7.206
2.452
2.408
2.209
1.957
1.912
1.575
9.5 9.0 8.5 8.0 7.5 7.0 6.5 6.0 5.5 5.0 4.5 4.0 3.5 3.0 2.5 2.0 1.5 1.0 ppm
1.845
0.926
2.767
1.960
1.056
2.000
3.885
2.009

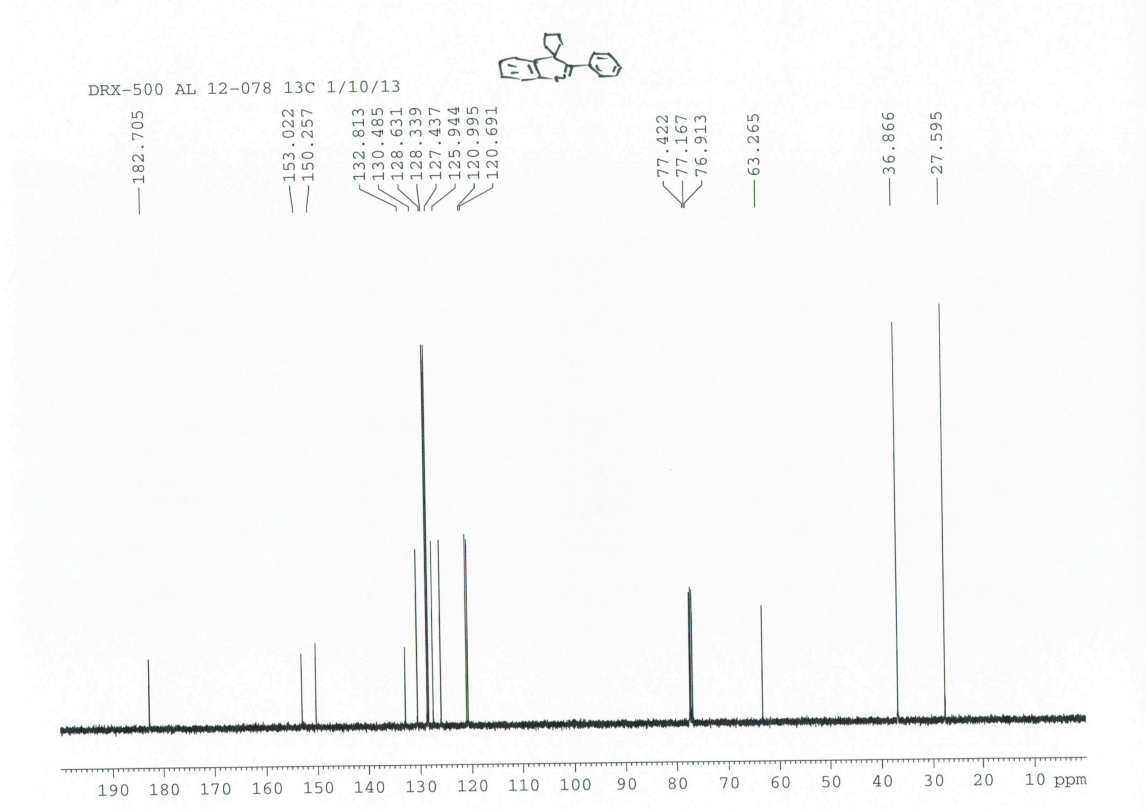
DRX-500 AL 12-078 13C 1/10/13
182.705
153.022
150.257
132.813
130.485
128.631
128.339
127.437
125.944
120.995
120.691
77.422
77.167
76.913
63.265
36.866
27.595
190 180 170 160 150 140 130 120 110 100 90 80 70 60 50 40 30 20 10 ppm

S3.1d

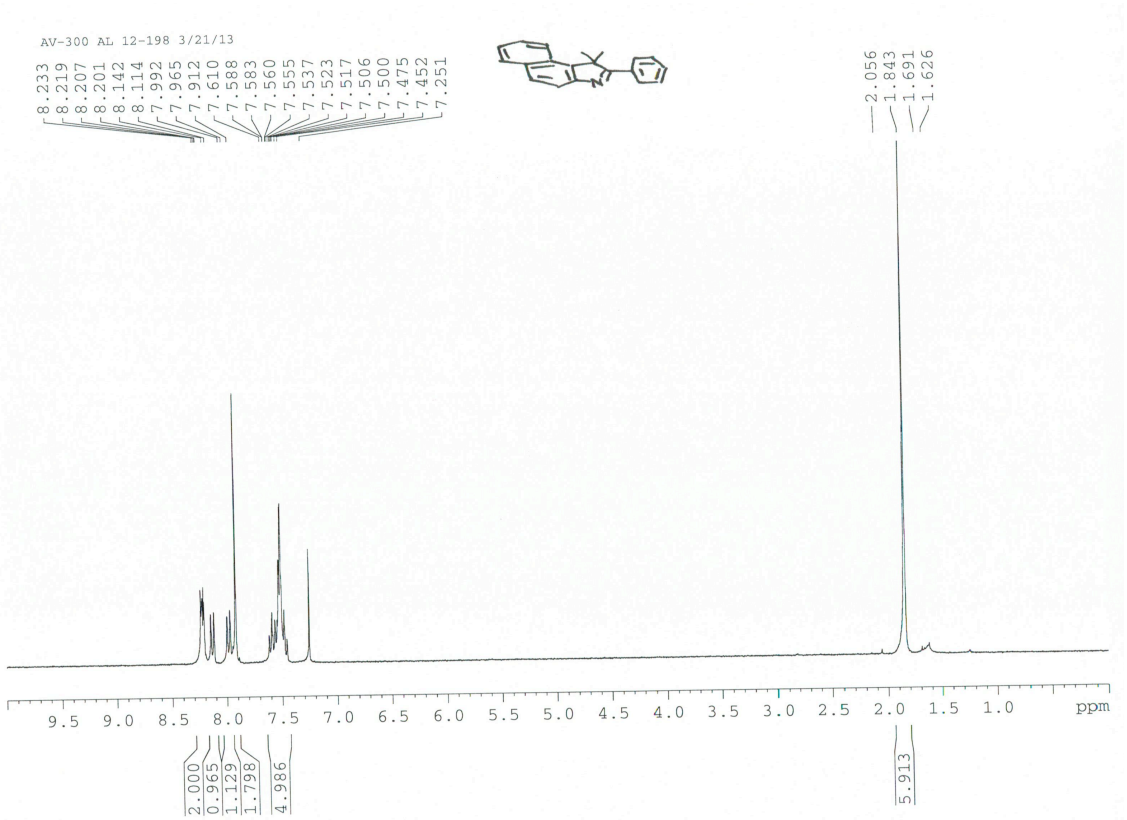
AV-300 AL 12-198 3/21/13
8.233
8.219
8.207
8.201
8.142
8.114
7.992
7.965
7.912
7.610
7.588
7.583
7.560
7.555
7.537
7.523
7.517
7.506
7.500
7.475
7.452
7.251
2.056
1.843
1.691
1.626
9.5 9.0 8.5 8.0 7.5 7.0 6.5 6.0 5.5 5.0 4.5 4.0 3.5 3.0 2.5 2.0 1.5 1.0 ppm
2.000
0.965
1.129
1.798
4.986
5.913

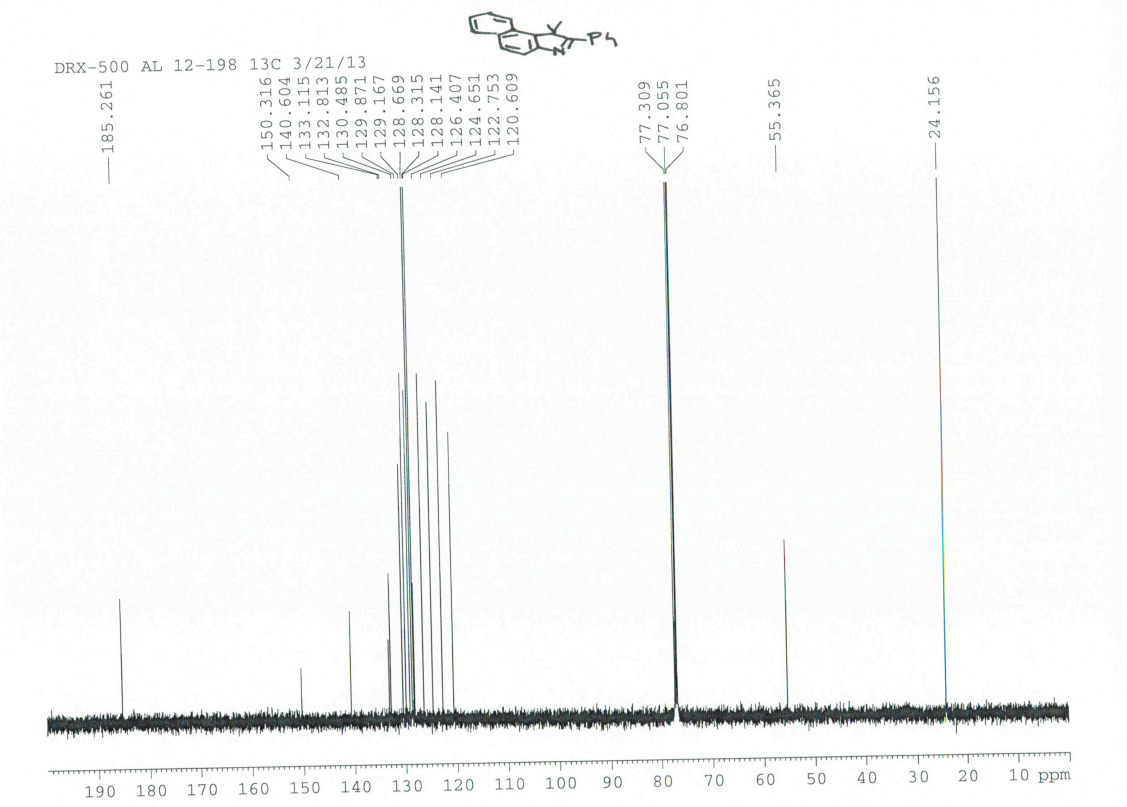
DRX-500 AL 12-198 13C 3/21/13
185.261
150.316
140.604
133.115
132.813
130.485
129.871
129.167
128.669
128.315
128.141
126.407
124.651
122.753
120.609
77.309
77.055
76.801
55.365
24.156
190 180 170 160 150 140 130 120 110 100 90 80 70 60 50 40 30 20 10 ppm

S3.1e

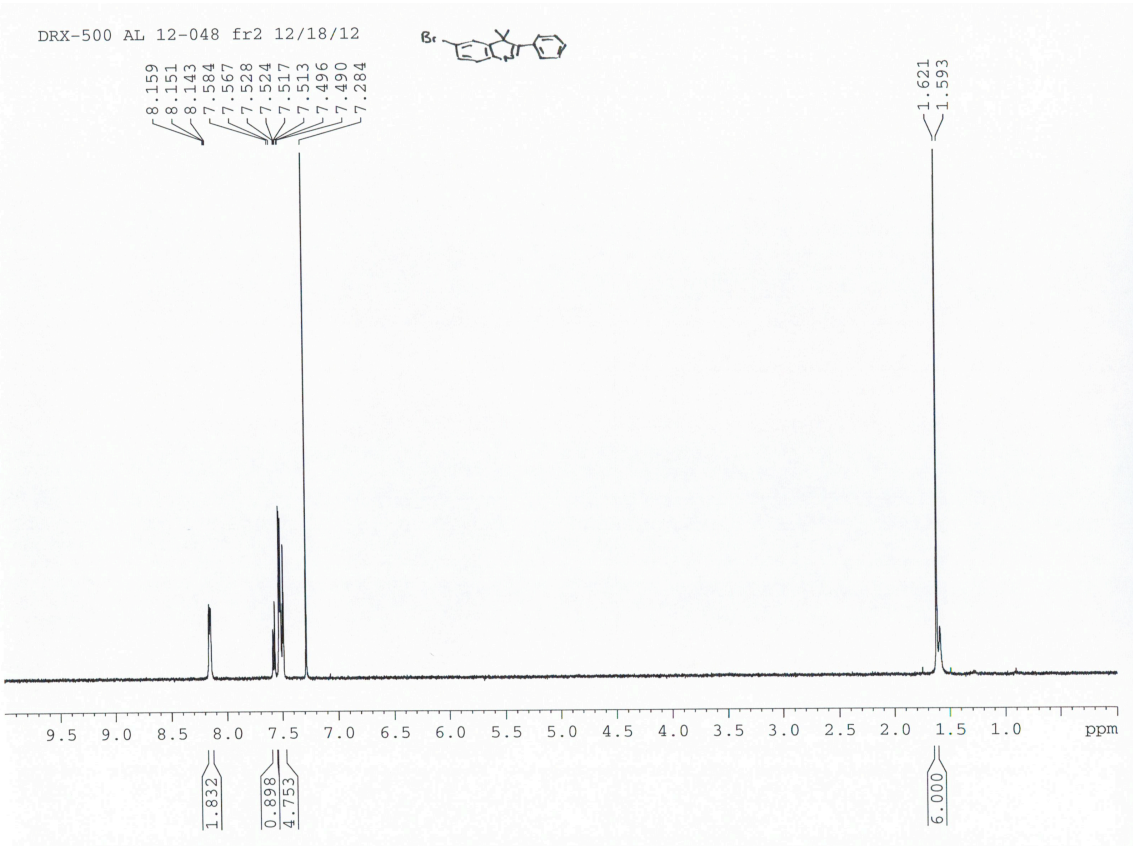
DRX-500 AL 12-048 fr2 12/18/12
8.159
8.151
8.143
7.584
7.567
7.528
7.524
7.517
7.513
7.496
7.490
7.284
1.621
1.593
9.5 9.0 8.5 8.0 7.5 7.0 6.5 6.0 5.5 5.0 4.5 4.0 3.5 3.0 2.5 2.0 1.5 1.0 ppm
1.832
0.898
4.753
6.000

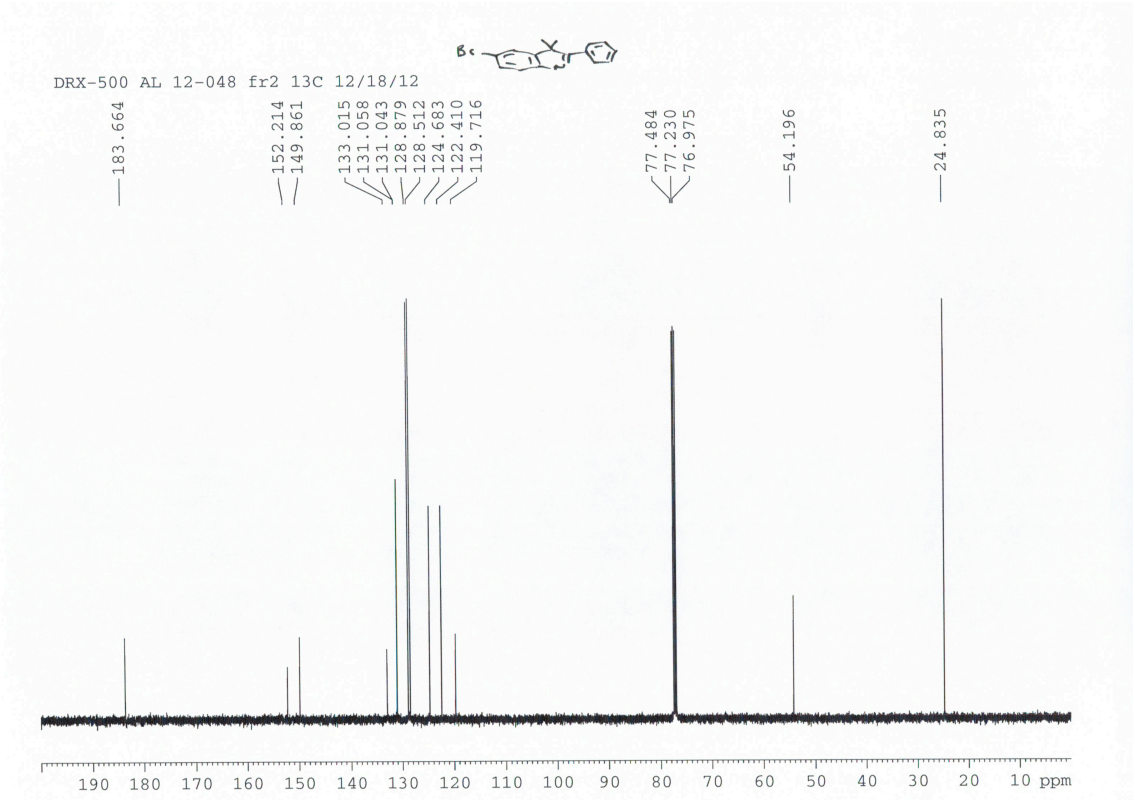
DRX-500 AL 12-048 fr2 13C 12/18/12
183.664
152.214
149.861
133.015
131.058
131.043
128.879
128.512
124.683
122.410
119.716
77.484
77.230
76.975
54.196
24.835
190 180 170 160 150 140 130 120 110 100 90 80 70 60 50 40 30 20 10 ppm

S3.1f

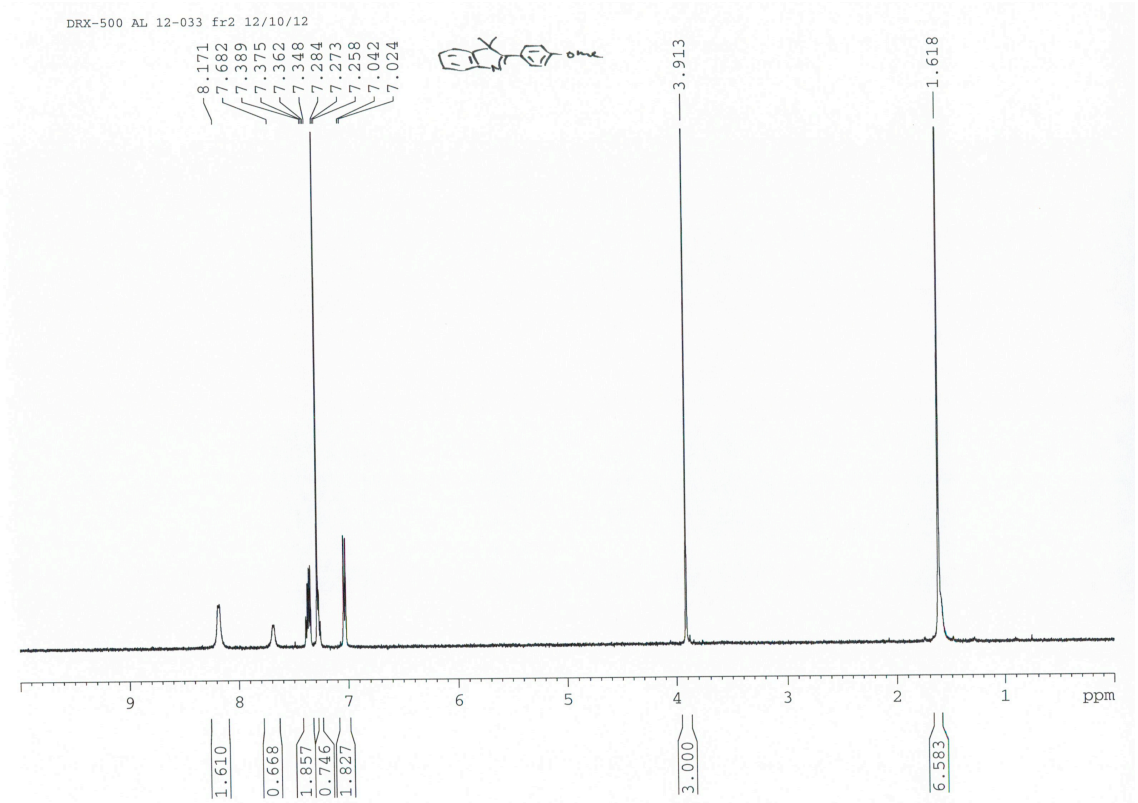
DRX-500 AL 12-033 fr2 12/10/12
8.171
7.682
7.389
7.375
7.362
7.348
7.284
7.273
7.258
7.042
7.024
3.913
1.618
ppm
1.610
0.668
1.857
0.746
1.827
3.000
6.583

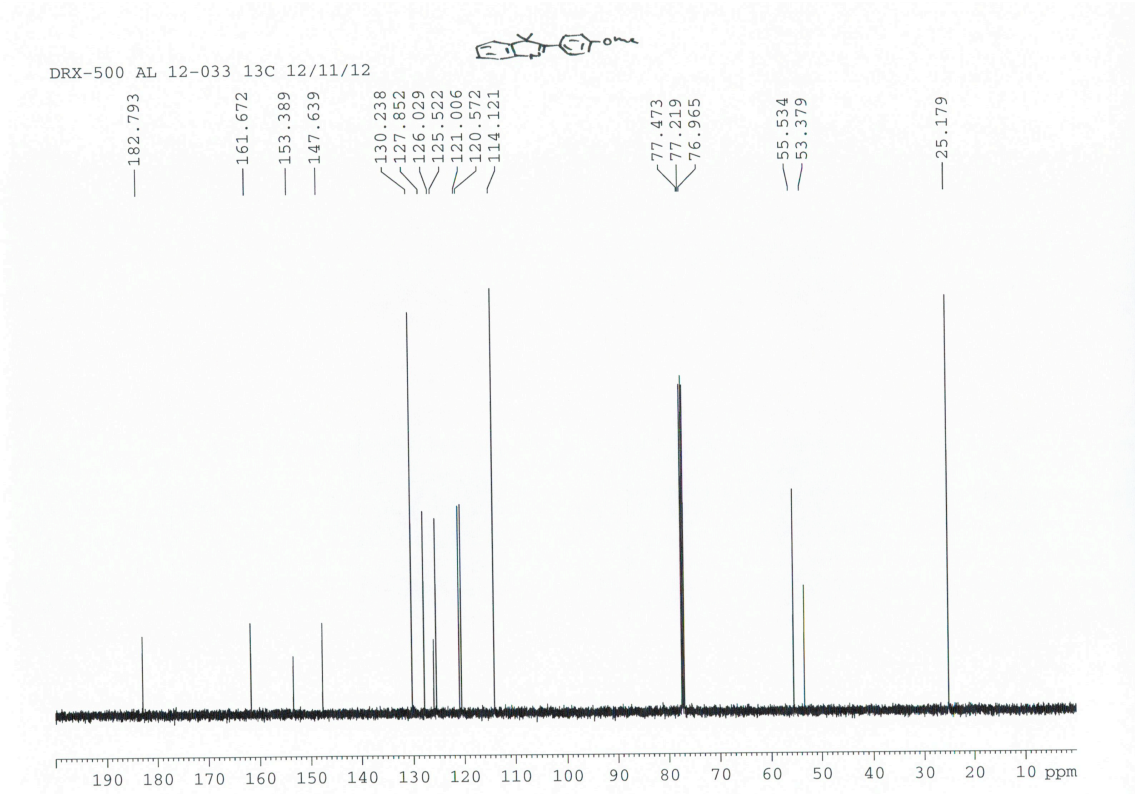
DRX-500 AL 12-033 13C 12/11/12
182.793
161.672
153.389
147.639
130.238
127.852
126.029
125.522
121.006
120.572
114.121
77.473
77.219
76.965
55.534
53.379
25.179
ppm

S3.1g

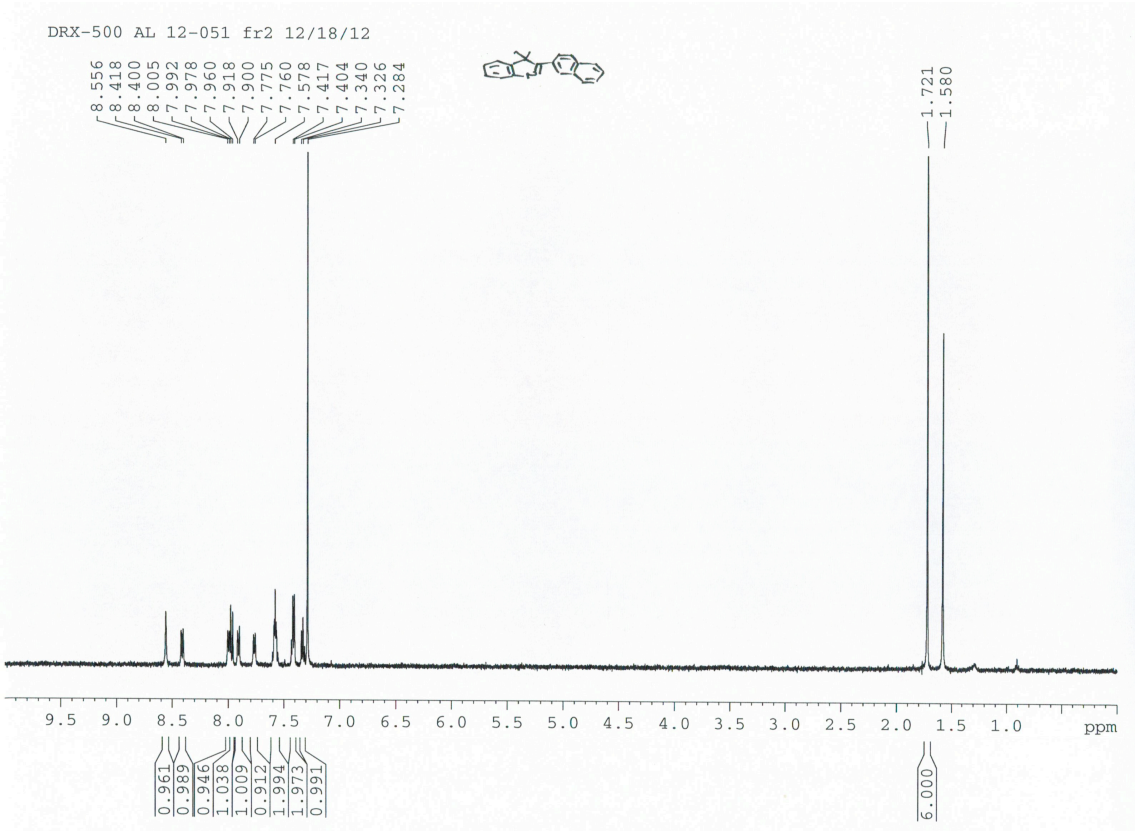
DRX-500 AL 12-051 fr2 12/18/12
8.556
8.418
8.400
8.005
7.992
7.978
7.960
7.918
7.900
7.775
7.760
7.578
7.417
7.404
7.340
7.326
7.284
1.721
1.580
9.5 9.0 8.5 8.0 7.5 7.0 6.5 6.0 5.5 5.0 4.5 4.0 3.5 3.0 2.5 2.0 1.5 1.0 ppm
0.961
0.989
0.946
1.038
1.009
0.912
1.994
1.973
0.991
6.000

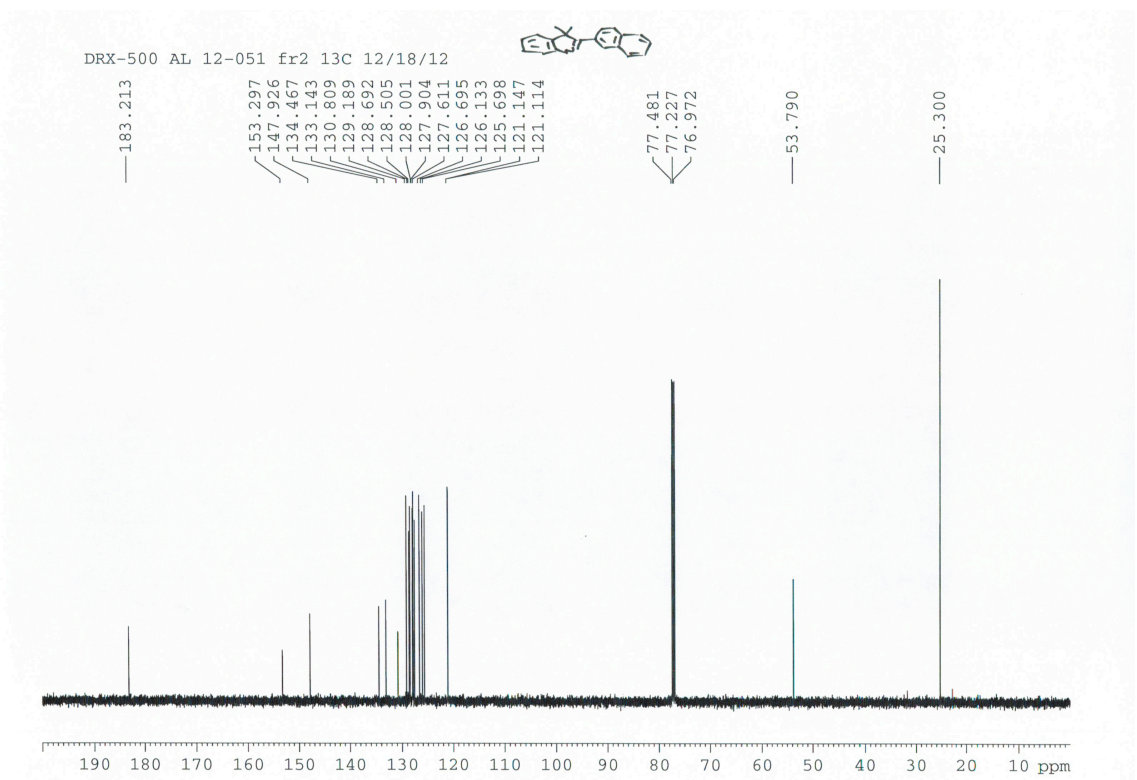
DRX-500 AL 12-051 fr2 13C 12/18/12
183.213
153.297
147.926
134.467
133.143
130.809
129.189
128.692
128.505
128.001
127.904
127.611
126.695
126.133
125.698
121.147
121.114
77.481
77.227
76.972
53.790
25.300
190 180 170 160 150 140 130 120 110 100 90 80 70 60 50 40 30 20 10 ppm

S3.1h

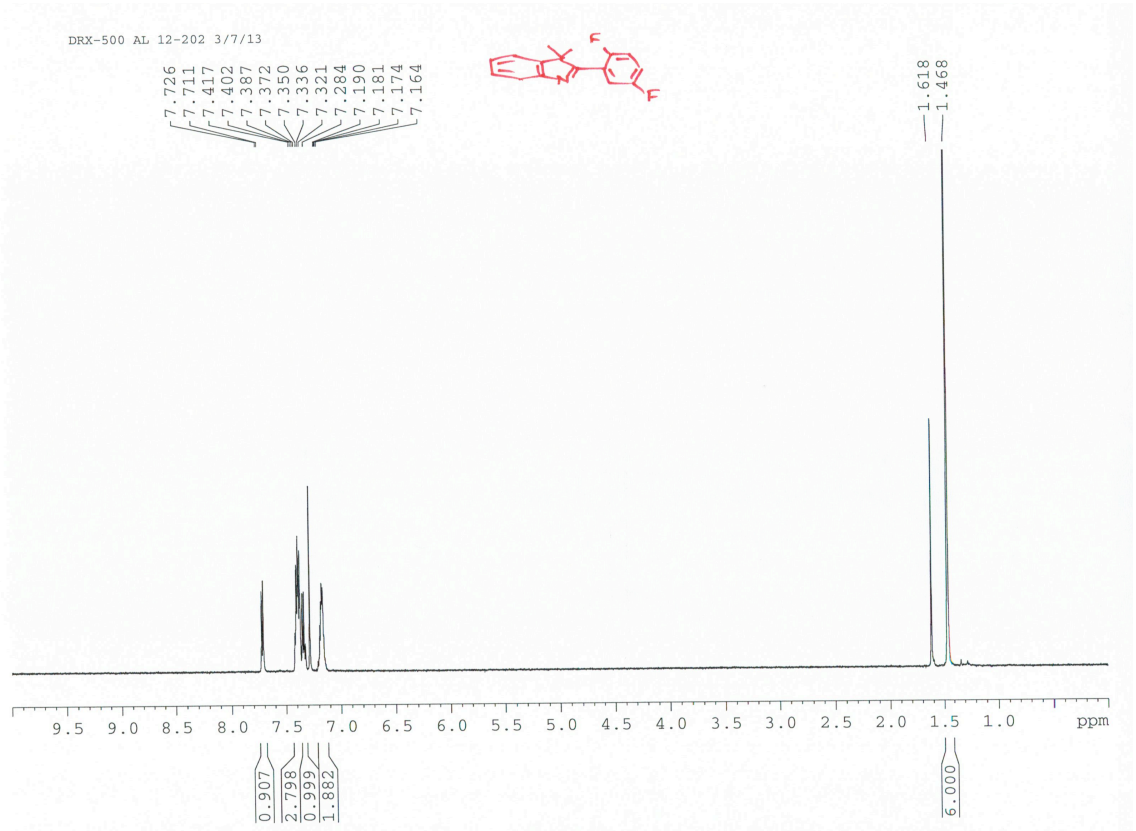
DRX-500 AL 12-202 3/7/13
7.726
7.711
7.417
7.402
7.387
7.372
7.350
7.336
7.321
7.284
7.190
7.181
7.174
7.164
1.618
1.468
9.5 9.0 8.5 8.0 7.5 7.0 6.5 6.0 5.5 5.0 4.5 4.0 3.5 3.0 2.5 2.0 1.5 1.0 ppm
0.907
2.798
0.999
1.882
6.000

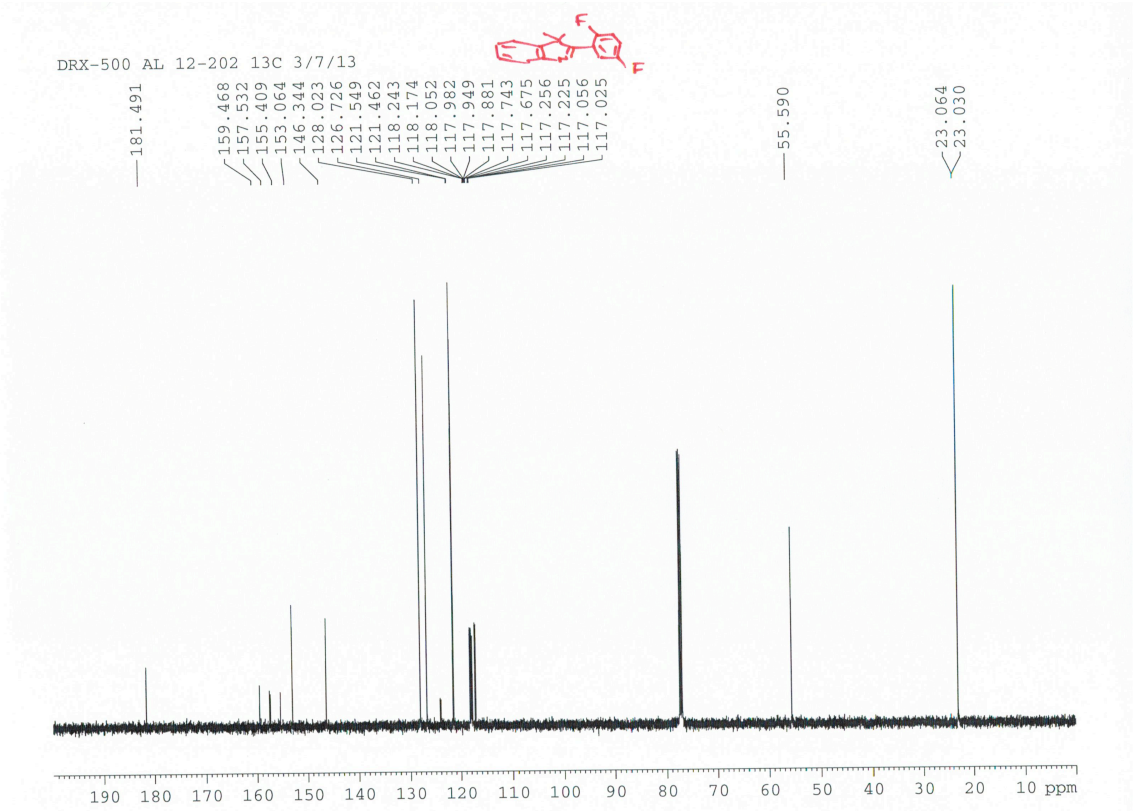
DRX-500 AL 12-202 13C 3/7/13
181.491
159.468
157.532
155.409
153.064
146.344
128.023
126.726
121.549
121.462
118.243
118.174
118.052
117.982
117.949
117.881
117.743
117.675
117.256
117.225
117.056
117.025
55.590
23.064
23.030
190 180 170 160 150 140 130 120 110 100 90 80 70 60 50 40 30 20 10 ppm

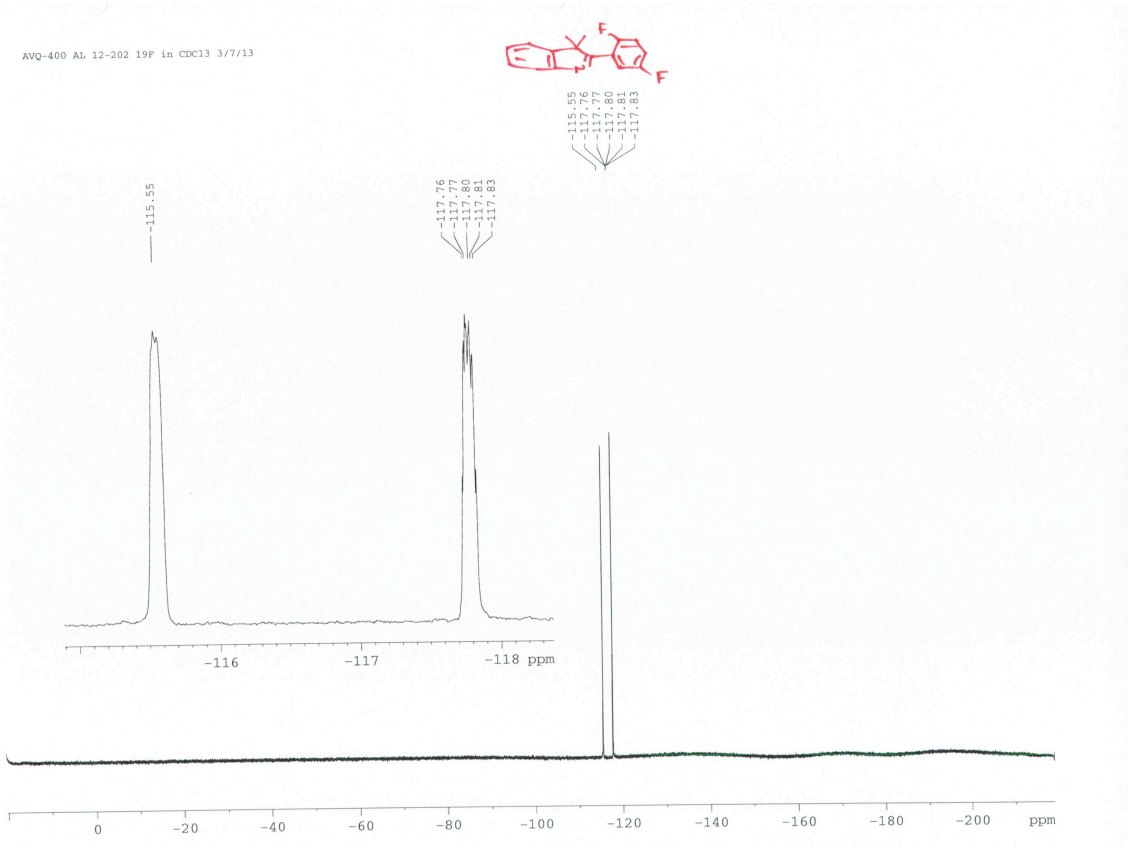
AVQ-400 AL 12-202 19F in CDCl3 3/7/13
F
F
-115.55
-115.76
-117.77
-117.80
-117.81
-117.83
-115.55
-117.76
-117.77
-117.80
-117.81
-117.83
-116
-117
-118 ppm
0
-20
-40
-60
-80
-100
-120
-140
-160
-180
-200
ppm

S3.2h

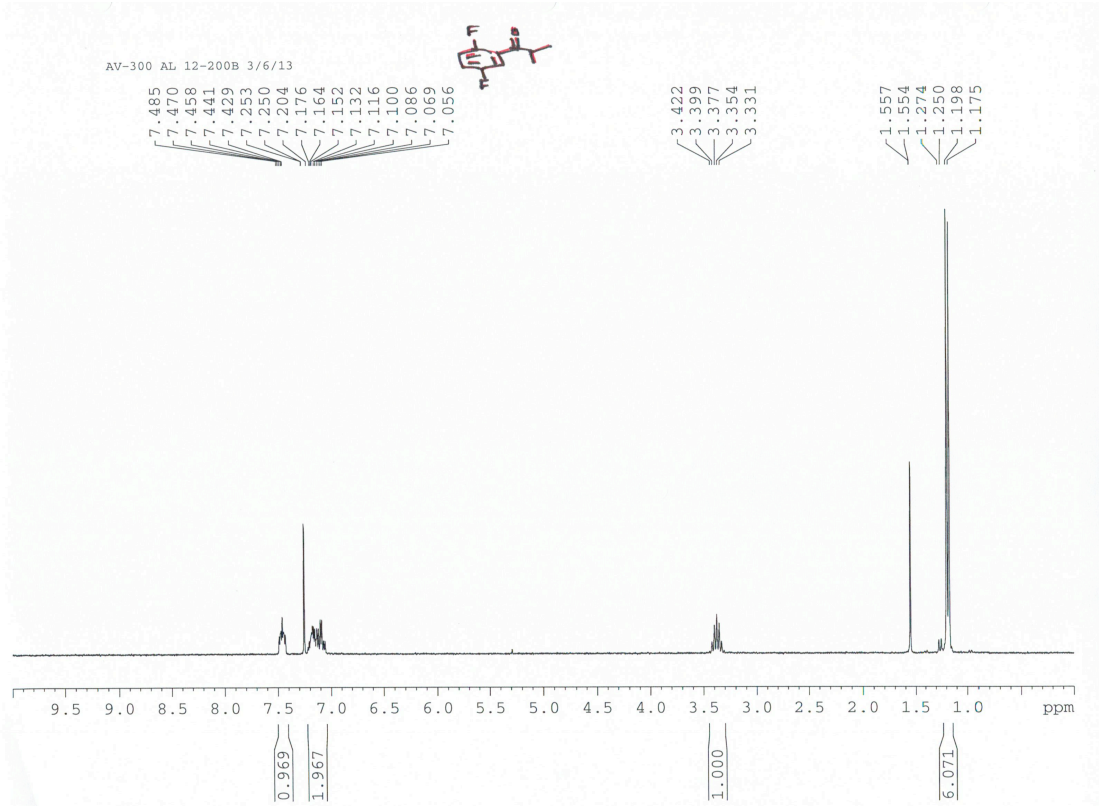
AV-300 AL 12-200B 3/6/13
7.485
7.470
7.458
7.441
7.429
7.253
7.250
7.204
7.176
7.164
7.152
7.132
7.116
7.100
7.086
7.069
7.056
3.422
3.399
3.377
3.354
3.331
1.557
1.554
1.274
1.250
1.198
1.175
9.5 9.0 8.5 8.0 7.5 7.0 6.5 6.0 5.5 5.0 4.5 4.0 3.5 3.0 2.5 2.0 1.5 1.0 ppm
0.969
1.967
1.000
6.071

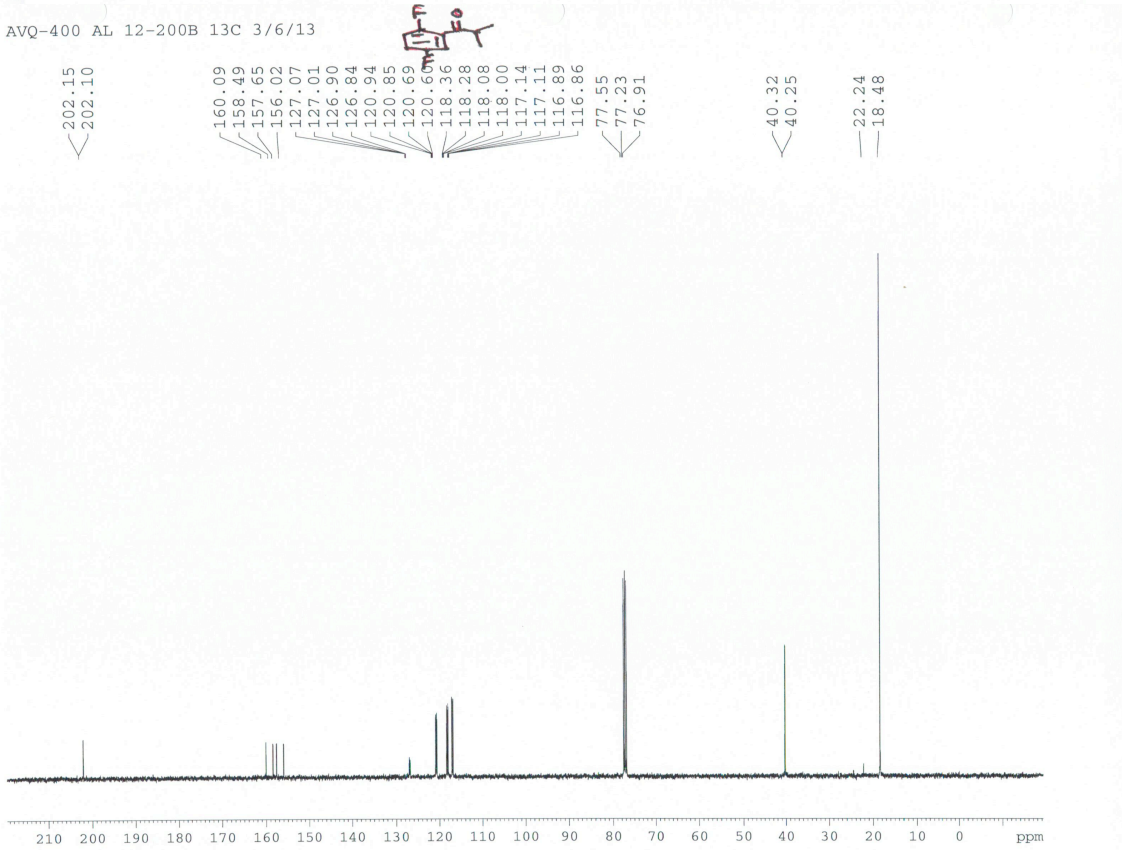
AVQ-400 AL 12-200B 13C 3/6/13
202.15
202.10
160.09
158.49
157.65
156.02
127.07
127.01
126.90
126.84
120.94
120.85
120.69
120.60
118.36
118.28
118.08
118.00
117.14
117.11
116.89
116.86
77.55
77.23
76.91
40.32
40.25
22.24
18.48
210 200 190 180 170 160 150 140 130 120 110 100 90 80 70 60 50 40 30 20 10 0 ppm

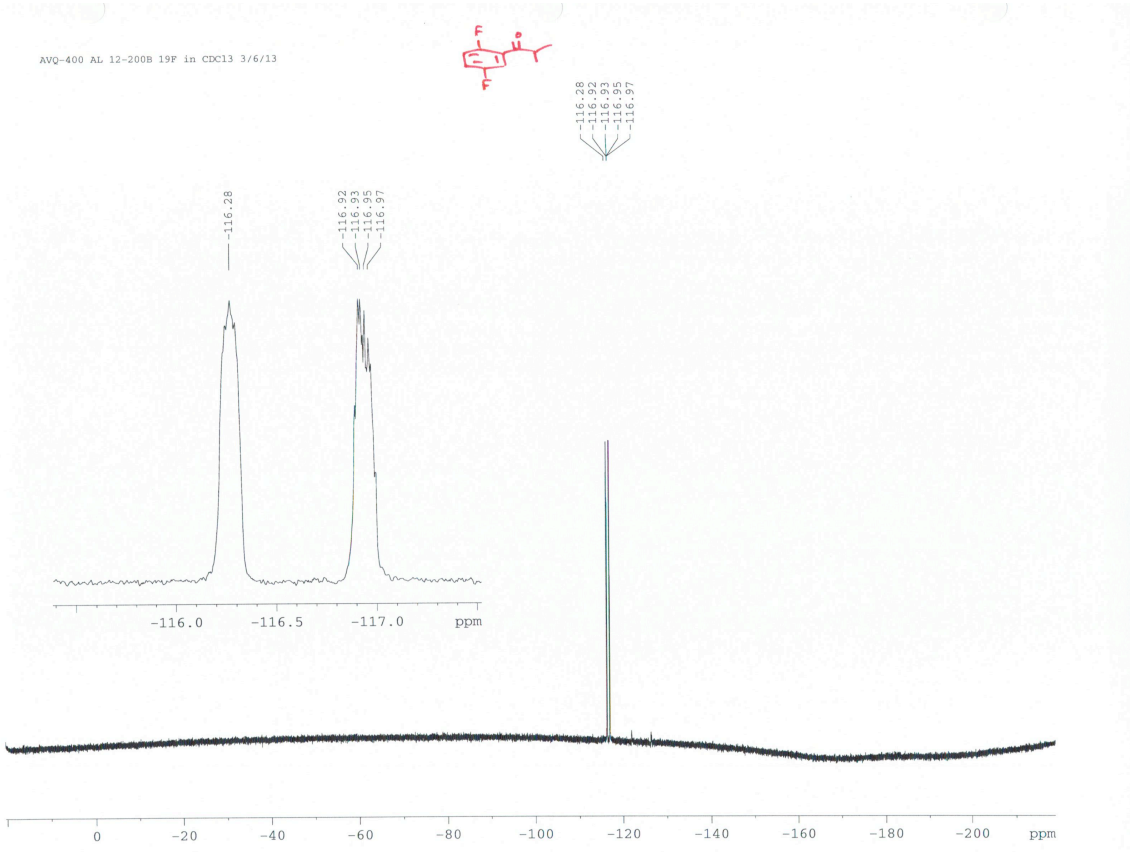
AVQ-400 AL 12-200B 19F in CDCl3 3/6/13
F
F
O
-116.28
-116.92
-116.93
-116.95
-116.97
-116.0
-116.5
-117.0
ppm
0
-20
-40
-60
-80
-100
-120
-140
-160
-180
-200
ppm

S3.1i

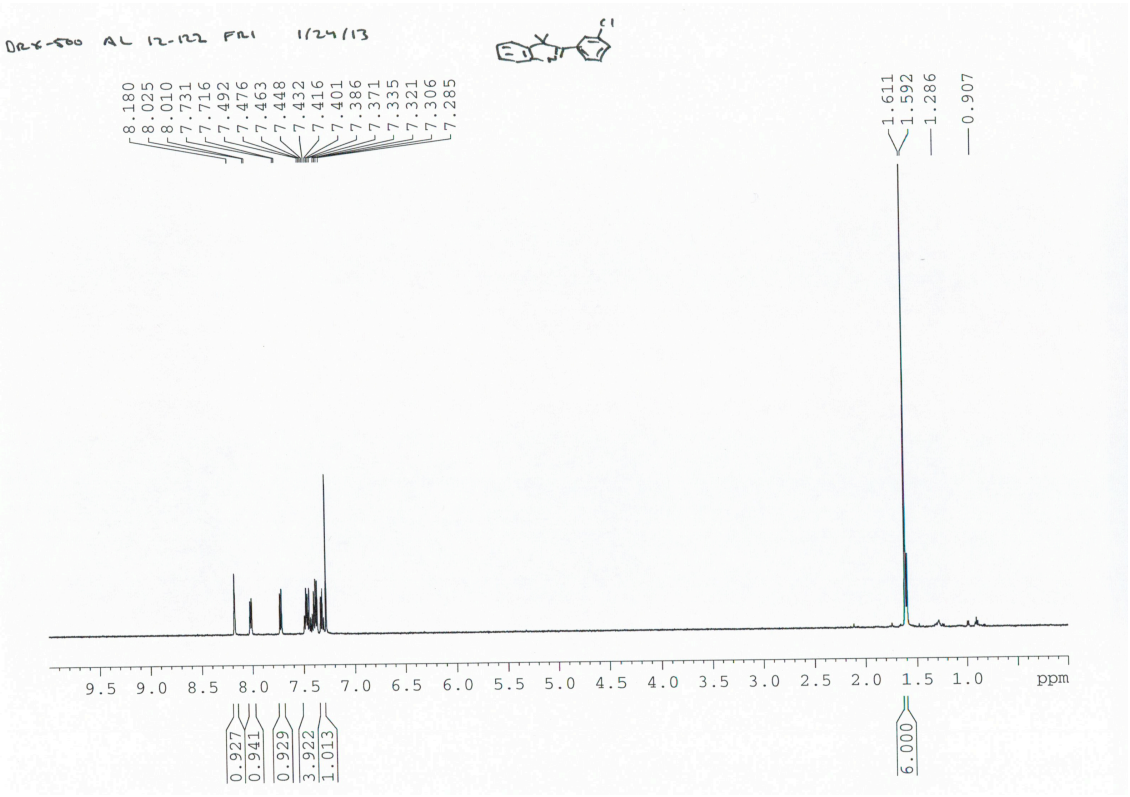
DRX-500 AL 12-122 FR1 1/24/13
8.180
8.025
8.010
7.731
7.716
7.492
7.476
7.463
7.448
7.432
7.416
7.401
7.386
7.371
7.335
7.321
7.306
7.285
1.611
1.592
1.286
0.907
9.5 9.0 8.5 8.0 7.5 7.0 6.5 6.0 5.5 5.0 4.5 4.0 3.5 3.0 2.5 2.0 1.5 1.0 ppm
0.927
0.941
0.929
3.922
1.013
6.000

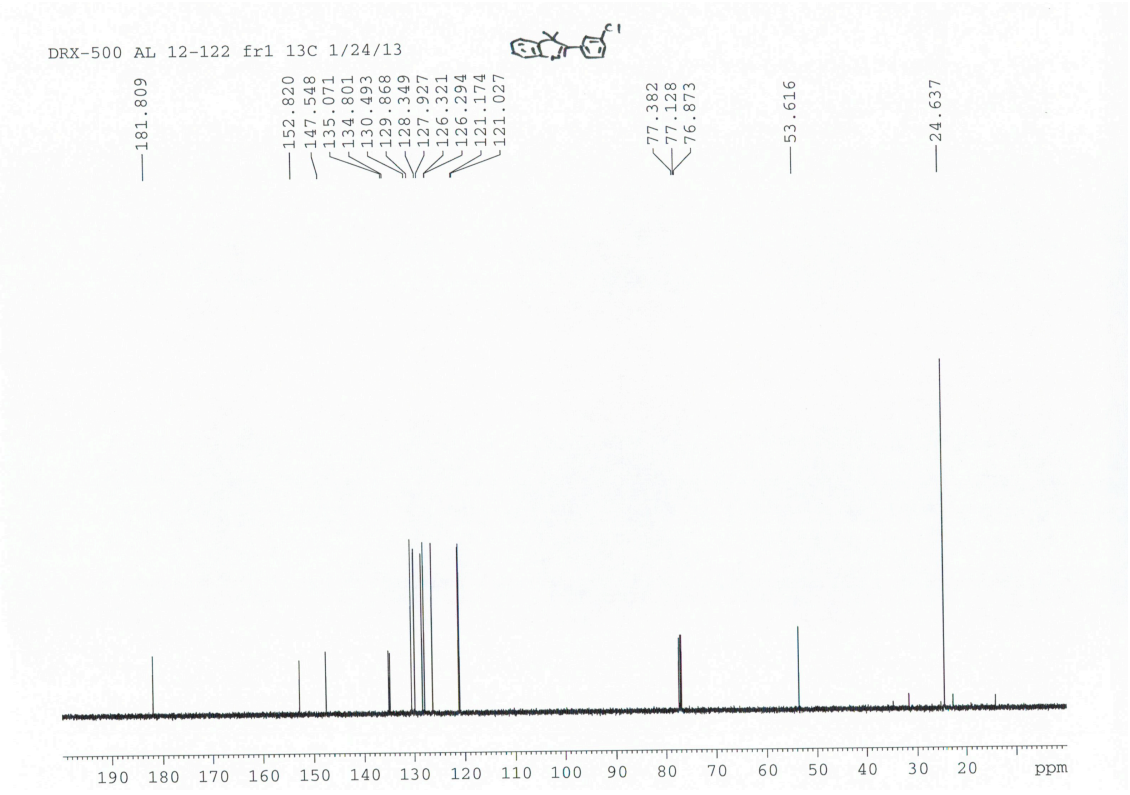
DRX-500 AL 12-122 fr1 13C 1/24/13
181.809
152.820
147.548
135.071
134.801
130.493
129.868
128.349
127.927
126.321
126.294
121.174
121.027
77.382
77.128
76.873
53.616
24.637
190 180 170 160 150 140 130 120 110 100 90 80 70 60 50 40 30 20 ppm

S3.1j

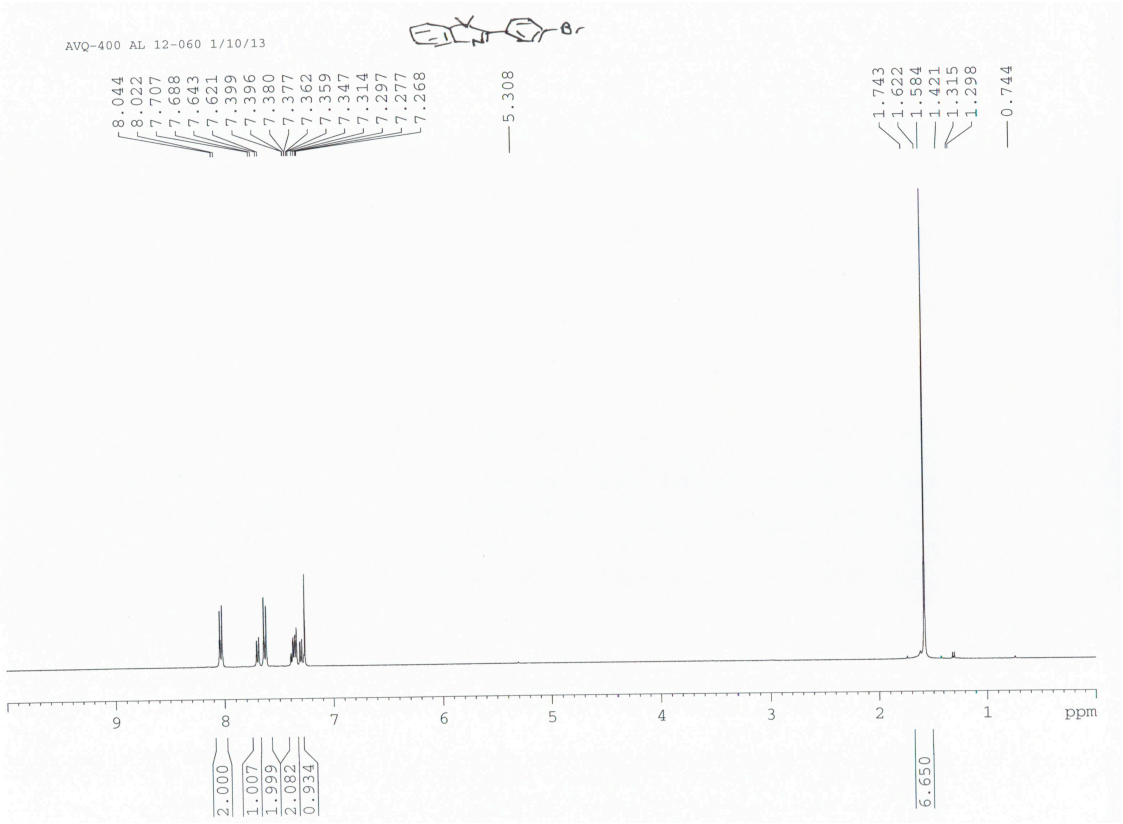
AVQ-400 AL 12-060 1/10/13
8.044
8.022
7.707
7.688
7.643
7.621
7.399
7.396
7.380
7.377
7.362
7.359
7.347
7.314
7.297
7.277
7.268
5.308
1.743
1.622
1.584
1.421
1.315
1.298
0.744
9
8
7
6
5
4
3
2
1
ppm
2.000
1.007
1.999
2.082
0.934
6.650

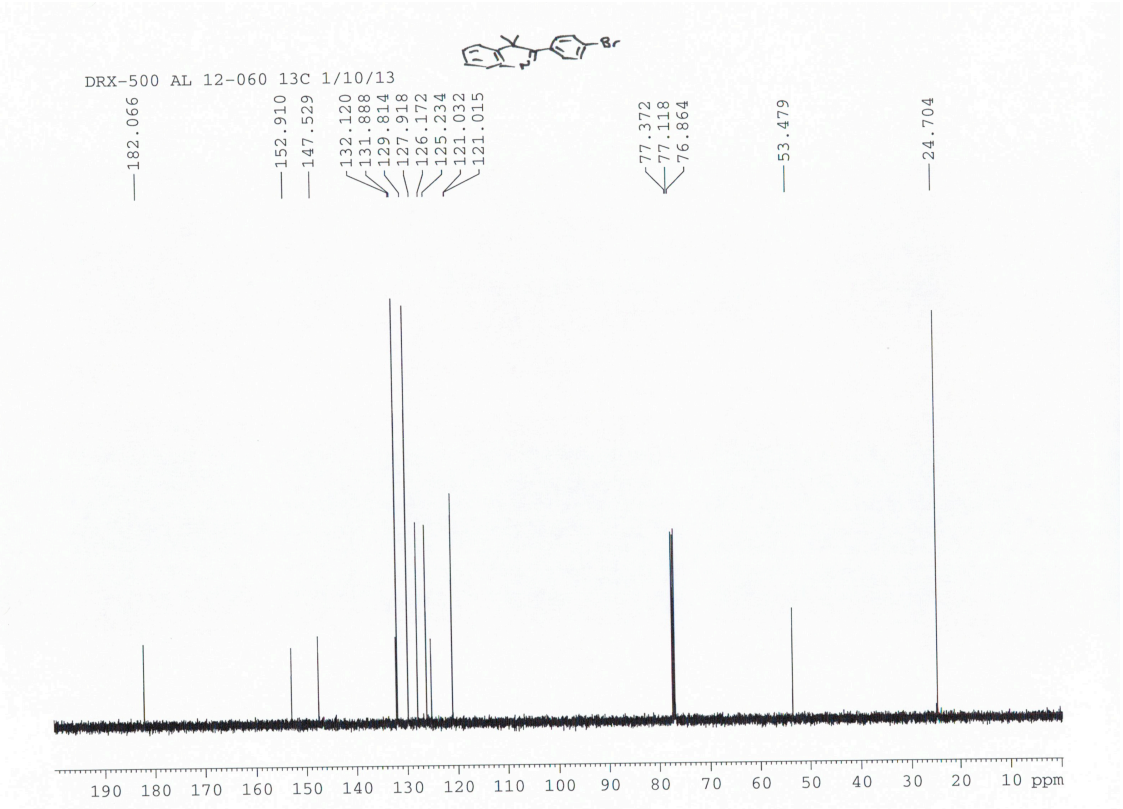
DRX-500 AL 12-060 13C 1/10/13
182.066
152.910
147.529
132.120
131.888
129.814
127.918
126.172
125.234
121.032
121.015
77.372
77.118
76.864
53.479
24.704
190
180
170
160
150
140
130
120
110
100
90
80
70
60
50
40
30
20
10 ppm

S3.1k

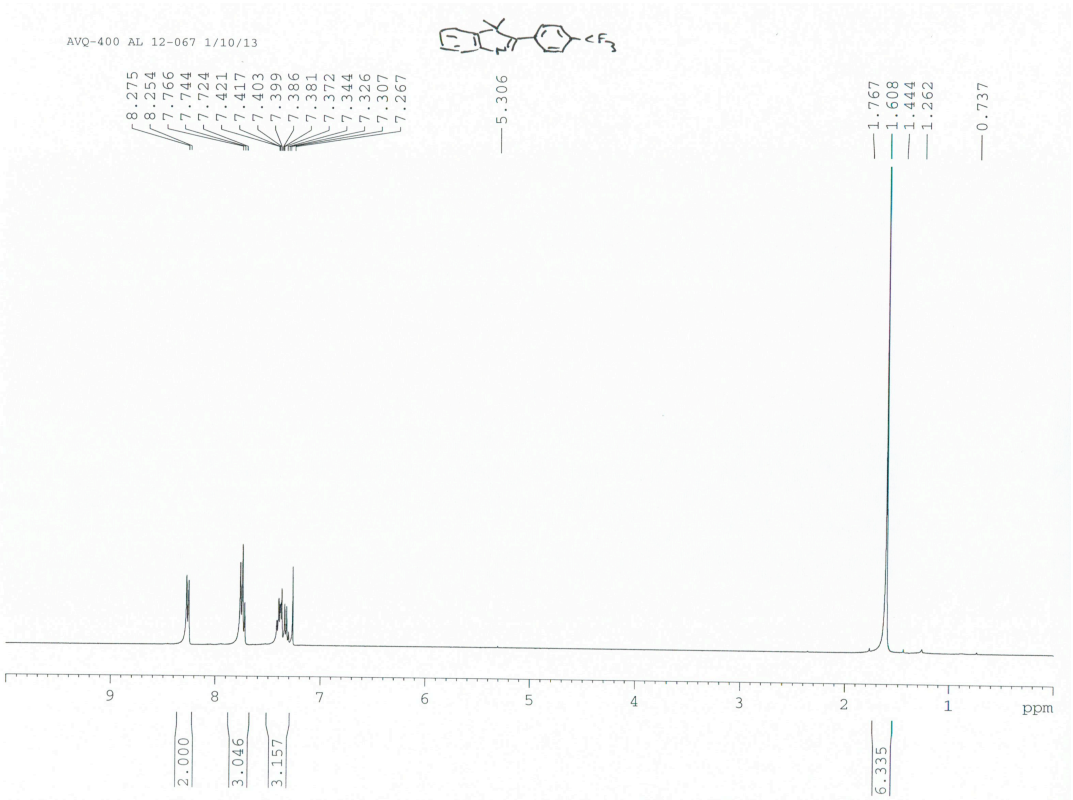
AVQ-400 AL 12-067 1/10/13
8.275
8.254
7.766
7.744
7.724
7.421
7.417
7.403
7.399
7.386
7.381
7.372
7.344
7.326
7.307
7.267
5.306
1.767
1.608
1.444
1.262
0.737
9
8
7
6
5
4
3
2
1
ppm
2.000
3.046
3.157
6.335

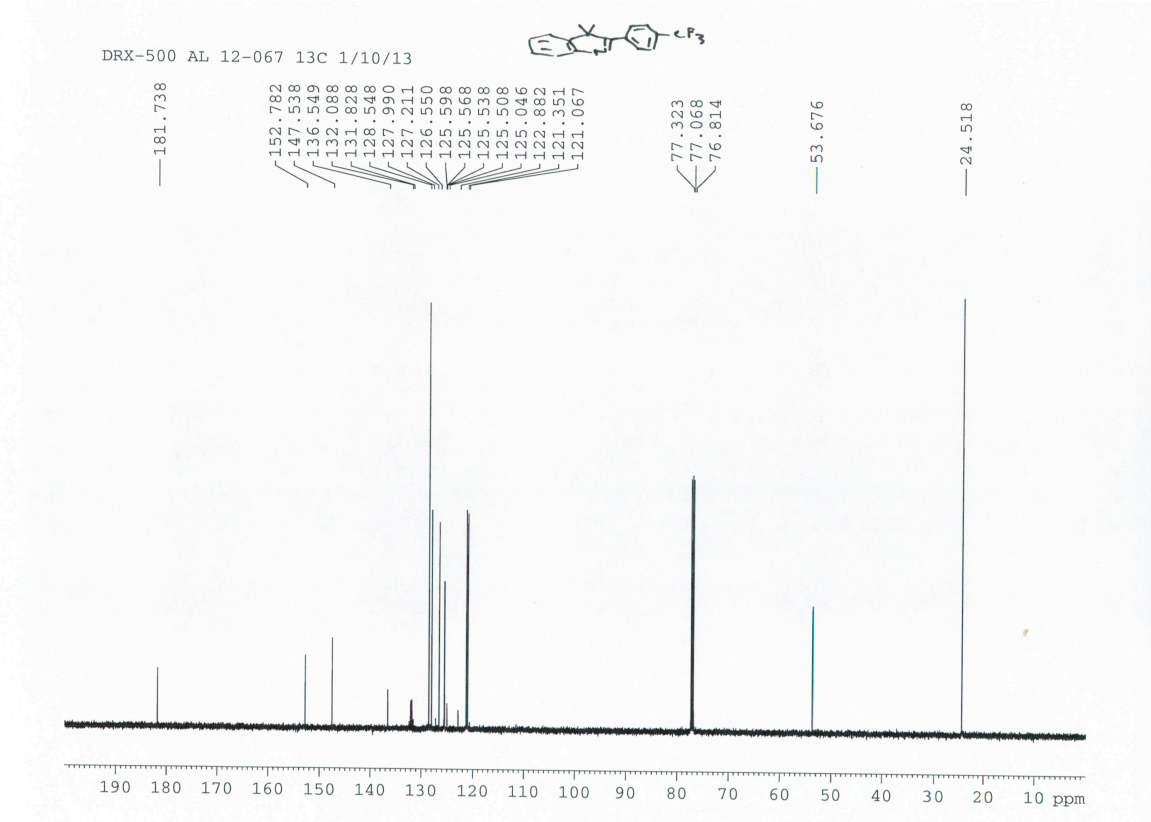
DRX-500 AL 12-067 13C 1/10/13
181.738
152.782
147.538
136.549
132.088
131.828
128.548
127.990
127.211
126.550
125.598
125.568
125.538
125.508
125.046
122.882
121.351
121.067
77.323
77.068
76.814
53.676
24.518
190
180
170
160
150
140
130
120
110
100
90
80
70
60
50
40
30
20
10 ppm

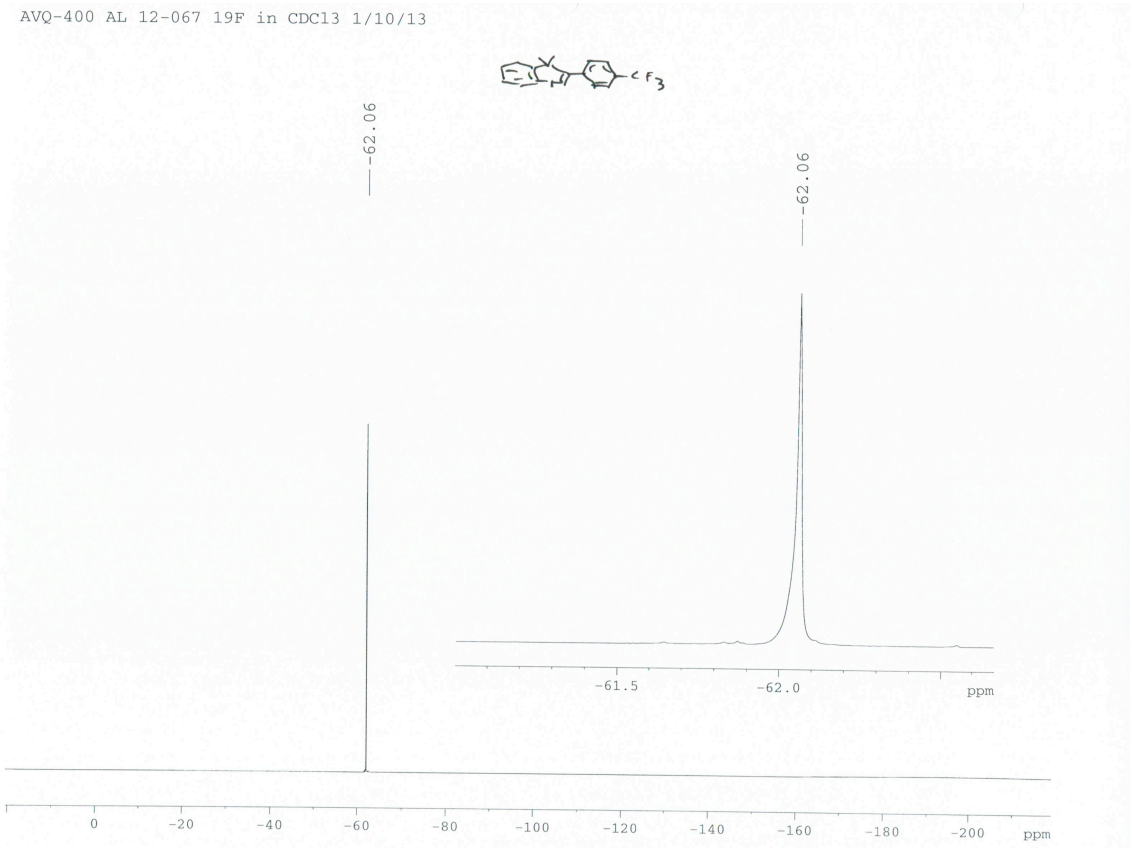
AVQ-400 AL 12-067 19F in CDCl3 1/10/13
-62.06
-62.06
-61.5
-62.0
ppm
0
-20
-40
-60
-80
-100
-120
-140
-160
-180
-200
ppm

3.17a-D

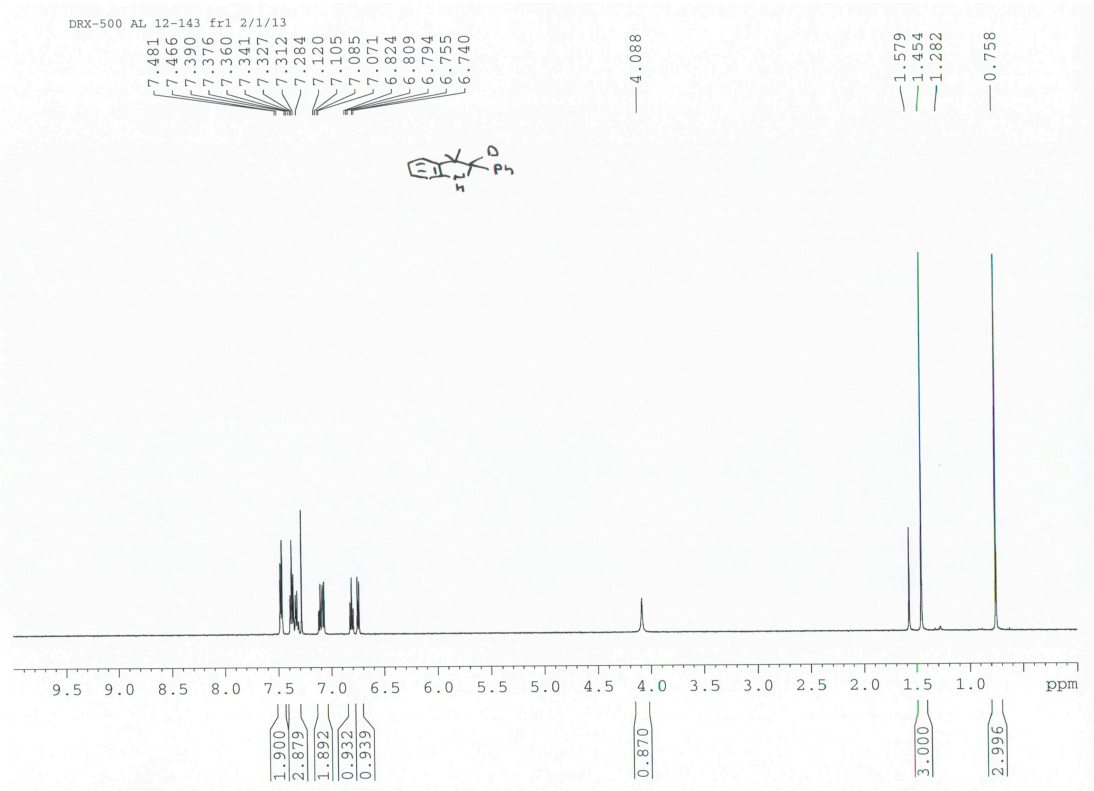
DRX-500 AL 12-143 fr1 2/1/13
7.481
7.466
7.390
7.376
7.360
7.341
7.327
7.312
7.284
7.120
7.105
7.085
7.071
6.824
6.809
6.794
6.755
6.740
4.088
1.579
1.454
1.282
0.758
D
Ph
9.5 9.0 8.5 8.0 7.5 7.0 6.5 6.0 5.5 5.0 4.5 4.0 3.5 3.0 2.5 2.0 1.5 1.0
ppm
1.900
2.879
1.892
0.932
0.939
0.870
3.000
2.996

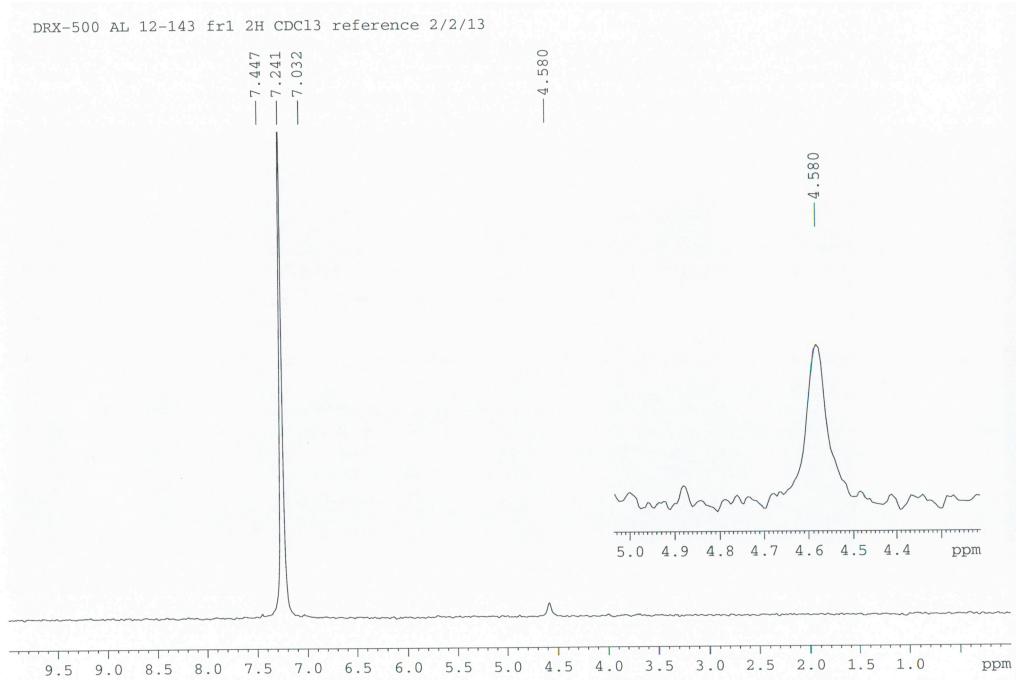
DRX-500 AL 12-143 fr1 2H CDCl3 reference 2/2/13
7.447
7.241
7.032
4.580
4.580
5.0 4.9 4.8 4.7 4.6 4.5 4.4 ppm
9.5 9.0 8.5 8.0 7.5 7.0 6.5 6.0 5.5 5.0 4.5 4.0 3.5 3.0 2.5 2.0 1.5 1.0 ppm

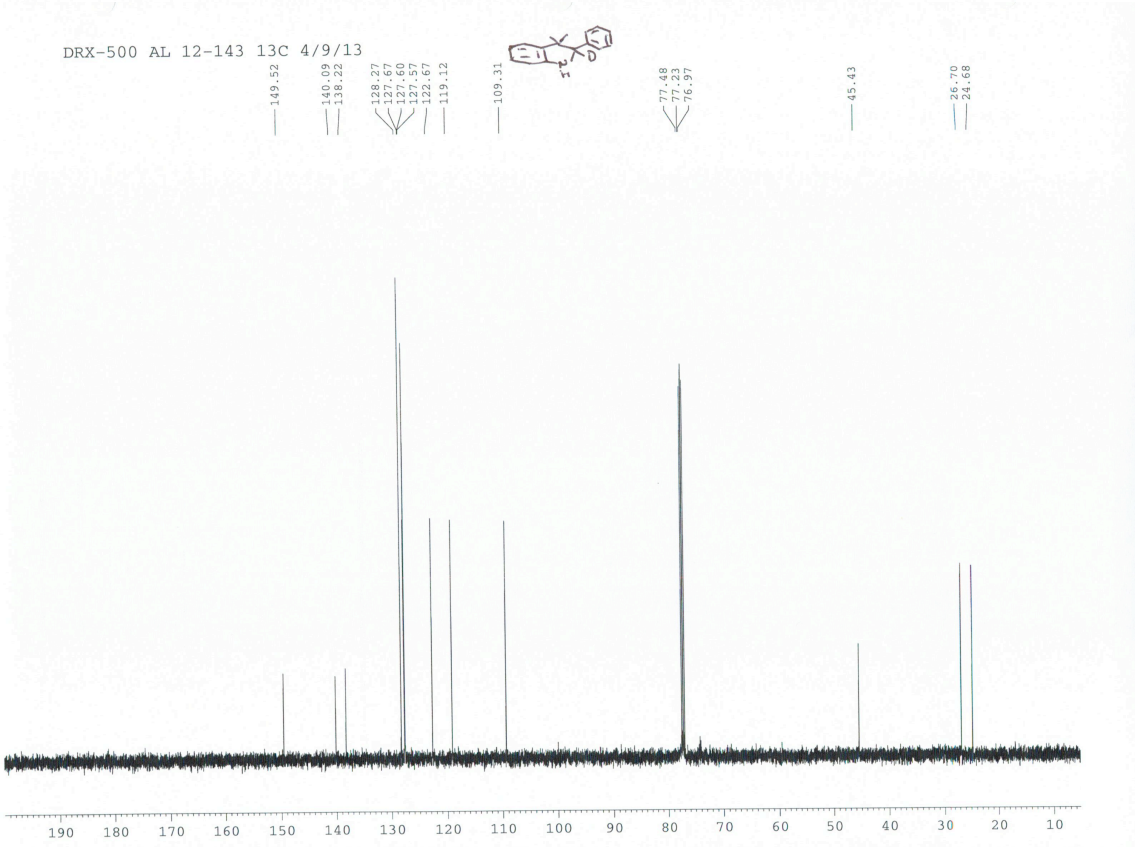
DRX-500 AL 12-143 13C 4/9/13
149.52
140.09
138.22
128.27
127.67
127.60
127.57
122.67
119.12
109.31
77.48
77.23
76.97
45.43
26.70
24.68
190 180 170 160 150 140 130 120 110 100 90 80 70 60 50 40 30 20 10

3.17a

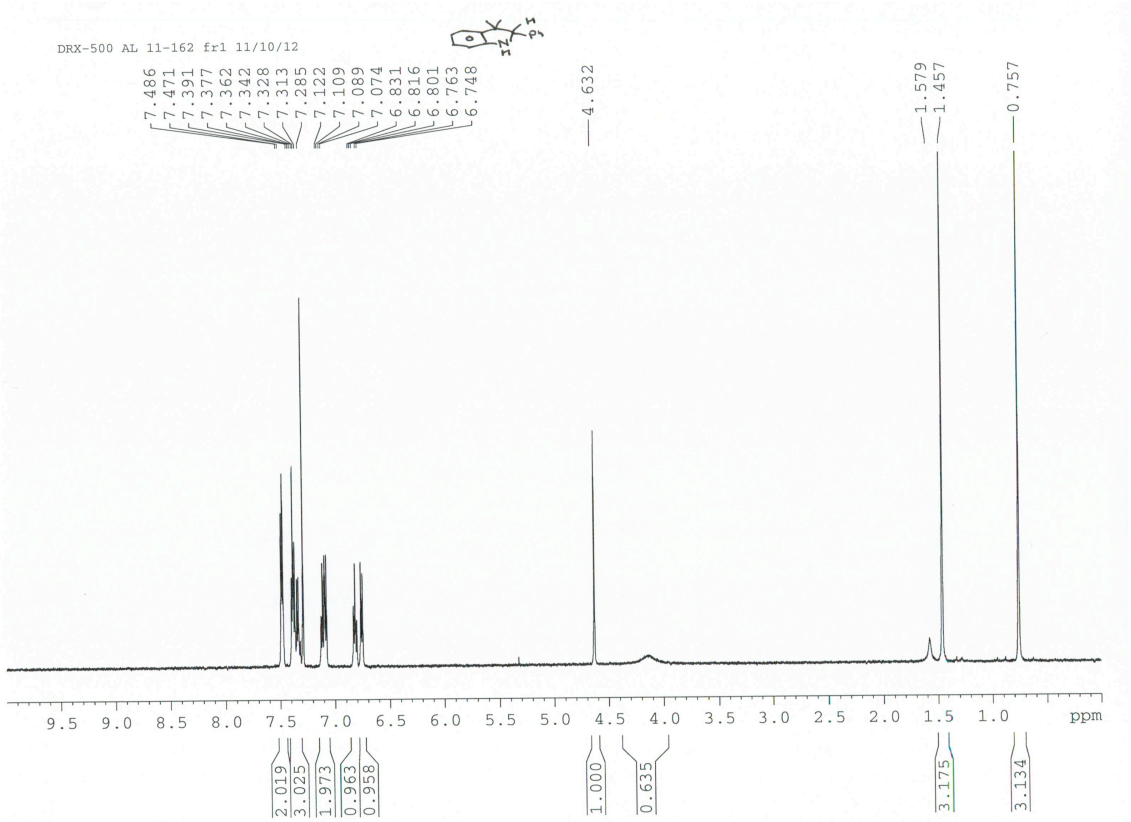
DRX-500 AL 11-162 fr1 11/10/12
7.486
7.471
7.391
7.377
7.362
7.342
7.328
7.313
7.285
7.122
7.109
7.089
7.074
6.831
6.816
6.801
6.763
6.748
4.632
1.579
1.457
0.757
ppm
2.019
3.025
1.973
0.963
0.958
1.000
0.635
3.175
3.134

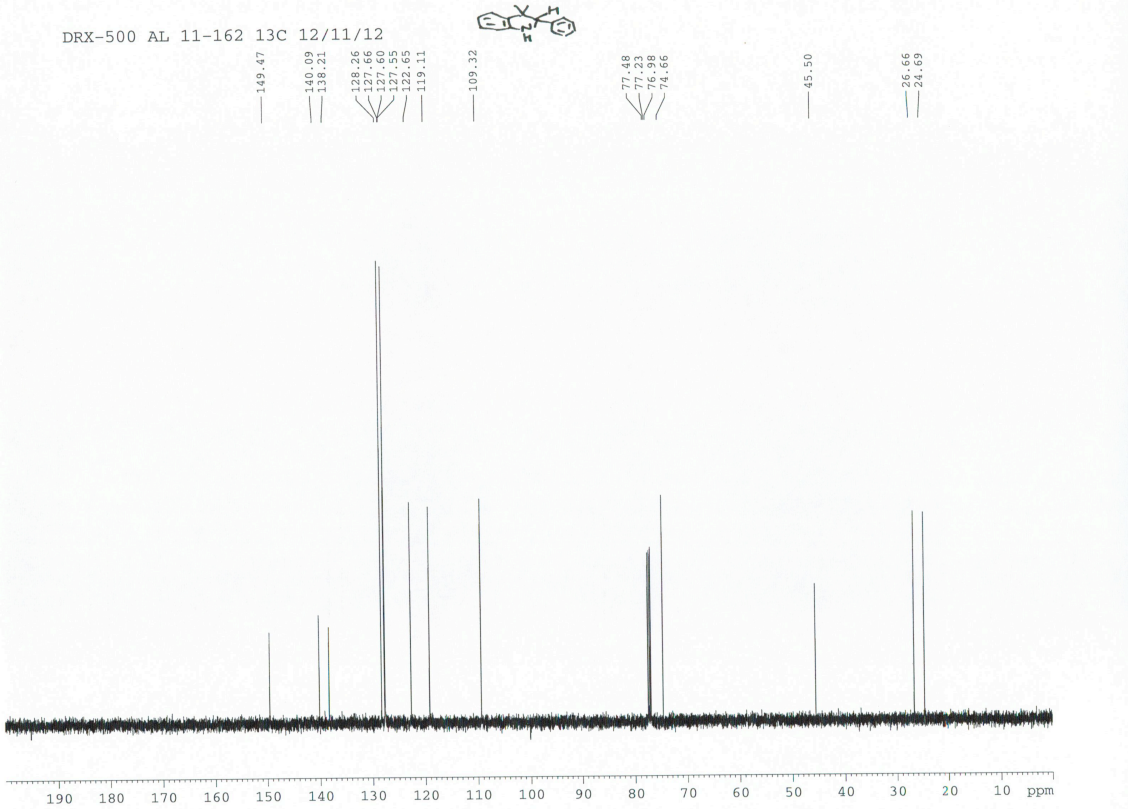
DRX-500 AL 11-162 13C 12/11/12
149.47
140.09
138.21
128.26
127.66
127.60
127.55
122.65
119.11
109.32
77.48
77.23
76.98
74.66
45.50
26.66
24.69
ppm

3.17b

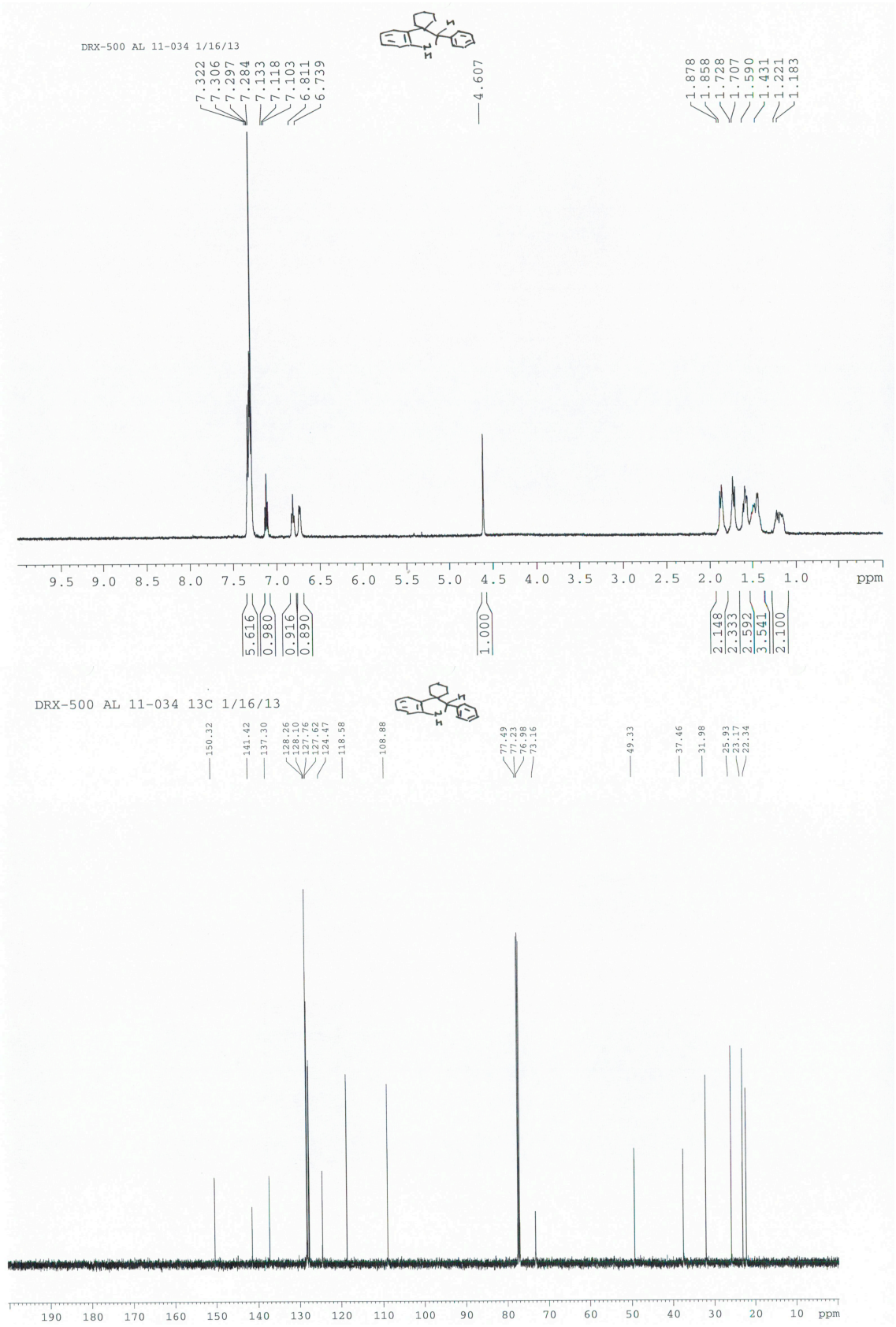
DRX-500 AL 11-034 1/16/13
7.322
7.306
7.297
7.284
7.133
7.118
7.103
6.811
6.739
4.607
1.878
1.858
1.728
1.707
1.590
1.431
1.221
1.183
ppm
5.616
0.980
0.916
0.890
1.000
2.148
2.333
2.592
3.541
2.100
DRX-500 AL 11-034 13C 1/16/13
150.32
141.42
137.30
128.26
128.10
127.76
127.62
124.47
118.58
108.88
77.49
77.23
76.98
73.16
49.33
37.46
31.98
25.93
23.17
22.34
ppm

3.17c

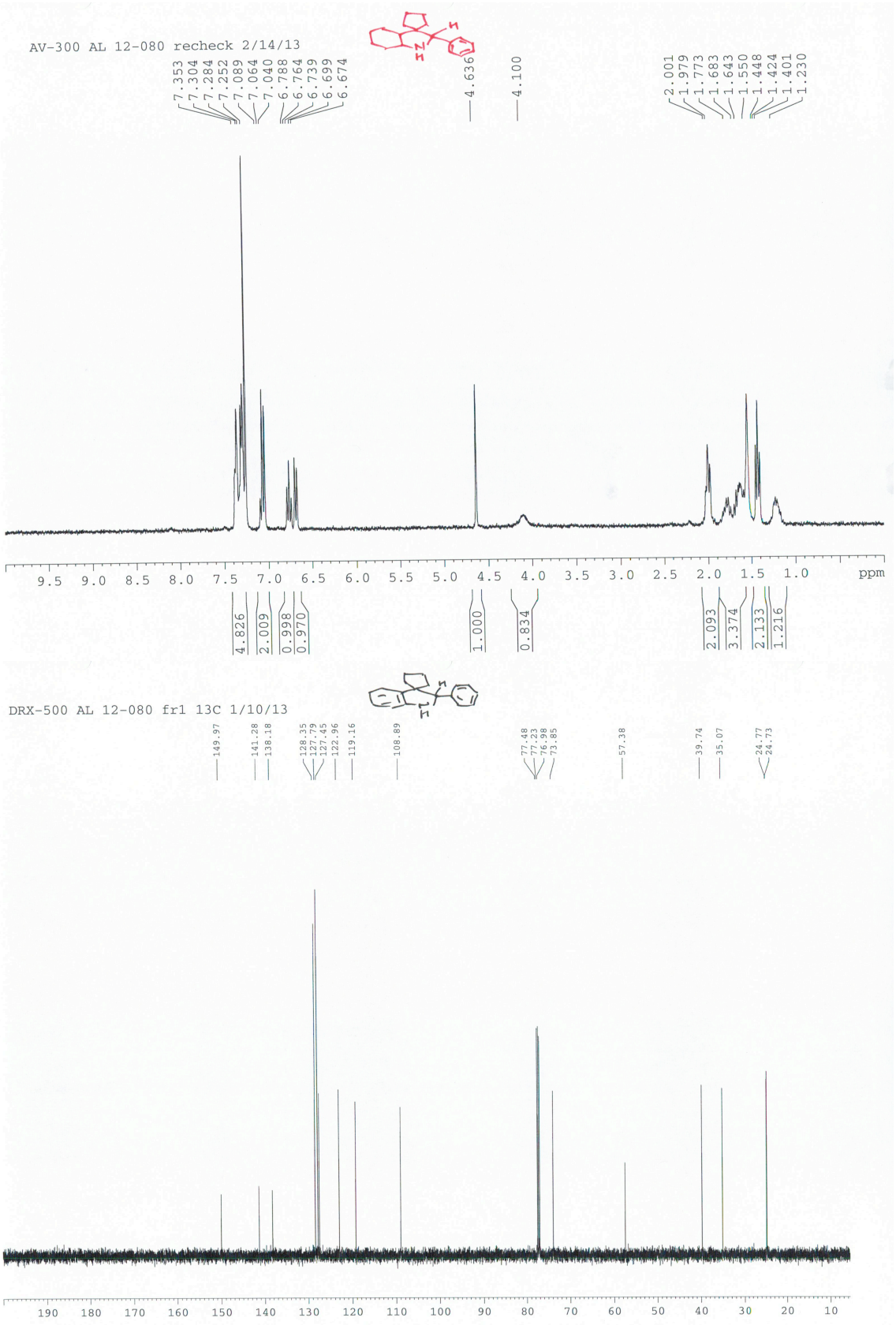
AV-300 AL 12-080 recheck 2/14/13
7.353
7.304
7.284
7.252
7.089
7.064
7.040
6.788
6.764
6.739
6.699
6.674
4.636
4.100
2.001
1.979
1.773
1.683
1.643
1.550
1.448
1.424
1.401
1.230
ppm
4.826
2.009
0.998
0.970
1.000
0.834
2.093
3.374
2.133
1.216
DRX-500 AL 12-080 fr1 13C 1/10/13
149.97
141.28
138.18
128.35
127.79
127.45
122.96
119.16
108.89
77.48
77.23
76.98
73.85
57.38
39.74
35.07
24.77
24.73

3.17d

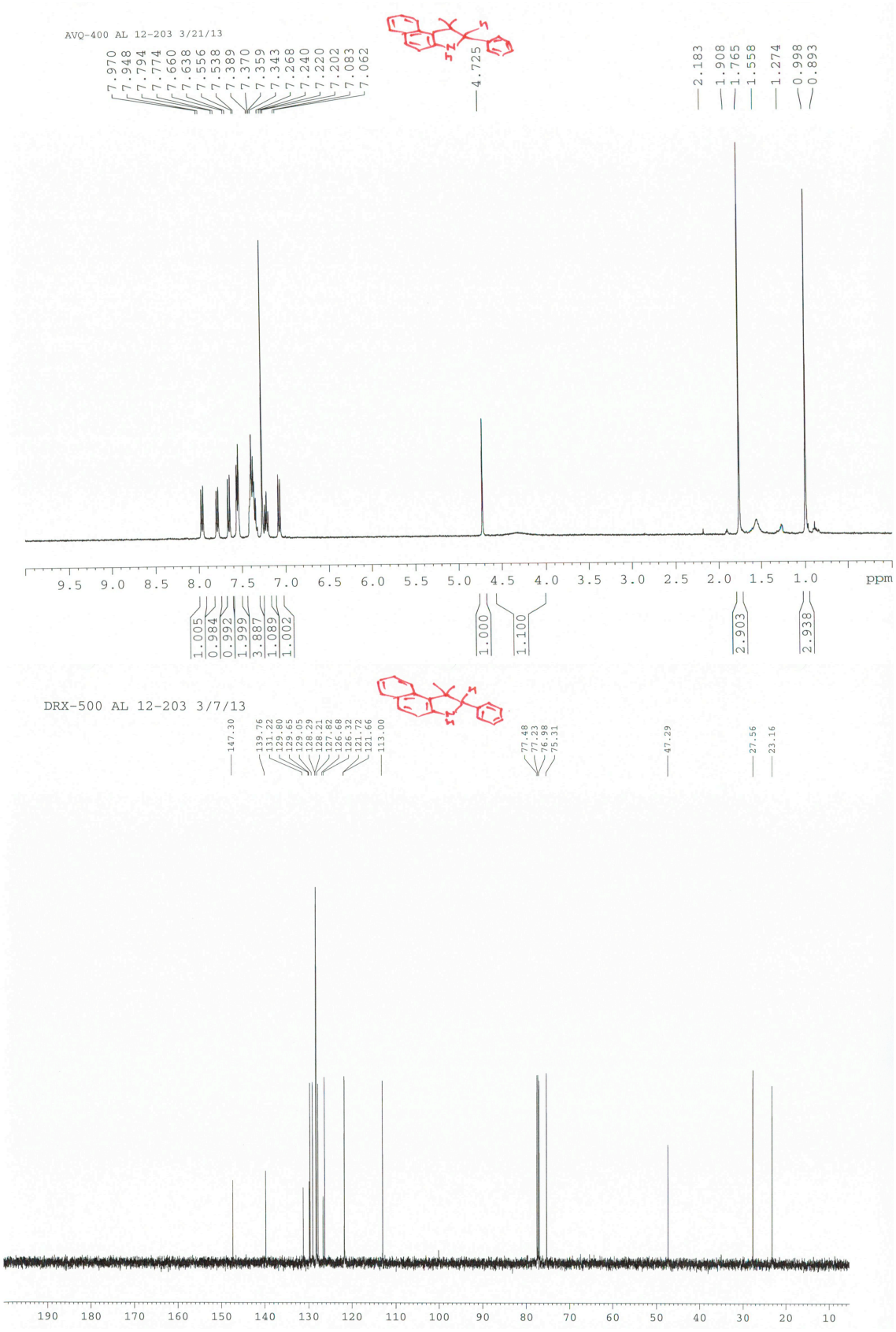
AVQ-400 AL 12-203 3/21/13
7.970
7.948
7.794
7.774
7.660
7.638
7.556
7.538
7.389
7.370
7.359
7.343
7.268
7.240
7.220
7.202
7.083
7.062
4.725
2.183
1.908
1.765
1.558
1.274
0.998
0.893
ppm
1.005
0.984
0.992
1.999
3.887
1.089
1.002
1.000
1.100
2.903
2.938
DRX-500 AL 12-203 3/7/13
147.30
139.76
131.22
129.80
129.65
129.05
128.29
128.21
127.82
126.68
126.32
121.72
121.66
113.00
77.48
77.23
76.98
75.31
47.29
27.56
23.16

3.17e

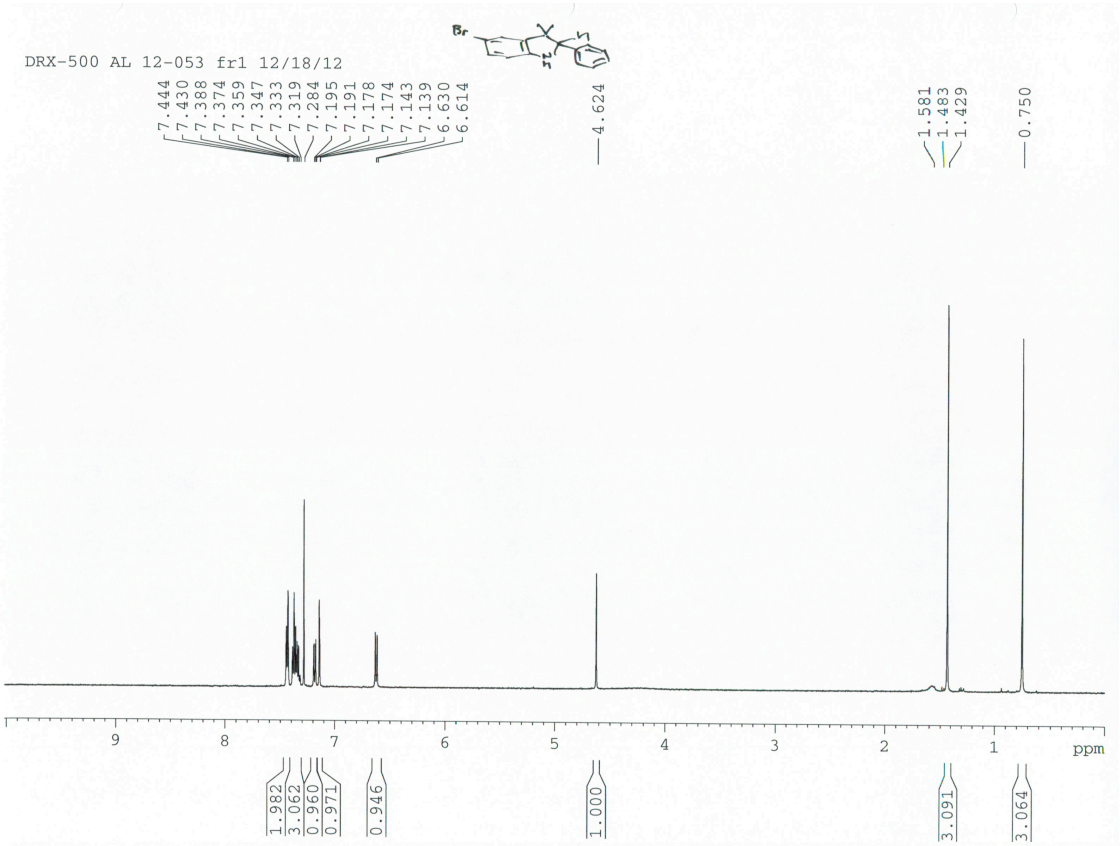
DRX-500 AL 12-053 fr1 12/18/12
7.444
7.430
7.388
7.374
7.359
7.347
7.333
7.319
7.284
7.195
7.191
7.178
7.174
7.143
7.139
6.630
6.614
4.624
1.581
1.483
1.429
0.750
ppm
1.982
3.062
0.960
0.971
0.946
1.000
3.091
3.064

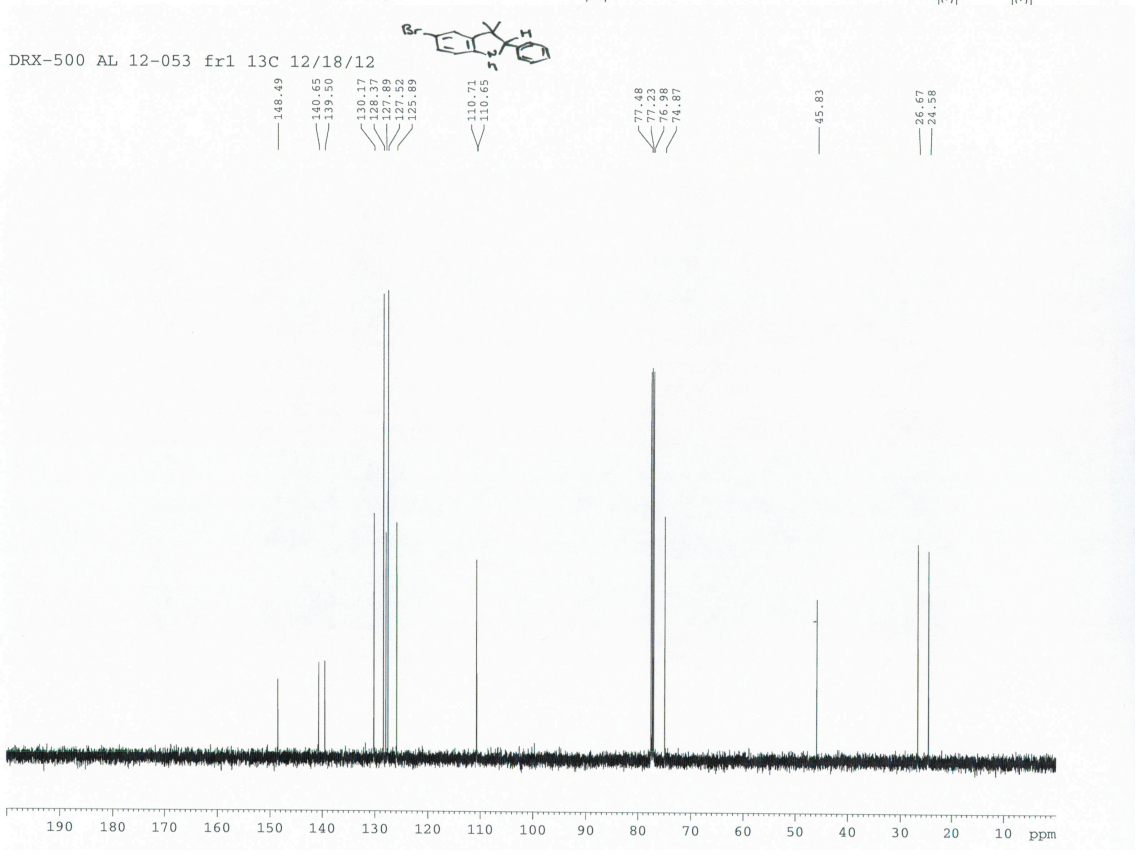
DRX-500 AL 12-053 fr1 13C 12/18/12
148.49
140.65
139.50
130.17
128.37
127.89
127.52
125.89
110.71
110.65
77.48
77.23
76.98
74.87
45.83
26.67
24.58
ppm

3.17f

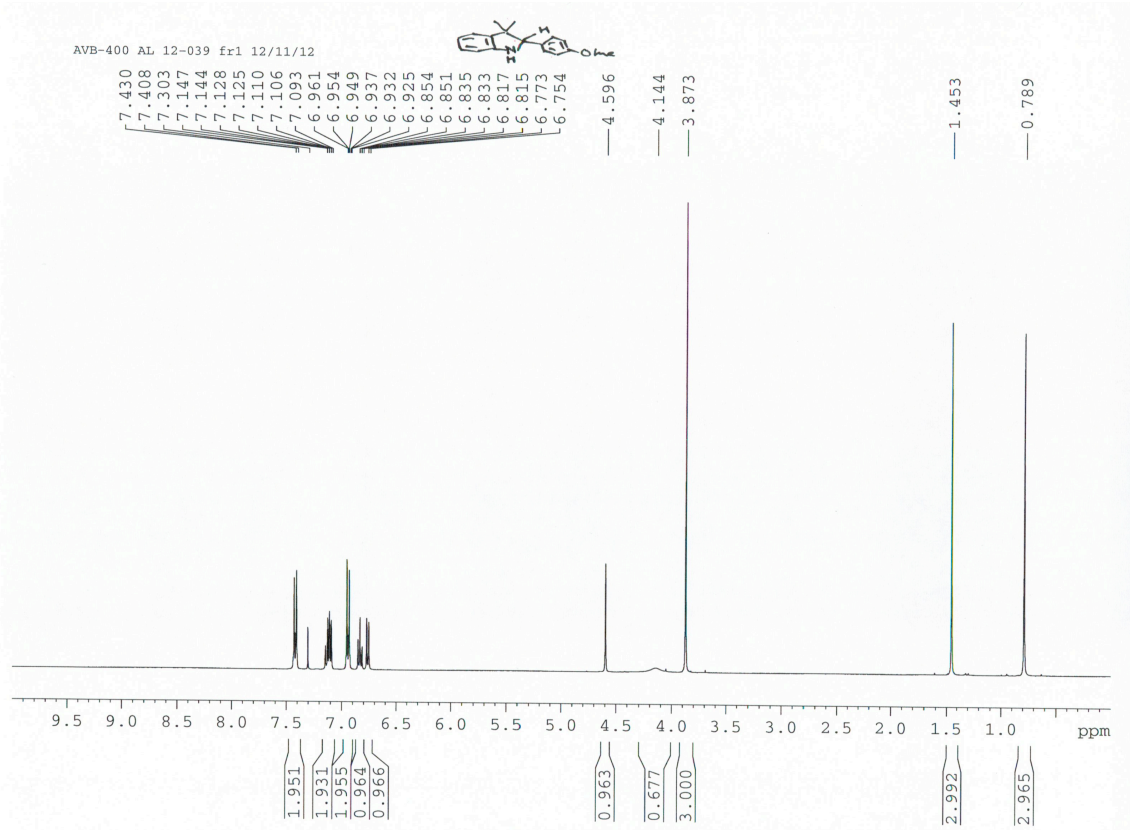
AVB-400 AL 12-039 fr1 12/11/12
7.430
7.408
7.303
7.147
7.144
7.128
7.125
7.110
7.106
7.093
6.961
6.954
6.949
6.937
6.932
6.925
6.854
6.851
6.835
6.833
6.817
6.815
6.773
6.754
4.596
4.144
3.873
1.453
0.789
9.5 9.0 8.5 8.0 7.5 7.0 6.5 6.0 5.5 5.0 4.5 4.0 3.5 3.0 2.5 2.0 1.5 1.0 ppm
1.951
1.931
1.955
0.964
0.966
0.963
0.677
3.000
2.992
2.965

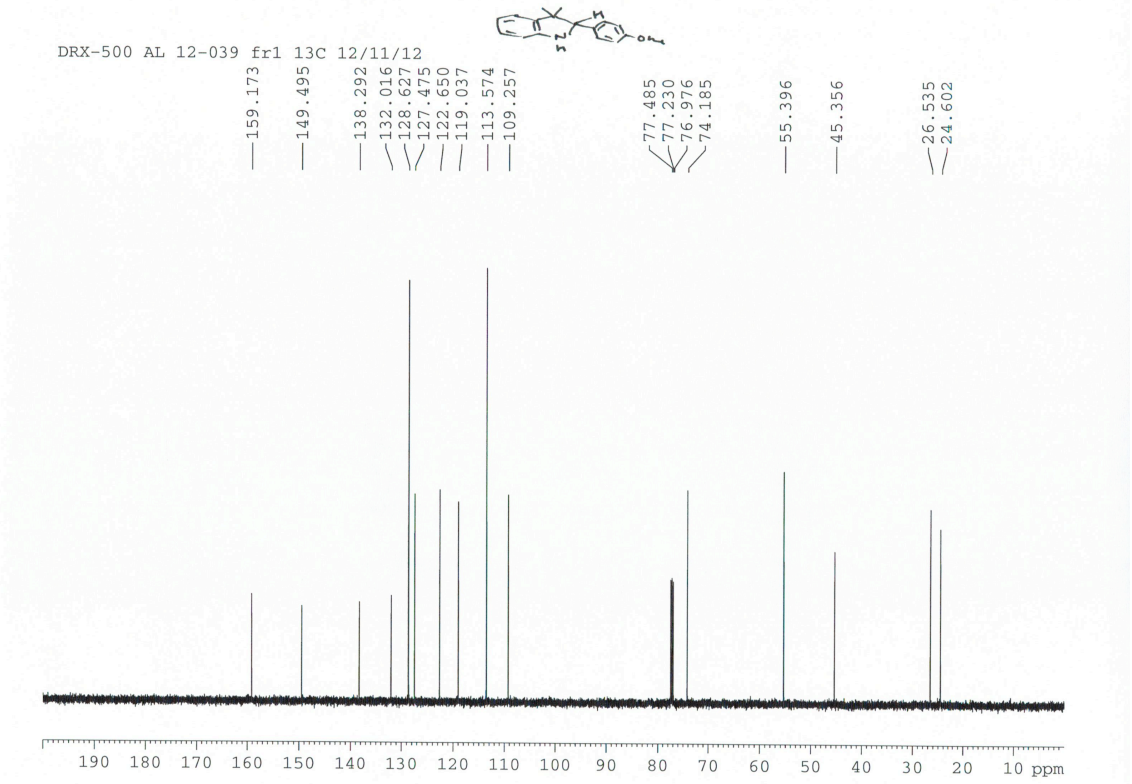
DRX-500 AL 12-039 fr1 13C 12/11/12
159.173
149.495
138.292
132.016
128.627
127.475
122.650
119.037
113.574
109.257
77.485
77.230
76.976
74.185
55.396
45.356
26.535
24.602
190 180 170 160 150 140 130 120 110 100 90 80 70 60 50 40 30 20 10 ppm

3.17g

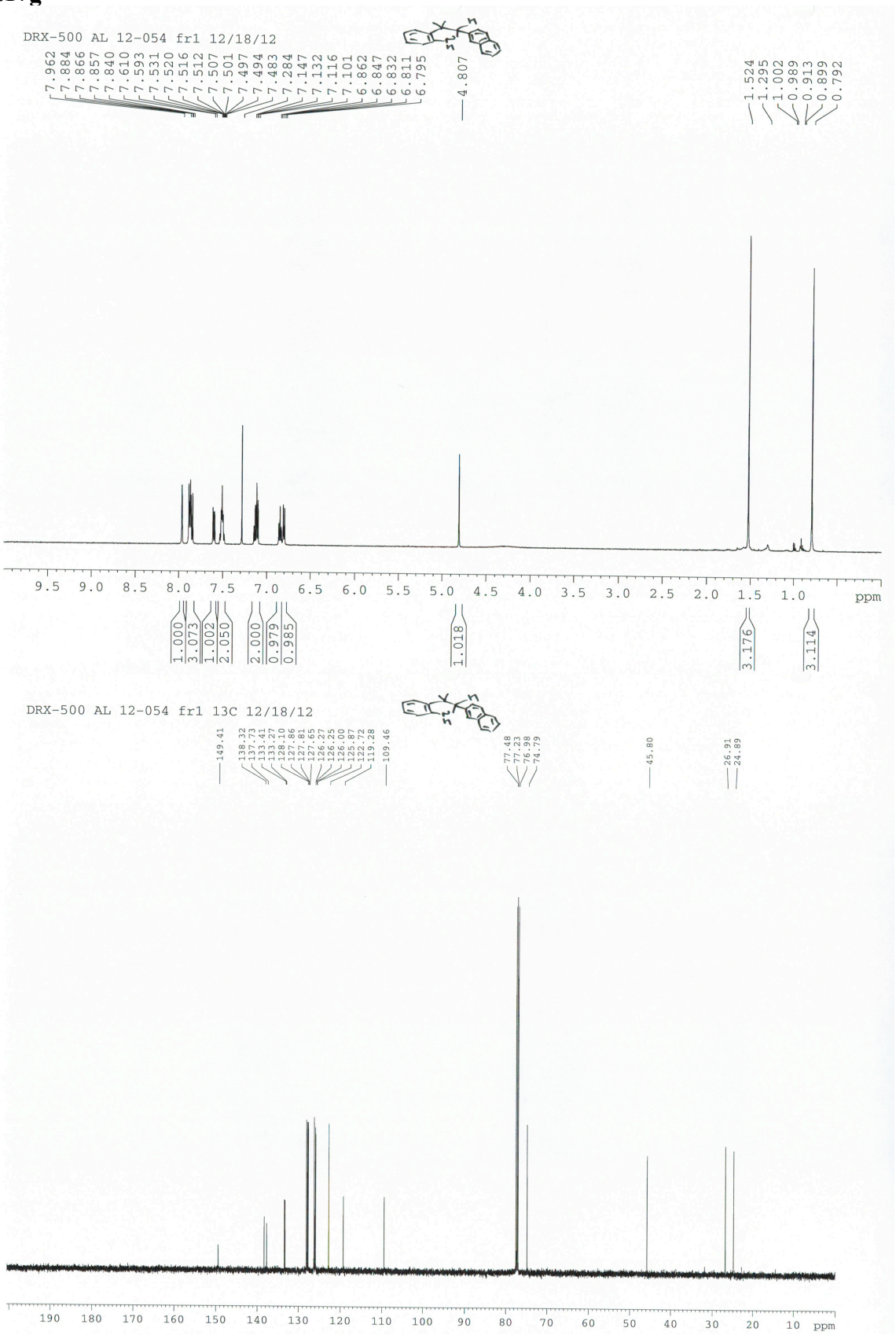
DRX-500 AL 12-054 fr1 12/18/12
7.962
7.884
7.866
7.857
7.840
7.610
7.593
7.531
7.520
7.516
7.512
7.507
7.501
7.497
7.494
7.483
7.284
7.147
7.132
7.116
7.101
6.862
6.847
6.832
6.811
6.795
4.807
1.524
1.295
1.002
0.989
0.913
0.899
0.792
ppm
1.000
3.073
1.002
2.050
2.000
0.979
0.985
1.018
3.176
3.114
DRX-500 AL 12-054 fr1 13C 12/18/12
149.41
138.32
137.73
133.41
133.27
128.10
127.86
127.81
127.65
126.27
126.25
126.00
125.87
122.72
119.28
109.46
77.48
77.23
76.98
74.79
45.80
26.91
24.89
ppm

3.17h

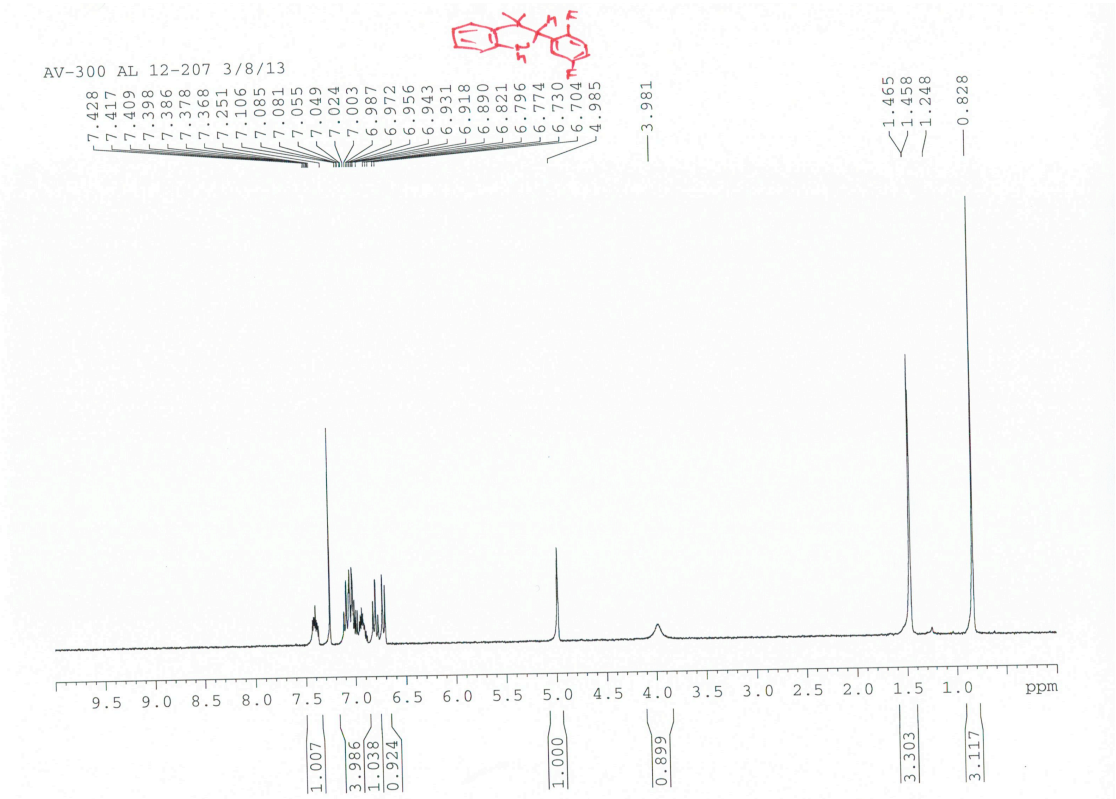
AV-300 AL 12-207 3/8/13
7.428
7.417
7.409
7.398
7.386
7.378
7.368
7.251
7.106
7.085
7.081
7.055
7.049
7.024
7.003
6.987
6.972
6.956
6.943
6.931
6.918
6.890
6.821
6.796
6.774
6.730
6.704
4.985
3.981
1.465
1.458
1.248
0.828
9.5 9.0 8.5 8.0 7.5 7.0 6.5 6.0 5.5 5.0 4.5 4.0 3.5 3.0 2.5 2.0 1.5 1.0
ppm
1.007
3.986
1.038
0.924
1.000
0.899
3.303
3.117

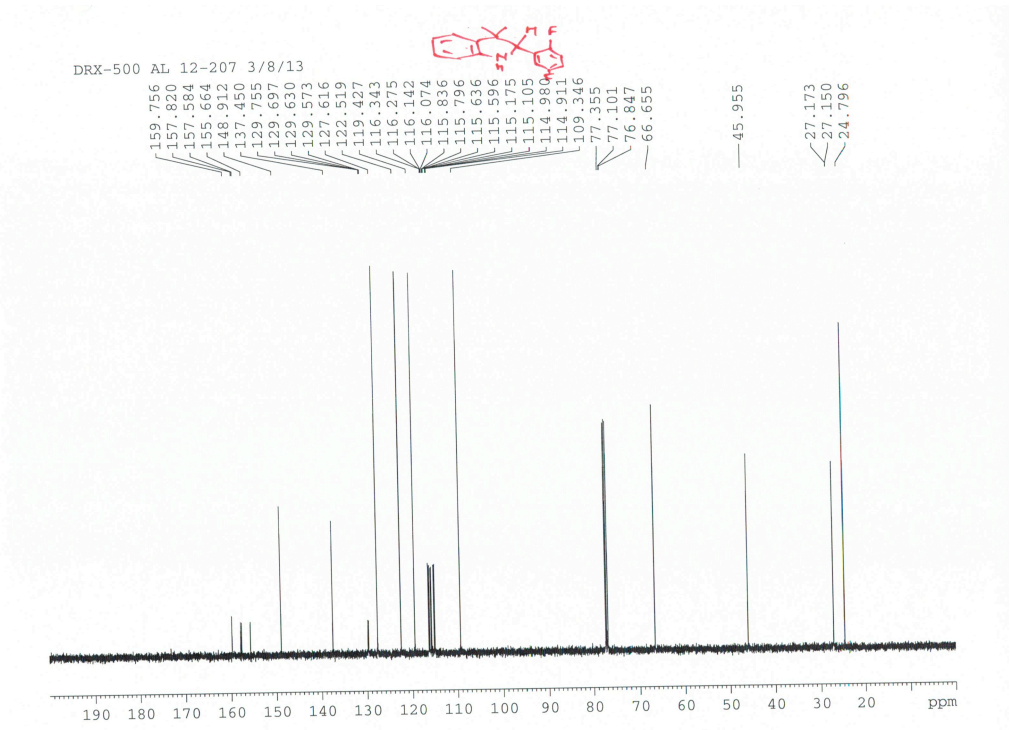
DRX-500 AL 12-207 3/8/13
159.756
157.820
157.584
155.664
148.912
137.450
129.755
129.697
129.630
129.573
127.616
122.519
119.427
116.343
116.275
116.142
116.074
115.836
115.796
115.636
115.596
115.175
115.105
114.980
114.911
109.346
77.355
77.101
76.847
66.655
45.955
27.173
27.150
24.796
190 180 170 160 150 140 130 120 110 100 90 80 70 60 50 40 30 20 ppm

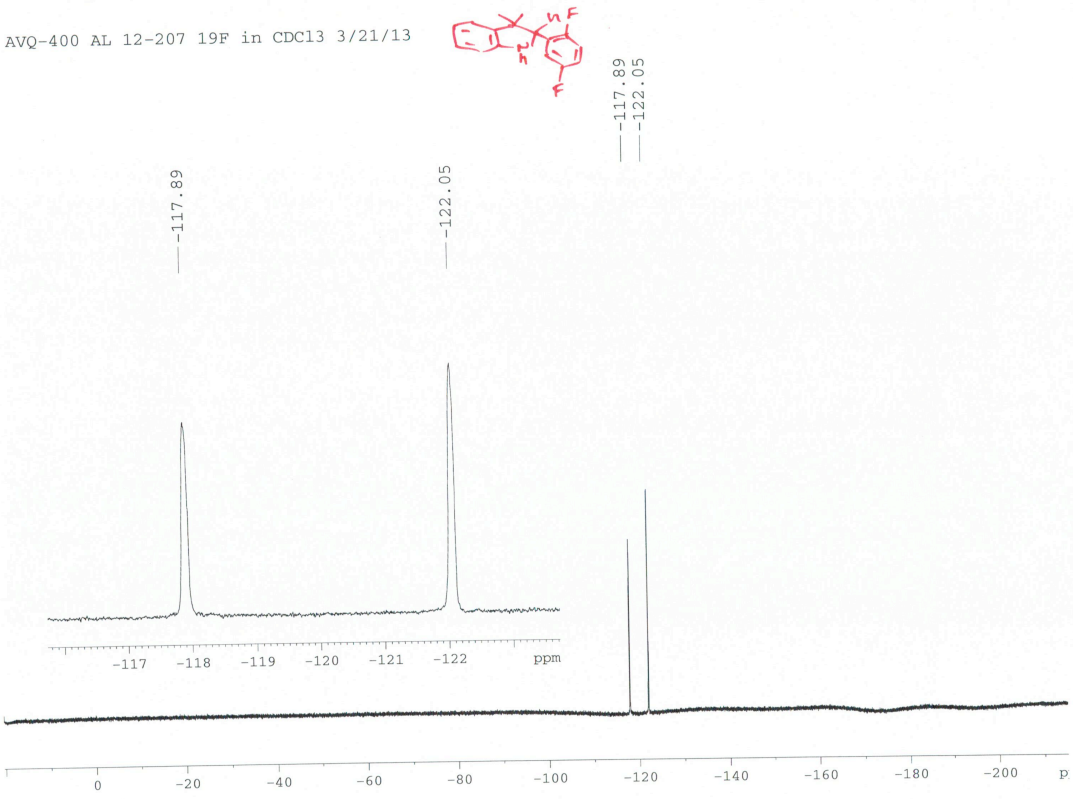
AVQ-400 AL 12-207 19F in CDCl3 3/21/13
-117.89
-122.05
-117.89
-122.05
-117 -118 -119 -120 -121 -122 ppm
0 -20 -40 -60 -80 -100 -120 -140 -160 -180 -200 p

3.17i

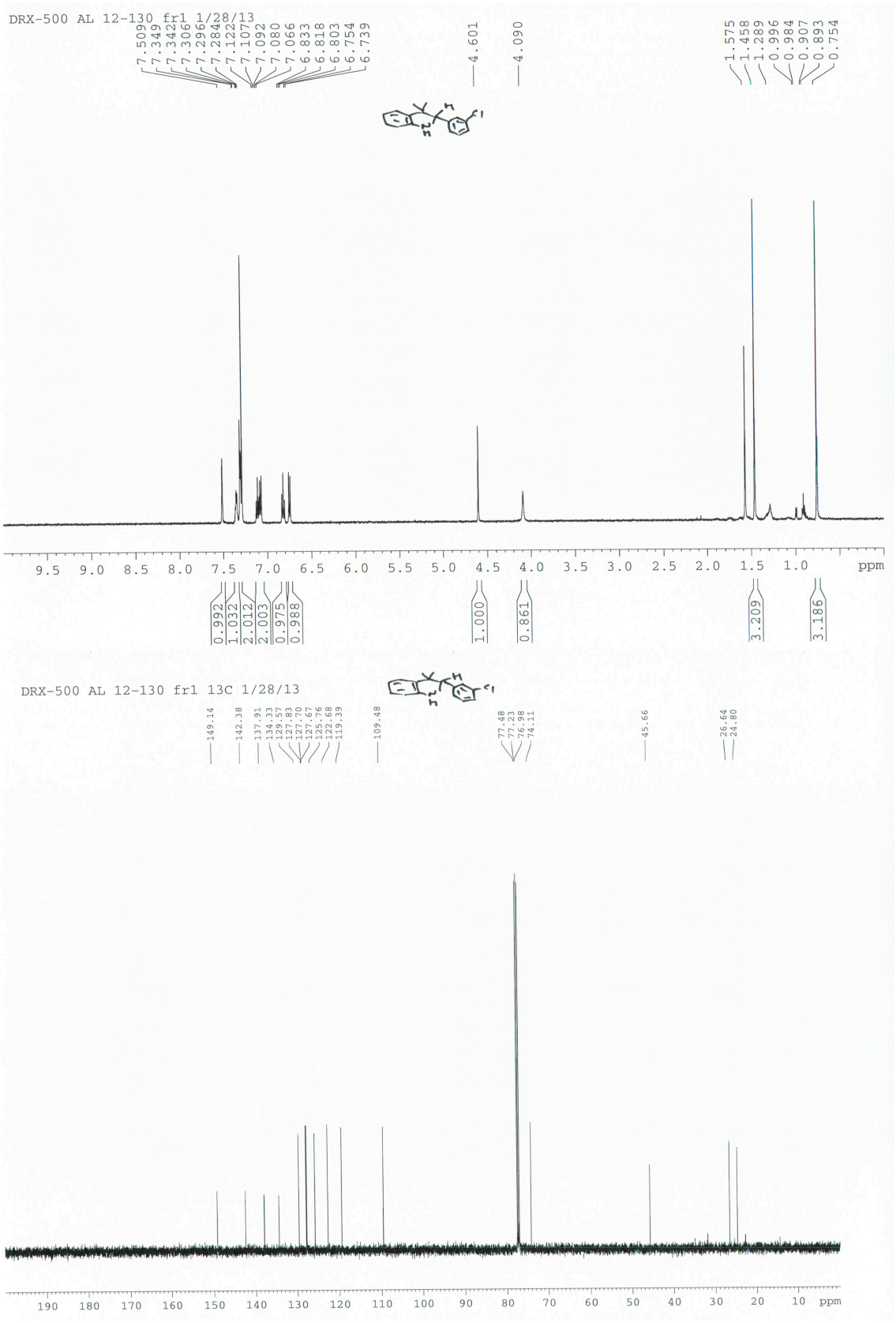
DRX-500 AL 12-130 fr1 1/28/13
7.509
7.349
7.342
7.306
7.296
7.284
7.122
7.107
7.092
7.080
7.066
6.833
6.818
6.803
6.754
6.739
4.601
4.090
1.575
1.458
1.289
0.996
0.984
0.907
0.893
0.754
ppm
0.992
1.032
2.012
2.003
0.975
0.988
1.000
0.861
3.209
3.186
DRX-500 AL 12-130 fr1 13C 1/28/13
149.14
142.38
137.91
134.33
129.57
127.83
127.70
127.67
125.76
122.68
119.39
109.48
77.48
77.23
76.98
74.11
45.66
26.64
24.80
ppm

3.17j

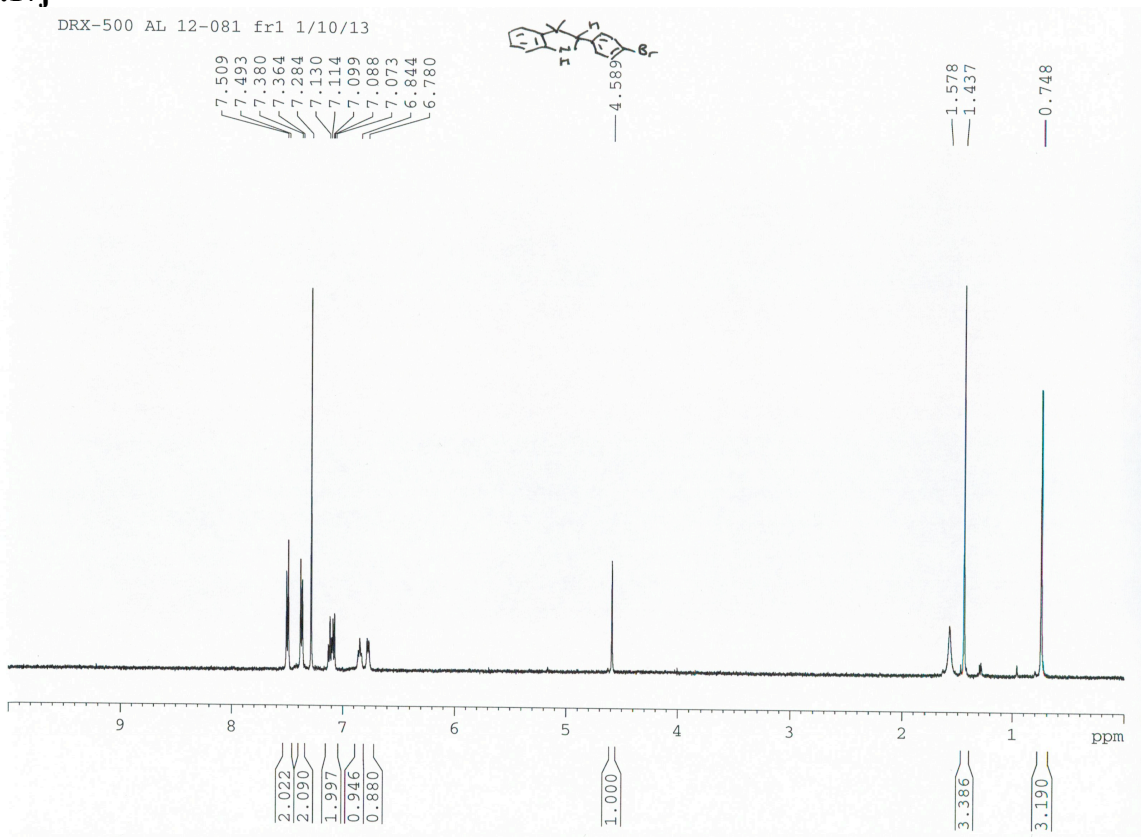
DRX-500 AL 12-081 fr1 1/10/13
7.509
7.493
7.380
7.364
7.284
7.130
7.114
7.099
7.088
7.073
6.844
6.780
4.589
1.578
1.437
0.748
9
8
7
6
5
4
3
2
1
ppm
2.022
2.090
1.997
0.946
0.880
1.000
3.386
3.190

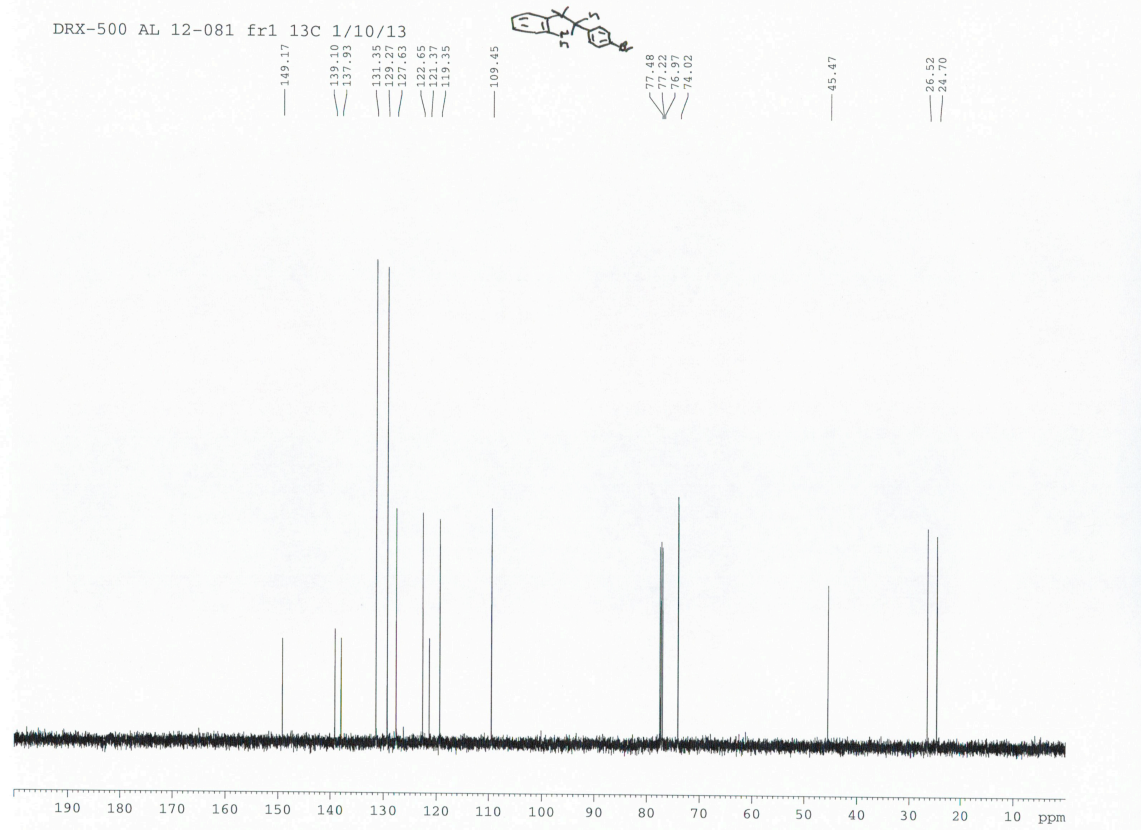
DRX-500 AL 12-081 fr1 13C 1/10/13
149.17
139.10
137.93
131.35
129.27
127.63
122.65
121.37
119.35
109.45
77.48
77.22
76.97
74.02
45.47
26.52
24.70
190
180
170
160
150
140
130
120
110
100
90
80
70
60
50
40
30
20
10
ppm

3.17k

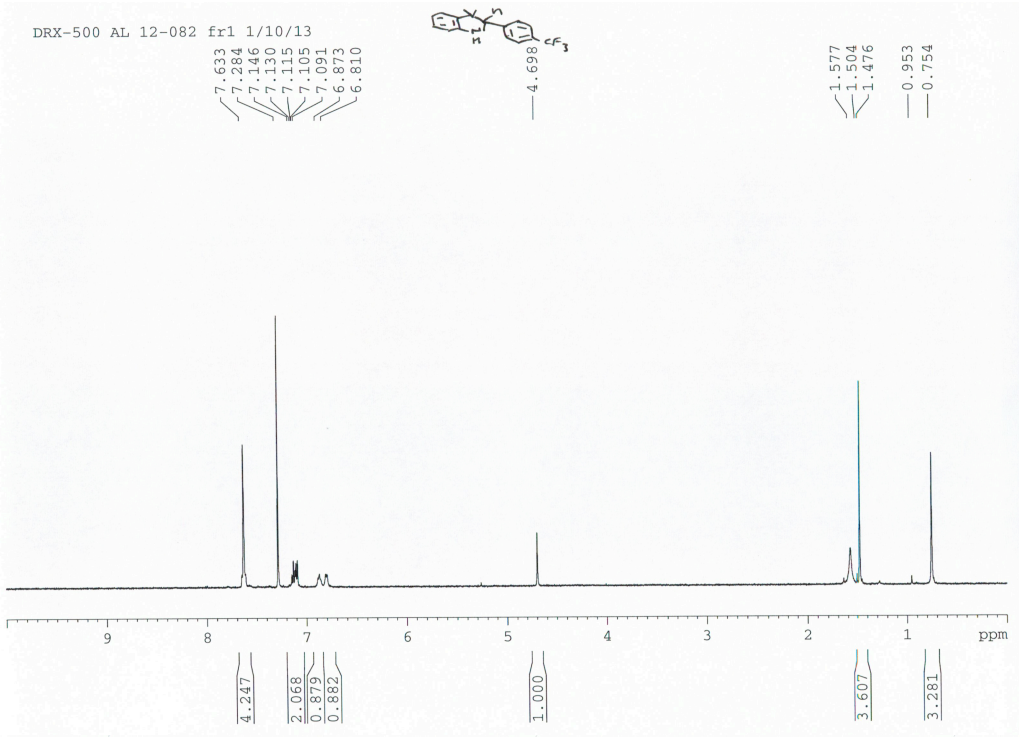
DRX-500 AL 12-082 fr1 1/10/13
7.633
7.284
7.146
7.130
7.115
7.105
7.091
6.873
6.810
4.698
1.577
1.504
1.476
0.953
0.754
9
8
7
6
5
4
3
2
1
ppm
4.247
2.068
0.879
0.882
1.000
3.607
3.281

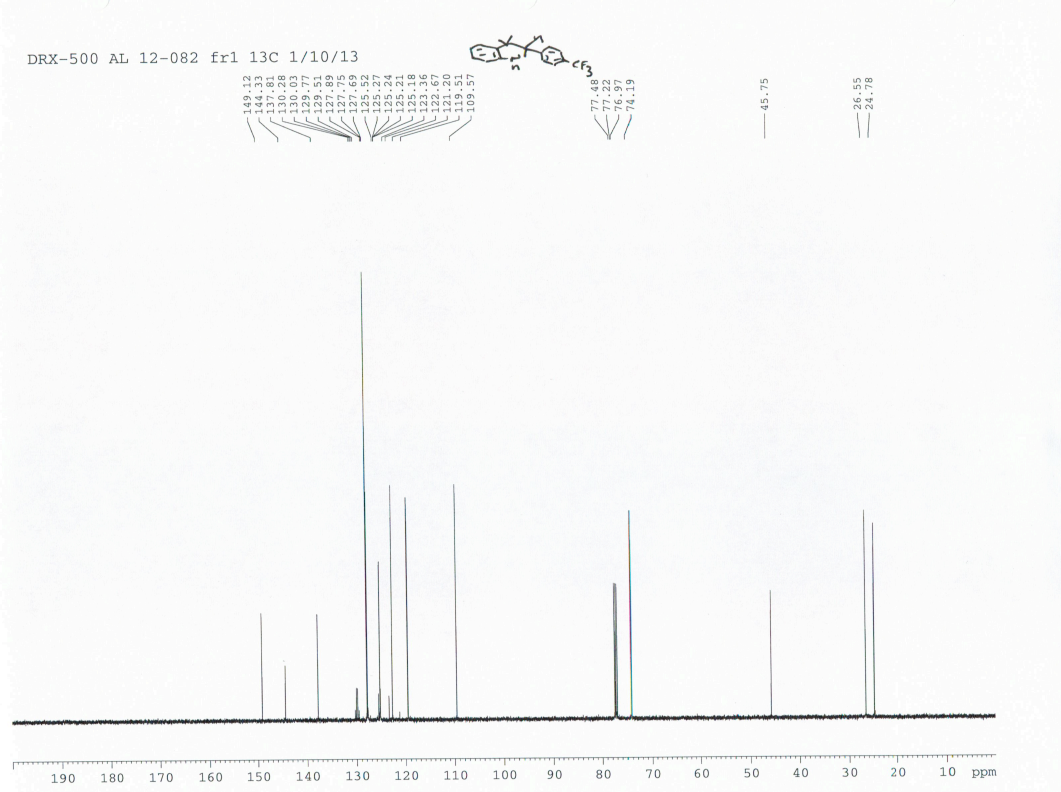
DRX-500 AL 12-082 fr1 13C 1/10/13
149.12
144.13
137.81
130.28
130.03
129.77
129.51
127.89
127.72
127.69
125.52
125.27
125.24
125.21
123.18
123.36
122.67
121.20
119.51
109.57
77.48
77.22
76.97
74.19
45.75
26.55
24.78
190
180
170
160
150
140
130
120
110
100
90
80
70
60
50
40
30
20
10
ppm

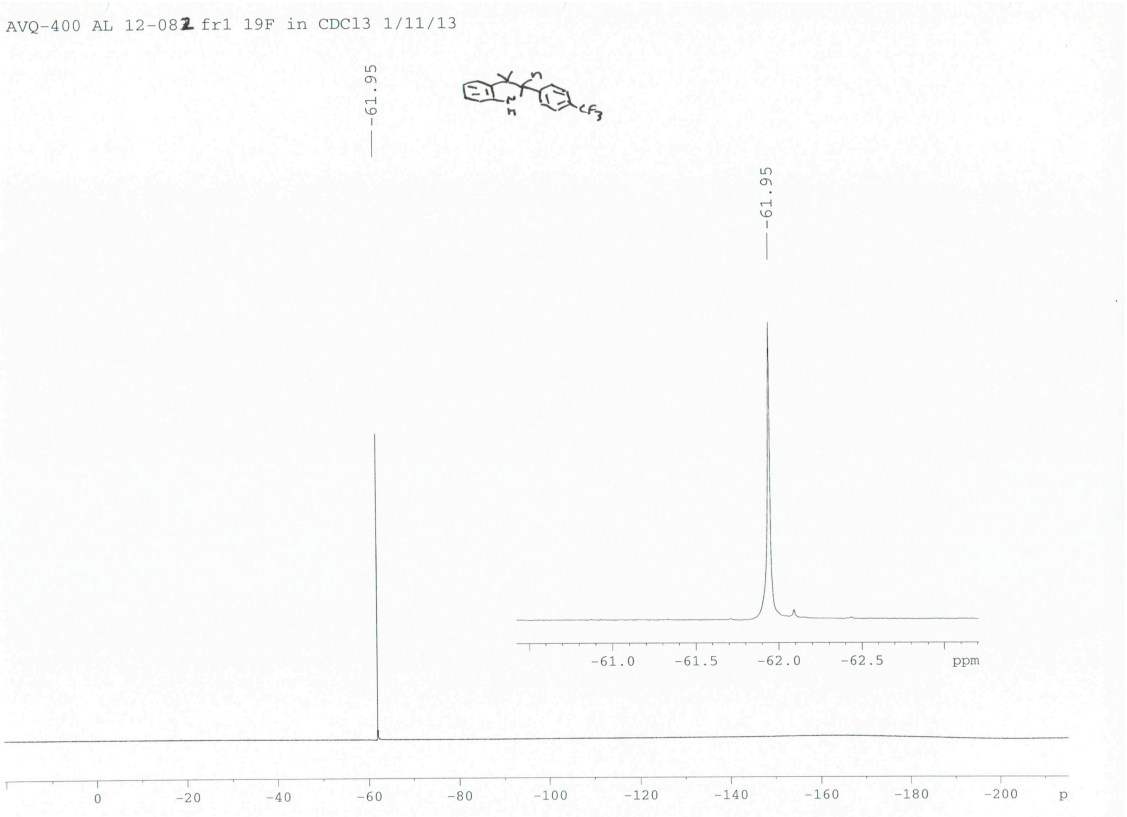
AVQ-400 AL 12-082 fr1 19F in CDCl3 1/11/13
-61.95
-61.95
-61.0
-61.5
-62.0
-62.5
ppm
0
-20
-40
-60
-80
-100
-120
-140
-160
-180
-200

HPLCs

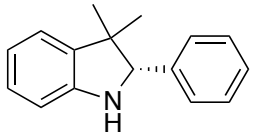

(*S*)-**3.17a**

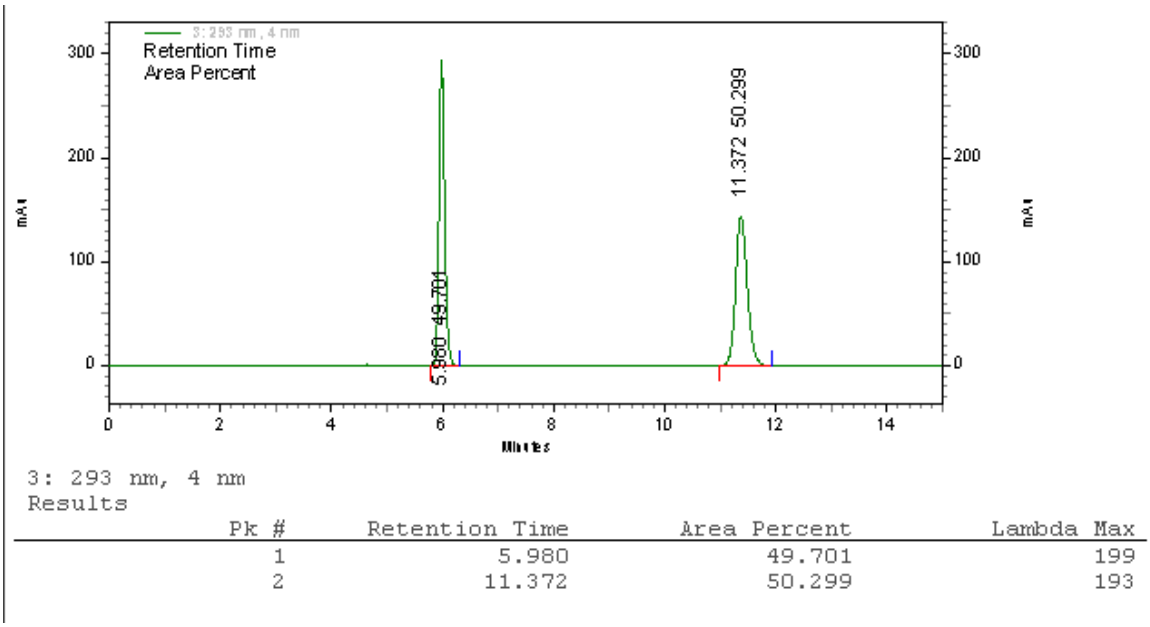

3: 293 nm, 4 nm
Results

Pk #	Retention Time	Area Percent	Lambda Max
1	5.980	49.701	199
2	11.372	50.299	193

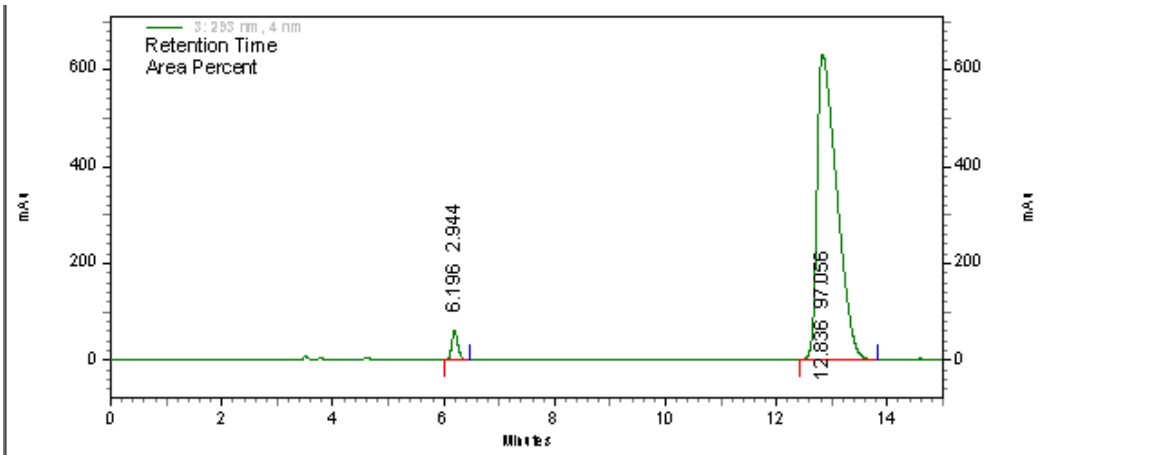

3: 293 nm, 4 nm
Results

Pk #	Retention Time	Area Percent	Lambda Max
1	6.196	2.944	207
2	12.836	97.056	212

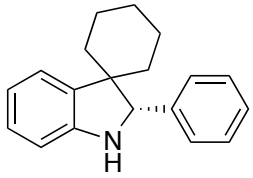

(*S*)-**3.17b**

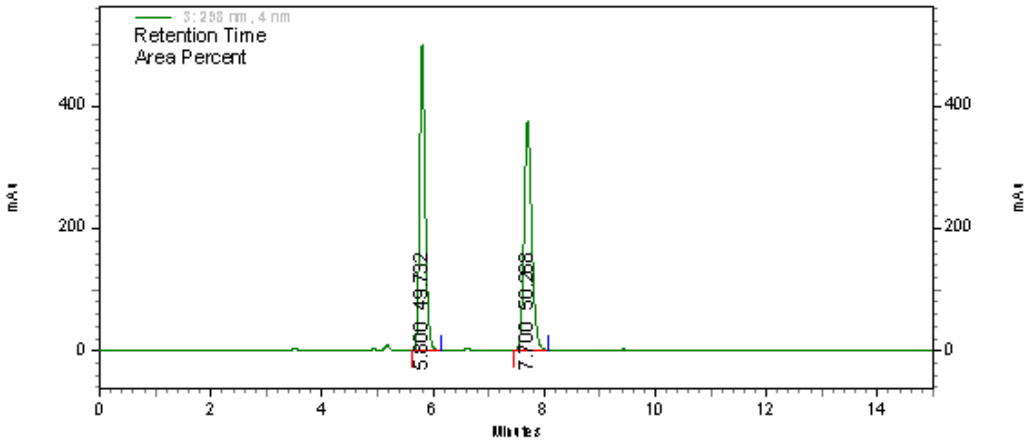

3: 298 nm, 4 nm
Results

Pk #	Retention Time	Area Percent	Lambda Max
1	5.800	49.732	210
2	7.700	50.268	205

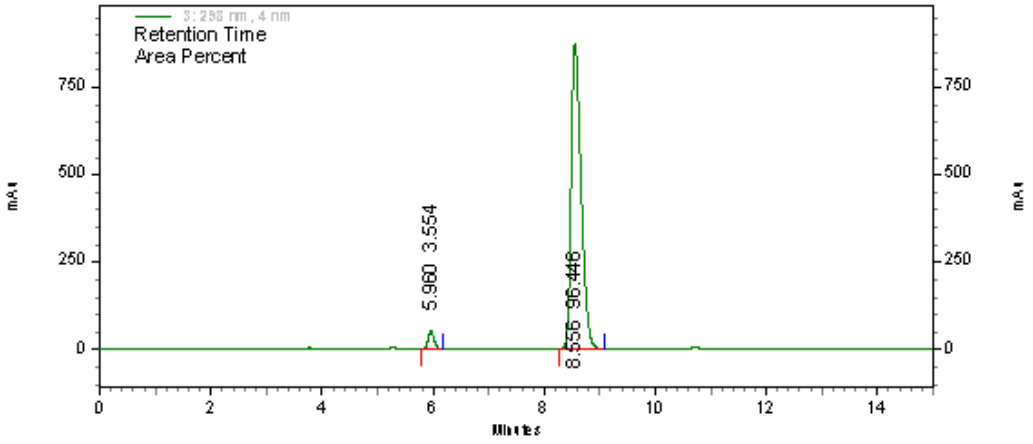

3: 298 nm, 4 nm
Results

Pk #	Retention Time	Area Percent	Lambda Max
1	5.960	3.554	207
2	8.556	96.446	215

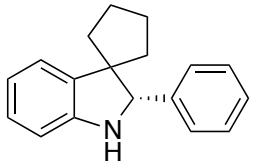

(*S*)-**3.17c**

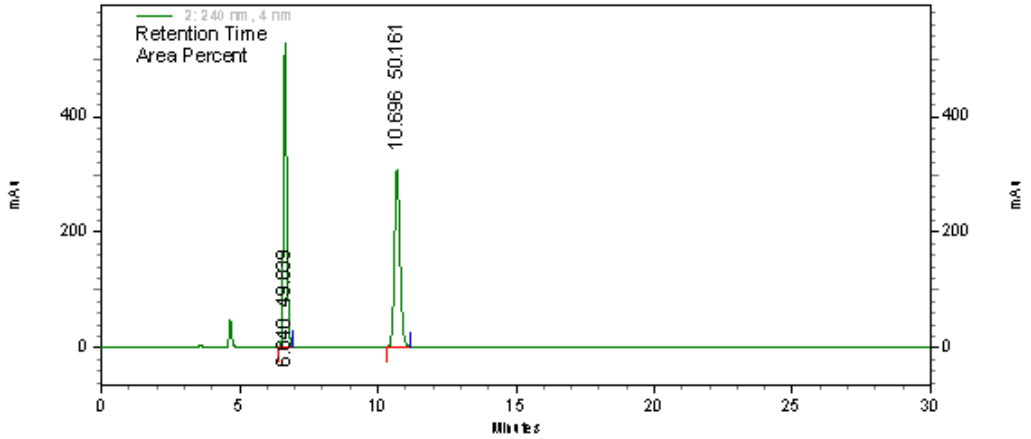

2: 240 nm, 4 nm
Results

Pk #	Retention Time	Area Percent	Lambda Max
1	6.640	49.839	197
2	10.696	50.161	194

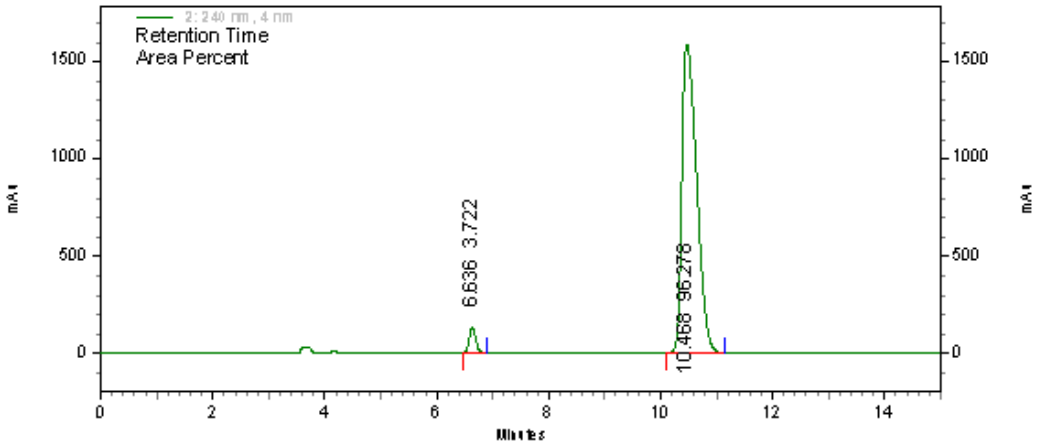

2: 240 nm, 4 nm
Results

Pk #	Retention Time	Area Percent	Lambda Max
1	6.636	3.722	207
2	10.468	96.278	213

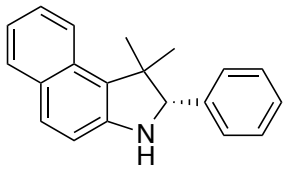

(*S*)-**3.17d**

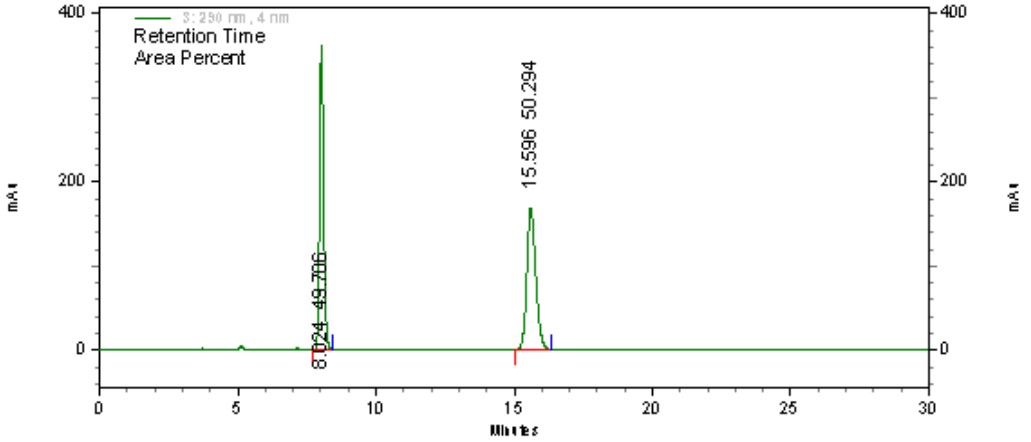

3: 290 nm, 4 nm
Results

Pk #	Retention Time	Area Percent	Lambda Max
1	8.024	49.706	201
2	15.596	50.294	195

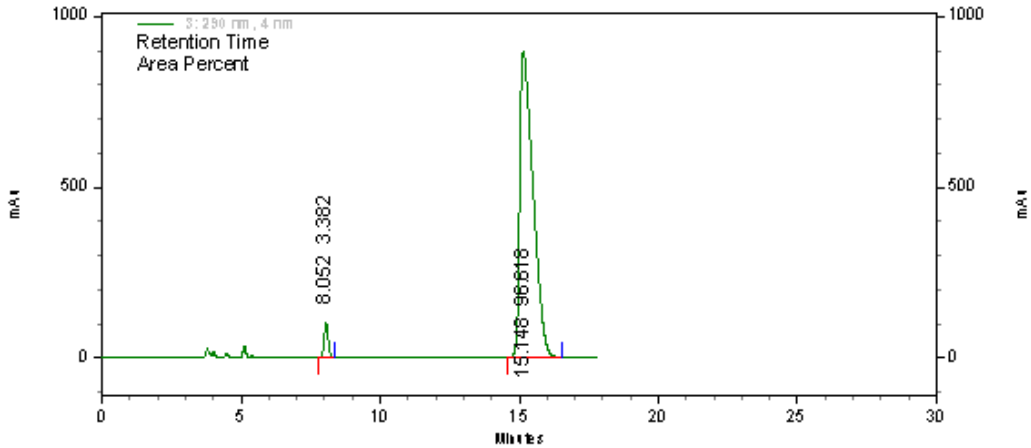

3: 290 nm, 4 nm
Results

Pk #	Retention Time	Area Percent	Lambda Max
1	8.052	3.382	244
2	15.148	96.618	223

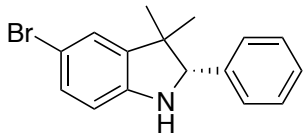

(*S*)-**3.17e**

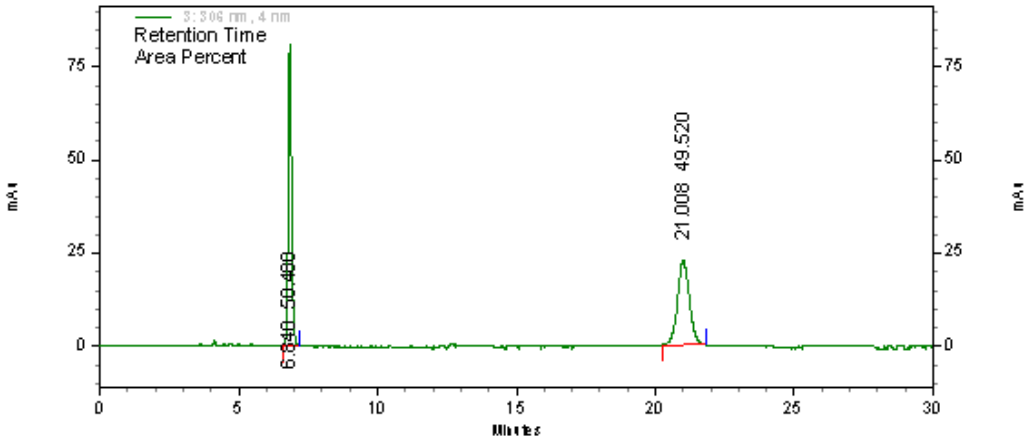

3: 306 nm, 4 nm
Results

Pk #	Retention Time	Area Percent	Lambda Max
1	6.840	50.480	191
2	21.008	49.520	208

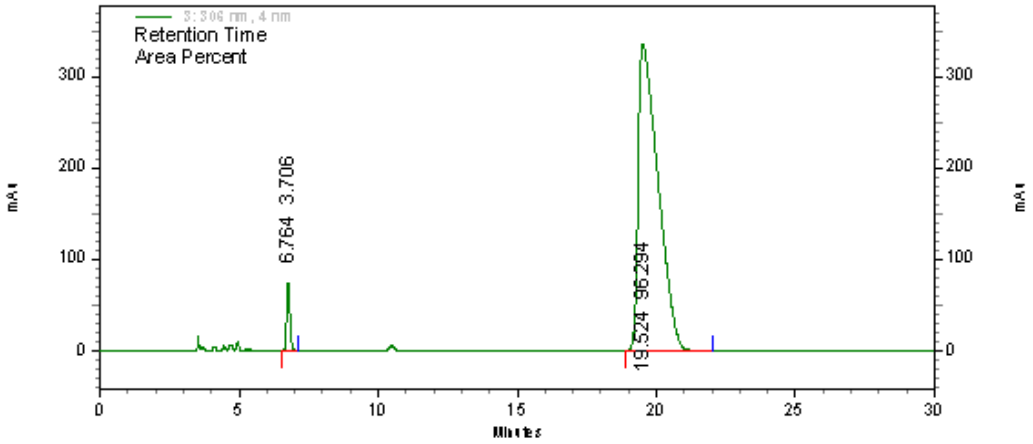

3: 306 nm, 4 nm
Results

Pk #	Retention Time	Area Percent	Lambda Max
1	6.764	3.706	191
2	19.524	96.294	203

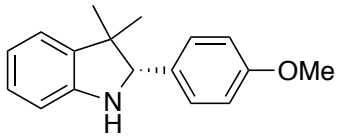

(*S*)-**3.17f**

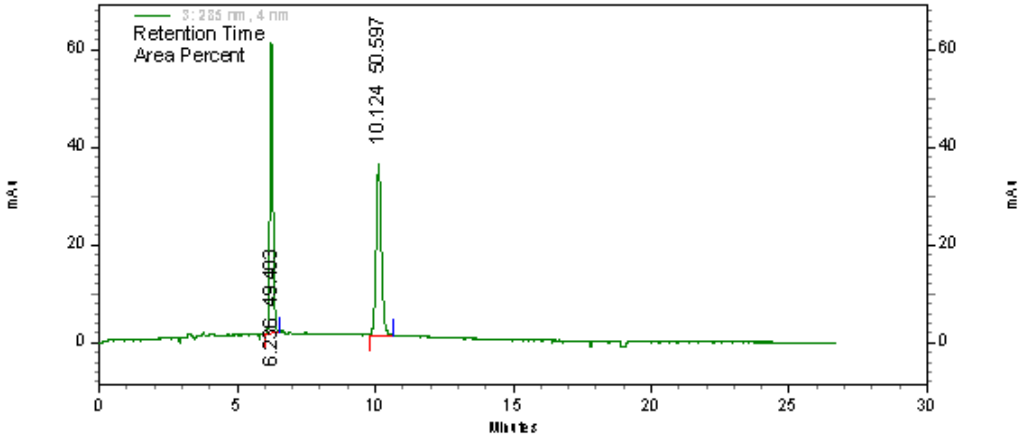

3: 285 nm, 4 nm
Results

Pk #	Retention Time	Area Percent	Lambda Max
1	6.236	49.403	205
2	10.124	50.597	205

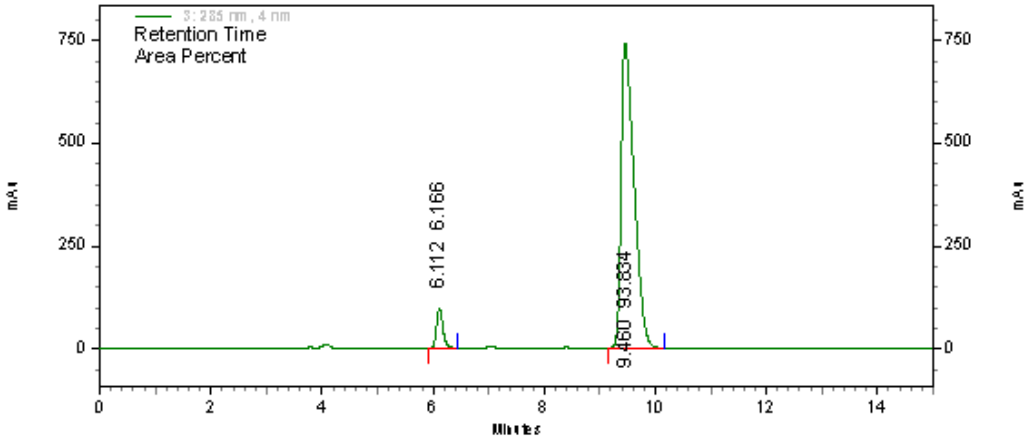

3: 285 nm, 4 nm
Results

Pk #	Retention Time	Area Percent	Lambda Max
1	6.112	6.166	190
2	9.460	93.834	223

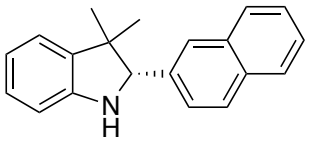

(*S*)-**3.17g**

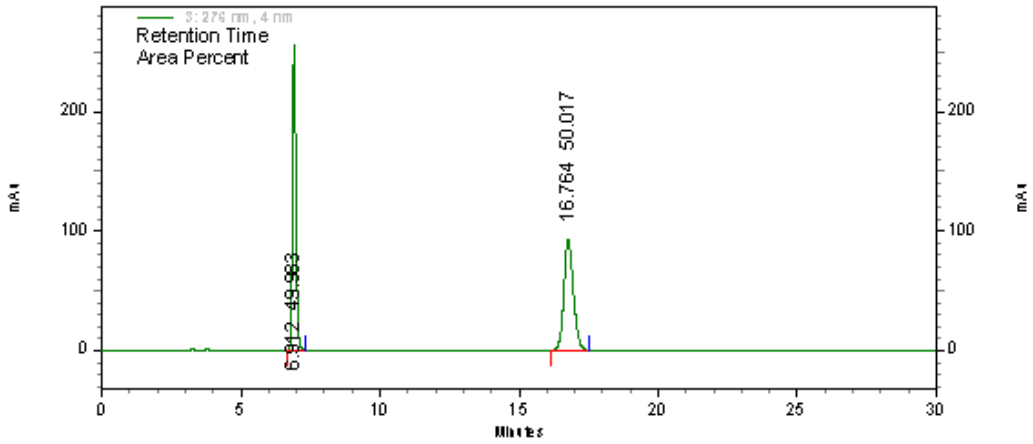

3: 276 nm, 4 nm
Results

Pk #	Retention Time	Area Percent	Lambda Max
1	6.912	49.983	201
2	16.764	50.017	223

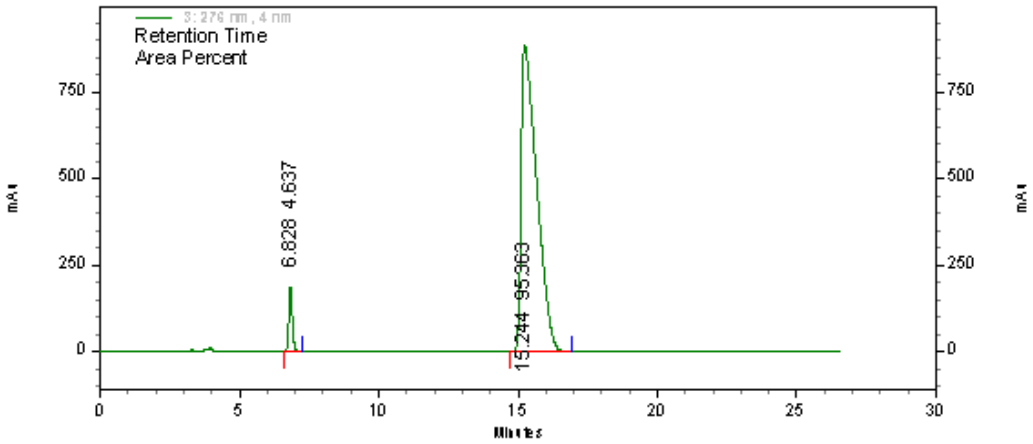

3: 276 nm, 4 nm
Results

Pk #	Retention Time	Area Percent	Lambda Max
1	6.828	4.637	198
2	15.244	95.363	223

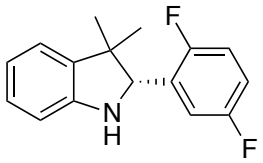

(*S*)-**3.17h**

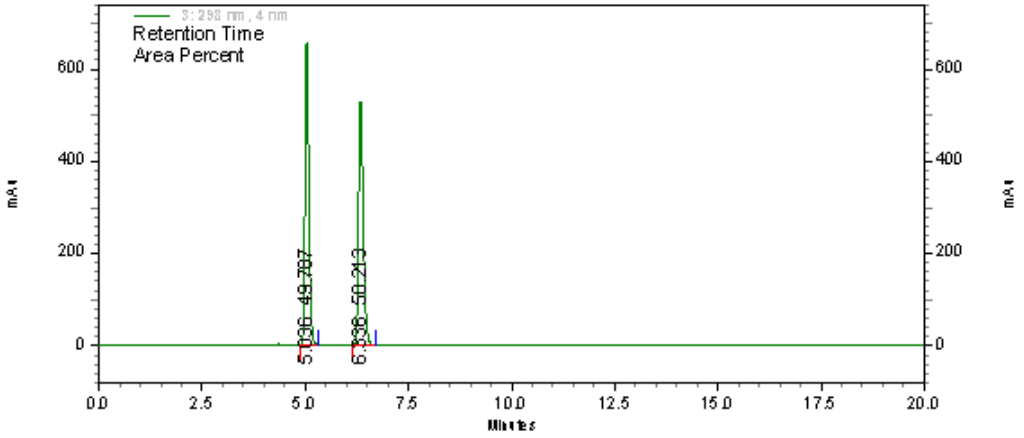

3: 298 nm, 4 nm
Results

Pk #	Retention Time	Area Percent	Lambda Max
1	5.036	49.787	211
2	6.336	50.213	210

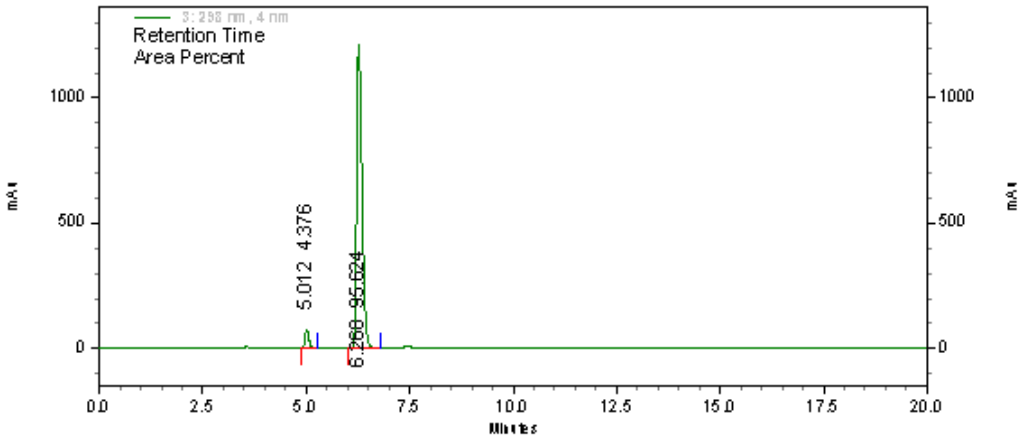

3: 298 nm, 4 nm
Results

Pk #	Retention Time	Area Percent	Lambda Max
1	5.012	4.376	207
2	6.268	95.624	223

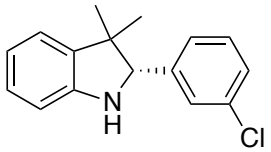

(*S*)-**3.17i**

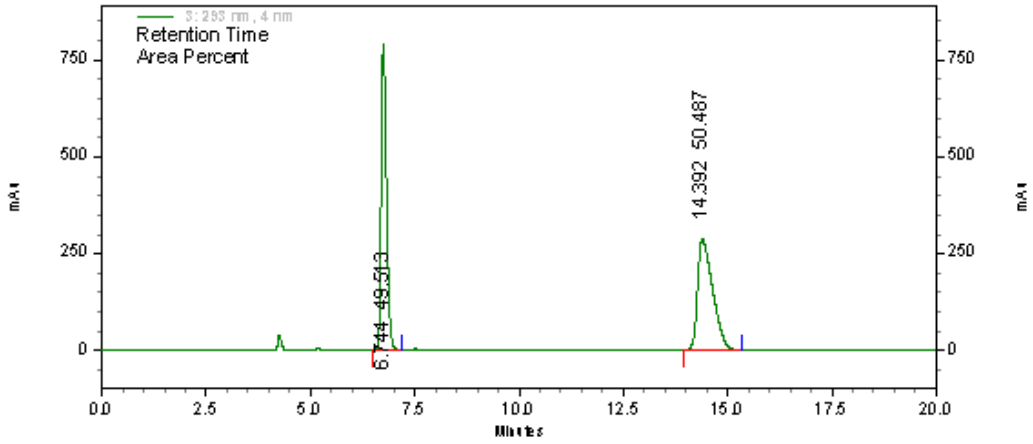

3: 293 nm, 4 nm
Results

Pk #	Retention Time	Area Percent	Lambda Max
1	6.744	49.513	218
2	14.392	50.487	205

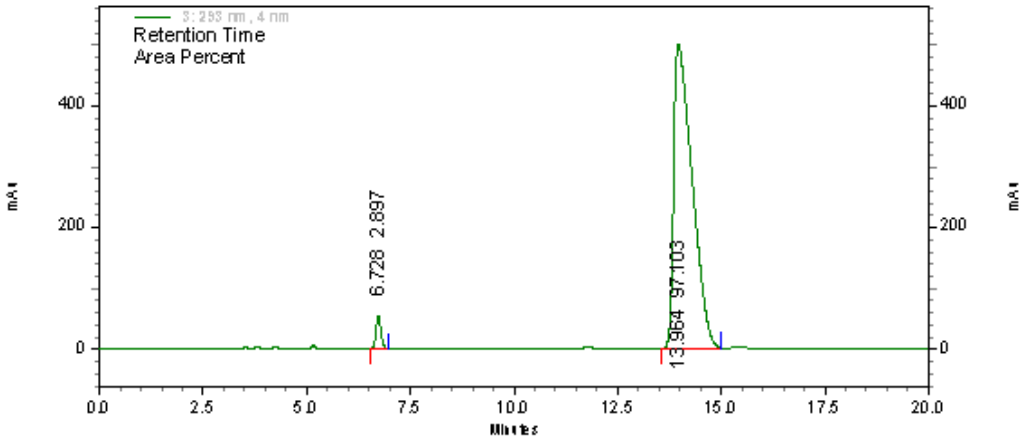

3: 293 nm, 4 nm
Results

Pk #	Retention Time	Area Percent	Lambda Max
1	6.728	2.897	206
2	13.964	97.103	211

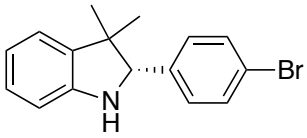

(*S*)-**3.17j**

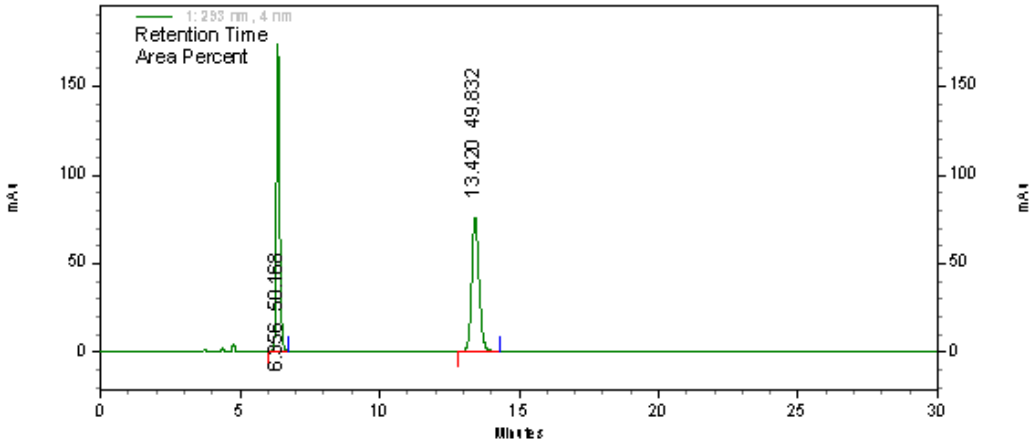

1: 293 nm, 4 nm
Results

Pk #	Retention Time	Area Percent	Lambda Max
1	6.356	50.168	202
2	13.420	49.832	205

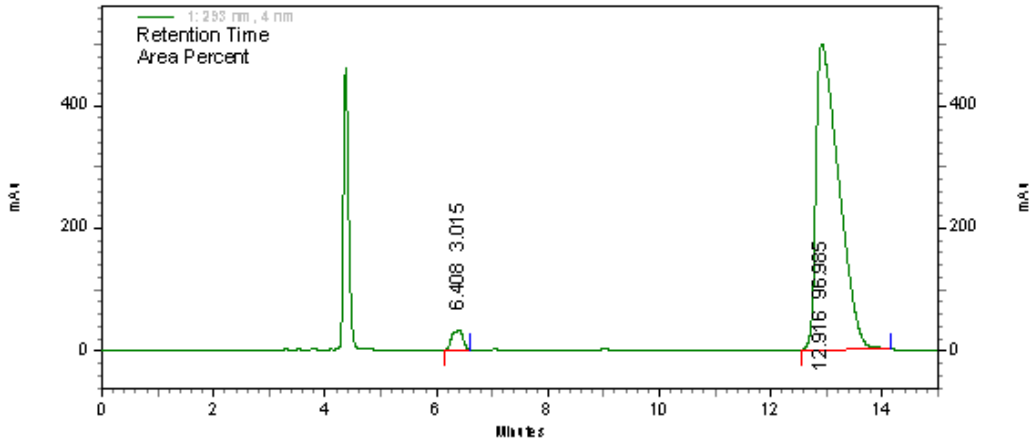

1: 293 nm, 4 nm
Results

Pk #	Retention Time	Area Percent	Lambda Max
1	6.408	3.015	206
2	12.916	96.985	221

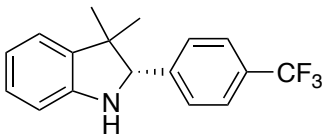

(*S*)-**3.17k**

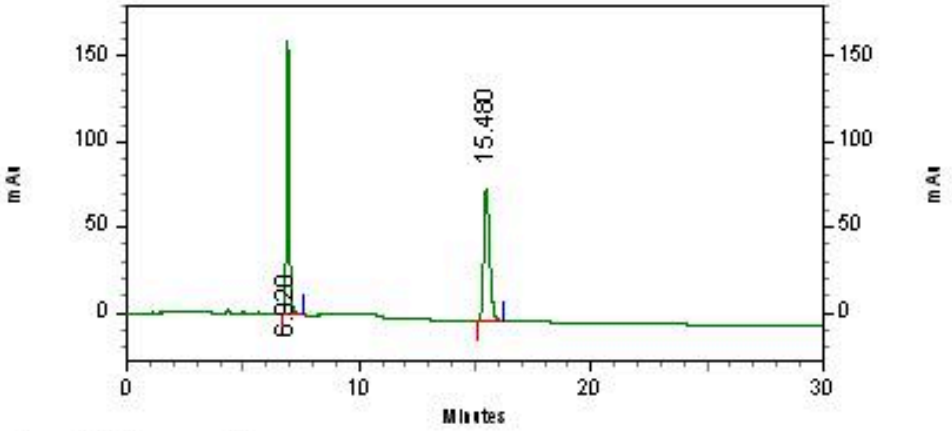

2: 248 nm, 4 nm Results

Retention Time	Area	Area Percent	Lambda Max
6.920	1351967	49.756	207
15.480	1365226	50.244	207

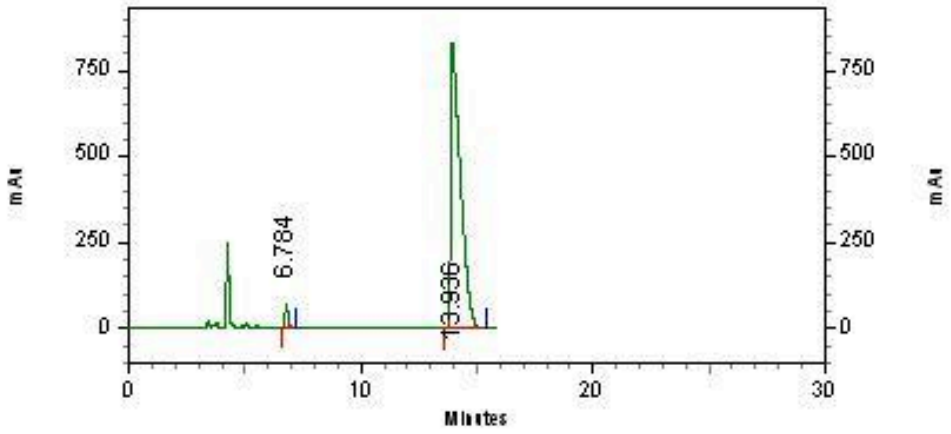

2: 248 nm, 4 nm Results

Retention Time	Area	Area Percent	Lambda Max
6.784	643872	2.604	207
13.936	24083669	97.396	199

Inversion of (*S*)-3.17a to (*R*)-3.17a

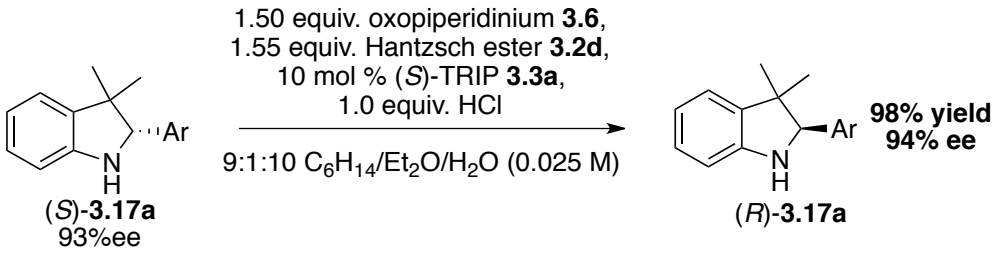

(*S*)-**3.17a**
93%ee

(*R*)-**3.17a**

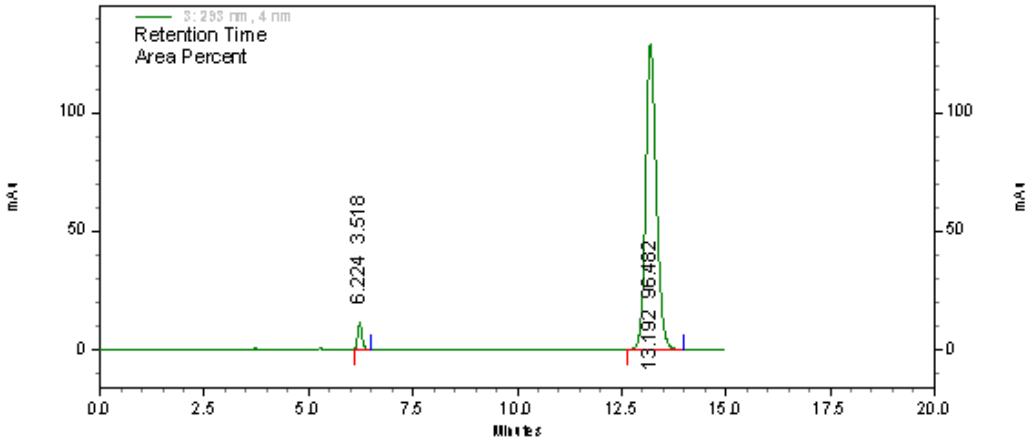

3: 293 nm, 4 nm
Results

Pk #	Retention Time	Area Percent	Lambda Max
1	6.224	3.518	206
2	13.192	96.482	193

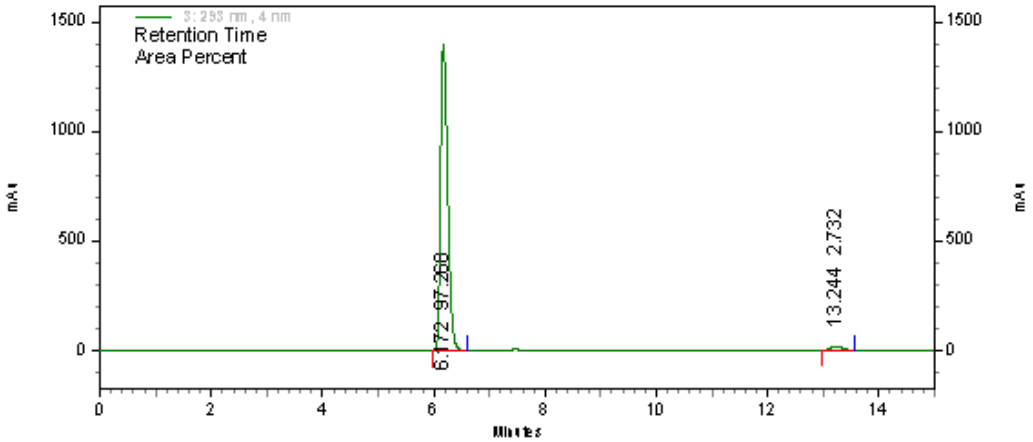

3: 293 nm, 4 nm
Results

Pk #	Retention Time	Area Percent	Lambda Max
1	6.172	97.268	223
2	13.244	2.732	206